

THE INDIAN JOURNAL OF TECHNICAL EDUCATION

Published by
INDIAN SOCIETY FOR TECHNICAL EDUCATION
Near Katwaria Sarai, Shaheed Jeet Singh Marg,
New Delhi - 110 016



INDIAN JOURNAL OF TECHNICAL EDUCATION

Volume 47 • Special Issue • No. 1 • March 2024

Indexed in the UGC-Care Journal list

Editorial Advisory Committee

Prof. Pratapsinh K. Desai - Chairman
President, ISTE

Prof. N. R. Shetty
Former President, ISTE, New Delhi

Prof. (Dr.) Buta Singh Sidhu
Vice Chancellor, Maharaja Ranjit Singh
Punjab Technical University, Bathinda

Prof. G. Ranga Janardhana
Vice Chancellor
JNTU Anantapur, Ananthapuramu

Prof. D. N. Reddy
Former Chairman
Recruitment & Assessment Centre
DRDO, Ministry of Defence, Govt. of India
New Delhi

Prof G. D. Yadav
Vice Chancellor
Institute of Chemical Technology, Mumbai

Dr. Akshai Aggarwal
Former Vice Chancellor
Gujarat Technological University,
Gandhinagar

Prof. M. S. Palanichamy
Former Vice Chancellor
Tamil Nadu Open University, Chennai

Dr. D. B. Shinde
Vice Chancellor
Shivaji University
Kolhapur

Editorial Board

Dr. Vivek B. Kamat
Director of Technical Education
Government of Goa, Goa

Dr. E. B. Perumal Pillai
Director-HRDC & Professor of Civil Engg.
Vel Tech. University, Chennai

Prof. C. C. Handa
Professor & Head, Dept. of Mech.Engg.
KDK College of Engineering
Nagpur

Prof. S. Mohan
Chief Executive, Innovation Centre (SID)
Indian Institute of Science, Bangalore

Prof. Y. Vrushabhendrapa
Director
Bapuji Institute of Engg. & Technology,
Davangere

Dr. Anant I Dhattrak
Associate Professor, Civil Engineering
Department, Government College of
Engineering, Amravati, Maharashtra

Dr. Jyoti Sekhar Banerjee
Associate Editor

Dr. Rajeshree D. Raut
Associate Editor

Dr. Y. R. M. Rao
Editor

Copyright (c) Indian Society for Technical Education, The Journal articles or any part of it may not be reproduced in any form without the written permission of the Publisher.

INDIAN JOURNAL OF TECHNICAL EDUCATION

Published by
INDIAN SOCIETY FOR TECHNICAL EDUCATION
Near Katwaria Sarai, Shaheed Jeet Singh Marg
New Delhi - 110 016



Editorial

Technology played a crucial role in developing modern world. In the recent years Artificial Intelligence (AI) and Machine Learning (ML) stand at the forefront of innovation and transformation. Artificial Intelligence refers to the simulation of human intelligence processes by machines, encompassing a wide range of techniques such as machine learning, natural language processing, computer vision, and robotics. Machine Learning, a subset of AI, focuses on the development of algorithms that enable computers to learn from and make predictions or decisions based on data, without explicit programming.

As we delve deeper into the realms of intelligent systems, the need for comprehensive understanding and critical analysis becomes paramount. This journal aims to provide a platform for exploring the intricate landscapes of AI and ML, unraveling their complexities, and examining their profound implications across various domains. Through meticulous research and analysis, the articles in this journal shed light on the evolution of AI and ML, tracing their origins, milestones, and contemporary applications. From classical algorithms to cutting-edge deep learning architectures, each contribution dissects a facet of AI and ML to uncover underlying principles and paradigms. Moreover, this journal seeks to elucidate the societal, ethical, and economic ramifications of AI and ML proliferation. As these technologies permeate industries and reshape societal structures, it is imperative to discern both their promises and perils. By delving into ethical considerations, regulatory frameworks, and potential socio-economic impacts, the articles in this journal foster informed discourse and responsible innovation.

In curating this journal, the contributions of research scholars, academicians, and practitioners are commendable whose insights have enriched this discourse. Their collective wisdom has served as a guiding beacon throughout this exploration, illuminating pathways for further inquiry and discovery. We are sure that the articles published in this journal aspires to serve as a compendium for scholars, practitioners, and enthusiasts alike, navigating the intricate intersections of AI and ML with rigor, technical depth, and conscientiousness.

New Delhi

Editor

31st March 2024

Jawahar Education Society's Institute of Technology, Management and Research

Survey No 48, Gowardhan, Gangapur Road
Nashik - 422 222, Maharashtra

Chief Patron

Hon. Shri. Rohidasji. C. Patil, (Founder, Jawahar Education Society)

Patrons

Hon. Shri. Vinay R. Patil
(President, Jawahar Education Society)

Hon. Shri. Kunal R. Patil
(Secretary, Jawahar Education Society)

Conference Chair

Dr. M.V. Bhatkar

Convener

Mrs. Swati A.Thete

Editorial Advisory Committee

Dr. H. A. Shahane
PhD, Post-Doc School of Civil and Environmental Engineering
University of the Witwatersrand, Johannesburg, South Africa

Dr. S. D. Kalpande
Head, Mechanical Engg., MET, Institute of Engg., Nashik.

Dr. Vishwas Khare
Head, Mathematics Department.
SSR, College of Arts, Commerce and Science, Silvassa

Dr. R. K. Munje
Head, Electrical Engg., KKW Institute of Engineering
Education & Research, Nashik

Dr. Amol Potgantwar
Board of Studies, Computer Engg., S.I.E.M. Nashik

Dr. M. P. Kadam
COE, KBT College of Engineering, Nashik

Editorial Board

Dr. S. K. Sonkar
Amrutvahini College of Engineering, Sanganmner

Dr. Sahebrao Pagar
Dept. of Physics, HPT Arts & RYK Science College Nashik

Dr. M. A. Waghchaure
Amrutvahini College of Engineering, Sanganmner

Prof. P. A. Lahare
PVG COE & SSD IOM, Nashik

Dr. S. J. Aswar
Head, Mechanical Engineering
Jawahar Education Society's Institute of Technology
Management and Research, Nashik

Mrs. G. P. Mohole
Head, Computer Engineering
Jawahar Education Society's Institute of Technology
Management and Research, Nashik

Mr. S. B. Patil
Head, IT Engineering
Jawahar Education Society's Institute of Technology
Management and Research, Nashik

Mr. S. B. Kajbe
Head, Civil Engineering
Jawahar Education Society's Institute of Technology
Management and Research, Nashik

Dr. D. D. Deshmukh
MET, Bhujbal Nashik

Dr. Rupesh Mahajan
Dr.D .Y .Patil Institute of Technology ,Pimpri, Pune

Dr. J.V.Shinde
K. K. Wagh Institute of Engg. Education and Research, Nashik

Dr. B. S. Shirole
Sanghavi College of Engineering, Nashik

Mr. Ganesh B. Patil
Assistant Professor (Mechanical Engineering)
Jawahar Education Society's Institute of Technology
Management and Research, Nashik

Mrs. Shalmali N.Botekar
Assistant Professor (Computer Engineering)
Jawahar Education Society's Institute of Technology
Management and Research, Nashik

Mr. Nadim B. Shaikh
Assistant Professor (Electrical Engineering)
Jawahar Education Society's Institute of Technology
Management and Research, Nashik

Mr. Santosh D. Nagare
Assistant Professor (Civil Engineering)
Jawahar Education Society's Institute of Technology
Management and Research, Nashik

Dr. Anita K. Sanap
Associate Editor
Head, Applied Science & Humanities

Mrs. Swati A. Thete
Associate Editor
Head, Electrical Engineering

Dr. M. V. Bhatkar
Editor
Principal

Jawahar Education Society's
Institute of Technology Management and Research, Nashik

Contents

1	The Development of Contraction Mappings in Metric Space Referencing Megha Subhash Pingale, Renu Praveen Pathak	1
2.	The Novel Santiagonamine Alkaloid Skeleton Fused-Coumarins as Exclusive Anti-breast Cancer Agents Jigar Patel	7
3.	Environmentally Conscious Production of TiO₂ using Aloe Vera Gel Extract Alkesh Bhavsar, Mahendra Shinde, Basilio Jose, Kinnari Patil, D. R. Patil, A. M. Patil	15
4.	The Introduction of LiOH for the Replacement of NaOH by the Green Chemistry Method for the Reduction of COD and BOD in the Effluents Jigar Patel, Sachin Pawar, Khanderao Pagar, Hiranman Udgar	20
5.	Eco-Friendly Synthesis of Zinc Oxide Nanostructures from Chicken Eggshell: Exploring Electrical and Colloidal Properties Basillio Jose Augusto Jose, Mahendra D. Shinde, Alkesh Bhavsar	24
6.	Synthesis of Conjugated Polymeric Nano Materials and Evaluation of their Antimicrobial Potential Against Human Pathogens Jyoti P. Mahashabde, Jayvant P. Sonawane, Arun M. Patil, Sandip P. Patil	29
7.	Assessing the Impact of Socio-Economic Factors on Indian Agriculture: A Mathematical Modelling Approach Avinash V. Khambayat, Neetu M. Sharma	37
8.	Studies in the Synthesis of Fluorescent 4-styrylcoumarins by Conventional and Green Method Kailas K. Sanap, Anita K. Sanap	45
9.	The Impact of Elevated Temperature on the Mechanical Characteristics of Concrete Containing GGBS A. J. Pawar, S. R. Suryawanshi	56
10.	Evaluation of Seismic Performance of Silo Supporting Structure for Joint Rotation Requirements as per IS 800:2007 Bhavinkumar Shah, Vijay Panchal	62
11.	Comparison of PCU Values in Mixed Traffic by Different Methods at Low Volume Road Gulshan Chauhan, Tripathi Bishnukumar B	70
12.	Study on Black Cotton Soil Stabilized with Class C Fly Ash for Use in Flexible Road Pavements: An Experimental Study Hrishikesh A. Shahane, Sachin L. Desale	74
13.	Use of Bio-Coagulant for Removal of Turbidity P. L. Pathak, Dr. P. D. Jadhao, Mohd. H. A. A., S. S. Suryawanshi	81
14.	Verification of Technical Feasibility for Construction and Demolition Waste and RCA with Sustainability of SW Material for Flexible Pavement P. L. Pathak, P. D. Jadhao, F. I. Chavan	87
15.	Machine Learning Approach for Cyber-attack Detection: A Comprehensive Review Swati Gawand, Meesala Sudhir Kumar	94

16. An AI based Interactive and Intelligent Museum Exhibit Based on Attention Analysis	100
Kunal Chanda, Souvik Banik, Washef Ahmed	
17. Nutritional Analysis Using Deep Learning: A Revolution in Understanding Dietary Patterns	108
Pragati Pandit, Nagama Kazzi	
18. Near Nexus Commerce Strengthening Buyers and Sellers through Regional Nexus Based on Data Analytics and Web Technology	115
Harshal Ashok Sonawane, Kunal Manik Walshete, Sahil Sachin Gujarathi, Ashutosh Sanjay Gangurde	
19. A Review Paper on Trusted Crowdfunding Platform Using Smart Contract	120
Bhagyashree Kadam, Sajal Bagade, Sohel Momin, Saurabh Satpute, Sarfraj Mulla, Niraj Chavan	
20. Coupons Code Exchange Platform	124
G. P. Mohole, Avanti Bhamare, Yogesh Bhavsar, Rahul Raundal, Swapnil Ranmale	
21. An Extensive Review of Cloud Security: Challenges Threats & Intrusions	130
J. P. Patil, S. B. Patil, D. D. Survase	
22. Supply Chain Management in Agriculture using Blockchain Technology	136
Mundhe Bhalchandra B, Dere Kapil D	
23. The Jio Revolution: Transforming India's Digital Landscape	139
Mahesh Sanghavi, Kainjan Sanghavi, Bhavana Khivsara, Santosh Sancheti	
24. COVID19 Pandemic from Machine Learning Perspective	145
Pooja R. Shastri, Rohan Kulkarni, Suhas Kakade	
25. Applications & Scope of Artificial Intelligence in All Branch of Engineering	151
Sandip Ramdasrao Mokle, Sachin Gangadhar Tathe	
26. Representations of Graceful Labeling of a Graph Using Python Programming Language	157
V. T. Dhokrat, S. B. Gaikwad, P. G. Jadhav	
27. Disk Space Rental System	164
Dhanshree Gavankar, Vaishnavi Khairnar, Prajwal Pahilwan, Jayesh Ughade, Shalmali Botekar	
28. A Comprehensive Survey on Enhancing Blockchain Data Security through the Integration of IoT and AI	167
Yogesh Arjun Shinde, S. K. Sonkar	
29. CryptoBoost: Empowering Crowdfunding through Blockchain Technology	175
Rameshwar Navarange, Roshan Kate, Kshitij Sonawane, Vipul Katale, Ajit Patil	
30. SMART Interview System	180
K. M. Sanghavi, Pranita Borse, Sanjeevani Gandhakse, Swayam Dugaje, Sakshi Vyas	
31. Digital Evolution in Construction: Exploring the Impact of eCommerce Platforms on Efficiency and Collaboration	187
Uday C. Patkar, Om Bhamare, Tejal Abhivant	
32. A Comprehensive Research Review on Attendance System (SPA)	195
U. C. Patkar, Digvijay Jadhav, Tejas Kulkarni, Dhruv Kurliye, Mayuresh Gajalwar	
33. Automating Analogue Gauge Measurements with Computer Vision Strategies	200
U. C. Patkar, Suhas Pawar, Hrishikesh Bari, Rushikesh Shinde, Kaveti Nani Kartik	

34.	Eco-Friendly Farming: Strategies for Waste Reduction and Tree Health Uday C. Patkar, Om Bhamare	205
35.	Developing a High-Performance Malware Prediction Model through Autoencoder and Attention-enhanced Recurrent Graph Analysis Mahesh T. Dhande, Sanjaykumar Tiwari	211
36.	Enhancing Engineering Pedagogy to Elevate the Quality of Engineering Education in India Santosh Sancheti, Kainjan Sanghavi, Mahesh Sanghavi	218
37.	A Paradigm Shift in Higher Education in India from Classroom Learning to Real-World Application Dipak Sancheti, Santosh Sancheti, Kainjan Sanghavi, Mahesh Sanghavi	224
38.	Reliability Assessment of Distributed Generation under Islanding Operation Swati Warungase, Priyanka D.Jawale, M. V. Bhatkar	232
39.	An Extensive Review of Wind Turbine Emulators to Promote the Integration of Renewable Energy A. P. Kulkarni, V. S. Jape, Haripriya H. Kulkarni, Deepa S. Bhandare	241
40.	Optimizing Economic Strategies for Alternative Energy Sources in Electric Power Generation V. S. Jape, Deepa S. Bhandare, Haripriya H. Kulkarni, Varad Chavare	248
41.	Design and Implementation of a Novel Intelligent FFOPI Controller for a Coupled Tank Liquid Level Control System by Simulation Deepa S. Bhandare, Neelima R. Kulkarni, Mayuresh V. Bakshi	256
42.	Automated Crop Monitoring and Surveillance Device using Remote Sensing and Deep Learning Techniques Deepa S. Bhandare, Shayan Chakraborty, Yash Kshirsagar, Avinash More, Tanishq Shelke, Atharva Baramkar	264
43.	Impact of Inverter Interfaced Distributed Generation on Distance Protection Gajanan S. Sarode, M. V. Bhatkar	272
44.	Real Time Monitoring System Representing Offset Machine Page Counting and Report Generation Abhijit Kulkarni, Santosh Agnihotri, Arjun Kapile, Pratik Junagade	281
45.	Detection of Inter-turn Short-circuit Fault in Induction Machine Using Vibration Analysis Deepak M. Sonje, Shrunkhala G.Khadilkar, M. V. Reddy, Ravindra K Munje	285
46.	Review: Congestion management by Distributed Generation with its Hosting Capacity Swati Warungase, M. V. Bhatkar	291
47.	Selection of Traction Motor and Battery Capacity for Design and Development of 249 Kg Electric Two wheeler Pooja Shastri, Mugdha Kulkarni, Devendra J. Goyar	303
48.	Quantitative Analysis of the Impact of Phantom Power on Voltage Stability in Electrical Power System Networks Manish Parihar, Dharmendra Jain, M. K. Bhaskar	310
49.	IoT Enhanced 3 Phase Induction Motor Control and Protection with PLC Amruta J. Takawale, Himanshu S. Nalawade, Mayuresh P. Patil, Shubham S. Gholap	317

50. Comparative Analysis of MPPT Schemes for Optimized Fuel Cell Operation	324
Bodke Mahesh Prakash, M V Bhatkar	
51. Estimation of Very Fast Transient Overvoltage's in GIS	332
Rahul S. Patil, M. V. Bhatkar	
52. Analysis of EM Waves Emitted from Multiple Partial Discharge Sources in a GIS Using FDTD Method	338
Mahesh A. Patil, Sonali Borase, M. V. Bhatkar	
53. Intermittent Nature of Distributed Generation and its Impact on Electricity Market	342
Swati K. Warungase, M. V. Bhatkar	
54. Structural Analysis of Bobbin Thread Removal Mechanism	353
Rahul R Gurpude, Ankush Hatwar	
55. Comparative Study of Parallel Plate Fin Heat Sinks with Three and Four Perforation on Circular Pin Fins Between the Plate Fins in Natural Convection	357
Rahul R. Sonawane, Sagarkumar J. Aswar, Ganesh B. Patil	
56. Helical Spring and It Dimensional Optimization used in Tractor Seat	361
Ganesh B Patil, Rahul Sonawane, Y. R. Girase	
57. Experimental Analysis on Laser Cutting of Hastelloy C 276: Effects of Process Parameters on Kerf Width	368
Sagarkumar J. Aswar, Chaitali S. Deore, Rahul R. Sonawane	
58. Design & Fabrication of Coconut Shell Crusher	375
Chaitali S. Deore, Sagarkumar J. Aswar	

The Development of Contraction Mappings in Metric Space Referencing

Megha Subhash Pingale

Mathematics Department

Sandip University

Nasik, Maharashtra

✉ meghakothawade17@gmail.com

Renu Praveen Pathak

Mathematics Department

Sandip University

Nasik, Maharashtra

ABSTRACT

The research into metric space has advanced greatly during the last few years. We have versions of metric spaces and b-metric spaces since few researchers have sought to change metric spaces. While others explored metric fixed-point theory to develop an infinite number of different contraction mappings. The goal of the research piece is to analyse and improve different contraction mappings with respect to metric spaces.

Subject Classification: 30L15, 30L99

KEYWORDS : Contraction mappings, weakly contractive map, multivalued mappings, rational contraction mapping, Ciric's Contraction Mapping.

INTRODUCTION

In 1905, Maurice Fréchet, a French mathematician, began exploring metric spaces. Metric space continues to exist in mathematics as an abstract set with a distance function known as a metric, only in the division topology. Let's analyze the different contraction mappings in metric space.

SUMMARY OF PRIOR RESEARCH

Definition: metric space (M.S.)

Assume metric or distance function $d: \wp \times \wp \rightarrow \mathbb{R}^+$ for non-empty set \wp . If

$$(1) d(v_1, w_1) = 0 \Leftrightarrow v_1 = w_1 \quad (2) d(v_1, w_1) = d(w_1, v_1) \quad (3) d(v_1, w_1) \leq [d(v_1, u_1) + d(u_1, w_1)]$$

for all $v_1, w_1, u_1 \in \wp$ Suppose d is a metric on \wp , we state, (\wp, d) is metric space. [1]

Backthin had a thought about b-metric space in 1989, and Czerwik later wrote that thought down in terms of b-metric space in 1993. Czerwik thus established b-metric space as the first concept.

Definition: b-metric space (b-M.S.)

Assume \wp is a set and take $s \geq 1, s \in \mathbb{R}$. A function $d: \wp \times \wp \rightarrow \mathbb{R}^+$ is considered a b-metric if $\forall v_1, w_1, u_1 \in \wp \Rightarrow$

$$(1) d(v_1, w_1) = 0 \Leftrightarrow v_1 = w_1 \quad (2) d(v_1, w_1) = d(w_1, v_1)$$

$$(3) d(v_1, w_1) \leq s [d(v_1, u_1) + d(u_1, w_1)]$$

A couple (\wp, d) is denoted as a b-metric space. [14]

Example: -

The space L_p ($0 < p < 1$) pertaining to all real functions $v(t), t \in [0, 1]$ so that:

$$\int_0^1 |v(t)|^p dt < \infty$$

$$d(v, w) = \left(\int_0^1 |v(t) - w(t)|^p dt \right)^{1/p}$$

for each $v, w \in L_p$, where $a = 2^{(1/p)}$

Augustin Louis Cauchy, a French mathematician, developed the Cauchy sequence idea. According to his theories, a series is said to be Cauchy if its terms arbitrarily approach one another as it moves forward. [8]

Definition: Cauchy Sequences & convergence in b-metric Spaces: -

Consider the sequence $(v_n)_{n \in \mathbb{N}}$ in b-metric space is called:

: Cauchy whenever $\epsilon > 0$ one can find, $n(\epsilon) \in \mathbb{N} : \forall n, m \geq n(\epsilon)$, we have $d(v_n, v_m) < \epsilon$

: Convergent whenever $\exists v \in \mathcal{X}$ to each $\epsilon > 0$, $\exists n(\epsilon) \in \mathbb{N}$ for each $n \geq n(\epsilon)$

We have $d(v_n, v) < \epsilon$ i. e. $\lim_{n \rightarrow \infty} v_n = v$ [8]

Definition: Complete b-Metric Space: -

(1) Assume that the space (\mathcal{X}, d) is b-metric. Subsequently a subset $\mathcal{K} \subset \mathcal{X}$ is then referred to as compact if and only if there is a Subsequence approaching an element in \mathcal{K} ." for every sequence of \mathcal{K} 's elements.

: Closed whenever every sequence $(v_n)_{n \in \mathbb{N}}$ in Y converges to $v \Rightarrow v \in \mathcal{K}$

: The b-metric space is complete whenever each Cauchy sequence converges. [8]

Definition: b-Convergent Sequence: -

Let (\mathcal{X}, d) is a b-metric space. Then the sequence $\{v_n\}$ in \mathcal{X} is called:

: b- Convergent if and only if there exists $v \in \mathcal{X}$ such that

$$d(v_n, v) \rightarrow 0 \text{ as } n \rightarrow \infty \text{ symbolically } \lim_{n \rightarrow \infty} v_n = v$$

: b- Cauchy $\Leftrightarrow d(v_n, v_m) \rightarrow 0$ as $n, m \rightarrow \infty$ [6].

Theorem: Every sequence in a metric space that converges is a Cauchy.

Remark: Not every Cauchy sequence in a metric space necessarily converges.

Example: Cauchy sequence

Assume sequence $v_1 = 1.41, v_2 = 1.414, v_3 = 1.4142, v_4 = 1.41421, \dots$ in usual metric space \mathbb{Q} , converging to $\sqrt{2} \Rightarrow$ it is Cauchy but $\sqrt{2} \notin \mathbb{Q}$.

Let $\mathcal{X} = (0,1]$ and $d(v, w) = |v - w|$ is metric and $\{v_n\} = \{\frac{1}{n} : n \in \mathbb{N}\} \Rightarrow$ is a Cauchy $\forall \epsilon > 0$ we have

$$d(v_m, v_n) = \left| \frac{1}{m} - \frac{1}{n} \right| < \epsilon$$

for all $m, n > 1/\epsilon$ on other hand $v_n \rightarrow 0$ but 0 does not belong to \mathcal{X} hence sequence is not convergent.

However, if $\mathcal{X} = [0,1]$ the sequence is Cauchy and is convergent. [4,5]

Definition: - Fixed point

Assume a nonempty set \mathcal{X} and $\mathcal{K} : \mathcal{X} \rightarrow \mathcal{X}$. If $\mathcal{K}(v_1) = v_1 \Rightarrow$ It's a fixed point. [7]

Table1: Fixed point of functions

Function	Fixed point	Contraction mapping	Metric space
e^v	No fixed point	Yes	(0,1)
$\log v$	No fixed point	Yes	\mathbb{R}^+
v^2	0 and 1	Yes, only in metric [0,1/2]	[0,1/2]
$\sinh v$	0	No	----
$\tanh v$	0	Yes	\mathbb{R}^+
$v + 1$	No	Yes	\mathbb{R}^+
$\frac{1}{v + 1}$	0.618033	No	\mathbb{R}
$mv + b$	$b/[1-m]$	Yes	\mathbb{R}

Definition: Fixed point of multivalued mapping

Nadler (1969): Assume $v_0 \in \mathcal{X}$ is a fixed point of the multivalued mapping f if, $v_0 \in \mathcal{K}v_0$ [19]

The term "contractive mapping" was initially introduced by Edelstein for the metric space.

Definition: Contraction mapping (C.M.)

Assume $\mathcal{K} : \mathcal{X} \rightarrow \mathcal{X}$ in metric space (\mathcal{X}, d) is C.M. if $v_1 \neq w_1$ entails $d(\mathcal{K}(v_1), \mathcal{K}(w_1)) < d(v_1, w_1)$ [18]

Example 1: Contraction Mapping (C.M.)

Define $\mathcal{X} = (0,1]$ alongwith, $d(v, w) = |v - w|$

Let $\mathcal{K} : \mathcal{X} \rightarrow \mathcal{X} \mid \mathcal{K}(v) = 1/2v$ is contraction mapping.

In the research Ciric [12], [13] investigated C.M., also known as Ciric's type C.M. In one research article "A generalization of Banach's contraction principle", author defined quasi C.M.

Definition: Ciric’s type C.M.

Consider $\aleph: \wp \rightarrow \wp$ in b-metric space named as Ciric’s type contraction $\Leftrightarrow \forall v, w \in \wp \exists h < 1$ so as

$$d(\aleph(v), \aleph(w)) \leq h \cdot \max\{d(v, w), d(v, \aleph v), \frac{d(v, \aleph w) + d(w, \aleph v)}{2}\}$$

Example2: Ciric’s C.M.

Define $\wp = [1, \infty)$ with $d(v, w) = |v - w|$. Assume $\aleph(v) = 1/v$ is Ciric’s C.M. where $h = 0.8$

Proof: $LHS = d(\aleph(v), \aleph(w)) = \left| \frac{1}{v} - \frac{1}{w} \right| = \left| \frac{v-w}{v \cdot w} \right| < |v - w|$

RHS = $0.8 |v - w|$ Hence $LHS \leq RHS$

Let’s point out that Ciric [14] invented and researched quasi-C.M. According to the well-known Ciric finding having unique fixed point (U.F.P) [12], [13]

Example: 4:

Let $\aleph, \varrho: \wp \rightarrow \wp$ as $\aleph(v) = v$ and $\varrho(v) = v^2$ then Clearly 1 is the coincidence point.

Definition: [17]

- Let $\psi_1: [0, \infty) \rightarrow [0, \infty)$ that fulfills the given requirements:
- Assures continuity of ψ_1
 - Non-decreasing is the function ψ_1
 - $\psi_1(\tau) = 0 \Leftrightarrow \tau = 0$

Alber and Guerre-Delabriere [16] first described the idea of the weak contraction in 1997.

Definition: Weakly contractive map (W.C.M.)

A self-map \aleph is considered a W.C.M. if $\exists \varphi_1: [0, +\infty) \rightarrow [0, +\infty)$ such that non-decreasing is the function φ_1 and assuring its continuity, and $\varphi_1(\tau) = 0 \Leftrightarrow \tau = 0$ satisfying $d(\aleph(v_1), \aleph(w_1)) \leq d(v_1, w_1) - \varphi_1(d(v_1, w_1)), \forall v_1, w_1 \in \aleph$ [17]

Remark 1

Consider the set $\aleph = [1, \infty)$, $\varphi_1: [0, \infty) \rightarrow [0, \infty)$ with $\varphi_1(\tau) = \tau^2$, $\aleph(v_1) = v_1$, $d(v_1, w_1) = |v_1 - w_1|$ φ_1 fails to be a W.C.P.

Remark 2:

Whereas for the set $\aleph = [1, \infty)$, $\varphi_1: [0, \infty) \rightarrow [0, \infty)$, $\varphi_1(\tau) = \tau/2$, $\aleph(v) = 1/v$, $d(v_1, w_1) = |v_1 - w_1|$

Undoubtedly φ_1 is a W.C.M.

Remark 3:

The set $\wp = [2, \infty)$, with $\varphi(\tau) = \frac{\tau}{6}$, $\psi(\tau) = \frac{\tau}{3}$, $\aleph(v) = v$

Where $d(v, w) = |v - w|$ it is not (ψ, φ) -W.C.

Remark 4:

The set $\wp = [3, \infty)$, $\psi, \varphi: [0, \infty) \rightarrow [0, \infty)$ with $\varphi(t) = \frac{t}{6}$, $\psi(\tau) = \frac{t}{3}$, $f(v_1) = \frac{1}{v_1}$, $d(v_1, w_1) = |v_1 - w_1|$ It is (ψ, φ) - weak contraction map.

Definition: - Altering distance function (A.D.F.)

Consider $\psi: [0, \infty) \rightarrow [0, \infty)$ It is termed as an A.D.F. if:

- i) Assures continuity of ψ (ii) It is nondecreasing
- ii) $\psi(\tau) = 0$ exactly when $\tau = 0$ [16]

Remark 5:

$\psi(t) = t^2$ and te^t are A.D.F.

Definition: - Infinite altering distance function (I.A.D.F.)

An A.D.F. is an I.A.D.F. if is defined on \mathbb{R} [16]

Kirk et al. [24] worked on cyclic contraction mappings.

Definition: - Generalized cyclic contractive mapping (G.C.C.M.) [16], [6]

Let $\mathfrak{A} = A \cup B$, Assume, $\aleph: \mathfrak{A} \rightarrow \mathfrak{A}$, $A \subseteq \wp$, $B \subseteq \wp$: $A \neq \emptyset$, $B \neq \emptyset$, and (\wp, d, s) be a b-metric space. A G.C.C.M. is \aleph if:

- i) $\mathfrak{A} = A \cup B$ represents Y cyclically with regard to \aleph , that is, $\aleph(A) \subset B$ and $\aleph(B) \subset A$
- ii) There exist $\psi_1 \in \Psi$, $\varphi_1 \in \Phi$, $L \geq 0$ (constant) such that $\psi(s^d(\aleph v, \aleph w)) \leq \varphi(\psi(M(v, w))) + LN(v, w), \forall (v, w) \in A \times B$ or $(v, w) \in B \times A$ wherever

$$M(v, w) = \max\{d(v, w), d(v, \aleph v), d(w, \aleph w), \frac{d(v, \aleph w) + d(w, \aleph v)}{2s}\}$$

$$\frac{d(\aleph^2 v, v) + d(\aleph^2 v, \aleph w)}{2s}, d(\aleph^2 v, \aleph v), d(\aleph^2 v, w), d(\aleph^2 v, \aleph w)\}$$

$$N(v, w) = \min\{d(v, \aleph v), d(w, \aleph w), d(\aleph^2 v, \aleph^2 w)\}$$

In 1998, Jungck and Rhoades [20] developed the idea of weakly compatible maps and demonstrated that weakly

compatible maps are compatible maps, but the reverse is not necessarily accurate.

Definition: - Weakly Compatible

Consider $\mathfrak{N}, \varrho: \wp \rightarrow \wp$. in metric space (\wp, d) If $\mathfrak{N}u = \varrho u \Rightarrow \mathfrak{N}\varrho u = \varrho\mathfrak{N}u$ for some $u \in \wp$. Then \mathfrak{N} and ϱ are identified as weakly compatible. [2]

Definition: - K-contraction

Assuming $\mathfrak{N}: \wp \rightarrow \wp$ in metric space (\wp, d) is referred to as K-contraction if there can be found $a \in (0, 1/2)$: $\forall v, w \in \wp$ the subsequent inequality is valid:

$$d(\mathfrak{N}v, \mathfrak{N}w) \leq a[d(v, \mathfrak{N}v) + d(w, \mathfrak{N}w)] \quad [3]$$

In 1968, Kannan demonstrated that any K contraction on complete metric space (\wp, d) has a U.F.P.

A fixed-point theorem for C-contraction mappings was developed by Chatterjee in 1972. According to this theorem, a mapping \mathfrak{N} is a C-contraction if a \exists point at $\alpha \in (0, 1/2)$ where it fulfills condition below for every values of v and w :

$$d(\mathfrak{N}v, \mathfrak{N}w) \leq \alpha[d(v, \mathfrak{N}w) + d(w, \mathfrak{N}v)]$$

Definition: q-set-valued α -quasi-contraction

Assume b-metric space (\wp, d) and $\varphi: \wp \times \wp \rightarrow (0, \infty)$ is a mapping. The set-valued mapping

$\mathfrak{N}: \wp \rightarrow P_{b,d}(\wp)$ termed as q-set-valued α -quasi-contraction if

$$\varphi(v_1, w_1) H(\mathfrak{N}v_1, \mathfrak{N}w_1) \leq qM(v_1, w_1), \text{ for all } v_1, w_1 \in \wp, 0 \leq q < 1 \text{ and}$$

$$M(v_1, w_1) =$$

$$\max \{d(v_1, w_1), d(v_1, \mathfrak{N}v_1), d(w_1, \mathfrak{N}w_1), d(v_1, \mathfrak{N}w_1), d(w_1, \mathfrak{N}v_1)\} \quad [16]$$

Definition: - Multivalued mappings (M.P.)

Assume $\wp \neq \emptyset, \mathbb{I} \neq \emptyset$ and $\mathfrak{N}: \wp \rightarrow 2^{\mathbb{I}}$ then \mathfrak{N} is known as M.P. [19]

By applying a control function, Sessa et al. [23] established an altering distance function in the year 1984.

Definition: - Comparison Function (C.F.)

Suppose $\varphi_1: [0, \infty) \rightarrow [0, \infty)$ φ_1 is termed as a C.F. if

(i) Assurance of increasing and

(ii) $\varphi_1^n(\tau) \rightarrow 0$ as $n \rightarrow \infty$ for any $\tau \in [0, \infty)$. [10]

Definition: - b-comparison function (b-C.F.)

Let $s \geq 1$ a real number. Suppose $\varphi_1: [0, \infty) \rightarrow [0, \infty)$ is a b-C.F. if

(1) If φ_1 is monotonically increasing and

(2) $\exists n_0 \in \mathbb{N}, a \in (0, 1)$ and a convergent series of nonnegative terms $\sum_{n=1}^{\infty} V_n$ so that $s^{n+1} \varphi_1^{n+1}(\tau) \leq a s^n \varphi_1^n(\tau) + V_n$ For $n \geq n_0$ and any $\tau \in [0, \infty)$ [10]

Definition: - α - ψ contractive mappings

Assume $\mathfrak{N}: \wp \rightarrow \wp$ in metric space (\wp, d) . Then \mathfrak{N} is α - ψ contractive mappings. Supposing there are two functions

\exists functions $\varphi: \wp \times \wp \rightarrow [0, \infty)$ and $\psi \in \Psi$:

$$\varphi(v, w)d(\mathfrak{N}v, \mathfrak{N}w) \leq \psi(d(v, w)) \text{ for all } v, w \in \wp \quad [10]$$

Authors Arsalan Hojat Ansari, Vishal Gupta, Naveen Mani in the year as 2010 had newly defined the infinite altering distance function.

Definition: - Infinite altering distance function (I.A.D.F.) [6]

Suppose $\psi: \mathbb{R} \rightarrow \mathbb{R}$ termed as an I.A.D.F. if the following criteria are met:

i) ψ is non-decreasing as well as continuous

ii) $\psi(\tau) = 0 \Leftrightarrow \tau = 0$

In the year 2012 Samet et al originated concept α admissible mapping as mentioned below.

Definition: - α admissible mapping

If for, $\mathfrak{N}: \wp \rightarrow \wp, \exists \varphi: \wp \times \wp \rightarrow [0, \infty)$ f is α -admissible mapping if $\forall v, w \in \wp, \varphi(v, w) \geq 1 \Rightarrow$

$$\varphi(\mathfrak{N}v, \mathfrak{N}w) \geq 1 \quad [10]$$

Remark 11

Let $\wp = (0, \infty)$ and $\mathfrak{N}: \wp \rightarrow \wp, \exists \varphi: \wp \times \wp \rightarrow [0, \infty)$ by

$\mathfrak{N}v_1 = \sqrt{(v_1)} \forall v_1 \in \wp$. Then f is α admissible mapping where

$$\varphi(v_1, w_1) = \begin{cases} e^{v_1 - w_1}, & v_1 \geq w_1 \\ 0, & v_1 < w_1 \end{cases} \quad [22]$$

Definition: - C-comparison function (C-C.F)

The function $\varphi_1: [0, \infty) \rightarrow [0, \infty)$ is a C-C.F.

- (i) where it is increasing and
- (ii) $\exists n_0 \in \mathbb{N}, a \in (0,1)$ and a convergent series of nonnegative terms $\sum_{n=1}^{\infty} V_n$ so that $\varphi_1^{n+1}(\tau) \leq a\varphi_1^n(\tau) + V_n$

For $n \geq n_0$ and any $\tau \in [0, \infty)$ [8]

Definition: - Ordered - ψ -Suzuki type rational contractive mapping

For partially ordered b-metric space (\wp, d, \preceq) . $\aleph: \wp \rightarrow \wp$ is an ordered - ψ -Suzuki type rational contractive mapping if $1/2s d(v_1, \aleph v_1) \leq d(v_1, w) \Rightarrow sd(\aleph v_1, \aleph w) \leq \psi(M(v_1, w))$ where

$$M(v_1, w_1) = \max \left\{ \begin{aligned} & d(v_1, w_1), \frac{d(v_1, \aleph v_1)d(w_1, \aleph w_1)}{1 + s[d(v_1, w_1) + d(v_1, \aleph w_1)]} \\ & \frac{d(v_1, \aleph w_1)d(v_1, w_1)}{1 + s[d(v_1, \aleph v_1) + d(w_1, \aleph w_1)} \end{aligned} \right\}$$

$\forall (v_1, w_1) \in X$ with $v_1 \preceq w_1$ [25]

Later, Karapinar [21] changed admissible mappings by including additional requirements to create a triangular admissible mapping.

Authors Piyachat Borisut, Poom Kumam, Vishal Gupta and Naveen Mani [9] introduced A class of generalized (ψ, α, β) – weak contraction.

Definition: [9]

Suppose $\aleph, Q, S: \wp \rightarrow \wp$ are generalized (ψ, α, β) – weak contraction if $\forall v, w \in \wp$

$\psi(d(\aleph v, Qw) \leq \alpha(d(Sv, Sw) \beta(d(Sv, Sw))$ for all $v \geq w$ Where $\alpha \in F, \psi \in \Psi, \beta: [0, \infty) \rightarrow [0, \infty)$ is a continuous function with condition $0 < \beta(\tau) < \psi(\tau)$

Example: [9]

Let $\wp = \mathbb{N} \cup \{0\}$ Defined $d(v_1, w_1) = \begin{cases} v_1 + w_1, & \text{if } v_1 \neq w_1 \\ 0, & \text{if } v_1 = w_1 \end{cases}$

Definition: - [6]

A mapping $F: [0, \infty)^2 \rightarrow \mathbb{R}$ is C-class function if it is continuous and

- (i) $F(v_1, w_1) \leq v_1$

- (ii) $F(v_1, w_1) = v_1 \Rightarrow$ either $v_1 = 0$ or $w_1 = 0$ for all $v_1, w_1 \in [0, \infty)$ Moreover $F(0, 0) = 0$.

Authors [15] defined F-contractive type mappings in b-metric spaces as mentioned below.

Definition: [15]

Assume $Q: \wp \rightarrow \wp$ in b-metric space (X, d, s) , is F-contractive type mapping if $\exists \tau > 0 \mid d(v, Qv)d(w, Qw) \neq 0$ implies

$$\tau + F(sd(Qv, Qw)) \leq 1/3 [Fd(v, w) + Fd(v, Qv) + Fd(w, Qw)]$$

and $d(v, Qv)d(w, Qw) = 0$ implies

$$\tau + F(sd(Qv, Qw)) \leq 1/3 [Fd(v, w) + Fd(v, Qw) + Fd(w, Qv)]$$

for all $v, w \in \wp$

CONCLUSION

Various scholars studied and worked in field of metric space. In the scholarly article we tried to rescript the various contraction mappings and the basic concepts in the reference of metric space. There are other further contraction mappings in the body of literature. The goal of this essay was to summaries the limited literature that was available.

REFERENCES

1. Aggarwal Jeetendra and Rajesh Singh, "Introduction to Metric Spaces", <https://www.researchgate.net/publication/311589083>
2. Akkouchi M., "Common Fixed-point theorem for two self-mappings of a B metric space under an implicit relation" Hacettepe Journal of Mathematics and statistics volume 40(6) (2011), 805-810
3. Ansari A.H., Chandok S. and Lonescu C., "Fixed point theorems on B-Metric spaces for weak Contraction with auxiliary functions" Ansari et el Journal of inequalities and applications, 2014;2014: 429
4. Mani N., Beniwal S., Shukla R., Pingale M., "Fixed point theory in extended parametric Sb- metric spaces and its applications", symmetry, (2023) 15:2136. <https://doi.org/10.3390/sym15122136>.
5. Mani N., Pingale M., Shukla R., Pathak R., "Fixed point theorems in fuzzy b- metric spaces using two different t -norms", Adv. Fixed Point Theory, (2023) 13:29. <https://doi.org/10.28919/afpt/8235>.
6. Ansari A.H., Gupta V., And Mani N., "C-Class Functions on Some Coupled Fixed-Point Theorems in

- Partially Ordered S-Metric Spaces” Commun. Fac. Sci. Univ. Ank. Ser. A1 Math. Stat., Volume 68, Number 2, Pages 1694-1708 (2019), ISSN 1303.5991 E-ISSN 2618-6470
7. Ansari Q.H., “Metric Spaces -Including fixed point theory and Set valued maps”, Narosa Publishing House Private Limited, ISBN 10: 818487099X / ISBN 13: 9788184870992, 2010
 8. Boriceanu M., “Fixed point theory for multivalued contractions on a set with two B metrics” Creative math and Inf 17(2008), No 3,326-332
 9. Borisut P., Kumam P., Gupta V. and Mani N., “Generalized (ψ, α, β) – Weak Contractions for Initial Value Problems” MDPI, Mathematics 2019, 7, 26
 10. Bota M.F., Karapinar E. and Mlesnite O., “Ulam Hyers Stability results for Fixed point problems via α - ψ contractive mappings in B-Metric spaces” Hindawi Publishing corporation Abstract and applied analysis Vol 2013, Article ID 825293
 11. Chugh R. and Kumar S., “Common fixed points for weakly compatible maps”, Proc. Indian Acad. Sci. (Math. Sci.), Volume 111, No 2, May 2001, pp, 241-247, Printed in India.
 12. Ćirić Lj. B., “On contraction type mappings”, Math. Balkanica. 1 (1971) 52–57.
 13. Ćirić Lj. B., “A generalization of Banach’s contraction principle”, Proc. Amer. Math. Soc. 45 (1974) 267 – 273.
 14. Czerwik S., “Contraction Mappings in B metric Spaces” Acta Mathematica et Informatica Universities, Vol1 (1993), No-1, 5—11
 15. Goswami N., Haokip N. and Mishra V.N., “F-contractive type mappings in b-metric spaces and some related fixed-point results”, Fixed Point Theory and Applications (2019) 2019:13
 16. Han Bui T.N., Hieu N. T., “A fixed point theorem for generalized cyclic contractive mappings in b metric space”, Facta Universitatis (NIS), Ser, Math, Inform, Vol, 31, No 2(2016), 399-415
 17. Iqbal M., Batool A., Ege O., and Sen M, “Fixed Point of Generalized Weak Contraction in b-Metric Spaces.” Hindawi Journal of Function Spaces, Volume 2021, Article ID 2042162.
 18. Janos L., “On the Edelstein Contractive Mapping Theorem”, Canad. Math. Bull. Vol. 18 (5), 1975
 19. Joseph M., Roselin D. and Marudai M, “Fixed point theorems on multi valued mappings in b metric spaces.”, Springer Plus (2016) 5:217
 20. Jungck G and Rhoades B. E., “Fixed point for set valued functions without continuity”, Indian J. Pure Appl. Math. 29(3) (1998) 227–238
 21. Karapinar E., “ α - ψ -Geraghty contraction type mappings and some related fixed-point results,” Filomat, vol. 28, no. 1, pp. 37–48, 2014.
 22. Kaushik P, Kumar S., and Tas K., “A New Class of Contraction in b -Metric Spaces and Applications” Hindawi, Abstract and Applied Analysis, Volume 2017, Article ID 9718535, 10 pages
 23. Khan M.S., Swalech M. and Sessa S., “Fixed point theorem by altering distances between the points”, Bull. Aust. Math. Soc. 30, 1–9 (1984)
 24. Kirk W.A., Srinivasan, P.S., Veeramani, P, “Fixed points for mapping satisfying cyclic contractive conditions.” Fixed Point Theory 4, 79-89 (2003)
 25. Latif A., Salimi P., Parvaneh V., Mazrooei A., “Various Suzuki type theorems in b-Metric spaces”, Journal of Nonlinear analysis and Applications JULY 2015.

The Novel Santiagonamine Alkaloid Skeleton Fused-Coumarins as Exclusive Anti-breast Cancer Agents

Jigar Patel

Department of Chemistry
SSR College of Arts, Commerce and Science
Union Territory Administration of Dadra and Nagar Haveli and Daman and Diu
Department of Chemistry
Sardar Patel University
Vallabh Vidya Nagar, Anand, Gujarat
✉ drjigar.myself@gmail.com

ABSTRACT

The synthesis of various fused coumarins have been carried out by the reaction of various 4-hydroxy coumarins with appropriate chalcones in the presence of ammonium acetate in refluxing acetic acid. The products are screened for MCF-7 anti-breast cancer activity.

KEYWORDS : 4-hydroxy coumarin, Fused coumarin, MCF-7 anti-breast cancer activity.

INTRODUCTION

Santiagonamine¹ is the first phenanthridine alkaloid, has been isolated from Hook (Berberidaceae). Alkaloids are a class of basic, naturally occurring organic compounds that contain at least one nitrogen atom. Coumarins² are large number of valuable species used commonly as medicinal plants, aromatic plants, and edible plants for human and animal feeding belongs to coumarin-rich plant families. Among them are species with well-documented biological activity, in which coumarins are part of the active principles³⁻⁵. The 1,4-Michael addition, *q.v.*, of α -pyridinium methyl ketone salts to α,β -unsaturated ketones, generating the 1,5-dicarbonyl compounds which undergo ammonium acetate-promoted ring closure, to yield substituted pyridines is known as Kröhnke⁶⁻⁷ Pyridine Synthesis. The pyrido[2,3-*c*]coumarin skeleton constitutes the backbone of Santiagonamine. Considering the importance of fused coumarins, it has been considered for anti-cancer activity study. A cancer that forms in the cells of the breasts is known as Breast Cancer. Breast Cancer can occur in women and rarely in men. Symptoms of breast cancer include a lump in the breast, bloody discharge from the nipple and changes in the shape or texture of the nipple or breast. MCF-7 is a breast cancer cell line isolated in 1970 from a 69-year-old Caucasian woman⁸. MCF-7 is the acronym of Michigan Cancer

Foundation-7, referring to the institute in Detroit where the cell line was established in 1973 by Herbert Soule and co-workers⁹.

BREAST CANCER

A cancer that forms in the cells of the breasts is known as Breast Cancer. Breast Cancer can occur in women and rarely in men. Symptoms of breast cancer include a lump in the breast, bloody discharge from the nipple and changes in the shape or texture of the nipple or breast.

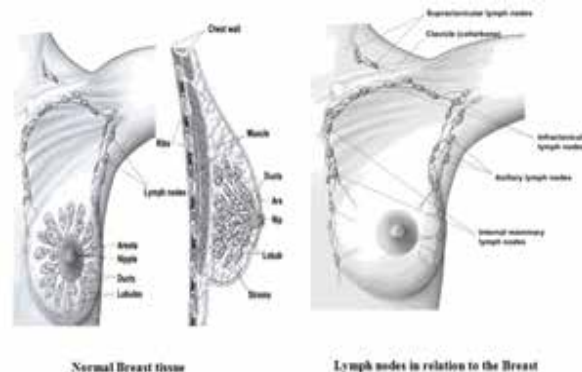


Figure 1 The normal Breast tissue and lymph nodes in relation to the breast

(Credits: <https://www.cancer.org/cancer/breast-cancer/about/what-is-breast-cancer.html>)

Breast cancer can spread when the cancer cells get into the blood or lymph system and are carried to other parts

of the body. The lymph system is a network of lymph (or lymphatic) vessels found throughout the body that connects lymph nodes (small bean-shaped collections of immune system cells). The clear fluid inside the lymph vessels, called lymph, contains tissue by-products and waste material, as well as immune system cells. The lymph vessels carry lymph fluid away from the breast. In the case of breast cancer, cancer cells can enter those lymph vessels and start to grow in lymph nodes (Figure 1).

Most of the lymph vessels of the breast drain into:

- i. Lymph nodes under the arm (axillary nodes)
- ii. Lymph nodes around the collarbone (supraclavicular [above the collar bone] and infraclavicular [below the collar bone] lymph nodes)
- iii. Lymph nodes inside the chest near the breast bone (internal mammary lymph nodes)

If cancer cells have spread to your lymph nodes, there is a higher chance that the cells could have traveled through the lymph system and spread (metastasized) to other parts of your body. The more lymph nodes with breast cancer cells, the more likely it is that the cancer may be found in other organs. Because of this, finding cancer in one or more lymph nodes often affects your treatment plan. Usually, you will need surgery to remove one or more lymph nodes to know whether the cancer has spread². The two main categories of breast cancer are invasive and noninvasive. Non-invasive breast cancers stay within the milk ducts and lobules of the breast. Invasive cancers spread beyond these areas and invade normal tissue. Unlike DCIS, LCIS is not considered a cancer, but it does mean that a woman has a higher risk of developing breast cancer³.

COUMARIN (A NATURAL PRODUCT)

Coumarin, the name is coming from the word coumarou. It is the French word for the tonka beans. The word tonka for the tonka bean is taken from the Galibi (Carib) tongue spoken by natives of French Guiana (one source for the plant); it also appears in Old Tupi, another language of the same region, as the name of the tree. The old genus name, Coumarouna, was formed from another Tupi name for tree, kumarú⁷.

Coumarins are the best known aromatic lactones. The isolation of coumarin was first reported by Vogel in Munich in 1820. He associated the pleasant

odour of the tonka bean from Guiana with that of clover, *Melilotus officinalis*, which gives rise to the characteristic aroma of new-mown hay. Vogel then concluded that the long colorless crystals which he discovered on slicing open Tonka Beans and which crystallized as glistening needles from aqueous alcohol were identical with similar crystals he obtained, albeit in much lower yield, by extracting fresh clover blossoms.

A large number of valuable species used commonly as medicinal plants, aromatic plants, and edible plants for human and animal feeding belongs to coumarin-rich plant families. Among them are species with well-documented biological activity, in which coumarins are part of the active principles⁸.

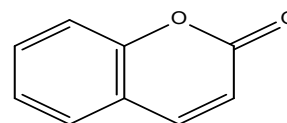


Figure 3 Chemical structure of natural product coumarin

Now, in continuation of interest in the introduction of newer fused coumarin derivatives as anti-breast cancer drugs, it was thought worthwhile to synthesize fused coumarins having coumarin and pyrazole substitution in pyridine ring and therefore in the present work coumarin and pyrazole substituted fused coumarins have been carried out.

MATERIALS AND METHODS

Synthesis and Characterisation

All chemicals were purchased from Sigma-Aldrich, Germany. Melting points were determined by the open capillary method and were uncorrected. FTIR spectra of the synthesized compounds were recorded on a Shimadzu-8400S, using KBr pellets in 10-4 resolution and 30 scans. ¹H NMR spectra were recorded on a Varian spectrometer, USA at 400 MHz at room temperature. Samples were prepared in CDCl₃ containing TMS as an internal standard. Splitting patterns were designated as follows: s, singlet; d, doublet; t, triplet; m, multiplet. Chemical shift values were given in parts per million (ppm). ¹³C NMR were recorded on Varian 400 spectrometer, operating at 400 MHz. The Liquid Chromatography Mass Spectra (LC-MS) were recorded on a Varian Inc, USA, 410 Prostar Binary LC with 500 MS IT PDA detectors.

Cell lines

MCF-7 (breast cancer) cell were cultured in DMEM medium and supplemented with 10% of fetal bovine serum (FBS) then the culture flasks were incubated for 3-4 days at 37°C in 5% CO₂ incubator.

Analysis of cell viability by MTT assay

Cell viability was measured quantitatively by using MTT, showed the activity of living cells [Plumb et al., 1989]. MCF-7 was seeded into 24 well plates and treated with 100 µl/ml, 150 µl/ml, 200 µl/ml, 250 µl/ml and 300 µl/ml, 350 µl/ml, 400 µl/ml, 450 µl/ml and 500 µl/ml of various fusedcoumarins mixture dissolved in CHCl₃ and dried extracts were used as triplicate. The DMSO was used as control in each experiment. The treated mixture was then incubated at 37°C with 5% CO₂ for 24 hours. After incubation, 2 µl/ml of the labeled reagent was added to each well followed by incubation for 3 hours at 37°C with 5% CO₂ and then the medium was discarded and the crystals were dissolved in 1.0 ml of 0.04N HCl. The absorbance of cells was measured at 570 nm with an ELISA reader. MTT assay was performed in the Department of Microbiology, SSR College of Arts, Commerce and Science, Silvassa.

Statistical Analysis

Each data point was obtained by making at least 3 independent measurements. All data are expressed as mean + S.D. Data were analyzed by an analysis of variance (p<0.05) and the means separated by one way ANOVA.

EXPERIMENTAL

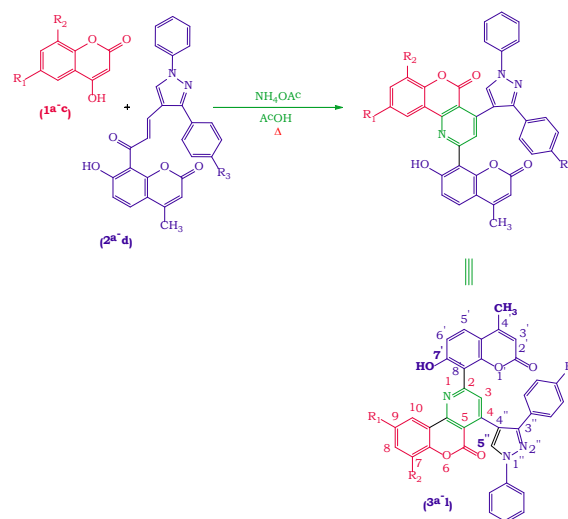
Preparation of various fusedcoumarins

The synthesis of 2-(7'-hydroxy-4'-methyl-coumarin-8'-yl)-4-(1''-phenyl-3''-aryl-1H-pyrazol-4''-yl) fusedcoumarins (3a-l) has been carried out by the reaction of various 4-hydroxy coumarins10 (1a-c) with appropriate 7-hydroxyl-4-methyl-8-(3-(1-phenyl-3-aryl-1H-pyrazol-4-yl)acryloyl)coumarin11-12 (2a-d) in the presence of ammonium acetate in refluxing acetic acid (Scheme 1).

The required chalcones, 7-hydroxy-4-methyl-8-[3'(1''-phenyl-3''-aryl-1''H-pyrazol-4''-yl)-acryloyl] coumarins (2a-d) were prepared by the reaction of 4-methyl-7-hydroxy-8-acetyl coumarin with appropriate 1-phenyl-

3-aryl-1H-pyrazole-4-carbaldehyde in the presence of piperidine in ethanol.

The condensation of various 4-hydroxy coumarins (1a-c) with appropriate 7-hydroxyl-4-methyl-8-(3-(1-phenyl-3-aryl-1H-pyrazol-4-yl)-acryloyl) coumarin (2a-d) in the presence of ammonium acetate in refluxing acetic acid proceeded smoothly and gave the expected products (3a-l) in 60-77% yield. The detailed mechanism for the formation of compounds (3a-l) is shown in (Scheme 2).



	R ₁	R ₂	R ₃		R ₁	R ₂	R ₃
3a:	H	H	H	3g:	H	H	OCH ₃
3b:	CH ₃	H	H	3h:	CH ₃	H	OCH ₃
3c:	H	CH ₃	H	3i:	H	CH ₃	OCH ₃
3d:	H	H	CH ₃	3j:	H	H	Cl
3e:	CH ₃	H	CH ₃	3k:	CH ₃	H	Cl
3f:	H	CH ₃	CH ₃	3l:	H	CH ₃	Cl

(Scheme-1)

The following general procedure was used for the synthesis of compounds (3a-l).

In a 100 mL round bottom flask equipped with a dropping funnel, condenser, guard tube and magnetic needle, an appropriate 4-hydroxy coumarin (1a-c) (0.005 mole) was taken in glacial acetic acid (15 mL). To this, ammonium acetate (0.05 mole) was added with stirring at room temperature. Then a solution of

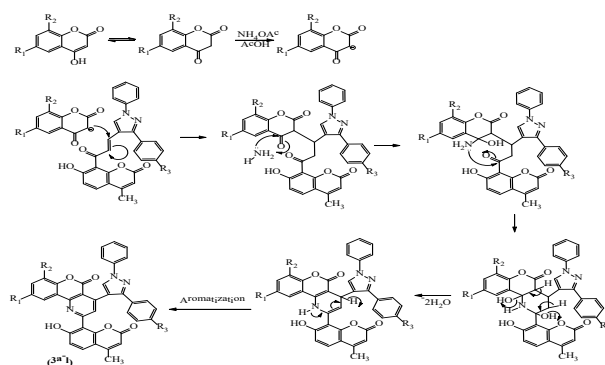
an appropriate 7-hydroxy-4-methyl-8-[3'-(1''-phenyl-3''-aryl-1''H-pyrazol-4''-yl)-acryloyl]- coumarin (2a-d) (0.005 mole) in acetic acid (15 mL) was added with stirring at room temperature. The reaction mixture was further stirred for 45 minutes at room temperature and then refluxed in an oil bath at 140°C for 12 hours. It was then allowed to come to room temperature and poured into ice cold water (75 mL). The gummy mass obtained was extracted with chloroform (3 x 30 mL). The combined chloroform extract was washed with 10% sodium bicarbonate solution (3 x 20 mL) and then with water (3 x 20 mL). It was then dried over anhydrous sodium sulfate. The removal of chloroform under vacuum gave a solid product. This was further purified by column chromatography using silica gel and chloroform-ethyl acetate (8:2) as an eluent. Thus products (3a-l) were obtained as white solid, which were recrystallized from chloroform-hexane.

The structures of all the compounds (3a-l) were confirmed by analytical and spectral data.

Analytical and Spectral Data

The IR spectrum of compound 3a ($C_{37}H_{23}N_3O_5$) (Yield = 65%, mp 231°C) showed a strong band at 1736 cm^{-1} which is due to carbonyl stretching of δ -lactone ring present in coumarin nucleus. The bands observed at 1597 and 1538 cm^{-1} are due to aromatic C=C and C=N stretching vibrations respectively. The sharp bands observed at 690 and 779 cm^{-1} are due to C-H out of plane bending vibrations for mono substituted benzene ring. The bands observed at 2925 and 3073 cm^{-1} are due to aliphatic C-H stretching and aromatic C-H stretching vibrations respectively. A broad band observed around 3414 cm^{-1} is due to O-H stretching.

The 1H NMR spectrum of compound 3a (in $CDCl_3$) showed a singlet at 2.43 δ integrating for three protons which is due to methyl group. A singlet appeared at 6.09 δ integrating for one proton, is due to proton attached at C3'. A singlet appeared at 8.70 δ integrating for one proton, is due to proton attached at C5''. The hydroxyl group proton of coumarin separated out from other signals and appeared as a broad singlet in the most downfield region at 15.09 δ . The presence of hydroxyl group proton was confirmed by D2O exchange. The remaining seventeen aromatic protons appeared as a multiplet between 6.30-7.81 δ .



(Scheme-2)

The ^{13}C NMR spectrum of compound 3a (in $CDCl_3$) showed signals at 19.41, 101.34, 112.50, 114.12, 114.46, 118.62, 119.71, 119.96, 120.84, 123.25, 124.81, 126.02, 126.29, 127.50, 127.70, 128.71, 129.21, 129.31, 129.47, 130.60, 131.65, 133.01, 143.69, 145.86, 147.51, 148.12, 150.99, 152.70, 154.90, 158.35, 158.45, 158.55 and 160.85 δ . Thus, total thirty three carbon signals are seen. The compound is having thirty three types of non-equivalent carbon atoms and hence expected number of signals is observed. The most downfield signals appeared at 158.55 and 160.85 δ can be assigned to the carbonyl carbon of the δ -lactone ring of two coumarin rings. The DEPT-135 spectrum of compound 3a (in $CDCl_3$) showed signals at 19.41, 112.50, 114.46, 118.62, 119.96, 123.25, 124.81, 126.02, 126.29, 127.49, 127.70, 128.71, 129.22, 129.31, 130.58 and 131.64 δ . The signal at 19.41 δ is due to methyl carbon. The signals appeared at 112.50, 114.46, 118.62, 119.96, 123.25, 124.81, 126.02, 126.29, 127.49, 127.70, 128.71, 129.22, 129.31, 130.58 and 131.64 δ are due to fifteen tertiary carbons.

The mass spectrum of compound 3a showed M^+ peak at 589(75%) (m/z %) along with some other fragments peaks at 501 (63%), 220(30%), 77(100%), 51(40%) etc. The appearance of molecular ion peak at 589 mass unit supports the structure of compound 3a.

3b ($R_1 = CH_3$, $R_2 = R_3 = H$) ($C_{38}H_{25}N_3O_5$) (Yield = 77% mp 216°C) IR: λ_{max} 1735 ($C=O$ stretching of δ -lactone of coumarin), 1599 and 1449 (aromatic C=C and C=N stretching), 2926 and 3070 (aliphatic C-H stretching and aromatic C-H stretching), 757 and 693 (C-H bending vibrations of mono substituted benzene ring), 3448 (O-H stretching). 1H -NMR: (δ , ppm) ($CDCl_3$) 2.41 and 2.43 (6H, two singlets, $2 \times CH_3$), 6.08 (1H, singlet, proton at C3'), 6.30-7.83 (16H, multiplet, aromatic protons except proton at C5''), 8.69 (1H , singlet, proton at C5''),

15.46(1H, broad singlet, D₂O exchangeable -OH proton). ¹³C NMR: (δ, ppm) (CDCl₃) 19.41(CH₃), 21.69(CH₃), 101.32(C), 112.49(CH), 114.11(CH), 114.45(C), 116.92(CH), 118.62(CH), 119.68(CH), 119.95(CH), 120.83(CH), 124.81(CH), 126.28(CH), 127.50(CH), 128.00(C), 128.70(CH), 129.22(CH), 129.30(CH), 130.87(C), 131.63(CH), 133.00(C), 135.69(C), 143.68(C), 144.81(C), 145.85(C), 147.51(C), 148.49(C), 150.99(C), 152.70(C), 154.90(C), 155.51(C), 158.34(C), 158.54(CO of coumarin), 160.83(CO of Coumarin).

3c (R₂ = CH₃, R₁ = R₃ = H) (C₃₈H₂₅N₃O₅) (Yield = 63%, mp 224-226°C) IR: λ_{max} 1735 (C=O stretching of δ-lactone of coumarin), 1599 and 1501 (aromatic C=C and C=N stretching), 2926 and 3067 (aliphatic C-H stretching and aromatic C-H stretching), 757 and 693 (C-H bending vibrations of mono substituted benzene ring), 3433 (O-H stretching). ¹H-NMR: (δ, ppm) (CDCl₃) 2.41 and 2.46 (6H, two singlets, 2 × CH₃), 6.09 (1H, singlet, proton at C3'), 6.30-8.11 (16H, multiplet, aromatic protons except proton at C5''), 8.70 (1H, singlet, proton at C5''), 15.09 (1H, broad singlet, D₂O exchangeable -OH proton). ¹³C NMR: (δ, ppm) (CDCl₃) 15.61(CH₃), 19.41(CH₃), 101.33(C), 112.50(CH), 114.12(C), 114.61(CH), 118.63(CH), 119.72(CH), 119.97(CH), 120.83(C), 123.24(C), 124.81(CH), 126.03(CH), 126.28(CH), 127.48(CH), 127.70(CH), 128.71(CH), 129.20(CH), 129.32(CH), 129.46(CH), 131.63(CH), 132.26(C), 133.00(C), 143.68(C), 145.86(C), 147.50(C), 148.12(C), 150.95(C), 152.69(C), 154.89(C), 155.57(C), 158.33(C), 158.55(CO of coumarin), 160.84(CO of coumarin).

3d (R₃ = CH₃, R₁ = R₂ = H) (C₃₈H₂₅N₃O₅) (Yield = 72%, mp 200-202°C) IR: λ_{max} 1728 (C=O stretching of δ-lactone of coumarin), 1598 and 1504 (aromatic C=C and C=N stretching), 2922 and 3068 (aliphatic C-H stretching and aromatic C-H stretching), 756 and 688 (C-H bending vibrations of mono substituted benzene ring), 825 (C-H bending vibrations of p-disubstituted benzene ring), 3510 (O-H stretching). ¹H-NMR: (δ, ppm) (CDCl₃) 2.35 and 2.41 (6H, two singlets, 2 × CH₃), 6.11 (1H, singlet, proton at C3'), 6.30-7.82 (16H, multiplet, aromatic protons except proton at C5''), 8.70 (1H, singlet, proton at C5''), 15.01 (1H, broad singlet, D₂O exchangeable -OH proton). ¹³C NMR: (δ, ppm) (CDCl₃) 19.43(CH₃), 21.31(CH₃), 101.33(C), 112.50(CH), 114.12(C), 114.45(CH), 118.62(CH), 119.70(C), 119.96(CH), 120.83(C), 123.24(CH), 124.82(CH), 125.71(CH), 126.03(CH), 126.28(CH), 127.70(CH), 129.33(CH),

129.48(C), 129.51(CH), 130.61(CH), 131.64(CH), 131.73(C), 131.75(C), 143.68(C), 145.86(C), 147.51(C), 148.13(C), 150.99(C), 152.70(C), 154.89(C), 158.35(C), 158.45(C), 158.54(CO of coumarin), 160.85(CO of coumarin).

3e (R₂ = H, R₁ = R₃ = CH₃) (C₃₉H₂₇N₃O₅) (Yield = 71%, mp 175°C) IR: λ_{max} 1728 (C=O stretching of δ-lactone of coumarin), 1597 and 1504 (aromatic C=C and C=N stretching), 2924 and 3071 (aliphatic C-H stretching and aromatic C-H stretching), 754 and 688 (C-H bending vibrations of mono substituted benzene ring), 825 (C-H bending vibrations of p-disubstituted benzene ring), 3448 (O-H stretching). ¹H-NMR: (δ, ppm) (CDCl₃) 2.24, 2.35 and 2.41 (9H, three singlets, 3 × CH₃), 6.11 (1H, singlet, proton at C3'), 6.30-7.82 (15H, multiplet, aromatic protons except proton at C5''), 8.70 (1H, singlet, proton at C5''), 15.01 (1H, broad singlet, D₂O exchangeable -OH proton). ¹³C NMR: (δ, ppm) (CDCl₃) 19.41(CH₃), 21.34(CH₃), 21.64(CH₃), 101.32(C), 112.49(CH), 114.12(C), 114.50(CH), 116.89(C), 118.61(CH), 119.70(CH), 119.96(CH), 120.80(C), 124.79(CH), 125.69(CH), 126.28(CH), 128.01(CH), 129.30(CH), 129.51(CH), 130.32(C), 130.88(CH), 131.64(CH), 131.71(C), 135.65(C), 143.70(C), 144.82(C), 145.85(C), 147.51(C), 148.00(C), 150.99(C), 152.67(C), 154.89(C), 155.41(C), 158.32(C), 158.54(CO of coumarin), 160.84(CO of coumarin).

3f (R₁ = H, R₂ = R₃ = CH₃) (C₃₉H₂₇N₃O₅) (Yield = 60%, mp 186-188°C) IR: λ_{max} 1728 (C=O stretching of δ-lactone of coumarin), 1598 and 1505 (aromatic C=C and C=N stretching), 2922 and 3067 (aliphatic C-H stretching and aromatic C-H stretching), 756 and 688 (C-H bending vibrations of mono substituted benzene ring), 825 (C-H bending vibrations of p-disubstituted benzene ring), 3482 (O-H stretching). ¹H-NMR: (δ, ppm) (CDCl₃) 2.35, 2.41 and 2.44 (9H, three singlets, 3 × CH₃), 6.11 (1H, singlet, proton at C3'), 6.30-7.83 (15H, multiplet, aromatic protons except proton at C5''), 8.70 (1H, singlet, proton at C5''), 15.01 (1H, broad singlet, D₂O exchangeable -OH proton). ¹³C NMR: (δ, ppm) (CDCl₃) 15.62(CH₃), 19.40(CH₃), 21.33(CH₃), 101.28(C), 112.47(CH), 114.09(C), 114.45(CH), 118.68(CH), 119.67(C), 119.89(CH), 120.87(C), 123.24(CH), 124.82(CH), 126.03(CH), 126.31(CH), 127.49(C), 127.71(CH), 128.71(C), 129.23(C), 129.28(CH), 129.48(CH), 131.66(CH), 132.27(CH), 133.11(C), 143.70(C), 145.83(C), 147.45(C), 148.11(C),

150.99(C), 152.68(C), 154.91(C), 155.48(C), 158.30(C), 158.55(CO of coumarin), 160.86 (CO of coumarin).

3g ($R_3 = \text{OCH}_3$, $R_1 = R_2 = \text{H}$) ($\text{C}_{38}\text{H}_{25}\text{N}_3\text{O}_6$) (Yield = 75%, mp 218-220°C) IR: λ_{max} 1735 (C=O stretching of δ -lactone of coumarin), 1599 and 1503 (aromatic C=C and C=N stretching), 2926 and 3070 (aliphatic C-H stretching and aromatic C-H stretching), 757 and 690 (C-H bending vibrations of mono substituted benzene ring), 836 (C-H bending vibrations of p-disubstituted benzene ring), 3447 (O-H stretching). 1H-NMR: (δ , ppm) (CDCl_3) 2.41 (3H, singlet, CH_3), 3.87 (3H, singlet, OCH_3), 6.10 (1H, singlet, proton at C3'), 6.30-7.81 (16H, multiplet, aromatic protons except proton at C5''), 8.70 (1H, singlet, proton at C5''), 15.05(1H, broad singlet, D2O exchangeable -OH proton). 13C NMR: (δ , ppm) (CDCl_3) 19.41(CH_3), 55.84(OCH_3), 101.32(C), 112.50(CH), 114.13(C), 114.44(CH), 114.83(CH), 118.62(CH), 119.62(CH), 119.97(C), 120.82(C), 123.23(CH), 124.87(CH), 125.30(C), 126.03(CH), 126.28(CH), 127.69(CH), 128.51(CH), 129.31(CH), 129.50(C), 130.57(CH), 131.66(CH), 143.68(C), 145.79(C), 147.52(C), 148.11(C), 150.97(C), 152.66(C), 154.91(C), 158.35(C), 158.45(C), 158.56(C), 160.62(CO of coumarin), 160.85(CO of coumarin).

3h ($R_1 = \text{CH}_3$, $R_2 = \text{H}$, $R_3 = \text{OCH}_3$) ($\text{C}_{39}\text{H}_{27}\text{N}_3\text{O}_6$) (Yield = 74%, mp 210-212°C) IR: λ_{max} 1734 (C=O stretching of δ -lactone of coumarin), 1599 and 1503 (aromatic C=C and C=N stretching), 2928 and 3071 (aliphatic C-H stretching and aromatic C-H stretching), 757 and 690 (C-H bending vibrations of mono substituted benzene ring), 836 (C-H bending vibrations of p-disubstituted benzene ring), 3448 (O-H stretching). 1H-NMR: (δ , ppm) (CDCl_3) 2.41 and 2.46 (6H, two singlets, $2 \times \text{CH}_3$), 3.84 (3H, singlet, OCH_3), 6.08 (1H, singlet, proton at C3'), 6.29-7.80 (15H, multiplet, aromatic protons except proton at C5''), 8.68 (1H, singlet, proton at C5''), 15.08(1H, broad singlet, D2O exchangeable -OH proton). 13C NMR: (δ , ppm) (CDCl_3) 19.41(CH_3), 21.62(CH_3), 55.83(OCH_3), 101.32(C), 112.50(CH), 114.14(C), 114.43(CH), 114.84(CH), 116.93(CH), 118.62(CH), 119.71(CH), 119.96(CH), 120.84(C), 124.82(CH), 125.30(C), 126.29(CH), 128.50(CH), 129.31(CH), 130.90(CH), 131.65(CH), 135.70(C), 143.69(C), 144.89(C), 145.86(C), 147.51(C), 148.12(C), 150.99(C), 152.71(C), 154.90(C), 155.40(C), 158.35(C), 158.45(C), 158.55(C), 160.62(CO of coumarin), 160.86(CO of coumarin).

3i ($R_1 = \text{H}$, $R_2 = \text{CH}_3$, $R_3 = \text{OCH}_3$) ($\text{C}_{39}\text{H}_{27}\text{N}_3\text{O}_6$) (Yield = 62%, mp 225-227°C) IR: λ_{max} 1734 (C=O stretching of δ -lactone of coumarin), 1599 and 1503 (aromatic C=C and C=N stretching), 2931 and 3070 (aliphatic C-H stretching and aromatic C-H stretching), 757 and 690 (C-H bending vibrations of mono substituted benzene ring), 889 (C-H bending vibrations of p-disubstituted benzene ring), 3433 (O-H stretching). 1H-NMR: (δ , ppm) (CDCl_3) 2.41 and 2.44 (6H, two singlets, $2 \times \text{CH}_3$), 3.80 (3H, singlet, OCH_3), 6.10 (1H, singlet, proton at C3'), 6.30-7.81 (15H, multiplet, aromatic protons except proton at C5''), 8.70 (1H, singlet, proton at C5''), 15.05(1H, broad singlet, D2O exchangeable -OH proton). 13C NMR: (δ , ppm) (CDCl_3) 15.62(CH_3), 19.41(CH_3), 55.84(OCH_3), 101.32(C), 112.49(CH), 114.11(C), 114.44(CH), 114.45(CH), 118.61(CH), 119.68(C), 119.95(CH), 120.85(C), 123.24(C), 124.79(CH), 125.31(C), 126.03(CH), 126.30(CH), 127.77(CH), 128.48(CH), 129.35(CH), 129.50(CH), 130.59(C), 131.66(CH), 143.69(C), 145.91(C), 147.49(C), 148.12(C), 150.98(C), 152.67(C), 154.88(C), 158.34(C), 158.44(C), 158.55(C), 160.62(CO of coumarin), 160.85(CO of coumarin).

3j ($R_1 = \text{H}$, $R_2 = \text{H}$, $R_3 = \text{Cl}$) ($\text{C}_{37}\text{H}_{22}\text{ClN}_3\text{O}_5$) (Yield = 65% mp 233°C) IR: λ_{max} 1735 (C=O stretching of δ -lactone of coumarin), 1599 and 1503 (aromatic C=C and C=N stretching), 2926 and 3070 (aliphatic C-H stretching and aromatic C-H stretching), 757 and 690 (C-H bending vibrations of mono substituted benzene ring), 890 (C-H bending vibrations of p-disubstituted benzene ring), 3447 (O-H stretching). 1H-NMR: (δ , ppm) (CDCl_3) 2.42 (3H, singlet, CH_3), 6.25 (1H, singlet, proton at C3'), 6.32-8.14 (16H, multiplet, aromatic protons except proton at C5''), 8.72 (1H, singlet, proton at C5''), 15.11(1H, broad singlet, D2O exchangeable -OH proton). 13C NMR: (δ , ppm) (CDCl_3) 19.41(CH_3), 101.34(C), 112.49(CH), 114.11(C), 114.42(CH), 118.63(CH), 119.72(C), 119.95(CH), 120.78(C), 123.30(CH), 124.75(CH), 126.04(CH), 126.28(CH), 127.48(CH), 127.67(C), 128.93(CH), 129.29(CH), 129.31(CH), 129.47(C), 130.60(CH), 131.70(CH), 134.30(C), 143.70(C), 145.87(C), 147.55(C), 148.11(C), 150.99(C), 152.70(C), 154.91(C), 158.29(C), 158.45(C), 158.48(CO of coumarin), 160.87(CO of coumarin).

3k ($R_1 = \text{CH}_3$, $R_2 = \text{H}$, $R_3 = \text{Cl}$) ($\text{C}_{38}\text{H}_{24}\text{ClN}_3\text{O}_5$) (Yield = 61%, mp 232-234°C) IR: λ_{max} 1735 (C=O stretching of δ -lactone of coumarin), 1597 and 1528 (aromatic C=C and C=N stretching), 2926 and 3066 (aliphatic C-H

stretching and aromatic C-H stretching), 755 and 690 (C-H bending vibrations of mono substituted benzene ring), 836 (C-H bending vibrations of p-disubstituted benzene ring), 3448 (O-H stretching). ¹H-NMR: (δ , ppm) (CDCl₃) 2.39 and 2.45 (6H, two singlets, 2 × CH₃), 6.08 (1H, singlet, proton at C3'), 6.30-7.99 (15H, multiplet, aromatic protons except proton at C5''), 8.61 (1H, singlet, proton at C5''), 13.87 (1H, broad singlet, D₂O exchangeable -OH proton). ¹³C NMR: (δ , ppm) (CDCl₃) 19.41(CH₃), 21.62(CH₃), 101.32(C), 112.50(CH), 114.13(C), 114.46(CH), 116.95(CH), 118.62(CH), 119.68(C), 119.89(CH), 120.77(C), 124.82(CH), 126.28(CH), 128.03(CH), 128.90(CH), 129.28(CH), 129.29(CH), 130.88(CH), 131.11(CH), 131.31(C), 134.29(C), 135.69(C), 143.55(C), 144.77(C), 145.46(C), 147.48(C), 148.15(C), 150.94(C), 152.88(C), 154.48(C), 155.46(C), 158.32(C), 158.53(CO of coumarin), 160.84(CO of coumarin).

3l (R₁ = H, R₂ = CH₃, R₃ = Cl) IR: λ_{\max} 1726 (C=O stretching of δ -lactone of coumarin), 1600 and 1502 (aromatic C=C and C=N stretching), 2925 and 3071 (aliphatic C-H stretching and aromatic C-H stretching), 756 and 689 (C-H bending vibrations of mono substituted benzene ring), 830 (C-H bending vibrations of p-disubstituted benzene ring), 3448 (O-H stretching). ¹H-NMR: (δ , ppm) (CDCl₃) 2.42 and 2.45 (6H, two singlets, 2 × CH₃), 6.11 (1H, singlet, proton at C3'), 6.31-7.82 (15H, multiplet, aromatic protons except proton at C5''), 8.70 (1H, singlet, proton at C5''), 14.91(1H, broad singlet, D₂O exchangeable -OH proton). ¹³C NMR: (δ , ppm) (CDCl₃) 15.43(CH₃), 19.41(CH₃), 101.34(C), 112.50(CH), 114.11(C), 114.38(CH), 118.58(CH), 119.72(C), 119.97(CH), 120.78(C), 123.23(C), 124.75(CH), 126.03(CH), 126.28(CH), 127.51(C),

Table 1

Compounds	Cell viability (%)									
	Concentration	100 μ l/ml	150 μ l/ml	200 μ l/ml	250 μ l/ml	300 μ l/ml	350 μ l/ml	400 μ l/ml	450 μ l/ml	500 μ l/ml
	Control	100	100	100	100	100	100	100	100	100
3a		61.12 \pm 1.13	53 \pm 1.12	41 \pm 1.13	35 \pm 1.12	31 \pm 1.11	25 \pm 1.13	22 \pm 1.12	17 \pm 1.14	15 \pm 1.13
3b		60.21 \pm 1.1	32.14 \pm 1.4	41.12 \pm 1.4	33.11 \pm 1.12	32.4 \pm 1.13	24.23 \pm 1.15	21.27 \pm 1.12	18 \pm 1.13	15 \pm 1.13
3c		66.35 \pm 1.16	33.21 \pm 1.14	42.17 \pm 1.1	36.13 \pm 1.1	33.14 \pm 1.15	23.22 \pm 1.1	20.11 \pm 1.1	16.1 \pm 1.17	14.12 \pm 1.14
3d		63.27 \pm 1.12	31.14 \pm 1.14	43.27 \pm 1.14	36.21 \pm 1.14	31.23 \pm 1.13	25.14 \pm 1.13	22.14 \pm 1.13	17.22 \pm 1.14	12 \pm 1.14
3e		61.24 \pm 1.14	31.26 \pm 1.11	41.21 \pm 1.14	36.3 \pm 1.14	31.4 \pm 1.15	26.2 \pm 1.15	24.1 \pm 1.14	16 \pm 1.14	14 \pm 1.14
3f		62.3 \pm 1.14	32.3 \pm 1.1	41.3 \pm 1.14	33.4 \pm 1.14	32.1 \pm 1.13	23.1 \pm 1.13	22.3 \pm 1.13	16.4 \pm 1.14	14 \pm 1.14
3g		63.2 \pm 1.14	33.1 \pm 1.12	42.4 \pm 1.14	37 \pm 1.14	33 \pm 1.14	24.6 \pm 1.12	21.4 \pm 1.17	17 \pm 1.13	16.4 \pm 1.16
3h		61.23 \pm 1.14	30.17 \pm 1.12	44.26 \pm 1.17	34.24 \pm 1.14	32.2 \pm 1.12	25.1 \pm 1.11	22.5 \pm 1.14	18.2 \pm 1.15	13.4 \pm 1.17
3i		62.2 \pm 1.1	34 \pm 1.14	41.7 \pm 1.13	33.4 \pm 1.13	31.5 \pm 1.14	26.2 \pm 1.13	21.7 \pm 1.14	16 \pm 1.14	13.4 \pm 1.14
3j		63.5 \pm 1.13	32.5 \pm 1.17	42.5 \pm 1.16	33.5 \pm 1.14	32.4 \pm 1.17	23.4 \pm 1.15	20.4 \pm 1.14	17.2 \pm 1.11	9 \pm 1.13
3k		61.4 \pm 1.18	32.8 \pm 1.18	42.5 \pm 2.1	36.5 \pm 2.1	35 \pm 2.1	24.7 \pm 1.9	20.8 \pm 1.7	16.34 \pm 1.9	10.44 \pm 1.8
3l		62.23 \pm 1.14	31.24 \pm 1.16	43.24 \pm 1.14	33.26 \pm 1.14	30.23 \pm 1.14	23.12 \pm 1.10	20.1 \pm 1.1	15 \pm 1.1	10 \pm 1.1

127.68(CH), 128.94(CH), 129.28(CH), 129.31(CH), 129.48(CH), 130.57(C), 131.63(CH), 134.28(C), 143.66(C), 145.85(C), 147.52(C), 148.12(C), 150.96(C), 152.73(C), 154.33(C), 158.31(C), 158.43(C), 158.52(CO of coumarin), 160.84(CO of coumarin).

RESULTS

Various fused-coumarins (3a-l) were screened at concentration of 100 μ l/ml, 150 μ l/ml, 200 μ l/ml, 250 μ l/ml and 300 μ l/ml, 350 μ l/ml, 400 μ l/ml, 450 μ l/ml and 500 μ l/ml. The most of compounds significantly reduced the growth of MCF-7 cell line.

The evaluation of reduction for MCF-7 cell line treated with fusedcoumarins (3a-l) mixture at 570nm using ELISA reader data are shown in Table 1.

The assay describes that all the compounds fusedcoumarins (3a-l) shows visible effects Chart 2.

CONCLUSION

Thus, to gain a better understanding of the beneficial biological activities of fusedcoumarins upon cancer prevention, a greater knowledge of the metabolism of fusedcoumarins is needed. More research is clearly needed to identify and characterize additional fusedcoumarins metabolites and their biological activities, which will potentially provide invaluable insights into the mechanisms underlying the beneficial effects of fusedcoumarins to humans, especially in terms of cancer prevention. The synthesized compounds can also be screened with non-cancerous cell lines such as CHO or HEK293 cell lines in future. If such studies succeed in identifying an active fusedcoumarins derivative, it could be used as a parent compound for the development of potent anticancer drugs.

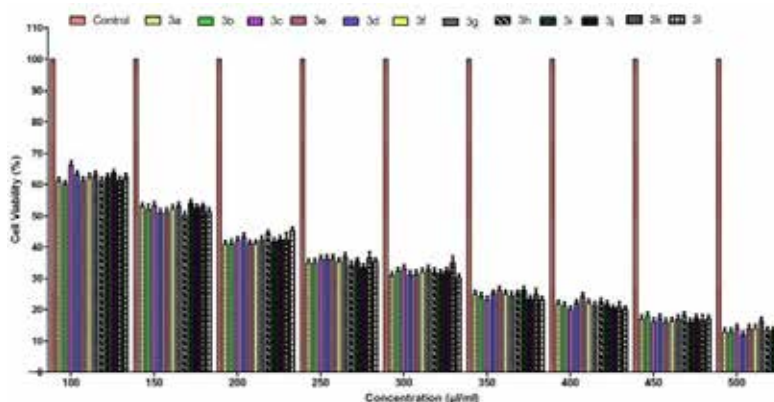


Chart 1

ACKNOWLEDGMENT

I am thankful to Department of Chemistry, Sardar Patel University, Gujarat for all the Laboratory facilities and Spectral Analysis.

I Have to be Thankful to Shree Vinoba Bhav Civil Hospital, Health Administration of UT Dadra and Nagar Haveli for Sample Analysis.

I am Thankful to the Principal, SSR College of Arts, Commerce and Science and SSR Memorial Trust for the continuous motivations. I am Thankful to my parents; wife and my son for always keep me energetic for every endeavor.

REFERENCES

- Emir Valencia, Amarendra Patra, Alan J. Freyer, Maurice Shamma, Victor Fajardo, Santiagonamine: A New Aporphinoid Alkaloid Incorporating A Phenanthridine Skeleton, *Tetrahedron Letters*, Volume 25, Issue 30, 1984, Pages 3163-3166, Issn 0040-4039, [https://doi.org/10.1016/S0040-4039\(01\)90998-0](https://doi.org/10.1016/S0040-4039(01)90998-0).
- Jigar L P, *The Introduction of Coumarin: Concise Reference Book*, First Edition, Bluerose Publication, ISBN: 978-93-5347-587-1 (2019).
- Jigar Patel, *Antimicrobial Evaluation of Some New Pyrazolyl Pyridinyl Coumarins*, *Der Pharma Chemica* (2018) Volume 10, Issue 8, Issn-0975-413x, Doi: 10.13140/Rg.2.2.33240.55040.
- Jigar Patel, *Pyrano Fused Coumarins: An Exclusive Synthesis From Simple Micheal Addition of 4-Hydroxy Coumarin To A,B –Unsaturated Carbonyl Compound And Screening of MCF-7 Cell Viability By MTT Assay*, *International Journal Of Solid State Technology*, Vol. 12, No. 3, 2019, Issn: 0038-111x.
- Jigar Patel, *Introduction Of Modified Fused Coumarin And Screening of Biological Activity Against Breast Cancer Cell Lines*, *Advances In Applied Science Research*, Vol.12 No.2:13, 2021, Issn: 0976-8610.
- W. Zecher, F. Kröhnke, *Ber.* 94, 690, 698 (1961); *Eidem, Angew. Chem. Int. Ed.* 1, 626 (1962).
- F. Kröhnke, *Synthesis* 1976, 1-24. *Synthetic Applications: J. N. Chatterjea Et Al.*, *Indian J. Chem.* 15b, 430 (1977).
- Lee, Adrian V.; Et Al. (1 July 2015). "MCF-7 Cells-Changing The Course of Breast Cancer Research And Care For 45 Years". *Journal Of The National Cancer Institute*. 107 (7): D1v073. Doi:10.1093/Jnci/D1v073. Pmid 25828948. *Breast Carcinoma*". *Journal of The National Cancer Institute*. 51 (5): 1409–1416. Doi:10.1093/Jnci/51.5.1409.
- Soule, Hd; Vazquez J; Long A; Albert S; Brennan M. (1973). "A Human Cell Line From A Pleural Effusion Derived From A Breast Carcinoma". *Journal Of The National Cancer Institute*. 51 (5): 1409–1416. Doi:10.1093/Jnci/51.5.1409.
- Jigar L P, *The Introduction of Coumarin: Concise Reference Book*, First Edition, Bluerose Publication, Page 250, ISBN: 978-93-5347-587-1 (2019).
- Jigar Lp, *The Introduction of Coumarin: Concise Reference Book*, First Edition, Bluerose Publication, Page 251, ISBN: 978-93-5347-587-1 (2019).
- Jigar L P, *The Introduction of Coumarin: Concise Reference Book*, First Edition, Bluerose Publication, Page 252, ISBN: 978-93-5347-587-1 (2019).

Environmentally Conscious Production of TiO₂ using Aloe Vera Gel Extract

Alkesh Bhavsar

Nanomaterial Research Laboratory
Department of Physics
School of Science, Sandip University
Nashik, Maharashtra

Kinnari Patil, D. R. Patil,

A. M. Patil

Department of Physics
R. C. Patel Arts, Commerce and Science College,
Shirpur, Maharashtra

Mahendra Shinde, Basilio Jose

Nanomaterial Research Laboratory
Department of Physics
School of Science
Sandip University
Nashik, Maharashtra

✉ mahendrashinde989@gmail.com

ABSTRACT

Titanium dioxide (TiO₂) stands out as a significant semiconductor material in the realm of solar energy conversion technologies. Despite its potential, its inherent limitations, such as a high band gap and a propensity for rapid charge carrier recombination under light, have posed challenges for its effective utilization. In this context, this study explores a novel approach to mitigate these constraints by tailoring the particle size using an environmentally friendly manufacturing method that harnesses the properties of Aloe Vera gel. This method not only addresses the kinetics and thermodynamics of TiO₂ synthesis but also aligns with sustainable practices. Several approaches such as X-ray diffraction (XRD), UV-visible spectroscopy, and others, were employed to comprehensively assess the properties of the synthesized TiO₂ particles. The outcomes of this investigation promise to contribute significantly to the advancement of more robust synthesis methodologies for the production of highly uniform and monodisperse TiO₂ nanoparticles. These tailored nanoparticles hold immense promise for a wide array of applications in diverse fields, particularly those requiring precise control over TiO₂ properties, including solar energy conversion technologies and beyond.

KEYWORDS : *Green synthesis, Aloe Vera gel, TiO₂ nanoparticles.*

INTRODUCTION

Due to the fast growth of industrialization and urbanization, an increasing amount of dangerous chemicals, gasses, or other substances are being released into the environment, severely harming our ecosystem [1]. Thus, it is essential to get knowledge regarding the application of natural ingredients in the creation of specialized functional nanomaterials [2]. The manipulation of matter at the atomic, molecular, and super molecular scales—with dimensions ranging from 1 to 100 nm—is known as nanotechnology. In contemporary material science, it is one of the most active research fields. It is the study of minuscule objects and has applications in all branches of research,

including engineering, chemistry, biology, physics, and material science. An inorganic solid is titanium dioxide [3]. The metal oxide is white in colour. TiO₂ shows poor solubility, non-flammability, and the heat stability. It is not considered hazardous by the United Nations (UN) according to the Universally Coordinated Scheme of Classification and Labelling of Elements [4]. It will show three dissimilar stages in the nanometer range at dissimilar high temperature: anatase, rutile and brookite. Anatase may be a specific one of these stages that has illustrated remarkable chemical and physical qualities for natural cleanup [5]. As a result, it finds usage in a wide range of industrial applications, including textiles, microelectronics, electrochemistry, charge spreading

devices, dye-sensitized solar cells, photocatalysis, self-cleaning, and chemical sensors [6].

Historically, the vast majority of metal and metal oxide nanoparticles were routinely produced using various physical and chemical processes. Non-sputtering, solvothermal methods, reduction, sol-gel technology, and electrochemical technique are some of the commonly utilized synthetic methods [7-10]. However, these procedures are costly, hazardous, interest tremendous pressure and energy, are difficult to separate, and are possibly hazardous [11]. The green synthesis process is an environmentally friendly technology that uses plant extracts (leaves, flowers, seeds and bark), fungi, bacteria and enzymes to synthesize titanium dioxide nanoparticles instead of many drugs [12]. Green synthesis has advantages over chemical and physical processes. Since it is more economical, easy to usage, and enables large-scale production.

The present investigation is based on an extract of the Aloe Vera plant. Aloe Vera is the earliest known curative herb [13]. He is the most often used medicinal plant amongst moist plant species.

It is stated that the plant has been used for medicinal purposes since the 1st century AD. I It is a vigorous herbal rising to 60–100 cm (24–39 in) high, through thick, ample green to grey-green leaves and white markings on the higher and inferior sides of the stem [14]. Aloe vera lotion covers vitamin B12, vitamin A, extra B vitamins, vitamin C, vitamin E, folic acid, and 19 of the 20 essential amino acids. Aloe vera has powerful detoxifying, antibacterial, nerve tonic, strong immune and antiviral properties and helps the digestive system. Aloe vera extract is an established skin naturopath that helps heal casing damage caused by skin irascibilities, insect tastes, burns and wounds. Water-soluble compounds found in aloe vera extract include aloe-emodin, Chrysophonal and Helmin-thosor [15-18]. This chemical acts as a reducing agent during the TiO₂ formation mentioned earlier. The nanoparticles produced will be rummage-sale in photocatalytic applications such as colorant squalor and aquatic piercing. Crystal violet dye and titanium matrix were chosen to study degradation and disintegration of water [19].

EXPERIMENTATIONS

Arrangement of Aloe Vera Herbal Extricate

New and well Aloe Vera plants were calm from R. C. Patel Art's, Commerce and Science College Campus, Shirpur, Maharashtra. Cut unique of the certain greeneries and wash it double with blow aquatic, shadowed by purified marine, to eliminate dirt and other contaminants. Weigh 50 g of leaves using an electronic scale and transfer to a 450 ml beaker containing 250 ml of refined marine [20]. The fillings were cooked on 90°C for 2 hours. The excerpt stood clean through What-man sieve paper 40. The remainder was saved for nanoparticle production.

Preparation Of Titanium Dioxide Nanoparticles

Titanium Isopropoxide (C₁₂H₂₈O₄Ti) (0.1 M) was synthesized using double distilled water. To achieve a pH 7 solution, aloe vera leaf extract was added drop by drop while continuously stirring [20]. For three hours, the mixture was constantly stirred. During this process, nanoparticles are melded then detached by means of Whatman sieve tabloid 40. Rinse the pellet several times with double distilled water to remove particles from the product. The nanoparticles remained dehydrated on 100°C for 6 h then calcined at 300 °C for 1 h [21-23].

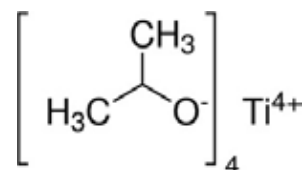


Fig. 1: Assembly of TTIP

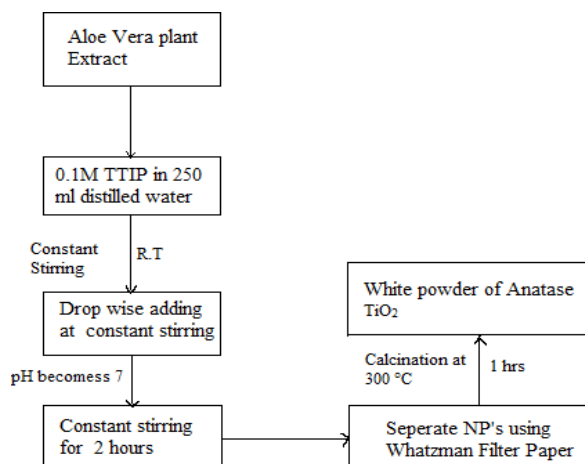


Fig. 2: Flow chart representation of synthesis of TiO₂ nanoparticles

CONCLUSIONS

The current study reaches the following conclusions:

- 1) Green synthesis method is used to produce high quality TiO₂ nanoparticles.
 - By XRD scrutiny, the usual crystallite magnitude of the trial remained determined as 12 nm. It was practical that a tetragonal arrangement through anatase phase developed. The SEM picture showed the structure of tetragonal irregular particles.
 - SEM is used to determine the size and properties of nanoparticles.
 - The absorption spectrum of the TiO₂ sample shows an absorption onset at approximately 393 nm, very close to the gap between the anatase stage (~3.2 eV).
- 2) This modest, economical, time redeemable and environmentally approachable synthesis process opens up new possibilities for many applications.
- 3) An environmentally friendly green chemistry strategy using aloe vera leaf extract to produce nanoparticles would improve the economics of this process.

ACKNOWLEDGMENT

We are grateful to the Nanomaterial Research Laboratory, Department of Physics, R. C. Patel Art's, Commerce and Science College Shirpur (Maharashtra) and Nanomaterial Research Laboratory, Department of Physics, School of Science, Sandip University, Nashik (Maharashtra) for XRD and UV characterization. Also, we are grateful to the Central Instrumentation Facility, Department of Chemistry, SPPU for SEM Characterization.

REFERENCES:

1. K. Zakrzewskal and M. Radecka. TiO₂-Based Nanomaterials for Gas Sensing Influence of Anatase and Rutile Contributions, *Nanoscale Research Letter*, 12:89, 2017.
2. Siti Amaniah Mohd Chachuli1, Mohd Nizar Hamidon1, Mehmet Ertugrul, TiO₂/B₂O₃ thick film gas sensor for monitoring carbon monoxide at different operating temperature, *Journal of Physics: Conference Series*, 1432 012040, 2020.
3. Yuan Wang, et al., TiO₂-Based Nano heterostructures for Promoting Gas Sensitivity Performance: Designs, Developments, and Prospects, 17, 1971; doi:10.3390/s17091971, 2017.
4. Jamal Malallah Rzajj. Et al, Review on: TiO₂ Thin Film as a Metal Oxide Gas Sensor. *Journal of Chemical Reviews*, Volume 2, Issue 2, Pages 114-121, 2020.
5. Vardan Galstyan, Porous TiO₂-Based Gas Sensors for Cyber Chemical Systems to Provide Security and Medical Diagnosis, *Sensors*, 17(12), 2947, 2017.
6. Kavitha Thangavelu. Et al, Synthesis and Characterization of Nanosized TiO₂ Powder Derived Fro A Sol-Gel Process in Acidic Conditins. Volume 4, Issue 2, pp: 90-95 ©IJESSET Rouxel D, 2017.
7. Synthesis of Nanoparticles of Titanium Dioxide TiO₂ for Toxicological Studies. Volume 3 . Issue 1 - October 2017.
8. R. Vijayalakshmi and V. Rajendran, Synthesis and characterization of nano-TiO₂ via different methods. *Archives of Applied Science Research*, 4 (2):1183-1190, 2012.
9. M. A. Gondal, S. G. Rashid, Sol-Gel Synthesis of Au/Cu-TiO₂ Nanocomposite and Their Morphological and Optical Properties, Volume 5, Number 3, June 2013.
10. Xiuzhen Wei, Guangfeng Zhu, Jinfeng Fang, and Jinyuan Chen. Synthesis, Characterization, and Photocatalysis of Well-Dispersible Phase-Pure Anatase TiO₂ Nanoparticles. *International Journal of Photoenergy* Volume 2013, Article ID 726872, 6 pages, 2013.
11. Eneyew Tilahun Bekele. Et. al, Synthesis of Titanium Oxide Nanoparticles Using Root Extract of Kniphofia foliosa as a Template, Characterization, and Its Application on Drug Resistance Bacteria. *Hindawi Journal of Nanomaterials* Volume 2020, Article ID 2817037, 10, 2020.
12. GM. Aravind. Et al, Synthesis of TiO₂ nanoparticles by chemical and green synthesis methods and their multifaceted properties. *SN Applied Sciences* 3:409, 2021.
13. Akinnowo. Et al. Synthesis, Modification, Applications and Challenges of Titanium Dioxide Nanoparticles. *Research Journal of Nanoscience and Engineering* Volume 3, Issue 4, PP 10-22, 2019.

14. Bruna Andressa Bregadiolli, et al, Easy and Fast Preparation of TiO₂ - based Nanostructures Using Microwave Assisted Hydrothermal Synthesis. *Materials Research.*; 20(4): 912-919, 2017.
15. Yuan Wang, Tao Wu, Chuanmin Meng, et al, TiO₂-Based Nano heterostructures for Promoting Gas Sensitivity Performance: Designs, Developments, and Prospects, *Sensors*, 17, 1971, 2017.
16. Jinhong Noh, Soon-Hwan Kwon, et al, TiO₂ Nanorods and Pt Nanoparticles under a UV-LED for an NO₂ Gas Sensor at Room Temperature, 1826, 2021.
17. Xu Tian, Xiuxiu Cui, et al., Gas sensors based on TiO₂ nanostructured materials for the detection of hazardous gases, 390–403, 2021.
18. Naresh Kumar Sethy and Pradeep Kumar, Green synthesis of TiO₂ nanoparticles from *Syzygium cumini* extract for photo-catalytic removal of lead (Pb) in explosive industrial wastewater, *De Grunter*; 9: 171–181, 2020.
19. Waseem Ahmad and et. Al., Green synthesis of titanium dioxide (TiO₂) nanoparticles by using *Mentha arvensis* leave extract and its antimicrobial properties, *Inorganic and Nano metal chemistry*, 2470-1564, 2020.
20. Ghulam Nabi, Qurat Al-In and Et.al., Green synthesis of TiO₂ nanoparticles using lemon peel extract: their optical and photocatalytic properties, *International Journal of Environmental Analytical chemistry*, ISSN: 0306-7319, 2020.
21. Yanjing Li and Yujhi Fu, Green synthesis of 3D tripyramid TiO₂ architectures with assistance of aloe extracts for highly efficient photocatalytic degradation of antibiotic ciprofloxacin, *Applied catalysis B: Environmental*, 0926-3373, 2020.
22. Rakesh Sonkar and Gaurav Hitkari, Green synthesis of TiO₂ nanosheet by chemical method for the removal of Rhodamin B from industrial waste, *Material Science and Engineering B*, 0921-5107, 2020.
23. Rosana Conclaves and Nirav Joshi, *Green Synthesis and Applications of ZnO and TiO₂ Nanostructures*, MDPI, 26, 2236, 2021.
24. Achudhan D and Vijaykumar S, the antibacterial, antibiofilm, antifogging and mosquitocidal activities of titanium dioxide (TiO₂) nanoparticles green-synthesized using 14 multiple plants extracts, *Environmental Chemical Engineering*, S2213-3437(20)30870-8, 2020.
25. Surya Pratap Goutam and Varunika Singh, Green synthesis of TiO₂ nanoparticles using leaf extracts of *Jatropha curcas* L. for photocatalytic degradation of tannery wastewater, *Chemical Engineering Journal*, S1385-8947(17)32142-3, 2017.
26. Tentu Nageswara Rao and P. Babji, Green synthesis and structural classification of *Acacia nilotica* mediated-silver doped titanium oxide (Ag/TiO₂) spherical nanoparticles: Assessment of its antimicrobial and anticancer activity, *Suadi Journal of Biological Science*, 1319-562, 2019.
27. Ishwar Chandra Maurya and Shalini Singh, Green synthesis of TiO₂ nanoparticles using *Bixa orellana* seed extract and its application for solar cells, *Elsevier Solar Energy*, 0038-092, 2019.
28. Muna Abu Dalo and Azza Zaradat, Green synthesis of TiO₂ NPs/pristine pomegranate peel extract nanocomposite and its antimicrobial activity for water disinfection, *Journal of Environmental Chemical Engineering*, 103370, 2019.
29. R. Ranjith and Shen Ming Chen, Green synthesis of reduced graphene oxide supported TiO₂/Co₃O₄ nanocomposite for photocatalytic degradation of methylene blue and crystal violet, 0272-8842, 2019.

The Introduction of LiOH for the Replacement of NaOH by the Green Chemistry Method for the Reduction of COD and BOD in the Effluents

Jigar Patel, Sachin Pawar

Khanderao Pagar, Hiranman Udar

SSR College of Arts, Commerce and Science
(affiliated to Savitribai Phule Pune University)
Silvassa, UT of Diu
Daman & Dadra Nagar Haveli
✉ drjigar.myself@gmail.com

ABSTRACT

The conventional method for the synthesis of chalcones includes the use of sodium hydroxide, which is hazardous in nature. The use of lithium hydroxide gives similar results for the synthesis of same chalcones. The various acetyl pyridines and various benzaldehydes reacted in presence of ethanol, water and lithium hydroxide gives chalcones. The water samples from the effluents have been studied by chemical oxygen demand (COD) and biological oxygen demand (BOD). In this green chemistry method, the use of Sodium Hydroxide is replaced by Lithium Hydroxide and in both case, the effluents are screened for its COD and BOD.

KEYWORDS : Green chemistry method, NaOH, LiOH, Chalcones, COD and BOD.

INTRODUCTION

The chalcones are very useful for the development of newer structure development¹⁻⁹. Green Context in of this procedure is free from use of hazardous organic solvents. The Lithium hydroxide (LiOH) is easy to handle as it is comparatively less hygroscopic than other alkali metal hydroxide (NaOH) and also it is less hazardous. Here, the catalytic amount of base gives better results. The reaction of Acetyl Pyridine with Benzaldehyde in presence of catalytic amount of LiOH in alcohol-water system, gives pyridine substituted chalcones, the same chalcones were prepared by using NaOH and reported earlier¹⁰. The results of biological hazard from its effluents were studied for conventional method (use of sodium hydroxide) and green chemistry method (use of lithium hydroxide).

Chemical oxygen demand [11-13] (COD) is an indirect measurement of the amount of organic matter in a sample. With this test, you can measure virtually all

organic compounds that can be digested by a digestion reagent. COD contrasts with Biochemical Oxygen Demand [14-15] (BOD), which relies on the use of microorganisms to break down the organic material in the sample by aerobic respiration over the course of a set incubation period (typically five days). As gauges of organic matter in a sample, BOD and COD are critical in wastewater for determining the amount of waste in the water.

MATERIALS AND METHODS

All chemicals were purchased from Sigma- Aldrich, German. Melting points were determined by the open capillary method and were uncorrected. FT-IR spectra of the synthesized compounds were recorded on a Shimadzu-8400S, using KBr pellets in 10^{-4} resolution and 30 scans. ¹H NMR spectra were recorded on a Varian spectrometer, USA at 400 MHz at room temperature. Samples were prepared in CDCl₃ containing TMS as an internal standard.

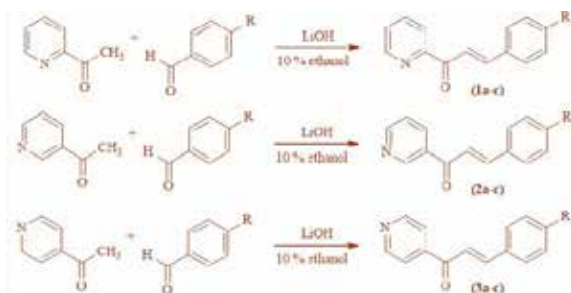
EXPERIMENTAL

The Synthesis of various chalcones (1a-3c) Scheme-1

The Conventional Method: In a 100 mL three necked flask equipped with a thermometer and magnetic needle, an aqueous 10% sodium hydroxide solution (25 ml) and ethanol (20 ml) were added with stirring and the mixture was cooled to 0-10°C in an ice bath. An appropriate aromatic aldehyde (0.02 mol) was introduced in one portion. Then appropriate acetyl pyridine (0.02 mol) was added in small portions over a period of 10 minutes. The mixture was stirred for three hours at 10°C under stirring. The resulting solid was isolated by filtration. The solid was collected and purified. The resulted effluent was collected for COD [11-13] and BOD [14-15] analysis.

The Green Chemistry Method (Scheme- 1)

In a 25 mL round bottom flask containing a small magnetic bar, the aldehyde (0.02 mol) and acetyl pyridine (0.02 mol) were taken with ethyl alcohol (15 ml) and lithium hydroxide (0.01 mol) monohydrate was added into it. The reaction mixture was magnetically stirred vigorously for 8-10 minutes. The pale yellow solid precipitated out, 5 g of crushed ice was added and the solid was allowed to settle down. The solid was collected [16-17] and purified. The resulted effluent was collected for COD [11-13] and BOD [14-15] analysis.



1a	R = CH ₃	(E)-1-(pyridin-2-yl)-3-p-tolylprop-2-en-1-one
1b	R = OCH ₃	(E)-3-(4-methoxyphenyl)-1-(pyridin-2-yl)prop-2-en-1-one
1c	R = Cl	(E)-3-(4-chlorophenyl)-1-(pyridin-2-yl)prop-2-en-1-one
2a	R = CH ₃	(E)-1-(pyridin-3-yl)-3-p-tolylprop-2-en-1-one
2b	R = OCH ₃	(E)-3-(4-methoxyphenyl)-1-(pyridin-3-yl)prop-2-en-1-one
2c	R = Cl	(E)-3-(4-chlorophenyl)-1-(pyridin-3-yl)prop-2-en-1-one
3a	R = CH ₃	(E)-1-(pyridin-4-yl)-3-p-tolylprop-2-en-1-one
3b	R = OCH ₃	(E)-3-(4-methoxyphenyl)-1-(pyridin-4-yl)prop-2-en-1-one
3c	R = Cl	(E)-3-(4-chlorophenyl)-1-(pyridin-4-yl)prop-2-en-1-one

(Scheme 1)

Chemical Oxygen Demand

$$\text{COD} = \frac{(A - B) N \times 8000}{S} \frac{\text{mg}}{\text{L}}$$

Where:

A = Milliliters of Fe(NH₄)₂(SO₄)₂ solution required for titration of the blank,

B = Milliliters of Fe(NH₄)₂(SO₄)₂ solution required for of the sample,

N = Normality of the Fe(NH₄)₂(SO₄)₂ solution, and

S = Milliliters of sample used for the test.

Biological Oxygen Demand

$$\text{BOD} = \frac{(D1 - D2) - (S)V_s}{P} \frac{\text{mg}}{\text{L}}$$

Where:

D1 = DO of diluted sample immediately after preparation, mg/L,

D2 = DO of diluted sample after 5 d incubation at 20°C, mg/L,

S = Oxygen uptake of seed (5 days)

V_s = Volume of seed in the respective test bottle, mL, and

P = Decimal volumetric fraction of sample used (Dilution Factor)

	Conventional Method		Green Chemistry Method	
	COD mg/L	BOD mg/L	COD mg/L	BOD mg/L
1a	56	42	49	36
1b	61	38	53	34
1c	79	51	71	45
2a	50	40	45	37
2b	61	32	54	29
2c	85	58	78	51
3a	58	45	52	39
3b	60	32	56	28
3c	81	56	72	52

Table 1: The measurement of COD & BOD in the Effluents of the various chalcones Products in Conventional & Green Chemistry Method

RESULTS

The effluents from conventional method and green chemistry methods collected from compound (1a-3c) have been screen with COD and BOD analysis 11-15. The Conventional Method gives results of effluent COD ranges from 56 mg/L to 81 mg/L. The Conventional Method gives results of effluent BOD ranges from 42

mg/L to 56 mg/L. The Green Chemistry Method gives results of effluent COD ranges from 49 mg/L to 72 mg/L. The Green Chemistry Method gives results of effluent BOD ranges from 36 mg/L to 28 mg/L.

CONCLUSIONS

The Chart 1 describes the comparison of Chemical Oxygen Demand for effluents from compounds (1a-3c) from Conventional Method and Green Chemistry Method, which shows visible reduction in COD of each effluent. While Chart 2 describes the comparison of Biological Oxygen Demand for effluents from compounds (1a-3c) from Conventional Method and Green Chemistry Method, which shows visible reduction in BOD of each effluent.

Thus, the COD of the chalcones effluents from green chemistry method (GC Method) has visible reduction in the Chemical Oxygen Demand (mg/L) as well as the BOD of the chalcones effluents from green chemistry method (GC Method) has visible reduction in the Biological Oxygen Demand (mg/L).

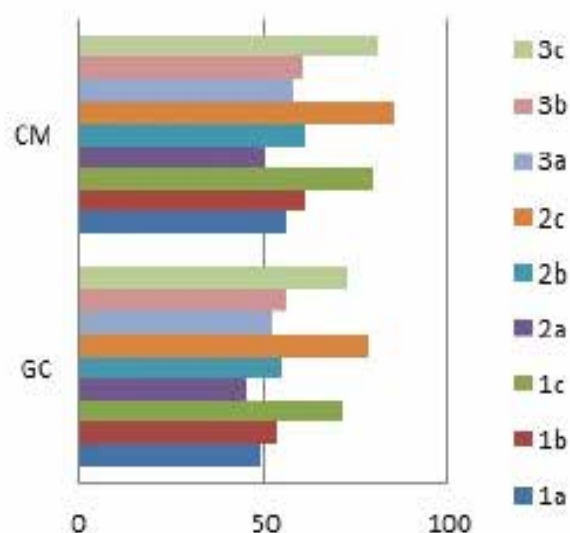


Chart 1: Chemical Oxygen Demand Results from effluent of compounds 1a to 3c

CM: Chemical Oxygen Demand (mg/L) measured for Conventional Method Effluents.

GC: Chemical Oxygen Demand (mg/L) measured for Green Chemistry Method Effluents.

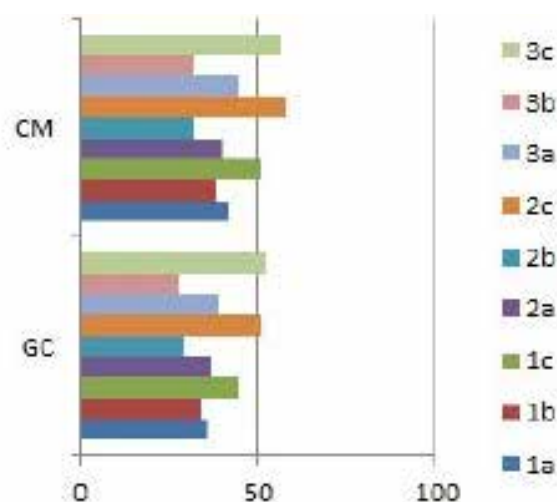


Chart 2: Biological Oxygen Demand Results from effluent of compounds 1a to 3c

CM: Chemical Oxygen Demand (mg/L) measured for Conventional Method Effluents

GC: Chemical Oxygen Demand (mg/L) measured for Green Chemistry Method Effluents

So here we can observe that if the wide use of NaOH (sodium hydroxide) can be replaced by LiOH (Lithium Hydroxide), the intention of the Green Chemistry can be fulfilled in the all types of the chalcones synthesis. Clearly it's a better option for the replacement of Hazardous NaOH.

ACKNOWLEDGEMENTS

The authors are thankful to the Principal & The Management of SSR Memorial Trust for all financial aid and laboratory uses.

REFERENCE

1. J. Patel, International Journal of Solid State Technology, Vol. 12, No. 3, 2019.
2. J. Patel, Der Pharma Chemica, 10(8): 67- 81, 2018.
3. D. I. Brahmhatt, J. Patel, International Journal of Research and Analytical Reviews, Volume 6, Issue 1, March 2019.
4. J. Patel, International Journal of Research and Analytical Reviews, Volume 6, Issue 2, May 2019.
5. J. Patel, International Journal of Advance Research and Development, Volume3, Issue 6, 2018.

6. J. Patel, International Journal of Advance Research and Development, Volume3, Issue 7, 2018.
7. J. Machhi, J. Patel, Chem Sci Rev Lett 7(26), 501-508, 2018.
8. J. Machhi, J. Patel, International Journal of Chemical Science, Volume 3; Issue 2; March, PP No. 43-46, 2019.
9. J. Patel, International Journal of Engineering Science Invention (IJESI), Volume 7 Issue 7 Ver III, PP 12-23, 2018.
10. Jigar L P, The Introduction of Coumarin: Concise reference book, First Edition, BlueRose Publication, page 165, ISBN: 978-93-5347-587-1 (2019).
11. <https://blog.hannainst.com/cod-testing>
12. Standard Methods for the Examination of Water and Wastewater, 14th Edition, p 550, Method 508 (1975).
13. Annual Book of ASTM Standards, Part 31, "Water", Standard D 1252-67, p 473 (1976).
14. YOUNG, J.C. 1973. Chemical methods for nitrification control. J. Water Pollut. Control Fed. 45:637.
15. U. S. ENVIRONMENTAL PROTECTION AGENCY, OFFICE OF RESEARCH AND DEVELOPMENT. 1986. Method-by-Method Statistics from Water Pollution (WP) Laboratory Performance Evaluation Studies. Quality Assurance Branch, Environmental Monitoring and Support Lab., Cincinnati, Ohio.
16. S. Bhagat, R. Sharma, and A.K. Chakraborti, J. Mol. Cat. A: Chemical 260, 235-240, 2006. Monograph on Green Chemistry
17. Laboratory Experiments by Green Chemistry Task Force Committee, DST.

Eco-Friendly Synthesis of Zinc Oxide Nanostructures from Chicken Eggshell: Exploring Electrical and Colloidal Properties

Basillio Jose Augusto Jose

Faculty of Science and Technology
Licungo University, Beira, Mozambique
✉ bjose@unilicungo.ac.mz

Mahendra D. Shinde

Nanomaterial Research Laboratory
Department of Physics, School of Science
Sandip University
Nashik, Maharashtra
✉ mahendrashinde989@gmail.com

Alkesh Bhavsar

Nanomaterial Research Laboratory
Department of Physics
R.C. P. A. C. S. College
Shirpur, Maharashtra

ABSTRACT

In response to the escalating environmental degradation, climate change, and extreme weather events, scientific research has shifted its focus toward sustainable and eco-friendly practices. This heightened attention to materials with minimal environmental impact aligns with the pursuit of Sustainable Development Goals. In this study, zinc oxide nanostructures were successfully synthesized using zinc acetate dehydration and chicken eggshell extract as the reaction mediators. XRD patterns confirmed the formation of ZnO NPs with an average size of 21.9 nm calculated from the Scherer formula and 19.1 nm determined from the W-H plot procedure. UV-Vis spectroscopy, coupled with the Kubelka-Munk method, determined the bandgap width to be 3.21 eV. Surface examination by FESEM revealed rod-like and spherical particle formations with well-defined grain boundaries and a markedly rough texture, further corroborated by AFM imaging. The Zeta potential test exhibited a negative surface charge of -26.72 mV related to stability in colloidal suspension. The i-v curve of the thin film, produced via pulsed laser deposition, displayed a negative temperature coefficient, indicating semiconductor behavior with decreasing resistance as temperature rose. This property suggests versatile applications in electronics, leveraging the film's adaptability to temperature changes. The thorough characterization of synthesized zinc oxide nanostructures offers valuable insights into their potential for sustainable and versatile technological uses.

KEYWORDS : *Eco-friendly synthesis, Zinc oxide nanostructures, Eggshell extract, Electrical and colloidal properties.*

INTRODUCTION

In the face of escalating environmental degradation, climate change, and extreme weather events, the scientific community has pivoted its research focus towards sustainable and eco-friendly practices. This redirection aligns with the global commitment to the Sustainable Development Goals (SDGs) and underscores the urgency to develop materials with minimal environmental impact [1].

This paper intricately delves into the synthesis of zinc oxide nanostructures, propelled by the fundamental pursuit of sustainable technological solutions that

demand a conscientious reduction in chemical usage. Aligned with the imperative for eco-friendly practices, our methodology is centered on the meticulous application of zinc acetate dehydration. It strategically leverages the distinctive properties embedded in chicken eggshell extract, which serves not only as a reaction mediator but also assumes multiple crucial roles—acting as a capping agent, a reducing agent, and a stabilizer. These varied functions play a pivotal role in orchestrating the formation of ZnO nanostructures, adding depth to the eco-conscious approach adopted in our research. This strategic choice aligns with the commitment to minimizing the environmental footprint

associated with traditional synthesis methods, as depicted in Fig. 1.

To our best understanding, limited studies have explored the synthesis of ZnO from eggshell extract and the subsequent analysis of their colloidal and electrical behavior, as well as morphologies. This research paper addresses this research gap by providing comprehensive insights into these aspects.



Fig. 1: Eco-friendly Synthesis Approach [14]

For instance, a molar concentration of 0.25 M eggshell was employed as a template for the green synthesis of ZnO using three zinc precursors (acetate, nitrate, and chloride). This process resulted in a favorable band gap of 3.25 eV, showcasing distinct emissions attributed to crystal effects [2]. Interwoven meshwork at three dimensions of ZnO of 5nm was obtained from zinc nitrate and eggshell membranes (ESM) with potential application in catalysis and electrochemical devices [3]

Regarding antibacterial and antifungal (*Bacillus subtilis* and *Aspergillus*) activity, bio-waste eggshell was utilized as a template for synthesizing ZnO nanoparticles of 14.7 nm through a soaking and calcination method. The prepared ZnO demonstrated both good colloidal stability (-42.7 mV) and UV properties (302-372 nm), with the observation of peaks at 449 cm^{-1} and 550 cm^{-1} attributed to stretching vibrations [12].

Eggshell membranes served as templates for synthesizing versatile ZnO nanocomposites, with applications spanning pharmaceuticals, catalysis, electrode materials, mechanochemical treatment, and building industry applications [13].

Table 1: Survey on Synthesis of ZnO Using Eggshell

N	Synthesis	Cryst.	Application	Rf
1	Zn/Eggshell powder/Felulago macrocarpa	25nm	Photocatalytic, Antibacterial and water disinfection	[4]
2	Eggshell/ZnO/NiO	14.12nm; 14.70nm	Antibacterial and antifungal activity	[5]
3	Different precursors of Zn/Eggshell	25.65-48.18nm	Comparison of physical properties	[6]
4	Functionalization Eggshell CuO-ZnO	15nm-20nm	Antibacterial activity	[7]
5	Zinc precursor/Eggshell	5nm	Study of physical properties of ZnO	[8]
6	Zinc precursor/Eggshell	6nm-40nm	Study of physical properties of ZnO	[9]
7	Eggshell/V ₂ O ₅ /ZnO	39.66nm	Antibacterial activity	[10]
8	Artemisia Eggshell/Zinc precursor	50nm	Photocatalytic activity	[11]

The eco-friendly synthesis approach (Fig. 1a) was selected for its utilization of abundant natural materials, often discarded as waste, thereby mitigating environmental hazards [14]. This method's cost-effectiveness is underscored by its single-pot synthesis capability, which requires minimal machinery and is devoid of costly environmental prerequisites. Notably, the plant-mediated synthesis method operates at ambient temperatures, enhancing practicality and affordability [15]

MATERIALS AND METHODS

The chicken eggshell was meticulously cleaned using tap water followed by deionized water rinses to remove surface impurities and ensure cleanliness. After drying for 6 hours, the eggshells were ground to increase surface area. A 6g powder was then mixed with 200 ml of deionized water and boiled for 45 minutes to extract active components. The resulting mixture was filtered and centrifuged to separate the liquid phase from the residues. The filtered solution, 100ml, was stored for subsequent use. The Zinc precursor, Zn(CH₃COO)₂·2H₂O, procured from Merck Life Science

Private Limited, with a purity of over 98% and a molecular weight of 219.49 g/mol, was used as the primary material. For thin film preparation, 2 grams of ZnO powder were compressed at 50 KN for 5 minutes, forming a 2 mmx25 mm pallet, then sintered at 900°C for 5 hours. The dense pallet was used as a target in pulse laser deposition onto a p-Si (100) substrate at 700°C for 30 minutes under 1mb pressure, followed by annealing at 500°C for 1 hour in an oxygen atmosphere.

RESULTS AND DISCUSSION

XRD

Fig. 2 illustrates the XRD structural analysis that utilized Cu K α radiation ($\lambda=1.5418\text{\AA}$) with a scanning angle (2θ) of $[20^\circ-80^\circ]$, revealing 11 peaks in alignment with JCPDS (36-1451) [16]. Peak intensity analysis, with a COD (R2) of 0.98011, determined a crystallite size of 21.9 nm via the Debye-Scherrer formula and 19.151 nm through the Williamson-Hall plot method. Fig. 4 depicts peaks at 11 distinct angles, matching specific diffraction planes, with FWHM ranging from 0.4181 to 0.39366, indicating a uniform crystallite size distribution.

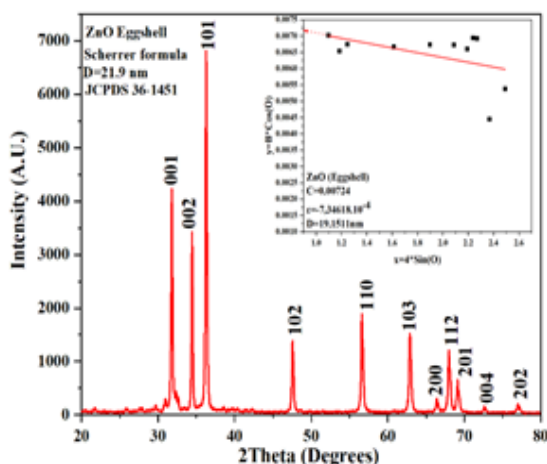


Fig. 2: XRD patterns of ZnO using Eggshell

UV-VIS Spectroscopy

The eggshell template's effect on ZnO NPs was investigated via UV-Spectroscopy, revealing a narrowed band gap at approximately 377 nm in Fig. 3. The Kubelka-Munk transformation of diffuse reflectance spectroscopy data determined a band gap of 3.21 eV, indicating direct electron transitions. This value, within the range of 3.0 to 3.7 eV reported in the literature,

underscores the efficacy of eco-friendly synthesis methods like eggshell-mediated ZnO production in modifying ZnO's optical properties.

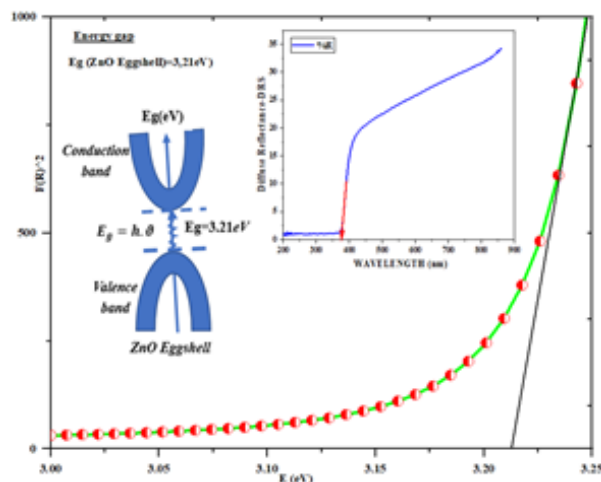


Fig. 3: UV-Vis spectroscopy

Raman Spectrograph

Fig. 4 illustrates Raman spectroscopy analysis of ZnO, conducted with a HORIBA Jobin LabRAM HR800 instrument using a 473 nm laser. Various vibrational modes, including polar modes (A_1 and E_1) and E_2 modes, are identified, shedding light on crystal structure and impurities. Notably, peaks at 328.96 cm^{-1} (E_2H-E_2L) and 434.523 cm^{-1} (E_2H) correspond to longitudinal and transversal optical phonon modes, respectively, indicative of ZnO's wurtzite phase. The appearance of a peak at 563.383 cm^{-1} further elucidates ZnO's crystallographic properties.

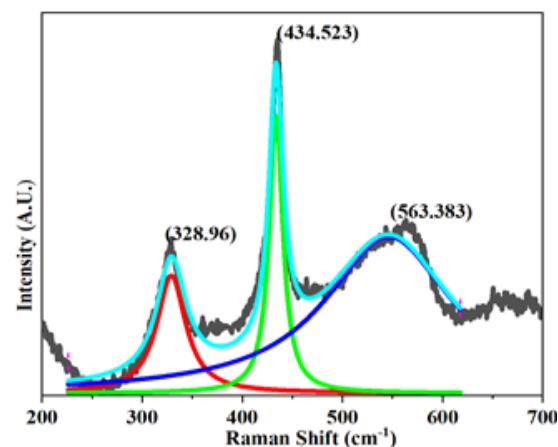


Fig. 4: Raman spectrograph of ZnO

FESEM and AFM

Surface analysis (FE-SEM), and AFM, (Fig. 5) revealed diverse ZnO particle structures with well-defined grain boundaries and high crystallinity, averaging 15.1 nm in size. AFM imaging unveiled surface features including grains, valleys, and peaks, while nanoindentation tests established a correlation between surface roughness, continuity, and material hardness. These observations offer valuable insights into potential applications in materials engineering and biomimetics, indicating a significant influence on electrical properties. The ZnO thin films were deposited on a silicon p-Si (100) substrate using PLD, and continuous film deposition was monitored, as evidenced by the absence of vacancies along the diagonal line indicated by pulse waves.

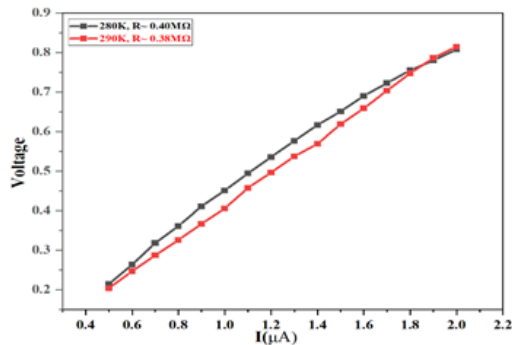


Fig. 5: i-v characteristics of ZnO thin film

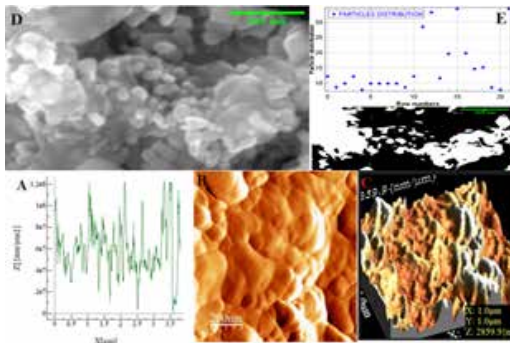


Fig. 6: FESEM and AFM patterns of ZnO

Zeta potential

Zeta potential analysis (Fig. 6) was conducted on synthesized ZnO nanofluids using eggshell extract. The experimental setup involved mixing 0.2 mg of nanostructures with 20 ml of deionized water (pH 7) followed by 3 minutes of negative surface charge, the particles displayed stability (Zeta potential ~

-26.09 mV) in the deionized water medium, yet their colloidal suspension state compromised their practical application efficacy.

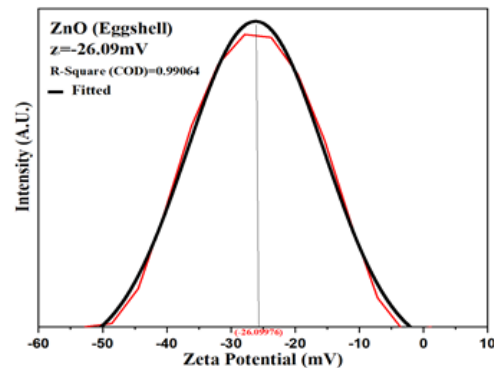


Fig. 6: Zeta potential of ZnO

Electrical study

The electrical properties of ZnO rectangular thin films (10 mm x 5 mm) were analyzed for current-voltage characteristics at 280 K and 290 K. The results depicted in (Fig. 7) indicate a direct correlation between increasing voltage and current at both temperatures. The average resistance decreased from 0.40 MΩ at 280 K to 0.38 MΩ at 290 K, suggesting a negative temperature coefficient typical of semiconductors like zinc oxide. This behavior provides insights into the material's response to temperature variations.

CONCLUSIONS

This study demonstrates the successful synthesis of zinc oxide using an eco-friendly method involving zinc acetate dehydration and eggshell extract incorporation, yielding parameters typical of ZnO properties. The achievement highlights reduced chemical usage and underscores a commitment to environmental sustainability. Colloidal tests revealed weak stability in suspensions, vital for applications requiring stable colloids. Additionally, thin film electrical behavior exhibited a negative temperature coefficient, aligning with semiconductor classification and offering insights into material response to varying temperatures. These findings advance understanding of ZnO behavior, paving the way for sustainable synthesis and diverse electronic applications.

Disclosure Statement

The authors assert their research integrity, emphasizing a purpose-driven path devoid of conflicting interests.

ACKNOWLEDGEMENT

We sincerely thank UGC-DAE-CSR Indore, India, for their invaluable support in providing laboratory facilities and library access, Sandip University, India, for essential equipment contribution, and Licungo University, Mozambique, for their unwavering support.

REFERENCES

1. F. Fusco Nerini et al., "Connecting climate action with other Sustainable Development Goals," *Nature Sustainability* 2019 2:8, vol. 2, no. 8, pp. 674–680, Jul. 2019, doi: 10.1038/s41893-019-0334-y.
2. R. Camaratta, J. Orozco Messana, and C. Pérez Bergmann, "Synthesis of ZnO through biomimetization of eggshell membranes using different precursors and its characterization," *Ceram Int*, vol. 41, no. 10, pp. 14826–14833, Dec. 2015, doi: 10.1016/J.CERAMINT.2015.08.005.
3. H. Su, F. Song, Q. Dong, T. Li, X. Zhang, and D. Zhang, "Bio-inspired synthesis of ZnO polyhedral single crystals under eggshell membrane direction," *Appl Phys A*, vol. 104, pp. 269–274, 2011, doi: 10.1007/s00339-010-6122-1.
4. F. Lashkarizadeh, "Green synthesis of ZnO/eggshell nanocomposite using ferulago macrocarpa extract and its photocatalytic and antimicrobial activity in water disinfection," *Inorganic and Nano-Metal Chemistry*, pp. 1–12, doi: 10.1080/24701556.2021.1983837.
5. S. Prashanna Suvaiha, P. Sridhar, T. Divya, P. Palani, and K. Venkatachalam, "Bio-waste eggshell membrane assisted synthesis of NiO/ZnO nanocomposite and its characterization: Evaluation of antibacterial and antifungal activity," *Inorganica Chim Acta*, vol. 536, p. 120892, Jun. 2022, doi: 10.1016/J.ICA.2022.120892.
6. R. Camaratta, J. Orozco Messana, and C. Pérez Bergmann, "Synthesis of ZnO through biomimetization of eggshell membranes using different precursors and its characterization," *Ceram Int*, vol. 41, no. 10, pp. 14826–14833, Dec. 2015, doi: 10.1016/j.ceramint.2015.08.005.
7. N. Preda et al., "Functionalization of eggshell membranes with CuO–ZnO based p–n junctions for visible light induced antibacterial activity against *Escherichia coli*," *Sci Rep*, vol. 10, no. 1, Dec. 2020, doi: 10.1038/s41598-020-78005-x.
8. Q. Dong, H. Su, J. Xu, D. Zhang, and R. Wang, "Synthesis of biomorphic ZnO interwoven microfibers using eggshell membrane as the biotemplate," *Mater Lett*, vol. 61, no. 13, pp. 2714–2717, May 2007, doi: 10.1016/J.MATLET.2006.06.091.
9. H. Su, F. Song, Q. Dong, T. Li, X. Zhang, and D. Zhang, "Bio-inspired synthesis of ZnO polyhedral single crystals under eggshell membrane direction," *Applied Physics A*, vol. 104, no. 1, pp. 269–274, 2011, doi: 10.1007/s00339-010-6122-1.
10. P. S. Sundara Selvam, G. S. Chinnadurai, D. Ganesan, and V. Kandan, "Eggshell membrane-mediated V2O5/ZnO nanocomposite: synthesis, characterization, antibacterial activity, minimum inhibitory concentration, and its mechanism," *Appl Phys A Mater Sci Process*, vol. 126, no. 11, Nov. 2020, doi: 10.1007/s00339-020-04076-2.
11. C. Qian et al., "Facile preparation and highly efficient photodegradation performances of self-assembled Artemia eggshell-ZnO nanocomposites for wastewater treatment," *Colloids Surf A Physicochem Eng Asp*, vol. 610, p. 125752, Feb. 2021, doi: 10.1016/J.COLSURFA.2020.125752.
12. S. Prashanna Suvaiha, P. Sridhar, T. Divya, P. Palani, and K. Venkatachalam, "Bio-waste eggshell membrane assisted synthesis of NiO/ZnO nanocomposite and its characterization: Evaluation of antibacterial and antifungal activity," *Inorganica Chim Acta*, vol. 536, p. 120892, Jun. 2022, doi: 10.1016/J.ICA.2022.120892.
13. A. Gomaa et al., "State-of-the-Art of Eggshell Waste in Materials Science: Recent Advances in Catalysis, Pharmaceutical Applications, and Mechanochemistry," *Frontiers in Bioengineering and Biotechnology* | www.frontiersin.org, vol. 1, p. 612567, 2021, doi: 10.3389/fbioe.2020.612567.
14. B. J. A. José, M. D. Shinde, and C. A. C. Azuranahim, "Zinc oxide nanostructures: review of eco-friendly synthesis and technological applications," *Nanomaterials and Energy*, vol. 12, no. 3, pp. 117–130, Jul. 2023, doi: 10.1680/jnaen.23.00018.
15. B. J. A. José and M. D. Shinde, "Colloidal stability and dielectric behavior of eco-friendly synthesized zinc oxide nanostructures from Moringa seeds," *Sci Rep*, vol. 14, no. 1, p. 2310, 2024, doi: 10.1038/s41598-024-52093-5.
16. A. A. A. Mohammed, A. B. Suriani, and A. R. Jabur, "The Enhancement of UV Sensor Response by Zinc Oxide Nanorods / Reduced Graphene Oxide Bilayer Nanocomposites Film," in *Journal of Physics: Conference Series*, Institute of Physics Publishing, May 2018. doi: 10.1088/1742-6596/1003/1/012070.

Synthesis of Conjugated Polymeric Nano Materials and Evaluation of their Antimicrobial Potential Against Human Pathogens

Jyoti P. Mahashabde, Jayvant P. Sonawane

Department of Chemistry
R. C. Patel Arts, Commerce and Science College
Shirpur, Maharashtra

Arun M. Patil

Department of Physics
R. C. Patel Arts, Commerce and Science College
Shirpur, Maharashtra

Sandip P. Patil

Department of Microbiology and Biotechnology
R. C. Patel Arts, Commerce and Science College,
Maharashtra

✉ patilsandip3@gmail.com

ABSTRACT

One pot syntheses of copolymer of thiophene with para substituted benzaldehydes were carried out in laboratory under normal conditions. This technique uses POCl_3 in 1, 4 dioxane as a solvent for neutralization. This one pot method takes only 24 h to get the desired product. The doped copolymers were synthesized in presence of 0.1gm cobalt chloride whereas the final products were obtained using menthol. The physical characterizations of doped and undoped copolymers were carried out by using FTIR and $^1\text{HNMR}$. The polycrystalline phase was also confirmed by using structural analysis. The synthesized polymeric nanomaterial showed strong antimicrobial activities against human pathogens that cause multiple life-threatening diseases, including *A. niger*, *C. albicans*, *B. subtilis*, *S. aureus*, *E. coli*, and *P. vulgaris*. This property of synthesized materials can be used in the preparations of potent and effective antimicrobial substances.

KEYWORDS : *Conjugated polymers, Nanomaterial, Antimicrobial, Pathogens.*

INTRODUCTION

Conjugated polymers are widely utilized in several altered specific fields [1-3]. Their shared repetition is linked to the typical constant movement of π -bonding electrons in carbons, which are in regulator for their essential optical and electronic properties [4, 5]. Conjugated polymers, such PPy and PEDOT have verified enormous ability as materials for biological tissue interfaces with electrically conducting devices [6] excellent absorption of light [7-9] steady and brilliant light output [10]. Conjugated polymers such as PEDOT and PPy have shown wonderful potential as materials for interfacing electrically conducting devices with biological tissue [6] good light absorption [7-9] stable and bright light emission [10]. Conjugated polymers have many valuable properties that are also related to

their ease of handling. These contain the capacity to be shared with electromechanically energetic devices, produce flexible light-emitting displays, and solar cells [11], in addition to study biomedical applications of nanoparticles [15,16]. They have since been verified to be effective antimicrobial compounds due to their ability to absorb visible light, sensitize the production of reactive oxygen species (ROS), and selectively associate with and damage negatively charged cell envelopes [17]. Due to their remarkable fluorescence for bio sensing, cationic polythiophene was first used in biology [18, 19]. Conducting polymer fabrics exhibit antibacterial activity, signifying probable uses in many smart materials and the biological field. Enriching the H_2O_2 level can stimulate the generation of hydroxyl radicals, so producing an antimicrobial property [20]. Materials

based on conjugated polymers are most operative as bio imaging analyses [1], cancer controlling research [21–23], drug delivery systems [24, 25], and agents which are light-responsive in antimicrobial activity [26–28]. The research on decomposable conjugated polymers demonstrates the growing awareness in these capable organic materials [29, 30]. Their basic ability to create heat, which damages bacteria through a variety of targeted pathways, is related to their test as antibacterial agents initiated by light [1-3]. Antibiotic-resistant microorganisms have power and act as severe threat to human health because of the overuse of antibiotics and the slow development of new medicines. We created a new conjugated polymer with a backbone made of benzaldehyde and thiophene with the intention of creating new antibacterial agents. Its cationic backbone allows it to interact significantly with bacterial membranes, giving it a stronger antibacterial effect than a conjugated polymer with a neutral backbone.

Recent years have seen a lot of interest in the cationic conjugated polymers antibacterial capabilities. These polymers work by disrupting the bacterial cell membrane and by photosensitizing, which boosts the generation of reactive oxygen species by the backbone when exposed to light. Stronger interactions between the negatively charged bacterial membrane and the cationic backbone would result in increased antimicrobial activity under both light and dark irradiation conditions [36].

Conjugated polymers must have positive charges in order to interact with the negatively charged bacterial membrane. By oxidative polymerizing thiophene and substituted benzaldehydes, a number of thiophene-based conjugated microporous polymeric cationic nanoparticles have been created. Using ^1H NMR, and Fourier-transform infrared spectroscopy, their structures were verified.

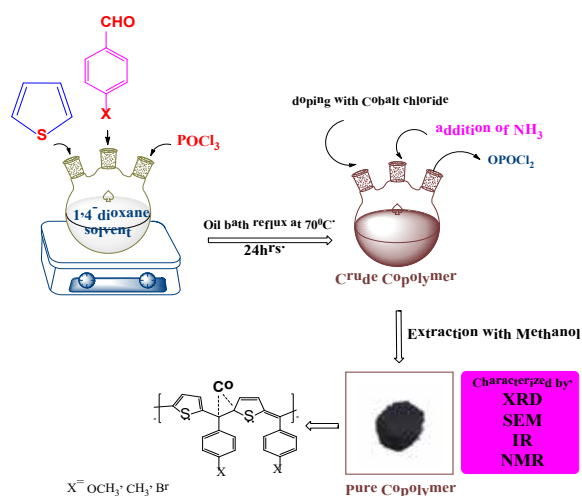
MATERIALS & METHODS

In present study, one pot synthesis of copolymerization of thiophene with p-substituted benzaldehydes was carried out in laboratory under normal conditions as previously reported article [31]. The same method of polycondensation is used for the synthesis of three undoped and three doped different conjugated copolymers of thiophene with p-methoxy benzaldehyde, p-methyl benzaldehyde and p-bromo benzaldehyde respectively.

A substituted para substituted benzaldehydes as well as dopant cobalt chloride are used to study which is different from previously published work.

Thiophene and para substituted benzaldehydes were obtained from Sigma Aldrich. POCl_3 , a dehydrating agent, was employed as a catalyst, and the reaction was conducted in 1, 4 dioxane. To extract the product, ammonia and methanol are added to the reaction mixture. Reaction is a straightforward condensation-based single-step polymerization process. Using catalyst phosphorous oxychloride, a moderate dehydrating agent, 0.02 mmoles of thiophene and 0.02 mmoles of p-substituted benzaldehydes were condensed separately in 1, 4 dioxane solvent in a 100 ml round-bottom flask. Reaction mixes were then refluxed in an oil bath that had been heated to 70°C for 24 hours. Using TLC, the responses were tracked. Following the completion of the reaction, methanol was added to produce a fine, dark black-brown powder. This was then repeatedly cleaned with methanol and allowed to dry in a vacuum for a full day.

Similar procedures were used to synthesize doped polymers, but 0.1 gm was added after the reaction was finished. Each reaction flask had cobalt chloride added as a dopant, which was then refluxed for an additional two hours. The crude products were dried, and then column chromatography was used to purify them. The methine bridge polymer's production is seen in Scheme 1.



Scheme-1: Synthesis of conjugated polymeric nanomaterials

CHARACTERIZATION OF SYNTHESIZED CONJUGATED POLYMERIC NANOMATERIALS

Fourier Transform Infrared Spectra (FTIR)

The materials' infrared (IR) spectra were obtained in the 4000-400 cm^{-1} range using the FTIR and IR Affinity 1 SHIMADZU instrument and DRX sampling technique.

Nuclear Magnetic Resonance (NMR) Spectroscopy

Using CDCl_3 as a solvent and a TMS as an internal reference, nuclear magnetic resonance (^1H NMR) spectra were acquired at 25°C on a Bruker ADVANCE II 400 NMR spectrometer.

X-Ray Diffraction Analysis (XRD)

Structural analysis is one of the most common techniques in the characterization of material. In the field of material characterization, X-ray diffraction is a crucial technique for obtaining information on an atomic scale from both crystalline and nanocrystalline (amorphous) materials. Using a Bruker D8 Advance diffractometer with a $\text{CuK}\alpha$ incident beam with $\lambda = 1.5406 \text{ \AA}$ in a 2θ range of 20 to 80 degrees, X-ray diffraction (XRD) measurements were performed.

Antimicrobial Study by Using Disc Diffusion Assay (Kirby-Bauer Method)

The antibacterial and antifungal properties of the conjugated polymeric nanoparticles produced above were assessed against a range of harmful bacterial and fungal species. The Department of Microbiology at R. C. Patel Arts, Commerce and Science College in Shirpur, India provided the pure cultures of bacterial pathogens, both Gram positive (*Staphylococcus aureus*, *Bacillus subtilis*) and Gram negative (*Escherichia coli*, *Proteus vulgaris*), as well as fungal strains of *Aspergillus niger* and *Candida albicans*. At 4 °C, fungal and bacterial cultures were kept on Czapek dox agar slants and Nutrient agar slants, respectively. The antibacterial activity of test compounds was assessed using the disc diffusion method [34]. The negative control was the solvent DMSO. After being transferred into Czapek dox broth and Nutrient broth, the microbial strains were revived from stock cultures and cultured for 24 hours at 37 °C. The sterile Nutrient agar and Czapek dox agar plates were made following

standard microbiological procedures. Using the spread plate approach, the bacterial and fungal strains were distributed independently on sterile nutritional media plates [35]. Commercially available paper discs (6 mm in diameter) with various test compound concentrations were added to the agar surface containing distinct pathogens in addition to DMSO as a negative control. The antibacterial plates were incubated for 24 hours at 37 °C, whereas the antifungal plates were incubated for 48 hours at the same temperature. The plates were incubated, and afterward, the creation of an inhibition zone surrounding the wells was monitored. Each experiment was carried out three times.

RESULTS AND DISCUSSION

In total six polymeric nanomaterials were synthesized by using the scheme-1 described previously. The synthesized nanomaterials (A1, A2, B1, B2, C1 and C2) are designated as follow in Table 1.

Table 1. Synthesized Polymeric Nanomaterials

Nanomaterial	Doped / Undoped	Name of Nanomaterial
A1	Undoped	Poly (Thiophene-2,5-diyl)-co-p-methoxy benzylidene
A2	Doped	Poly (Thiophene-2,5-diyl)-co-p-methoxy benzylidene
B1	Undoped	Poly (Thiophene-2,5-diyl)-co-p-methyl benzylidene
B2	Doped	Poly (Thiophene-2,5-diyl)-co-p-methyl benzylidene
C1	Undoped	Poly (Thiophene-2,5-diyl)-co-p-bromo benzylidene
C2	Doped	Poly (Thiophene-2,5-diyl)-co-p-bromo benzylidene

TABLE 2. Analysis of Functional Groups of Nanomaterials by Using FT-IR

Fun. Gp.	p-OMe undoped	p-OMe doped	p-Me undoped	p-Me doped	Standard frequency cm^{-1}
C=C	1606	AB	1513	AB	1500-1600
C-S-C	1106	1070	1181	1180	100-1200
Aromatic C-H	2957	2922	2850	2920	2900-3000
C=O	AB	AB	AB	AB	1720

Functional gp.	C-O	C-O	C-C	C-C	-
I.R. frequency	1174	1228	2920	2900	-
C-Co	-	503	-	549	500-700

Fun. Gp.	p-Br undoped	p-Br doped	Standard frequency cm ⁻¹
C=C	1597	AB	1500-1600
C-S-C	1074	1070	1000-1200
Aromatic C-H	3024	2924	2900-3000
C=O	AB	AB	1720
Functional gp.	C-Br	C-Br	-
I.R. frequency	802	800	-
C-Co	-	551	500-700

The KBr technique is used to measure the FT-IR spectra of polythiophene benzylidene derivatives. With a resolution of 4 cm⁻¹, the spectra are captured in the 400-4000 cm⁻¹ area. Disappearance of aldehyde carbonyl stretching frequency peak in the polymer spectrum indicates that the monomers are polymerized and polythiophene benzylidene derivatives are produced. Peaks at 503, 549, and 551 cm⁻¹ are thought to be caused by the polymer's C-Co stretching modes. The C-S-C vibration modes are thought to be responsible for the peaks at 1070, 1180, and 2924 cm⁻¹.

A. Nuclear Magnetic Resonance (NMR) Spectroscopy

¹H NMR Spectroscopy: Nuclear Magnetic Resonance at 400 MHz. on Bruker Advance in CDCl₃ Solvent.

¹H NMR Para Methoxy Undoped Polymer Composite

7.33δ(d)2H, 7.33δ(d)1H, 7.29δ, dd(m)2H, 6.97δ, dd(m)4H, 6.44δ, dd(m)1H, 6.22(d)2H, 3.83δ, (s,q)2H.

¹H NMR Para methoxy doped polymer composite

7.21δ(d)1H, 7.00δ, dd(m)2H, 7.00δ, dd(m)1H, 6.89δ, dd(m)2H, 6.83δ, (d)1H, 4.55δ, dd(m)1H, 4.42δ, (s,q)1H, 3.75δ, (s)3H.

¹H NMR Para methyl undoped polymer composite

7.28δ, (d)1H, 7.22δ, (d)1H, 7.18δ, dd(m)2H, 7.14δ, dd(m)1H, 7.12δ, dd(m)2H, 6.70δ, (d)1H, 6.10δ, dd(m)1H, 3.90δ(s,q)1H.

¹H NMR Para methyl doped polymer composite

7.25δ, (d)1H, 7.14δ, dd(m)2H, 7.10δ, dd(m)2H, 7.14δ,

(d)1H, 7.10δ, dd(m)2H, 6.70δ(d)1H, 6.40δ, dd(m)1H, 3.70δ(s,q)1H.

¹H NMR Para bromo undoped polymer composite

7.76δ, dd(m)2H, 7.72δ,(d)1H, 7.63δ, dd(m)2H, 7.43δ, (d)1H, 7.19δ, dd(m)1H, 6.37δ, (d)1H, 5.80δ, dd(m)1H, 3.31δ, (s,q)1H.

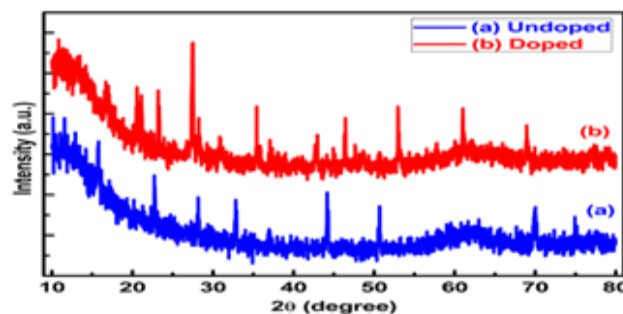
¹H NMR Para bromo doped polymer composite

7.72δ, (d)1H, 7.50δ, dd(m)2H, 7.36δ, (d)1H, 7.29δ, dd(m)2H, 7.17δ, dd(m)1H, 6.39δ, (d)1H, 5.80δ, dd(m)1H, 3.36δ, (s,q)1H.

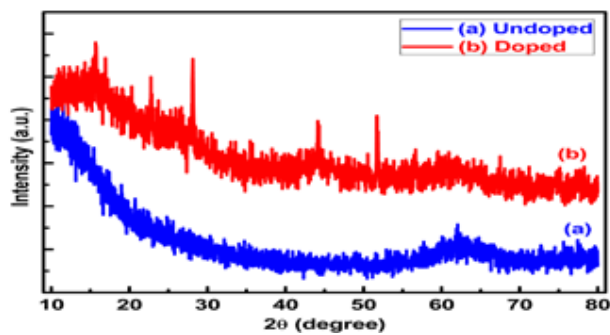
NMR data confirmed formation of copolymer of thiophene and para substituted benzaldehydes. Due to electron withdrawing sulphur containing heterocycles shifts the adjacent proton value towards high δ value. Due to steric interactions between thiophene protons also shifts at high δ value.

The ¹H NMR data obtained from spectra confirmed that single step polymerization of polymer composites by oxidative polymerization. The peaks were assigned by comparison with the spectra of monomer and polymer composite.

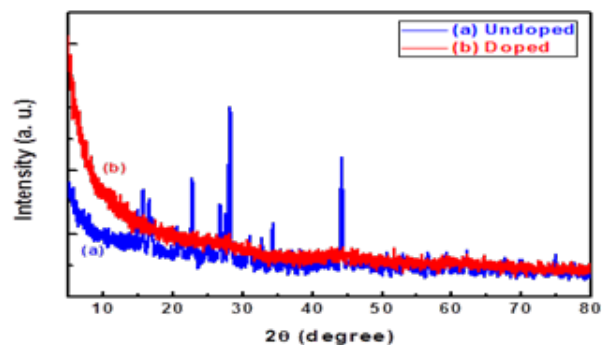
Polymer benzylidene derivatives' ¹H NMR spectra were acquired in order to examine and validate the suggested structure in more detail. Phenyl protons are represented by the protons that emerge at 3.72 ppm (3H, s), 6.85 ppm (2H, d, J = 7.15 Hz), and 7.11 ppm (2H, d, J = 7.35 Hz). The location of the thiophene protons is 7.49 ppm (2H, d, J = 4.11 Hz). The terminal protons at the conclusion of the polymer chain are responsible for the tiny peak at 1.82 ppm (2H, s). The attachment of two monomers was alternating, as shown by the quasi-equality of the aromatic protons integration curves of benzene and thiophene protons.



(a) p-methoxy benzylidene



(b) p-methyl benzylidene



(c) p-methoxy benzylidene

Fig. 1: XRD spectra of synthesized nanomaterials [Scherrr’s equation $D = (0.9\lambda)/\beta\cos\theta$]

Table 3. Crystallinity and Crystallite Size Values from XRD

Polymer composite	Crystallinity Undoped (%)	Crystallinity CoDoped (%)	Crystallite size Undoped (nm)	Crystallite size Codoped (nm)
Poly [(Thiophene-2,5-diyl)-co-p-methoxy benzylidene	37.2	52.3	44	55
Poly [(Thiophene-2,5-diyl)-co-p-methyl benzylidene	55.3	54.3	58	56
Poly [(Thiophene-2,5-diyl)-co-p-bromo benzylidene	72.3	48.1	127	45

The X-ray diffraction (XRD) patterns were used to examine the structural characteristics of both doped and undoped polymers. The produced material exhibited a strong XRD peak, suggesting that the undoped polymer is crystalline. The crystallinity values in the polymer

composites are roughly 37.2 to 72.3% for undoped polymer and 52.3 to 48.1 for doped polymer, indicating a decrease in crystallinity caused by cobalt doping. The cobalt peak in the doped polymer composite is found at 44.22°, as verified by JCPDS card number 89-4307. Using the well-known Scherrer's equation, the crystallite sizes were determined to be around 44 nm, 58 nm, and 127 nm for the undoped sample and 55 nm, 56 nm, and 45 nm for the doped sample. $D = (0.9\lambda)/\beta\cos\theta$ along peak at 44.3° is Scherrer's equation [32]. It is observed that for bromo substituted benzaldehyde cobalt doping decrease the crystallinity effectively and showed remarkable decrease in crystallite size from 127nm to 45 nm. More antibacterial activity was demonstrated by the powder samples with smaller crystallite sizes than by those with larger crystallite sizes [33].

Evaluation of antimicrobial activity

The disc diffusion method was utilized to investigate the in vitro antimicrobial activities of conjugated polymeric nanomaterials against fungal strains of *Aspergillus niger* and *Candida albicans*, as well as Gram positive (*Staphylococcus aureus*, *Bacillus subtilis*) and Gram negative (*Escherichia coli*, *Proteus vulgaris*) bacterial pathogens. The zone of inhibition surrounding the disc served as a proxy for the antibacterial properties of these drugs. The zone of inhibition developed as a result of the test substance under examination interfering with the growth and reproduction of microbial cells, which inhibits the growth of bacteria surrounding the disc. Table 4 shows the zones of inhibition for the test drugs.

Table 4. Zones of inhibition for the test compounds

Comp	<i>E. coli</i>	<i>P. vulgaris</i>	<i>S. aureus</i>	<i>B. subtilis</i>	<i>A. niger</i>	<i>C. albicans</i>
A1	7.25	-	6.43	-	9.52	-
A2	6.49	-	-	-	-	-
B1	7.38	-	7.52	-	-	-
B2	7.61	-	-	-	-	-
C1	-	8.47	7.50	8.84	-	9.92
C2	-	9.64	-	8.56	9.95	9.75
*CHL	30.79	29.36	38.11	19.87	NA	NA
*AMP	NA	NA	NA	NA	34.38	37.21

*CHL-Chloramphenicol, *AMP-Amphotericin-B

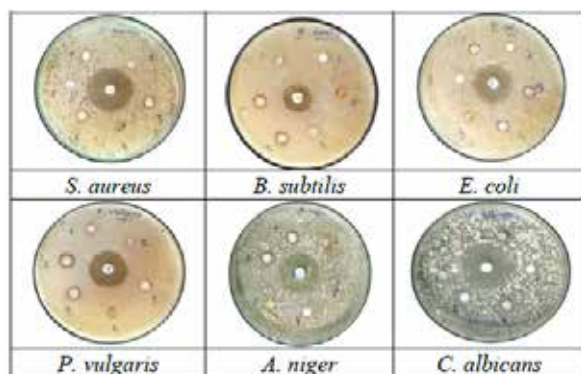


Fig.2: Antimicrobial activity of synthesized nanomaterials against human pathogens (A) *S. aureus* (B) *B. subtilis* (C) *E. coli* (D) *P. vulgaris* (E) *A. niger* and (F) *C. albicans*

These results revealed a strong antimicrobial potential of compounds under investigation against the selected strains of human bacterial and fungal pathogens. The growth of microorganisms around the disc was inhibited effectively by the test compounds by certain mechanisms.

CONCLUSIONS

In conclusion, six conjugated polymeric nanomaterials (three undoped and three doped) of thiophene with p-methoxy benzaldehyde; p-methyl benzaldehyde and p-bromo benzaldehyde were successfully synthesized by polycondensation method. These nanomaterials were characterized by using advanced analytical methods viz. FTIR, NMR and XRD. The absence of C=O frequency in both the undoped and doped samples indicated that the condensation reaction had finished and that the initial aldehyde carbonyl group had not been present. It has been noted that only doped samples contain the C-Co group in the 500–550 cm⁻¹ range.

When tested against specific human infections, all six of the nanomaterials shown possible antibacterial activity. The most powerful broad spectrum activity against bacterial and fungal infections was demonstrated by the nanomaterials C1 (Poly (Thiophene-2, 5-diyl)-co-p-bromo benzylidene) and C2 (Poly (Thiophene-2, 5-diyl)-co-p-bromo benzylidene). On the other hand, considerable activity against bacterial pathogens was also demonstrated by undoped A1 (Poly (Thiophene-2,5-diyl)-co-p-methoxy benzylidene) and B1 (Poly (Thiophene-2,5-diyl)-co-p-methyl benzylidene). The

least successful at preventing the growth of bacterial and fungal human diseases were the doped nanomaterials A2 (Poly (Thiophene-2, 5-diyl)-co-p-methoxy benzylidene) and B2 (Poly (Thiophene-2, 5-diyl)-co-p-methyl benzylidene). In this study, the nanomaterials C1 and C2 showed promise as therapeutic candidates against a range of serious illnesses brought on by human pathogens. Conjugated polymeric nanoparticles have practical clinical uses that require further study for the benefit of humankind.

ACKNOWLEDGMENT

Authors would like to thank R. C. Patel Arts, Commerce and Science College, Shirpur, KBCNMU, Jalgaon, and SAIF Chandigarh for providing FTIR, XRD and NMR facilities. SPP also acknowledges the financial assistance provided by RGSTC, KBCNMU Center, Jalgaon.

REFERENCES

1. T. Abelha, C. Dreiss, M. Green, and L. A. Dailey, Conjugated polymers as nanoparticle probes for fluorescence and photoacoustic imaging, *J. Mater. Chem. B*, 8, 592, 2020.
2. J. Burroughes, D. Bradley, A. Brown, R. Marks, K. Mackay, R. Friend, P. Burns, and A. Holmes, Light-emitting diodes based on conjugated polymers, *Nature*, 347, 539, 1990.
3. L. Zhou, F. Lv, L. Liu, and S. Wang, Water-Soluble Conjugated Organic Molecules as Optical and Electrochemical Materials for Interdisciplinary Biological Applications, *Acc. Chem. Res.*, 52, 3211, 2019.
4. A. Heeger, Semiconducting polymers: the Third Generation, *Chem. Soc. Rev.*, 39, 2354, 2010.
5. Z. Qiu, B. Hammer, and K. Müllen, Conjugated polymers – Problems and promises, *Prog. Polym. Sci.*, 100, 101179, 2020.
6. L. Povlich, K. Feldman, B. Wei, T. Eom, and B. Shim, Electroactive Polymeric Biomaterials, D.C. Martin, Volume 1, 547-561, 2011.
7. J. Hou, H. Chen, S. Zhang, G. Li, and Y. Yang, Synthesis, Characterization, and Photovoltaic Properties of a Low Band Gap Polymer Based on Silole-Containing Polythiophenes and 2,1,3-Benzothiadiazole, *Am. Chem. Soc.*, 130, 16144, 2008.

8. G. Schulz, F. Fischer, D. Trefz, A. Melnyk, A. Hamidi-Sakr, M. Brinkmann, D. Andrienko, and S. Ludwigs, The PCPDTBT Family: Correlations between Chemical Structure, Polymorphism, and Device Performance, *Macromolecules*, 50, 1402, 2017.
9. S. Chang, T. Muto, T. Kondo, M. Liao, and M. Horie, Double acceptor donor-acceptor alternating conjugated polymers containing cyclopentadithiophene, benzothiadiazole and thienopyrroledione: toward subtractive color organic photovoltaics, *Polym. J.*, 49, 113, 2017.
10. C. Wu, B. Bull, C. Szymanski, K. Christensen, J. McNeill, and Multicolor conjugated polymer dots for biological fluorescence imaging, *ACS Nano*, 2, 2415, 2008.
11. D. Melling, J. Martinez, and E. Jager, Conjugated Polymer Actuators and Devices: Progress and Opportunities, *Adv. Mater.*, 31, 1808210, 2019.
12. K. Coakley, and M. McGehee, Conjugated Polymer Photovoltaic Cells, *Chem. Mater.*, 16, 4533, 2004.
13. K. Yu, B. Park, G. Kim, C. Kim, S. Park, J. Kim, S. Jung, S. Jeong, S. Kwon, H. Kang, J. Kim, M. Yoon, and K. Lee, Direct Observation of Confinement Effects of Semiconducting Polymers in Polymer Blend Electronic Systems, *Proc. Natl. Acad. Sci. USA*, 8(14), 2100332, 2021.
14. C. Ou, N. Cheetham, J. Weng, M. Yu, J. Lin, X. Wang, C. Sun, J. Gonzalez, L. Xie, L. Bai, Y. Han, D. Bradley, and W. Huang., Hierarchical Uniform Supramolecular Conjugated Spherulites with Suppression of Defect Emission, 16: 399–409, 2019.
15. Z. Wang, C. Wang, Y. Fang, H. Yuan, Y. Quan, and Y. Cheng, Color-tunable AIE-active conjugated polymer nanoparticles as drug carriers for self-indicating cancer therapy via intramolecular FRET mechanism, *Polym. Chem.*, 9, 3205, 2018.
16. R. Dmitriev, S. Borisov, H. Dössmann, S. Sun, B. Müller, J. Prehn, V. Baklaushev, I. Klimant, and D. Papkovsky, Versatile Conjugated Polymer Nanoparticles for High-Resolution O2 Imaging in Cells and 3D Tissue Models, *ACS Nano*, 9, 5275, 2015.
17. D. Brown, J. Yang, E. Strach, M. Khalil, and G. David., Size and Substitution Effect on Antimicrobial Activity of Polythiophene Polyelectrolyte Derivatives Under Photolysis and Dark Conditions, *Photochem Photobiology*, Nov; 94(6):1116-1123, 2018.
18. P. S. Heeger, and A. J. Heeger, Making sense of polymer-based biosensors, *Proc. Natl. Acad. Sci. USA*, 96, 12219, 1999.
19. L. Chen, D. McBranch, H. Wang, R. Helgeson, F. Wudl, and D. Whitten, Highly sensitive biological and chemical sensors based on reversible fluorescence quenching in a conjugated polymer *Proc. Natl. Acad. Sci. USA*, 96, 12287, 1999.
20. K Namsheer and C. Rout, Conducting polymers: a comprehensive review on recent advances in synthesis, properties and applications, *RSC Adv.* 10, 5659-5697, 2021.
21. Y Wu, Y Zhen, Y Ma, R Zheng, Z Wang, and H Fu. Exceptional Intersystem Crossing in Di (perylene bisimide)s: A Structural Platform toward Photosensitizers for Singlet Oxygen Generation *J. Phys. Chem. Lett.* 2010; 1:2499–2502.
22. D. Zhang, M. Wu, Y. Zeng, N. Liao, Z. Cai, G. Liu, X. Liu, and J. Liu, Lipid micelles packaged with semiconducting polymer dots as simultaneous MRI/photo acoustic imaging and photodynamic/photo thermal dual-modal therapeutic agents for liver cancer, *J. Mater. Chem. B*, 4, 589, 2016.
23. G. Jin, R. He, Q. Liu, Y. Dong, M. Lin, W. Li, and F. Xu, Graphene-based heterojunction photocatalysts, *ACS Appl. Mater. Interfaces*, 10, 10634, 2018.
24. C Schmidt, and R Bodmeier., Incorporation of polymeric nanoparticles into solid dosage forms, *J. Control Release*. 57:115–25, 1999.
25. T. Senthilkumar, L. Zhou, Q. Gu, L. Liu, F. Lv, and S. Wang, Conjugated Polymer Nanoparticles with Appended Photo-Responsive Units for Controlled Drug Delivery, Release, and Imaging, *Angew. Chem., Int. Ed.*, 57, 13114, 2018.
26. A. Morena, and T. Tzanov, Antibacterial lignin-based nanoparticles and their use in composite materials, *Nanoscale Advances*, 22, 2022.
27. K. Das, V. Singh, and R. Gardas. Cationic Amphiphilic Molecules as Bactericidal Agents, 277-302, 2022.
28. P. Parvathy, A. Ayobami, A. Raichur, and S. Sahoo, Methacrylated alkali lignin grafted P(Nipam-Co-AAc) copolymeric hydrogels: Tuning the mechanical and stimuli-responsive properties, *International Journal of Biological Macromolecules*, 192, 180-196, 2021.
29. T. Repenko, A. Rix, S. Ludwanowski, D. Go, F. Kiessling, W. Lederle, and A. Kuehne, Bio-degradable

- highly fluorescent conjugated polymer nanoparticles for bio-medical imaging applications, *Nat. Commun.*, 8, 8, 2017.
30. M. Twomey, E. Mendez, R. K. Manian, S. Lee, and J. Moon, Mitochondria-specific conjugated polymer nanoparticles, *Chem. Commun.*, 52, 4910, 2016.
 31. J. Mahashabde, S. Patel, and P. Baviskar, Physical properties of poly [(thiophene-2, 5-diyl)-co-para-chloro benzylidene] doped with cobalt sulphate: synthesis and characterization, *Polymer bulletin*, 75(2), 255-265, 2018.
 32. B Sankapal, P Baviskar, and D Salunkhe, Room temperature chemical synthesis of highly oriented PbSe nanotubes based on negative free energy of formation, *J. Alloy Compd.* 506:268–270, 2010.
 33. T. Ohira, and O. Yamamoto, Correlation between antibacterial activity and crystallite size on ceramics, *Chemical Engineering Science*, vol. 68(1), 355-361, 2012.
 34. F. Gonelimali, J. Lin, W. Miao, J. Xuan, F. Charles, M. Chen, and S. Hatab, Antimicrobial Properties and Mechanism of Action of Some Plant Extracts Against Food Pathogens and Spoilage Microorganisms, *Frontiers in microbiology*, 9, 1639, 2018.
 35. D. Hartman, Perfecting Your Spread Plate Technique, *Journal of Microbiology and Biology Education: JMBE*, 12(2), 204, 2011.
 36. X. Qingling, H. Ping, J. Wang, H. Chen, F. Lv, L. Liu, S. Wang, and J. Yoon., Antimicrobial activity of a conjugated polymer with cationic backbone, *Dyes and Pigments*, Volume 160, January 2019, Pages 519-523.

Assessing the Impact of Socio-Economic Factors on Indian Agriculture: A Mathematical Modelling Approach

Avinash V. Khambayat

Professor

Department of Mathematics School of Science

Sandip University

Nasik, Maharashtra

✉ avinash.khambayat@sandipuniversity.edu.in

Neetu M. Sharma

Research Scholar

Department of Mathematics School of Science

Sandip University

Nasik, Maharashtra

✉ neetu.sharma@sandipuniversity.edu.in

ABSTRACT

Mathematical modelling has been extensively used in agricultural yield prediction for ages. Indian Economy rests on the shoulders of agricultural activities directly or indirectly. In this present study, we discussed the impact of socio-economic factors such as urbanization, population rise and total crop area on gross food production in India. The study is performed based on the relevant data of 30 years from 1980-81 to 2009-10 in the Indian state of Telangana, which was part of Andhra Pradesh till 2014. Multiple Linear Regression (MLR) has been used to find the relationship among these variables and Autoregressive Integrated Moving Average (ARIMA) models for developing predictive models to predict the variables up to 2020. Further, the predicted food grain production value from MLR and ARIMA's expected value were compared from 2010-11 to 2020-21. It has been observed that there is a positive trend, and the overall Indian economy may face a slight effect in the next decade which will also affect the gross food production.

KEYWORDS : *Socio-Economic Factors; Urbanization; Multiple Linear Regression; ARIMA; Mathematical Prediction model.*

INTRODUCTION

The Indian Economy rests on the shoulders of Agriculture and its allied activities. Agriculture facilitates the livelihoods of approximately 60 % to 70% of its population and employs more than 50% of the people, contributing around 18.3% to the overall GDP(Fig.1) as of 2022 [1]. The percentage share of GVA by different Economic sectors for 2022-23 is shown in Table 1. India, the second most populated country, has an alarming challenge to feed its population of over 1383 million. Irregular rainfall, changing climatic and non-climatic conditions, and low farm yield prices are causing a shift in the urban population [2]. Over the past two decades, Urbanization has witnessed a significant rise with intense implications for agricultural changes and land use.

In their study, [3] highlighted the positive impact of urbanization on agricultural eco-efficiency. They

suggested that the migration of rural surplus labour to urban areas was a promising solution to excessive agricultural labour input. [4] highlighted that the continuous loss of agricultural land due to urbanization, is directly through land purchase and indirectly through the conversion of agricultural land for non-agricultural purposes. Both studies in [3], [5] found that urbanization positively impacts crop production, considering changes in cropland area and crop yield. Many researchers studied how Mathematical modelling is widely used in agriculture to forecast crop yield, promoting sustainability goals[6][7][8][9].

Amidst the turmoil of COVID-19, Telangana's nominal GSDP was 21.8% higher in 2021-22 as compared to the pre-pandemic levels in 2019-20 while India's nominal GDP had only increased by 17.8% in these two years (Fig.1).

The present study is based on assessing the impact of

urbanization, population rise, and the total crop area on gross food grain production in India. In Table 2, the data for the state of Telangana was collected for the analysis during the period of 30 years from 1980-81 to 2009-10. that was obtained from www.data.icrisat.org and RBI, GOI annual reports. For Data Analysis, Multiple Linear Regression and Autoregressive Integrated Moving Average (ARIMA) were applied. The tests were performed over the state of Telangana, which indicated that urbanization and population growth affect agricultural food production adversely. This research is mainly conducted to determine if these results can help generalize for overall Indian economy [10].

Growth Rate of Gross Domestic Product at Current Prices for Telangana and India (2014-15 to 2021-22)

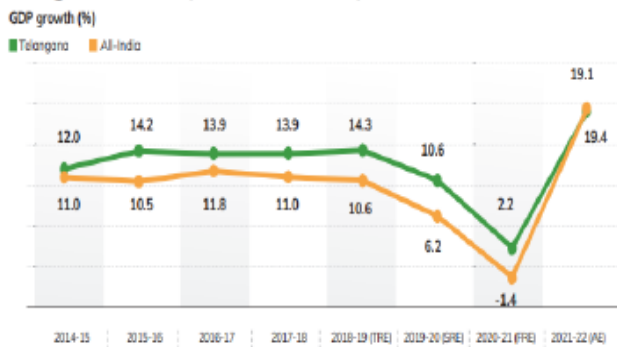


Fig.1 GDP Growth Rate (2014-15 to 2021-22)

Table 1. Share of Gross Value Added(GVA)

Sector	% Share
Agriculture, Forestry, Fishery	18.39
Real Estate	16
Manufacturing	15.8
Others	49.2

Authors compilation Source: National Accounts Statistics 2023

PROPOSED METHODOLOGY

Telangana, declared as the 29th Indian state in the year 2014 has an area of 1,12,077 sq. km and has a population of 3,50,03,674(2011 Census) with a Decadal Growth rate of 13.58 %. Around 33 districts inhabit 61.12 %(approx.) of the population in rural areas. The State has a 66.54% Literacy rate, and 163.42 Lakh people are engaged as workers for their livelihood(www.telangana.gov.in). The state is a leading IT exporter spread over

its capital city Hyderabad. Agriculture is one of its important sectors covering 53.51 Lakh hectares of arable land growing Rice, Maize, Groundnut, Cotton, Sugarcane, etc. As per the Govt reports, the state has seen a Positive trend in total production (Fig.3).

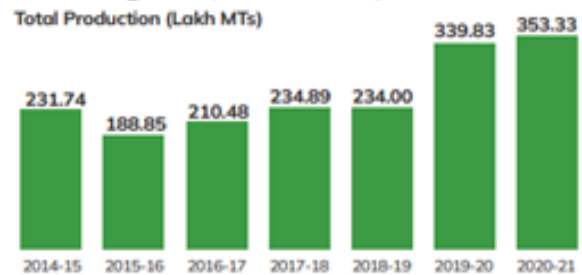
Sectoral Contribution to Telangana GSVA from 2014-15 to 2021-22 (AE) (at Current Prices)



Source: Directorate of Economics and Statistics, GoTS

Fig.2 Percentage Share of Gross State Value Added by Different Economic Sector for 2021-22(AE) Source: National Accounts Statistics 2023, First Advance Estimates (FAE) of National Income, 2023-24

Trends in Total Agriculture Production in Telangana (in Lakh MT)



Source: Directorate of Economics and Statistics, GoTS

8 As per 4th advance estimates 2019-20.

Fig.3 Gross Agricultural Production

As per the Govt. records of 2021-22 estimates, the Gross Sown Area between 2019-20 and 2020-21 has increased (Fig.4). As per estimates, 46.8% of the state's population resides in urban areas, which is more than the country as whole, with only 34.7% of the total population living in urban areas.

According to the population projections published by the Ministry of Health and Family Welfare, Telangana is urbanizing at a faster rate than the rest of India

combined. It is expected that the share of urban residents in the state's population will reach 57.3% by the year 2036(Fig. 5).

For this study, the crop-related data have been collected online from www.data.icrisat.org, and MOSPI, GOI reports. The duration of 1980-81 to 2009-10 was taken as a Training set on Gross Food Grain Crop production (GFGCP), Total Cultivated Land Area (TCLA), Area Urbanized (AU), and Population (PP). A Multiple Linear Regression (MLR) model based on 30 years of crop data has been fitted taking GFGCP as the dependent variable and TCLA, AU, and PP as independent variables. The statistical significance of the model is determined based on the Coefficient of Determination (R2). The significance of the predicted independent variables is verified on the respective p-value at 0.05 level.

ARIMA models are fitted after fitting the MLR equation, to predict the independent variables in the study. The values of GFGCP, TCLA, AU and PP are predicted based on the respective ARIMA models for the next 11 years (2010-11 to 2020-21).

Further, MLR equations are used to predict the values of independent variables for 2010-11 to 2020-21 as a Testing Set. The difference values of these two sets of GFGCP values are calculated and then fitted with a suitable trend equation. The predicted GFGCP values based on MLR show the relationship of TCLA, AU, and PP which signifies the possible GFGCP. The predicted value is based on the ARIMA method up to 2020-21 which signifies the expected GFGCP value considering the available trend of GFGCP.

The differences between the two sets of GFGCPs signify the availability gap of Gross Food Grain Crop production due to the present trend of AU, TCLA, and PP.

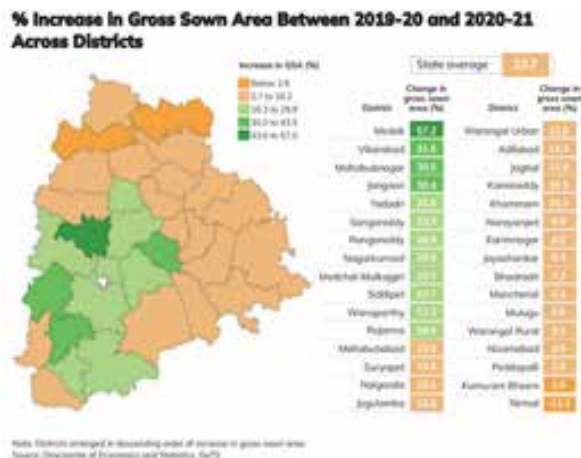


Fig.4 Increase in Area Sown (Source; DoES, GOI, 2021-22)

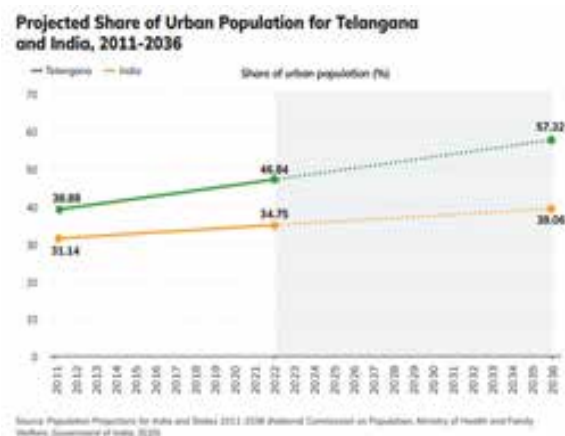


Fig.5 Projected Urban Population till 2036

MATHEMATICAL MODEL

Multiple Linear Regression analysis (MLR) is used to formulate a relationship between the GHGCP and TCLA, AU, and PP variables [11]. A method of Ordinary Least Square (OLS) has been used to obtain the coefficients of independent variables. The coefficient of Determination (R2) is calculated to evaluate the significance of the MLR equation. The coefficient of determination is p-value which is used to assess the significance of the estimates of independent variables.

The general form of the MLR equation is as follows:

$$Y=B_0+B_1 X_1+B_2 X_2+...+B_k X_k \tag{1}$$

where,

Y = Dependent variable

X_i = Independent variable (i =,1,...,k)

B₀ = Constant term

B_i = Regression coefficient of X_i

Table 2 Data of GFGCP, TCLA, AU, PP, and up from 1980-81 To 2009-10

Year	GFGCP (Y)	TCLA Foodgrains (X1)	AU (X2)	PP (X3)	Urban Population (X4)
1980-81	9,991.7	1266.7	1,726.3	696828385	160953420
1981-82	11,413.1	1291.4	1,767.5	712869298	166932604
1982-83	11,172.3	1250.9	1,727.5	729169466	172426704
1983-84	11,881.3	1311.6	1,795.6	745826546	178095921
1984-85	9,615.1	1266.7	1,763.3	762895156	183956909
1985-86	10,373.8	1280.3	1,784.6	780242084	189973343
1986-87	9,678.6	1272	1,764.1	797878993	196158550
1987-88	10,482.0	1196.9	1,707.4	815716125	202485214
1988-89	13,487.6	1276.7	1,822.8	833729681	208957670
1989-90	13,330.6	1267.7	1,822.7	852012673	215601807
1990-91	12,882.9	1278.4	1,857.4	870452165	222374415
1991-92	12,319.3	1218.7	1,822.4	888941756	229151406
1992-93	12,282.8	1231.5	1,857.0	907574049	235824041
1993-94	12,752.2	1227.6	1,865.8	926351297	242620668
1994-95	12,212.6	1237.1	1,880.5	945261958	249539704
1995-96	12,253.7	1210.1	1,874.7	964279129	256565748
1996-97	13,675.2	1235.8	1,895.0	983281218	263686524
1997-98	10,913.5	1238.5	1,899.9	1002335230	270911166
1998-99	14,905.0	1251.6	1,916.5	1021434576	278238779
1999-00	13,696.2	1231.1	1,884.0	1040500054	285648480
2000-01	16,029.2	1210.5	1,853.4	1059633675	293168849
2001-02	14,835.5	1227.7	1,880.1	1078970907	301227098
2002-03	10,653.6	1138.7	1,738.9	1098313039	310207535
2003-04	13,697.0	1234.5	1,896.6	1117415123	319267849
2004-05	13,396.0	1200.8	1,911.0	1136264583	328414552
2005-06	16,951.0	1216	1,927.4	1154638713	337558628
2006-07	16,229.0	1237	1,923.8	1172373788	346659205
2007-08	19,303.0	1240.6	1,952.2	1189691809	355789232
2008-09	20,421.0	1228.3	1,953.3	1206734806	364989009
2009-10	15,295.0	1213.3	1,891.9	1223640160	374274816

(SOURCE RBI, INDIA)

Fitting of Auto-Regressive Integrated Moving Average (ARIMA) Model

Time series models are applied with the assumption that the data points are stationary. In a stochastic process, the term Stationarity refers to the phase where the average and variability remain constant over time,

and the covariance between two time periods depends only on the lag or disturbance at which the correlation is calculated [12]. The ARIMA model combines Autoregressive (AR) and Moving Average (MA) models with appropriate differencing orders. Therefore, it is important to understand AR and MA models before applying the description of the ARIMA model.

Auto Regressive (AR) Model:

$$Y_t = a + b_1 Y_{t-1} + \dots + b_p Y_{t-p} + U_t \tag{2}$$

where, Y_t = Values of the variable for forecasting at time 't', A = Constant. U_t = Random Error, b_i = i th regression Coefficient, ($i = 1, 2, \dots, p$)

In the analysis of Time Series data, the AR model helps to express the current value with the previous ones, along with a noise error term. It plays a significant role in trend analysis.

This model is called the AR(p) model.

2) Moving- Average (MA) Model: Sometimes residuals with different lags may exhibit relationships with the dependent variable, as follows:

$$Y_t = \mu + \phi U_t + \phi_1 U_{t-1} + \phi_2 U_{t-2} + \dots + \phi_q U_{t-q} \tag{3}$$

where, Y_t = Values of the variable for forecasting at time 't', μ = Constant, ϕ_i = Partial regression coefficient, ($i = 0, 1, 2, \dots, q$)

This model is known as the MA (q) model.

3) Auto Regressive Moving Average (ARMA) Model: In this model, Y_t depends on AR as well as MA variables and can be specified as:

$$Z_t - b_1 Z_{t-1} - \dots - b_p Z_{t-p} = U_t - \phi_1 U_{t-1} - \dots - \phi_q U_{t-q} \tag{4}$$

where, $Z_t = Y_t - \bar{Y}$ (deviation of Y_t from mean \bar{Y})

The above model is the ARMA(p,q) model.

Auto-Regressive Integrated Moving Average (ARIMA) Model: The previous models assumed that the error U_t is random, and the data is stationary. However, the data is non-stationary many times, which shows repetitive changes in the trends.

To solve this issue, the regression coefficients can be estimated while repetitions can be eliminated through successive differencing. The difference stationary model leads to the ARIMA model, which transforms the non-stationary time series into a stationary one by applying appropriate differencing (Box and Jenkins, 1978).

The ARIMA model is an ARMA model with the added step of differencing, requiring identification of the order

of AR terms (p), order of differencing (d), and order of MA terms (q). Thus, based on these constants, an ARIMA (p, d, q) model can be formulated.

$$Z_t - b_1 Z_{t-1} - \dots - b_p Z_{t-p} = U_t - \phi_1 U_{t-1} - \dots - \phi_q U_{t-q} \tag{5}$$

where, $Z_t = Y_t - \bar{Y}$ (deviation of Y_t from mean \bar{Y})

RESULTS AND DISCUSSIONS

A Multiple Linear Regression (MLR) equation has been fitted by taking Gross Food Grain Crop Production (GFGCP) production as the dependent variable and Total Cultivated Land Area (TCLA), Area Urbanized (AU) and Population (PP) as independent variables based on 30 years of data (1980-81 to 2009-10). As Table 5 shows, the MLR equation is as follows:

$$GFGCP = -159119909.30 + 1.10 * TCLA - 0.62 * AU + 0.21 * PP \tag{6}$$

Table 3. MLR Model Summary

Parameter	Estimate	Standard Error	t-Statistic	P-Value
Constant	159119909.30	37445949.11	-4.25	< 0.0001
AU	-0.62	1.77	-0.35	0.7245
TCLA	1.10	0.35	3.33	0.0015
PP	0.21	0.03	8.03	< 0.0001

Table 4. MLR-ANOVA

Source	Degrees of freedom	Sum of Squares	Mean Square	F-Ratio	P-Value
Model	3	1.70*10 ¹⁷	5.68*10 ¹⁶	696.929	< 0.0001
Residual	56	4.56*10 ¹⁵	8.15*10 ¹³		
Total	59	1.75*10 ¹⁷			

The Standard Error of the estimate is an important measure of accuracy of the predictions. It is square root of the sum of squared errors ((SSE) divided by the degrees of freedom (df). The regression estimates shows the change in the dependent variable for each unit change in the independent variable.

In MLR, the t-value measures the significance of the partial correlation between the variables reflected by regression coefficients.

$$t - statistic = \frac{Regression\ Coefficient}{Standard\ Error} = \frac{\bar{x} - \mu}{s/\sqrt{n}} \tag{7}$$

A high value of t gives a high level of assurance to the researcher. The ANOVA analysis gives the statistical test for overall model fit in terms of F-Ratio as shown in Table 4.

$$F = \frac{(Sum\ of\ Equares\ of\ Regression/DfRegression)}{(Sum\ of\ Equares\ of\ Residuals/DfResiduals)} = \frac{SST/k-1}{SSE/n-k} \quad (8)$$

The high value of F-Ratio gives a high level of significance.

Here the Coefficient of Determination, R2 = 0.9709 which proves that 97.09% variation of GFGCP is explained by PP, AU, and TCLA. The main reason for the remaining variation of 2.91% of GFGCP may be due to some errors or other influencing factors that are involved but are not included in the model.

Explanation of the estimates:

- Gross Food Grain Crop production (GFGCP)

production must be increased by 0.21 Tonnes per person to meet the food demand every year.

- For an increase in 1 hectare of an urbanized area, 0.62. Tonnes of Total Food Grain production will be reduced.
- For the 1 hectare increase in Total Cultivated Land Area (TCLA), in the present trend, 1.10 Tonnes of Gross Food Grain Crops (GFGC) production can be increased.

Now based on the forecasted values of TCLA, AU, and PP, GFGCPs are estimated by using the equation (6) for 11 years, 2010-11 to 2020-21 as shown in Table 6 and Fig.6.

Table 5 ARIMA Models – Summary of Values for AU, TCLA, PP & GFGCP

Variables	ARIMA(p,d,q)	ARIMA Model Summary				
		Parameter	Estimate	Std. Error	t-statistic	P-value
AU	ARIMA(1,1,2)	AR(1)	0.96037	0.0393	24.4114	< 0.0001
		MA(1)	1.10111	0.1657	6.6467	< 0.0001
		MA(2)	-0.32670	0.1618	-2.0194	0.0664
TCLA	ARIMA(1,0,1)	AR(1)	0.98660	0.0241	40.9075	< 0.0001
		MA(1)	0.30218	0.1522	1.9853	0.0705
		Intercept	132456083	11900195	11.1306	< 0.0001
PP	ARIMA(1,2,1)	AR(1)	-0.05113	0.1875	-0.2727	0.7893
		MA(1)	0.80934	0.1175	6.8883	< 0.0001
GFGCP	ARIMA(0,1,1)	MA(1)	0.68246	0.1216	5.6146	< 0.0001
		Intercept	3054288	440476	6.9341	< 0.0001

Table 6. Predicted Values of Different Variabes based on ARIMA Models

Year	GFGCP	TCLA	AU	PP
2010-11	229675474.8	140868248.9	25791525.01	1239186469
2011-12	232729762.5	140755490.7	25931822.87	1261932520
2012-13	235784050.2	140644243.9	26066560.91	1284671012
2013-14	238838337.9	140534488.3	26195959.45	1307409892
2014-15	241892625.7	140426203.9	26320230.09	1330148751
2015-16	244946913.4	140319370.9	26439576.04	1352887611
2016-17	248001201.1	140213970	26554192.47	1375626471
2017-18	251055488.8	140109981.9	26664266.79	1398365332
2018-19	254109776.5	140007387.6	26769979	1421104192
2019-20	257164064.2	139906168.6	26871501.98	1443843052
2020-21	260218352.0	139806306.3	26969001.73	1466581913

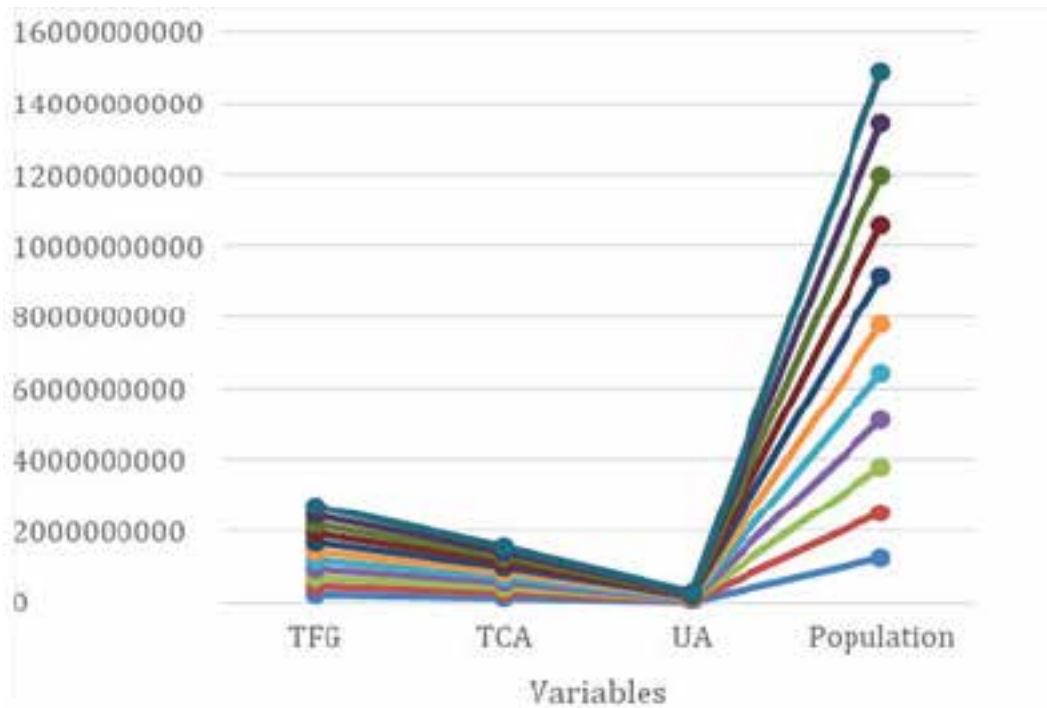


Fig. 6. Predicted values of different variables based on ARIMA Models

Table 7. Comparative Study of Two Sets of Predicted GFGC Vaues based on MLR & ARIMA

Year	GFGCP (MLR Model- (I) (in tonnes)	GFGCP (ARIMA Model) -(II) (in tonnes)	D (I)-(II) (in tonnes)
2010-11	241924814.8	229675474.8	12249340.06
2011-12	246317526.6	232729762.5	13587764.12
2012-13	250713966.5	235784050.2	14929916.32
2013-14	255115584.0	238838337.9	16277246.07
2014-15	259522140.6	241892625.7	17629514.97
2015-16	263933490.1	244946913.4	18986576.76
2016-17	268349487.2	248001201.1	20348286.11
2017-18	272769991.9	251055488.8	21714503.09
2018-19	277194869.2	254109776.5	23085092.67
2019-20	281623988.9	257164064.2	24459924.63
2020-21	286057225.3	260218352.0	25838873.30

The values in Table 7 shows the comparative results of GFGCP as calculated from the two methods, MLR and ARIMA. The difference value(D) is then computed from these two method results. The difference (D) values as shown in Table 8, follows a linear trend which is given by:

$$D = 10855451.32 + 1359046.57 * T, \text{ where, } T = \text{time... (9)}$$

Table 8. D- Trend Model Summary

Parameter	Estimate	Standard Error	t-statistic	P-value
Constant	10855451.32	14558.07	745.67	< 0.0001
Slope	1359046.57	2146.47	633.15	< 0.0001

Thus, it is quite evident that the differences of the possible and expected GFGCPs are increasing in a steep linear trend. Hence if the same trend of TCLA, AU and PP exists there will be no serious problem regarding food security in the next 10 years.

CONCLUSION

The present study shows that urbanization and population growth have serious concerns on agricultural food grain production in the coming decades. Telangana, besides agriculture, also contributes extensively to the software industries. People prefer this place for better career perspectives. Further, it has been observed that there is a positive trend, and the state may face a slight effect in the next decade which will also affect the overall Indian economy. The present study will be extended in the future to find the Gross food production in the other states of the country.

ACKNOWLEDGEMENT

The authors would like to acknowledge their sincere gratitude to the authorities of the Government of India E-portals/Annual reports for providing the relevant data that played a crucial role in performing this study.

REFERENCES

1. National Accounts Statistics 2023 | Ministry of Statistics and Program Implementation | Government of India (mospi.gov.in), DBIE (rbi.org.in)
2. "Climate Change Is Altering Rainfall Patterns Worldwide." 12 Nov. 2013, <https://www.scientificamerican.com/article/climate-change-is-altering-rainfall-patterns-worldwide/>.
3. Zhao X, Yang J, Chen H, Zhang X and Xi Y (2023) "The effect of urbanization on agricultural eco-efficiency and mediation analysis". *Front. Environ. Sci.* 11:1199446. doi: 10.3389/fenvs.2023.1199446
4. Veronique Beckers, L. Poelmans, A. Van Rompaey & N. Dendoncker (2020) "The impact of urbanization on agricultural dynamics: a case study in Belgium, *Journal of Land Use Science*", 15:5, 626-643, DOI: 10.1080/1747423X.2020.1769211
5. Wang, Hao & Cui, Peng & Carling, Paul. (2021). Wang et al 2021. *Earth Science Frontiers*. 28. 140-167. https://www.researchgate.net/publication/355164916_Wang_et_al_2021
6. Neetu Sharma, Naveen Kumar Mani. (2020). "Analysis of different Methodology behind the Crop Yield Prediction. *International Journal of Advanced Science and Technology*, 29(05), 13535 – 13543". Retrieved from <http://sersc.org/journals/index.php/IJAST/article/view/35355>
7. Sharma, Neetu. (2020). "Analysis on Present Mathematical Model for Predicting the Crop Production. *International Journal of Innovative Technology and Exploring Engineering*". 9. 10.35940/ijitee.L7946.1091220.
8. Sharma, N., & Mani, N. K. (2020). "Innovative practices for food security & sustainable agriculture: a forecasting challenge to the post-pandemic economy". *THE BOOK OF*, 25.
9. Dey S. K., C Pramanik, and C Dey. "Mathematical Modelling of Effects of Urbanization and Population Growth on Agricultural Economics". *Journal of Intellectual Economics*. 2(8), 7-20,2014
10. Pramanik Chanchal, S K Dey and Sarkar A. (2010). "Effect of Urbanization on Agriculture: A Special Scenario on Andhra Pradesh, India. *International Journal of Applied Science & Computations*", 17(2), 121-128.
11. Ferguson C. E. (1958). A Statistical Study on Urbanization. *Social Forces*, 37(1), 19-26.
12. Dobre I and Alexandru A A M (2008). Modelling unemployment rate using Box-Jenkins Procedure. *Journal of Applied Quantitative Methods*, 3(2), 156-166.

Studies in the Synthesis of Fluorescent 4-styrylcoumarins by Conventional and Green Method

Kailas K. Sanap

Department of Chemistry
HPT Arts and RYK Science College
Nashik, Maharashtra
✉ ksanap100@gmail.com

Anita K. Sanap

Jawahar Education Society's, Institute of Technology,
Management & Research
Nashik, Maharashtra
✉ ghuge.anita@gmail.com

ABSTRACT

Reaction of coumarin-4-acetic acids with different aldehydes by piperidine gives substituted-4-styrylcoumarins. The same reaction is carried out in choline chloride-urea DES gives mixture of 4-styrylcoumarin and corresponding decarboxylated 4-methylcoumarin. The styrylcoumarins are yellow to orange-red in colour and show strong emission under UV light (365 nm). They show good stoke shift. The effect of substituent of the coumarin ring at 7-position on the Stoke shift is studied. Similarly, the effect of substituent on pendent phenyl ring is investigated.

KEYWORDS : *Coumarin-4-acetic acid, 4-styrylcoumarin, DES, Fluorescence, Chromophore.*

INTRODUCTION

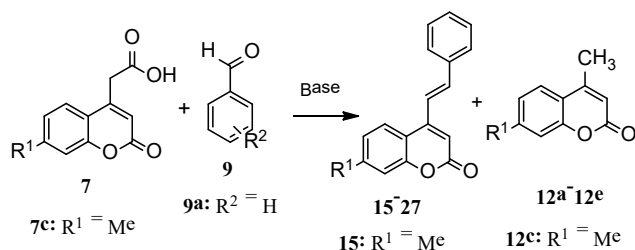
4-Styrylcoumarins and their derivatives are of considerable interest because of their wide range of biological activities, such as antifungal [1-3], antimicrobial [4], anti-bacterial [5], antifeedant [6-7], anti-inflammatory, antitubercular [8], antiproliferative, proapoptotic and anticancer activities [9]. In addition, coumarin derivatives with electron donor substituent at the 7-position are of interest as organic luminophores [10] and they are effective laser dyes in the blue green region of the spectrum [11]. 7-Diethylamino-4-styrylcoumarin and its analogues show good fluorescence properties [12-13]. 4-Styrylcoumarins are also good starting materials for annulation of the 3,4-double bond through Diels-Alder reaction [15-19]. Synthesis of 4-styrylcoumarins is reported mainly by the condensation of coumarin-4-acetic acids with aryl aldehydes using homogenous classical bases. It was also synthesized by the reaction of coumarin-4-acetic acid and aryl aldehydes using acetic acid as a catalyst and solvent as well for longer reaction time at higher temperature [1-2]. One of the alternative approaches involves the condensation reaction of 4-methylcoumarin and aryl aldehydes by using piperidine at room temperature [8, 20] for longer reaction time which gives lower yield of the product, and the same condensation reaction was also carried out

at higher temperature using piperidine to give product in lower yield [4, 16, 21-23]. *KotBu* was also employed in the synthesis of 4-styrylcoumarin to give lower yield [12]. Moderate yields of products were obtained in the reaction of coumarin-4-acetic acid and benzaldehyde in presence of piperidine [5, 15, 24]. Wittig and Wittig type reactions of chalcone and phosphorane were also reported to give 4-styrylcoumarin in moderate to good yield at higher temperature [3, 9, 14, 25, 26]. In some cases, phosphonic acid diethyl ester of coumarin, and aryl aldehyde were reacted using *NaOMe* to give corresponding styryl product at higher temperature. Reverse Wittig reaction attempt i.e. by using coumarin-4-carbaldehyde and Wittig salt using *NaH* in *DMF* was also made to synthesize 4-styrylcoumarin [14]. Coumarin 4-acetic acid and aromatic aldehydes were also condensed in presence of piperidine at room temperature and at higher temperature. These methods, however, suffer from one or another drawback, such as the use of metal mediated catalysis, a larger number of steps, strong acidic or basic conditions, longer reaction times, moisture sensitive catalysts or expensive reagents, and low conversions, which limit their practical utility in organic synthesis. Our protocols describe a simple method for the synthesis of 4-styrylcoumarin from coumarin-4-acetic acids and aryl aldehydes. In recent

years, the use of environmentally benign catalysts has received tremendous interest in different areas of organic synthesis. choline chloride-urea DES is an environmentally benign, easy to prepare, which displays strong basicity. It has received considerable interest as an economical, easily available, and recyclable catalyst for various organic transformations. It was thought worthwhile to explore the catalytic potential of choline chloride-urea DES for this conversion. In view of the above and as a part of our ongoing program to develop viable protocols, we report herein a CHOH catalyzed, mild, simple, and efficient procedure for the construction of 4-styrylcoumarins.

RESULTS AND DISCUSSION

We needed coumarin-4-acetic acids (7) for the synthesis of 4-styrylcoumarins. Reaction of phenols (6) with acetone dicarboxylic acid (5) is reported to give coumarin-4-acetic acids (7) [27]. Acetone dicarboxylic acid (5) is prepared in situ by the reaction of concentrated H_2SO_4 on citric acid (4), which is further reacted in situ with phenols (6) to obtain coumarin-4-acetic acids (1) (Pechmann reaction). Thus, a series of 7 was prepared and they were confirmed from known literature melting points. For phenols with electron donating group good yields of the products were obtained. Reaction of 7-methylcoumarin-4-acetic acid (7c) with benzaldehyde (9a) in different conditions were tried and summarized in the Scheme 1. and Table no. 1.



Scheme 1: Reaction of 7-methylcoumarin-4-acetic acid (7c) with benzaldehyde (9a)

Table 1 Reaction of 7-methylcoumarin-4-acetic acid (7c) with benzaldehyde (9a) in the presence of different bases

Entry	Base	Solvent	Time	Yield of 15	Yield of 12c
1	KOH	EtOH	2.5	0	69
2	NaOH	EtOH	3	0	62

3	Pyridine	Pyridine	16	0	54
4	NaH	THF	16	N.R	-
5	CH ₃ COONa	AcOH	18	Trace	Trace
6	Et ₃ N	EtOH	18	Trace	Trace
7	Piperidine	MeOH	2	41	23
8	Piperidine	MeOH	16	66	7

Reaction conditions: 7c (0.218 g, 1 mmol), 9a (0.106 g, 1 mmol), aBase (1 mmol), bReflux temp, cIsolated yield

7c decarboxylated under reflux conditions in the presence of KOH, NaOH and pyridine, possibly through the decarboxylation.

The reaction was successful in the presence of piperidine at room temperature as well as at reflux condition to give the expected product 15. At reflux condition, the yield was low possibly due to high lability of 7c to undergo decarboxylation.

Using the above optimized conditions, a series of 7-substituted coumarin-4-acetic acids was condensed with different aromatic aldehydes to obtain the corresponding 4-styrylcoumarins [Table 2]. Compound 20 was methylated by using DMS and K_2CO_3 to obtain 27 (27 was prepared for UV-Vis absorption and emission study). All the coumarin-4-acetic acids were reactive and gave the condensation products at ambient temperature in good yield; however, the time required for complete consumption of the coumarin-4-acetic acid varied. The aldehydes with electron withdrawing group gave good yield of the products, while the aldehydes with electron donating group gave less yield of the products.

Reaction in DES: Recently Perkin condensation and Knoevenagel reaction have been carried out in Deep Eutectic Solvent (DES) [28-29]. Taking inspiration from this, the reaction of coumarin-4-acetic acid with benzaldehyde was carried out. The DES were prepared by the reported method [28, 30]. Reaction of 7-methyl coumarin-4-acetic acid and benzaldehyde was attempted in 4 mL of different DES at 75 °C [Scheme 1, where instead of base DES was used. Choline chloride/Urea (DES A) Choline chloride/Phenol (DES B) Choline chloride/Glycerol (DES C) Choline chloride/Malonic acid (DES D) were prepared by the reported method [28, 30]. Only in DES A, 15 was obtained in low yield

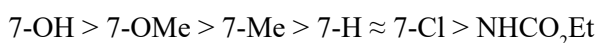
along with substantial amount of 12c. All other DES gave only 12c. Hence, for further work choline chloride/urea (DES A) was used.

Thus, different coumarin-4-acetic acids were reacted with different benzaldehydes in DES A [Table 2, Method B]. We have earlier noted the tendency of coumarin-4-acetic acids to undergo decarboxylation. In the case of DES A, the reaction did not take place at room temperature and hence the reaction was carried out at 75 °C. However, at this temperature there was more decarboxylation than that observed in the case of piperidine method. The aldehydes with electron donating group gave good yield of the products, while the aldehydes with electron withdrawing group gave poor yield.

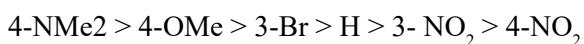
Reusability of DES A: In the reaction of 7-hydroxycoumarin-4-acetic acid (7d) and 4-N,N-dimethylaminobenzaldehyde (9e), DES A was separated from the reaction mixture by filtration and the water from the filtrate was removed at 80°C under vacuum. The recovered DES A was used for successive runs to test its reusability. The DES A was reusable without loss in activity up to three runs.

Photophysical properties: Compounds (13-27) were yellow to orange red in colour and showed good emission under UV light (365 nm). The compounds

were poorly soluble in solvents- n-hexane, chloroform, carbon tetrachloride, methanol, water but freely soluble in dimethyl sulfoxide. Hence, their UV-Vis absorption and emission properties were studied in dimethyl sulfoxide [Table 3]. UV-Vis absorption and emission spectra are shown in Figure 2 and 3 respectively. UV-Vis absorption ($\lambda_{\text{abs max}}$) and emission ($\text{Em } \lambda_{\text{max}}$) depended upon the nature of substituents on the coumarin ring and the pendant phenyl ring. The effect of substituents on the coumarin ring at 7-position on the Stoke shift was

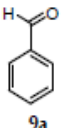
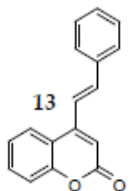
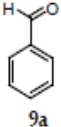
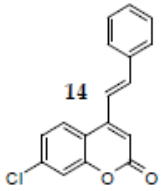


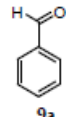
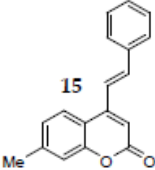
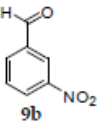
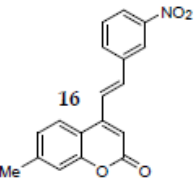
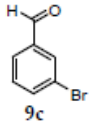
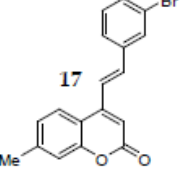
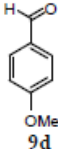
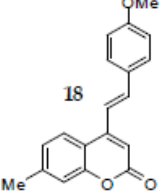
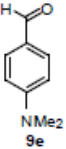
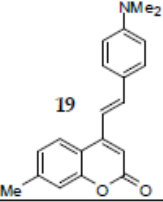
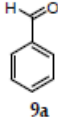
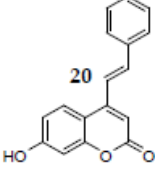
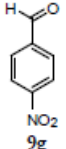
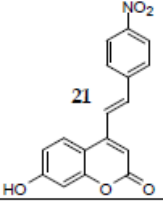
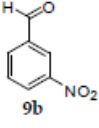
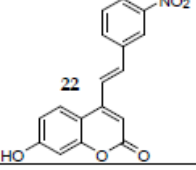
This may be ascribed to the increased π -electron density on the coumarin ring, due to the presence of electron donating groups. The effect of substituent on the pendant phenyl ring of 7-hydroxy-4-styrylcoumarins (20-25) on the Stoke shift was

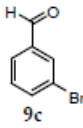
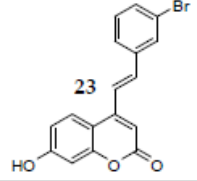
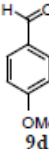
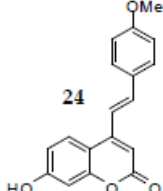
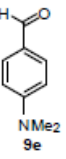
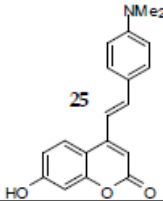
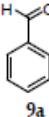
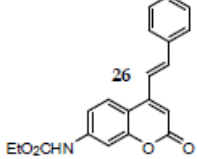
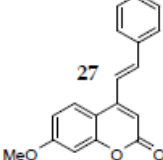


π -electron delocalization from the donor group at para position in the pendant phenyl ring to the acceptor carbonyl group in coumarin took place through the ethylene bridge. Electron donating group on the pendant phenyl ring increased the emission $\text{Em } \lambda_{\text{max}}$. Diethylamino and methoxyl groups on the pendant phenyl ring were significant and showed higher stoke shifts.

Table 2 Reaction of coumarin-4-acetic acids (7) with benzaldehydes (9) in the presence of piperidine (Method A) or in DES A (Method B)

Entry	(7) R ¹	(9)	Styrylcoumarin (13-27)	Method A Time ^a (h), (Yield ^b , %)	Method B Time ^a (h), (Yield ^b , of 13-27 %) [Yield ^b , of 12a-12e %]
1	7a, H			16 (61)	1.8 (29) [45]
2	7b, Cl			16 (77)	1.8 (31) [47]

3	7c, Me			16 (69)	1.8 (27) [46]
4	7c, Me			14 (74)	2.1 (14) [53]
5	7c, Me			13 (54)	1.7 (34) [34]
6	7c, Me			19 (49)	1.5 (44) [26]
7	7c, Me			22 (37)	1 (76) [04]
8	7d, OH			18 (62)	1.8 (21) [52]
9	7d, OH			14 (72)	3 (00) [62]
10	7d, OH			14 (67)	2 (11) [54]

11	7d, OH			16 (47)	1.7 (34) [33]
12	7d, OH			19 (44)	1.7 (41) [27]
13	7d, OH			32 (29)	1 (71) [07]
14	7e, NHC ₂ O ₂ Et			14 (71)	2 (22) [49]
15	-----	-----		-	-

Reaction conditions: a) Time for total consumption of 7, b) Isolated yield, Method A: 7 (1 mmol), 9 (1 mmol), Methanol: 5 mL, Piperidine (0.085 g, 1 mmol), Temp: RT; Method B: 7 (1 mmol), 9 (1 mmol); DES A: 4 mL, Temp: 5 °C

Table 3 UV-Vis absorption ($\lambda_{\text{abs max}}$) and emission (λ_{max}) of 4-styrylcoumarins

Product	Substrates		UV-vis absorption λ_{max} (nm)	Fluorescence λ_{max} (nm)	Stoke shift $\Delta\lambda\text{E-A}$ (nm)
	R ₁	R ₂			
13	H	H	326	436	110
14	Cl	H	287	397	110
15	Me	H	326	454	128
16	Me	3-NO ₂	313	348	35
17	Me	3-Br	323	462	139
18	Me	4-OMe	265	414	149
19	Me	4-NMe ₂	297	576	279
20	OH	H	324	478	154
21	OH	4-NO ₂	341	396	55
22	OH	3-NO ₂	312	394	82

23	OH	3-Br	324	490	166
24	OH	4-OMe	262	432	170
25	OH	4-NMe ₂	297	571	274
26	NHCO ₂ Et	H	318	404	86
27	OMe	H	327	464	137

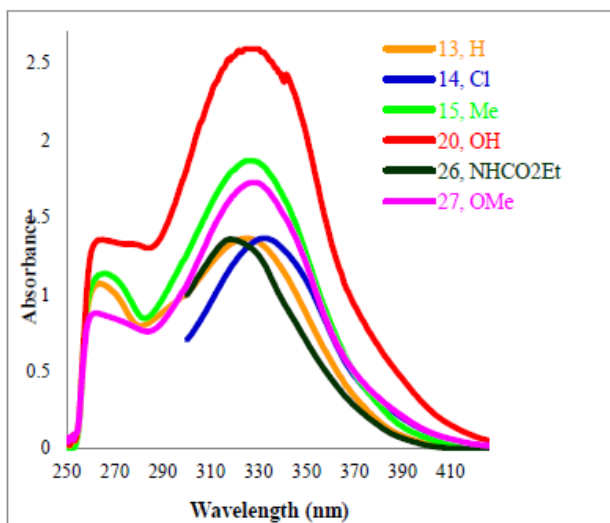


Figure 2(a) UV-Vis absorption spectra of 4-styrylcoumarins bearing different substituent at 7-position

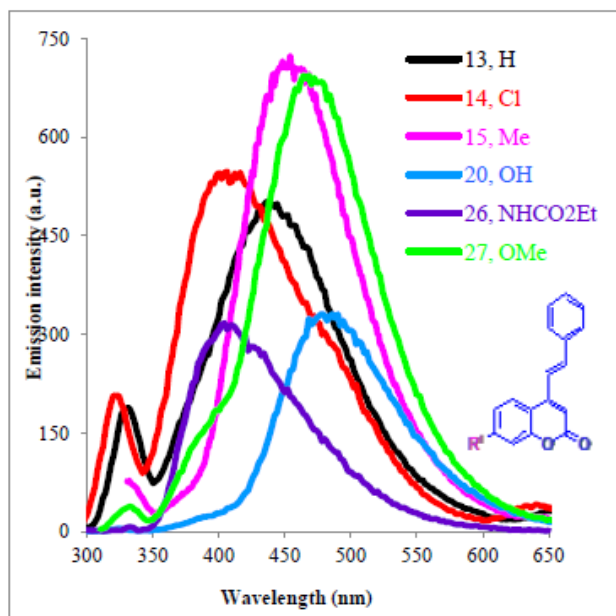


Figure 3 (a) Emission spectra of 4-styrylcoumarins bearing different substituent at 7-position

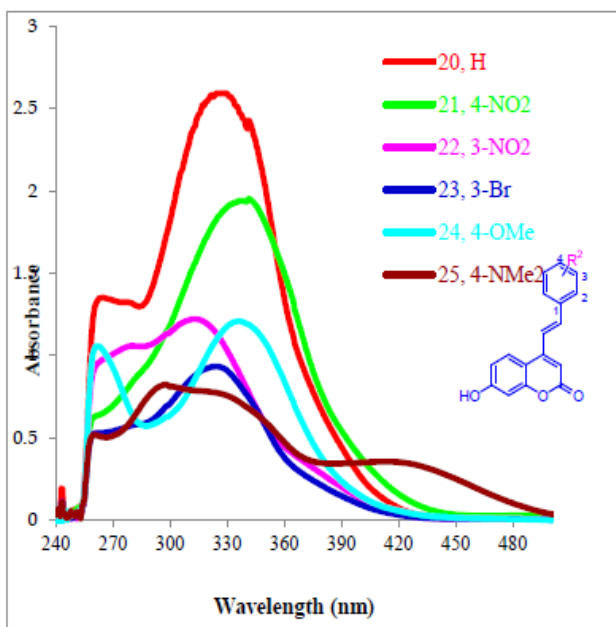


Figure 2 (b) UV-Vis absorption spectra of 7-hydroxy-4-styrylcoumarins (20-25) bearing different substituent at pendant phenyl ring

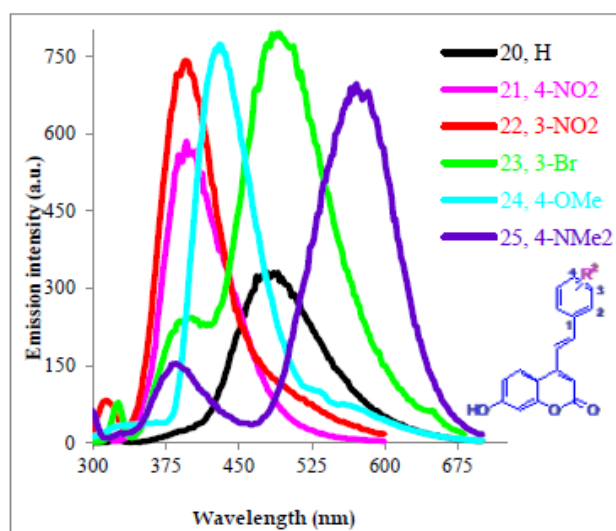


Figure 3 (b) Emission spectra of 7-hydroxy-4-styrylcoumarins (20-25) bearing different substituent at pendant phenyl ring

CONCLUSIONS

4-Styrylcoumarins are prepared by the reaction of different coumarin-4-acetic acids with substituted benzaldehydes in the presence of piperidine. The same reaction can be carried out using choline chloride-urea DES. Though the yields in the case of some aldehydes are less than piperidine method the DES method is environment friendly, as DES can be recovered and recycled and no hazardous substance is involved. The styrylcoumarins are yellow to orange-red in colour and show strong emission under UV light (365 nm). They show good stoke shift. They show UV-visible absorption in the range of 262-341 nm and emission in the range of 348-576 nm. The effect of substituent on the coumarin ring at 7-position on the Stoke shift decreases in the order of 7-OH > 7-OMe > 7-Me > 7-H \approx 7-Cl > NHCO₂Et. The effect of substituent on pendent phenyl ring decreased in the order of 4-NMe₂ > 4-OMe > 3-Br > H > 3-NO₂ > 4-NO₂.

ACKNOWLEDGMENT

Author KKS is thankful to research supervisor Prof. S. D. Samant (ICT, Mumbai) for his constant and encouraging support.

EXPERIMENTAL

7-methylcoumarin-4-acetic acid (7c)

A mixture of anhydrous citric acid (192 g, 1 mol) and conc. H₂SO₄ (280 mL) was stirred at room temperature for 1 h and then slowly heated (rate of heating governed by foaming) to 70 °C. After 30-35 min at this temperature, with stirring throughout, the evolution of carbon monoxide slackened. The clear solution was rapidly cooled to 0 °C. To the cooled solution, m-cresol (86.4 g, 0.8 mol) and conc. H₂SO₄ (112 mL) were added with stirring, each in three equal portions, at such a rate that the internal temperature did not exceed 10 °C. The resulting mixture was stirred at room temperature for 16 h, poured into ice and the resulting precipitate was filtered and washed thoroughly with water. The precipitate was stirred with saturated NaHCO₃ solution (1000 mL) for 15 min at 65 °C. The solution was filtered and the insoluble material was washed with water. Acidification of the combined filtrate and washings gave 7-methylcoumarin-4-acetic acid (7c).

Using the above procedure different substituted phenols (6) were condensed with acetone dicarboxylic acid to obtain a series of 7-substituted coumarin-4-acetic acids (7).

Preparation of 7-methyl-4-styrylcoumarin (15) by the reaction of 7-methyl coumarin-4-acetic acid (7c) and benzaldehyde (9a) in the presence of piperidine

7c (0.218 g, 1 mmol) and piperidine (0.085 g, 1 mmol) were stirred in methanol (5 mL) for 15 min and 9a (0.106 g, 1 mmol) was added slowly at room temperature. After complete consumption of 7c, the precipitated solid was collected by filtration and washed with small quantity of cold methanol followed by water to remove piperidine. The solid (15) was washed with ethyl acetate. The second crop of 15 was obtained from the filtrate by evaporating it to obtain a sticky mass which was purified by column chromatography on silica gel using pet ether - ethyl acetate (80: 20 v/v).

Using the above procedure different substituted coumarin-4-acetic acids (7) were condensed with different benzaldehydes (9) to obtain a series of substituted-4- styrylcoumarins (13-26).

Preparation of deep eutectic solvent DES A

Choline chloride (100 g, 71 mmol) and urea (86 g, 143 mmol) were placed in a round bottom flask and heated with stirring to 80 °C, until a liquid began to form. After 25-30 min, a homogenous colourless liquid (186 g, 100%) formed, which was used directly for the reaction without purification.

Using the above procedure different DES B, DES C and DES D were prepared.

Preparation of 7-methyl-4-styrylcoumarin (15) by the reaction of 7-methylcoumarin-4-acetic acid (7c) and benzaldehyde (9a) in DES A

7c (0.218 g, 1 mmol) and 9a (0.106 g, 1 mmol) were heated in DES A (4 mL). After complete consumption of 7c, the precipitated solid was collected by filtration and washed with small quantity of water. The second crop of 15 was obtained from the filtrate by extracting it with ethyl acetate (20 mL). The solvent was evaporated to obtain a sticky mass. The entire mass was purified by column chromatography on silica gel using pet ether - ethyl acetate (80:20 v/v).

Using the above procedure, different 7-substituted coumarin-4-acetic acids (7) were condensed with different benzaldehydes (9) to obtain a series of 7-substituted-4-styrylcoumarins (13-26).

Preparation of 7-methoxy-4-[(E)-2-phenylethenyl]-2H-benzopyran-2-one (27)

20 (0.264 g, 1 mmol) and K₂CO₃ (0.276 g, 2 mmol) were stirred in acetone (6 mL) at reflux temperature for 5 min. DMS (0.252 g, 2 mmol) was added slowly. After complete consumption of 20, the precipitated solid was collected by filtration and washed with water to obtain 27.

4-methyl-2H-1-benzopyran-2-one (12a)

Off white solid, 140-141 °C.

FT-IR (neat) in cm⁻¹: 2921 (aliphatic C-H), 1714 (C=O); 1625, 1605, 1568 (aromatic C=C), 1185, 1033, 849.

7-chloro-4-methyl-2H-1-benzopyran-2-one (12b)

Off white solid, 148-149 °C.

FT-IR (neat) in cm⁻¹: 3068 (aromatic C-H), 2916 (aliphatic C-H), 1742 (C=O), 1598, 1556, (aromatic C=C), 1487, 1378, 1246, 1173, 1060, 950, 877.

4,7-dimethyl-2H-1-benzopyran-2-one (12c)

White solid, 130-131 °C.

FT-IR (neat) in cm⁻¹: 2918 (aliphatic C-H), 1764 (C=O), 1622, 1578, 1504 (aromatic C=C), 1410, 1238, 1154, 965, 818.

7-hydroxy-4-methyl-2H-1-benzopyran-2-one (12d)

White solid, 179-180 °C.

FT-IR (neat) in cm⁻¹: 3483 (O-H), 2981 (aliphatic C-H), 1665 (C=O), 1597, 1518 (aromatic C=C), 1454, 1392, 1276, 1159, 1135, 1056, 1032, 838, 749.

7-[(ethoxycarbonyl)amino]-4-methyl-2H-1-benzopyran-2-one (12e)

Off white solid, 189-190 °C.

FT-IR (neat) in cm⁻¹: 3418 (N-H), 3091 (aromatic C-H), 1699 (broad, C=O), 1617, 1588, 1528 (aromatic C=C), 1487, 1355, 1228, 1009, 1020, 848.

4-[(E)-2-phenylethenyl]-2H-benzopyran-2-one (13)

Yellow solid, mp 180-181 °C (ethyl acetate).

FT-IR (neat) in cm⁻¹: 3075 (aromatic C-H), 1712 (C=O); 1601, 1556 and 1495 (aromatic C=C); 1447, 1378, 1319, 1259, 1215, 1183, 1127, 965, 935.

¹H NMR (CDCl₃): 6.61 (s, 1H, C₃H), 7.32-7.46 (m, 7H, C₁'H, C₂'H, C₄'H, C₅'H, C₆'H, C₆H and C₈H), 7.53-7.61 (m, 3H, C₃'H, C₇'H and C₇H) 7.80 (dd, 1H, C₅H, J = 1.2 and 7.95 Hz).

7-chloro-4-[(E)-2-phenylethenyl]-2H-benzopyran-2-one (14)

Yellow solid, mp 130-132 °C (ethyl acetate).

FT-IR (neat) in cm⁻¹: 3062 (aromatic C-H), 1705 (C=O); 1602, 1548 and 1494 (aromatic C=C); 1450, 1379, 1244, 1181, 1083, 967, 755 (C-Cl).

¹H NMR (DMSO): 6.85 (s, 1H, C₃H), 7.39-7.49 (m, 4H, C₁'H, C₂'H, C₅'H and C₆H), 7.62 (d, 1H, C₈H, J = 1.8 Hz), 7.69 (s, 2H, C₄'H and C₆'H), 7.82 (dd, 2H, C₃'H and C₇'H, J = 2.1 and 8.4 Hz), 8.26 (d, 1H, C₅H, J = 8.4 Hz).

7-methyl-4-[(E)-2-phenylethenyl]-2H-benzopyran-2-one (15)

Yellow solid, mp 132-134 °C (lit[15]. 132-134 °C).

FT-IR (neat) in cm⁻¹: 2923 (aliphatic C-H), 1686 (C=O); 1618, 1592, 1545 and 1496 (aromatic C=C); 1449, 1381, 1266, 1231, 1215, 1146, 759, 709

¹H NMR (CDCl₃): 2.48 (s, 3H, CH₃), 6.55 (s, 1H, C₃H), 7.15 (d, 1H, C₆H, J = 8 Hz), 7.19 (s, 1H, C₈H), 7.28-7.34 (m, 2H, C₄'H and C₆'H), 7.38-7.47 (m, 3H, C₁'H, C₂'H and C₅'H) 7.60-7.62 (d, 2H, C₃'H and C₇'H, J = 8 Hz), 7.69 (d, 1H, C₅H, J = 8 Hz).

7-methyl-4-[(E)-2-(3-nitrophenyl)ethenyl]-2H-benzopyran-2-one (16)

Yellow solid, mp 181-183 °C (ethyl acetate).

FT-IR (neat) in cm⁻¹: 3093 (aromatic C-H), 2923 (aliphatic C-H), 1698 (C=O); 1621, 1594 and 1531 (aromatic C=C); 1569 and 1351 (NO₂); 1274, 1151, 962.

¹H NMR (CDCl₃+DMSO): 2.19 (s, 3H, CH₃), 6.27 (s, 1H, C₃H), 6.86 (d, 2H, C₆H and C₈H, J = 8 Hz), 7.13

(d, 1H, C₁'H, J = 16 Hz), 7.27-7.38 (m, 2H, C₂'H and C₆'H), 7.48 (d, 1H, C₇'H, J = 8 Hz), 7.67 (d, 1H, C₅'H, J = 8.0 Hz), 7.91 (d, 1H, C₅H, J = 8 Hz), 8.22 (s, 1H, C₃'H).

7-methyl-4-[(E)-2-(3-bromophenyl)ethenyl]-2H-benzopyran-2-one (17)

White solid, mp 124-125 °C.

FT-IR (neat) in cm⁻¹: 3036 (aromatic C-H), 2918 (aromatic C-H), 1707 (C=O); 1624, 1597 and 1471 (aromatic C=C); 1429, 1380, 1259, 1230, 1147, 988.

¹H NMR (DMSO): 2.44 (s, 3H, CH₃), 6.74 (s, 1H, C₃H), 7.25 (dd, 1H, C₆H, J = 1 and 8.1 Hz), 7.27 (s, 1H, C₈H), 7.41 (t, 1H, C₆'H, J = 7.8 Hz), 7.58 (m, 1H, C₇'H), 7.63 (d, 1H, C₁'H, J = 16.1 Hz), 7.7950 (d, 1H, C₂'H, J = 16 Hz), 7.7964 (d, 1H, C₅'H, J = 7.7 Hz) 8.14 (m, 1H, C₃'H, J = 1.8 and 8.1 Hz), 8.15 (d, 1H, C₃H, J = 8.1 Hz).

7-methyl-4-[(E)-2-(4-methoxyphenyl)ethenyl]-2H-benzopyran-2-one (18)

Pale yellow solid, mp 161-162 °C (ethyl acetate), [lit[15], 180-181 °C (ethanol)]

FT-IR (neat) in cm⁻¹: 3072 (aromatic C-H), 2923 (aromatic C-H), 1712 (C=O); 1625, 1594, 1572 and 1515 (aromatic C=C), 1424, 1384, 1324, 1249, 1177, 1031, 958, 837.

¹H NMR (CDCl₃ + DMSO): 2.15 (s, 3H, CH₃), 3.53 (s, 3H, OCH₃), 6.17 (s, 1H, C₃H), 6.61 (d, 2H, C₄'H and C₆'H, J = 8.0 Hz), 6.79-6.86 (m, 2H, C₁'H and C₈H), 6.95 (d, 2H, C₃'H and C₇'H, J = 6 Hz), 7.17-7.25 (m, 2H, C₆H and C₂'H), 7.42 (d, 1H, C₅H, J = 8 Hz).

7-methyl-4-[(E)-2-[4-(dimethylamino)phenyl]ethenyl]-2H-benzopyran-2-one (19)

Red Solid, mp 170-171 °C (ethyl acetate), [lit[23], 190 °C (ethanol)].

FT-IR (neat) in cm⁻¹: 3038 (aromatic C-H), 2914 (aromatic C-H), 1704 (C=O); 1611, 1586 and 1543 (aromatic C=C); 1452, 1371, 1325, 1271, 1224, 1188, 1148.

¹H NMR (CDCl₃ + DMSO): 2.44 (s, 3H, Ar-CH₃), 3.04 (s, 6H, N-(CH₃)₂), 6.49 (s, 1H, C₃H), 6.69 (d, 2H, C₄'H and C₆'H, J = 8 Hz), 7.05-7.15 (m, 3H, C₁'H, C₆H and C₈H), 7.29 (d, 1H, C₂'H, J = 16 Hz), 7.45 (d, 2H, C₃'H

and C₇'H, J = 8 Hz), 7.69 (d, 1H, C₅H, J = 8 Hz).

7-hydroxy-4-[(E)-2-phenylethenyl]-2H-benzopyran-2-one (20)

Yellow solid, mp 205-206 °C (ethyl acetate), [lit[23], 175 °C (ethanol)].

FT-IR (neat) in cm⁻¹: 3182 (O-H), 1679 (C=O); 1619 and 1591 (aromatic C=C); 1449, 1383, 1296, 1273, 1144.

¹H NMR (DMSO): 6.55 (s, 1H, C₃H), 6.75 (d, 1H, C₈H, J = 2.0 Hz), 6.83 (dd, 1H, C₆H, J = 2.0 and 8.8 Hz), 7.36-7.45 (m, 3H, C₁'H, C₂'H and C₅'H), 7.58-7.67 (m, 2H, C₄'H and C₆'H), 7.80 (d, 2H, C₃'H and C₇'H, J = 7.2 Hz), 8.02 (d, 1H, C₅H, J = 8.8 Hz), 10.42 (bs, 1H, OH exchangeable with D₂O).

7-hydroxy-4-[(E)-2-(4-nitrophenyl)ethenyl]-2H-benzopyran-2-one (21)

Yellow solid, mp 266-267 °C (ethyl acetate).

FT-IR (neat) in cm⁻¹: 3266 (O-H), 1705 (C=O); 1627, 1594, 1515 and 1496 (aromatic C=C); 1443, 1388; 1547 and 1341 (NO₂); 1275, 1206, 1144, 970.

7-hydroxy-4-[(E)-2-(3-nitrophenyl)ethenyl]-2H-benzopyran-2-one (22)

Yellow solid, mp 291-293 °C (ethyl acetate).

FT-IR (neat) in cm⁻¹: 3221 (O-H), 1698 (C=O); 1626, 1556 and 1520 (aromatic C=C); 1446, 1388; 1556 and 1359 (NO₂); 1272, 1227, 1140, 967.

¹H NMR (DMSO): 6.60 (s, 1H, C₃H), 6.76 (d, 1H, C₈H, J = 2.3 Hz), 6.84 (dd, 1H, C₆H, J = 2.3 and 8.7 Hz), 7.74 (d, 1H, C₆'H), 7.76 (d, 1H, C₁'H, J = 16.1 Hz), 7.89 (d, 1H, C₂'H, J = 16 Hz), 8.12 (d, 1H, C₃H, J = 8.8 Hz), 8.22 (dd, 1H, C₇'H, J = 2.2 and 8 Hz), 8.28 (d, 1H, C₅'H, J = 7.72 Hz), 8.67 (s, 1H, C₃'H), 10.61 (s, 1H, OH, exchangeable with D₂O).

7-hydroxy-4-[(E)-2-(3-bromophenyl)ethenyl]-2H-benzopyran-2-one (23)

White solid, mp 228-229 °C (ethyl acetate).

FT-IR (neat) in cm⁻¹: 3196 (O-H), 1707 (C=O); 1623, 1594 and 1551 (aromatic C=C); 1445, 1384, 1270, 1227, 1148, 962.

¹H NMR (DMSO): 6.55 (s, 1H, C₃H), 6.75 (d, 1H, C₈H, J = 2.3 Hz), 6.83 (dd, 1H, C₆H, J = 2.3 and 8.4 Hz),

7.40 (t, 1H, C₆'H, J = 7.9 Hz), 7.57 (m, 1H, C₅'H), 7.59 (d, 1H, C₁'H, J = 16.5 Hz), 7.74 (d, 1H, C₂'H, J = 16.5 Hz), 7.77 (d, 1H, C₇'H, J = 8.2 Hz), 8.08 (d, 1H, C₅H, J = 8.8 Hz), 8.12 (s, 1H, C₃'H), 10.60 (bs, 1H, OH, exchangeable with D₂O).

7-hydroxy-4-[(E)-2-(4-methoxyphenyl)ethenyl]-2H-benzopyran-2-one (24)

Yellow solid, mp 179 °C, [lit[23], 179 °C].

FT-IR (neat) in cm⁻¹: 3254 (O-H), 2847 (aromatic C-H), 1683 (C=O); 1598 and 1515 (aromatic C=C); 1426, 1387, 1268, 1225, 1140, 1024, 834.

7-hydroxy-4-[(E)-2-[4-(dimethylamino)phenyl]ethenyl]-2H-benzopyran-2-one (25)

Red solid, mp 229-230 °C (ethyl acetate), [lit[23], 171 °C (ethanol)].

FT-IR (neat) in cm⁻¹: 3079 (O-H), 1666 (C=O); 1599, 1586 and 1543 (aromatic C=C); 1444, 1374 1220, 1184, 1141, 958, 825.

¹H NMR (DMSO): 2.98 (s, 6H, 2xCH₃), 6.45 (s, 1H, C₃H), 6.75 (m, 2H, C₆H and C₈H, J= 8 Hz), 6.81 (d, 2H, C₄'H and C₆'H, J = 8 Hz), 7.32 (d, 1H, C₁'H, J = 16 Hz), 7.56 (d, 1H, C₂'H, J = 16 Hz), 7.64 (d, 2H, C₃'H and C₇'H, J = 8 Hz), 8.05 (d, 1H, C₅H, J = 8 Hz), 10.53 (s, 1H, OH, exchangeable with D₂O).

7-[(ethoxycarbonyl)amino]-4-[(E)-2-phenylethenyl]-2H-benzopyran-2-one (26)

Yellow solid, mp 179-181 °C.

FT-IR (neat) in cm⁻¹: 3302 (NH), 1722 (C=O); 1708 (C=O of NHCO₂Et), 1618, 1572 and 1512, (aromatic C=C), 1382, 1226.

¹H NMR (DMSO): 1.27 (t, 3H, CH₃, J = 8 Hz), 4.17 (q, 2H, CH₂, J = 8 Hz), 6.64 (s, 1H, C₃H), 7.42-7.45 (m, 4H, C₁'H, C₂'H, C₅'H and C₆'H), 7.58 (s, 1H, C₈H), 7.64 (s, 2H, C₄'H and C₆'H), 7.80 (d, 2H, C₃'H and C₇'H), 8.11 (d, 1H, C₅H, J = 10 Hz), 10.18 (s, 1H, NH).

7-methoxy-4-[(E)-2-phenylethenyl]-2H-benzopyran-2-one (27)

Yellow solid, mp 136-137 °C

FT-IR (neat) in cm⁻¹: 3028 (aromatic C-H), 1728 (C=O); 1618 and 1542 (aromatic C=C); 1452, 1384, 1284, 1269, 1133.

¹H NMR (CDCl₃): 3.89 (s, 3H, OCH₃), 6.46 (s, 1H, C₃H), 6.88 (dd, 1H, C₆H, J = 2.4 and 7 Hz), 6.91 (d, 1H, C₈H, J = 2.4 Hz), 7.32 (s, 2H, C₄'H and C₆'H), 7.38-7.47 (m, 3H, C₁'H, C₂'H and C₅'H), 7.60 (d, 2H, C₃'H and C₇'H, J = 6.8 Hz), 7.71 (d, 1H, C₅H, J = 8.8 Hz).

REFERENCES

- G. R. Kokil, P. V. Rewatkar, S. Gosainc, S. Aggarwal, A. Verma, A. Kalra, S. Thareja. Lett. Drug Des. Discov. 2010, 7, 46.
- S. Thareja, A. Verma, A. Kalra, S. Gosainc, P. V. Rewatkar, G. R. Kokil, ACTA POL PHARM, Drug Research 2010, 67, 423.
- V. K. Ahluwalia, N. Kaila, S. Bala, Indian J. Chem. 1987, 26B, 700.
- M. E. El-Fattah, M. Y. El-Kady, S. M. El-Rayes, M. K. Mohammed, Rev. Chim. (Bucharest) 2011, 62, 881.
- D. R. Shridhar, C. V. Reddy Sastry, N. K. Vaidya, S. R. Moorty, G. S. Reddi, G. S. Thapar, Indian J. Chem. 1978, 16B, 704.
- B. Sreenivasulu, P. N. Sarma, Synth. Commun. 1997, 27, 2281.
- P. Rao, Sampath, V. V. K. Reddy, K. V Reddy, Synth. Commun. 1997, 27, 3361.
- K. Upadhyay, A. Bavishi, S. Thakrar, A. Radadiya, H. Vala, S. Parekh, D. Bhavsar, M. Savant, M. Parmar, P. Adlakha, A. Shah, Bioorg. Med. Chem. Lett. 2011, 21, 2547.
- F. Belluti, G. Fontana, L. Dal Bo, N. Carenini, C. Giommarelli, F. Zunino, Bioorg. Med. Chem. 2010, 18, 3543.
- B. M. Krasovitskii, B. M. Bolotin, Organic Luminophores [in Russian], Khimiya, Moscow 1984, 145.
- L. K. Denisov, B. M. Uzhinov, Khim Geterotsikl. Soedin. 1980, 723.
- I. I. Tkach, N. A. Andronova, L. P. Savvina, E. A. Luk'yanets, Khim Geterotsikl. Soedin. 1991, 319.
- M. A. Kirpichënok, N. S. Patalakha, L. Y. Fomina, I. I. Grandberg, Khim Geterotsikl. Soedin. 1991, 1170.

14. S. Valente, E. Bana, E. Viry, D. Bagrel, G. Kirsch Bioorg. Med. Chem. Lett. 2010, 20, 5827.
15. A. Y. Soliman, A. F. El-Karawawy, F. K. Mohamed, H. M. Baker, A. M. Abdel-Gawad, Indian J. Chem. 1991, 30B, 477
16. A. El-Shafei, A. A. Fadda, A. M. Abdel-Gawad.; E. H. E. Youssif, Synth. Commun. 2009, 39, 2954.
17. D. K. Bhardwaj, S. Neelakantan, T. R. Seshadri, Indian J. Chem. 1969, 7B, 325.
18. A. Mustafa, M. Kamel, M. A. Allam, J. Am. Chem. Soc. 1955, 77, 1828.
19. A. Mustafa, M. Kamel, M. A. Allam, J. Am. Chem. Soc. 1956, 78, 4692.
20. A. S. A. Youssef, K. A. Kandeel, H. M. F. Madkour, J. Indian Chem. Soc. 1995, 72, 103.
21. H. M. F. Madkour, Heterocycles 1993, 36, 947.
22. A. D. Gharde, B. J. Ghiya, J. Indian Chem. Soc. 1992, 69, 397.
23. E. Dimitrova, Y. Anghelova, Synth. Commun. 1986, 16, 1195.
24. J. N. Moorthy, K. Venkatesan, Bull. Chem. Soc. Jpn. 1994, 67, 1.
25. B. Henkel, Synlett. 2008, 3, 355.
26. P. D. Lokhande, B. J. Ghiya, J. Indian Chem. Soc. 1989, 66, 314.
27. S. C. Laskowski, R. O. Clinton, J. Am. Chem. Soc. 1950, 72, 4692.
28. P. M. Pawar, K. J. Jarag, G. S. Shankarling, Green Chem. 2011, 13, 2130.
29. Y. A. Sonawane, S. B. Phadtare, B. N. Borse, A. R. Jagtap, G. S. Shankarling, Org. Lett. 2010, 12, 1456
30. Abbott, A. P.; Barron, J. C.; Ryder, K. S. Wilson D. Chem. Eur. J. 2007, 13, 6495

The Impact of Elevated Temperature on the Mechanical Characteristics of Concrete Containing GGBS

A. J. Pawar

Assistant Professor
Department of Civil Engineering
Jawahar Education Society's, Institute of Technology,
Management and Research, Nashik.
Savitribai Phule Pune University
Pune, Maharashtra
✉ akshay4592@gmail.com

S. R. Suryawanshi

Associate Professor
Department of Civil Engineering
S. V. National Institute of Technology, Surat, Gujarat.
(Deemed University)

ABSTRACT

The incorporation of Ground Granulated Blast Furnace Slag (GGBS) into concrete is supported by economic, environmental, and technical considerations. The present study examined the impact of increased temperatures on the characteristics of concrete produced using GGBS as a substitute to Ordinary Portland Cement (OPC). The replacement ratios were corresponded to 20%, 40%, and 60% of the cement weight. The concrete specimens were exposed to a range of increased temperatures, from 200° C to 1200° C. Afterwards, the residual compressive strength, split tensile strength, and flexural strength of the concrete were measured. Standard cubes, cylinders, and prisms with dimensions of 150 x 150 x 150 mm, 150 x 300 mm, and 100 x 100 x 500 mm, respectively, were manufactured and subjected to testing. The test findings demonstrate that substituting 20% of cement with GGBS yield comparable outcomes.

KEYWORDS : GGBS, Replacement ratio and Elevated temperature.

INTRODUCTION

Fire is a prevalent natural hazard that poses a threat to building structures. Exposing concrete to elevated temperatures, such as those resulting from unintentional fires, can result in significant degradation and ultimately compromise the structural integrity of buildings. The structural integrity of building components is significantly compromised when exposed to elevated temperatures. This includes a decrease in compressive strength, split tensile strength, flexural strength, as well as a reduction in durability [1]. Additionally, the high temperature exposure leads to structural cracking and alters the colour of associated aggregates. In the process of design, it is often overlooked that a building may be subjected to elevated temperatures, resulting in alterations to the characteristics and load-bearing capacity of its materials. Hence, it is imperative to familiarize oneself with the behaviour of various materials when exposed to elevated temperatures, as this might potentially lead to structural failure in buildings.

Concrete possesses exceptional fire resistant capabilities in comparison to alternative materials due to its low thermal conductivity and high specific gravity [2]. Consequently, it can effectively serve as a protective barrier for other structural components, such as steel. Concrete intermittently needs to withstand the impact of intentionally generated elevated temperatures, which can arise in close proximity to furnaces or atomic reactors, on pavements exposed to jet engine blasts, and in fire-prone environments. The utilization of concrete in scenarios requiring exceptionally great temperatures, such as the construction of landing pads for missiles, is typically regarded as disposable. However, in the majority of cases, it is preferable to minimize the degradation of the concrete physical characteristics to the greatest extent feasible.

The examination of the residual design strength of concrete under high temperatures has become a crucial aspect for engineers. This is necessary in order to establish a comprehensive database that can be

utilized for practical research applications, specifically focusing on the performance of concrete at elevated temperatures. Concrete possesses intrinsic fire-resistant qualities, which confers it with a distinct advantage over alternative construction materials. Nevertheless, it is imperative to consider the impact of fire on concrete structures during the design process. Despite the loss in strength caused by the rise in temperature, it remains essential for structural elements to possess the ability to withstand both dead and applied loads without experiencing structural failure. The topic of interest pertains to the strength and modulus of elasticity in concrete and steel reinforcement materials. In order to accurately forecast the reaction of a building following exposure to elevated temperatures, it is important to possess a comprehensive understanding of the strength characteristics of concrete when subjected to high temperature.

Ground Granulated Blast Furnace Slag

Blast furnace slag is a residual material generated during the production of iron in the manufacturing industry. The furnace is charged with iron ore, coke, and limestone, which undergo a process culminating in the formation of molten slag. This slag, characterized by its ability to float above the molten iron, is observed at a temperature range of around 1500°C to 1600°C [3]. The molten slag is composed of approximately 30% to 40% silicon dioxide (SiO₂) and about 40% calcium oxide (CaO), which closely resembles the chemical composition of Portland cement [4]. Once the molten iron is extracted, the residual molten slag, primarily composed of siliceous and aluminous remnants, is promptly subjected to water quenching, leading to the creation of a glassy granular material [5]. The glassy granulate is subjected to a process of drying and grinding in order to attain the necessary particle size, which yields a substance known as ground granulated blast furnace slag. The energy demand for the manufacturing of GGBS is quite low in comparison to that of Portland cement production. The substitution of Portland cement with GGBS is expected to result in a substantial decrease in the emission of carbon dioxide gas. Hence, GGBS can be regarded as a construction material that is environmentally sustainable [6].

The impact of increased temperature on concrete

The increase in temperature induces a phase transition

of the unbound water within concrete, transitioning it from a liquid phase to a gaseous phase. The alteration in state induces modifications in the rate at which thermal energy is transferred from the surface to the inner regions of the concrete element. When the temperature rises over a certain threshold, the cement paste experiences shrinkage, leading to an overall expansion of the concrete. This expansion causes a drop in the strength and modulus of elasticity for both the concrete and the steel reinforcement. The rate of strength and modulus reduction is contingent upon the pace of temperature growth in the fire and the insulating characteristics of concrete.

Advantages of GGBS Concrete

GGBS concrete has enhanced water impermeability properties, along with better resistance to corrosion and sulphate attack [7]. Consequently, the longevity of a structure is increased, leading to a decrease in maintenance expenses. Additionally, it has the capacity to decrease thermal energy in concrete structures. The utilization of high-volume eco-friendly replacement slag has resulted in the advancement of concrete technology, enabling the incorporation of industrial waste materials. This innovative approach not only contributes to the sustainable management of industrial by products but also offers substantial benefits in terms of conservation of natural resources and energy efficiency. As a result, there is a decrease in the utilization of cement. The utilization of GGBS as cementitious constituents necessitates solely the process of grinding, hence resulting in significant energy savings in comparison to the manufacturing of OPC. The utilization of GGBS has garnered increasing interest due to its ability to enhance the characteristics of blended cement concrete, reduce costs, and mitigate adverse environmental impacts [8]. Concrete using GGBS is expected to exhibit comparable or marginally worse characteristics in comparison to OPC concrete.

The purpose of this study is to examine the impact of increased temperature on both ordinary concrete and concrete containing GGBS as a mineral additive. The aim of this study is to investigate the influence of elevated temperature on the compressive strength, flexural strength, and tensile strength of traditional concrete and concrete incorporating GGBS as a mineral

additive. In order to examine the most appropriate combination, it is necessary to conduct an investigation.

EXPERIMENTAL INVESTIGATION

Material

The cement utilized in this study was Ordinary Portland (53 grade) cement, and its corresponding physical characteristics are presented in Table 1. The product complied with the specifications outlined in the Indian Standard Specifications, namely IS: 12269-2013 [9]. A fine aggregate consisting of natural sand with a maximum size of 4.75 mm was utilized. The characteristics of the sand are presented in Table 2. The coarse aggregate utilized in the study consisted of crushed stone, with a maximum particle size of 20 mm. The specimens underwent testing in accordance with the IS: 383- 2016 [10], and their respective physical attributes are presented in Table 2. The water utilized in this study was potable water, characterized by its absence of harmful levels of detrimental substances. The GGBS used in this study was sourced from JSW Cement Limited. Detailed information regarding its qualities can be found in Table 1 and Table 3.

Table 1: Physical Properties of Cement and GGBS

Sr. No.	Properties	Cement	GGBS
1	Colour	Grey	White
2	Specific Gravity	3.15	2.87
3	Fineness (retained on 90 micron sieve)	8 %	0 %
4	Fineness (retained on 45 micron sieve)	--	0.8 %
5	Soundness (mm)	5	1

Table 2: Physical Properties of FA and CA

Sr. No.	Properties	FA	CA
1	Type	Natural	Natural
2	Specific Gravity	2.62	2.75
3	Fineness Modulus	2.47	7.2
4	Surface Texture	Smooth	Rough
5	Particle Shape	Rounded	Angular

Mix Proportion and Mix Details

This study focuses on the examination of M25 mix concrete using a weight-based approach. Specifically, the analysis involves the substitution of 20%, 40%, and 60% of cement with GGBS. The mix proportion that has been adopted is 1:1.6:2.85.

The study involved the utilization of four distinct concrete mixtures in order to examine the impact of increased temperature on the characteristics of concrete that incorporates GGBS. Table 4 provides a comprehensive overview of the specific characteristics and components of the various concrete mixtures.

A control mixture of conventional concrete was formulated in accordance with the Indian Standard Specifications IS:

Table 3: Chemical Composition of GGBS

Sr. No.	Parameters	JSW GGBS	As per IS: 12089-1987 [11]
1	CaO	37.34%	--
2	Al ₂ O ₃	14.42%	--
3	Fe ₂ O ₃	1.11%	--
4	SiO ₂	37.73%	--
5	MgO	8.71%	Max. 17%
6	MnO	0.02%	Max. 5.5%
7	Sulphide Sulphur	0.39%	Max 2%
8	Insoluble Residue	1.59%	Max. 5%
9	Glass content in %	92%	Min. 85%
10	Chemical Moduli: 1. $\frac{CaO+MgO+1/3Al_2O_3}{SiO_2+2/3Al_2O_3}$	1.07	≥ 1
	2. $\frac{CaO+MgO+Al_2O_3}{SiO_2}$	1.60	≥ 1

The presence of major oxides with granulated slag shall satisfy at least one of the equation

Table 4: Concrete Mix Proportions

Sr. No.	Combinations	Specimen	Temperature °C
1	Conventional Concrete	Cube	200°C, 400°C, 600°C, 800°C, 1000°C,1200°C
		Cylinder	
		Prism	
2	20% GGBS (RB1)	Cube	Exposure time 1 hour
		Cylinder	
		Prism	
3	40% GGBS (RB2)	Cube	Exposure time 1 hour
		Cylinder	
		Prism	
4	60% GGBS (RB3)	Cube	Exposure time 1 hour
		Cylinder	
		Prism	

10262-2019 [12], with the objective of achieving a 28-day compressive strength. The remaining concrete combinations, namely RB1, RB2, and RB3, were formulated by substituting 20%, 40%, and 60% of GGBS in relation to the weight of cement. The water-to-cementitious materials ratio was maintained at a constant level during the experiment to examine the impact of substituting cement with GGBS while keeping all other variables same.

Cooling and Heating regimes

Following a curing period of 28 days, the specimens were extracted from the tank and subjected to the process of air drying. Subsequently, the specimens underwent thermal treatment in an electric oven, wherein they were subjected to incremental temperatures of 200° C, 400° C, 600° C, 800° C, 1000° C, and 1200° C. The temperature was held constant at its respective value for a duration of one hour in order to establish a state of thermal equilibrium. Subsequently, the furnace door was unlatched, enabling the specimens to undergo a gradual cooling process until they reached the ambient temperature of the surrounding environment.

Test specimens and the corresponding test procedure

Following the cooling of the concrete specimens to ambient temperature, various tests were conducted to determine their compressive strength, split tensile strength, and flexural strength. The experiments were conducted in accordance with the applicable Indian norms.

Test specimens consisting of 150 mm concrete cubes and cylinders with dimensions of 150 x 300 mm were employed in order to assess the compressive strength and split tensile strength of concrete. This evaluation encompassed two scenarios: standard concrete and GGBS concrete. The components of concrete were meticulously blended until a homogeneous texture was attained. The cubes and cylinders underwent effective compaction by the utilization of machine mixing. The process of demoulding the concrete cubes and cylinders was completed within a 24-hour timeframe subsequent to their casting. The test specimens, after being removed from the mould, were adequately cured in the potable water for a duration of 28 days. A compression test was performed using a compression testing machine that was present in the laboratory, following the guidelines outlined in the IS 516-1959 [13] standard. The force was consistently and evenly distributed until the specimen failure. The split tensile strength test was carried out in accordance with the specifications stated in IS 5816-1999 [14]. The specimen was positioned in a horizontal orientation between the loading surfaces of the compression testing equipment, and a gradual application of force was administered until the specimen failure. The flexural strength of concrete

prism measuring 100 mm x 100 mm x 500 mm was evaluated in accordance with the guidelines specified in IS 516-1959 [13]. The stress was exerted by means of two identical rollers positioned at intervals of one third along the supporting span. The load was gradually added without any sudden impact until the point of failure was reached.

RESULTS AND DISCUSSION

Compressive Strength

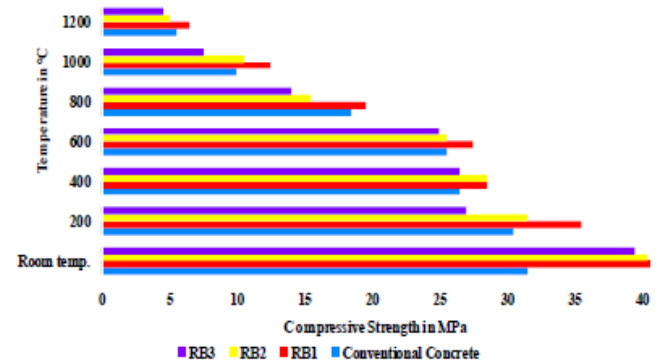


Fig. 1: Compressive strength of concrete at elevated temperature

The results of the compressive strength test are depicted in Fig. 1. The test findings indicate a decrease in the compressive strength of both conventional and GGBS concrete with an increase in temperature. The compressive strength exhibits a reduction as the content of GGBS increases. The utilization of a concrete mixture including 20% GGBS has been observed to yield a greater compressive strength when compared to alternative combinations. The decrease in compressive strength is greater in concrete containing 60% GGBS in comparison to other combinations.

Split Tensile Strength

The results of the split tensile strength test are depicted in Fig 2. The test findings indicate a drop in the split tensile strength of both conventional and GGBS concrete with an increase in temperature. The split tensile strength likewise exhibits a decrease when the content of GGBS increases. The combination of concrete containing 20% GGBS exhibits superior split tensile strength when compared to alternative combinations. The decrease in split tensile strength is greater for concrete containing 60% GGBS when compared to other combinations,

specifically at temperatures ranging from 1000° C to 1200° C.

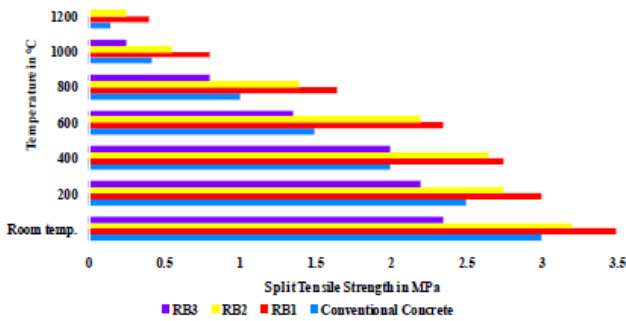


Fig. 2: Split tensile strength of concrete at elevated temperature

Flexural Strength

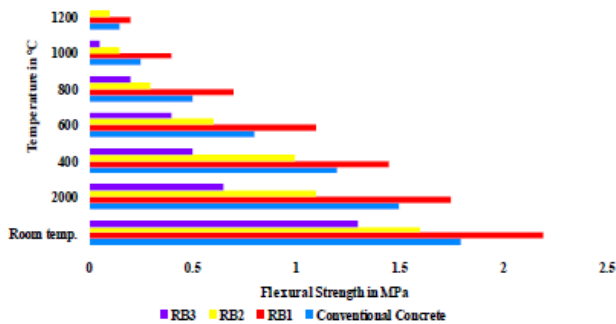


Fig. 3: Flexural strength of concrete at elevated temperature

The results of the Flexural Strength test are depicted in Fig 3. The test findings indicate a decline in the flexural strength of both conventional and GGBS concrete as the temperature increases. The flexural strength is shown to diminish as the content of GGBS increases. The utilization of concrete containing 20% GGBS exhibits superior flexural strength in comparison to alternative combinations. The decrease in flexural strength is greater in concrete containing 60% GGBS in comparison to other combinations.

CONCLUSIONS

The present study examined the impact of increased temperature on the characteristics of concrete incorporating GGBS as a cementitious material. The present study aimed to explore the compressive strength, split tensile strength, and flexural strength of concrete. Based on the findings reported in this research, it is possible to infer the following conclusions.

1. The compressive strength, split tensile strength, and flexural strength of concrete are negatively affected by the elevated temperature of 1200° C. This is due to the drying process that occurs, resulting in the hardening of the cement paste. Consequently, the link between cementitious elements is weakened, leading to a reduction in strength.
2. The findings indicate that the use of GGBS in concrete has resulted in a notable enhancement in strength when 20% of the cement is replaced with a GGBS. The observed enhancement in strength can be attributed to the heightened reactivity between GGBS and cement, as well as the filling effect exerted by GGBS.
3. The reduction in strength is greater when 60% of cement is replaced by a GGBS, as compared to other combinations. This can be attributed to the delayed reactivity of GGBS during the early stages of curing.
4. As the temperature and exposure time increase, the impact of elevated temperature on concrete becomes more pronounced.
5. At higher temperatures, the concrete exhibits increased brittleness and has a greater decline in strength.
6. The utilization of GGBS as a substitute for cement contributes to the mitigation of energy consumption during the cement manufacturing process.
7. The reutilization of slag contributes to environmental protection by mitigating pollution, namely reducing CO₂ emissions, and also aids in the conservation of natural resources.

ACKNOWLEDGMENT

It was a great privilege to conduct this research under the guidance of Dr. Valsson Varghese and Prof. V. D. Vaidya. I am grateful for his unwavering support, guidance, and encouragement.

REFERENCES

1. Q. Li, Z. Li, and G. Yuan, "Effects of elevated temperatures on properties of concrete containing ground granulated blast furnace slag as cementitious material," *Constr. Build. Mater.*, vol. 35, pp. 687–692, 2012, doi: 10.1016/j.conbuildmat.2012.04.103.

2. R. Kumar, A. K. Samanta, and D. K. S. Roy, "Characterization and development of ecofriendly concrete using industrial waste –A review," *J. Urban Environ. Eng.*, vol. 8, no. 1, pp. 98–108, 2014, doi: 10.4090/juee.2014.v8n1.098108.
3. R. K. Pareek and V. Singh, "Utilization of Ground Granulated Blast Furnace Slag to Improve Properties of Concrete," *Int. J. Emerg. Technol.*, vol. 6, no. 2, pp. 72–79, 2015.
4. V. Awasare and M. V Nagendra, "Analysis of strength characteristics of GGBS concrete," *Int. J. Adv. Eng. Technol. E- Int J Adv Engg Tech V/Issue II*, vol. 12, no. 4, pp. 82–84, 2014.
5. A. Dubey, R. Chandak, and P. R. K. Yadav, "Effect of blast furnace slag powder on compressive strength of concrete," *Int. J. Sci. Eng. Res.*, vol. 3, no. 8, pp. 1–5, 2012.
6. C. Garg and A. Khadwal, "Behavior of Ground Granulated Blast Furnace Slag and Limestone Powder as Partial Cement Replacement," *Int. J. Eng. Adv. Technol.*, no. 6, pp. 2249–8958, 2014.
7. P. P. Saklecha, R. S. Kedar, and A. Professor, "Review on Ground Granulated Blast-Furnace Slag as a Supplementary Cementitious Material," *Int. J. Comput. Appl.*, pp. 975–8887, 2015.
8. K. Lal and J. A. Professor, "To effect on strength properties of concrete of by using GGBS by Partial Replacing cement and addition of GGBS without replacing cement," *SSRG Int. J. Civ. Eng.*, vol. 3, no. 5, pp. 116–120, 2016, [Online].
9. IS 12269-2013 "Ordinary Portland cement 53 grade-specification", Bureau of Indian Standards, New Delhi.
10. IS 383-2016 "Coarse and fine aggregates for Concrete-Specification", Indian Standards, New Delhi.
11. IS 12089-1987 "Specification for Granulated Slag for Manufacture of Portland cement", Bureau of Indian Standards, New Delhi, India.
12. IS 10262-2019 "Concrete Mix Proportioning-Guidelines", Bureau of Indian Standards, New Delhi.
13. IS 516-1959 "Methods of Tests for strength of concrete", Bureau of Indian Standards, New Delhi.
14. IS 5816-1999, "Splitting Tensile Strength of Concrete Method of Test", Bureau of Indian Standards, New Delhi.

Evaluation of Seismic Performance of Silo Supporting Structure for Joint Rotation Requirements as per IS 800:2007

Bhavinkumar Shah

Vijay Panchal

M.S. Patel Department of Civil Engineering
Chandubhai S. Patel Institute of Technology Charotar
University of Science and Technology (CHARUSAT),
CHARUSAT Campus, Changa
✉ bhavin@sqveconsultants.com

ABSTRACT

For design of the industrial steel structures, generally, first order elastic analysis or second order elastic analysis is performed. However, during the seismic event the actual displacement in the structure may be significantly higher as compared to the analytical results. Accordingly, the current approach in IS 800:2007 for special concentrically braced frames is to ensure that joints should be shown to withstand rotation of 0.04 rad and the frame should be able to withstand corresponding inelastic displacement without degradation in strength and stiffness below the full yield value. To achieve high value of joint rotation as 0.04 rad, the connected members at a joint should be able to withstand the rotation. For heavy industrial steel structures, conventional brace (CB) is one of the most popular structural systems. Buckling restrained brace (BRB) are not yet explored extensively for the heavy industrial steel structures. In the present study, seismic performance of CB & BRB frames of silo supporting steel structure are compared with reference to the joint rotation requirements. Nonlinear static analysis is performed for total 16 nos. of frames to derive the maximum feasible joint rotation in each frame. The maximum joint rotation observed for BRB frames is approximately 2.7 times greater than the maximum joint rotation achieved for CB frames. However, practically, it is very difficult to achieve the joint rotation of 0.04 rad for braced frames. Therefore, it is suggested to relook in to the provision of the IS code.

KEYWORDS : Earthquake resistant design, Silo supporting steel structures, Joint rotation, Conventional brace, Buckling restrained brace.

INTRODUCTION

India had witnessed major earthquakes in the past and likely to face even higher intensity of the earthquakes in the future. The Indian plate is subducting below the Eurasian plate and the entire contact region between two plates are vulnerable to earthquakes. Himalaya is one of the most seismically active international regions of the world [1]. Global tectonics plate reconstruction data suggests that the NE moving Indian plate is obliquely converging with the Eurasian plate at 54mm/year [2]. GPS observations between Bangalore and Port Blair (capital of Andaman Nicobar Islands) suggest that the Indian plate is approaching the Burmese plate at a rate of 15.3 mm/year [3]. Sukhija et. al. (1999) reported the result of paleo-liquefaction evidence on the periodicity

of large pre- historic earthquake in shillong region. The finding for shillong plateau suggested a recurrence interval of around 400-600 years. India has already witnessed major earthquake ($M_w > 7$) in Himalaya region, near Andaman and near Kutch. The peninsular India was earlier considered to be “seismically safe”. But, large earthquakes M6.2 Killari (1992), M6.6 Koyna (1967) & M 5.8 – Jabalpur (1997) have proven it wrong. With this, the industrial structures are highly vulnerable in India, as they are highly irregular. The irregularity in the industrial structures arise to meet the different functional requirements which leads to uneven distributions of mass and stiffness in the structures. As per IS code provisions there are couple of stringent requirements to be satisfied for the industrial steel structures along with the other details mentioned in the

design standards. Firstly, section 12 of IS800:2007, require that Special Concentrically Braced Frames (SCBF) to be used in seismic zones 4 & 5. As per the code, SCBF should be shown to withstand inelastic deformation corresponding to a joint rotation of 0.04 radians without degradation in strength and stiffness below the full yield value [5]. Secondly, IS 1893 (Part 4) : 2015 require that non-linear analysis of structures shall be performed to verify the collapse mechanism [6]. The requirement of joint rotation for braced frames along with verification of the collapse mechanism is not yet addressed appropriately in the different researches. Aim of the present research it to evaluate performance of conventional braces (CB) and buckling restrained braces (BRB) with reference to joint rotation requirements of the design standard.

One of the examples of such industrial structure is silo supporting steel structure which is required in Fuel Gas Desulfurization (FGD) package. FGD packages are required in the existing thermal power plants to reduce or remove sulphur from the flue gases after the combustion process to meet environmental requirements [7]. There is significant amount of mass irregularity in the silo supporting structure. Generally, CB is most popular structural system for the silo supporting steel structure. In the present study, performance of CB and BRB frames are compared with reference to joint rotation requirements of the code. Two different types of brace arrangements are considered. Total 16 nos. of frames are analysed accordingly. BRB frames are not yet fully explored for heavy industrial steel structures in India. For BRB, the axial load carrying capacity is almost similar in compression and tension. In fact, the compression carrying capacity is bit higher due to friction between debonding gap material and high strength mortar [8]. With this, the seismic demand on the structure will reduce as the yielding cross section area of BRB member will be lesser than CB.

In the following section, BRB is reviewed with reference to earthquake resistant design.

REVIEW OF BUCKLING RESTRAINED BRACE

BRB was invented due to basic limitation of steel brace which is very less compressive force carrying capacity as compared to the tension force, mainly due

to buckling under compressive load. Because of the same, the conventional steel brace does not exhibit the symmetric hysteresis. BRB also known as unbonded brace having the major components as steel core, restrainer, & debonding material/gap. Steel core is the main component resisting the axial load. The function of restrainer is to prevent buckling of the steel core in the lower modes. Generally, the restrainer is filled up with high strength mortar. The filled mortar serves as an elastic spring which restrains low mode buckling of the steel core [9]. Debonding material/gap is vital for ensuring poisson's effect in the steel core, i.e. allowing expansion and contraction of steel core which is independent of the restrainer. The steel core will be connected to the gusset plate through transition piece which is non yielding and also known as neck since there is a possibility of rotation or global buckling of BRB at the neck location. To achieve similar capacity in compression, debonding gap between core steel member and mortar results in range of 1mm to 3mm [10]. The higher debonding gap than designed gap would result in the lesser compressive capacity as compared to the tensile force. Hence, the strict fabrication control is required while manufacturing BRB. In certain cases, the BRB are also used as Buckling Restrained Columns (BRC) [11].

The following shows overall design philosophy for BRB [8]:

- Restrainer doesn't allow first mode flexural buckling of core.
- Debonding mechanism to allow for poisson's effect of steel core
- Higher mode of buckling of steel core should not result in to bulging of restrainer wall
- Global out of plane stability to be ensured including connections.
- Low cycle fatigue capacity should be sufficient for the expected demand.

Numerous experiments were conducted on BRB across the world and still number of experiments are in progress for further improvement of BRB. Few of the experiments are mentioned below for reference.

Tsai et al. (2004) conducted full scale study on different types of debonding materials. In-plane local bulging failure & out of plane bulging failure for BRB was investigated ([13], [14]). Takeuchi et al. (2013) performed experiments to study the global buckling of BRB. Matsui et al. (2008) performed experiments and found that restrainer specimen having diameter-to-thickness ratio 65 buckled locally and the specimens having diameter-to-thickness ratio of 25 did not buckle. Chen et al. (2004) added stiffeners during testing of full scale BRB which prevented out of plane buckling of the gusset connection with beam-column. Koetaka et al. (2008) defined the stiffness requirements of the connection as well as of the girder (where BRB is connected) to prevent out of plane buckling of BRB and to ensure that it achieves its full strength. Hikino et al. (2013) performed large scale shake table tests for BRB placed in chevron arrangement. BRBs having transition segment embedded in the restrainer by 1.5 times the depth of yielding section did not buckle and exhibited the excellent seismic behaviour. Takeuchi et al. (2013) studied and proposed restrainer moment transfer capacity for different types of connections and the same were checked with full scale BRB test. Takeuchi et al. (2013) proposed the concept of spine frame for controlling the residual drifts which is popular for tall buildings. Wang et al. (2019) evaluated Damage Concentration Effect (DCE) on high rise structures using numerical analysis and it is observed for the considered examples that structures with BRBs will have higher DCE as compared to the CB or Moment Resisting Frames. Hence, it is suggested that for the structures having BRBs, DCE should be considered in the design. Li et al. (2019) has proposed variable cross section BRB, termed as BRB-VCC. Six BRB-VCC specimens were tested and mathematical formulae are suggested for design of the braces. Chen and Lou (2019) critically evaluated full scale testing requirements of BRB with different connection types of welded, bolted and pinned. Hoveidae (2019) has proposed hybrid BRB having different material for core (stainless steel) and restrainer (steel). Shah and Panchal (2022) listed down few of the areas wherein more researches are required for effective use of BRB. The same may be also helpful for codification in the country. Following section shows the geometry and property considered for the study.

GEOMETRY & PROPERTY CONSIDERED FOR CB AND BRB FRAMES

The weight of silo is considered as approximately 6300 KN (including self weight of the silo and lime stone filled up to the full capacity of silo) supported at 20m height. Plan dimension of the structure is considered as 10m X 10m with storey height of 4m each. 3D models are generated for different frames. The sizes of the columns are derived using conventional process of analysis and design. Due to presence of heavy loading, the built-up columns are provided. Also, to avoid formation of plastic hinge at support location of the silo, larger sizes of main beam and brace is considered in the top storey of the structure. With this, the plastic hinges will be generated initially in the lower braces. For all the frames, sizes of columns, beam at silo supporting level and brace in top storey are kept constant. Fig. 1 shows elevation view of the silo supporting structure with Type-A brace arrangement.

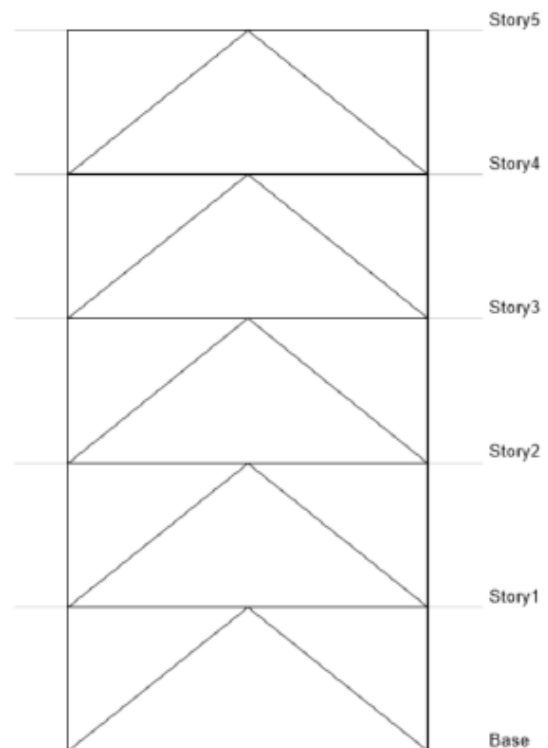


Fig. 1: Elevation view of Silo supporting steel structure (TYPE-A brace arrangement)

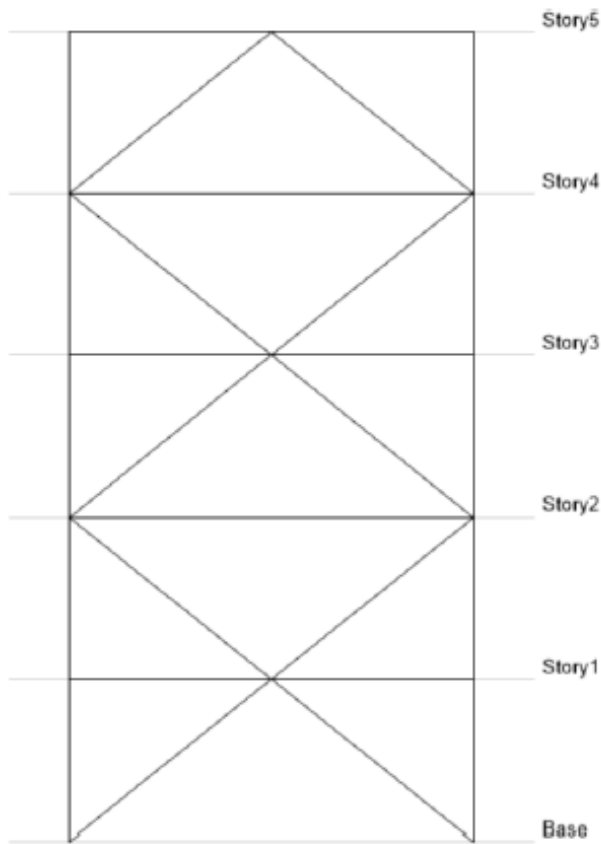


Fig. 2: Elevation view of Silo supporting steel structure (TYPE-B brace arrangement)

In the study, for braces in the lower storeys, size, type and arrangement are varied. In each frame, size and type of brace are considered as identical from 1st storey to 4th storey. Table 1 shows sizes of the braces in the lower storeys for CB & BRB frames. In the present study, properties of COREBRACE manufacturer are considered. For all steel members, tensile yield strength is defined as 250 N/mm² and ultimate tensile strength is considered as 410 N/mm².

Table 1: Sizes of the Braces from 1st Storey to 4th Storey

No.	Sizes of the braces from 1st storey to 4th Storey		
	Section name	Cross sectional area (cm ²)	Type of frame
1	UC203X203X86.1	109.6	CB

2	UC254X254X107.1	136.4	CB
3	UC305X305X117.9	150.2	CB
4	UC305X305X240	305.8	CB
5	BRB-8	51.61	BRB*
6	BRB-9	58.1	BRB*
7	BRB-10	64.5	BRB*
8	BRB-11	71	BRB*

* For BRB frames, cross-section area is mentioned for the yielding core

METHODOLOGY AND IMPORTANT ASSUMPTIONS

Following shows important assumptions and methodology for the analysis:

- For mass calculation, the load from silo and self-weight of structure is considered. Mass at intermediate floors is ignored as relatively it is very small value. Total mass from the silo is lumped at the point of support location.
- Support condition is considered as pinned at bottom of the structure.
- For the analysis, commercial software ETABS (version 19.1.0) is used.
- Nonlinear properties of I sections & conventional brace are considered as per ASCE 41-17 [26] which are automatically calculated from the software based on section properties. For columns, two hinges are assigned at top and bottom. For beams, two hinges are assigned at start and end of the beam. For CB, the hinge is assigned to a center of the bracing.
- BRB is modelled as a single line element having two nodes at ends. The moments are released at the ends so that only axial forces can be transferred to BRB. The cross-sectional area of the BRB is considered as yielding steel core area (A_c) for the entire length of the member in the analytical model.
- BRB is having mainly three components as yielding steel core region, transition region and elastic region. In the analytical model, BRB is modelled as a single line member from working point to working point having uniform cross sectional area

equal to yielding steel core area. To account for the stiffness from transition region and elastic region, stiffness modification factor of 1.4 is considered in the software [27].

- For nonlinear analysis, formation of hinge is considered at center of the BRB and degree of freedom is considered as only axial compression and tension force. In the present study, the backbone curves of the BRB manufacturer which are available in the software are used for nonlinear analysis of BRB system.
- Nonlinear static (pushover) analysis is performed to observe behaviour of the structure beyond elastic limit for all frames. In this analysis, the frames are pushed in the horizontal direction considering the earthquake load pattern and restricting the maximum displacement at top of the structure as 300mm or the collapse mechanism whichever is reached earlier. To consider P-delta effect in nonlinear static analysis, firstly, nonlinear static analysis is carried out for the load combination for gravity load (self weight + vertical load from silo). For pushover analysis, state of the structure based on gravity load is considered as an initial condition as shown in Fig. 3.

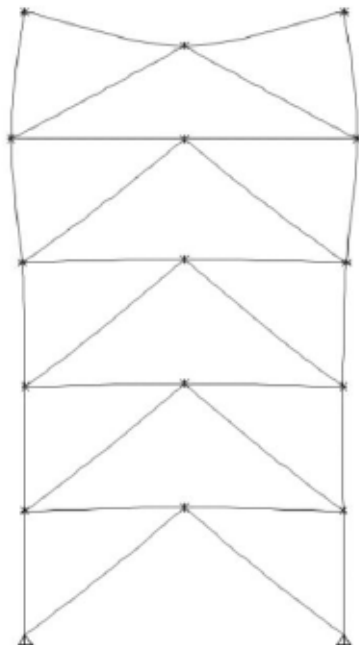


Fig. 3: Initial conditions considered for Push Over analysis

- Performance level is restricted as Life Safety for all frames based on ASCE 7-16 [27].

RESULTS AND DISCUSSIONS

Non-linear static analysis is performed for all the frames wherein the frames were pushed in the horizontal direction with maximum displacement of 300mm at top of the structure. All the frames reached performance level of life safety before reaching the displacement of 300mm at top of the structure. Performance level of life safety (LS) is measured based on plastic deformation in the braces, in line with the limits specified in ASCE 7-16. Fig. 4 & Fig. 5 shows typical deformation shape of CB & BRB frames respectively when the performance level of LS is reached. As shown in Fig. 4, for CB frames non-linear hinges are generated only in couple of braces wherein buckling capacity of the brace is reached. However, for BRB frames, as shown in Fig. 5, non-linear hinges are well distributed in the lower storey braces.

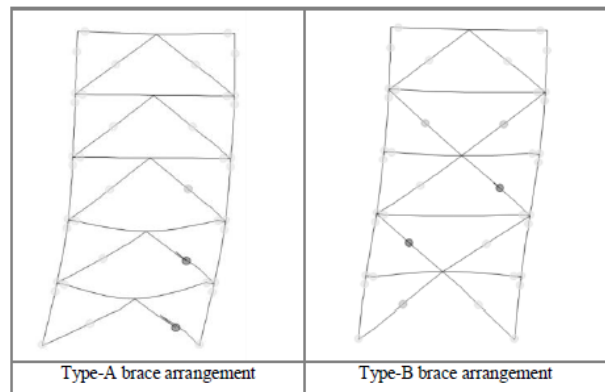


Fig. 4: Deformation of CB frame with brace size of UC203X203X86.1

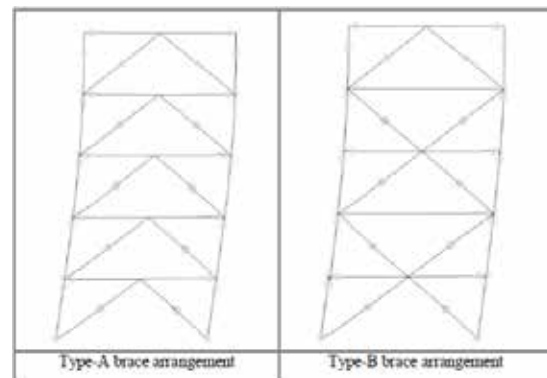


Fig. 5 Deformation of BRB frame with brace size of BRB-8

Joint rotation of all the frames were observed when performance level of LS was reached. Maximum joint rotation observed between 1st storey to 5th storey are summarised below.

TABLE 2 shows maximum joint rotation obtained for CB frame with Type-A brace arrangement. The maximum joint rotation was observed at 1st storey. Maximum joint rotation obtained is 0.0054 rad for brace size of UC305X305X117.9. For brace size, UC305X305X240, results are not mentioned since the initial plastic hinges were generated in the column which is not acceptable.

Table 2: Joint Rotation for CB Frames with Type-A Brace Arrangement

No.	For Type-A brace arrangement		
	Section name	Joint rotation at 1st storey (radians)	Type of frame
1	UC203X203X86.1	0.0043	CB
2	UC254X254X107.1	0.0047	CB
3	UC305X305X117.9	0.0054	CB
4	UC305X305X240	**	CB

** Collapse mechanism is not desired.

Table 3 shows the maximum joint rotation observed for CB frames with Type-B brace arrangement. The maximum joint rotations are observed at 2nd storey. The maximum joint rotation is observed for the brace size of UC305X305X117.9 as 0.0046 rad. For brace size, UC305X305X240, results is not mentioned since the initial plastic hinges were generated in the column which is not acceptable. The joint rotation obtained with Type-A brace arrangement is nearly 17% higher than Type-B brace arrangement.

Table 3: Joint Rotation for CB Frames with Type-B Brace Arrangement

No.	For Type-B brace arrangement		
	Section name	Joint rotation at 2nd storey (radians)	Type of frame
1	UC203X203X86.1	0.0039	CB
2	UC254X254X107.1	0.0043	CB
3	UC305X305X117.9	0.0046	CB
4	UC305X305X240	**	CB

** Collapse mechanism is not desired.

Table 4 shows maximum joint rotation values for BRB frames with Type-A brace arrangement. The maximum joint rotation is observed as 0.0151 rad for brace size of BRB-10.

Table 4: Joint Rotation for BRB Frames with Type-A Brace Arrangement

No.	For Type-A brace arrangement		
	Section name	Joint rotation at 1st storey (radians)	Type of frame
1	BRB-8	0.0145	BRB
2	BRB-9	0.0149	BRB
3	BRB-10	0.0151	BRB
4	BRB-11	0.015	BRB

Table 5 shows maximum joint rotation values for BRB frames with Type-B brace arrangement. The maximum joint rotation is observed as 0.0136 rad for brace size of BRB-10.

Table 5: Joint Rotation for BRB Frames with Type-B Brace Arrangement

No.	For Type-B brace arrangement		
	Section name	Joint rotation at 1st storey (radians)	Type of frame
1	BRB-8	0.013	BRB
2	BRB-9	0.0135	BRB
3	BRB-10	0.0136	BRB
4	BRB-11	0.0133	BRB

BRB frames withstand higher values of joint rotation as compared to CB frames. Type-A brace arrangement reported higher values of joint rotation for both type of frames. For CB frames, the maximum joint rotation obtained was only 0.0054 rad which is significantly lower than the requirement of 0.04 rad as per IS 800:2007. It is observed that by increasing size of the brace for CB frames joint rotation increases. However, when the braces in the lower storey will become relatively stiffer than columns, then the initial plastic hinges will be generated in the column which is not desirable collapse mechanism. For BRB frames, the maximum joint rotation observed is nearly 2.7 times higher than the joint rotation values of CB frames. For BRB frames, still the desired collapse mechanism can be achieved by

increasing the size of the brace beyond BRB-11. With increase in size of BRB, the value of joint rotation will increase. However, it appears as practically difficult to achieve joint rotation of 0.04 rad even for BRB frames. As it is observed in the study that the structural systems with the bracing arrangement for resisting lateral loads is relatively rigid system. Therefore, to achieve joint rotation value of 0.04 rad is extremely difficult. It is suggested that the code requirement related to joint rotation for special concentrically braced frames to be revisited.

CONCLUSIONS

India witnessed major earthquakes in the past and it is likely that even higher intensity of the earthquakes may strike in future. Earthquake resistant design of industrial steel structures is very crucial since the failure of the structure may cause loss of lives, interruption of the emergency services or substantial financial losses. IS 800:2007 requires that the special concentrically braced frames should achieve joint rotation of 0.04 rad before reaching the collapse mechanism. In the study, silo supporting steel structure was analysed with conventional braces (CB) and buckling restrained braced frames (BRB) having type-A and type-B brace arrangements. Total 16 frames are analysed and values of maximum joint rotations are observed at the verge of reaching the performance of life safety. It is observed for CB & BRB frames that the structures are relatively rigid with bracing arrangement of Type-B as compared to the bracing arrangement of Type-A. Based on the results of the study, CB frame could achieve the maximum joint rotation of only 0.0054 rad as against the maximum value of 0.015 rad for BRB frames. For CB frames, it is impossible to achieve the joint rotation of 0.04 rad because the collapse mechanism will reach well before reaching the required value of joint rotation. If we increase the lower brace size significantly (as in case of UC305X305X240) then the initial plastic hinges will be generated in the column which is not desirable. Cross section area of BRB is ~2.3 times lesser which resulted in ~2.7 times of more joint rotation as compared to CB frame. BRB frames still can achieve, the larger values of joint rotation by increasing the sizes of the braces in lower storeys. However, it appears as practically difficult to achieve the joint rotation of 0.04 rad even with BRB frames. It is suggested that the requirement

of joint rotation in IS 800:2007 of 0.04 rad for special concentrically braced frames shall be revisited. Either the required joint rotation values may be reduced or the same may be removed from the design standard. The similar exercises may be carried out for the other irregular industrial structures such as pipe rack, equipment supporting structure, etc. BRB appears as a good alternative to CB for the industrial steel structures. The same should be explored further for the earthquake resistant design of industrial structures in India.

REFERENCES

1. Malik, J.N., Shah, A.A., Sahoo, A.K., Puhan, B., Banerjee, C., Shinde, D.P., Juyal, N., Singhvi, A.K. and Rath, S.K. (2010), 'Active fault, fault growth and segment linkage along the Janauri anticline (frontal foreland fold), NW Himalaya, India', *ELSEVIER – Tectonophysics* 483 (2010), pp 327-343.
2. DeMets, C., Gordon, R. G., Argus, D. F., & Stein, S. (1994). Effect of recent revisions to the geomagnetic reversal time scale on estimates of current plate motions. *Geophysical Research Letters*, 21(20), 2191-2194. <https://doi.org/10.1029/94GL02118>
3. Paul, J., Bürgmann, R., Gaur, V. K., Bilham, R., Larson, K., Ananda, M. B., Jade, S., Mukul, M., Anupama, T. S., Satyal, G., and Kumar, D., (2001). The motion and active deformation of India, *Geophysical Research Letters* 28, 647–651.
4. Sukhija, B.S., Rao, M.N., Reddy, D.V., Nagabhushanam, P., Hussain, S., Chadha, R.K., and Gupta, H. K. (1999), 'Paleoliquefaction evidence and periodicity of large prehistoric earthquakes in Shillong Plateau, India', *Earth Planet. Sci. Lett.*, 199, 167, pp 269-282.
5. Bureau of Indian Standards (2007) IS 800 : 2007 : Indian Standard – General construction in steel – Code of practice, New Delhi, BIS.
6. Bureau of Indian Standards (2015) IS1893 (Part-4) : 2015 : Indian Standard – Criteria for earthquake resistant design of structures – Part 4 Industrial structures including Stack-like structures, New Delhi, BIS.
7. Butalia, T. S., Wolfe, W., Amaya, P. (2017), "The utilization of flue- gas desulfurization materials", DOI: <https://doi.org/10.1016/B978-0-08-100945-1.00006-X>
8. Takeuchi, T. and Wada, a. (2017), "Buckling-Restrained Braces and Applications", 1st ed., The Japan Society of Seismic Isolation.

9. Watanabe, A., Hitomi, Y., Saeki, E., Wada, A., Fujimoto, M. (1988), "Properties of brace encased in Buckling-Restraining concrete and steel tube", Paper presented at Proceedings of Ninth World Conference on Earthquake Engineering, August 2-9, 1988, Tokyo-Kyoto, Japan (Vol. IV)
10. Takeuchi, T. (2018), "Buckling restrained brace : History, Design and Applications", Paper presented at 9th International Conference on Behavior of Steel Structures in Seismic Areas, 14-16 February 2018, Christchurch, Newzealand.
11. Bruneau, M., Uang, C. and Sabelli, R. (2011), 'Ductile design of steel structures', McGraw- Hill, New York, NY.
12. Tsai, K.C., Lai, J.W., Hwang, Y.C., Lin, S.L. and Weng, C.H. (2004), "Research and application of double-core buckling restrained braces in Taiwan". Paper presented at 13th World Conference on Earthquake Engineering, August 1-6, 2004, Paper No. 2179, Vancouver, B.C., Canada
13. Takeuchi, T., Hajjar, J.F., Matsui, R., Nishimoto, K. and Aiken, I.D. (2010), 'Local buckling resistant condition for core plates in buckling restrained braces', Journal of Constructional Steel Research, 2010, 66(2), pp 139-149.
14. Lin, P.C., Tsai, K.C., Chang, C.A., Hsiao, Y.Y. and Wu, A.C. (2016), 'Seismic design and testing of buckling-restrained braces with a thin profile', Earthquake Engineering and Structural Dynamics, 2016, 45(3), pp 339-358.
15. Takeuchi, T., Ozaki, H., Matsui, R., and Sutcu, F. (2013), 'Out-of- plane stability of buckling-restrained braces including moment transfer capacity', Earthquake engineering & Structural Dynamics (2013). Published online in Wiley Online Library (wileyonlinelibrary.com). DOI: 10.1002/eqe.2376
16. Matsui, R., Takeuchi, T., Hajjar, J.F., Nishimoto, K. and Aiken, I. (2008), "Local buckling restrained braces", Paper presented at the 14th world conference on earthquake engineering, 12-17, October, 2008, Beijing, China.
17. Chen, C.H., Hsio, P.C., Lai, J.W., Lin, M.L., Weng, Y.T., and Tsai, K.C. (2004), "Pseudo-dynamic test of a full-scale CFT/BRB frame : Part 2 – Construction and testing", Paper presented at 13th World Conference on earthquake engineering, Paper no. 2175, 1-6 August, 2004, Vancouver, B.C., Canada.
18. Koetaka, Y., Kinoshita, T., Inoue, K., and Iitani, K. (2008), "Criteria of buckling-restrained braces to prevent out-of-plane buckling". Proceedings of 14th World Conference on Earthquake Engineering, October 12-17, 2008, Beijing, China
19. Hikino, T., Okazaki, T., Kajiwar, K. and Nakashima, M. (2013), "Out-of-Plane Stability of Buckling-Restrained Braces Placed in Chevron Arrangement", American Society of Civil Engineers, Vol. 139, No. 11, November 1, 2013, DOI: 10.1061/(ASCE)ST.1943-541X.0000767
20. Takeuchi, T. & Wada, A. (2018), "Review of Buckling-Restrained Brace Design and Application to Tall Buildings", International Journal of High-Rise buildings, September 2018, Volume 7, Number 3, pp 187-195.
21. Wang, H., Feng, Y., Wu, J., Jiang, Q. and Chong, X. (2019), "Damage Concentration Effect of Multistory Buckling-Restrained Braced Frames". Hindawi, Advances in Civil Engineering, Volume 2019, Article ID 7164373, 15 pages, <https://doi.org/10.1155/2019/7164373>
22. Li, L., Zhou, T., Chen, Junwu., and Chen, Jianfeng (2019), "A New Buckling-Restrained Brace with a Variable Cross-Section Core Advances in Civil Engineering", Hindawi, Advances in Civil Engineering, Volume 2019, Article ID 4620430, 15 pages <https://doi.org/10.1155/2019/4620430>
23. Chen, W. and Lou, G. (2019), IOP Conference Series.: Earth and Environmental Science 304 032027, IOP Publishing doi:10.1088/1755- 1315/304/3/032027
24. Hoveidae, N. (2019), 'Numerical Investigation of Seismic Response of hybrid Buckling Restrained Braced Frames', Periodica Polytechnica Civil Engineering, vol. 63, no. 1, pp. 130-140, <https://doi.org/10.3311/PPci.12040>
25. Shah, B. S. and Panchal, V. R., "Review of buckling restrained braces for earthquake resistant design of industrial structures in India", Int. J. Structural Engineering, Vol. 12, No. 1, 2022.
26. American Society of Civil Engineers (2017) ASCE 41-17, Seismic evolution and retrofitting of existing buildings, Virginia, America. www.asce.org/bookstore | ascelibrary.org.
27. American Society of Civil Engineers (2016) ASCE 7-16, Minimum Design Loads and Associated Criteria for Buildings and Other Structures, Virginia, America. www.asce.org/bookstore | ascelibrary.org.

Comparison of PCU Values in Mixed Traffic by Different Methods at Low Volume Road

Gulshan Chauhan

Civil Engineering Department
Gujarat Technological University
✉ gulshanchauhan63550@gmail.com

Tripathi Bishnukumar B

Shri K J Polytechnic
Bharuch Bolav, Bharuch
Gujarat

ABSTRACT

The developing country like India has mixed traffic, the composition of road traffic is heterogeneous. As per Indo-HCM (2018) we have ten class of motorized vehicle and three classes of non-motorized vehicles. The traffic flow is simply measure in vehicles or vehicles/hr, this does not provide any meaning unless we mention type of vehicles for that, in order to fill this gap there is term called PCU or PCE, since different type of vehicle have different characteristics like speed, weight, dimension etc. In India, we have ten class of motorized vehicle and three classes of non-motorized vehicles are specified in Indo- HCM (2018). In this paper, PCU values are calculated by using three methods, which are speed based from the literature. The first method, Chandra method based on speed and area of vehicle type. The second method speed ratio based on space mean speed of vehicles. The third method homogenization coefficient method based length and speed of the vehicle, the By considering Chandra method as standard method PCU values are compare for each vehicle type with Indo-HCM, 2018 values. The results shows the PCU values are within limits of Highway Capacity Manual, 2018, while other methods values varying differentially. Data is collected manually from the field by using license plate survey technique and classified volume count for six hours for three days at state highway of Bharuch.

KEYWORDS : PCU, Speed-Ratio method, Chandra method, Homogenization coefficient method.

INTRODUCTION

Road Traffic in developing nations like India, Bangladesh etc has to gratify to the needs of a different types of vehicles. The difference in vehicle is not the how they drive but also their variation in their dimensions, weight and power. Due to this reason a challenge has been created for traffic engineers to give them a mathematical form and also estimating the capacity of a facility. Thus it became necessary to convert this heterogeneous or mixed traffic mixture to a homogeneous one. This can be done by multiplying the volume of each vehicle type by a corresponding factor termed as Passenger Car Unit (PCU).

The homogeneous and mixed traffic shows the complications in execution of traffic operations and designing roads. To overcome this, a uniform measure of vehicle called passenger car unit (PCU), also

known as passenger car equivalent (PCE) is used for converting traffic stream composed of two or more vehicle types into an equivalent traffic stream consists of passenger cars only. The Highway Capacity Manual (Highway Research Board, 1965) first defined PCU as “the number of passenger cars displaced in the traffic flow by a truck or a bus, under the prevailing roadway and traffic conditions.” Indian Roads Congress (IRC 1990) suggests static PCUs for different vehicle types in India based on traffic composition. INDO-HCM (2018) defines PCU as, ‘It is the amount of interaction (impedance) caused by the vehicle to the traffic stream with respect to standard passenger car. It is used to convert a heterogeneous traffic stream into a homogeneous equivalent to express flow and density in a common unit’. PCU factors estimation used different performance measures like average speed, modified density, area occupancy, headway, flow rate, time

occupancy etc. Thus, for accuracy of PCU values the selection performance measures is very important.

Variables used in estimation of PCU for different roadway facility types are different under homogeneous and mixed traffic. For homogeneous traffic, researchers have used several parameters such as speed (e.g., Aerde and Yagar 1984), headway (e.g., Greenshields et al. 1947), density (e.g., Huber 1982), delay (e.g., Craus et al. 1980), travel time (e.g., Keller and Saklas 1984), and queue discharge flow (QDF) (e.g., Al- Kaisy et al. 2002). Besides these parameters, for mixed traffic, Chandra et al. (1995) developed an equation considering speed-area ratio to estimate PCUs for different vehicle types. Other parameters such as density (e.g., Tiwari et al. 2000), queue discharge (e.g., Mohan and Chandra 2017), headway (e.g., Saha et al. 2009), area occupancy (e.g., Kumar et al. 2017), time occupancy (e.g., Mohan and Chandra 2018), influence area (e.g., Paul and Sarkar 2013), effective area (e.g., Pooja et al. 2018).

The review from the past revealed that many people had work on PCU values in Indian context but low volume roads or rural roads are not at par. So this paper presents three methods to derive PCU values of SH-6 road from Bharuch to Ankleshwar. All this three methods use speed as performance measure. Detailed explanation of these methods is given in different sections of this paper.

METHODOLOGY

This paper discusses three different approaches to estimate PCU in Indian Traffic Condition.

Based on Speed-Area Ratio (Chandra Method): For the present study the PCU values were estimated by using the Equation (1) which was introduced by Chandra and Kumar (2003).

$$PCU_i = \frac{V_c/V_i}{A_c/A_i}$$

PCU_i = Passenger Car Unit of ith Vehicle

Where, V_c = mean speed of standard passenger car

V_i = Mean speed of ith vehicle

A_c = Projected Area of Standard Passenger Car A_i = Projected Area of ith Vehicle type

Length, Width and Projected Area is used in this study is as given in Indo-HCM, 2018.

Speed Ratio Method

Patil and Adavi (2015) estimated PCUs for urban midblocks in Pune, India using mean speed ratio of passenger cars to any vehicle class using the following equation Eq. 2.

$$F_u = \frac{U_c}{U_v}$$

where Fu = PCU factor for speed of vehicle class v; U_c = mean speed of car c; and U_v = mean speed of the vehicle class v.

Homogenization coefficient method

Permanent International Association of Road Congress (PIARC) proposed a model to determine ‘Homogeneous Coefficient’ (or PCU) of a vehicle category present in a mixed traffic stream. The speed, as well as the length of a vehicle, were considered to formulate the Homogeneous Coefficient (HC_i) as given in Eq. (3).

$$HC_i = \frac{L_i/V_i}{L_c/V_c}, \text{ Where}$$

L_i = length of vehicle ‘i’ (m)

V_i = average speed of vehicle ‘i’ (km/h)

L_c = length of passenger car (m)

V_c = average speed of passenger car (km/h)

DATA COLLECTION AND EXTRACTION:

The SH-6 (Bharuch-Ankleshwar) at Narmada Maiya bridge was selected for data collection. The road is state highway four-lane divided carriage with median 1.2m and road width 7m both the side along with paved shoulders 0.5m. Data were collected on a weekday through license plate survey for three days (i.e. Tuesday, Wednesday and Thursday) while classified volume count is done in a day. The length of bridge is 5 kms including both approaches Surat end and Bharuch end Figure 1 shows the road stretch selected for the present

study. The effect of upgrade and downgrade is not considered here. Total six hours for two days of survey has been done by 3 hours in morning and evening to get proper sample size in order to calculate space mean speed of each type of vehicle, where as length and width of vehicle type are taken from Indo-HCM, 2018 for this study. In this section of road there exists two points diverging and merging whose effect is ignored. During survey the vehicle enter from approach bharuch end and exit on approach Surat end is considered. During one hour 30 to 40 observations were made in license plate survey.

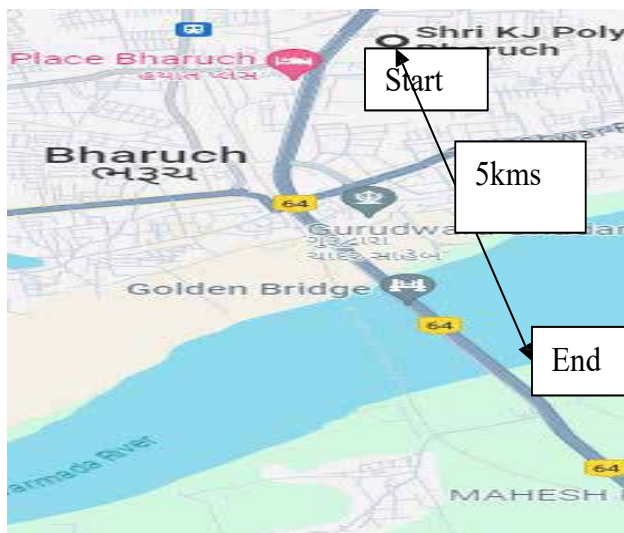


Figure1: Narmada Maiya Bridge

For each vehicle type start time is recorded with license plate number and stop watch, message is conveyed to other recorder with the help of Whatsapp or text message.. For each type difference of time is recorded. Spot speed is calculated by distance by time taken by the vehicle. Thereafter mean speed is calculated. Traffic composition shows (Table:1) 2W and 4W as major vehicle type while 3W is relatively less and LCV, BUS are very less, other Motorized class such as mini- bus, truck, tractor, van etc and Non-motorized class like bicycle, pedal rickshaw, pedestrian etc. are in very negligible in composition so they are not included in this work. The no of 2W and 4W is high and Heavy Vehicles are very negligible since they are not allowed in numbers. 3W and Bus are very low as per traffic composition. The following Table1 show the details of traffic composition of study area.

Table 1 :Traffic Composition At Selected Road

Morning, Traffic Composition in Percentage					
Vehicle Type	2W	3W	4W	LCV	BUS
Hour-1(8am to 9am)	50.43	4.51	39.70	3.00	2.36
Hour-2(9am to 10am)	45.62	4.58	42.83	3.78	3.19
Hour-3(10am to 11am)	31.01	6.15	55.31	5.59	1.96
Evening, Traffic Composition in Percentage					
Vehicle Type	2W	3W	4W	LCV	BUS
Hour-1(4pm to 5pm)	47.73	12.59	36.90	0.50	2.27
Hour-2(5pm to 6pm)	51.41	11.62	36.15	0.12	0.70
Hour-3(6pm to 7pm)	54.29	8.22	36.25	0.18	1.06

ESTIMATION OF PCU

The data collected in this study were used to calculate PCU factors using three methods proposed in this paper.

Based on Speed-Area Ratio Method

In this study mean speed is calculated by using Eq.4.

$$V_m = n / \sum_i^n (1/V_i)$$

where n is no of observations, V_i is spot speeds of ith vehicle.

Table 2: PCU Values by Chandra Method in this Study

Vehicle Type	L(m)	W(m)	A_i	$A_r (A_i/A_i)$	V_i	$V_r (V_i/V_i)$	PCU _i
2W	1.84	0.64	1.2	4.50	51.95	1.040	0.23
3W	3.2	1.4	4.5	1.20	52.38	1.032	0.86
4W	3.72	1.44	5.4	1.00	54.05	1.000	1.00
LCV	6.1	2.1	12.8	0.42	50.87	1.063	2.52
BUS	10.1	2.43	24.5	0.22	54.06	1.000	4.54

Speed Ratio Method

Mean speed is calculated as per Eq.4 and Table3 Shows the PCU values.

Table 3: PCU Values by Speed-Ratio Method

Vehicle Type	U_c	U_v	F_u
2W	54.05	51.95	1.040

3W	54.05	52.38	1.032
4W	54.05	54.05	1.000
LCV	54.05	50.87	1.063
BUS	54.05	54.06	1.000

Homogenization Coefficient Method

In this method mean speed is calculated by Eq.4 and Length of ith type of vehicle is taken from Indo-HCM, 2018.

Table 4: Shows the Value of PCU

Vehicle Type	Lm)	V _i	V _c	Li/Vi	Lc/Vc	PCUi
2W	1.84	51.95	54.05			
3W	3.2	52.38	54.05	0.0354	0.069	0.51
4W	3.72	54.05	54.05	0.0611	0.069	0.88
LCV	6.1	50.87	54.05	0.069	0.069	1.0
BUS	10.1	54.06	54.05	0.1199	0.069	1.73
				0.1868	0.069	2.70

RESULTS AND DISCUSSION

The PCU values found by Chandra Methods in this study was found to be within the limits of Indo-HCM Range since both are same, except 3W which is 0.86, the reason might be driving behavior and traffic characteristics are expected to be more different among each other.

Table 5: Comparison of PCU Values with Indo-HCM, 2018

Methods/Class of Vehicle	2W	3W	4W	LCV	BUS
Speed-Area Ratio	0.23	0.86	1	2.52	4.54
Speed-Ratio	1.04	1.03	1	1.06	1
Homogeneous Coefficient Method	0.51	0.88	1	1.73	2.7
Indo-HCM Range	0.20-0.50	1.10-2.0	1	2.0-5.0	2.80-4.80

CONCLUSION

Some studies also suggested the static PCU values for different types of vehicle but they are found to be inconsistency due to traffic, road geometric and other conditions. PCU estimation is a complex phenomenon and depends on many factors and also methods of estimation. Therefore, it has been suggested further research is required by using modified density method, space-occupancy for traffic in countries like India.

REFERENCES

1. Al-Kaisy, A., Y. Jung, and H. Rakha. 2005. "Developing passenger car equivalency factors for heavy vehicles during congestion." *J. Transp. Eng.* 131 (7): 514–523. [https://doi.org/10.1061/\(ASCE\)0733-947X\(2005\)131:7\(514\)](https://doi.org/10.1061/(ASCE)0733-947X(2005)131:7(514)).
2. Chandra, Satish, and Upendra Kumar(2003). "Effect of lane width on capacity under mixed traffic conditions in India." *Journal of transportation engineering* 129(2), 155-160.
3. Chandra, S.,Kumar, V.,Sikdar, P. K., 19995.Dynamic PCU and estimation of capacity of urban roads. *Indian Highw. Indian Road Congr.* 23(4), 17–28.
4. Chandra, S., and P. K. Sikdar. 2000. "Factors affecting PCU in mixed traffic situation in urban roads." *Road Transp. Res.* 9 (3): 40–50.
6. Craus,J.,Polus,A.,Grinberg, I.,1980.A revised method for the determination of passenger care equivalencies. *Transp.Res.PartA:Gen.*14(4),241–246.
7. Highway Research Board (1965). *Highway Capacity Manual*. Washington D.C.
8. Indian Highway Capacity Manual (Indo-HCM), CSIR,2017, New Delhi
9. IRC (Indian Roads Congress). 1990. *Guidelines for capacity of urban roads in plain areas. IRC 106*. New Delhi, India: Indian Code of Practice.
10. Keller, E. L., Saklas, J. G., 1984. Passenger care equivalents from network simulation. *J. Transp.Eng., ASCE* 110(4),397–411.
11. Raj, Pooja, et al(2019). "Review of methods for estimation of passenger car unit values of vehicles." *Journal of Transportation Engineering, Part A: Systems* 145.6: 04019019.
12. Sharma, Manjul, and Subhadip Biswas(2020). "Estimation of Passenger Car Unit on urban roads: A literature review." *International Journal of Transportation Science and Technology*
13. Huber,M.J.,1982.Estimation of passenger care equivalents of trucks intraffic stream. *Transp.Res. Rec.*869,60–68.
14. Tiwari, G., J. Fazio, and S. Pavitravas. 2000. "Passenger car units for heterogeneous traffic using a modified density method." In *Proc. 4th Int. Symp. on Highway Capacity*, 246–257. Washington, DC: Transportation Research Board, National Research Council .
15. Van Aerde, M., Yagar, S., 1984 Capacity, speed, and platooning vehicle equivalents for two-lanerural highways. *Transp.Res.Rec.*911,58–67.

Study on Black Cotton Soil Stabilized with Class C Fly Ash for Use in Flexible Road Pavements: An Experimental Study

Hrishikesh A. Shahane

Post Doctoral Fellow
School of Civil and Environmental Engineering
Faculty of Engineering and Built Environment
University of the Witwatersrand
Johannesburg, South Africa
✉ shahane.hrishi@gmail.com

Sachin L. Desale

Assistant Professor
Department of Civil Engineering
Jawahar Education Society's
Institute of Technology, Management and Research
Nashik, Maharashtra

ABSTRACT

Excessive heave associated with swelling of expansive soils can cause considerable distress to light weight civil engineering structures. Development of adequate road network is very important for the socio economic development of a country. For construction, maintenance and widening of roads, a large quantum of construction material is required. Also presence of expansive soil causes distress to these road pavements. The most commonly used method is addition of stabilizing agents, such as lime or cement to the expansive soil. Consequently several methods have been suggested to control this problem so that black cotton soil can be replaced with class C fly ash to be used as subgrade and subbase of flexible road pavements. In this study, class C fly ash is used for stabilization of an expansive soil. An evaluation of the expansive soil-fly ash and fly ash systems is presented.

The scope of the present research consists of two main parts, namely, experimental investigations on engineering properties of different soil- fly ash combinations and two dimensional finite element analysis of five layer flexible pavement system. The experimental program is carried out in two parts. First, compaction characteristics, swelling characteristics, unconfined compressive strength, CBR, shear characteristics and elastic modulus of different trial mixes of the soil-fly ash combinations are investigated and the optimum mixes are determined. Next, unconsolidated undrained triaxial tests and scanning electron microscopy (SEM) tests and pavement model tests are performed on the optimum mixes. The tests are carried out on different combinations of soil-fly ash mixes. For subgrade and sub base material, class C fly ash is chosen as the stabilizer. These mixes were chosen based on their strength characteristics and availability of the fly ash in the vicinity of the proposed site for road construction. The behaviour of the these soil-fly ash mixes for the sub base course is compared with that of the conventional Granular Sub base (GSB) and the waste mixes for subgrade course are compared with that of the conventional black cotton soil. Based on the engineering properties obtained for the different trial mixes of the proposed subgrade materials the optimum mix proportion is adopted as per the strength requirements of Indian Road Congress are 20%Fly ash + 80% Black Cotton soil. And 40%Fly ash+ 60% Black Cotton soil. The service life of a flexible pavement having the optimum mixes in the subgrade and sub base course vis-a-vis the conventional Granular Subbase (GSB) layer and black cotton soil subgrade is also evaluated in the present study through finite-element analyses of a five layer flexible pavement system. The service life of the pavement with optimum mixes as the sub base course and subgrade course is higher than that of the pavement with GSB as subbase course as per failure criterion.

KEYWORDS : Fly Ash, Soil stabilization.

INTRODUCTION

In design and construction of any structure, the role of soil is very crucial. Since the soil is in direct contact with the structure, it acts as a medium of load transfer and hence for any analysis of forces acting on structure, one has to consider the aspect of stress distribution through soil, as stability of structure itself depends on soil properties. Geotechnical study of site is crucial at feasibility stage, taking place before the design begins (a critical design input) in order to understand the characteristics of subsoil upon which the structure will stand. Structures need a stable foundation for their proper construction and lifelong durability. Foundation needs to rest on soil ultimately, transferring whole load to the soil. If weak soil base is used for construction, with passage of time it compacts and consolidates, which results in differential settlement of structure. It may result in cracks in structure which can have catastrophic affect too. To avoid these future problems in weak soil, stabilized soil should be considered.

Expansive soils (Black Cotton soil) covers nearly 20% of the total landmass in India. This includes almost the entire Deccan plateau, Western Madhya Pradesh, parts of Gujarat, Andhra Pradesh, Uttar Pradesh, Karnataka and Maharashtra (Gourav and Dhiraj, 2015). These soils show extensive volume and strength changes with change in moisture content due to the presence of a mineral called Montmorillonite in it. Highway construction on cohesive/clayey soils has been a confront to engineers and designers because of its high swelling and shrinkage behaviour due to the presence of inorganic clays of medium to high compressibility, which results in cracks in the pavement structure. Expansive soil failures exhibit damage ranging from minimal cracking in a slab to large cracking of a monolithic wall from floor to ceiling. Regions with hot and dry to cold and rainy seasons that have a high content of sandy clay to clay like soils are susceptible to this type of damage.

Expansive Soil

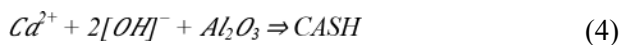
The term expansive soil applies to soils that have the tendency to swell when their moisture content is increased. Expansive soils are generally characterized by the presence of a clay mineral of the smectite

group. These soils can give rise to problems in civil engineering works because of their capacity to undergo large volume changes with changes in the moisture content or suction. Excessive heave associated with swelling of expansive soils can cause considerable distress to lightweight civil engineering structures. (Cokca 2001). The moisture may come from rain flooding, leaking water or sewer lines or from reduction in surface evapotranspiration when an area is covered by a building or pavement. Soils containing the clay mineral montmorillonite (a smectite) generally exhibit these properties (Chen 1975). The kaolinite group is generally non expansive. The mica-like group, which includes illites and vermiculites, can be expansive, but generally does not pose significant problems (Nelson and Miller 1992). Damage caused by expansive soils is almost entirely restricted to light structures and is a particular problem when they are encountered in road construction.

Fly Ash Stabilization

Fly ash is defined as the material extracted from the flue gases of a furnace fired with coal. Fly ash consists of often hollow spheres of silicon, aluminum, and iron oxides and unoxidized carbon. Fly ash can be regarded as non plastic fine silt by the Unified Soil Classification System. The composition of fly ash varies considerably depending on the nature of the coal burned and the power plant operational characteristics (Cabrera and Woolley 1994; Rollings and Rollings 1996). There are two major classes of fly ash. Class F fly ash is produced from burning anthracite or bituminous coal. Class C fly ash is produced from burning lignite and sub bituminous coal. Both classes of fly ash are pozzolans, which are defined as siliceous or siliceous and aluminous materials. Fly ash can provide an adequate array of divalent and trivalent cations (Ca^{2+} , Al^{3+} , Fe^{3+} , etc.) under ionized conditions that can promote flocculation of dispersed clay particles. Thus, expansive soils can be potentially stabilized effectively by cation exchange using fly ash. The fly ash is highly heterogeneous material where particles of similar size may have different chemistry and mineralogy. There is variation of fly ash properties from different sources, from same source but with time and with collection point and variation in load generation.

When binders such as lime, cement, and fly ash are blended with soil in the presence of water, a set of reactions occur that result in dissociation of lime (CaO) in the binders and the formation of cementitious and pozzolanic gels [calcium silicate hydrate gel (CSH) and calcium aluminate silicate hydrate gel (CASH)]:



These reactions are referred to as cementitious and/ or pozzolanic reactions that result in the formation of cementitious gels. The increase in strength was found to be roughly related to the type and quantity of possible reaction products (i.e., cement reaction product, CSH for short-term strength and pozzolanic reaction product, CASH for long-term strength gain). The source for the pozzolans (a siliceous or aluminous material) is either the soil or the binding agent. These reactions contribute to stabilization of soils in two ways. First, plasticity of the soil is reduced by the exchange of calcium ions in the pore water with monovalent cations on clay surfaces and by compression of the adsorbed layer because of the elevated ionic strength of the pore water (Rogers and Glendinning 2000). Second, the CSH or CASH gels formed by cementitious and pozzolanic reactions bind the solid particles together, and this binding produces a stronger soil matrix (Arman and Munfakh 1972).

Significance of Research

The objectives of the study are:

1. To study the effect of curing period, curing condition and fly Ash (class C) content on various engineering properties such as index properties, free swell UCS, Resilient Modulus, Permanent strain etc. of the various Fly Ash mixes.
2. To study the micro structural behavior of various soil Fly ash mixes.
3. To study the feasibility of above mixes for the planning of road subgrade and sub base.
4. To study the service life of flexible road pavements for the proposed mix using finite element analysis.

EXPERIMENTAL PROGRAM

An easy way to comply with the conference paper formatting requirements is to use this document as a template and simply type your text into it.

Expansive Soil

Soil sample is collected from SAC Ground in Sardar Vallabhbai National Institute of Technology. The properties of the soil sample are given in Table 1.

Class C Fly Ash

Fly ash belonging to Class C classification was obtained from the lignite power plant, Tadkeshwar, Surat. The following table gives the chemical composition of fly ash. As the $Fe_2O_3 + Al_2O_3 + SiO_2$ is more than 50, it belongs to class C fly ash. Table 1 lists the index properties and compaction characteristics of Fly ash.

Table 1: Properties of Materials

Index Properties	BC Soil	Fly Ash
Natural water content, W _n (%)	12.22	0.3
Liquid Limit, WL(%)	66.5	-
Plastic Limit, W _p (%)	35	-
Plasticity Index (%)	31.5	-
Specific Gravity	2.27	2.094
Percentage Fines (%)	92.7	89
Classification	CH	NP
CBR	2.3	365
FSI	58	0
UCS(MPa)	0.404	1.02
Compaction Characteristics		
Optimum Moisture Content (%)	19	27.4
Maximum Dry Density(g/cc)	1.75	1.404
Grain Size Distribution		
Gravel	0	0
Sand	7.3	0
Silt	39	11
Clay	53.7	89

Table 2: Chemical Composition of Fly Ash

Sr. No.	Parameter	Result (%)	Test Method
1	CaO	3.82	IS:1727-1967
2	Fe ₂ O ₃	14.78	IS:1727-1967
3	Al ₂ O ₃	3.82	IS:1727-1967
4	Silicon Dioxide as SiO ₂	36.8	IS:1727-1967
5	Magnesium Oxide as MgO	0.895	IS:1727-1967
6	Total Sulphur as Sulphur Trioxide SO ₃	10.03	IS:1727-1967
7	Available alkalis as Na ₂ O	0.55	IS 3812 RA:2013
8	Total Chloride	0.24	IS4032:1985 RA:2014
9	Loss on Ignition	7.71	IS:1727-1967

Mix Proportion

Expansive soil was mixed with various dosages of additives. The different mix proportions adopted are:

Class C Fly ash at dosages of 10%, 20%, 30%, 40% and 50% by weight of dry soil.

RESULTS AND DISCUSSION

Plasticity Characteristics

The observed liquid and plastic limits of all binder combinations for 7 days curing period were recorded. Plasticity index was calculated and compared with the A-line value to know about the changes in plasticity and soil nature. Changes to the plasticity of the soil are a result of the cation exchange resulting in particle flocculation and aggregation. This increases the effective particle size of the fine-grained soil resulting in a more silt-like material. This typically increases the plastic limit and decreases the liquid limit. There occurs a reduction in LL and slight increase in PL causing a decrease in the

plasticity index. The trend of PI is similar to that of LL. The decrease in LL and increase in PL resulted in a net decrease of PI which reduced the plasticity of soil.

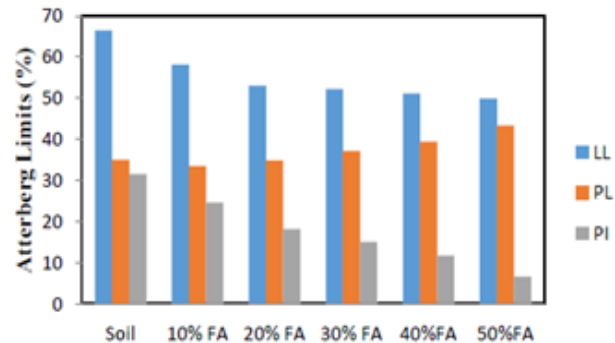


Fig. 1 Variation of LL, PL and PI with fly ash content

Compaction Characteristics

Modified Proctor test (heavy compaction) was conducted on various mixes of Class C Fly ash and soil by varying the proportion of water in every mix. Optimum moisture content and maximum dry density were determined as per IS 2720 (Part 8)-1983.

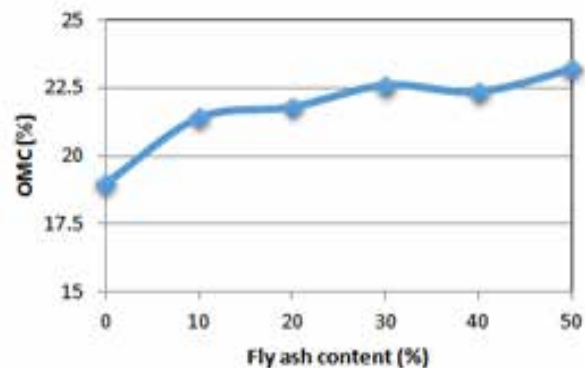


Fig. 2 Variation of OMC with fly ash content

When class C fly ash is added to pure black cotton soil it can cause a decrease in MDD and an increase in OMC. This is attributed to the low specific gravity of Class C Fly ash compared to the black cotton soil. Class C fly ash has an OMC and MDD of 27% and 1.404 g/cc.

The variation of OMC with variation of binder content is shown in fig.4.13. The OMC of treated soil goes on increasing for binder contents 10,20,30,40 and 50%. The OMC increases due to the hydration effect and the affinity for more moisture during this reaction process.

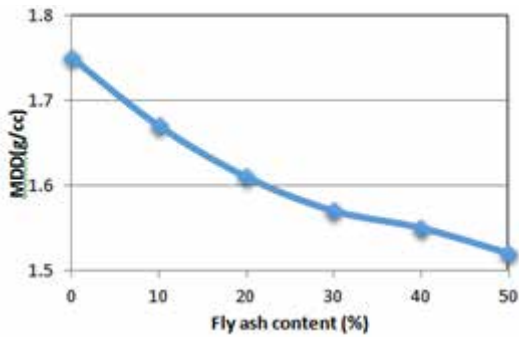


Fig. 3 Variation of OMD with fly ash content

The variation of OMC with variation of binder content is shown in fig.4.13. The OMC of treated soil goes on increasing for binder contents 10, 20, 30, 40 and 50%. The OMC increases due to the hydration effect and the affinity for more moisture during this reaction process.

Discussing about MDD, the value the value goes on decreasing for the addition of binders from 10 to 50%. Decrease in density is directly attributed to the flocculation/aggregation and the formation of weak cementitious products. Flocculation/aggregation of the soil offers greater resistance to densification at a given level of compactive effort. The net result is a reduction in the MDD and the affinity for more moisture during this reaction process.

Free Swell Test

Excessive swelling and shrinkage is the main drawback of black cotton soil. The swelling of soil when immersed in water and Kerosene for 24 hours were compared. The extent of swelling of host soil was tested using free swell index test and reported value was 58, which falls under „very high expansiveness“ category. FSI values goes on decreasing with the increase of Fly ash content with the minimum occurring at 40 % Fly ash.

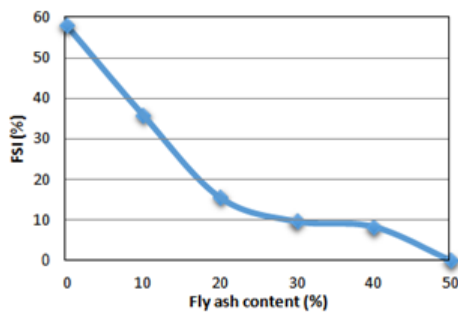


Fig. 4 Variation of FSI with fly ash content

Wet Sieve Analysis

Wet sieve analysis was done on soil-fly ash mixes after 7 days of curing. The results show that the finer particle percentage shows a decreasing trend with the increase in fly ash content. This can be attributed to the formation of larger particles when soil reacts with fly ash.

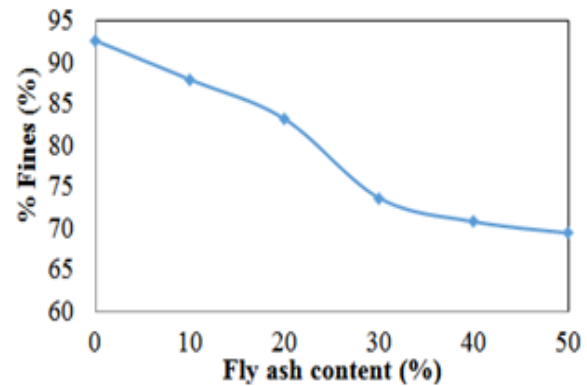


Fig. 5 Variation of Percentage Fines with fly ash content

Unconfined Compressive Strength

The UCS tests were conducted on the fly ash treated black cotton soil at curing periods of 7 days and 28 days for the fly ash contents of 10, 20, 30, 40 and 50%.

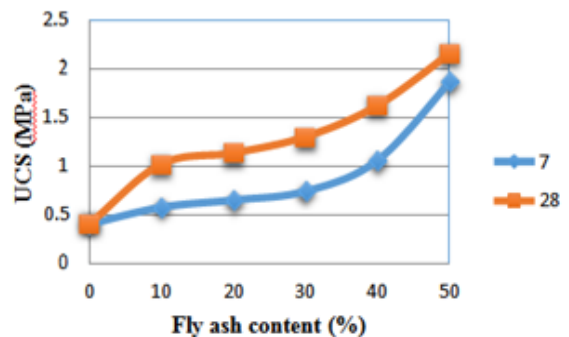


Fig. 6 Variation of UCS with Fly ash content with curing period

From the above UCS results, it can be seen that the UCS value shows an increasing trend with the increase in fly ash content. Also with the increase in curing period also the trend of UCS value is increasing. From comparing the UCS values after 7 days and 28 days curing, there is a significant difference for the 10, 20 and 30% Fly ash mixes. But for the 40 and 50% Fly ash mix combination there was not that much a prominent change occurs.

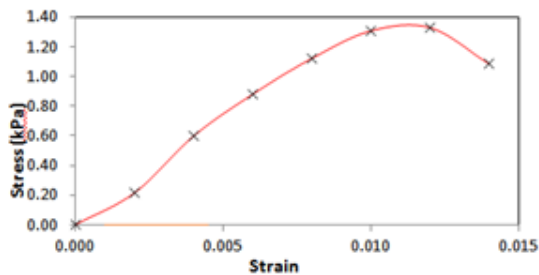


Fig. 7 Typical stress strain curve for soil mixed with 40% fly ash

This can be attributed to the significance of fly ash content in the mix. The class c fly ash acquires an early strength during the initial periods and after that there occurs retardation. This can be explained from the UCS values of the fly ash sample cured for 7 days and 28 days.

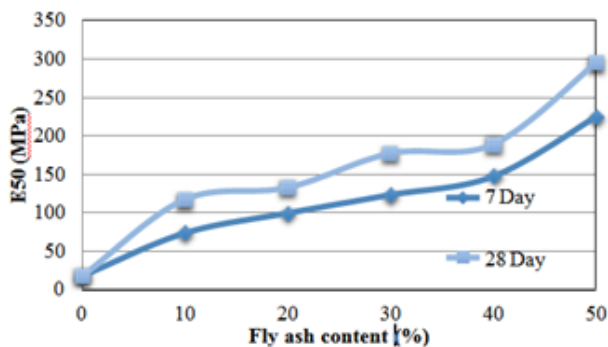


Fig. 8 Variation of Elastic Modulus with Fly ash content at 7 day and 28 day curing period

CONCLUSION

Experimental and numerical studies were conducted on expansive soil stabilized by class C Fly ash for use in flexible road pavements. The conclusions drawn from the study are stated below,

1. The stabilization of black cotton soil from the SVNIT Campus with Class C fly ash from the power plant resulted in the reduction in the plasticity of soil. The plasticity index got reduced with the increase of binder due to the decrease in liquid limit along with the increase in plastic limit.
2. The free swell index of the soil experienced a significant reduction of the expansiveness on treating with Fly ash. It got reduced its value from

58 to zero at 50 % Fly ash addition. This resulted in the degree of expansiveness of soil to reduce from very high to low.

3. The optimum moisture content goes on increasing with the addition of Fly ash but the maximum dry density showed a decreasing trend. This can be attributed to the low specific gravity of fly ash compared to the black cotton soil. For material used as a subgrade the OMC and MDD obtained is 21.8% and 1.61 g/cc. For material to be used as a sub base layer the OMC and MDD obtained is 22.36% and 1.55g/cc.
4. The UCS value of the soil increased with increase in fly ash content. The UCS value of the pure Black cotton soil is 404.5 kPa. It got increased to 1864.5kPa at a Fly ash content of 50% for 7 days curing period. For 28 days curing period the UCS value reached up to 2058.93 kPa. For material to be used as a subgrade and Sub base the 7 day UCS strength is obtained as 651.9 kPa and 1059.8 kPa respectively. For 28 days curing the values obtained are 1136.627 kPa and 1623.6 kPa.
5. The UCS value of the optimum mix showed an increasing trend with the change in curing condition .The curing condition adopted were 3 day curing+ 4day soaking,7 day curing + 4 day soaking and 10 day curing and 4 day soaking.
6. The 7 day cured and 4 day soaked CBR values of the soil increased up on addition of fly ash content. For the optimum mix of 20 % and 40 % the CBR values are respectively 30 % and 60%.As the CBR value for soil with 40%Fly ash is more than 30%, the material is suitable for sub base material for high volume roads.

REFERENCES

1. Bin-Shafiquea, S., Rahmanb, K., Yaykirana, M and Azfara, I. (2010).”The long term performance of two fly ash stabilized fine-grained soil subbases.” Resources, Conservation and Recycling 54 (2010) 666–672.
2. Brooks, R., Udoeyo, F. F and Takkalapelli, K. V. (2011). “Geotechnical Properties of Problem Soils Stabilized with Fly Ash and Limestone Dust in Philadelphia.” J. Mater. Civ. Eng., 23(5): 711-716.

3. Buhler, R.L., and Cerato, A.B.(2007).”Stabilization of Oklahoma expansive soils using lime and class C fly ash.”GSP 162 Problematic Soils and Rocks and In Situ Characterization.
4. Cokca, E. (2001).” Use Of Class C Fly Ashes For The Stabilization Of An Expansive Soil.” J. Geotech. Geoenviron. Eng., 127(7):568-573.
5. Consoli, N. C., Rosa, A. D and Saldanha, R. B. (2011).” Variables Governing Strength of Compacted Soil–Fly Ash–Lime Mixtures.” J. Mater. Civ. Eng., 23(4), 432-440.
6. Das, S. K and Yudhbir. (2005). “Geotechnical Characterization of Some Indian Fly Ashes.” 17(5):544-552.
7. Edil, T. B., Acosta, A. A., and Benson, C. H. (2006). “Stabilizing soft fine grained Soils with fly ash.” J. Mater. Civ. Eng., 18(2), 283–294.
8. Edil, T. B., Sandstrom, L. K and Berthouex., P. M. (1992). “Interaction of Inorganic Leachate with Compacted Pozzolanic Fly Ash.” ASCE J. Geotech. Eng., 118(9): 1410- 1430.
9. Fleming, L. N and Inyang, H. I. (1995).” Permeability Of Clay-Modified Fly Ash Under Thermal Gradients.” J. Mater. Civ. Eng., 7(3): 178-182.
10. IRC (Indian Road Congress). (2001). “Guidelines for the design of flexible pavements” IRC 37, New Delhi.
11. IRC (Indian Road Congress). (2012). “Tentative guidelines for the design of flexible pavements” IRC 37, New Delhi.
12. IS (Indian Standard). (1977).”Determination of free swell index” IS 2720 (Part 40), New Delhi.
13. IS (Indian Standard). (1980).”Determination of specific gravity” IS 2720 (Part III/Sec I), New Delhi.
14. IS (Indian Standard). (1983).”Determination of water content-dry density relation using heavy compaction” IS 2720 (Part VIII), New Delhi.
15. IS (Indian Standard). (1985).”Determination of liquid and plastic limit” IS 2720 (Part V), New Delhi.
16. IS (Indian Standard). (1985).”Grain size analysis” IS 2720 (Part IV), New Delhi.
17. Misra, A., Biswas, D., and Upadhyaya, S.(2005).” Physico-mechanical behavior of self- cementing class C fly ash–clay mixtures.” Fuel 84 (2005) 1410–1422.
18. Nalbantog˘lu, Z (2004).” Effectiveness of Class C fly ash as an expansive soil stabilizer. “Construction and Building Materials 18 (2004) 377–381.
19. Phanikumar, B. R and Sharma, R. S. (2007).” Volume Change Behavior of Fly Ash- Stabilized Clays.” J. Mater. Civ. Eng., 19(1):67-74.
20. Phanikumar, B.R and Sharma, R.S.(2004).“Effect of Fly Ash on Engineering Properties of Expansive Soils.” J. Geotech. Geoenviron. Eng., 2004, 130(7): 764-767.
21. Senol, A., Edil, T.B., Bin-Shafique, M.S., Acosta, H.A. and Benson, C.H.(2006).” Soft subgrades” stabilization by using various fly ashes.” Resources, Conservation and Recycling 46 (2006) 365–376.
22. Sezer, A., I˘nan,G., Yılmaz, H.R and Ramyar,K. (2006).”Utilization of a very high lime fly ash for improvement of Izmir clay.” Building and Environment 41 (2006) 150–155.
23. Shanthakumar, S., Singh, D. N and Phadke, R. C. (2010).” Methodology for Determining Particle-Size Distribution Characteristics of Fly Ashes.” J. Mater. Civ. Eng., 22(5), 435-442.
24. Sharma, N.K., Swain, S.K., and Sahoo, U.C.(2012).”Stabilization of a Clayey Soil with Fly Ash and Lime: A Micro Level Investigation.”Geotech Geol Eng (2012) 30:1197– 1205.
25. Solanki, P., Khoury, N and Zaman, M. M. (2009). “Engineering Properties and Moisture Susceptibility of Silty Clay Stabilized with Lime, Class C Fly Ash, and Cement Kiln Dust.” J. Mater. Civ. Eng., 21(12): 749-757

Use of Bio-Coagulant for Removal of Turbidity

P. L. Pathak, Dr. P. D. Jadhao

Mohd. H. A. A., S. S. Suryawanshi

Department of Civil Engineering
K.K. Wagh Institute of Engineering Education and Research, Nashik
✉ ppathak@kkwagh.edu.in

ABSTRACT

Clean and safe drinking water is essential requirement for all types of livelihoods, but it remains a significant challenge in rural areas. Many rural communities depend on rivers and wells directly for their daily water needs, but these sources of water not met with required standards of good quality water. Many urban water resources also get contaminated due to Industrialization, Rapid urbanization and unregulated human activities. All these activities results contamination of water resources by changing different properties of water and significantly increases turbidity of water. In this study natural coagulants are used for removal of turbidity. Natural coagulants are made by fruit peels of Pomelo and Banana by grinding and sieving fruit peel powder in particle size of 300μ after oven drying at $100\text{ }^{\circ}\text{C}$. This coagulant is added in different dosages such as 40mg/l, 50mg/l and 60mg/l. Among all dosage 50mg/l dose gives 90-95 percent turbidity removal efficiency without changing other properties of water much more.

KEYWORDS : Turbidity, Pomelo peels, Banana peels, Pectin, Coagulant.

INTRODUCTION

Access to clean and safe drinking water is a fundamental necessity, but it remains a significant challenge in many rural areas. One of the primary reasons for this challenge is the absence of adequate infrastructure for water treatment and distribution, as government-provided piping systems are often lacking. As a result, residents in these areas are often compelled to rely on alternative water sources, such as rivers and groundwater, for their daily water needs. Unfortunately, these alternative sources frequently fall short of meeting the stringent standards set for safe drinking water, leading to concerns about water quality and safety.

Surface waters, such as urban lakes, hold a pivotal role in our water resources, serving as crucial sources of water for the communities living in their vicinity. In recent years, however, many of these urban lakes have suffered from severe pollution due to various factors, including industrialization, rapid urbanization, and unregulated human activities. These environmental changes have caused significant alterations in the physical, chemical, and biological properties of the water in these lakes, ultimately resulting in issues such as increased turbidity.

Turbidity, which refers to the cloudiness or haziness of water caused by the presence of tiny particles and impurities, poses a significant challenge to ensuring that surface water meets the necessary quality standards for safe consumption.

To address these water quality concerns and make surface water sources suitable for human consumption, the process of flocculation and coagulation is employed. This process involves the addition of coagulants to water to aggregate and settle the suspended particles, thereby clarifying the water. Traditionally, synthetic or inorganic coagulants have been widely used for this purpose, but they come with certain disadvantages. For example, these coagulants can be sensitive to changes in the pH of the water, requiring precise control. Additionally, there is a risk of secondary contamination, as the use of synthetic polymers may introduce trace amounts of potentially harmful substances such as aluminium into the treated water. Moreover, the non-biodegradable nature of synthetic polymer coagulants makes the management and recycling of the sludge generated during the water treatment process a significant challenge.

In response to these issues, there is a growing interest in exploring natural coagulants as a safer and more environmentally friendly alternative. Natural coagulants, derived from sources like pomelo peels, are characterized by their eco-friendliness, primarily because they are biodegradable. These coagulants have the potential to revolutionize the flocculation-coagulation process, making it not only more effective but also safer for both human health and the environment. By utilizing natural coagulants, we aim to ensure that even in rural areas with limited access to clean water, residents can rely on readily available, clean, and safe drinking water, mitigating the challenges posed by surface water pollution and turbidity. This promising approach has the potential to significantly improve the quality of life and health in rural communities, addressing the critical issue of water scarcity.

LITERATURE REVIEW

Neha Arukia, et al., Natural materials should be used in the coagulant-flocculation process as much as possible. According to the literature, it is worthwhile to develop and, if possible, convert natural materials into commercial. On the other hand, natural coagulants are insufficient as a primary treatment since their efficacy is being hampered by increasing restrictions. Emerging technology and in-depth research contribute to the creation of these restricted settings as well as the success of chemicals. Natural coagulants are also commonly employed as coagulant aids in conjunction with manufactured coagulants. The type of coagulants used in the treatment of waste-water coagulation, in particular the usage of natural coagulants, is the subject of this investigation. Natural materials potential for future expansion as aids and as sustainable composite coagulants are also discussed in this analytical report.

Bahman Ramavandi, et al., A bio-coagulant was successfully extracted from *Plantago ovata* by using an FeCl₃-induced crude extract (FCE). The potential of FCE to act as a natural coagulant was tested for clarification using the turbid water of a river. Experimental tests were performed to evaluate the effects of turbidity concentration, coagulant quantity, water pH, and humic acid concentration on the coagulation of water turbidity by FCE. The maximum turbidity removal was occurred at water PH<8. At the optimum dosage of FCE, only

0.8 mg/L of dissolved organic carbon was released to the treated water. An increase in the humic acid led to the promotion of the water turbidity removal. Results demonstrated that the FCE removed more than 95.6% of all initial turbidity concentrations (50–300 NTU). High bacteriological quality was achieved in the treated water. FCE as an eco-friendly bio-coagulant was revealed to be a very efficient coagulant for removing turbidity from waters.

K. Subba Narasiah et al., A model turbid water was treated by coagulation, flocculation and sedimentation, with *Moringa oleifera* seeds as a coagulant, using jar tests. The quality of the treated water was analysed and compared with that of the water treated with alum. Experiments were conducted at various dosages of the crude 5% water extract of both dry, shelled and non-shelled *Moringa oleifera* seeds. Measurements of pH, conductivity, alkalinity, cation and anion concentrations, showed that coagulation with *Moringa oleifera* seeds did not significantly affect the quality of the treated water. However, concentration of organic matter in the treated water increased considerably with the dosage of *Moringa* solution. It is suggested that *Moringa oleifera* seeds be used as a coagulant in water and wastewater treatment, only after an adequate purification of the active proteins. Nuramidah Hamidon et al., Water is our most precious natural resource. Based on this study which was conducted in Kangkar Senangar, Johor, the majority of rural communities still drink superficial water that the ability of Pomelo Peel is tested as natural adsorbent, to remove Iron (Fe) from aqueous solution by adsorption was investigated. Characterization of adsorbent was done by SEM and FTIR analyses to observe the surface morphology and functional groups available on the adsorbent. Adsorption was most efficient when 0.20g of adsorbent was used with 50ml of water sample. 0.20g was the optimum weight of pomelo peel powder with contact time of 20 minutes to change the quality of water sample. Based on the results, the higher the adsorbent dosages, the higher the adsorption removal of Fe. The highest adsorption removal of Fe was 80.84%. After the adsorption, the water sample was treated using Bio-sand Filtration (BSF). The function of BSF was to reduce the turbidity, change the colour of water sample, increase the pH and dissolve oxygen. The BSF filtered all the suspended matters in the water samples after the adsorption and produced clearer water.

OBJECTIVE

1. To study the characteristics of surface water.
2. To know the effect of pH, contact time, particle size and coagulant dosage.
3. To analysis the effect of turbidity.
4. To analysis the effect and variations of surface water parameters like Turbidity, Hardness, Chloride & Alkalinity.

METHODOLOGY

Exp.: Determination of Turbidity in water sample.

Aim: To determine the turbidity of the given sample water by Nephelometric method.

Apparatus required: Jar test apparatus with at least 4 stirrers of adjustable speed. Glass ware and Miscellaneous Items:

Jars - 1 litre, 4 nos. 2) Measuring cylinder - 500 ml, 1 no. 2) Pipettes - 5 ml, 2 nos. 4) Beakers - 250 ml, 1 no. 5) pH papers 6) Raw water sample (2.5 liter) of known turbidity

Principle: Turbidity is a measure of the extent to which light is either absorbed or scattered by suspended material present in the water. Turbidity is surface waters results from the erosion of colloidal material such as clay, slit, rock fragments and metal oxides from soil, vegetable fibers and micro-organisms may also contribute to turbidity. Drinking water supplies requires special treatment by chemical coagulation and filtration before it may be used for public water supply. This turbidity can be brought down to required level by adding coagulants. Coagulants when added to water it will form a geletaneous substance known as floc and this will arrest the fine suspended and colloidal particles. These arrested particles will settle down rapidly because of increase in their size.

Procedure:

1. Take 500 ml of well mixed raw water, of known turbidity, in each of mixed raw water four one litre jars, A, B, C and D.

2. Shake well and add graded dosages of alum and lime to each jar, as illustrated, the range being consistent with the turbidity of the sample.
3. Flash mix., i.e., stir the contents vigorously, for one minute. (The speed of stirring should be sufficient to form a deep vortex without spilling).
4. Flocculate, by reducing the speed to be in the range of 20 - 40 rpm, for 20 minutes.
5. Stop the rotation of paddles. Take out the jars and allow them to settle for 20 minutes.
6. The recommended speed for a prototype is only 2 15 rpm, above which flocks may break, because of the difference between the model a and the prototype in respect of basin geometry and roughness.
7. Draw the supernatant from each jar. (Starting with the jar with maximum alum dosage) and determine its residual turbidity.
8. Plot a graph with alum dosage (mg/l) along X axis against residual turbidity (mg/l) along Y axis.
9. Determine the optimum dose of alum corresponding to a residual turbidity of 10 mg/l. (In some treatment plants a residual turbidity of 5 mg/l, after chemically assisted sedimentation, may be specified suitable load on filters.)

Table 1: Turbidity Results (1Hr Contact Time)

Sample No	Dosage	Initial Turbidity (NTU)	Final Turbidity (NTU)	% Efficiency
Pomelopeels powder				
1.a	2.0=40mg/l	40.7	6.6	83.37
1.b	2.5=40mg/l	40.7	8.8	78.37
1.c	3.0=40mg/l	40.7	9.1	77.64
2.a	2.0=50mg/l	40.7	5.2	87.22
2.b	2.5=50mg/l	40.7	3.7	90.90
2.c	3.0=50mg/l	40.7	4.1	89.92
3.a	2.0=60mg/l	40.7	6.3	84.52
3.b	2.5=60mg/l	40.7	5.6	86.24
3.c	3.0=60mg/l	40.7	4.8	88.26
Bananapeels powder				
4.a	2.0=40mg/l	40.7	15.5	61.91
4.b	2.5=40mg/l	40.7	18.3	55.03
4.c	3.0=40mg/l	40.7	22.1	45.70
5.a	2.0=50mg/l	40.7	13	68.05
5.b	2.5=50mg/l	40.7	10.1	75.18
5.c	3.0=50mg/l	40.7	12.3	69.77
6.a	2.0=60mg/l	40.7	21.8	46.43
6.b	2.5=60mg/l	40.7	17	58.23
6.c	3.0=60mg/l	40.7	15.2	62.32

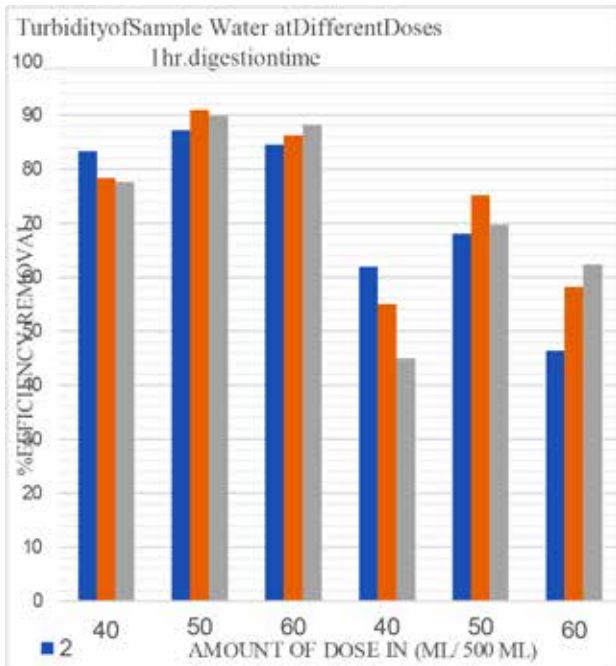


Fig 1. Turbidity graph (1hr contact time)

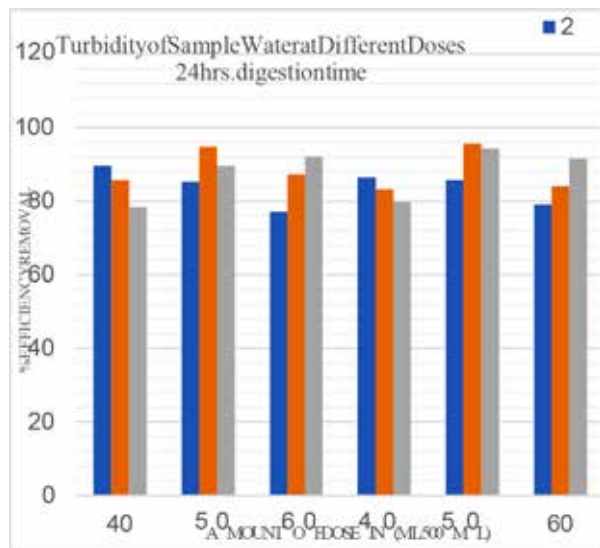


Fig 2. Turbidity graph (24hr contact time)

Table 3. Test Results (1hr Contact Time)

1hr.digestiontime	Amount of Pomelo eelsDose			AmountofBananaP PeelsDose			
	0	2.0	2.5	3.0	2.0	2.5	3.0
pH	7.5	7.90	7.95	7.93	7.94	7.67	7.90
Alkalinity(mg/lit)	80	100	120	84	112	80	100
Hardness(mg/lit)	784	574	560	490	525	455	560
ChlorideContent (mg/lit)	55.30	55.30	18.43	23.04	46.08	18.43	46.08

Table 4. Test Results (1hr Contact Time)

24hrs.digestiontime	AmountofPomelo PeelsDose			AmountofBananaP eelsDose		
	2.0	2.5	3.0	2.0	2.5	3.0
pH	7.90	7.95	7.93	7.94	7.67	7.90
Alkalinity(mg/lit)	100	80	80	100	88	88
Hardness(mg/lit)	420	420	420	560	455	560
ChlorideContent(mg/lit)	32.26	32.26	18.43	24.44	55.30	36.87

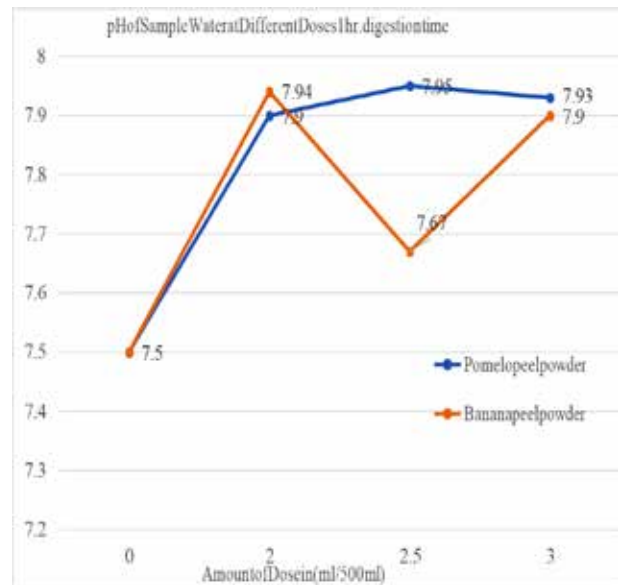


Fig 3. pH graph (1hr contact time)

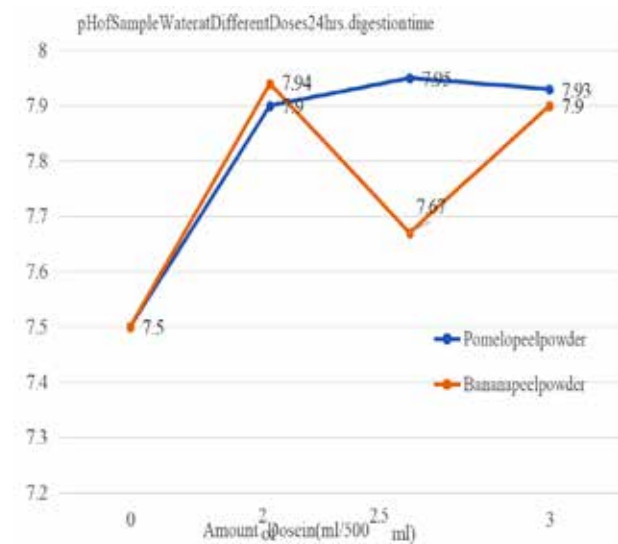


Fig 4. pH graph (24hr contact time)

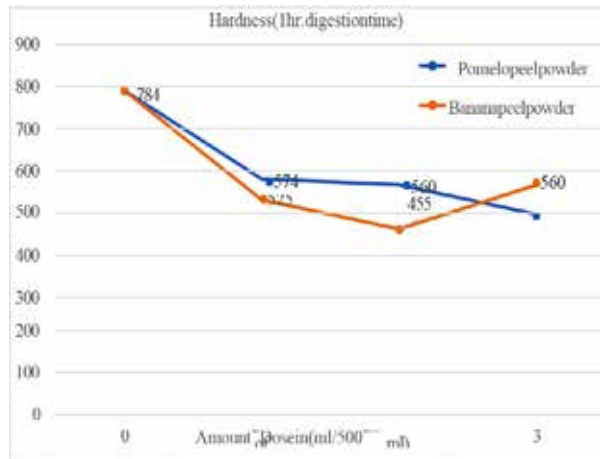


Fig 5. Hardness graph (1hr contact time)

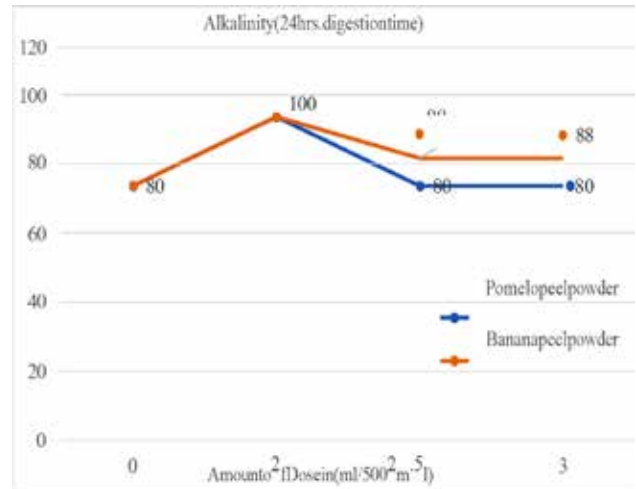


Fig 8. Alkalinity graph (24hr contact time)

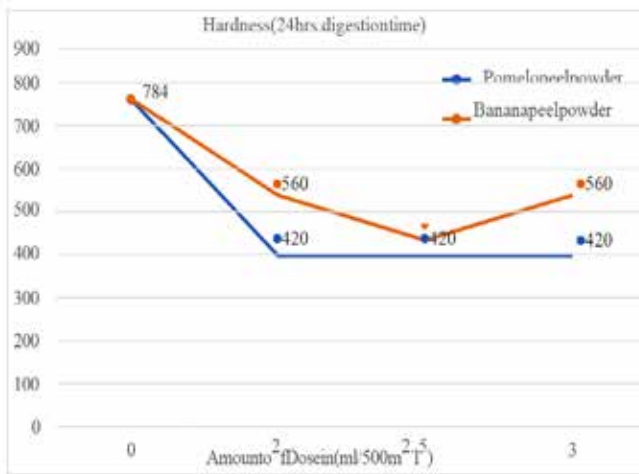


Fig 6. Hardness graph (24hr contact time)

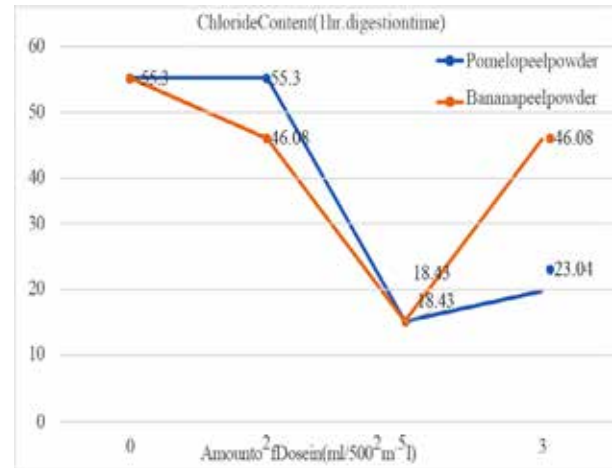


Fig 9. Chloride graph (1hr contact time)

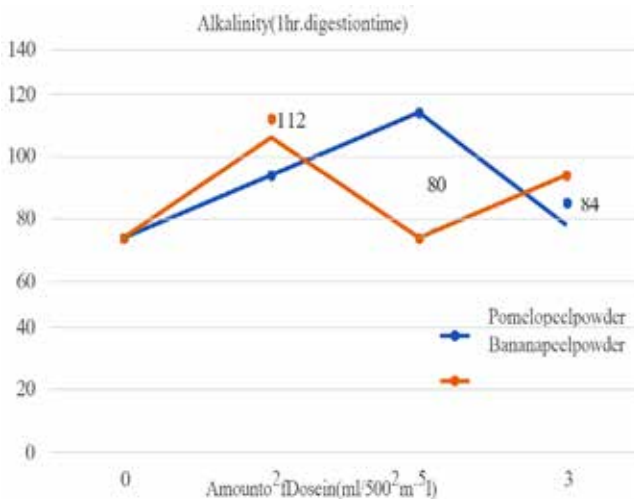


Fig 7. Alkalinity graph (1hr contact time)

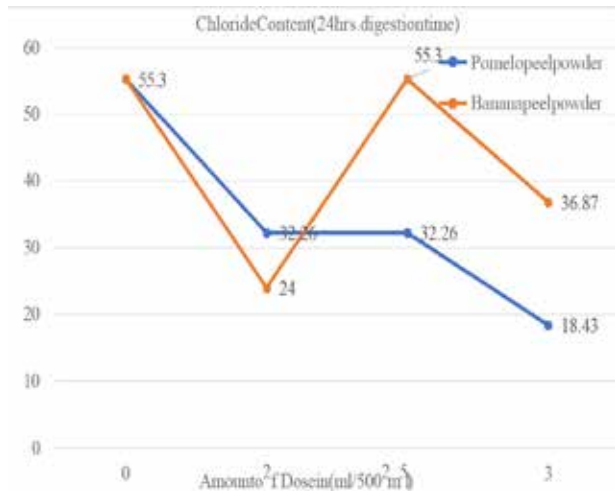


Fig 10. Chloride graph (24hr contact time)

CONCLUSIONS

The use of pomelo peels as a natural coagulant for turbidity removal represents a promising solution to the global challenge of providing clean and safe drinking water. This approach not only enhances water quality but also addresses environmental and health concerns associated with synthetic coagulants. By emphasizing the significance of this project, we recognize its potential to make a meaningful and positive impact on the lives of communities struggling with surface water pollution. It serves as a beacon of hope for a future where sustainable and accessible clean water is within reach for all.

ACKNOWLEDGMENT

The With all respect and gratitude, we would like to thank all the people who have helped us directly or indirectly for the progress of this work. We express our heartfelt appreciation towards our respected guide Prof. P.L. Pathak, for guiding us to understand the work conceptually and his constant encouragement to complete this Project on “Use of Bio-Coagulant for Removal of Turbidity”.

I also express my thanks to the head of the department, Prof. Dr. P.D. Jadhao of Civil engineering, for providing the necessary information and required resources.

With a deep sense of gratitude, I thank my principal Prof. Dr. K.N. Nandurkar of the K.K. Wagh Institute of Engineering Education and Research, Nashik. for providing all the necessary facilities and their constant encouragement and support.

I want to thank my parents and friends who supported and helped me. Last but not least, I would like to thank all the teaching and non-teaching staff member of the Civil engineering department for providing necessary information and required resources.

REFERENCES

1. Neha Arukia, Owais Khan, Palash Wanaskar, Pankaj Panchabhai, Prabodh Julm, Pragati Ingle “Study of Surface Water and Its Treatment Using Biocoagulant” ISSN: 2321-9653; IC Value: 45.98; Volume 10 Issue IV Apr 2022.
2. Nuramidah Hamidon, Nabilah Nazri, Mariah Awang, Norshuhaila Mohd Sunar, Mimi Suliza Muhamad, Nur Aini Mohd Arish, Hasnida Harun, Hazren A. Hamid, R. Ali, Mohammad Ashraf Abdul Rahman “Surface Water Treatment using Pomelo’s Peel (Citrus Grandis) and Biosand Filter as Iron (Fe) Adsorption in Kangkar Senangar’s River” ISSN: 2278-3075, Volume-8 Issue-8S, June 2019.
3. Bahman Ramavandi, “Treatment of water turbidity and bacteria by using a coagulant extracted from Plantago ovate” Water Resources and Industry 6 (2014) 36–50.
4. Anselme Ndabigengesere, K. Subba Narasiah “Quality Of Water Treated By Coagulation Using Moringa Oleifera Seeds” Wat. Res. Vol. 32, No. 3, pp. 781-791, 1998.
5. Dr.B G Mahendra, Ms. Firdous Sultana “Treatment of waste water using lemon and banana peel as natural coagulant.” International Research Journal of Engineering and Technology (IRJET): (2020)
6. Nuralhuda Aladdin Jasim, Jasim M. Azeez and Mohammed S. Shamkhi “A comparative study of different coagulants used in treatment of turbid water.” Research Article: (2022)
7. Vicky Kumar, Norzila Othman, Syazwani Mohd-Asharuddin “Partial Replacement of Alum by Using Natural Coagulant Aid to Remove Turbidity from Institutional Wastewater.” International Journal of Integrated Engineering Vol. 12 NO. 4 (2020) 241-251
8. Peck Loo Kiew, Kian Hen Chong “Development of Fruit Based Waste Material as Bio flocculants for Water Clarification.” Journal of Mechanical Engineering Vol SI 4(5), 1-10, 2017.

Verification of Technical Feasibility for Construction and Demolition Waste and RCA with Sustainability of SW Material for Flexible Pavement

P. L. Pathak, P. D. Jadhao

Department of Civil Engineering

K.K.W.I.E.E. & R

Nashik, Maharashtra

✉ plpathak@kkwagh.edu.in

✉ pdjadhao@kkwagh.edu.in

F. I. Chavan

Department of Civil Engineering

SSBT's COET

Jalgaon, Maharashtra

✉ farooqamaravati@gmail.com

ABSTRACT

The road construction using natural aggregate is a common phenomenon that leads to higher cost in construction and maintenance as availability of material is low and hence the gap between demand and supply is high. So it is necessary to find a better alternative without compromising on Strength. Day by day there is a huge scarcity of natural resources. Thus, it is necessary to alternate natural resources. This study verifies the technical viability of using C&D waste and RCA as material for flexible road pavement. The suitability of solid waste material is tested in flexible road pavement by conducting Geotechnical and Geo-environmental laboratory. Also, the field performance of new products C&D waste in the base and sub-base course is investigated.

The utilization of these waste materials in road construction will be enhanced and higher economic returns are expected. Also, the concrete waste needs to be separated from the C&D waste at the initial stage rather than using a mixed proportion of C&D waste, as result interpretation of the C&D waste failed in the impact, Crushing and Abrasion test.

KEYWORDS : *Recycled aggregates, Suitability, Solid waste material, Road pavement, C&D waste.*

INTRODUCTION

Construction and demolition (C&D) waste is generated from the cleanup, renovation, repair, and demolition of houses, buildings, roads, dams, etc. C&D waste is made up of plastic, wood, steel, cardboard, concrete, sheetrock, masonry, metal, tires, mattresses, furniture, and much more. It is observed that above 80% of C&D materials are inert, known as public fill. Public fill includes debris, rubble, earth, and concrete which is suitable for land reclamation and are used as filling material for site formation. When properly sorted, materials such as concrete and asphalt can be recycled for construction use. The remaining non-inert substances are known as C&D wastes including bamboo, timber, vegetation, packing waste, and other organic materials. Whereas, for public fill, non-inert waste is not suitable for land reclamation and subject

to recovery of reusable or recyclable items, is disposed of at landfills.

Recycling is the act of processing the used material for further use in developing new value-added products. The integral technique behind the recycling process includes the breaking of demolished concrete to produce smaller size fragments by subjecting to a series of performances such as removal of contaminants (reinforcement, wood, plastic, etc.), different stages of screening, and sorting. Higher-quality aggregates can also be processed in steps with time and effort involved in stockpiling, crushing, pre-sizing, sorting (pre-crushing and post crushing), screening, and contaminant elimination depending upon the level of contamination and the application for which the recycled materials will be used. Demolition debris can be crushed by several crushers such as jaw crusher, hammer mill, impact crusher, and cone crusher

or manually by a hammer. Different crushers have different consequences on the physical and mechanical properties of RAs depending upon the effectiveness of crushing processes and consequently it affects the concrete performance also. Jaw crushers are mainly used for primary crushing as it can crush oversized concrete pieces into comparable size for secondary crushing. Impact crushers are preferred for secondary crushing as they produce a better quality of aggregate with less adhered mortar content. Desirable grading for RAs can be achieved by crushing through primary crushers successively through secondary crushers. The selection of crushers at various stages depends on several factors such as maximum feed size, quality of output, desirable particle size, and shape of the various fractions, and the amount of fines produced.

LITERATURE REVIEW

A literature survey has been carried out with a broad approach to have a better understanding of the concept of Use of Construction and demolition waste in the construction of flexible road pavement. The effect of natural aggregate in conventional road construction is well known. However, the use of recycled aggregate from C&D waste in flexible road pavement has not created a significant situation in the research sector to date.

F. Lancieri, A. Marradi & S. Mannucci, C&D waste for road construction-long time performance of road constructed using recycled aggregate for unpaved layers. These field tests were integrated with laboratory tests performed in order to investigate the time evolution of mechanical characteristics of C&D materials and to evaluate the influence of compaction techniques on the improvement in resistance recorded with the gyratory compactor. The data and results presented confirm that road construction could offer a reliable use for C&D waste recycling. [1]

Rafaela Cardoso (2016), Use of recycled aggregates from construction and demolition waste in geotechnical applications. This paper presents a review of the most important physical properties of different types of C&D aggregate and their comparison with natural aggregates (NA), and how these properties affect their hydraulic and mechanical behavior when compacted, The results collected from the literature indicate that the performance of most C&D aggregate is comparable

to that of Natural aggregate and can be used in unbound pavement layers or in other applications requiring compaction.[2]

Arul rajah (2012), Geotechnical characteristics of recycled crushed brick blends for pavement sub-base applications. This paper presents the findings of a laboratory investigation on the characterization of recycled crushed brick when blended with recycled concrete aggregate and crushed rock for pavement sub-base applications. The engineering properties of the crushed brick blends were compared with typical state road authority specifications in Australia for pavement sub-base systems to ascertain the potential use of crushed brick blends in these applications[3]

Rosario Herrador (2012), Recycled construction and demolition waste aggregate for road course surfacing, the aim of this research study is to verify the technical viability of using construction waste as material for the base pavement layers of road surfaces. For this purpose, a field study was carried out, which included testing the performance of pavement composed of concrete, asphalt mix, and ceramic waste aggregate. This was done by analyzing the characteristics of the recycled material on a section of an actual road under real vehicle traffic conditions. It was observed that the load-bearing capacity of the recycled artificial CDW aggregate was satisfactory.[4]

Ozlem Bozyurt (2012), Resilient modulus of recycled asphalt pavement and recycled concrete aggregate. Review the mechanical properties of RCA and RAP as an unbound base including the relationships between resilient modulus (M_r) And compositions. A high degree of correlation between the predicted M_r and the physical properties of RCA and RAP.[5]

Cesare Sangiori (2014), Construction and demolition waste recycling: an application for road construction. This work focuses on studying the development of the stiffness of recycled materials during construction, as well as how it modifies over time. The study assessed also the correlation between testing systems. A purpose-built experimental embankment with four sections of different recycled materials was built and tested. The results show that recycled aggregates perform well when properly compacted and may show some positive self-cementing properties.[6]

Sherif Yehia, (2015), Strength and durability evaluation of recycled aggregate concrete. This paper discusses the suitability of producing concrete with 100 % recycled aggregate to meet durability and strength requirements for different applications. The results showed that concrete with acceptable strength and durability could be produced if high packing density is achieved.[7]

Chetna M. Vyas et al, 2013, Durability Properties of concrete with partial replacement of natural aggregates by recycled coarse aggregates. Different grades of concrete and different % of replacement of RA, water absorption, and porosity test as durability characteristics. Lower sorptivity and water absorption at 40% replacement for all grades, no significant change of sorptivity for grades of concrete.[8]

OBJECTIVE OF PROJECT

- i. The aim of this project study is to verify the technical viability of using C&D waste and RCA as material for the Flexible road pavement.
- ii. Checking the suitability of solid waste material in flexible road pavement by conducting Geotechnical and Geo-environmental laboratory testing.
- iii. The field performance of the new products C&D waste in the base and sub-base course will be investigated. iv. Construction costs as well as operating and maintenance costs of the pavement with the waste materials will be compared with that of the pavement with the conventional materials.

PROBLEM STATEMENT

The road construction using natural aggregate is a common phenomenon that leads to higher cost in construction and maintenance as availability of material is low and hence the gap between demand and supply is high. So it is necessary to find a better alternative without compromising on Strength. For a decade, many Researchers stated that the C&D waste materials are a suitable alternative for the problem that arises

- i. The constituents included in C&D waste like Ceramics, bricks, etc. cause issues regarding the strength. So, it is necessary to find out that particular constituent from the C&D waste which satisfies the strength and to eliminate the other constituents.

- ii. The rapid economic growth of the country has led to heavy investment in the construction of new infrastructure and the replacement of older infrastructure. This has led to a new variety of the solid waste that environmental engineers have to contend with namely, Construction & Demolition (C&D) waste.

METHODOLOGY

In the report, the emphasis was given on the strength assessment of construction and demolition waste. The properties like compaction value, impact value, specific gravity, abrasion value, etc. are compared with properties of natural aggregate as mentioned above and according to that, the suitability of replacement of natural aggregate with Recycled concrete aggregate is decided. C&D material was collected from a demolition site at Gangapur Road, Nashik, and this waste was crushed in the Crushing Facility in the Civil department of KKWIEER, Nashik in different sizes. Crushed waste of appropriate size was directly used in laboratory testing without recycling. RCA Material was collected from Ahmedabad Enviro Company Pvt. Ltd, Ahmedabad.

RESULTS AND DISCUSSION

Calculation of impact value test

Comparison between NA, C&D waste, RCA for Impact Value Test

Table 1. Comparison between NA, C&D Waste, RCA for Impact Value Test

Sr. No.	Natural Aggregate	C & D material	RCA
1	11.04%	15.12%	14.75%
2	10.11%	29.23%	13.67%
3	10.00%	20.12%	13.17%

Comparison between Concrete, Ceramic & Brick waste for Impact Value Test

Table 2 : Comparison between Concrete, Ceramic & Brick Waste for Impact Value Test

Sr. No.	Concrete waste	Ceramic waste	Brick waste
1	14.75%	10.31%	52.52%
2	15.67%	14.49%	51.32%
3	13.17%	12.38%	53.22%

Graphical representation of Impact value test

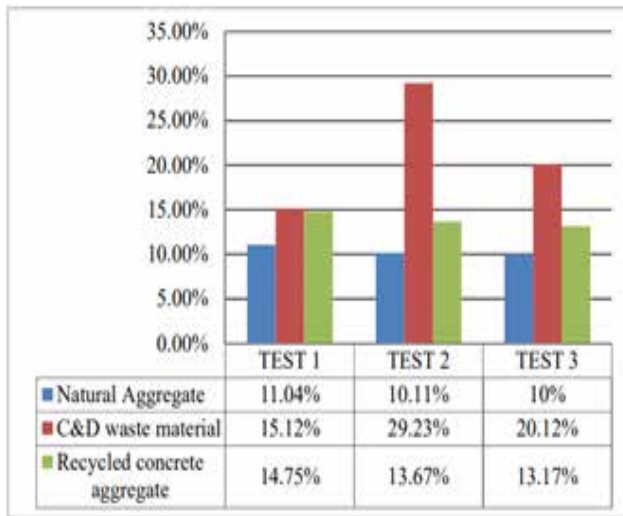


Fig 1 Graphical Representation of Impact Value Test

Graphical representation of impact value test

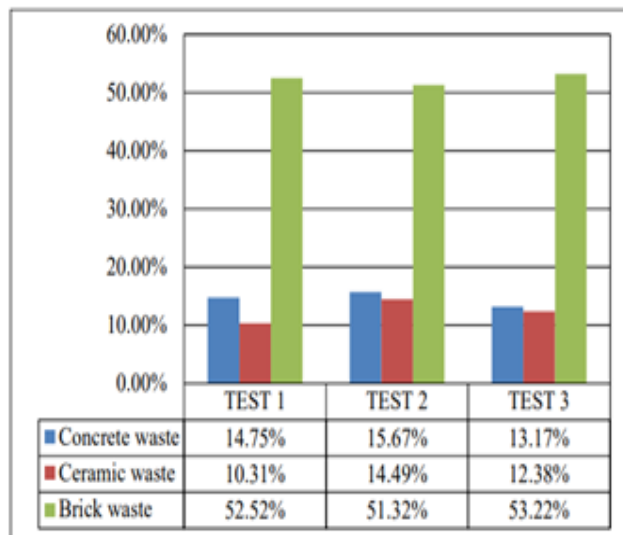


Fig 2 Graphical representation of Impact value test

Standard Result Table for Impact Value Test

Table 3 : Standard result table for Impact Value Test

Aggregate impact value	Classification
<10%	Exceptionally strong
10-20%	Strong
20-30%	Satisfactory for road surfacing
>30%	Weak for road surfacing

e Recycled Concrete Aggregate Impact Value is between 10-20%. Hence, classified as strong for flexible pavement.

Calculation of Crushing Value Test

Comparison between NA, C&D waste & RCA for Crushing Value Test

Table 4: Comparison between NA, C&D waste & RCA for Crushing Value Test

Sr. No.	Natural Aggregate	C & D material	RCA
1	17.99%	37.56%	26.30%
2	18.65%	41.78%	26.25%
3	17.29%	28.91%	25.29%

Comparison between Concrete, Ceramic & Brick waste for Impact Value Test

Table 5 : Comparison between Concrete, Ceramic & Brick waste for Impact Value Test

Sr. No.	Concrete waste	Ceramic waste	Brick waste
1	27.30%	17.50%	52.64%
2	26.25%	16.39%	51.58%
3	25.49%	18.25%	54.68%

Graphical representation of Crushing value test

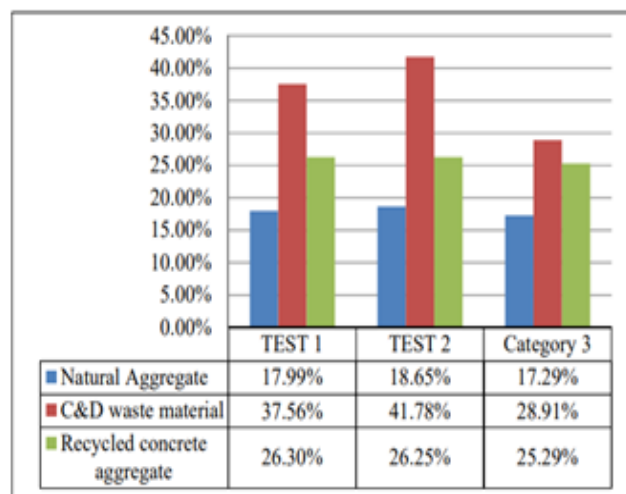


Fig. 3 Graphical representation of crushing value test

Graphical representation of Crushing value test

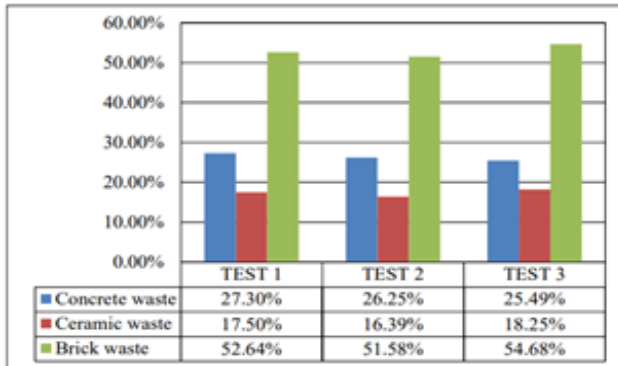


Fig. 4 Graphical representation of crushing value test

Standard Result Table for Crushing Value Test

Table 6 : Standard Result Table for Crushing Value Test

Type of road construction	A.C.V. Not more than(%)
Flexible pavements	
A)soling	50
B)water bound macadam	40
C)bituminous macadam	40
D)bituminous surface dressing or thin premix carpet	30
E)dense mix carpet	30
Rigid pavements	
A)other than wearing course	45
B)surface or wearing course	30

The Recycled concrete aggregate Crushing value is between 20-30%. Hence, classified as strong for flexible as well as rigid pavement. And the C&D waste material cannot be used due to high crushing value.

Alculation of Abrasion Test

Comparison between NA, C&D waste & RCA for Crushing Value Test

Table 7: Comparison between NA, C&D waste & RCA for Crushing Value Test

Sr. No.	Natural Aggregate	C & D material	RCA
1	19.24%	32.43%	23.50%
2	19.66%	43.39%	22.65%
3	20.24%	31.61%	23.41%

Comparison between Concrete, Ceramic & Brick waste for Impact Value Test

Table 8 : Comparison between Concrete, Ceramic & Brick waste for Impact Value Test

Sr. No.	Concrete waste	Ceramic waste	Brick waste
1	32.89%	40.12%	59.32%
2	33.45%	41.69%	58.54%
3	32.36%	41.56%	56.46%

Graphical representation of Abrasion test

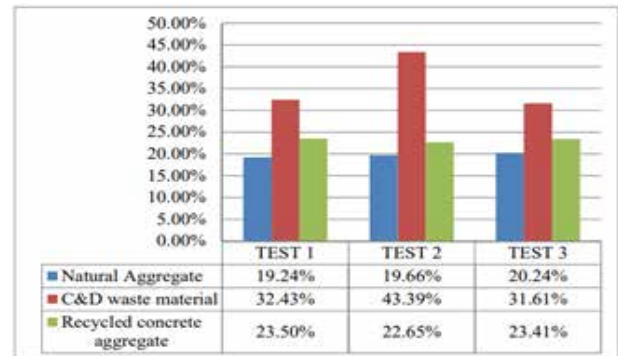


Fig. 5 Graphical representation of Abrasion test

Graphical representation of Abrasion test

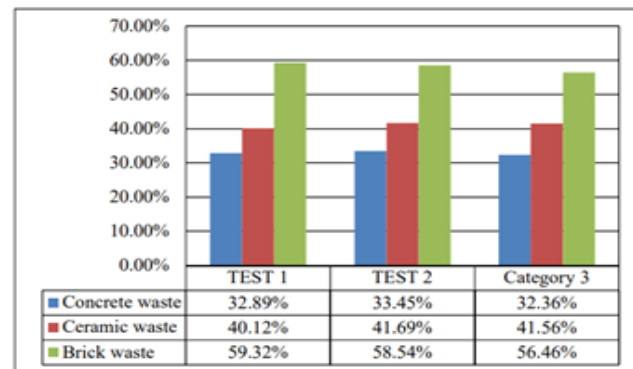


Fig. 6 Graphical representation of Abrasion test

Standard Result Table for Abrasion Test

Table 9 : Standard Result Table for Abrasion Test

Sr. No.	Type of pavement	Limiting value
1	W.B.M sub-surface course	60
2	W.B.M base course with the bituminous surfacing	50

3	Bituminous bound macadam	50
4	W.B.M surface course	40
5	Bituminous penetration macadam	40
6	Bituminous surface dressing, cement concrete surface course	35
7	Bituminous concrete surface course	30

The RCA Abrasion value is between 15-30%. Hence, classified as strong for a bituminous concrete surface course.

Specific Gravity and Water Absorption

Comparison between NA & RCA for Specific Gravity and Water Absorption Test

Table 10 Comparison between NA & RCA for Specific Gravity and Water Absorption Test

	Natural Aggregate	RCA
Specific Gravity	2.92	2.63
Water Absorption	2.12 %	2.89%

Graphical representation of the Specific gravity and Water absorption test

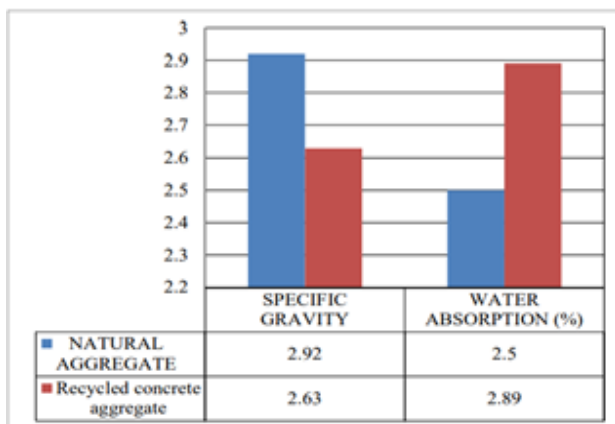


Figure 7 Graphical representation of the Specific gravity and Water absorption test

As per MORTH specifications, Water absorption up to 4% has been successfully used in the granular base course of road pavements.

Calculation of Shape Test

Result of FI and EI

Table 11 Result of FI and EI

	Flakiness Particles (FI)	Elongated Particles(EI)
RCA	16.59%	19.33%
Ceramic Waste	66.32%	73.23%
Brick waste	43.58%	36.58%
C&D waste	39.87%	51.37%

Flaky Particles: More than 30% of flaky particles are not allowed for construction of pavement as we got the flakiness index value 16.59% for RCA, so these aggregates are suitable for any type of pavement construction. But the FI of Ceramic, Brick and C&D waste is varying as compared to RCA. So the aggregates may affect the strength of the road pavement. For Elongated Particles: As there is no proper scale of measuring percentage ratio allowable for this test as per IRC but the particles not fit for FI is not fit for Elongated index. The shape test give only a rough idea of the relative shapes of the aggregates.

Stripping Value Test

Comparison between NA & RCA for Stripping Value Test

Table 12 Comparison between NA & RCA for Stripping Value Test

Test	Natural Aggregate	RCA
Stripping Value	4.92%	3.63%

Indian Roads congress (IRC) and MORTH have specified the allowable limits of stripping test values for the aggregates to be used in bituminous road construction is 25%. The stripping value of recycled concrete aggregate is 3.63% which is less than 25% and hence the RCA can be used for bituminous road construction.

CONCLUSION

It is observed that the results obtained from the natural aggregate and Recycled Concrete Aggregate of Impact value test, Crushing value test, Abrasion test, Specific gravity and water absorption test and Stripping value test are almost close enough and is also within limiting

value. Hence, replacing the natural aggregate with the Recycled Concrete Aggregate is the best feasible alternative. As the manufacturing cost of Recycled Concrete Aggregate is very cheap as compared to Mined Virgin aggregates. Hence, the utilization of these waste materials in road construction will be enhanced and higher economic returns are expected. Also, the concrete waste need to be separated from the C&D waste at initial stage rather than using mixed proportion of C&D waste, as result interpretation of the C&D waste failed in Impact, Crushing and Abrasion test.

REFERENCES

1. F. Lancieri, A. Marradi & S. Mannucci, "C&D waste for road construction- long time performance of road constructed using recycled aggregate for unpaved layers", WIT Transactions on Ecology and the Environment 92:559-569 · June 2006.
2. Rafaela Cardoso (2016), "Use of recycled aggregates from construction and demolition waste in geotechnical applications, Waste Management Volume 49, March 2016, Pages 131-145".
3. Arul rajah (2012), "Geotechnical characteristics of recycled crushed brick blends for pavement sub-base applications, Canadian Geotechnical Journal 49(7):796-811 · June 2012".
4. Rosario Herrador, (2012), "Recycled construction and demolition waste aggregate for road course surfacing Journal of Transportation Engineering 138(2):182-190 · February 2012".
5. Ozlem Bozyurt (2012), "Resilient modulus of recycled asphalt pavement and recycled concrete aggregate, Geotechnical Special Publication · March 2012".
6. Cesare Sangiori (2014), "Construction and demolition waste recycling: an application for road construction, International Journal of Pavement Engineering 16(6):1-8 · November 2014".
7. Sherif Yehia, (2015), "Strength and durability evaluation of recycled aggregate concrete".
8. Chetna M. Vyas, 2013, "Durability Properties of concrete with partial Replacement of natural aggregates by recycled coarse aggregates".
9. Use of Construction Demolition Waste in Pavement: ISSN: 2350-0328: International Journal of Advanced Research in Science, Engineering and Technology Vol. 4, Issue 12, December 2017
10. Sandeep Shrivastava and Abdol Chini M.E. Rinker, Construction Materials and C&D Waste in India: Sr. School of Building Construction University of Florida, USA.
11. Geotechnical Challenges in Highway Engineering in Twenty First Century: Lessons from the Past Experiences and New Technologies: (2013) - Seventh International Conference on Case Histories in Geotechnical Engineering

Machine Learning Approach for Cyber-attack Detection: A Comprehensive Review

Swati Gawand

Research Scholar
Department of Computer Science and Engineering
Sandip University, Mahiravani
Nashik Maharashtra
✉ swatigawand@gmail.com

Meesala Sudhir Kumar

Professor
Department of Computer Science and Engineering
Sandip University, Mahiravani
Nashik, Maharashtra

ABSTRACT

The Internet is being used by more people than ever before. The primary cause of this is the current trend of electronic devices and data bundles being more affordable. In actuality, people's daily lives in the modern world depend heavily on the Internet. People utilize the Internet for a variety of purposes, such as banking, gaming, business, education, sports viewing, entertainment, and travel. It leads to a modern, information-rich life where everything is at your fingertips. Conversely, excessive use causes our private information to be unknowingly disclosed online. These data can be misused in a number of different ways. The term "cyber security" refers to this, which is a large field of study that covers the fundamentals of misuse this is commonly referred to as "cyber security," which is a large topic of study that addresses risks associated with utilizing the Internet and the fundamentals of data misuse. Specifically, these dangers are known as cyber-attacks, and one of the oldest and most prevalent issues is identifying these types of hostile activity on a network. Recognizing and avoiding digital attacks can be challenging tasks. Every year, there is an increase in the severity of cybercrimes and their damage. Cybersecurity is important in every industry to protect company data and recognize attack techniques. Defending it's getting harder to protect data against cyber-attacks like denial-of-service (DoS), phishing, WannaCry, etc. Cyber-attacks are happening more frequently, which regularly causes major financial loss to both individuals and nations. Even though preventing and identifying cyber-attacks are still thought to be difficult undertakings, cyber security is constantly changing. A subset of artificial intelligence called machine learning (ML) is helpful in predictive analysis. In this review paper, we go over various ML algorithms and techniques for Cyber-attack detection. The primary goal of this work is to link the types of assaults to the types of machine learning algorithms that are used to identify them.

KEYWORDS : Denial of service attack (DoS), Wannacry attack, DoS attack, Algorithms.

INTRODUCTION

Security incidents have been reported more frequently recently all across the world. This issue is closely tied to the recent rise in mobile device users who make up the population of connect-from-anywhere terminals, which frequently push the conventional limits of network security. Moreover, the usage of Internet is growing exponentially nowadays. This is mainly due to the cheaper price of electronic gadgets and data packages as per the recent trend. In fact, Internet is playing a crucial role in everyday life of people in today's world.

For instance, people use Internet for browsing, banking, playing games, business, education, watching sports, entertainment, travel, etc. It leads to a sophisticated life where the information is available in the finger tips. On the other, the heavy usage incurs our personal data to be leaked elsewhere in the web without our knowledge. There are multiple ways through which these data can be misutilized. This field of study is generally termed as Cyber security which is a broad field of research covering the essentials of misutilization of data and threats of using Internet.

Cyber security is growing field and the percentage of Cyber-attacks is constantly increasing. Network protection is developing and the pace of Cyber-attacks is continually expanding. Refined assaults are thought of as exceptional, however the new ordinary as they may be turning out to be more regular and boundless. This steady advancement additionally calls for development in the network safety guard. Cyber security protects physical-digital data, networks, and technological systems from Cyber-attacks. Cyber-attacks such as distributed denial of service attacks by sending malicious packets have increased. Cyber-attacks such as distributed denial of service attacks by sending malicious packets have increased. In addition, increasingly, attackers are deploying malicious attack software that has been secretly placed on the victim's PC.

Basically, ML is a subset of Artificial Intelligence and it is useful in predictive analysis. In fact, ML abilities are used by numerous applications including Cyber security issues. In this review article, we discuss different approaches/methods of ML for identification of Cyber-attacks. The mapping between the kind of attacks and the type of ML algorithm used for detecting the respective attack is the main focus of this work.

The remainder of this paper is organized as follows. Section II is related to literature survey. Section III gives an overview of types of cyber-attacks. The various Machine Learning methods are discussed in section IV. Section V contains the conclusion of this research study and the future direction of works.

LITERATURE SURVEY

Today we live in a computerized time where all parts of our lives depend on the organization, computer and other electronic gadgets, and programming applications. All basic frameworks like the financial framework, medical services, monetary organizations, parliaments, and assembling businesses use gadgets associated with The Web as a center of their tasks. A portion of their data can be touchy for unapproved access or openness. This data allows gatecrashers and danger entertainers to invade them for monetary profit, coercion, political or social thought processes.

The act of trying to steal data or get unauthorized

access to computers and networks by using one or more computers is called a Cyber-attack. Before committing a data breach, an attacker would often launch a Cyber-attack to get unauthorized access to people or business computers or networks. Digital assaults are currently a global concern.

Machine Learning (ML) methods which are extensively used in Cyber security include Support Vector Machine Logistic Regression, K Nearest Neighbours, Decision Tree, and Random Forest Classification. The availability of large collection of past data with labels, Deep Learning classification models involving Restricted Boltzmann Machines (RBM), Convolution Neural Networks (CNN), Recurrent Neural Networks (RNN) cells for feature extraction followed by a densely connected neural network have become more efficient in solving complex tasks. Applicability of the above supervisory machine learning techniques is conditioned based on the availability of large collections of labelled data [1].

In this work [2], authors reviewed the primary commitments behind building this Digital Assault Location Model system are: Construct a computerized discovery system Digital Assault Location Model by utilizing database scan to work with multi-layered information and Rope to diminish dimensionality and picking the viable qualities of an organization for grouping of various sorts of assault.

In this paper [3], pre-handling is finished to eliminate the missing qualities, anomalies and so forth and from the pre-handled information, the huge highlights are found by applying right component determination calculation. From that point onward, the information with the chose highlights are grouped with the assistance of arrangement calculations. Outfit technique is utilized for arrangement since this strategy creates exceptionally confided in choices and works on by and large precision by cooperating. In this work [4] Authors plans to find spatial and fleeting criminal areas of interest utilizing a bunch of genuine world datasets of Cybercrimes. He will attempt to find the wrongdoing areas and their incessant event time Furthermore, will foresee what kind of wrongdoing could happen next in a particular area inside a specific time and which nations are probably going to get digital assaults.

Attack Forecast and Prediction [5] Working on guarded capacities in the internet for improving digital protection is one of the key moves that should be settled to empower versatile social orders and present day life, which is progressively entered by data innovation. Figuring out the past and foreseeing what's in store is a methodology being looked for over opportunity to foster new security profiles and programming to assist with safeguarding socially delicate information and basic framework from assailants. Foreseeing future digital assaults can help organizations, people and society. KNN grouping was the best with a precision of 78.9% [7].

ML approaches can work with us to stop delicate data releases, corporate leader interruption recognition framework and malware identification. ML rule will find and decide any new unprecedented example or conduct that might emerge from interruptions from outside. Security openings brought about by recompenses made to clients or developers or chiefs should be charmed a ton of care. Security holes caused by allowances created by users or programmers or directors should be infatuated with a lot of care [8].

In this work [9] authors discussed an online digital assault identification calculation utilizing the system of sans model Reinforcement Learning (RL). The proposed calculation is all inclusive, i.e., it does not need assault models. The proposed plot broadly appropriate and furthermore proactive as in new obscure assault types can be identified.

The danger of digital assaults is on the ascent in the computerized world today. Misclassification is a typical issue in machine for interruption identification, and the improvement of machine learning models is obstructed by an absence of understanding into the purposes for such misclassification. Intrusion Detection & prevention system is a software product application to identify network interruption utilizing different AI calculations. An ID screens an organization or framework for pernicious action and shields a PC network from unapproved access from clients, including maybe insider. The interruption indicator learning task is to fabricate a prescient model (for example a classifier) equipped for recognizing 'terrible associations' (interruption/assaults) and a 'decent (ordinary) associations [11].

We reviewed several papers on Cyber-attacks and

machine learning. Machine learning is used to identify and predict Cyber-attacks. Random Forest, Logistic Regression, K-Nearest Neighbors, Decision Tree, and Support Vector Machine are some of the algorithms.

TYPES OF CYBER ATTACKS

Cyber-attacks often aim to disable or obtain access to the target system. The objective can be accomplished by using a variety of attacks against the target system. Numerous Cyber- attacks exist and even change daily [12]. Following Figure 1 shows different types of attacks. Some of the common Cyber- attacks are explained below:



Figure 1: Types of Attacks [29]

From ransom ware attacks crippling entire systems to phishing scams targeting unsuspecting users, the range and complexity of cyber threats are ever-expanding. The repercussions of such attacks can be severe, leading to financial losses, compromised privacy, and even endangering national security. As society becomes increasingly reliant on digital infrastructure, combating cyber threats requires constant vigilance, robust cybersecurity measures, and collaborative efforts across sectors to safeguard against potential vulnerabilities.

Malware

Malware is a record or code, often conveyed over an organization, that taints, investigates, takes or leads practically any conduct that an aggressor needs. In spite of the fact that malware comes in countless variations, there are various techniques to taint PC

frameworks. Malware is "Noxious programming". It is an extraordinary kind of code or application explicitly created to hurt electronic gadgets

Phishing

Phishing is when aggressors try to fool clients into doing something unacceptable, for example clicking a terrible connection that will download malware, or direct them to a dodgy site. Phishing can be led through an instant message, online entertainment, or by telephone, but the term "phishing" is fundamentally used to describe assaults that show up by email. Phishing messages can arrive at a lot of clients easily, and stow away among the vast number of harmless messages that bustling clients get.

Man-in-the-middle Attack

A man in the middle attack is a type of digital assault where a client is presented with a gathering between the two gatherings by a vindictive person of some sort, controls the two players and gets admittance to the information that the two individuals were attempting to convey to one another. A man-in-the-center assault helps a noxious attacker, with no sort of member seeing until it's past the point of no return, to hack the transmission of information planned for another person and shouldn't be sent by any means.

Cryptojacking

Cryptojacking is a sort of Cyber-attack where a crook subtly uses a loss' ability to figure to make computerized cash This for the most part happens when the setback coincidentally presents a program with malignant items which grant the Cyber-attack to get to their PC or other Web related contraption, for example by tapping on a dark association in an email or visiting a defiled webpage. Programs called 'coin diggers' are then used by the criminal to make, or 'mine', advanced types of cash.

Denial-of-service Attack

A Denial-of-Service assault is an assault intended to shut down a machine or organization, making it impossible to reach its expected clients. DoS assaults achieve this by flooding the objective with traffic, or sending them data that sets off an accident.

Zero-Day

Zero-day weakness is a product weakness found by aggressors before the seller has become aware of it. No fix exists for zero- day weaknesses since the merchants are uninformed which make assaults prone to succeed. A zero-day exploit is the technique programmers use to go after frameworks with a formerly unidentified weakness.

In this segment we have talked about various kinds of digital assaults. A digital assault is a hostile, unapproved framework/network access by an outsider. It targets obliterating or taking private data from a PC organization, data framework, or individual gadget.

MACHINE LEARNING APPROACH

Machine Learning (ML) has acquired a wide interest on numerous applications and fields of study, especially in network safety. ML computations can be utilized to prepare and identify on the off chance that there has been a digital assault with equipment and figuring power turning out to be more open, machine learning techniques can be utilized to dissect and order troublemakers from a colossal arrangement of accessible information. Figure 2 shows the workflow of machine learning model. Machine learning model works with network traffic data or dataset. In data preprocessing step missing values of records are checked and that record will get deleted. Only distinct records are used for further processing. In feature extraction, highly correlated features are selected. Machine learning Algorithms are of two types i.e. supervised and unsupervised learning algorithm.



Figure 2: Machine Learning Workflow

Supervised Learning

Supervised machine learning algorithms are commonly used for cyber-attack detection. These algorithms learn from labeled training data, where the input data(features) are associated with corresponding labels indicating whether an attack is present or not. The trained model can then be used to make predictions on new, unseen data.

In the space of ML, the most famous managed learning procedures are known as order and relapse techniques. Navies Bayes, Decision Tree [16], K-Nearest Neighbours [20], support vector machines, adaptive boosting, and logistics regression are the notable grouping strategies. Relapse examinations can likewise be utilized to identify the underlying drivers of Cyber- attack and different sorts of misrepresentation. Straight relapse, support vector relapse are the well-known relapse strategies. Examples of supervised ML algorithms are, Decision Tree, Random Forest, Support vector machine, logistic regression, neural network.

Unsupervised Learning

Unsupervised machine learning algorithms can also be employed for cyber-attack detection. Unlike supervised learning, unsupervised learning doesn't require labelled training data; instead, it identifies patterns, anomalies, or clusters within the data without explicit guidance on what to look for. Unsupervised algorithms are particularly useful for detecting unknown or novel attacks that may not be well- defined or understood

In this section we have discussed about different types of ML algorithms Mainly, ML algorithms are classified as supervised learning and unsupervised learning. Supervised learning approaches are finished with regards to grouping where information matches to a result, or relapse where information is planned to a persistent result. Unsupervised learning is generally achieved through bunching and has been applied to exploratory investigation and aspect decrease. Both of these methodologies can be applied in network protection for examining malware in close to constant, hence fulfilling the shortcomings of customary discovery techniques.

CONCLUSIONS

This paper focuses on various types of Cyber-attacks and the usage of Machine Learning (ML) for those attacks. Basically digital protection is gaining knowledge with the expanded web utilization and wide assortment of organization applications. There are several ML algorithms which help in Cyber security. These ML algorithms basically differentiated in terms adopted strategies. Mainly the ML algorithms are divided into supervised and unsupervised learning. Both these types are observed to be potential solution for the

Cyber-attack detection. The field of this study can be expanded with additional Cyber-attacks types. Also, the special branch of ML, i.e., Deep Learning can be considered for the future studies. Mention that various Deep Learning algorithms are now in demand to solve the issues of Cyber security, especially for image and video encryptions.

REFERENCES

1. Jullian, O., Otero, B., Rodriguez, E. et al. Deep-Learning Based Detection for Cyber-Attacks in IoT Networks: A Distributed Attack Detection Framework. *J Netw Syst. Manage* 31, 33 (2023). <https://doi.org/10.1007/s10922-023-09722-7>
2. Devarakonda, Ananya & Sharma, Nilesh & Saha, Prita & Lokesh, Ramya. (2022). Network intrusion detection: a comparative study of four classifiers using the NSL-KDD and KDD'99 datasets. *Journal of Physics: Conference Series*. 2161. 012043. 10.1088/1742-6596/2161/1/012043.
3. Mr.S.S.Vasantharaja, Aakash B, Avinash M, "Predicton of Cyber-attack Using machine learning technique," *International Journal of creative thoughts*, Vol 10 Issue 6, pp 40-51, 2022
4. Arpitha. B, Sharan. R Brunda. B. M, Indrakumar. D. M, Ramesh. B. E" *Cyber Attack Detection and Notifying system using*
5. Techniques ", *Indian Journal of Computer Science and Engineering (IJCSE)*, pp 28153-28159, 2021
6. Fahima Hossain, Marzana Akter and Mohammed Nasir Uddin , " *Cyber Attack Detection Model (CADM) Based on Machine Learning*
7. Approach ", *2nd International Conference on Robotics, Electrical and Signal Processing Techniques (ICREST)*, pp 567-572, 2021
8. Abdulkadir Bilen and Ahmet Bedri Özer," *Cyber-attack method and perpetrator prediction using machine learning algorithms*", *Peer J Computer Science*, pp 475-496 ,2021
9. *Journal of Computer Science and Engineering (IJCSE)*, pp 28153- 28159, 2021
10. Fatima Hossain, Marzana Akhter and Mohammed Nasir Uddin , " *Cyber Attack Detection Model (CADM) Based on Machine Learning Approach "*, *2nd International Conference on Robotics, Electrical and Signal Processing Techniques (ICREST)*, pp 567-572, 2021

11. Abdulkadir Bilen and Ahmet Bedri Özer, "Cyber-attack method and perpetrator prediction using machine learning algorithms", peer Computer Science, pp 475-496, 2021
12. Florian Klaus Kaisera, Tobias Budiga, "Attack Forecast and Prediction", C&ESAR'21: Computer Electronics Security Application Rendezvous, pp 77-97, 2021
13. Twinkle Shah, Sagar Parmar, Kishan Panchal, "Cyber Crime Attack Prediction", International Research Journal of Engineering and Technology, pp 1037-1042, 2020.
14. Kumar, "Cyber-attack prediction using machine learning algorithms", International Conference on Advances in Computing, Communication and Control (ICAC3), pp 1-5, 2020
15. H. Alqahtani, I. Sarker, A. Kalim, S. Minhaz Hossain, S. Ikhlaq and S. Hossain, "Cyber Intrusion Detection Using Machine Learning Classification Techniques," In Proc. International Conference on Communications in Computer and Information Science, pp. 121-131, 2020
16. A. Ahmim, M. Ferrag, L. Maglaras, M. Derdour and H. Janicke, "A Detailed Analysis of Using Supervised Machine Learning for Intrusion Detection," Strategic Innovative Marketing and Tourism, pp. 629-639, 2020.
17. W. Zong, Y. Chow and W. Susilo, "Interactive three-dimensional visualization of network intrusion detection data for machine learning," Future Generation Computer Systems, vol. 102, pp. 292-306, 2020
18. O. Sarumi, A. Adetunmbi and F. Adetoye, "Discovering computer networks intrusion using data analytics and machine intelligence," Scientific African, vol. 9, p. p 1-5, 2020.
19. A. Nagaraja, B. Uma and R. Gunupudi, "UTTAMA: An Intrusion Detection System Based on Feature Clustering and Feature Transformation," Foundations of Science, vol. 25, no. 4, pp. 1049-1075, 2020.
20. A. Saleh, F. Talaat and L. Labib, "A hybrid intrusion detection system (HIDS) based on prioritized k-nearest neighbours and optimized SVM classifiers", Artificial Intelligence Review, vol. 51, no. 3, pp. 403-443, 2020.
21. H. Liu and A. Gegov, "Collaborative Decision Making by Ensemble Rule Based Classification Systems," Studies in Big Data, pp. 245-264, 2020. P. Negandhi, Y. Trivedi and R. Mangrulkar, "Intrusion Detection System Using Random Forest on the NSL- KDD Dataset," Emerging Research in Computing, Information, Communication and Applications, pp. 519-531, 2019.
22. C. Gayathri Harshitha, M. Kameswara Rao and P. Neelesh Kumar, "A Novel Mechanism for Host-Based Intrusion Detection System," In Proc. First International Conference on Sustainable Technologies for Computational Intelligence, pp. 527-536, 2019.
23. Y. Ever, B. Sekeroglu and K. Dimililer, "Classification Analysis of Intrusion Detection on NSL-KDD Using Machine Learning Algorithms," In Proc. International Conference on Mobile Web and Intelligent Information Systems, pp. 111-122, 2019.
24. T. Tang, D. McLernon, L. Mhamdi, S. Zaidi and M. Ghogho, "Intrusion Detection in SDN-Based Networks: Deep Recurrent Neural Network Approach," Deep Learning Applications for Cyber Security, pp. 175-195, 2019.
25. A. Gupta, G. Prasad and S. Nayak, "A New and Secure Intrusion Detecting System for Detection of Anomalies Within the Big Data," Studies in Big Data, pp. 177-190, 2018.
26. A. Saleh, F. Talaat and L. Labib, "A hybrid intrusion detection system (HIDS) based on prioritized k-nearest neighbors and optimized SVM classifiers", Artificial Intelligence Review, vol. 51, no. 3, pp. 403-443, 2017.
27. M. Ibrahim, "An empirical comparison of random forest-based and other learning-to-rank algorithms," "Pattern Analysis and Applications, vol. 23, no. 3, pp. 1133-1155, 2019.
28. <https://www.wallarm.com/what/what-is-a-cyber-attack>

An AI based Interactive and Intelligent Museum Exhibit Based on Attention Analysis

Kunal Chanda

Souvik Banik

Washef Ahmed

Centre for Development of Advanced Computing
Kolkata, West Bengal
✉ kunal.chanda@cdac.in

ABSTRACT

Present study aims to develop an AI based Interactive and Intelligent Museum Exhibit Based on Attention Analysis. Every year thousands of visitors visit Science Museums. The mission is to invoke a sense of awe and curiosity and use those emotions to educate and inform. In our own research, we have taken views from the visitors through a set of questionnaires to understand those objects in the exhibit which causes awe. The situational awe generated were either positive having a sense of connection, negative having feelings of disjointed or neutral. These were related to the assessed states and it was found direct correlation with the visitors response. The study was conducted at the Science Museum in Kolkata. A total of 201 visitors at Science City Museum participated in the current study. Recruitment occurred prior to entry into target exhibit spaces at the time of registration. It was found that to ignite interests towards different exhibits displayed in a museum among visitors our system was capable of understanding eye ball movement of a visitor towards an exhibit of interest in order to determine regions of attentions through gaze points on an exhibit. The system was also capable of identification of facial expression at the time of capturing attention by the visitor in order to categorize intensity and senses (positive, negative or neutral, etc.) of interest for that particular exhibit. Our AI based system was able to analyze based on the visual analytics parameters for out of the 201 visitors, 184 were correctly identified as to correlate with their interests captured through the questionnaires giving an accuracy of 92%.

KEYWORDS : *Interactive museum, Curiosity and awe, Visual analytics.*

INTRODUCTION

In the contemporary world, the fusion of technology and art has paved the way for revolutionary advancements in the way we interact with cultural exhibits. Among these innovations, the integration of Artificial Intelligence (AI) has brought forth a new era of interactive and intelligent museum experiences. This introduction of AI-driven attention analysis within museum exhibits represents a groundbreaking approach, transforming passive viewing into an engaging, personalized and insightful journey for visitors. The amalgamation of AI technology with traditional museum settings has given rise to a transformative experience—one that caters to the evolving preferences of a technologically- driven audience. Through the application of attention analysis, this exhibit harnesses the power of AI algorithms to discern and understand visitor behavior, preferences,

and engagement levels within the exhibition space.

This innovative approach fundamentally redefines the museum experience. It transcends the conventional static displays by creating a dynamic, responsive environment that adapts to the individual interests and engagement of each visitor. By leveraging attention analysis, the exhibit can intuitively adjust content delivery, offering a tailored experience that captures and sustains the attention of diverse audiences. Furthermore, this AI-based interactive exhibit serves as an educational tool by providing valuable insights into visitor interactions and preferences. The analysis of attention patterns and engagement metrics not only enhances the visitor experience but also enables curators and designers to refine future exhibitions based on empirical data. Moreover, the incorporation of AI-driven attention analysis aligns with the broader societal shift towards

personalized experiences. By creating a museum environment that dynamically responds to visitor preferences, this exhibit caters to the unique interests of each individual, fostering a deeper connection between the audience and the displayed artifacts or artworks.

Thus, this AI-based interactive and intelligent museum exhibit, founded on attention analysis, represents a pioneering advancement in the convergence of technology and culture. It marks a pivotal moment in redefining the museum experience, offering a personalized, engaging, and educational journey that resonates with diverse audiences, paving the way for a new era of immersive cultural exploration.

CONTRIBUTIONS

A novel method for an interactive and intelligent museum exhibit based on attention analysis is proposed.

Contributions in this paper are mainly:

- 1) Analysis of the time series generated by the eye ball tracker and detection of most attentive region by generating a heat map.
- 2) Creating an Attention Value Model relevant to exhibit of the museum.

RELATED WORK

The concept of AI-driven interactive museum exhibits is still in its early stages, but several research projects and initiatives demonstrate its potential. Here are some notable examples:

EyeSee [1] project developed an AI-powered museum exhibit that uses eye tracking technology to personalize the visitor experience. By analyzing visitor gaze patterns, the system highlights specific areas of interest and provides additional information about them. The Intelligent Museum [2] initiative aims to develop AI-powered museum experiences that are personalized, interactive, and engaging. It explores various approaches such as facial recognition, sentiment analysis, and visitor tracking to understand visitor behavior and tailor the exhibit accordingly. The Virtual Curator [3] project explores the use of virtual agents as AI-powered museum guides. These agents can answer visitor questions, provide additional information about exhibits, and even personalize the visitor experience

based on their preferences. Attention-Based Museum Exhibit Design [4] research investigated the potential of using attention analysis to design more engaging and informative museum exhibits. The study suggests that by understanding visitor attention patterns, exhibits can be designed to better capture and hold visitor interest. The Museum of the Future [5] in Dubai utilizes various AI technologies, including facial recognition, body language analysis, and personalized recommendations, to create a unique and dynamic visitor experience.

Millions of people visit science museums in our nation each year. Although each museum's goals differ greatly, they almost all share the same goal of inspiring wonder and curiosity and using such feelings to enlighten and educate [6]. Awe and related feelings are frequently intentionally cultivated in visitors through museum programming. The compression and expansion effect is a common technique used by museum builders to create awe in visitors by having them pass through small hallways and then enter a spacious, immersive area. "They expect to see wondrous things that they cannot see in their everyday lives," according to visitors to museums [7]. The mechanism could be in awe's role as one of the epistemological emotions, which have been shown to enhance learning and shape long-term memories of museum visits [8- 10]. Still another research intends to explore how Artificial Intelligence (AI) and computing technology can be used to create a more immersive and enjoyable experience within the context of a museum visit [11].

OVERVIEW

For understanding visitor's perception of the exhibit through Eye tracking the study is undergone with the objective of not confining eye-tracking to theoretical research, but bring this technology into the Indian museum space to understand how exhibits are consumed. Implementing eye-tracking in the museum space means giving the museum authorities the means to understand how visitors decode the exhibits and to use this knowledge to change the way they are explained. At present data collection and validation is being undergone on the visitor experience (what content was consumed) and also collect data on the very act of consuming the exhibit (how did the eye look at the exhibit? On which parts did the gaze stop?

How long was the exhibit contemplated?) The study proposes to understand in-depth on how exhibits are consumed and explanations taking into account the consumption pattern. These perspectives are innovative and promise to offer credible alternative to the traditional guided tour. The museums would also be able to increase the loyalty of their public by making the visit more enjoyable and didactic by offering them an evolving and personalized experience.

Museums and Awe

Every year thousands of visitors visit Science Museums. The mission is to invoke a sense of awe and curiosity and use those emotions to educate and inform. In our own research, we have taken views from the visitors through a set of questionnaires to understand those objects in the exhibit which causes awe. The situational awe generated were either positive having a sense of connection, negative having feelings of disjointed or neutral. These were related to the assessed states and there was found direct correlation with the visitors response.

Research setting

The study was conducted at the Science Museum in Kolkata. The current study focused on two exhibit spaces that were chosen based on characteristics that were likely to influence visitor’s experience of awe. Both spaces are physically vast, a factor known to induce awe, yet each space has unique awe. The Exhibit on Indian Classical Instrument had 10 different such instruments displayed in the most exquisite way with sounds emitting in a rhythmic form. The second exhibit is a diorama of Mohenjo-Daro Civilization with people wearing attires and carrying out errands of that time.

Scenario at Science City

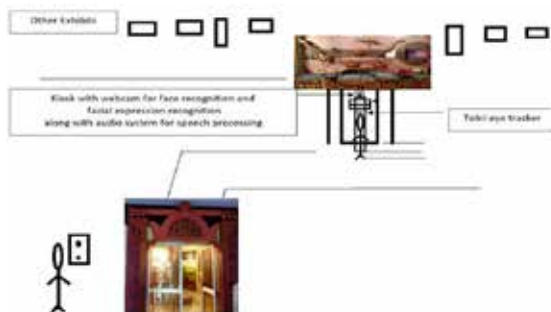


Fig 1. Scenario at Science City

A visitor enters the Heritage Gallery of Science City where the exhibits are located. The visitor stands in front of the exhibit with the sensor frame which will be automatically adjusted based on visitor’s height. The visitor will watch the exhibit through the Frame Window provided and automatic segmentation of the objects from the exhibit will be undergone. The visitor will watch different objects based on his/her interest and priority within a span of 30 secs.

Our developed system automatically collects required data using the webcam and tobii eye tracker and determine the most attentive regions. Based on the data collected machine learning algorithms is used to calculate and estimate the valence of the objects of the Exhibit based on the visitor’s priority.

PROPOSED METHODOLOGY

Creating an AI-based interactive and intelligent museum exhibit that utilizes attention analysis involves several key steps and methodologies. Block diagram shows the steps.

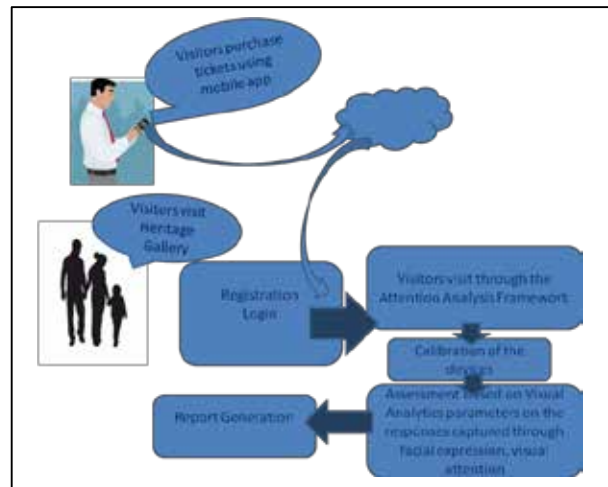


Fig 2. Block Diagram showing several steps

Here's a proposed methodology to develop such an exhibit:

Objectives and Audience

To ignite interests towards different exhibits displayed in a museum among visitors, the system must be capable of understanding eye ball movement of a visitor towards an exhibit of interest in order to determine regions of attentions through gaze points on an exhibit.

The system must also be capable of an identification of facial expression at the time of capturing attention by the visitor in order to categorize an intensity and senses (positive, negative or neutral, etc.) of interest for that particular exhibit.

The system should also have an auto calibration model to calibrate eyeball tracker for different visitors with different heights.

The system must be capable of automatic segmentation of objects of interest detected by identification of facial expression in order to facilitate an improved capture of regions of interests from the visitor.

Finally the system must be capable of determining and prioritizing the objects viewed and focus on the interested object with a narrative to the visitor.

A total of 201 visitors at Science City Museum participated in the current study. Recruitment occurred prior to entry into target exhibit spaces at the time of registration. A total of 148 visitors participated in this study on the Indian Classical Instrument Exhibit. And 53 visitors participated within the Mohenjo-Daro civilization exhibit space. Given that attention to the exhibit was a variable of interest, we avoided approaching families with small children and groups of four or more individuals.

Content and Interactive Elements

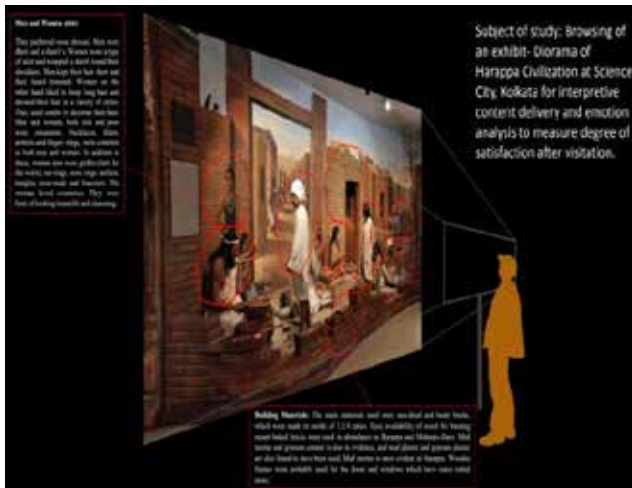


Fig 3. Exhibit of a Diorama

One of the exhibit is a diorama of Harappan Civilization at Science City Kolkata for interpretive content delivery

and emotion analysis to measure degree of satisfaction after visitation.

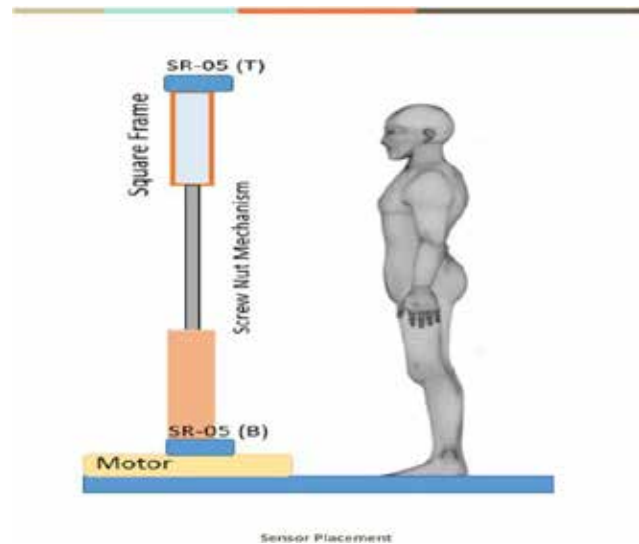


Fig 4. A sensing assembly and associated arrangement of the proximity sensors in the frame in order to facilitate operation of the system

A first proximity sensor mounted on a top edge of the frame and a second proximity sensor mounted on a bottom edge of a stand of the frame extending along a same line.

The proximity sensors are affixed to the frame via a screw nut mechanism.

Attention Analysis Framework

The data collection is performed using eye tracker and web camera to collect data on visitors' attention, gaze, and interactions within the exhibit.

For AI Attention Analysis, employment of machine learning algorithms to analyze attention patterns, identifying areas of high and low visitor engagement has been provided. The eye tracking parameters with the corresponding assessed states are provided in Table 1 below.

Table. 1. Eye Tracking parameters considered for AI Attention Analysis

Eye Tracking Parameters	Assessed States
Area of Visual Attention	Mental states
Number and durations of fixations	Mental states and information behavior

Fixation duration and saccade amplitude	Information search behavior and levels of mental load
Number of fixations, time to first fixation, fixation duration	Usability of product display structure
Attention heat map	Usability of a design concept
Fixation duration and saccade amplitude	Subjective sensation of presence
Scan path entropy	Meaningful perception of environment
Fixation number	Level of immersion
Fixation number and variability in fixation duration	Perceptual level
Facial Expression Analysis	Emotional state
Demographic Information	Gender and Age

Technology Implementation:

AI Integration is performed utilizing AI technologies (computer vision, machine learning models) to process and analyze real-time visitor data.

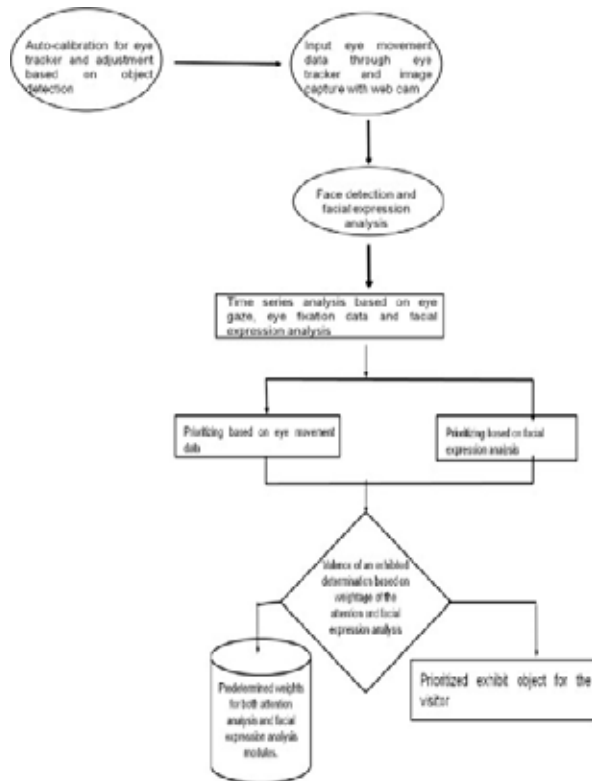


Fig 5. Flow diagram indicating operation of the integrated system



Fig 6. Auto calibration of the attention analysis framework in presence of visitor

The integrated system gets initiated with auto calibration for eye tracker and adjustment based on the visitor presence. The objects of interest of the exhibit are automatically segmented out and are visualized through the bounding box.



Fig 7. Automatic Object Detection and Segmentation for an Exhibit with different positions of the system for capture

Input eye movement data through eye tracker and image capture through webcam is next undergone based on face detection and facial expression analysis. This follows analysis of the time series based on eye fixation parameters revealing assessed states as depicted in Table 1.

Prioritization based on eye movement data and facial expression analysis is performed followed by determining Valence of the exhibit based on weightage of the attention and facial expression analysis. Finally

prioritized exhibit for the object is displayed for the visitor.

As a real time Interactive System is deployed that responses based on the attention analysis results.



Fig 8. Real time interactive system at work

Testing and Iteration

Prototype Testing is performed after deploying the prototype in controlled environments to observe visitor interactions and refine the exhibit based on feedback.

Iterative Improvements is continuously undergone to improve the exhibit based on observed attention patterns and visitor responses.

Visitor Feedback and Adaptation

Feedback Mechanism is done by implementing a system to collect visitor feedback for continuous improvement.

Visitors completed a demographic questionnaire and Situational Awe Scale(SAS) through paper survey once he had completed viewing the exhibit. The SAS was designed to measure all aspects of awe, including some of its negative connotations. It reflected basically on connection and disjointed. Participants rated the extent to which they disagreed versus agreed with each statement as it applied to how they felt while viewing through the apparatus.

For adaptation we use gathered feedback and additional attention analysis to adapt and enhance the exhibit over time.

By following these steps, we have been able to create an AI- based interactive and intelligent museum exhibit that not only captures visitors' attention but also offers a personalized and engaging experience based on attention analysis.

RESULT AND DISCUSSION

The system provides an immersive and a personalized experience to the visitor visiting the museum. The system analyzes cognitive aspects of the visitor and gathers information regarding taste and preferences of the visitor. It is found easy to implement requiring no skilled personnel for its operation in the field and user-friendly in nature. Finally the system is capable of providing a lively experience to the user.

Table. 2. Results for Exhibits 1 and 2.

Exhibit	No. of Data Collected	TP	FP	Precision	Accuracy
Exhibit1	148	127	21	0.86	86%
Exhibit2	53	44	9	0.83	83%

Visual Attention for the two exhibits were analyzed according to each of the 10 Area of Interests, AOIs. Although 85% cases correlated with our system's performance, but our search was to find the perceptual aspects in the data. For Exhibit 1 time attending to the three AOIs in the centre of the exhibit was more than the ones lying on the outer sides.

For Exhibit 2 time attending to the five AOIs closure to the apparatus with most of the contents in the diorama was more.

These instruments and objects connected to the mass more than the others. The data from the fixated, saccade vision as well as emotional state directly correlated with their perceptual level.

EXPLAINABLE FOR AI DISTRESS DETECTION

An AI-based interactive and intelligent museum exhibit that incorporates attention analysis has utilized Explainable AI (XAI) techniques to enhance visitor experience and comprehension. Here's an overview of how XAI has been integrated into such an exhibit:

Attention Analysis in Exhibit Interaction

AI algorithms analyzes visitors' attention through various eyetrackers and cameras, tracking visitors gaze or interaction patterns within the exhibit. This data

helps the AI understand which elements or information attract the most attention.

Explainable AI (XAI) for Interpretability

XAI techniques help in making the AI's decision-making process transparent and understandable to the visitors. It includes several approaches:

- i. Visualizations: Presenting visual heatmaps or overlays that show where visitors have focused their attention the most. These visual cues are displayed alongside the exhibit elements to reveal what attracted the most interest.
- ii. Natural Language Explanations: Using conversational AI interfaces or touch-screen displays to explain why certain aspects of the exhibit might be captivating is provided as another feature.

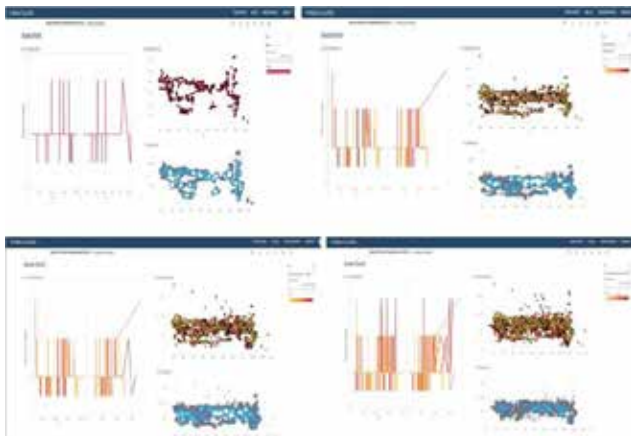


Fig 9. Visualization for Exhibit

FUTURE ACTIVITIES

Some of the future activities would be mobile eye tracking insights into awe in a science museum. Examine the ephemeral experience of awe across all the exhibits within a science museum. Extract the scan path of visit with time spent in front of exhibits through video analytics. The findings could help inform exhibit design to encourage a sense of connection by focusing visitor's attention to the current environment.

CONCLUSION

The development of an AI-based interactive and intelligent museum exhibit utilizing attention analysis represents a significant leap in enhancing visitor

engagement and enriching the overall museum experience. By harnessing cutting-edge technology, this exhibit not only captivates audiences but also personalizes interactions, catering to individual preferences and interests. This personalized approach ensures that each guest receives a unique and meaningful experience, fostering deeper connections with the exhibits and the museum's collections. Moreover, the integration of AI allows for real-time data collection and analysis, enabling museums to gain invaluable insights into visitor behavior and engagement patterns. This information can be leveraged to continually improve and refine the exhibit, ensuring its relevance and effectiveness over time. In conclusion, the AI-based interactive and intelligent museum exhibit driven by attention analysis stands as a beacon of innovation in the realm of cultural experiences.

REFERENCES

1. <https://mw2013.museumsandtheweb.com/paper/capturing-visitors-gazes-three-eye-tracking-studies-in-museums/index.html>
2. <https://zkm.de/en/project/intelligentmuseum>
3. <https://www.cooperhewitt.org/event/curator-computer-creator-a-discussion-on-museums-and-ai-in-the-21st-century-09-16-2019/>
4. https://www.researchgate.net/publication/237129973_Attention_Design_Eight_issues_to_consider
5. Link: <https://museumofthefuture.ae/en>
6. Valdesolo P, Shtulman A, Baron AS. Science is awe-some: The emotional antecedents of science learning. *Emot Rev.* 2017; 9: 215–21. <https://doi.org/10.1177/1754073916673212>
7. Smith JK. *The museum effect: How museums, libraries, and cultural institutions educate and civilize society.* Lanham, Maryland: Rowman & Littlefield; 2014
8. Anderson D. Visitors' long-term memories of world expositions. *Curator: The Museum Journal.* 2003; 46(4): 401–20. <https://doi.org/10.1111/j.2151-6952.2003.tb00106.x>
9. Falk JH, Gillespie KL. Investigating the role of emotion in science center visitor learning. *Visitor Studies.* 2009; 12(2): 112–32. <https://doi.org/10.1080/10645570903203414>

10. Staus NL, Falk JH. The role of emotion in informal science learning: testing an exploratory model. *Mind, brain, and education*. 2017; 11(2): 45–53. <https://doi.org/10.1111/mbe.12139> Tero Karras, Samuli Laine, Miika Aittala, Janne Hellsten, Jaakko Lehtinen, and Timo Aila. Analyzing and improving the image quality of stylegan. arXiv preprint arXiv:1912.04958, 2019.
- [11] Rani. S, Jining. D, Shah. D, Xaba. S. Exploring the Potential of Artificial Intelligence and Computing Technologies in Art Museums, 2023; 53(4):01004; DOI:10.1051/itmconf/20235301004

Nutritional Analysis Using Deep Learning: A Revolution in Understanding Dietary Patterns

Pragati Pandit

Nagama Kazzi

Department of Information Technology
K. K. Wagh Institute of Engineering Education & Research
✉ pvpandit@kkwagh.edu.in

ABSTRACT

Nutritional analysis using deep learning represents a ground-breaking approach to understanding and managing dietary patterns in the modern era. This essay explores the advancements and challenges in this field. Traditional methods of dietary assessment, fraught with subjectivity and error, have given way to the precision and convenience offered by deep learning. Deep learning models, such as Convolutional Neural Networks (CNNs) and Recurrent Neural Networks (RNNs), excel in image-based food recognition and nutrient prediction, enabling real-time tracking, personalized nutrition recommendations, and improved dietary planning. However, challenges persist, including data quality, portion estimation, privacy concerns, and regulatory considerations. Despite these obstacles, deep learning applications are already making significant impacts, from dietary monitoring apps to clinical nutrition and public health initiatives. The future holds promise, with efforts underway to enhance data quality, interpretability, cultural sensitivity, and ethical considerations. In conclusion, deep learning in nutritional analysis offers a transformative pathway to healthier lives, demanding continued research, and ethical considerations for its widespread adoption.

KEYWORDS : *Nutrition, Deep Learning, Dietary Assessment, Food Recognition, Nutrient Prediction, Image Analysis, Food Industry, Clinical Nutrition, Personalized Diet, Regulatory Frameworks.*

INTRODUCTION

The significance of nutrition is of utmost importance in promoting and maintaining human health and overall well-being. The ingestion of food has a crucial role in supplying our bodies with vital nutrients, energy, and nourishment, hence exerting a significant impact on our holistic well-being, encompassing both our physical and mental states. Given the escalating incidence of diet-related chronic ailments such as obesity, diabetes, and cardiovascular problems, there is a growing imperative for precise and individualised nutritional assessment to facilitate individuals in making well-informed dietary decisions. Conventional approaches to nutritional analysis, such as manual record-keeping and the use of food diaries, have been found to be burdensome and susceptible to inaccuracies. The use of deep learning into nutritional analysis has become a significant development in the era of technological progress.

Deep learning, which falls under the umbrella of

artificial intelligence (AI) and machine learning, has received considerable recognition due to its capacity to analyse extensive datasets and discern intricate patterns. In recent times, the use of deep learning techniques has significantly advanced the domain of nutrition, leading to transformative changes in the evaluation, tracking, and comprehension of dietary patterns. This essay explores the progress and obstacles related to nutritional analysis through the utilisation of deep learning, providing a comprehensive understanding of how this technology is transforming the trajectory of nutrition and its potential impact on human well-being.

LITERATURE REVIEW

Nutritional analysis is a critical component of public health, clinical practice, and personal wellness. Traditional methods of dietary assessment, such as food diaries and 24-hour recalls, have long been relied upon, but they suffer from limitations related to accuracy and user engagement. In recent years, deep learning has

emerged as a powerful tool to address these challenges and revolutionize the field of nutritional analysis. Deep learning, particularly Convolutional Neural Networks (CNNs), has shown significant promise in recognizing and categorizing foods from images. The Food-101 dataset, introduced by Bossard et al. in 2014, was an early milestone in training deep learning models for food recognition [1]. Subsequent research has built upon this foundation, achieving impressive accuracy in identifying individual food items and portion sizes from images [2] [3].

Deep learning models, including Recurrent Neural Networks (RNNs), have been employed to predict the nutrient content of foods. For example, Beijbom et al. demonstrated the feasibility of using deep networks to predict calorie content from food images [4]. These models leverage both image data and textual information, such as ingredient lists or recipes, to estimate the quantity of specific nutrients. Mobile applications equipped with deep learning algorithms have become increasingly popular tools for individuals interested in monitoring their diets. These applications, such as NutriSnap [5], allow users to capture images of their meals, with the deep learning model identifying and logging the nutritional information in real-time. Deep learning's ability to process large datasets and learn individual preferences has led to the development of personalized nutrition recommendations. Research by Eldeib et al. explored the use of deep learning to tailor dietary advice based on an individual's dietary preferences and restrictions [6]. This personalized approach has the potential to enhance dietary adherence and improve health outcomes. Despite the advancements, several challenges remain. Ensuring data quality and diversity in training datasets is crucial to improving the generalization of deep learning models [7]. Portion estimation, privacy concerns surrounding user-generated data, and the need for interpretable models are ongoing research areas [8]. Deep learning applications in nutritional analysis are already being deployed in various sectors. Clinical nutritionists are using deep learning tools to automate dietary assessments, facilitate personalized recommendations, and track patients' progress [9]. Public health initiatives are exploring large-scale dietary surveys powered by deep learning to inform evidence-based policies

[10]. The food industry is integrating deep learning into product development and quality control [11]. Researchers are actively working on enhancing data quality, interpretability, cultural sensitivity, and ethical considerations. Stricter regulations and guidelines will be necessary to protect individuals' personal and dietary information, ensuring that the benefits of deep learning in nutritional analysis are accessible and equitable for all [12].

PRECISE NUTRITIONAL ANALYSIS

Before delving into the role of deep learning in nutritional analysis, it is essential to comprehend the longstanding challenges associated with traditional methods of dietary assessment. For decades, individuals and healthcare professionals have relied on manual techniques like food diaries and 24-hour recalls to estimate daily nutrient intake. These methods, while informative, are labour-intensive, subjective, and prone to recall bias. Moreover, they often lack the granularity required to provide detailed insights into dietary habits.

Subjectivity and Human Error: Traditional dietary assessment methods heavily rely on individuals' memory and self-reporting, introducing subjectivity and recall bias into the analysis. Such errors can lead to inaccurate estimations of nutrient intake, potentially impacting health outcomes.

Cumbersome Data Collection: Maintaining food diaries or recalling every item consumed in a day can be cumbersome and impractical for most people, leading to incomplete or inconsistent records.

Lack of Real-time Monitoring: Traditional methods provide retrospective insights but fail to offer real-time monitoring capabilities. This limitation hampers the immediate identification of dietary imbalances or deviations from recommended nutritional guidelines.

Portion Size Estimation: Estimating portion sizes accurately is a significant challenge in traditional dietary assessments. Inaccurate portion estimations can distort the overall nutrient analysis.

Limited Personalization: Traditional methods do not account for individual preferences, dietary restrictions, or allergies effectively. They often provide generic recommendations that may not align with an individual's specific needs.

Resource-Intensive: Conducting large-scale dietary surveys or cohort studies using traditional methods demands substantial resources, including time, personnel, and finances.

Recognizing these limitations, researchers and technologists have turned to deep learning as a promising solution to revolutionize nutritional analysis.

THE RISE OF DEEP LEARNING IN NUTRITION

Deep learning, a subset of machine learning, has made significant strides in various domains, including computer vision, natural language processing, and speech recognition. Its success lies in its ability to automatically learn and extract complex patterns from large datasets, making it well-suited for tasks that involve vast amounts of unstructured data. In the context of nutritional analysis, deep learning has gained prominence primarily in two areas: image-based food recognition and nutrient prediction.

Image-Based Food Recognition

One of the most transformative applications of deep learning in nutrition is image-based food recognition. Convolutional Neural Networks (CNNs), a class of deep learning models designed for image analysis, have demonstrated remarkable accuracy in identifying and categorizing foods from images. These models can classify and label various food items present in a photograph, making it easier for individuals to track their dietary intake.

Accuracy: CNNs excel at recognizing foods even in complex and cluttered environments, surpassing the human eye in some cases. This level of accuracy is pivotal for precise nutritional analysis.

Portion Estimation: Some deep learning models have also made strides in estimating portion sizes from food images, addressing a significant challenge in traditional dietary assessment.

Real-time Tracking: Mobile applications equipped with deep learning algorithms enable real-time food tracking. Users can simply take a picture of their meal, and the app identifies and logs the nutritional information.

Personalization: Deep learning models can be tailored to consider individual dietary preferences and restrictions, offering personalized nutritional recommendations.

Nutrient Prediction

Deep learning models, particularly recurrent neural networks (RNNs), have shown promise in predicting the nutrient content of foods more accurately. By processing textual information, such as recipes or ingredient lists, these models can estimate the quantity of specific nutrients, including calories, protein, carbohydrates, and vitamins, present in a dish.

Improved Accuracy: Deep learning models can account for a broader range of factors that influence nutrient content, resulting in more accurate predictions than traditional methods. Recipe Analysis: With the ability to process recipe data, deep learning can provide nutrient analyses for entire meals or dishes, enabling users to understand the nutritional composition of their culinary creations.

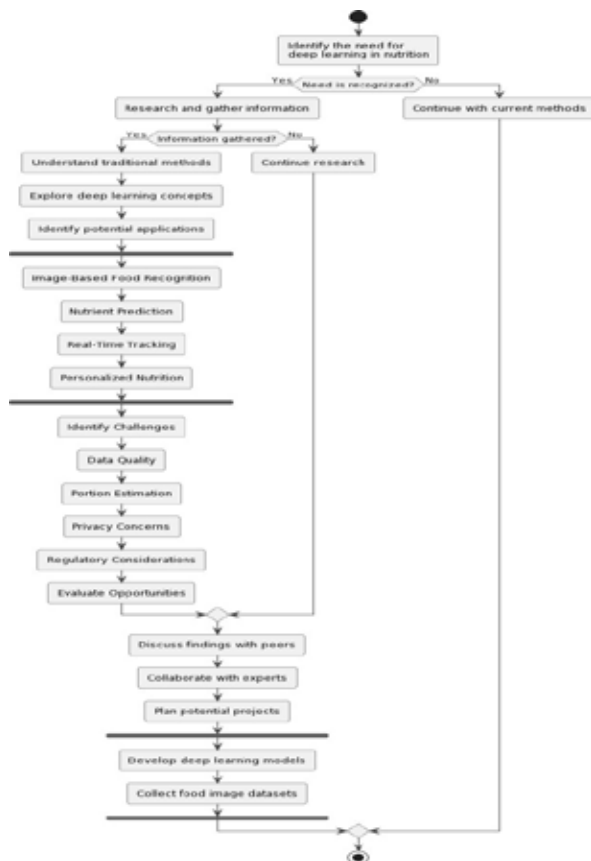


Fig 1. The Rise of Deep Learning in Nutrition

Dietary Planning: Accurate nutrient predictions allow for better dietary planning, helping individuals meet their nutritional goals and avoid deficiencies or excesses.

Integration with Wearables: Some wearable devices and smart kitchen appliances leverage deep learning to offer real-time feedback on nutrient intake, further enhancing dietary control. The integration of deep learning into nutritional analysis holds immense potential to transform the way we approach nutrition, with the promise of greater accuracy, personalization, and convenience. However, this revolutionary technology also faces several challenges that must be addressed to fully unlock its benefits.

ADVANCEMENTS AND CHALLENGES IN NUTRITIONAL ANALYSIS USING DEEP LEARNING

As the field of nutritional analysis using deep learning evolves, it presents a range of advancements and challenges that need to be carefully considered.

Advancements

Improved Accuracy: Deep learning models, particularly CNNs and RNNs, have shown remarkable accuracy in food image recognition and nutrient prediction. This precision is critical for accurate dietary assessment.

Large Datasets: The availability of large-scale food image datasets, such as Food-101, Open Food Facts, and NutriNet- Santé, has facilitated the development and training of deep learning models for nutritional analysis. These datasets encompass a wide range of foods, enabling models to generalize better.

Real-time Tracking: Mobile applications and devices equipped with deep learning algorithms offer real-time tracking of food consumption, making it easier for individuals to monitor their diets and make immediate adjustments.

Personalized Nutrition: Deep learning can help create personalized nutrition plans by considering an individual's dietary preferences, allergies, nutritional requirements, and health goals. This personalized approach can significantly enhance dietary adherence and health outcomes.

Nutrient Prediction: Deep learning models can predict the nutrient content of foods with greater accuracy,

making it easier for individuals to track their daily intake of specific nutrients such as calories, protein, fibre, and essential vitamins and minerals.

CHALLENGES

Data Quality and Diversity: The quality and diversity of food image datasets can significantly affect the generalization and accuracy of deep learning models. Variability in factors like lighting, presentation, and portion size can be challenging to address, leading to potential inaccuracies.

Portion Estimation: Estimating portion sizes accurately from images remains a significant challenge. While some progress has been made, it often requires additional sensors or manual input, limiting the seamless automation of nutritional analysis.

Nutrient Database: The availability of a comprehensive and up-to-date nutrient composition database is essential for accurate nutritional analysis. Incomplete or outdated databases can lead to errors in nutrient predictions.

User Engagement: Encouraging users to consistently use nutritional analysis tools or apps is a challenge. Many people find it tedious to log their food intake regularly, and sustaining user engagement is crucial for the effectiveness of these tools.

Privacy Concerns: Deep learning-based nutritional analysis often involves processing images of meals, raising concerns about data collection and usage. Ensuring privacy and data security is paramount.

Generalization to Cultural Foods: Deep learning models are typically trained on Western foods, which may not generalize well to diverse cultural cuisines with unique ingredients and preparation methods. This limitation hampers the applicability of deep learning-based tools in global contexts.

Interpretable Models: Deep learning models are often considered "black boxes," making it challenging to explain their predictions. Interpretable models are essential for building trust in nutritional recommendations, especially in healthcare settings.

Accessibility: Not everyone has access to smartphones or devices equipped with deep learning capabilities, limiting the reach of these technologies. Ensuring

accessibility to a broader population is crucial for equitable healthcare.

Regulatory Considerations: Regulations surrounding food labelling and nutritional analysis may not yet account for the use of deep learning, posing challenges for integrating these technologies into official dietary guidelines and labelling practices. Ensuring that deep learning-based tools meet regulatory standards is essential for their widespread adoption.

REAL-WORLD APPLICATIONS OF DEEP LEARNING IN NUTRITIONAL ANALYSIS

As deep learning continues to advance and overcome challenges in nutritional analysis, it is already finding practical applications across various domains. These real-world applications demonstrate the transformative potential of this technology in shaping dietary habits, healthcare, and research: **Dietary Monitoring Apps:** Mobile applications powered by deep learning algorithms are becoming increasingly popular tools for individuals interested in monitoring their dietary intake. Users can simply capture images of their meals, and the app provides detailed nutritional information, helping them make informed food choices. These apps also offer features such as meal planning, recipe suggestions, and personalized dietary recommendations.

Clinical Nutrition: Deep learning models are assisting healthcare professionals in clinical settings by automating dietary assessments. Nutritional analysis tools powered by deep learning can help dietitians and clinicians provide tailored dietary advice to patients, manage chronic conditions, and track the progress of dietary interventions.

Public Health Initiatives: Governments and public health organizations are exploring the use of deep learning in large-scale dietary surveys and nutritional research. These initiatives aim to collect data on dietary patterns across populations, identify dietary trends, and inform evidence-based policies for improved public health.

Food Labelling and Packaging: Deep learning can enhance food labelling accuracy, particularly in packaged foods. By automatically recognizing and verifying food product labels, deep learning algorithms

can help ensure that nutritional information is consistent and compliant with regulations.

Nutritional Education: Deep learning-powered educational tools can help individuals better understand their diets. Interactive platforms can offer insights into the nutritional content of foods, demonstrate the effects of different dietary choices, and promote healthier eating habits.

Research and Development: Food companies and research institutions are leveraging deep learning for product development. From optimizing ingredient combinations to predicting consumer preferences based on nutritional profiles, deep learning is driving innovation in the food industry.

Health and Fitness Wearables: Wearable devices equipped with deep learning capabilities are helping users monitor their nutrient intake in real time. These devices can track not only the foods consumed but also the nutritional quality of meals, providing immediate feedback and suggestions for improvement.

Clinical Trials and Drug Development: Deep learning plays a vital role in clinical trials and pharmaceutical research related to nutrition. It can help analyse dietary data collected during trials, identify correlations between diet and health outcomes, and contribute to the development of personalized nutrition-based therapies.

FUTURE DIRECTIONS AND ETHICAL CONSIDERATIONS

The future of nutritional analysis using deep learning holds immense promise, with numerous opportunities for further advancements. Researchers and practitioners are exploring several avenues to improve the accuracy, accessibility, and ethical implications of this technology:

Enhanced Data Quality: Addressing the challenges related to data quality is paramount. Collecting high-quality, diverse food image datasets and maintaining up-to-date nutrient databases are essential for improving the accuracy of deep learning models.

Interpretable Models: Researchers are actively working on making deep learning models more interpretable. Explainable AI (XAI) techniques aim to provide

transparency into model predictions, allowing users and healthcare professionals to understand the reasoning behind dietary recommendations.

Privacy and Data Security: As deep learning systems rely on user-generated data, ensuring robust privacy and data security measures is crucial. Stricter regulations and guidelines will be necessary to protect individuals' personal and dietary information.

Cultural Sensitivity: To make deep learning-based nutritional analysis universally applicable, efforts are being made to expand training datasets to include a broader range of cultural cuisines. This will ensure that the technology is relevant and effective across diverse populations.

Integration into Healthcare: Integrating deep learning-based nutritional analysis into healthcare systems and electronic health records will enhance the continuum of care. It can enable seamless communication between patients, healthcare providers, and nutritionists, facilitating collaborative approaches to health management.

Education and User Engagement: Promoting user engagement and education is critical for the long-term success of deep learning-powered nutritional analysis tools. Making these tools user-friendly, educational, and motivational will encourage individuals to adopt healthier eating habits.

Regulatory Frameworks: Governments and regulatory bodies will need to adapt to the evolving landscape of nutritional analysis using deep learning. Developing standardized guidelines for the use of deep learning in food labelling, dietary recommendations, and public health initiatives will be essential. **Ethical Considerations:** Ethical discussions surrounding deep learning in nutrition should encompass issues such as data ownership, consent, and transparency. Ensuring equitable access to technology and avoiding biases in algorithmic recommendations are also ethical imperatives.

CONCLUSION

Nutritional analysis using deep learning represents a transformative leap forward in our quest for precise, personalized, and data-driven dietary assessments.

By harnessing the power of deep learning algorithms, we have the potential to revolutionize the way we understand, manage, and optimize our diets. The combination of image-based food recognition, nutrient prediction, real-time tracking, and personalization promises to empower individuals to make informed dietary choices that align with their health goals and preferences. While the field has made significant strides in recent years, it also faces a host of challenges, from data quality and privacy concerns to the need for interpretability and cultural sensitivity. Addressing these challenges requires a multidisciplinary approach that brings together technologists, healthcare professionals, policymakers, and ethicists. As we navigate the evolving landscape of nutritional analysis using deep learning, it is imperative that we prioritize the ethical, equitable, and transparent deployment of this technology. By doing so, we can unlock its full potential to improve human health, reduce the burden of diet-related chronic diseases, and promote a future where everyone has access to personalized and evidence-based nutrition guidance. In this era of data-driven healthcare, deep learning is poised to be a cornerstone of our dietary well-being, offering a pathway to healthier lives for individuals and populations alike.

REFERENCES

1. Bossard, L., Guillaumin, M., & Van Gool, L. (2014). Food- 101 – Mining Discriminative Components with Random Forests. European Conference on Computer Vision (ECCV).
2. Chen, M., Dhingra, K., Wu, W., Yang, L., Sukthankar, R., & Yang, J. (2017). NutriNet: A Deep Learning Food and Drink Image Recognition System for Dietary Assessment. Proceedings of the 2017 CHI Conference on Human Factors in Computing Systems.
3. Zhang, N., Ye, H., Li, W., & Zhang, J. (2020). A Hierarchical Framework for Food Recognition and Volume Estimation from RGB Images Using Deep Networks. IEEE Transactions on Circuits and Systems for Video Technology.
4. Beijbom, O., Joshi, N., Morris, D., Saponas, S. C., Khullar, S., & McDuff, D. J. (2015). Menu-Match: Restaurant- Specific Food Logging from Images. Proceedings of the 2015 ACM International Joint Conference on Pervasive and Ubiquitous Computing.

5. NutriSnap. (n.d.). Retrieved from <https://play.google.com/store/apps/details?id=com.nutrisnap>
6. Eldeib, H., Atallah, L., Saeed, H., & Ahmed, M. (2017). An Intelligent Personalized Diet Recommender System Using Deep Learning. 2017 IEEE/RSJ International Conference on Intelligent Robots and Systems (IROS).
7. Bossard, L., Guillaumin, M., & Van Gool, L. (2014). Food-101 – Mining Discriminative Components with Random Forests. European Conference on Computer Vision (ECCV).
8. Eldeib, H., Atallah, L., Saeed, H., & Ahmed, M. (2017). An Intelligent Personalized Diet Recommender System Using Deep Learning. 2017 IEEE/RSJ International Conference on Intelligent Robots and Systems (IROS).
9. Boushey, C. J., Spoden, M., Zhu, F. M., Delp, E. J., & Kerr, D. A. (2017). New mobile methods for dietary assessment: Review of image-assisted and image-based dietary assessment methods. Proceedings of the Nutrition Society.
10. Geraci, F., Lanzarotti, R., & Papadopoulou, E. (2020). Applications of Deep Learning in the Food Industry: A Comprehensive Review. Computers in Industry.
11. Hu, Y., & Zhang, J. (2020). Privacy-Preserving Food Recognition and Volume Estimation for Dietary Assessment Using Convolutional Neural Networks. IEEE Journal of Biomedical and Health Informatics.
12. Lee, C., Song, Y., & Lee, J. (2020). Dietary Assessment Techniques Using Deep Learning: A Review.

Near Nexus Commerce Strengthening Buyers and Sellers through Regional Nexus Based on Data Analytics and Web Technology

Harshal Ashok Sonawane
Kunal Manik Walshete

Sahil Sachin Gujarathi
Ashutosh Sanjay Gangurde

Dept. of Information Technology
MET Institute of Engineering, Nashik
Savitribai Phule Pune University, Pune, Maharashtra
✉ harshalsonawane448@gmail.com

ABSTRACT

In today's rapidly evolving digital landscape, local businesses face a formidable challenge in establishing a robust online presence, hindering their capacity to effectively showcase a diverse range of products, services, and pricing structures to a broader audience. Concurrently, consumers grapple with the complexity of comparing offerings from various local shops. This disconnection presents a distinctive opportunity to invigorate local economies and enhance consumer decision-making. This research model seeks to develop an online platform that seamlessly connects local businesses with consumers, enabling businesses to prominently feature their products, services, prices, and reviews, while also providing consumers with the means to validate and compare these offerings. The proposed platform has the potential to foster local economic growth, support entrepreneurial endeavors, and empower consumers with the tools to make more informed and confident shopping choices.

KEYWORDS : *Regional commerce, E-commerce, Recommendation system.*

INTRODUCTION

In the contemporary landscape of the digital world, local businesses face a formidable challenge that significantly impacts their ability to thrive and consumers' capacity to make informed choices. This paper addresses the growing digital divide between local businesses and consumers, emphasizing the pressing need for a comprehensive solution to facilitate their symbiotic growth.

Local businesses have traditionally been the lifeblood of communities, providing an array of products and services tailored to their specific locales. Nevertheless, as the digital era advances, these businesses often find themselves struggling to establish a meaningful online presence. The absence of such an online presence not only hampers their growth but also results in missed opportunities, as consumers increasingly rely on the internet to discover and assess local offerings.

The primary challenge faced by local businesses is navigating the complexities of digital marketing and e-commerce, including the establishment of online stores, management of social media profiles, and search engine optimization. Smaller enterprises, in particular, encounter difficulties due to limited resources and expertise in navigating the digital landscape effectively. On the consumer side, the absence of a centralized platform to aggregate and compare information on local products and services poses significant challenges. Consumers often find it time-consuming and frustrating to compare offerings, prices, and reviews. This lack of transparency can lead to suboptimal choices, as consumers may settle for what is readily available rather than what best suits their preferences and needs.

This research model aims to present an innovative solution to bridge the digital gap between local businesses and consumers. Our platform offers a user-

friendly space for local businesses to establish an online presence, allowing them to comprehensively showcase their offerings, from product catalogs to service listings and pricing details. The objective is to empower local businesses to thrive in the digital age by providing support and guidance, simplifying the complexities of digital marketing.

The objective of our platform is not only to bolster local businesses but also to place a powerful set of tools in the hands of consumers. We recognize that the process of comparing and selecting products and services from local shops can often be convoluted and time-consuming. Our platform addresses this challenge by streamlining the comparison process. Users can easily conduct side-by-side comparisons of products, read user reviews, and consider ratings to make well-informed decisions. This level of transparency and convenience

is a substantial improvement over the traditional local shopping experience, where consumers might lack access to comprehensive product information and reviews.

This research project holds significant implications on multiple fronts. Firstly, it responds to the critical need for a digital solution that empowers local businesses to establish and strengthen their online presence. It offers them a digital marketplace where they can confidently assess and compare local offerings, ultimately leading to more informed purchasing decisions. Lastly, the project embodies a symbiotic relationship between local businesses and consumers, fostering a mutually beneficial ecosystem where both parties stand to gain. This initiative reflects the potential of the digital age to transform the dynamics of local commerce for the better, creating a win-win scenario for businesses and the communities.

LITERATURE SURVEY

Sr. no	Year	Title	Author	Feature	Limitation
1	2022	Social commerce from seller and region perspective: A data mining for indonesian e-commerce.	Gunawan University of surabaya, indonesia.	Connect commerce and seller in region perspective	Works in limited region.
2	2020	Reviewer credibility and sentiment analysis based user profile modelling.	Shigang hu, akshi kumar, shivam gupta	Profile modelling	Based on only product reviews for validation.
3	2021	Marketing strategies for e-commerce websites under the new media trend.	Yinlu li	New marketing strategies	New economic development model for e-commerce industry only for china country.
4	2022	The advancement of digitalization and its impact on the e-commerce trade.	John keats	Provide information of e-commerce trade	Selling and buying products and services online through social media platforms only.

[1] This research delves into the emerging field of social commerce within the Indonesian e-commerce landscape. Unlike previous studies that primarily focused on consumer behavior, it takes a unique approach by examining e-commerce sellers across various Indonesian regions. The primary goal is to categorize social commerce firms in these regions, with a particular emphasis on grouping provinces based on e-commerce and social commerce-related variables. This classification is achieved using data mining

techniques, the Cross-Industry Standard Process for Data Mining framework, and K-nime Analytics Platform. The research findings classify provinces into two categories - those with high social commerce activity and those with lower engagement. This information can be valuable for local governments in understanding their province's position and formulating policies to support social commerce entrepreneurs, shedding light on the regional dynamics of social commerce in Indonesia but the formal solution of this

technique is adding multiple regions to platform with wide variety of products. [2] Introducing the Credibility, Interest, and Sentiment Enhanced Recommendation (CISER) model, a sophisticated system designed to understand user purchase preferences and enhance the quality of product recommendations. The model combines heuristic-driven user interest profiling with reviewer credibility analysis and fine-grained feature sentiment analysis. It emphasizes the importance of sentiment expressions, customer preferences, and reviewer credibility, achieving high precision levels in recommendation systems, outperforming existing approaches. The CISER model represents a significant advancement in the realm of e-commerce and recommendation systems, offering a robust and data-driven approach to improving user experiences and product recommendations. [3] This paper focuses on the evolving landscape of e-commerce in China, specifically in the context of website marketing. It highlights the changing dynamics of e-commerce, influenced by continuous advancements in information technology. The study underscores the importance of website marketing in the e-commerce process, emphasizing that its effectiveness significantly impacts e-commerce businesses' overall performance. The research aims to improve the level of website marketing, enhance the influence of e-commerce enterprises, and provide marketing strategies within the context of new media technology. It promises an in-depth analysis of e-commerce website marketing, offering strategies to help businesses thrive in this evolving landscape. [4] This paper explores the profound impact of digitalization on the e-commerce trade. It provides an extensive overview of e-commerce, with a focus on transactions conducted through social media platforms. The research investigates the limitations and opportunities associated with conducting trade via social media, shedding light on the complexities and challenges in e-commerce's increasingly digital world. The paper offers valuable insights into how digitalization is transforming the e-commerce landscape and its implications for both businesses and consumers. the limitation of given paper is Selling and buying products and services online through social media platforms but to avoid this problem it needs to make responsive online platform for Local businesses and customers.

OBJECTIVES

To establishing a user-friendly platform

The initial step is to create a user-friendly website platform. This involves crafting an intuitive and visually appealing platform with a strong focus on user experience. Navigational ease is paramount, and the platform will be designed to adapt

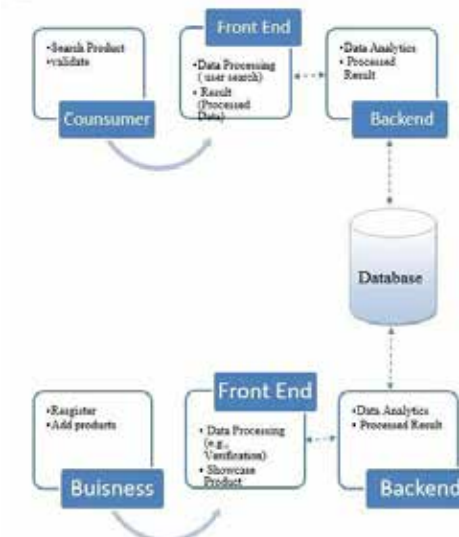
To analyze and aggregating data

Another critical aspect is the analysis and aggregation of data. to provide valuable insights and trends, a data aggregation mechanism will be developed to collect and consolidate pertinent information from diverse sources. utilizing data analysis techniques, we will extract meaningful information from the collected data, and establish a structured data repository that's readily accessible for decision-making.

To enabling informed decision-making

Informed decision-making is at the core of our mission. users will have access to data-driven insights, reviews, and comparisons that empower them to make well-informed choices. features facilitating easy comparisons of products, services, and reviews from various sources will be implemented. real-time updates and notifications will keep users informed about changes and relevant information, further enhancing the decision-making process.

SYSTEM ARCHITECTURE



METHODOLOGY

The system is designed to address the challenges faced by local businesses in establishing a robust online presence and to empower consumers to make informed choices. The system combines web development and analytics to achieve this. The methodology can be divided into several key components as follows -

User Registration and Business Profile Creation: This component focuses on user registration and how local businesses create profiles. Users provide personal information, and businesses create profiles with product listings, prices, and reviews. These profiles are stored in a database, allowing businesses to manage their online presence effectively.

Product Search and Comparison: To facilitate product search and comparison, businesses add their products, which are treated as objects in a database. Users can search and compare products based on various criteria, such as price and rating. The system employs an Object-Relational Mapping (ORM) model to map these objects to the database table, making it easier to retrieve and display relevant product information.

Location-Based Filtering: To facilitate location-based filtering, the system employs a combination of user-provided location data and geospatial algorithms. Users provide their location data during registration, which includes details such as city, postal code, or GPS coordinates. This information is securely stored in the system and local businesses also provide location data when creating their profiles, specifying their service areas or physical store addresses. The system utilizes geospatial techniques (GIS Algorithm) to determine the proximity of businesses to a user's location. These techniques calculate distances and define proximity zones. When a user performs a search, the system cross-references the location data of businesses with the user's location. It then filters and prioritizes results based on proximity. Businesses that are closer to the user's location are presented first in the search results. This approach ensures that users see relevant businesses and services nearby, enhancing their local shopping experience.

Recommendation Using Web Analytics Tools: Web analytics tools are used to monitor and analyze user

interactions within the platform. Data collection, storage, preprocessing, user profiling, behavioral analysis, and collaborative filtering are employed to understand user behavior and preferences. The system also utilizes content-based filtering and machine learning to provide personalized recommendations to users.

This methodology outlines the technical and data-driven approach to address the challenges faced by local businesses and consumers. It empowers businesses to establish an online presence and consumers to make informed decisions while fostering local economies and supporting entrepreneurship. The system aims to bridge the digital gap between local businesses and consumers, creating a thriving ecosystem for both parties.

CONCLUSION

In conclusion, this model represents a comprehensive solution that not only bridges the gap between local businesses and consumers in the digital age but also serves as a testament to the potential of technology to drive positive change in our communities. Through the utilization of HTML, CSS, React, Spring Boot, MySQL,

and data analytics tools, we've crafted a versatile platform that empowers local businesses to flourish in an increasingly competitive market. The integration of these technologies not only enables local businesses to showcase their offerings but also adapt to evolving consumer preferences with ease. This model underscores the critical significance of equipping consumers with the information they require to make informed decisions, thereby enhancing their overall shopping experience.

Beyond its immediate economic impact on local communities, this initiative possesses the potential to cultivate a sense of community and support that extends beyond the digital realm. By facilitating connections between businesses and consumers, we strengthen the very bonds that hold our neighborhoods together.

In essence, this model transcends the realm of a mere digital platform; it stands as a catalyst for positive change, a bridge that unites people, and a testimony to the transformative power of technology in enhancing our local economies and communities. As we look ahead, we anticipate the exciting journey that lies

before us, one that involves continuous evolution and adaptation to the ever- changing landscape of the digital age. Together, we move forward, bound by the shared vision of empowering local businesses and enriching the lives of our communities.

REFERENCES

1. Gunawan Saurabhas – “social commerce from seller and region perspective: A data mining for indonesian e-commerce” 2022 international conference on data science and its applications (icodsa)
2. Shigang Hu, Akshi Kumar, Shivam Gupta – “Reviewer credibility and sentiment analysis based user profile modelling for online product recommendation” IEEE Special section on cloud - fog - edge computing in cyber-physical-social systems (cpss) 2022
3. Yinlu li’s – “Marketing strategies for e-commerce websites under the new media trend” proceedings of the 2021 international conference on social development and media communication (SDMC 2021)
4. Katharina buchholz, “social commerce caputures online markets in asia,” statista, 2021.
5. Liu fang – “Analysis of e-commerce network soft marketing strategy under new media conditions.” Journal of chaohu college 2022.

A Review Paper on Trusted Crowdfunding Platform Using Smart Contract

Bhagyashree Kadam
Sajal Bagade
Sohel Momin

Saurabh Satpute
Sarfraj Mulla
Niraj Chavan

JSPMs' Bhivarabai Sawant Institute of Technology and Research
Wagholi, Pune, Maharashtra

ABSTRACT

Crowdfunding has become a revolutionary method for individuals and organizations to secure funds for their initiatives. This project review explores the development of a web-based crowdfunding system that leverages Custom Blockchain smart contracts and the Solidity programming language. By employing blockchain technology, the project addresses several critical issues encountered by traditional crowdfunding platforms. One significant advantage of this system is its decentralized nature, ensuring that all information related to campaigns, contributions, and transactions is securely stored on a transparent blockchain network accessible to everyone. The review identifies limitations in existing systems, such as high fees associated with some crowdfunding platforms, risks of scam campaigns, lack of transparency, and centralized authorities controlling and managing data.

KEYWORDS : *Crowdfunding, Blockchain, Smart contracts, Decentralize, Transparency, Trust, Security, Scam prevention.*

INTRODUCTION

Crowdfunding has emerged as a revolutionary method for raising capital and support for various projects, businesses, and charitable causes. However, despite its potential, it is plagued by issues of trust, transparency, and security. To address these challenges, innovative platforms are turning to custom blockchains and smart contracts, offering a new level of trust and reliability in crowdfunding campaigns.

Traditional crowdfunding platforms have limitations in terms of accountability, as the control over funds and project progress is centralized. This opens the door to potential misuse, fraud, and disputes. By implementing blockchain technology and smart contracts, a new era of crowdfunding platforms is emerging, characterized by trust, transparency, and automation.

The integration of custom blockchains and smart contracts results in a new breed of crowdfunding platforms. These platforms offer an ecosystem where

backers can confidently support projects, knowing that their funds are protected and will only be disbursed when specific project milestones are achieved. Creators benefit from a streamlined fundraising process and greater credibility.

As the world of crowdfunding evolves, these platforms aim to revolutionize the industry by setting a new standard for transparency and trust.

LITERATURE SURVEY

A comprehensive literature survey on trusted crowdfunding platforms leveraging smart contracts on custom blockchains reveals a growing body of research that underscores the transformative potential of blockchain technology in revolutionizing the crowdfunding landscape. These platforms offer a compelling solution to the long-standing issues of trust, transparency, and security that have been persistent challenges in traditional crowdfunding models.

[1] This paper outlines the development of a

crowdfunding decentralized application (dApp) on the Ethereum blockchain. It describes the architecture, smart contracts, and functions for campaign creation, investment, and management. The paper also discusses the cost of transactions and potential scalability issues, with a reference to alternative blockchain platforms.

[2] The research paper discusses the innovative potential of "Internet + Educational Crowdfunding" in the realm of education. It explores how educational crowd funding can foster innovation and access to educational resources. This approach harnesses social capital, promotes education equity, nurtures creative talents, and enhances educators' involvement. However, further studies are needed to address issues like intellectual property protection and participant engagement. The document highlights the growing role of crowd funding in education and references key research in the field.

[3] This paper discusses how crowd-funding can reduce housing costs and presents an optimization model for planning such projects. It emphasizes the importance of a reasonable housing plan for successful implementation and highlights the benefits for both developers and home buyers.

[4] This paper discusses the implementation of blockchain technology in crowdfunding platforms to enhance transparency and security, using Ethereum's smart contracts. It aims to prevent fraud and ensure efficient fund allocation.

[5] The paper explores post-investment activities of crowd equity investors in equity crowdfunding. It identifies low and high-involvement activities and investigates their antecedents, providing insights into the dynamics of crowdfunding and its potential benefits for technology startups.

[6] The paper explores crowdfunding using blockchain technology. It discusses the potential of blockchain to address issues in crowdfunding, such as fraud and lack of regulation. The platform presented, Supporttroops, focuses on charitable initiatives, social causes, and business capital. It also aims to minimize transactional slippage and reduce transaction fees in the future. Blockchain's transparency and smart contracts are seen as key in revolutionizing crowdfunding.

[7] The paper discusses blockchain-based crowdfunding platforms, emphasizing transparency, security, and decentralization. It highlights advantages like transparency and reduced fraud risk while acknowledging complexities and volatility as challenges. The study concludes that blockchain's potential in crowdfunding is growing.

[8] This paper, published in December, explores the viability of crowdfunding as an alternative funding mechanism for youth entrepreneurs. It discusses the perception of crowdfunding, types of crowdfunding models, and the preferences of youth entrepreneurs. The study found that donation-based and reward-based crowdfunding models were most preferred by the respondents, indicating that crowdfunding has the potential to support youth entrepreneurs in accessing financing.

[9] This paper is a study of donation-based crowdfunding platforms, focusing on factors influencing donation behavior. It explores the impact of website quality, trust, privacy, technology, and social networking on donation intention and behavior. Numerous references support the research findings.

EXISTING SYSTEM

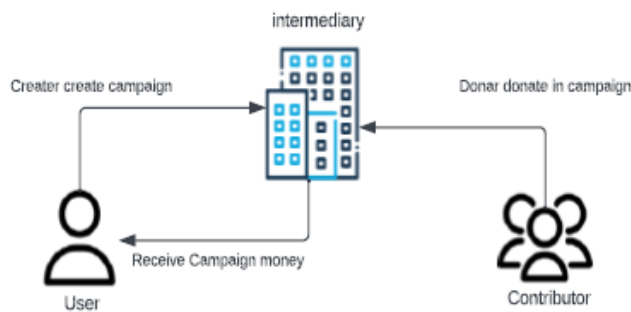
Ethereum-based Crowdfunding Platforms: Kickstarter: Kickstarter, one of the most well-known crowdfunding platforms, was exploring blockchain technology to improve transparency and accountability in its campaigns. They were considering the integration of smart contracts on the Ethereum blockchain to automate the disbursement of funds when project milestones were met. Tezos-based Crowdfunding Platforms: Tezsure: Tezsure aimed to create a decentralized crowdfunding platform using the Tezos blockchain. It leveraged Tezos' smart contract capabilities to automate fund releases and ensure trust among backers and creators. Cardano-based Crowdfunding Platforms: Liquid Finance: Liquid Finance explored Cardano's blockchain to build a decentralized crowdfunding platform. Cardano's smart contracts allowed for the creation of customizable funding rules and milestones, enhancing transparency and trust. EOS-based Crowdfunding Platforms: EOS Crowdfunding: EOS blockchain-based platforms emerged to facilitate crowdfunding campaigns using smart contracts. These platforms allowed project

creators to create their tokens, set conditions for fund release, and foster trust among their backers. Polkadot-based Crowdfunding Platforms: Polkaswap: While primarily a decentralized exchange, Polkaswap is a part of the Polkadot ecosystem and may contribute to the development of crowdfunding platforms on Polkadot. Custom blockchains in the Polkadot network provide flexibility and security for such applications.

Decentralized Autonomous Organizations (DAOs): Aragon: While not strictly a crowdfunding platform, Aragon provides a framework for creating DAOs. DAOs are smart contract-based organizations that can collectively decide on fund allocation, enabling decentralized and transparent decision-making in crowdfunding initiatives.

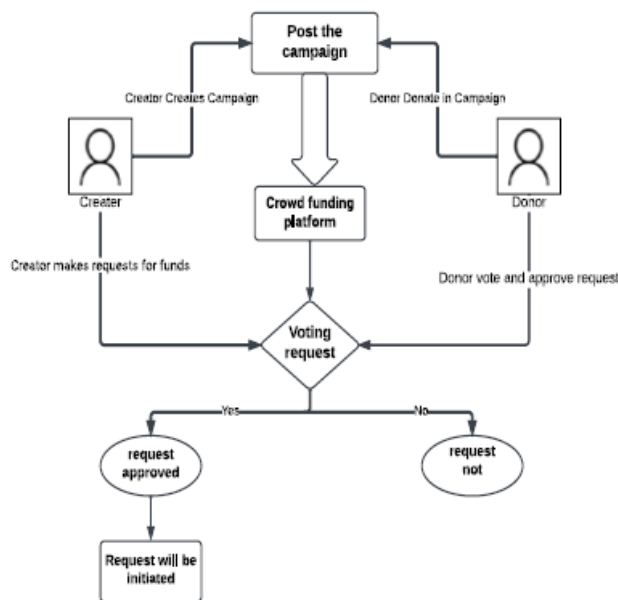
These platforms leverage the features of custom blockchains and smart contracts to create transparent and secure crowdfunding processes. They typically allow project creators to set conditions and milestones, and funds are automatically released when these milestones are met. This trustless execution minimizes the risks associated with traditional crowdfunding, where an intermediary often controls funds. Please note that the blockchain and cryptocurrency landscape is rapidly evolving. New platforms and developments may have emerged since my last knowledge update in 2021, so it's essential to conduct up-to-date research to explore the latest trusted crowdfunding platforms using custom blockchains and smart contracts. Additionally, regulatory environments can vary, so it's important to consider the legal and regulatory aspects when participating in or launching projects on these platforms.

and leverages smart contract technology to provide an environment where project creators and backers can engage with confidence. TrustedCrowd is designed to address the common challenges faced by traditional crowdfunding platforms, such as fraud, disputes, and lack of transparency. Key Features: Custom Blockchain: TrustedCrowd operates on a custom blockchain tailored to the specific needs of crowdfunding. This blockchain is designed for scalability, security, and efficiency, ensuring fast transaction processing and data immutability. User-Friendly Interface: The platform offers an intuitive and user-friendly interface for both project creators and backers. Users can easily navigate the platform, create campaigns, and contribute to projects. Smart Contracts: Smart contracts play a central role in TrustedCrowd. They automate the crowdfunding process and ensure trust by holding funds in escrow until predefined project milestones are met. This trustless execution reduces the risk of fraud and mismanagement. Transparency and Accountability: Every transaction and project update is recorded on the blockchain, providing complete transparency. Backers can track the progress of campaigns in real-time, ensuring accountability on the part of project creators. Decentralization: The use of custom blockchain technology eliminates the need for a central authority, promoting decentralization and reducing the risk of a single point of failure. Security: TrustedCrowd prioritizes the security of user data and funds. Blockchain's cryptographic mechanisms protect sensitive information, and multi-layered security measures are in place to safeguard the platform. Tokenization: To facilitate contributions and rewards, TrustedCrowd issues its native tokens. These tokens can be used for crowdfunding campaigns and as a means of exchange within the platform. Community and Support: The platform fosters a sense of community among backers and project creators. It offers support and resources to help creators launch successful campaigns. Services, covering operational costs and continual platform improvements to enhance user experience. TrustedCrowd aims to remain at the forefront of blockchain and crowdfunding innovations. Future developments may include expanding to mobile applications, integrating with more custom blockchains, and exploring decentralized finance (DeFi) features for backers and creators.



PROPOSED SYSTEM

The proposed crowdfunding platform, named "Trusted Crowd," is built on a custom blockchain infrastructure



CONCLUSION

In summary, a trusted crowdfunding platform utilizing smart contracts on a custom blockchain offers a promising solution to the longstanding issues of trust, security, and transparency in crowdfunding. It has the potential to redefine how projects are funded, empower creators, and provide backers with confidence in the crowdfunding process, contributing to the growth of innovative ideas and initiatives. The emergence and evolution of such platforms mark an exciting and transformative phase in the world of crowdfunding.

In conclusion, the concept of a trusted crowdfunding platform utilizing smart contracts on a custom blockchain represents a transformative shift in the crowdfunding landscape. Such a platform combines the strengths of blockchain technology and smart contracts to foster transparency, security, and trust in the crowdfunding process.

REFERENCES

1. A. Marotta, F. Martinelli, S. Nanni, A. Orlando, and A. Yautsiukhin, "Cyber- insurance survey," *Computer Science Review*, vol. 24, pp. 35– 61, 2019.
2. "Blockchain in insurance: applications and pursuing a path to adoption," [https://www.ey.com/Publications/vwLUAssets/EY-blockchain-in-insurance/\\$FILE/EY-blockchain-in-insurance.pdf](https://www.ey.com/Publications/vwLUAssets/EY-blockchain-in-insurance/$FILE/EY-blockchain-in-insurance.pdf), (Accessed on 09/03/2018).
3. M. M. Khalili, P. Naghizadeh, and M. Liu, "Designing cyber insurance policies: The role of pre-screening and security interdependence," *IEEE Transactions on Information Forensics and Security*, vol. 13, no. 9, pp. 2226– 2239, 2018.
4. S. Chekriy and Y. Mukhin, "i-chain.net.wpaper rev 005," <https://i-chain.net/i-chain.net.wpaper rev 005.pdf>, May 2018, (Accessed on 09/03/2018).
5. "Blockchain:An insurance focus-milliman insight," <http://www.milliman.com/in-sight/2016/Blockchain-An-insurance-focus/>, (Accessed on 09/03/2018).
6. Blockchain-Based Crowdfunding Application IEEE, <https://ieeexplore.ieee.org/document/9640888>, 2021 Fifth International Conference on I-SMAC (IoT in Social, Mobile, Analytics and Cloud) (I-SMAC), 11- 13 November 2021, 10.1109/I-SMAC52330.2021.9640888 at Palladam, India.
7. Blockchain-Based Crowdfunding: A Trust Building Model IEEE, <https://ieeexplore.ieee.org/document/9671003>, 2021 International Conference on Artificial Intelligence and Machine Vision (AIMV), 24-26 September 2021, 1109/RTEICT52294.2021.9573956 at Gandhinagar, India.
8. Blockchain Integrated Crowdfunding Platform for Enhanced Secure Transactions IEEE, <https://ieeexplore.ieee.org/document/9633380>, 2021 4th International Conference on Recent Developments in Control, Automation & Power Engineering (RDCAPE), 07-08, October 2021, 10.1109/RDCAPE52977.2021.9633380 at Noida, India.
9. O. Abedinia, D. Raisz, and N. Amjady, "Effective prediction model for hungarian small-scale solar power output," *IET Renewable Power Generation*, vol. 11, no. 13, pp. 1648–1658, 2017.

Coupons Code Exchange Platform

G. P. Mohole, Avanti Bhamare, Yogesh Bhavsar

Rahul Raundal, Swapnil Ranmale

Jawahar Education Society Institute of Technology, Management & Research
Nashik, Maharashtra
✉ gpmohole@gmail.com

ABSTRACT

In the digital age, where landfills groan under mountains of wasted paper and servers weep at unused coupon codes, a beacon of sustainability and savings rises: Share & Save. This MERN-powered web app isn't just another coupon aggregator; it's a revolutionary ecosystem where forgotten codes regain their magic and discarded deals dance again.

Imagine a world where users unearth a treasure trove of pre-vetted, verified coupons, their forgotten savings blossoming anew. Businesses whisper targeted promotions to engaged audiences, their brands blooming under the warm sun of customer delight. And Mother Earth? She finally catches a breath, the tide of coupon waste receding as Share & Save's innovative AI sleuths sniff out and disarm fraudulent offers before they wreak havoc.

Share & Save isn't just about convenience and cost-cutting; it's about rewriting the story of consumerism. It's about empowering individuals to unlock hidden discounts, businesses to connect with ideal customers, and the planet to heal one recycled barcode at a time. It's a community built on trust, transparency, and a shared vision of a future where every penny saved is a penny protected, and every coupon claimed is a victory for our collective well-being.

So join the Share & Save revolution. Unwrap the potential of forgotten deals, empower businesses with laser-targeted reach, and let the earth sigh with relief. Because with Share & Save, saving money and saving the planet are no longer mutually exclusive – they're just two sides of the same, beautifully sustainable coin.

KEYWORDS : *Coupon code exchange platform, Online coupons, Discounts, Savings, e-commerce.*

INTRODUCTION

Coupon code exchange platforms are online platforms that allow users to upload and redeem coupon codes. These platforms can be a valuable resource for both businesses and consumers. Businesses can use coupon code exchange platforms to promote their products and services and reach new customers, while consumers can use these platforms to save money on their purchases.

In the digital labyrinth of abandoned inboxes and overflowing discount folders, countless coupon codes lie forgotten, their promised savings yearning for redemption. These lost treasures, trapped in the purgatory of unused potential, represent not only missed opportunities for consumer joy but also a mounting

burden on our planet. But from the ashes of wasted paper and forgotten clicks rises Share & Save, a MERN-powered web app platform poised to revolutionize the way we experience deals and redefine the landscape of online shopping.

Share & Save transcends the tired trope of mere coupon aggregation. It's a vibrant ecosystem, a digital bazaar where pre-vetted coupons dance anew, whispers of targeted promotions reach eager ears, and Mother Earth breathes a sigh of relief as the tide of discarded discounts recedes. Imagine a world where:

Forgotten codes rise from the ashes: Users resurrect their slumbering savings, unleashing a torrent of discounts once thought lost to the void.

Deals blossom from a hidden garden: Advanced search

and filtering tools become treasure maps, guiding users to a bounty of hidden savings across a vast array of categories.

Confidence replaces confusion: Every claimed coupon shines with the assurance of pre-vetted authenticity, shielding users from the sting of fraudulent offers.

We leverage the MERN stack – a fortress of technological might – to craft a seamless and intuitive experience. Our interface is a welcoming oasis, beckoning users to navigate the world of deals with ease, upload forgotten codes with a swipe, and claim their rightful savings with a tap. But beneath this user-friendly veneer lies a bedrock of security, crafted from robust encryption and vigilant verification protocols, safeguarding data and ensuring platform integrity like an unbreachable digital moat.

Share & Save is more than just a platform for bargain hunters and savvy shoppers; it's a catalyst for change, a reimagining of the consumer experience. We champion resourcefulness, empowering users to take control of their digital discount ecosystems. We offer businesses a targeted megaphone, amplifying their promotions and connecting them with ideal customers who dance to the rhythm of their deals. We are the green knights of the digital age, wielding our platform as a shield against the wastefulness of forgotten coupons, reducing landfill burdens and promoting a more sustainable future.

This revolution, however, extends beyond individual savings and environmentalism. Share & Save fosters a community spirit, a digital agora where users gather to exchange tips, recommend hidden gems, and celebrate the thrill of a well-scored deal. In this online marketplace, trust reigns supreme, fueled by transparent reviews and genuine interactions.

Share & Save is a movement, a clarion call to unlock hidden savings, empower businesses, and contribute to a more sustainable tomorrow. Join us as we break free from the shackles of forgotten codes and rewrite the story of online shopping, one redeemed coupon at a time. Together, we can transform the digital landscape, turning forgotten discounts into shared triumphs and whispering deals into an echoing anthem of savings and sustainability.

This expanded introduction delves deeper into the project's vision, emphasizing its impact on users,

businesses, and the environment. It paints a vivid picture of the platform's potential and invites readers to join the movement for a more sustainable and rewarding online shopping experience. Remember, you can further personalize this introduction by incorporating specific details about your project's unique features and target audience.

BENEFITS OF COUPON CODE EXCHANGE PLATFORM

There are many benefits to using coupon code exchange platforms. For businesses, coupon code exchange platforms can help to:

- Increase brand awareness and reach new customers
- Generate leads and sales
- Boost website traffic
- Promote new products and services
- Increase customer loyalty

How Coupons Code Exchange Platform Work

Coupon code exchange platforms typically work as follows:

1. Users create an account on the platform.
2. Users upload the unused coupon codes to the platform.
3. When a user redeems a coupon code, the business that issued the coupon code is notified.
4. The business honors the coupon code and the user receives their discount.

Features of Coupons Code Exchange Platform

Coupon code exchange platforms typically offer a variety of features, such as:

- Search and filtering: Users can search for and filter coupon codes by category, score, and other criteria.
- Notifications: Users can receive notifications when new coupon codes are uploaded or when their favorite stores have new coupons available.
- Social media integration: Users can share coupon codes with their friends and followers on social media.

- Referrals: Coupon code exchange platforms often offer referral programs to encourage users to invite their friends to join the platform.

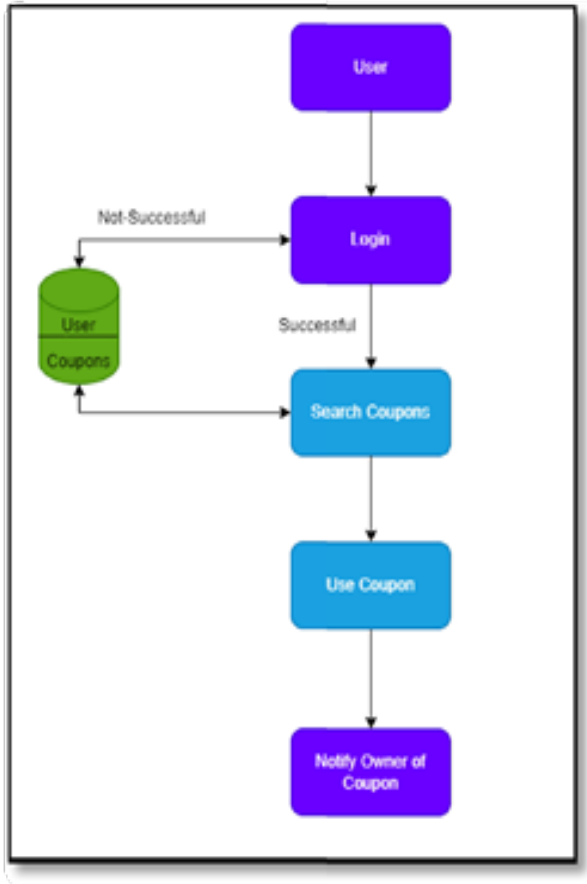


Fig. 1. Architecture Diagram

System Architecture

A description of the program architecture is presented below. The architecture follows a client-server model with distinct layers for presentation application logic and data storage. The Coupon Code Exchange Platform is designed to facilitate secure and efficient exchange of coupon codes among users. This architectural design aims to provide an overview of the system structure and functionality. The responsibilities of this architecture are to facilitate user interactions, submission of coupon codes, and display of exchange results. The platform includes user interfaces, an exchange engine, and logging capabilities.

It ensures a seamless and secure experience for users engaging in coupon code exchanges.

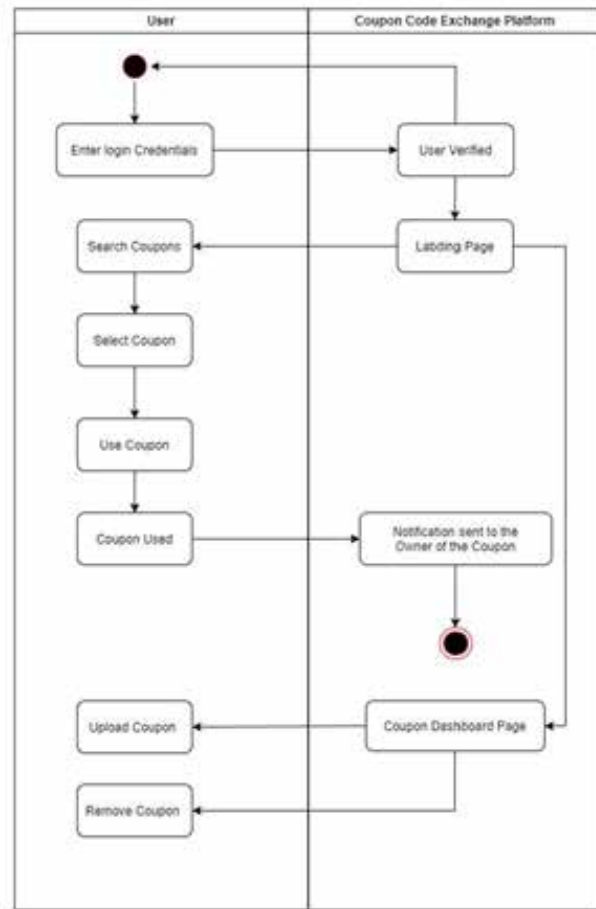


Fig. 2. Activity Diagram

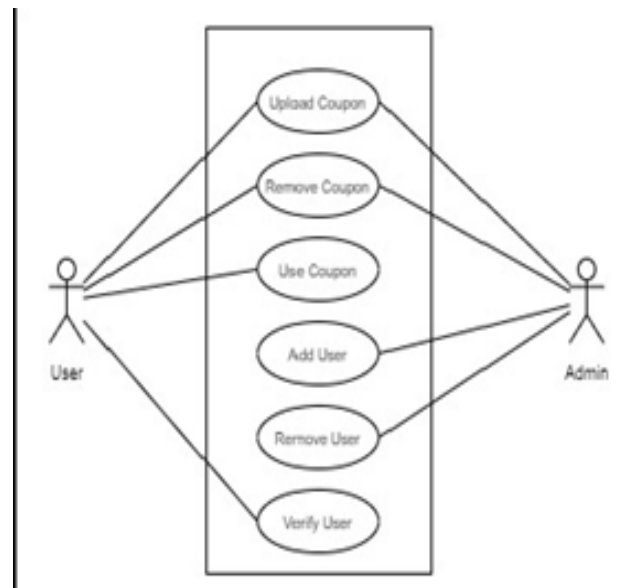


Fig. 2. Use Case Diagram

- Represents the interactions between system elements and external factors.
- Shows the system's functionality from a user's perspective.
- User authentication and authorization
- Coupon code management
- Admin panel
- Coupon code categories

NON-FUNCTIONAL REQUIREMENT

- Response time
- Throughput
- Availability
- Scalability
- Data encryption
- Input validation
- Access control
- Security monitoring
- Security patching

LITERATURE SURVEY

Benefits of Coupon Code Exchange Platforms

Cost savings for consumers: Sharing pre-vetted coupons unlocks a wider range of deals, maximizing purchasing power and offering a fresh avenue for financial resourcefulness.

Reduced environmental impact: Giving a second life to unused codes directly impacts sustainability by decreasing paper waste and curbing the environmental footprint associated with coupon production and circulation.

Brand awareness and customer engagement: Businesses can leverage these platforms to reach targeted audiences and promote their products and services through shared coupons, fostering brand loyalty and engagement.

Enhanced user experience: By providing a centralized hub for deal discovery and claiming, these platforms streamline the process, offering convenience and simplifying the journey from browsing to savings.

Challenges of Coupon: Code Exchange Platforms

Verification and fraud: Ensuring code legitimacy and validity is crucial for maintaining user trust and platform integrity. Robust verification mechanisms are needed to combat fraudulent activities and mitigate user disappointment.

Security and data privacy: Protecting user data and platform security are paramount to building trust and encouraging engagement. Secure systems and transparent data handling practices are essential.

Monetization and sustainability: Finding sustainable revenue models that do not compromise user experience or platform functionality is a key challenge for long-term viability. Striking a balance between value creation and revenue Competition and market saturation: Existing coupon aggregators and individual deal-sharing communities pose potential competition, necessitating unique value propositions and catering to specific user needs.

PROPOSED WORK

User Module

User Registration

- Implement a user registration module to facilitate user sign-up.
- Develop robust mechanisms for capturing and storing user details securely.
- User Login System
- Design and implement a secure user login system.

Employ industry-standard authentication protocols such as JWT tokens for enhanced security.

Home Page and Coupon Claiming

- Home Page Design
- Create an intuitive and visually appealing home page.
- Include a dedicated section for users to effortlessly claim available coupon codes.
- Coupon Claiming Process
- Develop the functionality for users to claim coupon codes seamlessly.

Implement any necessary validation and verification steps to ensure a smooth process.

Coupon Upload Module Dedicated Upload Page

Establish a dedicated page for users to upload coupon information.

Integrate a user-friendly form with fields for Coupon Name, Expiry Date, and Coupon Code.

Form Validation

Implement server-side form validation to ensure the accuracy and integrity of the uploaded coupon information.

Provide informative error messages for users during the submission process.

Server-Side Logic

- User Action Handling
- Develop robust server-side logic to handle user actions efficiently.
- Ensure seamless communication between the front end and back end.
- JWT Token Implementation
- Integrate JWT tokens to enhance the security of communication between the client and server.

Implement token-based authentication for user sessions.

MongoDB Database Integration

- Database Setup
- Configure and set up a MongoDB database to store user details and coupon information.
- Establish a clear database schema that aligns with the application's requirements.
- CRUD Operations
- Implement Create, Read, Update, and Delete (CRUD) operations for interacting with the MongoDB database.
- Ensure data consistency and integrity throughout the application.

Security Measures

- Authentication and Authorization

- Implement robust measures for user authentication and authorization.
- Enforce access controls to secure different parts of the application.
- Data Validation
- Apply stringent data validation techniques to prevent common security vulnerabilities.

Mitigate risks associated with malicious inputs and potential threats.

FUTURE SCOPE

Expand to mobile: Develop a mobile app for the platform, making it even more accessible and convenient for users to upload, search for, and claim coupons on the go.

- Personalization: Use AI and machine learning to personalize deal recommendations for users based on their purchase history, location, and other preferences.
- Community features: Encourage user interaction by adding features like forums, reviews, and ratings for coupons and businesses.
- Partnerships: Partner with businesses to offer exclusive deals and coupons on the platform.
- Social media integration: Allow users to share their coupon finds and savings with their friends and followers on social media
- Gamification: Implement gamification elements like points, badges, and leaderboards to incentivize user engagement and platform usage.
- International expansion: Expand the platform to other countries and regions to cater to a wider global audience.
- Subscription model: Offer a premium subscription tier with additional features, such as early access to deals, exclusive coupons, and personalized recommendations.
- Integrate with loyalty programs: Allow users to link their loyalty program accounts to the platform to earn points or rewards for using coupons
- Develop a charity component: Partner with charities and allow users to donate their unused coupons or a portion of their savings to a good cause.

- Invest in AI-powered coupon verification: Implement advanced AI algorithms to automatically detect and flag fraudulent coupons, ensuring platform security and user trust.
- Utilize blockchain technology: Explore the potential of blockchain technology to securely store and manage coupon data, further enhancing platform transparency and user confidence.

CONCLUSION

In a landscape choked by overflowing landfills and unused digital resources, "Share & Save" emerges as a beacon of environmental and economic responsibility. This MERN-powered web app platform tackles the twin challenges of coupon waste and consumer frustration by facilitating a vibrant ecosystem for exchanging pre-verified, verifiable discount codes.

"Share & Save" doesn't simply aggregate existing deals; it breathes new life into forgotten codes, empowering users to rediscover hidden savings and businesses to connect with targeted audiences. Robust security measures ensure user trust and data integrity, while advanced filtering and AI-powered verification combat fraud and misinformation.

This project transcends mere convenience and cost-cutting. It rewrites the narrative of consumerism by:

- Promoting sustainability: Reducing landfill waste and the environmental impact of unused coupons.
- Empowering individuals: Enabling users to unlock forgotten discounts and maximize their purchasing power.
- Supporting businesses: Offering targeted promotion tools to reach ideal customers and boost brand awareness.
- Fostering community: Encouraging a collaborative spirit of sharing and value discovery.

"Share & Save" isn't just a platform; it's a movement. It's a shift towards a future where saving money and

saving the planet go hand-in-hand. With its user-friendly interface, commitment to security, and impactful approach, "Share & Save" is poised to revolutionize the way we utilize and exchange discount codes, paving the way for a more sustainable and value-driven online shopping experience.

REFERENCES

1. Wikipedia: Ecoupon, 2019, [online] Available: <https://en.wikipedia.org/wiki/E-coupon> Show in Context Google Scholar
2. C. Blundo, S. Cimato and A. DeBonis, "Secure E-coupons", *Electron. Commerce Res.*, vol. 5, no. 1, pp.117-139, Jan. 2005. Show in Context Cross Ref Google Scholar
3. World Mobile Coupons Market to Grow at 73.1% CAGR to 2020, 2016, [online] Available: <https://www.prnewswire.com/news-releases/world-mobile-coupons-market-to-grow-at-7314-cagr-to-2020603320306.html> Show in Context Google Scholar
4. We are a four member team motivated to work on this coupon code exchange platform project for several reasons: Seventh International Conference on Information, Process, and Knowledge Management (eKNOW' 2015), At: Lisbon, Volume: 92-98 https://www.researchgate.net/publication/275641902_Discount_Coupons_Dematerialization_a_Comprehensive_Literature_Review
5. Four decades of coupon research in pricing: Evolution, development, and practice, August 2017, *Journal of Revenue and Pricing Management* 16 (4). https://www.researchgate.net/publication/310838471_Four_decades_of_coupon_research_in_pricing_Evolution_development_and_practice
- [6] F. Liu et al. Consumers' decision-making process in redeeming and sharing behaviors toward a pp-based mobile coupons in social commerce. *Int. J. Inf. Manag.* (2022) <https://www.sciencedirect.com/science/article/abs/pii/S0268401222000846>

An Extensive Review of Cloud Security: Challenges Threats & Intrusions

J. P. Patil

S. B. Patil

D. D. Survase

Department of Information Technology
Jawahar Education Society's Institute of Technology, Management & Research
Nashik, Maharashtra

ABSTRACT

The global adoption of cloud computing has revolutionized the organization and management of data storage, processing, and access. However, this technical advancement has raised significant concerns about data security and privacy in cloud computing environments. This abstract aims to provide a comprehensive review of the issues, potential solutions, and future developments related to data privacy and security in cloud computing. One of the main challenges in cloud computing systems is ensuring the privacy and security of data while it is being processed and stored in external data centers. This paper explores the potential dangers presented by internal threats, security breaches, and unauthorized entry into confidential data. As a result, data privacy and security in cloud computing environments continue to be major concerns for both organizations and individuals. The abstract provides an overview of global cloud storage usage, along with its challenges, potential solutions, and future innovations.

KEYWORDS : *Cloud computing, Cloud storage, Data integrity, Security, Privacy.*

INTRODUCTION

This paper examines data security in cloud computing, focusing on methods and approaches used worldwide to protect data and minimize risks and threats. While the availability of data in the cloud benefits many applications, it also poses risks by exposing data to potentially insecure applications. Additionally, the use of virtualization for cloud computing may risk data when a guest OS is run over a hypervisor without knowledge of its reliability. The paper also covers data security aspects for Data-in-Transit and Data-at-Rest, across all levels of SaaS, PaaS, and IaaS.

It is defined as a network solution that provides affordable, reliable, and easy access to IT resources. Unlike traditional applications, cloud computing is focused on providing services. This approach reduces infrastructure overhead and ownership costs while offering flexibility and improved performance for users. Security and privacy are major concerns when it comes to using cloud technology for data. It is crucial for cloud service providers to ensure data integrity, privacy, and

protection through various policies and mechanisms tailored to the nature, type, and size of the data. While one of the benefits of cloud computing is the ability to share data among organizations, this also presents risks to the data. Therefore, it is essential to secure data repositories and prevent potential risks.

SECURITY RESPONSIBILITIES FOR CLIENT/PROVIDER

Cloud security requires a shared responsibility between the client and provider. The cloud provider oversees physical infrastructure and application security, while the client manages authorization and cloud environment control. Service models like Infrastructure-as-a-Service (IaaS), Platform-as-a-Service (PaaS), and Software-as-a-Service (SaaS) offer different levels of responsibility for both parties. For example, in the IaaS model, the cloud service provider has authority over secure servers, storage, hypervisor, and virtualization, while the client is primarily responsible for data, applications, and network traffic.

Infrastructure-as-a-Service

Infrastructure-as-a-Service provides virtualized computing resources such as storage, networking, and accessible machines via the Internet. In this model, the cloud service provider (CSP) has full control over secure servers, storage, hypervisor, and virtualization, while the client is accountable for data, applications, and network traffic. The client bears the majority of the responsibilities in this model.

The IaaS cloud security models have these securities features:

- Evaluate and examine resources for misconfigurations.
- Prevent data loss using Data Loss Prevention tools.
- Detect suspicious user activity and behaviour.
- Find and eliminate malware.

Platform-as-a-Service

Platform-as-a-Service provides a secure platform for developers and organizations to create applications. In this model, the cloud service provider handles networking, storage, and hardware, while the client is responsible for application security, permissions, and configurations. This service model is an extension of IaaS for deploying applications in a cost-effective manner, eliminating the need to purchase all hardware and resources as required in the IaaS model.

Features included in PaaS:

- Cloud Access Security Brokers (CASB).
- Cloud Workload Protection Platforms (CWPP).
- Cloud Security Posture Management (CSPM).
- Logs, IP restrictions, and API gateways.
- Internet of Things (IoT).

In the PaaS model, the middleware and software are provided as part of the service to the application. Therefore, in this cloud security approach, the focus is on securing these services for application development, with both the CSP and the client being involved.

Software-as-a-Service

This model discusses the terms and conditions of

security ownership in the contract with the provider. For instance, Managed WordPress is a SaaS-based platform that hosts an organization's hardware, infrastructure, hypervisor, network traffic, and operating system, which are not visible to the user. The internal security system is a shared responsibility between the client and the cloud service provider, not solely the client's responsibility.

Features included in SaaS applications and infrastructure controls:

Organization of information misfortune avoidance.

- Evasion of unapproved sharing of weak information to informal people.
- Obstructing the download of corporate information to individual gadgets.
- ID of safety breaks, insider dangers, and malware.
- Perceivability into private applications.
- Survey for misconfiguration.

TOP CLOUD SECURITY FEATURES

For a profoundly gotten cloud stage, there are various devices that can be useful to safeguard classification and unwavering quality. The following are the security includes that should be available in your cloud security model.

Data Encryption

Encryption shields text and information by making an interpretation of them into figures that must be unraveled, got to, and altered by chosen parties. Information encryption is a valuable strategy to keep the most weak cloud information completely safe from the utilization of any unapproved person. Also, encryption brings down the gamble of taken information utilized for loathsome purposes. With information encryption, the CSP will get an opportunity to caution the client, and the client can do whatever it may take to safeguard their records.

Resilient Firmware

Firmware strength is a Field-Programmable Door Cluster (FPGA) based arrangement that aides in forestalling assaults to the firmware layer. It likewise

incorporates recuperation of the information after an assault to reestablish your framework to its past working state.

Advanced Perimeter Firewall

A firewall is a gadget that screens approaching and active traffic. It will permit or impede the traffic subsequent to filtering the traffic against security guidelines. Firewalls are significant as they guarantee a security hindrance for the organization traffic. Sadly, most of firewalls used to safeguard information are very essential since they just investigate the source and objective bundles.

Intrusion Detection Systems

An intrusion detection system (IDS) should be available in all IT security frameworks. With IDS, you can track and record a wide range of interruption endeavors. To forestall interruption endeavors, you should have excellent managed detection and response (MDR) security. MDR security will examine the malware present inside your framework and eliminate it.

Data Centers with Strong Physical Security

You or your CSP (contingent upon your administration model) need to protect your server farms with actual security like day in and day out CCTV checking, safety officers, and locked enclosures or cupboards for server racks.

Cloud Security Architecture Challenges and Threats

Information breaks and security dangers influence the trustworthiness of cloud administrations.

Here is a list of cloud security architecture challenges and threats to consider:

Insider Threats

Insider dangers incorporate the specialists inside your association who approach frameworks and cloud specialist organizations that can hole or take your significant information. For this reason it is important to pick a believed CSP administration and just permit chosen approved individuals to get to the information.

Denial-of-Service (DoS) or Distributed-Denial-of-Service (DDoS) Attacks

DoS or DDoS assaults try to crash a framework with rehashed demands until the help is inaccessible.

Security cutoff points can avoid these assaults utilizing network consistence approaches to take out rehashed demands. Furthermore, the CSPs can likewise move the information traffic to different assets while reestablishing the framework.

Password Issues

Regardless of whether you have a very much organized security design, frail passwords place your framework at likely gamble. Cloud security design helps in getting equipment, firmware, and programming. Nonetheless, all frameworks ought to constantly have areas of strength for an and two-factor confirmation to guard your information.

Confidentiality

Privacy is the capacity to stay quiet and indiscernible to individuals who shouldn't approach that information, for example, aggressors or individuals inside an association without the legitimate access level. Classification likewise incorporates security and trust, or when a business promises mystery in dealing with their clients' information.

Integrity

Trustworthiness is the possibility that the frameworks and applications are precisely exact thing you anticipate that they should be, and capability precisely as you anticipate that they should work. On the off chance that a framework or application has been compromised to create an obscure, startling, or misdirecting yield, this can prompt misfortunes.

Availability

Accessibility is the third capacity and is for the most part the most un-considered by cloud planners. Accessibility addresses disavowal of-administration (DoS) assaults. Maybe an aggressor can't see or change your information.

PRIVACY CHALLENGES IN CLOUD COMPUTING

Distributed computing is a generally very much examined point today with interest from all fields, be it exploration, the scholarly world, or the IT business. The cloud worldview rotates around comfort and simple the arrangement of a colossal pool of shared registering assets.

The fast advancement of the cloud has prompted greater adaptability, cost-cutting, and versatility of items yet additionally faces a colossal measure of protection and security challenges. Since it is a somewhat new idea and is developing step by step, there are unseen security gives that jerk up and should be dealt with when found. Here we talk about the main 7 security challenges experienced in distributed computing:

Data Confidentiality Issues

Classification of the client's information is a significant issue to be thought about while externalizing and re-appropriating incredibly fragile and delicate information to the cloud specialist organization. Individual information ought to be made inaccessible to clients who don't have legitimate approval to get to it and one approach to ensuring that privacy is by the utilization of extreme access control strategies and guidelines. The absence of trust between the clients and cloud specialist co-ops or the cloud information base specialist organization in regards to the information is a significant security concern and keeps down a many individuals from utilizing cloud administrations.

Data Loss Issues

Information misfortune or information burglary is one of the significant security challenges that the cloud suppliers face. In the event that a cloud merchant has revealed information misfortune or information robbery of basic or delicate material information before, in excess of a little over half of the clients would decline to utilize the cloud administrations given by the seller. Blackouts of the cloud administrations are regularly noticeable even from firms like Dropbox, Microsoft, Amazon, and so forth, which thus brings about a shortfall of confidence in these administrations during a crucial time.

Geographical Data Storage Issues

Since the cloud foundation is circulated across various geological areas spread all through the world, it is much of the time conceivable that the client's information is put away in an area that is out of the legitimate purview which prompts the client's interests about the lawful openness of neighborhood policing guidelines on information that is put away out of their district. Also, the client fears that nearby regulations can be disregarded because of the powerful idea of the

cloud makes it undeniably challenging to designate a particular server that will be utilized for trans-line information transmission.

Multi-Tenancy Security Issues

Multi-tenure is a worldview that follows the idea of sharing computational assets, information capacity, applications, and administrations among various occupants. This is then facilitated by a similar consistent or actual stage at the cloud specialist co-op's premises. While following this methodology, the supplier can boost benefits however puts the client at a gamble.

Transparency Issues

In distributed computing security, straightforwardness implies the eagerness of a cloud specialist organization to uncover various subtleties and qualities on its security readiness. A portion of these subtleties compromise strategies and guidelines on security, protection, and administration level. Notwithstanding the eagerness and demeanor, while ascertaining straightforwardness, it means quite a bit to see how reachable the security status information and data really are. It won't make any difference the degree to which the security realities about an association are within reach on the off chance that they are not introduced in a coordinated and effectively reasonable manner for cloud administration clients and reviewers, the straightforwardness of the association can then likewise be evaluated moderately little.

Hypervisor Related Issues

Virtualization implies the consistent deliberation of registering assets from actual limitations and requirements. In any case, this postures new difficulties for factors like client verification, bookkeeping, and approval. The hypervisor deals with numerous Virtual Machines and thusly turns into the objective of enemies. Unique in relation to the actual gadgets that are free of each other, Virtual Machines in the cloud as a rule dwell in a solitary actual gadget that is overseen by the equivalent hypervisor. The split the difference of the hypervisor will subsequently endanger different virtual machines.

Managerial Issues

There are specialized parts of cloud protection challenges as well as non-specialized and administrative ones. Indeed, even on carrying out a specialized answer

for an issue or an item and not overseeing presenting vulnerabilities appropriately is at last bound.

LITERATURE SURVEY

To comprehend the fundamentals of cloud computing and secure data storage on the cloud, we consulted multiple resources. This section presents a literature review to establish a basis for discussing different aspects of data security.

Wayne Jansen and Timothy Grance propose the concept of an Advanced Cloud Protection system (ACPS) to address security issues in virtualization. This system aims to safeguard guest virtual machines and distributed computing middleware, while also monitoring the behavior of cloud components through logging and periodic checks of executable system files. By implementing the ACPS, potential security attacks from guest VMs can be detected and blocked without detection, enhancing the overall security of the system [12].

Recent studies have been concentrating on the multi-cloud environment [12], [4], which oversees multiple clouds and eliminates reliance on any single cloud. Transitioning from a single cloud or intra-cloud to multiple clouds is logical and crucial for various reasons. According to Cachin et al. [7], "Services of single cloud are still subject to outage." Furthermore, Bowers et al. demonstrated that over 80% of company management "fear security threats and loss of control of data and systems." The shift of cloud computing from single to multi-clouds to safeguard user data is exceedingly important. The term "multi-clouds" is akin to the terms "intercloud" or "cloud-of-clouds" introduced by Vukolic [1], who also proposes that cloud computing should not culminate with a single cloud.

Vukolic [1] suggests that the primary reason for transitioning to intercloud is to enhance the capabilities provided by a single cloud, by spreading out the reliability, trust, and security across multiple cloud providers. Additionally, Vukolic [1] has proposed the use of dependable distributed storage that employs a portion of Byzantine fault tolerance (BFT) techniques for multi-cloud environments.

BFT protocols are not suitable for single clouds. According to Vukolic [1], one limitation of BFT for intra-cloud use is its requirement for a high level

of failure independence, as is the case with all fault-tolerant protocols. In the event of a Byzantine failure affecting a specific node in the cloud, it is necessary to have a different operating system, implementation, and hardware to prevent the spread of such a failure to other nodes within the same cloud. Furthermore, if an attack occurs within a specific cloud, it could potentially enable the attacker to take control of the inner-cloud infrastructure [1].

HAIL (High Availability and Integrity Layer) [8] is a protocol that manages multiple clouds. It is a distributed cryptographic system that enables a group of servers to verify the retrievability and integrity of a client's stored data. HAIL addresses the availability and integrity of stored data in an intercloud. However, it does not ensure data confidentiality, requires code execution in its servers, and does not handle multiple versions of data. In contrast, DepSky [11] does not have these limitations. The RACS system differs from the DepSky system by addressing "economic failures" and vendor lock-in but does not tackle cloud storage security issues. It also lacks mechanisms for ensuring data confidentiality or updating stored data. The DepSky system stands out for its experimental evaluation involving multiple clouds, distinguishing it from previous work on multi-clouds [12].

Providers and users have separate domains, each with a dedicated trust agent. Different trust strategies are employed for service providers and customers, taking into consideration time and transaction factors for trust assignment. Shantanu Pal suggests these approaches to establish a secure virtual network in a cloud environment, promoting interoperability and security across different clouds to protect customers from malicious suppliers and providers from malicious users. Josh Karlin has proposed a robust BGP (PGBGP) architecture to address cases where an Autonomous System may incorrectly announce itself as the destination for all data being transferred over the network. This architecture examines the Autonomous Systems (ASs) and conducts anomaly detection with a response system to prevent data from being routed to the wrong AS. It also allows for the deployment of the PGBGP protocol on select ASs to safeguard the entire network.

The issue of the insider threat in cloud infrastructure, the foundation of cloud computing, is addressed by Rocha

and Correia [9]. IaaS cloud providers offer users a set of virtual machines for running software, but traditional data encryption methods for ensuring confidentiality are inadequate because encrypted data cannot be processed within the cloud provider's virtual machines [9]. Administrators with remote access to servers pose a threat as malicious insiders, potentially compromising user data. Van Dijk and Juels [14] highlight drawbacks of data encryption in cloud computing, suggesting that it cannot guarantee privacy when data is processed from different clients. Despite cloud providers' awareness of insider threats, they believe they have effective solutions to mitigate the problem. Rocha and Correia [9] identify possible attackers targeting IaaS cloud providers, while Grosse et al. propose solutions such as preventing physical access to servers. However, Rocha and Correia [9] argue that the outlined attackers have remote access and do not require physical server access. Grosse et al. also suggest monitoring all server access in a cloud where user data is stored, but Rocha and Correia [9] dispute the effectiveness of this approach.

CONCLUSION

It is evident that despite the rapid growth in the adoption of cloud computing, security remains a significant concern in the cloud computing landscape. Users are reluctant to compromise their confidential data due to potential threats from both internal and external sources, as well as any unintended consequences arising from cloud service disruptions. Moreover, the recent surge in service unavailability has posed numerous challenges for a considerable customer base. Additionally, the intrusion of data further exacerbates the existing security issues.

REFERENCES

1. M. Vukolic, "The Byzantine empire in the intercloud", ACM SIGACT News, 41, 2010, pp. 105-111.
2. A. Bessani, M. Correia, B. Quaresma, F. André and P. Sousa, "DepSky: dependable and secure storage in a cloud-of-clouds", EuroSys'11: Proc. 6th Conf. On Computer systems, 2011, pp. 31-46.
3. H. Takabi, J.B.D. Joshi and G.-J. Ahn, "Security and Privacy Challenges in Cloud Computing Environments", IEEE Security & Privacy, 8(6), 2010, pp. 24-31.
4. M. Van Dijk and A. Juels, "On the impossibility of cryptography alone for privacy-preserving cloud computing", HotSec'10: Proc. 5th USENIX Conf. on Hot topics in security, 2010, pp.1-8.
5. C. Cachin, R. Haas and M. Vukolic, "Dependable storage in the Intercloud", Research Report RZ, 3783, 2010.
6. F. Rocha and M. Correia, "Lucy in the Sky without Diamonds: Stealing Confidential Data in the Cloud", Proc. 1st Intl. Workshop of Dependability of Clouds, Data Centers and Virtual Computing Environments, 2011, pp. 1-6.
7. Shantanu Pal, Sunirmal Khatua, Nabendu Chaki, Sugata Sanyal, "A New Trusted and Collaborative Agent Based Approach for Ensuring Cloud Security," Annals of Faculty Engineering Hunedoara International Journal of Engineering (Archived copy), scheduled for publication in vol. 10, issue 1, January 2012. ISSN: 1584-2665.
8. osh Karlin, Stephanie Forrest, Jennifer Rexford, "Autonomous Security for Autonomous Systems," Proc. Of Complex Computer and Communication Networks; vol. 52, issue. 15, pp. 2908- 2923, Elsevier, NY, USA, 2008.
9. Mohammed A. AlZain, Ben Soh and Eric Pardede, "MCDB: Using Multi-Clouds to Ensure Security in Cloud Computing", "2011 Ninth IEEE International Conference on Dependable, Autonomic and Secure Computing", 2011 IEEE, pp. 784-791.
10. Mohammed A. AlZain , Eric Pardede , Ben Soh , James A. Thom, "Cloud Computing Security: From Single to Multi-Clouds", 2012 45th Hawaii International Conference on System Sciences, 2012, pp. 5490-5499.
11. C. Wang, Q. Wang, K. Ren and W. Lou, "Ensuring data storage security in cloud computing", ARTCOM'10: Proc. Intl. Conf. on Advances in Recent Technologies in Communication and Computing, 2010, pp. 1-9.
12. H. Abu-Libdeh, L. Princehouse and H. Weatherspoon, "RACS: a case for cloud storage diversity", SoCC'10: Proc. 1st ACM symposium on Cloud computing, 2010, pp. 229-240.
13. Wayne Jansen, Timothy Grance, "NIST Guidelines on Security and Privacy in Public Cloud Computing," Draft Special Publication 800-144, 2011.
14. K.D. Bowers, A. Juels and A. Oprea, "HAIL: A high-availability and integrity layer for cloud storage", CCS'09: Proc. 16th ACM Conf. on Computer and communications security, 2009, pp. 187-198.

Supply Chain Management in Agriculture using Blockchain Technology

Mundhe Bhalchandra B

Dere Kapil D

Department of M. E. AI & D S Engineering
Jaihind College of Engineering
Kuran, Tal-Junnar
Pune, Maharashtra
✉ mundheraj.mundhe@gmail.com

ABSTRACT

Block chains, now firmly established, are a digital system that combines data management, incentive systems, cryptography, and networking to enable the execution, recording, and verification of transactions between parties. Even while the original goal of block chain technology was to facilitate new forms of digital currency that would enable easier and more secure payment methods, they have enormous promise as a new foundation for all kinds of transactions. Agribusiness stands to gain a lot from this technology by leveraging it as a platform to conduct "smart contracts" for transactions, especially for high-value goods. Before we go any further, it is important to distinguish between distributed ledger and block chain technologies and private digital currencies. Given the distributed and global character of digital currencies such as Bitcoin, it is improbable that central banks will be able to adequately oversee the underlying protocols. Monetary authorities are primarily concerned with understanding the "on-ramps" and "off-ramps" that comprise the links to the traditional payments system, rather than being able to monitor and manage the money itself. In contrast to the digital currency component of the block chain, the distributed ledger aspect holds great potential for application in trade and agriculture funding, especially in scenarios where multiple partners are involved and a dependable central authority is lacking.

KEYWORDS : *Advanced encryption standard, Block-chain.*

INTRODUCTION

Given the distributed and global character of digital currencies such as Bitcoin, it is improbable that central banks will be able to adequately oversee the underlying protocols. Monetary authorities are primarily concerned with understanding the "on-ramps" and "off-ramps" that comprise the links to the traditional payments system, rather than being able to monitor and manage the money itself. In contrast to the digital currency component of the block chain, the distributed ledger aspect holds great potential for application in trade and agriculture funding, especially in scenarios where multiple partners are involved and a dependable central authority is lacking. Since they demonstrate that existing strategies for fostering transparency and trust

have not been able to address or, in some cases, have made the problems of low transparency and trust in agri-food chains worse, these informational challenges pose a severe threat to food safety, food quality, and sustainability. The integrity of food in particular has become a major issue. In food value chains, food integrity pertains to the authenticity and fairness of food at both the physical and digital layers. It is anticipated that the digital layer would provide dependable and trustworthy information on the provenance and origin of food items at the physical layer. Blockchain technology provides a means of ensuring the durability of documents and could facilitate data sharing amongst many participants in the food value chain. This idea could lead to an exciting paradigm shift that ensures food integrity and fosters transparency and trust in food networks.

RELATED WORK

Agriculture Supply Chain Traceability of Soybeans By means of Blockchain, Raja Jayaraman, Nishara Nizamuddin, Khaled Salah, and Mohammed Omar additionally With a high degree of integrity, dependability, and security, the recommended method—which was published in IEEE Access (Volume: 7)—improves efficiency and safety by doing away with the need for intermediaries, centralized authority, and transaction records. The recommended approach focuses on using smart contracts to control and oversee all communications and exchanges between all stakeholders involved in the supply chain ecosystem. All transactions are documented and maintained thanks to connections to an immutable blockchain ledger and a decentralized file system (IPFS), providing everyone with access to a high degree of traceability and transparency into the supply chain ecosystem in a secure, dependable, and effective way. Integrating blockchain-driven traceability into the real-world agri-food supply chain Massimo Vecchio, Miguel Pincheira Caro, Raffaele Giaffreda, and Muhammad Salek Ali 2018 IoT Vertical and Topical Summit on Agriculture (IOT Tuscany) printed in In this article, AgriBlockIoT—a fully decentralized blockchain-based traceability system—is presented. It is designed to manage the agri-food supply chain by seamlessly integrating Internet of Things (IoT) devices that generate and use digital data along the entire chain. In order to appropriately assess Agri BlockET, we first created a conventional use-case inside the designated vertical area, specifically "from-farm-to-fork." Then, in order to ensure traceability, we built and implemented a use-case using Ethereum and Hyperledger Sawtooth, two alternative blockchain platforms. In conclusion, we evaluated and contrasted the installations' performance concerning latency, CPU, and network use, highlighting their principal benefits and drawbacks. A Dispersed Platform with Shared and Duplicate Bookkeeping for Agricultural Products Using Blockchain Provenance Mengzhen Wang, Fei-Yue Wang, Xiujuan Wang, Haoyu Wang, and Jing Hua Intelligent Vehicles Symposium (IV) 2018 IEEE In this work, we propose a blockchain-based agricultural provenance system that is characterized by decentralization, cooperative maintenance, consensus trust, and reliable data in order to tackle the trust problem in the supply chain

for commodities. The recorded information includes the management actions (fertilization, irrigation, etc.) with a specific data structure. Tracking the provenance of agricultural goods with blockchain technology not only broadens its potential applications but also fosters a reliable network among the many stakeholders in the agriculture sector. A blockchain and RFID-based approach to China's food and agriculture supply chain tracking 16th International Conference on Service Management and Systems Feng Tian (ICSSSM) First, we look at the current state of development and application of blockchain and RFID (Radio-Frequency IDentification) technologies in this study. Subsequently, we scrutinize the advantages and disadvantages of employing RFID and blockchain technology in the development of the agri-food supply chain traceability system. Lastly, we showcase the process of system creation. Food safety can be efficiently guaranteed by obtaining, transferring, and sharing authentic data about agri-food in the production, processing, warehousing, distribution, and selling linkages. This will enable traceability with trustworthy information along the whole agri-food supply chain. Food supply security with blockchain technology The 2017 IEEE International Conference on Industrial Engineering and Engineering Management (IEEM) featured a release by Bowen Zhang, Daniel Tse, Yuchen Yang, Chenli Cheng, and Haoran Mu. This article introduces blockchain technology, makes the case for its use to information security in the food supply chain, and compares it to the current supply chain architecture.

MOTIVATION

The last three years have seen a massive surge in interest in blockchain technology (BCT), with numerous companies and academic institutions focusing on the potential applications of this technology in a range of financial, industrial, and social domains. On the other hand, the technology has also been the subject of a great deal of exaggeration and hyperbole, which has created misconceptions and inflated expectations. Although BCT is still in its early stages of development, its commercial applications seem quite promising. Blockchain innovation is thought to challenge existing players in various industries through its applications, structures, and business concepts. It is often characterized by decentralized, open-source development.

PROBLEM STATEMENT AND OBJECTIVES

The last three years have seen a massive surge in interest in blockchain technology (BCT), with numerous companies and academic institutions focusing on the potential applications of this technology in a range of financial, industrial, and social domains. On the other hand, the technology has also been the subject of a great deal of exaggeration and hyperbole, which has created misconceptions and inflated expectations. Although BCT is still in its early stages of development, its commercial applications seem quite promising. Decentralized, open-source development is often associated with blockchain innovation, which is thought to upend existing players in numerous industries through its applications, business concepts, and structures.

SYSTEM ARCHITECTURE

A comprehensive process framework for the project is provided by a conceptual model called "system architecture". It describes each stage of the project's creation using a flow. Every step is explained in great depth. The system architecture is as follows: A hash value that acts as a record of each transaction that occurs in the system is contained in a block. When every block is connected to every other block, a virtual block chain is created. The hash value of a current block is created using the hash of the previous block and the data from the current block. In this way, the hashes of all subsequent blocks must be changed if one block is tampered. The many copies are stored across multiple servers, ensuring the confidentiality and integrity of the information. Since all transactions are made via an application interface, the management of the agricultural supply chain will continue to be transparent.



Figure 1: System Architecture

FUTURE WORK

In the future, we'll look into government sponsorship so that we can carry out a large-scale project with some domain and hosting space online.

CONCLUSION

We're planning to develop a Java web application prototype to implement BCT in supply chain management. We will implement blockchain features such as:

1. Disentanglement
2. The Hash Algorithm
3. A safe database.

Consequently, it is possible to monitor the agricultural supply chain and establish a minimum price for agricultural products.

REFERENCES

1. Niu, B., Dong, J., & Liu, Y. (2021a). Incentive alignment for blockchain adoption in medicine supply chains. *Transportation Research Part E: Logistics and Transportation Review*, 152(February), 102276. <https://doi.org/10.1016/j.tre.2021.102276>
2. O'Leary, D. E. (2019). Some issues in blockchain for accounting and the supply chain, with an application of distributed databases to virtual organizations. *Intelligent Systems in Accounting, Finance and Management*, 26(3), 137–149. <https://doi.org/10.1002/isaf.1457>
3. Oh, J., Choi, Y., & In, J. (2022). A conceptual framework for designing blockchain technology enabled supply chains. *International Journal of Logistics Research and Applications*. <https://doi.org/10.1080/13675567.2022.2052824>
4. Pandey, V., Pant, M., & Snasel, V. (2022). Blockchain technology in food supply chains: Review and bibliometric analysis. *Technology in Society*, 69(August 2021), 101954. <https://doi.org/10.1016/j.techsoc.2022.101954>
5. Patil, A., Shardeo, V., Dwivedi, A., & Madaan, J. (2021). An integrated approach to model the blockchain implementation barriers in humanitarian supply chain. *Journal of Global Operations and Strategic Sourcing*, 14(1), 81–103. <https://doi.org/10.1108/JGOSS-07-2020-0042>
6. Rainero, C., & Modarelli, G. (2021). Food tracking and blockchain-induced knowledge: A corporate social responsibility tool for sustainable decision-making. *British Food Journal*, 123(12), 4284–4308. <https://doi.org/10.1108/BFJ-10-2020-0921>

The Jio Revolution: Transforming India's Digital Landscape

Mahesh Sanghavi, Kainjan Sanghavi

Bhavana Khivsara

Department of Computer Engineering
SNJB's Late Sau KBJ CoE Neminagar
Chandwad

✉ sanghavi.mahesh@gmail.com

Santosh Sancheti

Department of Mechanical Engineering
SNJB's Late Sau KBJ CoE Neminagar
Chandwad

ABSTRACT

This paper explores the transformative effect of Reliance Jio on India's digital infrastructure during the last seven years. Through a comprehensive evaluation of seven key effects, the paper elucidates how Jio's access into the telecommunications quarter has reshaped the lives of common Indians and paved the way for a colorful virtual economy. From free outgoing calls to reducing the virtual divide, Jio's contributions were profound and some distance-achieving. The studies also discuss the destiny prospects, emphasizing the position of artificial intelligence inside the context of 5G technology.

KEYWORDS : *Telecommunication industry, Customer satisfaction, Digital India, Reliance Jio, 5G, AI.*

INTRODUCTION

Seven years in the past, in a momentous announcement, Mukesh Ambani, the owner of Reliance Industries, unveiled Reliance Jio to the arena. Little did all people envision at that point that this formidable endeavour could ultimately rework into the linchpin of India's virtual infrastructure. Today, as we stand on the seven-year mark of Reliance Jio's inception, it's abundantly clear that this telecom massive has essentially reshaped the landscape of the nation's digital ecosystem.

The ultimate seven years have borne witness to a profound and pervasive evolution, with Jio rising as a riding pressure behind a sequence of fantastic modifications that have left an indelible impact on the lives of everyday residents. This studies paper delves into the awesome journey of Reliance Jio. It dissects the seven important consequences it has wrought upon India's digital milieu, elucidating how those variations have touched the lives of limitless people, companies, and groups.

In essence, this research paper serves as a testimony to the top notch transformation added approximately via Reliance Jio in only seven years, illuminating its adventure from inception to turning into a harbinger of a digitally empowered India.

IMPACT OF JIO IN 7 YEARS

Free Outgoing Calls

On the historic day of September 5, 2016, Reliance Jio initiated a seismic shift within the telecommunications panorama of India by rendering outgoing calls freed from fee. This audacious move marked the give up of a technology characterized by means of exorbitant calling rates that had careworn clients for years. Reliance Jio emerged because the trailblazer, turning into the first employer in India to disencumber its subscribers from the shackles of high-priced outgoing calls, and this modern exercise stays in impact to these days.

The effect of this alteration changed into immediate and profound. Common people, who had previously hesitated to make calls because of high price lists, now should talk freely with their pals, circle of relatives, and co-workers. This newfound freedom fostered more exceptional connectivity and reinforced social bonds across the country.

Furthermore, the advent of loose outgoing calls had cascading outcomes on numerous sectors of the economic system. It led to improved smartphone adoption as extra individuals sought to take advantage of the newfound affordability of conversation. As a result,

the demand for cellular phones surged, stimulating the cellular production enterprise and creating activity opportunities.

Reliance Jio's dedication to free outgoing calls democratized verbal exchange and laid the muse for a more inclusive and digitally linked India. This first impact of Jio set the stage for a chain of transformative adjustments that might unfold over the following seven years, redefining the digital panorama and enhancing the excellence of life for millions of Indians.

Low Data and Mobile Bills

Reliance Jio's 2d profound impact at the Indian virtual panorama has been the sizable reduction in cellular information costs, resulting in substantially decreased cell payments for clients. Before Jio's entry, cell statistics was luxurious, with fees averaging around Rs 255 in keeping with gigabyte (GB), making it inaccessible to many. However, Jio, upon its launch, embarked on a project to democratize records and get right of entry by aggressively slashing statistics prices to much less than Rs 10 in keeping with GB.

This drastic discount in statistics costs has had a ripple effect, definitely impacting the lives of thousands and thousands of Indians in numerous approaches:

- 1) **Affordability for All:** With information turning into extra less expensive, even individuals from economically disadvantaged backgrounds could now get admission to the internet, opening up a global of information, amusement, and possibilities formerly out of reach.
- 2) **Increased Data Consumption:** Jio's aggressive pricing endorsed customers to consume more records. This surge in statistics intake led to a paradigm shift in how human beings accessed records, amusement, and conducted business.
- 3) **India Tops in Data Usage:** Before Jio's arrival, India languished on the one hundred and fifty fifth position globally concerning facts utilization. However, the dramatic drop in information prices catalyzed a facts revolution. India surged to grow to be one of the world's top two countries in facts utilization. Today, Jio's network by itself consumes an impressive 1,one hundred crore GB of data monthly.

- 4) **Industry-Leading Data Consumption:** Jio's customers, on average, devour an excellent 25 GB of statistics in step with month, setting a benchmark inside the telecom industry. This displays how low prices have empowered users to leverage virtual offerings for various purposes, inclusive of training, leisure, and e- trade.

The transformation of data from a luxurious to an affordable commodity has reshaped how people stay, work, and join in India. It has fueled the growth of online schooling, e-commerce, virtual leisure, and infinite other sectors. Jio's pioneering efforts in reducing records expenses and promoting facts utilization have lowered cell payments and extended India's progress in the direction of turning into a digitally inclusive nation. This 2d effect of Jio underscores the enterprise's commitment to making virtual access a fundamental right for all Indians.

The Digital Revolution - Everything in the Palm of Hand

Reliance Jio's 0.33 a long way-achieving impact has been the profound virtual transformation it ushered in, efficiently putting a whole international of offerings and leisure inside the compact display of a cell tool. This transformation became driven with the aid of the affordability and accessibility of information, which went hand in hand with Jio's disruptive access into the market.

- 1) **Entertainment at Fingertips:** With the appearance of lower priced statistics, enjoyment ceased to be a commodity reserved for special activities. It became an integral part of each day's existence, reachable with a simple click on a cellular device. Streaming platforms, online gaming, and virtual content material intake skyrocketed, offering humans with enjoyment choices restricted most effectively by their creativity.
- 2) **Seamless Travel Experience:** Jio's affect extended to the journey industry, wherein reserving train, plane, and cinema tickets transitioned into online experiences. The convenience of cellular bookings revolutionized tour making plans, making it extra available and green for human beings throughout the United states.

- 3) **Booming Hospitality and Food Services:** Jio@7 witnessed the proliferation of hotel reserving and meals transport platforms, capitalizing at the virtual wave. Ordering meals or booking accommodation have become a count of some faucets on a cell phone display, stimulating the hospitality and culinary sectors.
- 4) **Tourism and E-Commerce Thrive:** The ease of reserving and accessing facts online boosted tourism, encouraging greater human beings to explore new destinations. Simultaneously, e-commerce groups leveraged the ubiquity of cellular gadgets, imparting a full-size array of services and products accessible from anywhere, fuelling the boom of the virtual financial system.
- 5) **Online Classes and Remote Work:** The COVID-19 pandemic emphasized the essential role of lower priced facts quotes. With the surprising want for far flung training and work-from-home arrangements, the net became a lifeline. The availability of low-priced statistics ensured that individuals ought to retain their training and expert commitments even in the course of challenging instances.
- 6) **Imagine the opportunity scenario:** if information costs had remained as excessive as Rs 255 in keeping with GB, the virtual panorama might have been regarded as vastly distinctive. Access to online schooling, far off paintings possibilities, and digital leisure might have been limited, exacerbating the challenges faced in the course of the pandemic and hindering usual economic development.

Revolutionizing Financial Transactions - The Rise of Digital Payments

Reliance Jio's fourth transformative effect centers on its pivotal function in revolutionizing India's monetary panorama, ushering in a new era of digital payments and financial inclusion. The Government of India's Unified Payments Interface (UPI) Open Digital Payment System is at the coronary heart of this variation. This platform has basically altered the manner Indians conduct financial transactions.

- 1) **The Emergence of UPI:** The creation of UPI was a recreation-changer inside the Indian financial atmosphere. It introduced collectively financial

giants, including banks of all sizes, and progressive pockets groups inclusive of Paytm and PhonePe to enable seamless cash transactions thru the charge system available on every cellular tool.

- 2) **From Street Vendors to Five-Star Hotels:** The great adoption of UPI has democratized economic transactions, making digital bills on hand to individuals throughout the financial spectrum. Today, this machine is no longer best via tech-savvy urbanites however additionally with the aid of avenue vendors, small corporations, or even luxurious establishments like 5-famous person hotels.
- 3) **Telecom Companies' Role:** Reliance Jio performed a vital position in facilitating the success of UPI. The virtual infrastructure furnished by way of telecom groups, consisting of Jio, created the spine for secure and efficient virtual payments. This infrastructure ensured that people could get entry to and make use of digital fee offerings even in far off regions.
- 4) **The Catalyst: Low-Cost Data:** One of the driving elements at the back of the large adoption of virtual bills has been the drastic discount in information costs, the way to Jio's disruptive pricing strategy. Data fees plummeted with the aid of 25 instances following Jio's launch, making it low-cost for not unusual Indians to apply digital payment systems.

Financial Inclusion: The fulfilment of UPI has contributed considerably to economic inclusion in India. It has empowered people without traditional bank bills to participate within the formal economy, control their finances, and transact digitally.

Bridging the Generational Gap - Transitioning from 2G to 4G

Reliance Jio's fifth impactful contribution has been its concerted efforts to transition India's cellular person base from the preceding 2G technology to the advanced 4G community. This initiative became initiated in 2017 thru introducing the JioPhone, a characteristic smartphone designed to make 4G connectivity on hand to a massive demographic.

The JioPhone Revolution: In 2017, Reliance Jio launched the JioPhone. This characteristic cell phone

became aimed toward bringing the advantages of 4G connectivity to customers though reliant on 2G networks. This flow became instrumental in bridging the digital divide in India.

- 1) **Massive Adoption:** The JioPhone's affordability and 4G skills struck a chord with the loads. More than 13 crore JioPhones were sold, making it the highest-selling cellular phone version globally. This huge adoption of 4G-enabled feature phones extended the transition to virtual services.
- 2) **Jio Bharat Platform:** Building on the success of the JioPhone, Reliance added the Jio Bharat platform, which endured the venture of transitioning 2G users to 4G. This initiative aimed to increase digital inclusion even in addition, making sure every populace phase became included inside the virtual revolution.

Collaboration with Karbonn: Reliance's partnership with Karbonn, a cell cellphone producer, to create a 4G feature phone called 'Bharat' validated its commitment to presenting cheap 4G connectivity alternatives. This collaboration extended the variety of selections for consumers seeking to upgrade their cell experience.

Future Participation: The achievement of Reliance Jio's efforts to shift customers from 2G to 4G has set a precedent inside the industry. More corporations are predicted to sign up for this campaign, in addition accelerating the transition and expanding the attainment of 4G offerings.

Bridging the Digital Divide - Empowering Rural India

Reliance Jio's emergence in the Indian telecommunications panorama delivered about a profound and socially transformative impact with the aid of notably reducing the digital divide that had long endured within the use of a. This sixth impact underscores how Jio's innovative method to telecommunications has prolonged digital get entry to and its myriad benefits to each nook of India, which includes rural and faraway areas.

Before Jio's arrival, the exorbitant value of facts was a substantial barrier, proscribing virtual access on the whole to city, affluent populations. However, Jio's

disruptive pricing approach dramatically lowered statistics fees, making statistics usage less expensive for people across all socioeconomic strata. This pivotal shift prolonged the advantages of digital connectivity to millions who had formerly been excluded.

Furthermore, Jio's widespread community expansion ensured that 4G coverage reached a long way past cities, accomplishing even the remotest villages. This geographical enlargement became a recreation-changer, allowing rural populations, which had long been underserved in digital infrastructure, to access high-speed internet offerings.

As a result, rural groups won the capability to carry out a multitude of virtual obligations from the consolation in their villages. This consists of running Jan-Dhan money owed, enrolling in government welfare schemes, having access to online instructional resources, and engaging in e-trade sports. Reducing the digital divide has not best transformed monetary potentialities. However, it has also more desirable the overall first-rate of lifestyles in rural areas, enabling residents to access telemedicine offerings, government services, and academic assets without traveling long distances.

Fostering a Unicorn Ecosystem - Proliferation of Billion- Dollar Start-ups

Reliance Jio's 7th and profoundly transformative effect lies in its function as a catalyst for the proliferation of unicorn start-ups in India. Start-ups worth more than \$1 billion, regularly called "unicorns," have flourished in the wake of Jio's disruptive impact. This surge in entrepreneurial fulfilment has reshaped India's monetary panorama and placed the digital economy, with Reliance Jio, at its core, as a driving force. Before Jio's access, India boasted the handiest of a handful of unicorns—round 4-5. However, the digital revolution ignited by means of Jio@7 has seen this quantity skyrocket to an astounding 108 unicorns, a testament to the profound impact of inexpensive facts and extensive digital get right of entry to. Most of those unicorns function in the virtual financial system, which has emerged as the cornerstone of India's financial boom. The collective fee of Indian unicorns now surpasses 28 lakh crore rupees, reflecting the exquisite financial capability of these start-ups.

The influence of Jio in this unicorn phenomenon is plain. Notable figures inside the commercial enterprise international, consisting of Zomato's founder Dipendra Goyal and Netflix CEO Reed Hastings, have openly stated Jio's instrumental position in facilitating their businesses' increase in India. The symbiotic relationship between Jio's digital infrastructure and those start-ups has fuelled innovation, employment, and economic increase on an unprecedented scale. Indian economists are positive that the United States's digital economy, pushed specially by the Jio-led virtual revolution, will soon surpass the \$1 trillion mark. This projection underscores the profound and enduring impact of Reliance Jio on India's monetary landscape, wherein entrepreneurship, innovation, and virtual transformation force boom and prosperity.

SHAPING THE FUTURE - ARTIFICIAL INTELLIGENCE AND 5G

As we appear beforehand to the future, past the seven years of Reliance Jio's transformative journey, it will become glaring that the convergence of synthetic intelligence (AI) and 5G generation is poised to play a pivotal function in shaping the destiny of common Indians.

The destiny impact of Jio@7 underscores the developing importance of AI and the lightning-speed abilities of 5G. These technological advancements hold the capacity to usher in a brand new generation of innovation, connectivity, and development for the Indian population.

With its ability to process giant quantities of information and make actual-time choices, AI is already starting to expose its significance in numerous sectors, including healthcare, schooling, agriculture, and industry. Integrating AI into ordinary existence promises to enhance performance, productiveness, and first-class offerings.

When AI operates at the rate of 5G, the possibilities are simply limitless. The ultra-low latency and excessive-pace connectivity presented with the aid of 5G networks will allow AI-powered packages to supply immediate responses, transforming how human beings communicate, work, and engage with era. The synergy between AI and 5G will revolutionize multiple aspects of everyday existence, from self-reliant automobiles

and clever cities to telemedicine and personalized education.

Reliance Jio, with its robust digital infrastructure and commitment to technological advancement, is properly-located to guide the fee in harnessing the ability of AI and 5G for the advantage of all Indians. This roadmap for destiny envisions a digitally empowered India in which AI-pushed solutions enhance the right of entry to schooling, healthcare, and financial opportunities, ultimately raising the satisfaction of lifestyles for commonplace residents.

In conclusion, as Reliance Jio embarks on its adventure beyond the first seven years, the fusion of AI and 5G stands as a beacon of hope and development. This generation promises to shape a destiny where the opportunities are bound best with the aid of our imagination, fostering a digitally inclusive society wherein each Indian can participate and benefit from the fast advancements in the virtual landscape.

CONCLUSION

In the span of 7 amazing years, Reliance Jio has emerged as a transformative pressure in India's virtual panorama, leaving an indelible mark at the lives of tens of millions. This dialogue has illuminated seven pivotal influences of Jio's adventure, each representing a milestone in the enterprise's project to democratize virtual get entry to and reshape the state's destiny. Firstly, Jio's selection to provide unfastened outgoing calls shattered the generation of high priced telecommunication and ushered in a generation of communication freedom. The next reduction in statistics prices (Impact 2) revolutionized data intake, catapulting India to the leading edge of world information usage rankings. This newfound connectivity redefined enjoyment, journey, e-commerce, and even training (Impact 3), making these accessible with a faucet on a phone display.

Moreover, Jio's contributions extended to the realm of digital payments (Impact four), in which the Unified Payments Interface (UPI) became a ubiquitous device for financial transactions. This fulfilment turned into underpinned via Jio's affordability and its virtual infrastructure. Jio in addition facilitated the transition from 2G to 4G (Impact five), ensuring that everyone ought to participate inside the digital economy.

Jio's relentless efforts also bridged the virtual divide (Impact 6), extending virtual facilities to rural and underserved areas, permitting economic participation and enhancing high-quality lifestyles. Furthermore, the proliferation of Indian unicorns (Impact 7) pondered Jio's role as a using force at the back of the nation's digital economic system, raising India's global stature.

As we peer into destiny, the convergence of synthetic intelligence and 5G guarantees to redefine what's viable. Jio's sturdy virtual infrastructure places it at the leading edge of this technological evolution, positioning India for a destiny in which AI-pushed solutions decorate every facet of life.

In summation, the legacy of Jio@7 is one among empowerment, inclusion, and boundless capability. It exemplifies how a visionary organization, driven with the aid of the undertaking to bridge the digital divide, can shape a kingdom's future. As Reliance Jio keeps its journey, the promise of a digitally empowered India, in which era serves each citizen, remains ever closer to recognition.

REFERENCES

1. [Reliance Jio Infocomm] (<https://www.jio.com>): Official website of Reliance Jio providing information about the company's history, services, and impact.
2. Dey, S. (2020). "Telecom Sector in India: A Boon or a Bane for Digital India," *International Journal of Scientific and Research Publications*, 10(1), 57-62.
3. Sharma, A., & Kumar, S. (2019). "Impact of Jio on Digital India," *International Journal of Engineering Research & Technology*, 8(10), 35-38.
4. Gupta, P., & Jain, N. (2021). "Jio's Impact on Digital Payments in India," *International Journal of Scientific Research and Engineering Development*, 4(8), 207-210.
5. Arora, A., & Singh, H. (2018). "Impact of Jio on Rural India: A Study of Digital Divide Reduction," *International Journal of Management and Applied Science*, 4(5), 117-121.
6. Rajan, A. (2019). "Jio and the Unicorn Boom in India," *The Economic Times, Business News*.
7. Bhattacharyya, S., & Joshi, S. (2022). "The Future of AI in India: Opportunities and Challenges," *Journal of Artificial Intelligence Research*, 73(1), 245-263.

COVID19 Pandemic from Machine Learning Perspective

Pooja R. Shastri

Rohan Kulkarni

Suhas Kakade

Department of Electrical Engineering
K. J. College of Engineering Pune
Pune, Maharashtra
✉ poojashastri.kjcoemr@kjei.edu.in

ABSTRACT

COVID-19 is a global pandemic and has become the most urgent threat to the entire world. This pandemic has affected more than one million people and taken the lives of more than 50 thousand people. With the help of datasets from the Ministry of Health and Family Welfare of India, we can learn about the effect of COVID-19 on Indian citizens.

A better understanding of this pandemic situation can be carried out through various Machine Learning models. To analyse the current trend or pattern of COVID-19 transmission in India, various machine learning algorithms Polynomial Regression, Linear Regression, Ridge, LASSO can be applied. We are also studying various detection techniques of COVID-19 pandemic.

KEYWORDS : COVID-19.

INTRODUCTION

In Machine Learning program is as designed to perform tasks, and it is also learned from its experience if its measurable performance in these tasks improves as it gains more and more experience in executing these tasks. A computer program that learns to detect or predict cancer from the medical investigation reports of a patient. It will improve in performance as it gathers more experience by analysing medical investigation reports of a wider population of patients.

Machine Learning is applied in wide fields such as computer games, pattern recognition, natural language processing, data mining, traffic prediction, robotics, virtual personal assistants (Google), online transportation network (estimating surge price in peak hour by Uber app), product recommendation, share market prediction, medical diagnosis, online fraud prediction, agriculture advisory, search engine result refining (Google), BoTs (chatbots for online customer support), E- mail spam filtering, crime prediction through video surveillance system, social media services such as Facebook.

Machine Learning generally use for problems of

classification, regression, and clustering. Depending on the availability of types and categories of training data, one may need to select from the available techniques of “supervised learning,” “unsupervised learning,” “semi-supervised learning,” and “reinforcement learning.”

LITERATURE SURVEY

In [1], two machine learning models, namely, polynomial regression algorithm and support vector machine algorithm, analyze the COVID-19 pandemic. Exponential, linear, and 6th-degree polynomial regression models are used in [2] to best-fit regression models to actual data. They have also used the daily updates to construct a new polynomial function for error reduction. The curve fitting technique using polynomial regression reduces error. The convolutional neural networks (CNNs) are combined with consolidated machine learning methods, such as a k-nearest neighbor, Bayes, random forest, multilayer perceptron (MLP), and support vector machine (SVM) [3]. [4] Analyze dataset containing the day-wise actual past data and make predictions for upcoming days using machine learning algorithms. It is observed that linear regression

(LR), least absolute shrinkage, and selection operator (LASSO) also, perform well to predict death rate and confirm cases.

SOFTWARE USED

The software used for data processing of COVID-19 and implementation of algorithms is the Python programming language. Python is a high level, interpreted, and general-purpose dynamic programming language that focuses on code readability. The syntax in Python helps the programmer to do coding in fewer steps. The python community maintains a lot of official packages; including libraries (e.g. Numpy, pandas, and Matplotlib) providing scientific computing tools that are comparable to dedicated software such as MATLAB and R. The graphical python module Matplotlib supports 2D and 3D visualization. The programs written in python are intuitive, user-friendly, and simple in realization..

ANALYSIS

Regression

It is a statistical method used in finance, investing, and other disciplines that attempt to determine the strength and character of the relationship between one dependent variable (usually denoted by Y) and a series of other variables (known as independent variables) used to find out the relationship between independent and dependent variables and for forecasting.

Linear

Linear regression, a type of regression modeling, is the most usable statistical technique for predictive analysis in machine learning. Each observation in linear regression depends on two values; one is the dependent variable, and The second is the independent variable.

Linear regression determines a linear relationship between these dependent and independent variables. There are two factors (x; y) that are involved in linear regression analysis. The equation below shows how y is related to x, known as regression.

$$y = \beta_0 + \beta_1 x \tag{1}$$

$\beta_0 = y$ -intercept

$\beta_1 =$ slope

the machine learning finds the best value of β_0 and β_1 .

To put the concept of linear regression in the machine learning context, in order to train the model x is represented as input training dataset, y represents the class labels present in the input dataset.

LASSO

LASSO better and more stable and also reduces the error. LASSO is considered as a more suitable model for multicollinearity scenarios. Since the model performs L1 regularization and the penalty added in this case is equal to the magnitude of coefficients. So, LASSO makes the regression simpler in terms of the number of features it is using. It uses a regularization method for automatically penalizing the extra features. That is, the features that cannot help the regression results enough can be set to a very small value potentially zero.

In contrast, the LASSO regression attempts to add them one at a time and if the new feature does not improve the enough to out-way the penalty term by including that feature then it could not be added meaning as zero. Thus, the power of regularization by applying the penalty term for the extra features is that it can automatically do the selection for us.

Thus, the models are made sparse with few coefficients in this case of regularization since the process eliminates the coefficients when their values are equal to zero. LASSO regression works on an objective to minimize the following:

$$\sum_{i=1}^n (y_i - \sum_j x_{ij} \beta_j)^2 + \lambda \sum_{j=1}^p |\beta_j| \tag{2}$$

λ is where, slope is penalty term.

Polynomial

Polynomial is best for non-linear dataset. Polynomial Regression is a supervised Machine learning Algorithm that is trained based on prior data and then tested on another dataset to validate its accuracy.

$$y = \beta_0 + \beta_1 x + \beta_2 x^2 + \dots + \beta_n x^n \tag{3}$$

$x \in \mathbb{R}$

β_0 is bias,

$n =$ Degree of polynomial,

$\beta_1, \beta_2, \dots, \beta_n$, are the weights in the equation of polynomial regression.

Here, Degree of polynomial is varied according to obtain minimum mean square error.

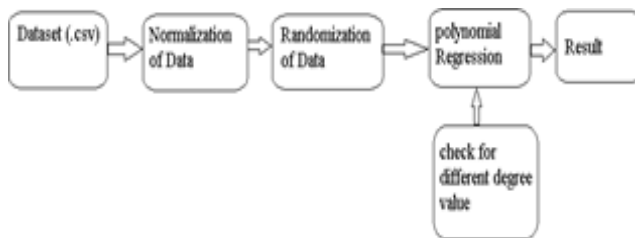


Fig. 1. Architecture of Polynomial Regression Based System

Ridge

Ridge regression is a variant of linear regression. Ridge regression is a method of estimating the coefficients of multiple-regression models in scenarios where independent variables are highly correlated.

It has uses in fields including econometrics, chemistry, and engineering. The theory was first introduced by Hoerl and Kennard in 1970 in their Technometrics papers “Ridge regressions: biased estimation of nonorthogonal problems” and “Ridge regressions: applications in nonorthogonal problems”. This was the result of ten years of research into the field of ridge analysis. Ridge regression was developed as a possible solution to the imprecision of least square estimators when linear regression models have some multicollinear (highly correlated) independent variables—by creating a ridge regression estimator (RR). This provides a more precise ridge parameters estimate, as its variance and mean square estimator is often smaller than the least square estimators previously derived.

An $n \times 1$ column vector y is to be projected onto the column, space of the $n \times p$ design matrix X (typically $p \ll n$) whose columns are highly correlated. The ordinary least squares estimator of the coefficients $\beta \in \mathbb{R}^{p \times 1}$ by which the columns are multiplied to get orthogonal projection $X\beta$ is

$$\beta = (X'X)^{-1} X' y \tag{4}$$

where X' is X transpose

By contrast Ridge estimator is

$$\beta_{\text{Ridge}} = (X'X + k I_p)^{-1} X' y \tag{5}$$

where I_p is the $p \times p$ identity matrix and $k > 0$.

k -NN

K Nearest Neighbour (KNN) An algorithm is a classification algorithm. It uses a database with data points grouped into several classes, and the algorithm tries to classify the sample data point given to it as a classification problem.

KNN does not assume any underlying data distribution, and so it is called non-parametric. The advantage of the KNN algorithm,

it is a simple technique that is easily implemented. Building the model is cheap. It is an extremely flexible classification scheme and well suited for Multi-modal classes. Records are with multiple class labels. The error rate is at most twice that of Bayes error rate. It can sometimes be the best method. Disadvantages of KNN are the following: classifying unknown records is relatively expensive. It requires distance computation of k -nearest neighbors. With the growth in training set size, the algorithm gets computationally intensive. Noisy/irrelevant features will result in degradation of accuracy. It is a lazy learner; it computes distance over k neighbours. It does not make any generalization on the training data and keeps all of them. It handles large data sets and hence expensive calculations. Higher-dimensional data will result in a decline in the accuracy of regions. KNN can be used in Recommendation systems, handwriting detection, analysis done by financial institutions before sanctioning loans, video recognition, forecasting votes for different political parties, and image recognition.

MEAN SQUARE ERROR (MSE)

Mean square error is another way to measure the performance of regression models. MSE takes the distance of data points from the regression line and squaring them. Squaring is necessary because it removes the negative sign from the value and gives more weight to larger differences. The smaller the mean squared error shows, the closer you are to finding the line of best fit. MSE can be calculated as:

$$MSE = \frac{1}{2} \sum_{i=1}^n (y_i - \hat{y}_i)^2 \tag{6}$$

Calculations

$$\text{Recovery rate} = (\text{Sum of Recovered cases} / \text{Sum of Confirmed Cases}) \tag{7}$$

$$\text{Death Rate/Mortality rate} = (\text{Sum of Death cases} / \text{Sum of Confirmed Cases}) \tag{8}$$

RESULTS

Dataset

Source link: <https://api.covid19india.org/csv/latest/states.csv> Link contain data online updated date wise state as following figure 2.

	Date	State	Confirmed	Recovered	Deceased	Tested
0	2020-01-30	Kerala	1	0	0	NaN
1	2020-01-30	India	1	0	0	NaN
2	2020-02-02	Kerala	2	0	0	NaN
3	2020-02-02	India	2	0	0	NaN
4	2020-02-03	Kerala	3	0	0	NaN
...
14575	2021-04-22	Tripura	34259	33242	391	669149.0
14576	2021-04-22	India	15931500	13449568	184679	272705103.0
14577	2021-04-22	Uttar Pradesh	942511	689900	10346	38892416.0
14578	2021-04-22	Uttarakhand	134012	104527	1953	3428170.0
14579	2021-04-22	West Bengal	688956	614750	10710	9950336.0

14580 rows x 6 columns

Fig. 2. Table of dataset of India

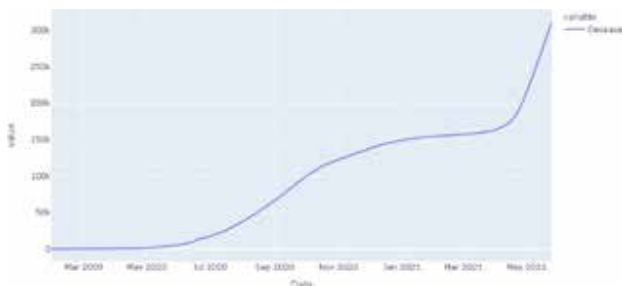


Fig. 3. Plot of All India death cases of India

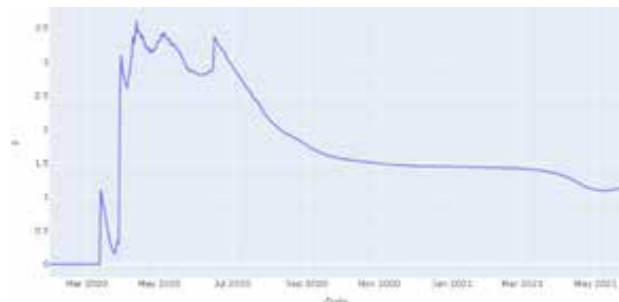


Fig. 4. Plot of All India death rate

X axis Date

Y axis percentage of Death

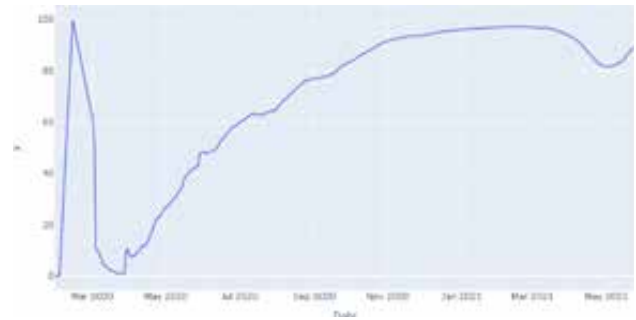


Fig. 5. Plot of recovery rate of India

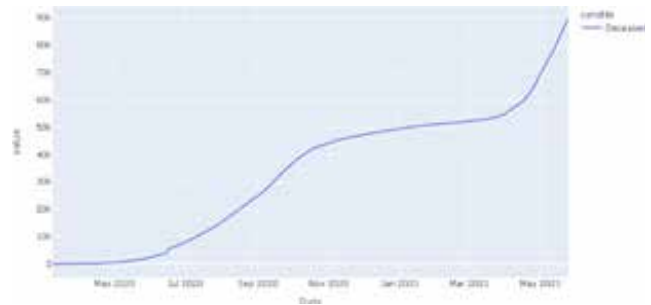


Fig. 6. Plot of Maharashtra state deceased cases

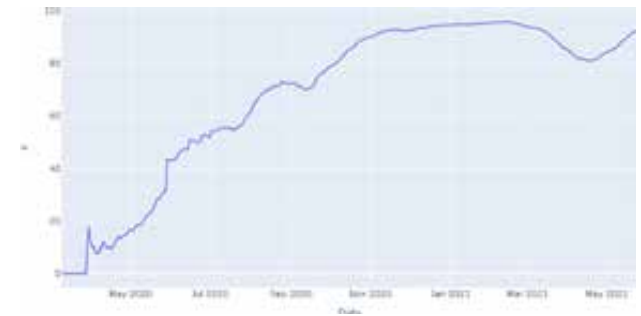


Fig. 7 Plot of Maharashtra state recovered rate

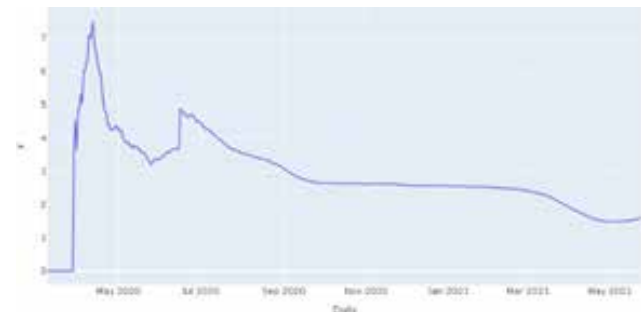


Fig. 8: Plot of Maharashtra state deceased rate

X axis Date

Y axis percentage of recovery

Regression result with error:

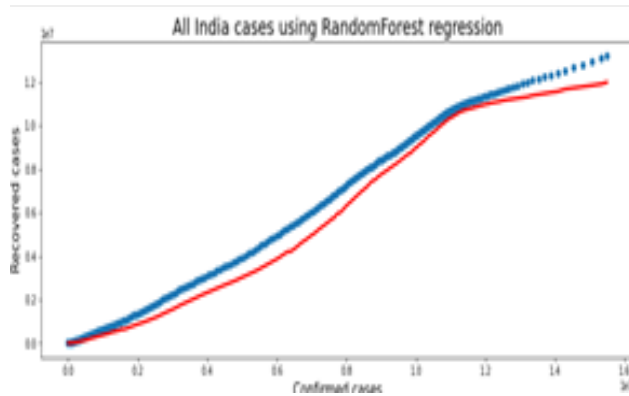


Fig. 9. Plot of recovered prediction of India using Random forest regression.

Mean Squared Error: 292181100627.6229 Accuracy means:0.05973330914368650

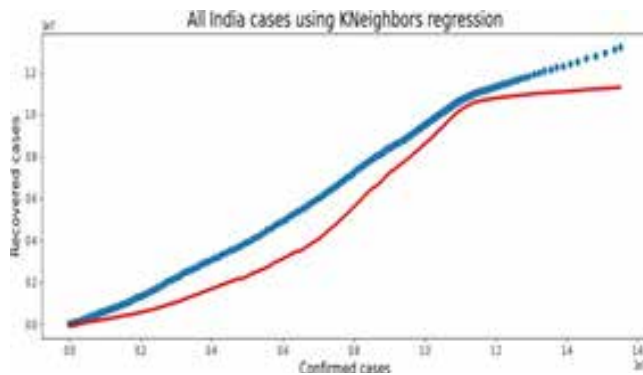


Fig. 10. Plot of recovered prediction of India using KNN regression Mean Squared Error: 875332092100.549

Accuracy means :0.04540094339622641

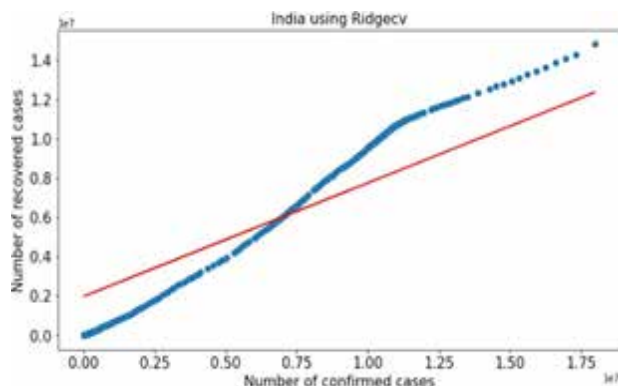


Fig. 11. Plot of recovered prediction of India using Ridge

Mean Squared Error: 4672581801336.149

Alpha = 2

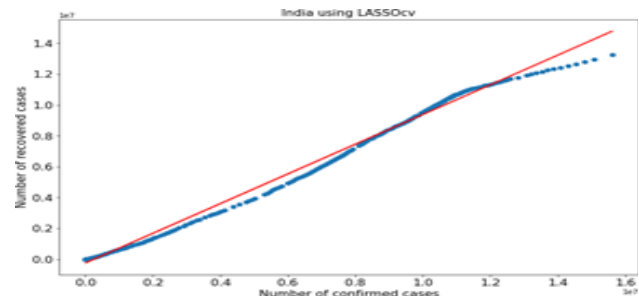


Fig. 12. Plot of recovered prediction of India using LASSO Mean Squared Error: 215176664379.85834

Alpha=5

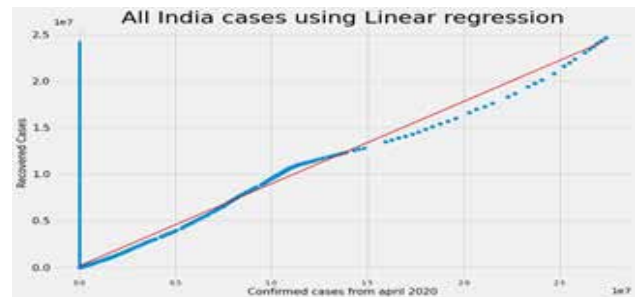


Fig. 13. Plot of recovered prediction of India using linear regression.

Mean Squared Error: 942412076526.2686

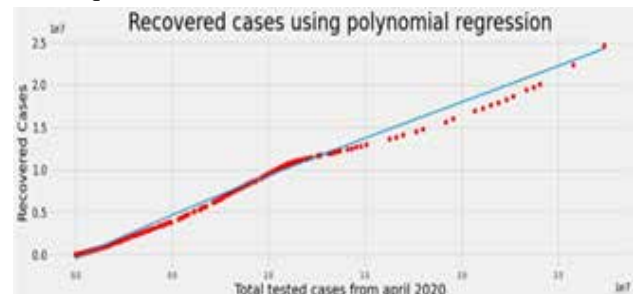


Fig. 14. Plot of recovered prediction of India using polynomial regression

Mean Squared Error: 265573275487.72855

Degree = 3

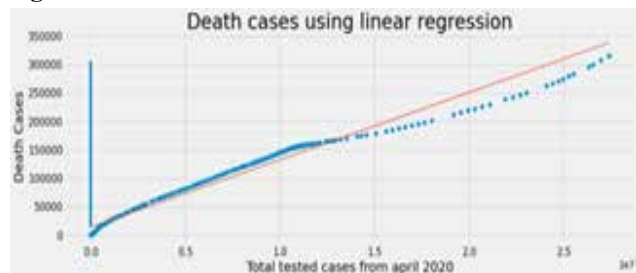


Fig. 15. Plot of death prediction of India using linear regression Mean Squared Error: 89173196332842.33

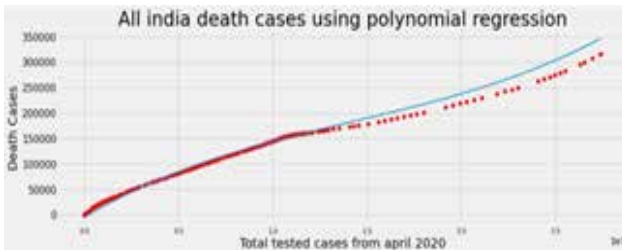


Fig. 16. Plot of death prediction of Maharashtra using polynomial regression.

Mean Squared Error: 65471758.8230277

Degree = 3

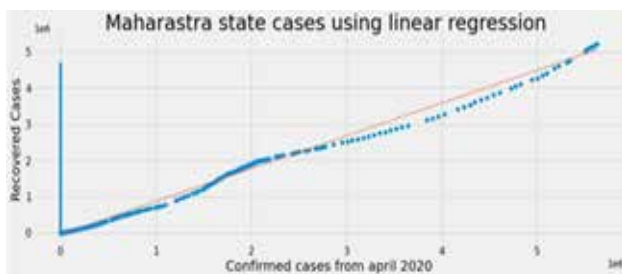


Fig. 17. Plot of recovered prediction of Maharashtra using linear regression.

Mean Squared Error: 52271884260.9528

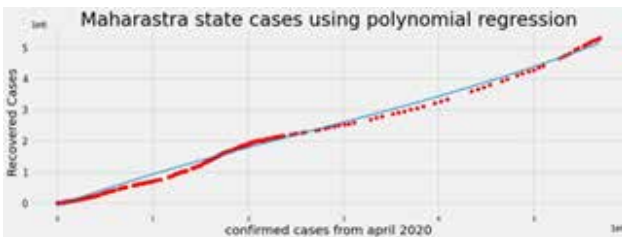


Fig. 18. Plot of positive prediction of Maharashtra using polynomial regression.

Degree = 3

Mean Squared Error: 62097245434.18521

CONCLUSION AND FUTURE WORK

The study gives insight into how machine learning algorithms can predict the recovered cases and death cases. Analyze the changes in the recovery rate and mortality rate. Daily updated data will be driven to construct a rate for error reduction. Due to the updated regression function, the resulting turning points will also be updated to contribute to predicting the curve's furtherance. In future regression model used to conclude lockdown period for reduction of COVID19 heat also for other business and research applications.

REFERENCES

1. Ekta Gambhir, Ritika Jain, Alankrit Gupta and Uma Tomer "Regression Analysis of COVID-19 using Machine Learning Algorithms" Proceedings of the International Conference on Smart Electronics and Communication (ICOSEC 2020) IEEE Xplore Part Number: CFP20V90-ART; ISBN: 978-1-7281-5461-9
2. Andreou Andreas, Constandinos X. Mavromoustakis, George Mastorakis, Shahid Mumtaz, Jordi Mongay Batalla and Evangelos Pallis "Modified Machine Learning Technique for Curve Fitting on Regression Models for COVID-19 projections" IEEE
3. Susmita Ray "A Quick Review of Machine Learning Algorithms Algorithms" 2019 International Conference on Machine Learning, Big Data, Cloud and Parallel Computing (Com-IT-Con), India, 14th -16th Feb 2019
4. Shreyas Setlur Arun and Ganesh Neelakanta Iyer "On the Analysis of COVID-19 – Novel Corona Viral Disease Pandemic Spread Data Using Machine Learning Techniques" Proceedings of the International Conference on Intelligent Computing and Control Systems (ICICCS 2020) IEEE Xplore Part Number: CFP20K74-ART; ISBN: 978-1-7281-4876-2.

Applications & Scope of Artificial Intelligence in All Branch of Engineering

Sandip Ramdasrao Mokle

Assistant Professor
S.N.D.College of Engineering & Research Centre
Yeola, Nashik, Maharashtra
✉ sandip.mokle@sndcoe.ac.in

Sachin Gangadhar Tathe

ABSTRACT

Artificial Intelligence (AI) is a multidisciplinary field of computer science that focuses on the development of intelligent agents capable of performing tasks that typically require human intelligence. It encompasses a broad range of techniques and methodologies, including machine learning, natural language processing, computer vision, robotics, and expert systems. The overarching goal of AI is to create systems that can learn, reason, perceive, and interact with their environment to achieve specific objectives.

KEYWORDS : *AI, Principles, Machine learning, Robotics.*

INTRODUCTION

Search algorithms play a crucial role in artificial intelligence (AI) for finding solutions to problems or making decisions. These algorithms are employed in various AI applications, including path finding, optimization, and problem-solving. Here are some common search algorithms used in AI:

Breadth-First Search (BFS): BFS explores a graph level by level, starting from the root or initial state. It uses a queue data structure to keep track of the nodes to be explored.

Depth-First Search (DFS): DFS explores a graph by going as deep as possible along one branch before backtracking. It uses a stack data structure or recursion to keep track of the nodes to be explored.

Uniform Cost Search (UCS): UCS is a variant of BFS that takes into account the cost of each path. It always expands the node with the lowest path cost, making it suitable for problems where the cost matters.

A Search Algorithm: *A* is an informed search algorithm that combines the benefits of both BFS and UCS. It uses a heuristic function to estimate the cost from the current state to the goal. The algorithm selects nodes based on a combination of the actual cost and the heuristic value.

Greedy Best-First Search: Greedy best-first search selects the node that appears to be the most promising based on the heuristic function. It doesn't consider the actual cost to reach the current node but only the estimated cost to reach the goal.

Depth-Limited Search: Depth-limited search is a variant of DFS that limits the depth of exploration. It helps address issues with infinite-depth graphs by restricting the search to a certain depth level.

Iterative Deepening Depth-First Search (IDDFS): IDDFS is a combination of depth-first search and Breadth-first search. It performs DFS repeatedly with increasing depth limits until the goal is found.

Bidirectional Search: Bidirectional search explores the search space from both the start and goal states simultaneously. It can be more efficient than traditional searches in some scenarios.

Beam Search: Beam search is a heuristic search algorithm that explores a limited set of the most promising paths. It keeps a fixed number of paths, called the beam width, and only expands nodes along those paths.

These search algorithms can be adapted and combined based on the specific requirements and characteristics of the problem at hand. The choice of a particular

algorithm depends on factors such as the nature of the transitions between states. The root node represents the initial state, and the leaf nodes represent terminal states (end of the game).

Artificial intelligence (AI) has significant applications across all branches of engineering, offering innovative solutions to various challenges and enhancing efficiency in different domains. Here's a brief overview of how AI is being utilized in different branches of engineering:

Civil Engineering

- AI is used in structural health monitoring to analyze data from sensors and predict potential failures in infrastructure such as bridges and buildings.
- It helps in optimizing construction processes through predictive analytics, resource allocation, and project management.
- AI-driven algorithms are employed in urban planning and traffic management for efficient city design and transportation systems.

Mechanical Engineering

- AI is applied in design optimization, allowing engineers to quickly generate and evaluate numerous design options to meet performance criteria.
- Predictive maintenance systems use AI to analyze sensor data from machinery and equipment to detect anomalies and prevent breakdowns.
- Robotics and automation leverage AI techniques for tasks such as object recognition, path planning, and autonomous control in manufacturing processes.

Electrical Engineering

- AI is used in power systems for demand forecasting, fault detection, and optimizing energy distribution.
- Smart grid technologies incorporate AI algorithms to manage electricity generation, transmission, and distribution efficiently.
- AI-driven control systems improve the performance of electrical devices and systems, such as in renewable energy systems and electric vehicles.

Computer Engineering

- AI is fundamental to the development of intelligent systems, including natural language processing, computer vision, and machine learning algorithms.
- AI is used in software engineering for code generation, testing, debugging, and software maintenance tasks.
- It plays a crucial role in cyber security, where AI-powered systems detect and respond to cyber threats in real-time.

Chemical Engineering

- AI is applied in process optimization and control to enhance the efficiency and safety of chemical processes, such as refining, petrochemicals, and pharmaceutical manufacturing.
- AI-driven models and simulations help in the design and development of new materials and chemicals with desired properties.
- Predictive analytics and machine learning techniques are used for quality control and product optimization in chemical production processes

Aerospace Engineering

- AI is employed in autonomous flight systems for unmanned aerial vehicles (UAVs), including navigation, obstacle avoidance, and mission planning.
- AI-based algorithms optimize aircraft design, aerodynamics, and structural analysis to improve performance and fuel efficiency.
- Predictive maintenance systems utilize AI to monitor aircraft health, predict component failures, and schedule maintenance proactively.

In summary, AI is transforming engineering disciplines by enabling automation, optimization, and intelligent decision-making across various applications and industries. Its integration into engineering processes promises to drive innovation and improve the performance, safety, and sustainability of engineered systems.

Minimax Algorithm

The minimax algorithm is a decision-making algorithm used in two-player games with perfect information (both players have full knowledge of the game state). The goal is to minimize the potential loss and maximize the potential gain. The algorithm explores the game tree recursively, evaluating each node based on the assumption that the opponent will make optimal moves.

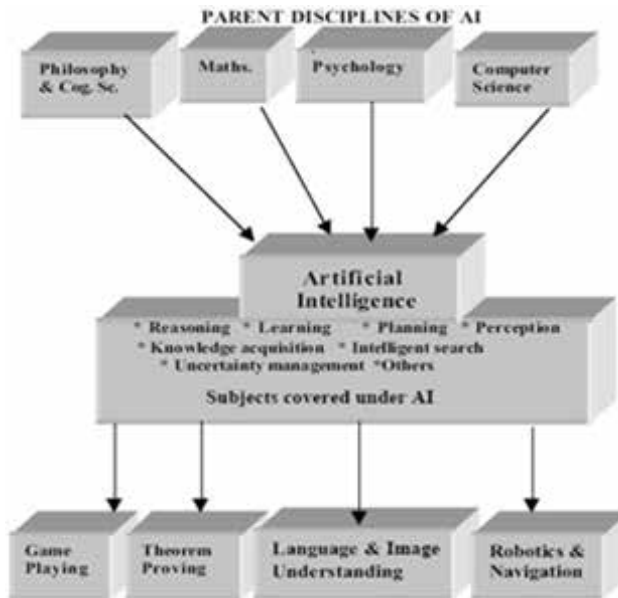


Figure 1.

certainly! Here's a simple example of a MATLAB program using artificial intelligence. This example demonstrates linear regression, a basic machine learning algorithm, using the built-in functions in MATLAB:

code

```
% Load sample data
data = load('ex1data1.txt');
X = data(:, 1); % Feature (input) y = data(:, 2); % Target (output)
% Plot the data
plot(X, y, 'rx', 'MarkerSize', 10); xlabel('Population of City in 10,000s'); ylabel('Profit in $10,000s');
% Add a column of ones to X for the intercept term X = [ones(length(y), 1), X];
```

```
% Initialize fitting parameters theta = zeros(2, 1);
% Set options for fminunc (an optimization algorithm)
options = optimset('GradObj', 'on', 'MaxIter', 1500);
% Run gradient descent to obtain the optimal theta
[theta, cost] = fminunc(@(t)(computeCost(X, y, t)), theta, options);
% Plot the linear fit hold on;
plot(X(:,2), X*theta, '-');
legend('Training data', 'Linear regression'); hold off;
% Function to compute the cost for linear regression
function J = computeCost(X, y, theta)
m = length(y); % number of training examples J = 1 / (2*m) * sum((X*theta - y).^2);
end
```

This code performs linear regression on a dataset (ex1data1.txt) to predict profit based on the population of a city. It uses the furnace optimization algorithm to find the optimal parameters (theta) that minimize the cost function.

Make sure to replace 'ex1data1.txt' with the path to your dataset if you're using a different dataset.

This is a basic example, and MATLAB offers various toolboxes for more advanced machine learning tasks such as classification, clustering, and neural networks. Depending on your interests, you can explore those functionalities for more complex AI applications in MATLAB.

Scope of artificial intelligence

The scope of artificial intelligence (AI) is vast and continually expanding as the technology advances. Here are some key areas where AI is currently making an impact and is expected to have significant growth and development in the future:

Machine Learning and Deep Learning: Machine learning algorithms, including deep learning, are at the forefront of AI research and applications. These techniques enable computers to learn from data, recognize patterns, and make decisions without being explicitly programmed. The scope of machine learning

spans various domains, including image recognition, natural language processing, recommendation systems, and predictive analytics.

Natural Language Processing (NLP): NLP focuses on enabling computers to understand, interpret, and generate human language. Applications of NLP range from language translation and sentiment analysis to chatbots and virtual assistants, revolutionizing how humans interact with computers and access information.

Computer Vision: Computer vision involves teaching computers to interpret and analyze visual information from the real world. AI-driven computer vision systems are used in object detection, image recognition, video analysis, autonomous vehicles, medical imaging, and augmented reality applications.

Robotics and Autonomous Systems: AI plays a crucial role in robotics and autonomous systems, enabling robots to perceive their environment, make decisions, and perform tasks autonomously. This includes industrial robots in manufacturing, service robots in healthcare and hospitality, drones for surveillance and delivery, and self-driving vehicles for transportation.

Healthcare: AI has vast potential in healthcare for tasks such as medical image analysis, disease diagnosis, drug discovery, personalized treatment planning, and health monitoring. AI-powered systems can

Inference Engine

The inference engine is responsible for reasoning with the knowledge stored in the knowledge base. It employs various reasoning mechanisms, such as deduction, induction, and abduction, to draw conclusions, make inferences, and answer queries. The inference engine is crucial for problem-solving and decision-making.

Domain-Specific Expertise

Knowledge agents are often designed for specific problem domains. They possess domain-specific expertise, allowing them to excel in particular tasks or areas of knowledge. This expertise is acquired during the knowledge acquisition phase and is used to guide the agent's behavior.

Learning Mechanisms

Knowledge agents may incorporate learning mechanisms to adapt and improve their performance over time. Machine learning algorithms, for example, can enable agents to automatically learn patterns, rules, or associations from data and experiences.

Communication and Interaction

Knowledge agents may need to communicate and interact with other agents, users, or systems. This involves the exchange of knowledge, sharing insights, and collaborating on tasks. Communication skills enhance the agent's ability to function effectively in collaborative environments.

Problem Solving and Decision Making

Knowledge agents are designed to solve problems and make decisions based on their knowledge. The ability to analyze situations, generate solutions, and evaluate possible actions is a crucial aspect of their functionality.

Adaptability

Knowledge agents should be adaptable to changing environments and evolving knowledge. They may need mechanisms to update their knowledge base, learn from new data, and adjust their behavior in response to changes in the problem domain.

Autonomy

Knowledge agents are often designed to operate autonomously, making decisions and taking actions without constant human intervention. Autonomy allows them to function in real-time and dynamic environments. Knowledge agents are applied in various domains including expert systems, decision support systems, natural language processing, and more. They are valuable tools for capturing and utilizing explicit knowledge to perform complex tasks in a wide range of applications.

A logical agent in artificial intelligence (AI) refers to an intelligent agent that uses logical reasoning and formal logic to represent and manipulate knowledge, make decisions, and perform problem-solving tasks. Logical agents are based on the

principles of symbolic AI, where information is represented using symbols, and logical rules are applied to manipulate these symbols. Here are key components and characteristics of a logical agent:

METHODOLOGY

Knowledge Representation: Logical agents represent knowledge using formal languages such as propositional logic or first-order logic. Knowledge is expressed through statements or sentences that can be manipulated logical operations.

Inference Mechanism: Logical agents use an inference mechanism to draw conclusions from the given knowledge. Inference involves applying logical rules to make logical deductions, inductions, or abductions. Common reasoning techniques include deduction (applying rules to derive new facts), induction (generalizing from specific instances), and abduction (inferring plausible explanations).

Knowledge Base: The knowledge base stores the agent's knowledge in a structured form. It includes information about the world, rules, and relationships between entities. The knowledge base serves as the foundation for the agent's reasoning and decision-making processes.

Logical Rules and Expressions: Logical agents use rules and expressions from formal logic to represent relationships and constraints in the domain. For example, in propositional logic, statements are represented as logical propositions, while in first-order logic, quantifiers and predicates are used to express more complex relationships.

Rule-Based Systems: Logical agents often operate as rule-based systems, where a set of rules governs the agent's behavior. These rules encode the agent's knowledge and guide its decision-making process. Rule-based systems are common in expert systems and knowledge-based applications.

Resolution and Proof Techniques: Logical agents may employ resolution and other proof techniques to determine the logical consequence of a set of statements. Resolution is a powerful inference rule used in logical reasoning to derive new statements from existing ones.

Predicate Calculus: In many logical agent systems, particularly those based on first-order logic, predicate calculus is used. Predicate calculus allows for the representation of relationships, quantification, and more complex logical structures.

Search and Planning: Logical agents may use search and planning algorithms to explore possible sequences of actions and find solutions to problems. Search algorithms help navigate through the space of possible states, while planning involves generating a sequence

Uncertainty Handling: Logical agents may need to deal with uncertainty and incomplete information. Extensions to classical logic, such as fuzzy logic or probabilistic logic, may be used to handle uncertainty in a more flexible manner.

Natural Language Processing: Some logical agents are designed to understand and process natural language. Logical representations are used to interpret and generate human-readable language, facilitating communication between humans and AI systems.

Logical agents are employed in various AI applications, including expert systems, knowledge-based systems, automated reasoning, and natural language processing. Their ability to represent and reason with symbolic knowledge makes them suitable for tasks that require high-level reasoning and decision-making.

Reasoning in artificial intelligence (AI) refers to the process by which an intelligent system draws conclusions, makes inferences, and reaches decisions based on available information and knowledge. It is a fundamental aspect of AI systems that enables them to understand, solve problems, and make informed decisions in complex environments. Different types of reasoning mechanisms are employed in AI, depending on the nature of the problem and the representation of knowledge. Here are some key types of reasoning in AI:

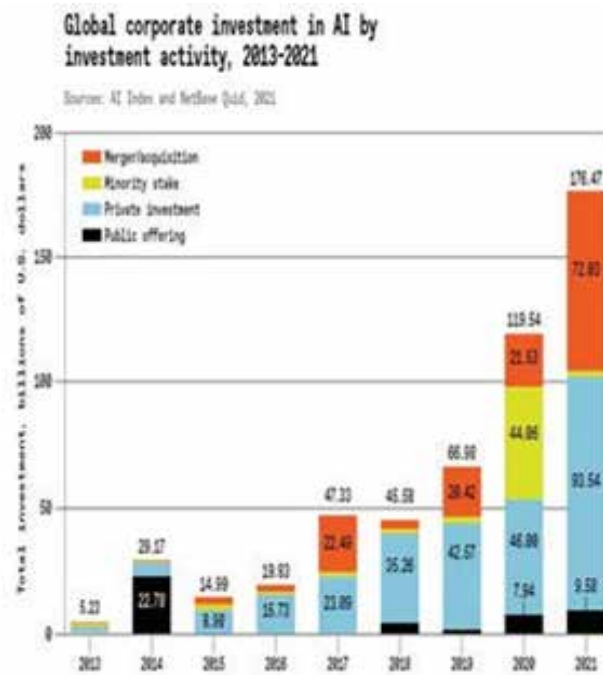
Deductive Reasoning

Deductive reasoning involves drawing specific conclusions from general statements or premises. In AI, deductive reasoning is often associated with formal logic, where rules and axioms are used to make logically valid deductions. The most common form of deductive reasoning in AI is theorem proving.

Inductive Reasoning

Inductive reasoning involves making generalizations from specific observations or examples. In AI, inductive reasoning is commonly used for learning from data. Machine learning algorithms, for instance, use inductive reasoning to generalize patterns and make predictions based on training data.

CONCLUSION & APPLICATIONS



A Graph showing investment of AI Globally in last decade i.e. (Scope of Artificial Intelligence)

Artificial intelligence (AI) represents a transformative and rapidly evolving field at the intersection of computer science, machine learning, and cognitive science. The advancements in AI have had profound impacts on various aspects of society, from healthcare and finance to education and entertainment. The development and deployment of intelligent systems capable of learning, reasoning, and interacting with the environment have opened new possibilities and challenges. AI technologies, such as machine learning and deep learning, have demonstrated remarkable capabilities in tasks ranging from image recognition and natural language processing to complex decision-making processes. These technologies have led to breakthroughs in areas like autonomous vehicles,

medical diagnosis, and personalized recommendations. As AI continues to evolve, it is critical for stakeholders, including researchers, policymakers, and the general public, to actively engage in discussions, collaborations, and regulations that shape the responsible and ethical development of AI. The journey of AI represents a dynamic and ongoing exploration of the possibilities and challenges that arise as we strive to create intelligent systems that enhance the quality of life and address complex global issues.

REFERENCES

1. Fjaer, E.; Horsrud, H.P.; Raaen, A.M.; Risnes, R. Petroleum Related Rock Mechanics; Elsevier B. V.: Amsterdam, The Netherlands, 2008.
2. Chang, C.; Zoback, M.D.; Khaksar, A. Empirical relations between rock strength and physical properties in sedimentary rocks. *J. Pet. Sci. Eng.* 2006, 51, 223–237. [CrossRef]
3. Gatens, J.M.; Harrison, C.W.; Lancaster, D.E.; Guldry, F.K. In-situ stress tests and acoustic logs determine mechanical properties and stress profiles in the devonian shales. *SPE Form. Eval.* 1990, 5, 248–254. [CrossRef]
4. Nes, O.M.; Fjaer, E.; Tronvoll, J.; Kristiansen, T.G.; Horsrud, P. Drilling time reduction through an integrated rock mechanics analysis. *J. Energy Res. Technol.* 2012, 134, 2802:1–2802:7. [CrossRef]
5. Larsen, I.; Fjar, E.; Renlie, L. Static and Dynamic Poisson's Ratio of Weak Sandstones. In Proceedings of the 4th North American Rock Mechanics Symposium, Seattle, WA, USA, 31 July–3 August 2000. ARMA- 2000-0077.
6. Bai, P. Experimental research on rock drillability in the center of junggar basin. *Electron. J. Geotech. Eng.* 2013 18, 5065–5074.
7. Khaksar, A.; Taylor, P.G.; Fang, Z.; Kayes, T.; Salazar, A.; Rahman, K. Rock strength from core and logs, wherewe stand and ways to go. In Proceedings of the EUROPEC/EAGE conference and exhibition, Amsterdam, The Netherlands, 8–11 June 2009. SPE-121972-MS.
8. Omran, M.G.H.; Salman, A.; Engelbrecht, A.P. Self-adaptive Differential Evolution. In *Computational Intelligence and Security*; Hao, Y., Liu, J., Wang, Y., Cheung, Y.-m., Yin, H., Jiao, L., Ma, J., Jiao, Y.-C., Eds.; CIS 2005. Lecture Notes in Computer Science; Springer: Berlin/Heidelberg, Germany, 2005; Volume 3801.

Representations of Graceful Labeling of a Graph Using Python Programming Language

V. T. Dhokrat

Research Scholar
Department of Mathematics
K.T.H.M. College
Nashik, Maharashtra
✉ vibhadhokrat@gmail.com

S. B. Gaikwad

Department of Mathematics
Dnyaneshwar Gramonnati Mandal Hon. Balasaheb
Jadhav Arts, Commerce and Science College
Pune, Maharashtra

P. G. Jadhav

Professor,
Department of Mathematics
New Art's, Comm. and Science College
Ahmednagar, Maharashtra

ABSTRACT

Many researchers have proved that every path has a graceful labeling. Also, there are various types of graph labeling techniques. Researchers to date have given some specific examples of graphs for different labeling techniques. But I have some questions in my mind. 1) Can we draw different graceful labeled graphs for the same graph? 2) How many such graphs can we draw? 3) Is it possible to use some computer programming language that helps us to draw distinct graphical structures for the same graph satisfying the labeling conditions? Getting the answers to these questions is the origin of this research work.

In this paper, we construct a program using Python, which helps us to draw different graceful labeled graphs for the same graph.

KEYWORDS : *Graph, graceful labeling, path, Python Programming, Latex.*

INTRODUCTION

The graph concept was invented in 1735 with the Koinsberg Seven Bridge problem. The phrase graph is derived from the Greek word 'graphein'. A "graph" in this paper consists of "vertices" or "nodes" and lines called edges that connect with vertices. Graph labeling was introduced within the mid-1960s by Alexander Rosa. Over the past six decades, the research in graph labeling developed very fast. Graph labeling is a flourishing as well as an application-oriented area of research in the theory of Graphs. To date, more than 200 types of graph labeling techniques had been introduced. Here we study mainly graph without loops and parallel edges, non-directed having the countable number of edges and vertices. Here we consider the terminology and symbols of graphs from Harary's Graph Theory.

Also, we use here Python programming and Latex code to draw graphs

Definition: Graph

A graph $G=G(V,E)$ consists of two sets: A non-empty set V called vertex set whose elements are called vertices or nodes and a set E called edge set whose elements are called edges such that each edge $e \in E$ is associated with an unordered pair (v_1, v_2) of vertices $v_1, v_2 \in V$.

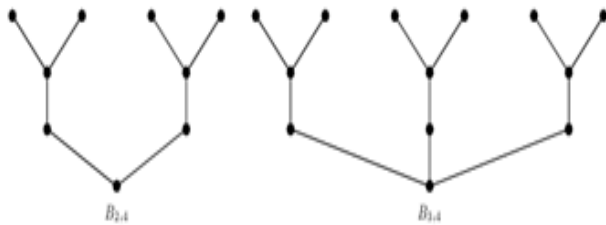
In this paper, we consider only those graphs that are finite, undirected, simple i.e. graphs without loops and parallel edges.

Graph labeling is an assignment of integers to the vertices or edges, or both, subject to certain conditions. If the domain of the mapping is the set of vertices, then the labeling is called vertex labeling. If the domain

of the mapping is the set of edges then the labeling is called an edge labeling

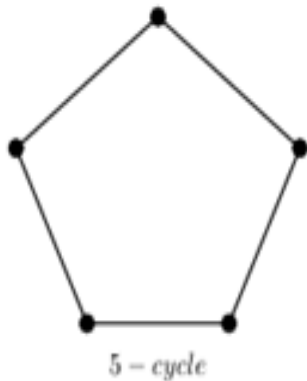
Definition: Graceful Labeling

A simple and finite graph $G = (V,E)$ is called graceful if there exists an injection $F;V(G) \rightarrow \{0,1,2,\dots,|E(G)|\}$ such that the induced function $F^*(uv) = |F(u)-f(v)|$, $uv \in E(G)$ is a bijection. The injection F is called a graceful labeling of G . The values of f and f^* are called graceful labels of vertex u and the edge uv resp. A graceful labeled graph is said to be a graceful graph. All symmetrical trees, trees with vertices ≤ 35 , Caterpillars, banana trees, etc. are always graceful.



Non-graceful graphs: A simple graph G is said to be non-graceful if there does not exist any graceful labelling.

Cycle graph on five vertices is a non-graceful graph



Python Programming

Python is a high-level, interactive, dynamic, general purpose computer programming language. Nokia, Google, You tube and NASA also preferred Python as it is simple and, has easy-to-use syntax. Python has a broader range of applications ranging from social networks, through automation to science calculations

Here in this paper we will construct a programme using

python which helps us to draw different graceful labeled graphs for the same graph.

Python is an exciting and powerful language with the right combination of performance and features that makes programming fun and easy. It is a high-level, interpreted, interactive, object-oriented and reliable language crafted in the 1980s by Guido Van Rossum. It has a vast library of modules to support the integration of complex solutions from pre-built components. It is a platform-independent, scripted language with complete access to operating system APIs.

Python has grown to become part of a plethora of Web-based, desktop-based, graphic design, scientific and computational applications. Python scripts can be used on different operating systems such as Windows, Linux, UNIX, Amigo, Mac OS, etc. We can move Python programs from one platform to another, and run it without any changes. Python is used to develop a wide range of applications including image processing, text processing, web and enterprise-level applications using scientific and numeric data from networks. It is also used for image processing and graphic design.[4]

We use this python programming to find different representations of a same graph for graceful labeling. Here using Itertool module of python we get a list of edge sequences and vertex sequences with the help of which we get different graceful labeled graphs for the same graph.

Itertool Module: It is a module in Python used for creating iterators for efficient looping. It produces complex iterators and help to solve problems easily and efficiently in terms of time as well as memory. It provides various ways to manipulate the sequence that we are traversing through.

Itertools.permutation() function comes under the Combinatoric Generators. The recursive generators that are used to simplify combinatorial constructs such as permutations, combinations, and Cartesian products are called combinatoric iterators. Itertool. permutations() provides all the possible arrangements that can be there for an iterator and all elements are assumed to be unique on the basis of their position and

not by their value or category. All these permutations are provided in lexicographical order. The function `itertools.permutations()` take an iterator and 'r' (length of permutation needed) as input and returns all possible permutations of length 'r' each.

In my investigation, I have continued the efforts of finding different graceful labeling for the same graph. Although difficult, the process became easier with the help of a python programming. When given the number of vertices, number of edges and list of endpoints of edges this program will able to find and list all graceful labelings of a graph. The outcome of this python programme is a list of edge sequences and vertex sequences with the help of which we get different graceful labeled graphs for the same graph.

Latex : In the year 1977 Donald E. Knuth developed a typesetting system which is used for preparing books that contains a lot of mathematical expressions. Later on American computer scientist and mathematician Leslie B. Lamport developed LaTeX in the early 1985. It is widely used for the communication and publication of scientific documents in many fields viz mathematics, computer science, engineering, physics, chemistry, economics, linguistics, quantitative psychology, Philosophy, and many more. It is also used in the preparation and publication of books, and articles that contain complex multilingual material.[3] In this research using a python programme we develop a Latex code to get different graceful labeling structures for a given graph. We apply these techniques to the basic graph labeling technique i.e. graceful labeling and also, we apply it to one simplest graph which contains a Triangle graph.

In this research, we first apply python programming to n vertices and n edges to create a vertex and edge sequence for graceful labeling. Then we develop a python programme to create a Latex code for different graceful labeling structures for a graph.

Python programme for graceful labeling

Programme

1] Graceful labeling of a graph having five vertices and five edges:

```
import itertools as it
def Check_diff(v1,v2,e):
    if abs(v1-v2)==e:
        return 1
    else:
        return 0
m=int(input("Enter no of edges = "))
edgeList=[]
for i in range(1,m+1):
    edgeList.append(i)
n=int(input("Enter no of vertices = "))
vertexList=[]
for i in range(m+1):
    vertexList.append(i)
print("Enter the list of endpoints of edges ")
edges=list(map(eval,input().split()))
edgeslen=len(edges)
for edgeSeq in it.permutations(edgeList,m):
    for vertexSeq in it.permutations(vertexList,n):
        j=0
        sm=0
        for i in range(0,edgeslen,2):
            t1=edges[i]-1
            t2=edges[i+1]-1
            sm=sm+Check_diff(vertexSeq[t1],vertexSeq[t2],edgeSeq[j])
            j=j+1
        if sm==len(edgeList):
            print(edgeSeq,vertexSeq)
```

Output:

```
(1, 2, 3, 4, 5) (1, 2, 4, 0, 5)
(1, 2, 3, 4, 5) (4, 3, 1, 5, 0)
(1, 2, 3, 5, 4) (2, 3, 5, 0, 4)
(1, 2, 3, 5, 4) (3, 2, 0, 5, 1)
(1, 3, 2, 4, 5) (2, 1, 4, 0, 5)
(1, 3, 2, 4, 5) (3, 4, 1, 5, 0)
(1, 3, 2, 5, 4) (2, 3, 0, 5, 1)
(1, 3, 2, 5, 4) (3, 2, 5, 0, 4)
(1, 4, 5, 3, 2) (0, 1, 5, 2, 4)
(1, 4, 5, 3, 2) (5, 4, 0, 3, 1)
(1, 5, 4, 3, 2) (1, 0, 5, 2, 4)
(1, 5, 4, 3, 2) (4, 5, 0, 3, 1)
(2, 1, 3, 4, 5) (1, 3, 4, 0, 5)
(2, 1, 3, 4, 5) (4, 2, 1, 5, 0)
(2, 3, 1, 4, 5) (2, 4, 1, 5, 0)
(2, 3, 1, 4, 5) (3, 1, 4, 0, 5)
(3, 1, 4, 5, 2) (1, 4, 5, 0, 2)
(3, 1, 4, 5, 2) (4, 1, 0, 5, 3)
(3, 2, 5, 4, 1) (0, 3, 5, 1, 2)
```

- (3, 2, 5, 4, 1) (5, 2, 0, 4, 3)
- (3, 4, 1, 5, 2) (1, 4, 0, 5, 3)
- (3, 4, 1, 5, 2) (4, 1, 5, 0, 2)
- (3, 5, 2, 4, 1) (2, 5, 0, 4, 3)
- (3, 5, 2, 4, 1) (3, 0, 5, 1, 2)
- (5, 1, 4, 3, 2) (0, 5, 4, 1, 3)
- (5, 1, 4, 3, 2) (5, 0, 1, 4, 2)
- (5, 4, 1, 3, 2) (0, 5, 1, 4, 2)
- (5, 4, 1, 3, 2) (5, 0, 4, 1, 3)

Using this python programme, we are able to find vertex sequence and edge sequence to get different graceful labeling.

Python programme to create latex code for different graceful labeling structures:

```

import itertools as it
import numpy as np
def Check_diff(v1,v2,e):
    if abs(v1-v2)==e:
        return 1
    else:
        return 0
n=int(input("Enter no of edges = "))
edgeList=[]
for i in range(1,n+1):
    edgeList.append(i)
m=int(input("Enter no of vertices = "))
vertexList=[]
for i in range(1,m+1):
    vertexList.append(i)
print("Enter the list of endpoints of edges ")
edges=list(map(eval, input().split()))
edgesLen=len(edges)
for edgeSeq in it.permutations(edgeList, m):
    for vertexSeq in it.permutations(vertexList, n):
        j=0
        sm=0
        for i in range(0,edgesLen,2):
            u1=edges[i]-1
            u2=edges[i+1]-1
            sm+=Check_diff(vertexSeq[u1],vertexSeq[u2],edgeSeq[j])
            j=j+1
        if sm==len(edgeList):
            #print(edgeSeq,vertexSeq)
            u1,u2,u3,u4,u5=vertexSeq[0],vertexSeq[1],vertexSeq[2],vertexSeq[3],vertexSeq[4]
            e1=np.abs(u1-u2)
            e2=np.abs(u2-u3)
            e3=np.abs(u1-u3)
            e4=np.abs(u3-u4)
            e5=np.abs(u4-u5)
            print("\begin{tikzpicture}[scale=1.5] \n \renewcommand{\VertexLineWidth}{1pc}\n
                \renewcommand{\EdgeLineWidth}{1pc}\n \graphIntr{style=Normal}\n
                \tikzset{EdgeStyle/.append style = {color = black, line width=4pc}}\n
                \tikzset{VertexStyle/.append style = {shape = circle, shading = ball,}
                ball color = white, very thin, inner sep=1pt, draw}\n \Vertex[=4d,x=1,y=2]{} \n
                \Vertex[=4d,x=1,y=0]{} \n \Vertex[=4d,x=2,y=0]{} \n \Vertex[=4d,x=4,y=0]{} \n
                \Vertex[=4d,x=6,y=0]{} \n \Edge[Label =4d] (1) (2)\n \Edge[Label =4d] (2) (3)\n
                \Edge[Label =4d] (3) (1)\n \Edge[Label =4d] (3) (4)\n \Edge[Label =4d] (4) (5)\n
                \end{tikzpicture}"%(u1,u2,u3,u4,u5,e1,e2,e3,e4,e5))
    
```

Using this python programme we are able to create a Latex code which gives different graceful labeling structures.

Output: Latex code

Enter no of edges = 5

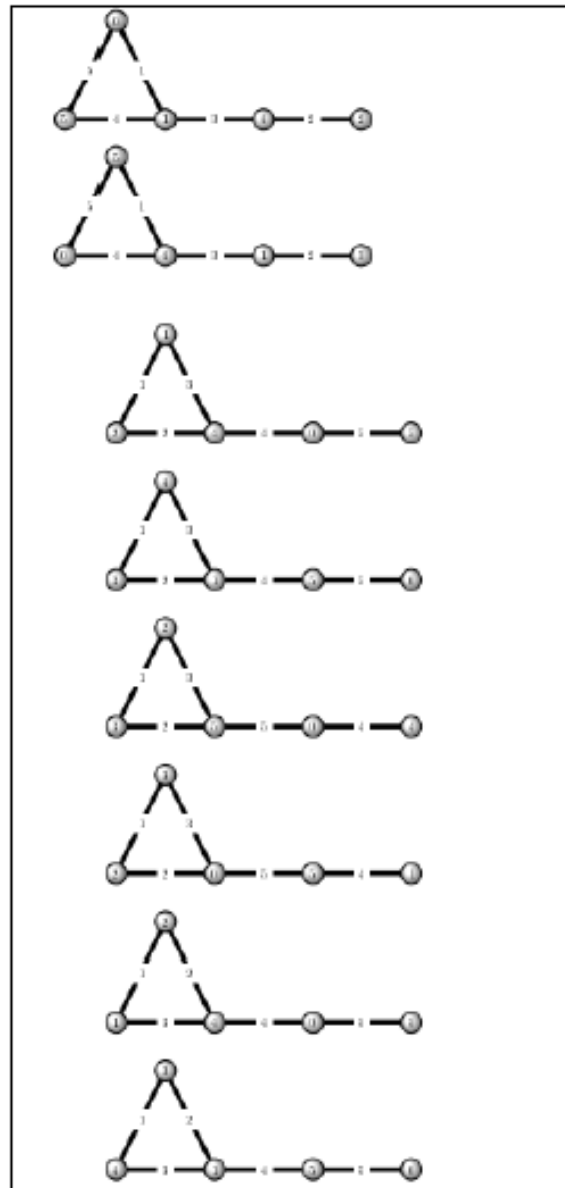
Enter no of vertices = 5

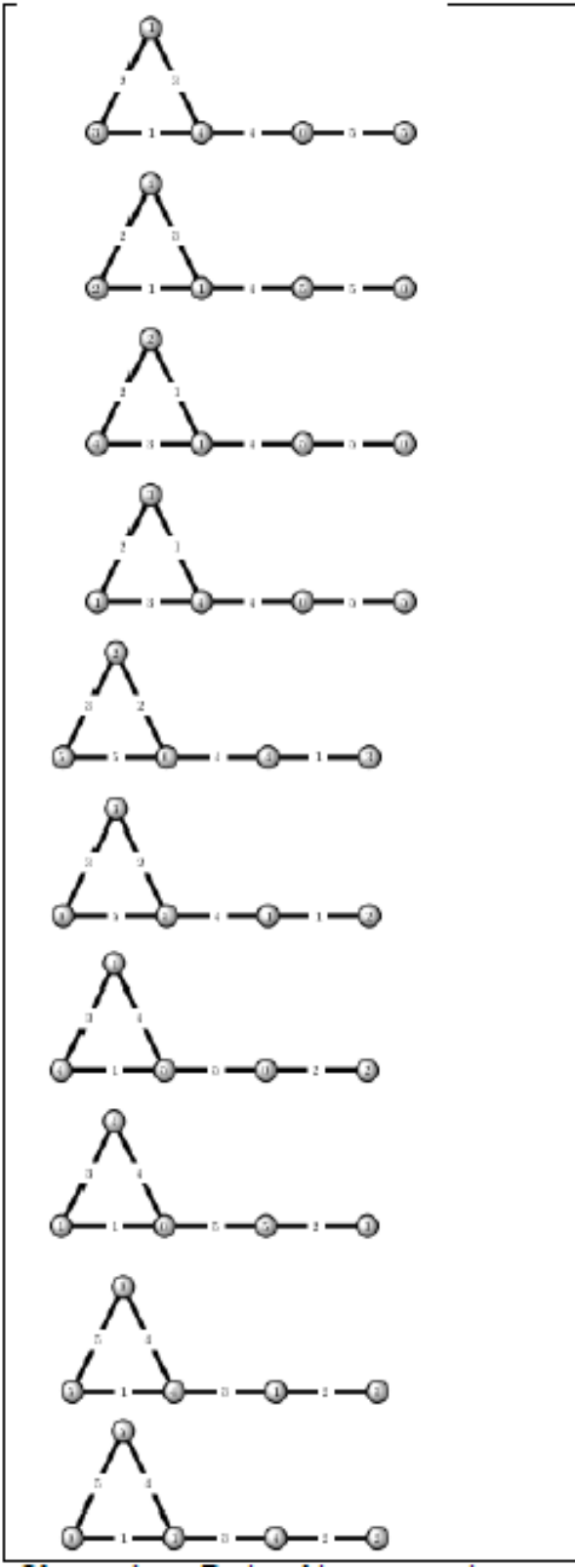
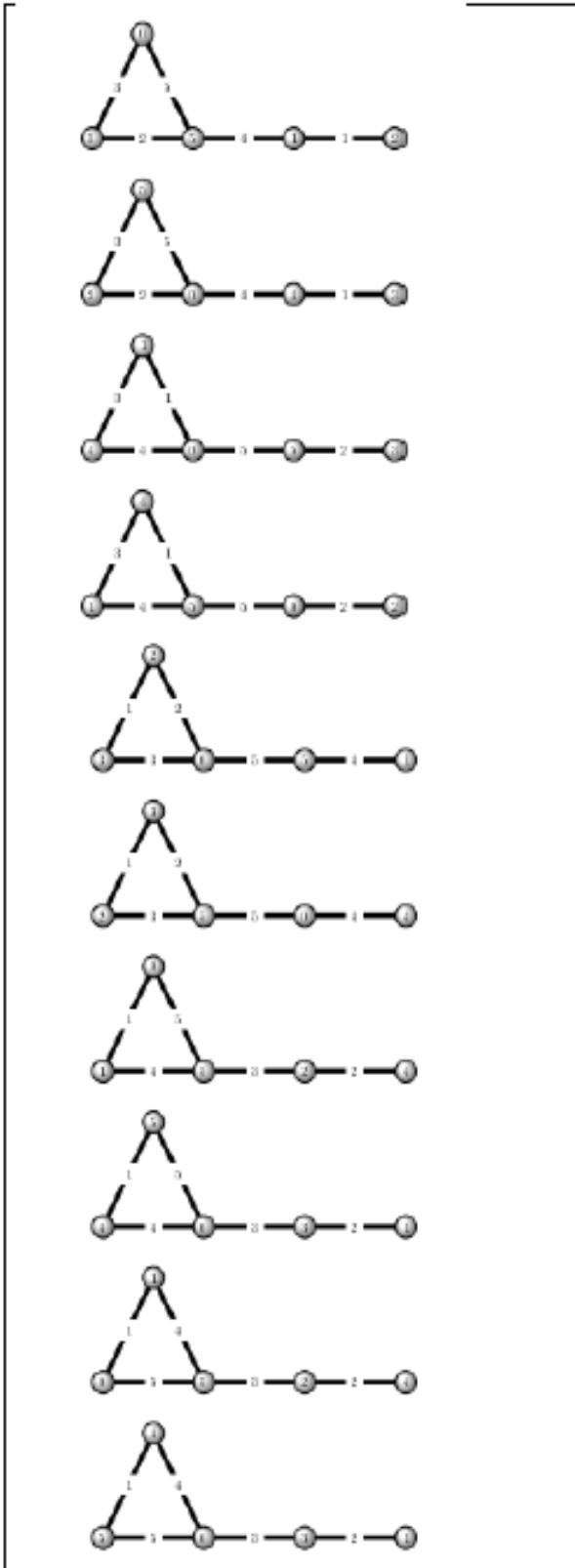
Enter the list of endpoints of edges

1 2 2 3 3 1 3 4 4 5

we get the following different graceful labeling graph structures.

FIGURE 1. Distinct graceful labeling of a graph with Five vertices





Observations: During this programming, we get the following observations

- 1) When we apply this python programme to a graph containing five vertices and five edges we get 28 graceful labeling structures. Due to the complementarity property, there are only 14 non-isomorphic graphical structures.
- 2) Each graph contains a triangle graph.
- 3) We get all the vertex and edge sequences in very short interval of time.
- 4) Due to latex code, we get all different graceful labeling structures within a short interval of time.

We apply all these programming techniques to different no. of vertices and edges, we get the vertex sequence, edge sequence, and latex code for different structures for graceful labeling.

We tabulate all findings during this investigation as:

Table 1. Relation between no. of vertices and no. of distinct graceful labeling

Number of vertices(n)	3	4	5	6	7	8	--
No. of graceful labeling of a graph obtained by Python program	12	20	28	52	84	152	-
Distinct graceful labeling	6	10	14	26	42	76	-
$\left(\frac{5}{3}\right)^n$	4.6	7.7 1	12. 86	21. 433 4	35. 72 24	59.5 37	-

We summarize all these results in a theorem as:

Theorem : The number of graceful labeling of a graph having equal number of vertices and edges is larger than $\left(\frac{5}{3}\right)^n$ where n is number of edges and $n \geq 3$.

This result matches with the corollary [1]

Corollary: The number of graceful labeling of paths P_n is larger than $\left(\frac{5}{3}\right)^n$ for sufficiently large n.

RESULT

From this python programme, regarding to graceful labeling we get the following results:

- 1) If the graph has m edges then each graceful labeling must contains vertex label as m.

- 2) The vertices having labels 0 and m are always adjacent.

- 3) Each graceful labeling graph contains a triangle graph.

- 4) As the number of vertices and number of edges increasing the programme takes more time but we are getting the different possible graceful labeling which we cannot find manually.

- 5) The complementarity property for graceful labeling is satisfied. That is for a given graph with a graceful labeling, if we swap every vertex label k with m-k, the resulting labeling is also graceful since the edge labels will not have changed the end vertices of an edge with labels a and b become m - a and m - b and $|a-b|=|(m-a)-(m-b)|$.

All these results obtained are coincides with previous known results. And we can check the generated vertex and edge sequence satisfies the graceful labeling conditions with the help of graph structures.

CONCLUSION

From this research we conclude that we can use python programme to get various representation of graceful labeling to same graph, which is quite tedious job to get the various representations manually. It also saves time and energy. Using these representations, we can think in different ways on any problem which helps us to get more reliable solution to the problem under study.

Scope: In this research, we only find the different possible graceful labeling in terms of vertex sequence and edge sequence. The interested researcher can construct a python programme to get directly the graphical structures for the various representations. In this research we only use python programme for graceful labeling, there is a scope to construct a python programme for other labeling techniques.

ACKNOWLEDGEMENT

I (first author) thanks Dr. P. G. Jadhav(second author) and Dr. S.B. Gaikwad (Third author) for his valuable guidance and encouragement. We acknowledge the Department of Mathematics, K.T.H.M College , Nashik for providing the basic infrastructure facilities.

REFERENCES

1. R.E.L. Aldred, Jozef Siran, Martin Siran 2003 'A note on the number of graceful labeling of paths', Discrete Mathematics 261,p.n. 27-30, ELSEVIER
2. B. Beavers, Golomb rulers and graceful graphs, http://webcourse.cs.technion.ac.il/236801/Spring2009/ho/WCFiles/Golomb_Rulers_and_Graceful_Graphs.pdf.
3. LaTeX in 24 Hours, A Practical Guide for Scientific Writing , Dilip Datta, Springer International Publishing AG, 2017
4. PYTHON BASICS, H. Bhasin, MERCURY LEARNING AND INFORMATION Dulles, Virginia Boston, Massachusetts New Delhi.
5. Ujwala N Deshmukh, August2015, 'APPLICATIONS OF GRACEFUL GRAPHS' International Journal of Engineering Sciences & Research Technology, <http://www.ijesrt.com>
6. Gallian, JA 2010, 'A dynamic survey of graph labeling', The Electronic Journal of Combinatorics, vol.17(DS6).
7. Harary, F 1988, 'Graph Theory', Narosa publishing House Reading, New Delhi.
8. K. R. Srinath, Dec-2017, 'Python – The Fastest Growing Programming Language', International Research Journal of Engineering and Technology (IRJET), Volume: 04,Issue: 12.
9. V. T. Dhokrat, Dr. P. G. Jadhav and Dr. S. B. Gaikwad, "A Survey Study of Association Between Graph and Graph Labeling Techniques",International Journal of Education, Modern Management, Applied Science & Social Science (IJEMASSS) 19 ISSN : 2581-9925, Volume 05, No. 03(II), July - September, 2023, pp. 19-30.

Disk Space Rental System

Dhanshree Gavankar, Vaishnavi Khairnar,
Prajwal Pahilwan

Jayesh Ughade, Shalmali Botekar

Jawahar Education Society Institute of Technology
Management & Research
Nashik, Maharashtra
✉ dhanashrijg08@gmail.com

ABSTRACT

Inadequate encryption and security protocols are a common problem with many information storage services, which raises privacy concerns and results in high-profile instances like the 2012 Dropbox attack and the 2014 iCloud breach. Traditional storage solutions, such centralized cloud services and physical data centers, have drawbacks like high costs, single points of failure, and security issues. As an alternative, a decentralized file storage marketplace makes use of blockchain technology to divide data among several renters, improving security and privacy. Data owners can rent space from disk space owners under the system's free-market operation. The corresponding Disk Space renting control system provides a decentralized marketplace for safe and efficient disk space renting while guaranteeing efficient resource allocation and security across several businesses.

KEYWORDS : *Storage service, Traditional storage solutions, Cloud, centralized, Decentralized, Blockchain, Disk Space renting.*

INTRODUCTION

The need for more storage due to the growing amount of data produced by electronic devices has resulted in the creation of cloud storage platforms such as Dropbox, AWS, and Google Drive. By leveraging the security advantages of blockchain technology, a decentralized alternative is provided by a blockchain-based disk rental system. The administrator of this system has access to transaction, payment, and disk utilization data and approves user requests for storage space. Users can browse for hard drive plans, establish accounts, and ask permission to rent space. The need of technical support and information security against theft and cyberattacks is emphasized, with constant monitoring and maintenance to guarantee server uptime and website upkeep.

BENEFITS OF DISK SPACE RENTAL SYSTEM

There are many benefits to using Disk Space Rental system:

- Blockchain is always secure because of its encryption characteristic.

- By lowering the chance of a single point of failure, blockchain data architectures strengthen network security and make database breaches more difficult.
- Since every user on the blockchain has a unique key, blockchain prevents unwanted access.
- It stops data manipulation.

HOW DISK SPACE RENTAL SYSTEM WORKS

Disk Space Rental system work as follows:

1. Users create an account on the platform.
2. The renter can search for disk spaces and plans posted by the provider.
3. Provider posts about their available disk spaces and plans they are providing.
4. Renter requests disk space from providers.
5. This transaction happens through a third party blockchain platform.
6. Provider accepts and gives permissions and access to the renter.

FEATURES OF DISK SPACE RENTAL SYSTEM

Disk Space Rental system typically offer a variety of features, such as:

- Search: User can search plans which suit their needs.
- Storage usage: User can check how much storage they've used and remaining storage
- User can add, update and view their data.
- User can cancel the transaction.
- If user need more space they can add to their existing rental space.

SYSTEM ARCHITECTURE

Three primary parts make up the Disk Renting System: disk providers, disk renters, and a third-party blockchain network. The disk supplier, who rents out their disk, is the main component. Users can share information more easily on the blockchain network, but in order to connect to the network, digital wallets are needed. A data integrity certificate is issued by the storage provider, and payments made with lightning network technology guarantee security and legality because all supporting documentation and payment information are kept on the blockchain. With login credentials in hand, the administrator examines and grants or rejects user requests while keeping an eye on transactions and disk usage. Users register, examine disk information, and ask the administrator for permission to rent space. Renters and suppliers must have a reliable internet connection because the system uses a client application using HTML, CSS, and React JS for user interaction and PHP to connect to the third-party blockchain network.

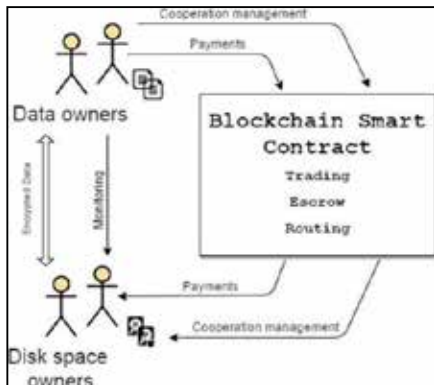


Fig. 1 Architecture Diagram

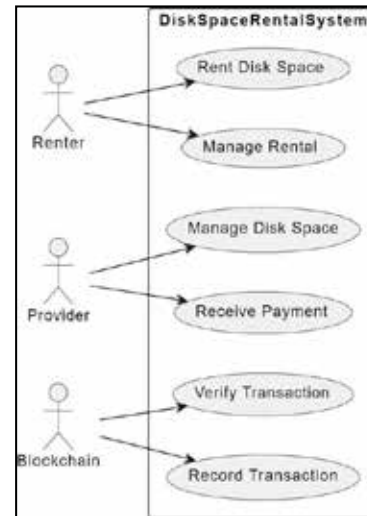


Fig. 2 Use Case Diagram

- Represents the interactions between system elements and external actors.
- Shows the system's functionality from a user's perspective.

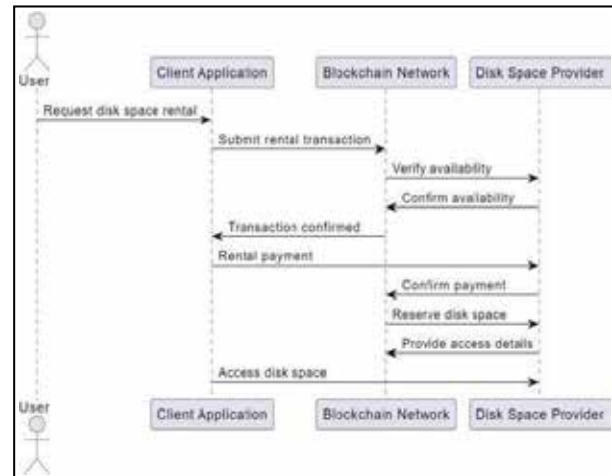


Fig. 3 Sequence Diagram

- Represents the flow of activities throughout the transaction.

FUNCTIONAL REQUIREMENT

- Registration / login
- Renting disk space
- Posting for available space
- Two-step verification

NON-FUNCTIONAL REQUIREMENT

- Internet
- Availability
- Verification
- Security
- Data encryption
- Access control

FUTURE WORK

- Enhanced Security Features: To strengthen data security, put modern encryption techniques and authentication processes into practice.
- Machine learning integration: Examine how machine learning techniques can be used to anticipate and optimize disk space needs based on usage trends.
- Blockchain integration: Examine how incorporating blockchain might improve data integrity and provide decentralized governance.
- Scalability improvements: Improve system scalability to meet the expanding needs of data-intensive applications and large-scale companies.
- User interface refinement: Make constant improvements to the user interface to make it more intuitive and user-friendly.
- Cross platform compatibility: Increase compatibility to provide accessibility across many operating systems and Support a larger variety of platforms.
- Comprehensive reporting and analysis: Provide thorough reporting capabilities and analytics options to give users insightful information about disk space trends and consumption.

CONCLUSION

The Disk Space Rental Management System emerges as a crucial tool for efficiently allocating and overseeing disk space resources. Its versatility is evident across diverse sectors, including data centers, cloud service providers, and educational institutions. The system's

efficacy is heightened through enhanced resource utilization, streamlined operations, and heightened security measures.

REFERENCES

1. Lu Meng, Bin Sun, "Research on Decentralized Storage Based on a Blockchain", Multidisciplinary Digital Publishing Institute, 2022.
2. Nabeel Khan, Hanan Aljoaey, Mujahid Tabassum, Ali Farzamia, Tripti Sharma, Yew Hoe Tung, "Proposed Model for Secured Data Storage in Decentralized Cloud by Blockchain Ethereum", Multidisciplinary Digital Publishing Institute, 2022.
3. Qazi Mazhar Ul Haq, Alfian Ma'arif, Wahyu Rahmaniari, "Blockchain technology", Jurnal Ilmiah Teknik Elektro Komputer dan Informatika, 2022.
4. Richa Shalom, Ganesh Rohit Nirogi, "Decentralized Cloud Storage Using Blockchain", International Journal for Research in Applied Science & Engineering Technology, 2022.
5. Yogita Sharma, Ayush Agarwalla, Dhananjay Joshi, Divyanshu Prasad, "A Secure Encrypted Digital Storage System Based on Blockchain", International Research Journal of Modernization in Engineering Technology and Science, 2021.
6. Pratima Sharma, Pajni Jindal, Malaya Dutta Borah, "Blockchain Technology for Cloud Storage: A Systematic Literature Review", ACM Computing Surveys, 2020.
7. Omar Ali, Ashraf Jaradat, Atik Kulakli, Ahmed Abuhalmeh, "A Comparative Study: Blockchain Technology Utilization Benefits, Challenges and Functionalities", Institute of Electrical and Electronics Engineers, 2020.
8. Yan Zhu, Chunli Lv, Zichuan Zeng, Jingfu Wang, Bei coupon ePei, "Blockchain-based Decentralized StorageScheme", IOP Publishing, 2019.
9. Subarna Shakya, Sagar Bhusal, Anish Shrestha, Bipin Khatiwada, "Decentralized Secure Cloud Storage using Blockchain", Tribhuvan University Institute of Engineering Pulchowk Campus, 2018.
10. Saqib Ali, Guojun Wang, Bebo White, Roger Leslie Cottrell, "A Blockchain-based Decentralized Data Storage and Access Framework for PingER", Institute of Electrical and Electronics Engineers, 2018.

A Comprehensive Survey on Enhancing Blockchain Data Security through the Integration of IoT and AI

Yogesh Arjun Shinde

Dept. of computer Engg, Research Scholar
MET's Institute of Engineering Nashik
(SPPU, Pune)
Pune, Maharashtra
✉ yogeshshinde599@gmail.com

S. K. Sonkar

Dept. of Computer Engineering
Amrutvahini College of Engineering
Sangamner, Maharashtra

ABSTRACT

Blockchain technology has significant transformation various multiple sectors through the provision of a secure and transparent decentralized ledger. However, as the adoption of blockchain continues to grow, concerns regarding data security become more pronounced. This survey paper aims to explore the intersection of blockchain, artificial intelligence (AI), and the Internet of Things (IoT) to address and enhance data security in blockchain ecosystems. The integration of AI and IoT into Blockchain systems have the capacity to mitigate security vulnerabilities, ensure privacy, and enhance overall system robustness.

KEYWORDS : *Blockchain, IOT, AI, Security, Cryptography, Hash, Smart contract.*

INTRODUCTION

Blockchain technology, heralded for its transformative potential across industries, has redefined the landscape of secure and transparent data management. As the adoption of blockchain continues to surge, so does the imperative to fortify its data security infrastructure. In this context, the convergence of two cutting-edge technologies, Artificial Intelligence (AI) and the Internet of Things (IoT), emerges as a compelling solution to bolster the resilience of blockchain ecosystems. This survey paper delves into the intricate fusion of blockchain, AI, and IoT, with a primary focus on enhancing data security. By exploring the synergies among these technologies, we aim to uncover novel approaches to address existing vulnerabilities, ensure privacy, and augment the overall robustness of blockchain systems.[1]

Background

Blockchain, initially conceptualized as the foundational technology for digital currencies such as Bitcoin, has transformed into a multifaceted technology with applications spanning finance, healthcare, supply

chain, and beyond. Its decentralized and immutable ledger architecture offers a paradigm shift in how data is stored and transactions are conducted. However, the rapid proliferation of blockchain has also exposed vulnerabilities, ranging from consensus algorithm weaknesses to smart contract exploits, prompting a critical examination of its data security mechanisms.[4]

Motivation

The impetus behind this survey stems from the recognition that as blockchain matures, so too must its defenses against an evolving landscape of cybersecurity threats. Traditional security measures, though robust, may not be sufficiently agile to counter novel and sophisticated attacks. In response to this challenge, the integration of AI and IoT holds promise as a dynamic and adaptive solution capable of fortifying blockchain networks against both known and emergent threats. The motivation lies in exploring how these synergies can proactively secure blockchain data, protect against unauthorized access, and ensure the long-term viability of decentralized ledger systems.[2][5]

This survey paper gives a comprehensive overview of the

current state of blockchain data security, the individual roles of AI and IoT in fortifying this security, and the collective impact of their integration. By dissecting the challenges, solutions, and real-world implementations, we aim to offer a roadmap for researchers, practitioners, and decision-makers navigating the intersection of blockchain, AI, and IoT in the pursuit of enhanced data security.

BLOCKCHAIN DATA SECURITY

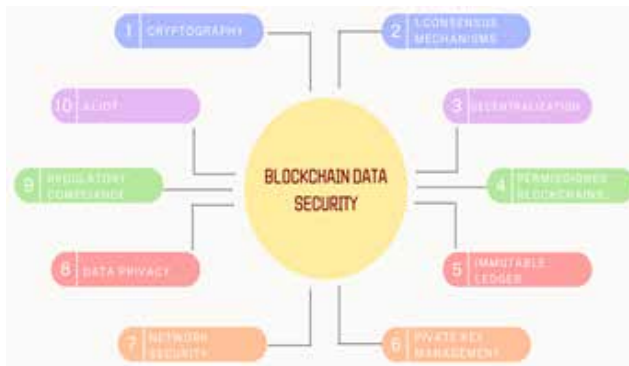


Fig. 1. Blockchain Data Security

Cryptography

Hash Functions: The blockchain uses cryptographic hash functions to generate fixed-size hash values that uniquely represent data. This ensures data integrity by making it extremely difficult to alter a block's information without changing all subsequent blocks.

Public-Key Cryptography: Digital signatures, a crucial part of blockchain security, are implemented using public-key cryptography. This enables secure transactions and authenticates participants.

Consensus Mechanisms

Proof of Work (PoW) and Proof of Stake (PoS): These consensus algorithms secure the network by requiring participants to solve complex mathematical problems (PoW) or stake a certain amount of cryptocurrency (PoS). Consensus mechanisms prevent malicious activities and maintain the integrity of the blockchain.

Decentralization

Decentralization is a core feature of blockchain, where data is distributed across a network of nodes. This minimizes the risk of a single point of failure and

enhances the security of the overall system.

Permissioned Blockchains

In addition to public blockchains, permissioned blockchains restrict access to a predefined group of participants. This control over network access enhances security and is particularly relevant in enterprise applications.

Smart Contract Security

Smart contracts, self-executing code on the blockchain, undergo thorough security audits. Vulnerabilities in smart contracts, if exploited, can lead to serious security breaches. Regular auditing and testing help identify and mitigate potential risks.

Immutable Ledger

The immutability of the blockchain ensures that once data is added to a block and the block is added to the chain, it cannot be altered. Immutability contributes to data integrity and transparency.

Private Key Management

Users' private keys, which grant access to their digital assets, must be securely managed. Secure storage solutions, like hardware wallets, and adherence to best practices in key management are crucial for preventing unauthorized access.

Network Security

Robust network security measures, including encryption and firewalls, protect against external threats. Network monitoring and anomaly detection help identify suspicious activities that may indicate a security breach.

Regular Software Updates

Regular updates to blockchain software and protocols are essential to address security vulnerabilities. Prompt implementation of patches and updates helps maintain a secure environment.

Data Privacy

Balancing transparency with data privacy is crucial. Techniques such as zero-knowledge proofs or privacy-focused blockchains are explored to enable private transactions while maintaining the overall transparency of the network.

Regulatory Compliance

Adherence to regulatory standards and compliance with legal frameworks are critical. Blockchain projects need to navigate evolving regulatory landscapes to ensure data protection and meet industry-specific requirements.

Blockchain data security encompasses a comprehensive set of measures, including cryptographic techniques, consensus mechanisms, decentralization, and proactive strategies to safeguard against potential threats. The continuous evolution of blockchain technology requires ongoing efforts in research, development, and collaboration to ensure the sustained integrity and security of decentralized systems.

ARTIFICIAL INTELLIGENCE IN BLOCKCHAIN SECURITY

AI is of the greatest significance in revolutionizing the landscape of blockchain security, offering innovative solutions to detect, prevent, and respond to evolving threats. This section explores the multifaceted contributions of AI to enhancing the security posture of blockchain networks.

Threat Detection and Prevention

One of the primary applications of AI in blockchain security is in the realm of threat detection and prevention. Machine learning algorithms can analyze vast datasets to identify patterns indicative of malicious activities within the blockchain network. This proactive approach allows for real-time monitoring, rapid threat identification, and the potential to thwart attacks before they escalate.

Machine learning models, ranging from supervised to unsupervised techniques, can be trained to recognize anomalous behavior, detect patterns associated with known attacks, and adapt to emerging threats. By using these models, blockchain systems can automatically find problems, like strange transaction patterns or strange network activity, and take immediate action to stop possible security breaches.

Anomaly Detection

AI-driven anomaly detection mechanisms are crucial for fortifying the security of blockchain networks. These systems leverage historical data and behavioral analytics to establish a baseline of normal network

activities. Deviations from this baseline, indicative of potential security threats or irregularities, trigger alerts or automated responses.

In the context of blockchain, anomaly detection powered by AI can identify abnormal transaction sizes, atypical consensus behaviors, or deviations in smart contract execution. This proactive approach enhances the overall resilience of the blockchain system by promptly identifying and mitigating potential vulnerabilities.

Smart Contract Security

Smart contracts, while integral to the functionality of many blockchain applications, pose unique security challenges. AI techniques can be applied to analyze smart contract code for vulnerabilities and potential exploits. Static analysis tools utilizing machine learning algorithms can identify patterns associated with common security flaws, helping developers rectify issues before deployment.

Furthermore, AI-enhanced dynamic analysis can simulate various execution scenarios to identify vulnerabilities that may not be apparent during static analysis. By leveraging machine learning to continuously learn from emerging threats and vulnerabilities, AI contributes to the ongoing improvement of smart contract security, reducing the risk of exploitation.

In summary, the integration of AI into blockchain security represents a dynamic and proactive approach to safeguarding decentralized networks. From real-time threat detection to enhancing the security of smart contracts, AI technologies contribute significantly to the resilience and adaptability of blockchain ecosystems. As the field continues to advance, the synergy between AI and blockchain security is poised to play a pivotal role in addressing the evolving challenges posed by malicious actors in the digital landscape.

THE INTERNET OF THINGS IN BLOCKCHAIN SECURITY

The Internet of Things (IoT) presents a transformative paradigm by connecting physical devices, sensors, and everyday objects to the digital realm. Integrating IoT with blockchain introduces novel approaches to enhance data security, particularly in the areas of device authentication, data integrity, and decentralized identity management.

Device Authentication and Authorization

Considering the issue of blockchain security, the authentication and authorization of devices participating in the network are critical components. IoT devices can be integrated into blockchain ecosystems to strengthen these processes. By leveraging unique device identifiers and cryptographic mechanisms, the integrity and authenticity of IoT devices can be assured.

Blockchain, acting as a decentralized ledger, ensures transparent and tamper-resistant records of device identities and permissions. This not only safeguards against unauthorized access but also establishes a trustworthy environment where IoT devices can seamlessly interact within the blockchain network. This integration contributes to the prevention of malicious actors attempting to compromise the system through unauthorized devices.

Data Integrity and Trustworthiness

IoT devices generate vast amounts of data, and ensuring the integrity and trustworthiness of this data is crucial for blockchain applications. Utilizing sensors and IoT devices, blockchain systems can create a secure and immutable record of data transactions. Each data transaction is cryptographically linked and timestamped, providing an auditable trail of the data's journey through the network.

This integration enhances the overall transparency and reliability of data in blockchain networks. In sectors such as supply chain management, where the provenance and authenticity of goods are paramount, the combination of IoT and blockchain ensures that data remains accurate and untampered throughout its lifecycle.

By establishing a direct link between the physical world and the blockchain, IoT contributes to the creation of a more robust and trustworthy ecosystem, addressing concerns related to data integrity and trust in blockchain applications.

INTEGRATION OF AI AND IOT IN BLOCKCHAIN DATA SECURITY

The integration of AI and the IoT within blockchain ecosystems represents a transformative synergy that holds the promise of significantly enhancing data security. This section explores the collaborative

impact of AI and IoT, focusing on privacy-preserving techniques, decentralized identity management, and their combined effect on blockchain security.

Privacy-Preserving Techniques

The marriage of AI, IoT, and blockchain addresses privacy concerns by incorporating sophisticated privacy-preserving techniques. One notable approach is the integration of homomorphic encryption. This cryptographic method enables computations on encoded information without decrypting it, preserving the confidentiality of sensitive information. AI algorithms operating on encrypted data can glean meaningful insights without exposing the raw data, ensuring robust privacy protection.

In scenarios where data privacy is paramount, such as healthcare or financial transactions, this amalgamation of technologies provides a robust framework. By employing homomorphic encryption in conjunction with AI and IoT, users can benefit from the analytical power of AI while maintaining the confidentiality of their data within the blockchain.

Decentralized Identity Management

Identity management is a critical aspect of blockchain security, and the integration of AI and IoT contributes to the development of decentralized identity solutions. Traditional identity systems are often centralized, creating vulnerabilities and privacy concerns. Through the combination of AI-driven biometric authentication and IoT-based device identity verification, decentralized identity management in blockchain becomes more secure and user-centric.

This integrated approach ensures that users maintain control over their personal information, selectively sharing attributes without revealing their entire identity. Furthermore, AI algorithms continuously adapt to evolving security threats, enhancing the resilience and adaptability of decentralized identity systems within blockchain networks.

CASE STUDIES AND IMPLEMENTATIONS

To illustrate the practical applications and benefits of integrating Artificial Intelligence (AI) and the Internet of Things (IoT) in enhancing blockchain data security,

we present real-world case studies and implementations across various industries.

Real-world Applications

Supply Chain Security

Case Study 1: VeChain (VeChainThor)

Objective: Ensuring transparency and security in the supply chain by leveraging IoT devices, AI analytics, and blockchain.

Implementation: VeChainThor integrates IoT sensors to collect real-time data on product conditions (temperature, humidity, location). AI algorithms analyze this data to predict potential issues in the supply chain. The information is then securely recorded on the VeChain blockchain, providing an immutable and transparent ledger of the product's journey.

Benefits: Enhanced traceability, reduced counterfeiting, and improved quality control. The combination of AI, IoT, and blockchain ensures data integrity, preventing tampering and unauthorized access.

Healthcare Data Management

Case Study 2: MedicalChain

Objective: Securing healthcare data and enabling interoperability through the integration of IoT devices, AI diagnostics, and blockchain.

Implementation: MedicalChain employs IoT devices for patient monitoring, collecting real-time health data. AI algorithms analyze the data for diagnostics and treatment recommendations. Patient records are securely stored on a blockchain, ensuring patient privacy and allowing authorized healthcare providers to access a patient's comprehensive medical history.

Benefits: Improved patient care, enhanced data security, and interoperability. The integration of AI, IoT, and blockchain ensures the integrity and confidentiality of sensitive healthcare information.

Smart Cities

Case Study 3: CitySense (Barcelona, Spain)

Objective: Enhancing urban security and efficiency by utilizing AI-driven IoT sensors and blockchain technology.

Implementation: Barcelona's CitySense project deploys IoT sensors for monitoring various aspects of urban life, including traffic flow, air quality, and noise levels. AI algorithms analyze the data to predict and respond to potential security threats. The collected data is stored securely on a blockchain, providing transparency and traceability.

Benefits: Improved urban planning, enhanced security, and optimized resource allocation. The integration of AI, IoT, and blockchain fosters a safer and more efficient urban environment.

These case studies demonstrate the tangible impact of integrating AI and IoT with blockchain in real-world scenarios. The collaborative use of these technologies contributes to improved security, transparency, and efficiency across diverse industries, showcasing the transformative potential of this interdisciplinary convergence. As research and development in this field continue, these implementations serve as valuable benchmarks for future applications of AI, IoT, and blockchain in enhancing data security.

CHALLENGES AND FUTURE DIRECTIONS

As the integration of AI, IoT, and blockchain in data security advances, several challenges and opportunities emerge. This section explores key challenges and proposes potential future directions for research and development in this interdisciplinary field.

Scalability

Challenge: The seamless integration of AI, IoT, and blockchain introduces scalability challenges, particularly concerning the processing and storage requirements for the massive amounts of data generated by IoT devices. As the volume of data increases, maintaining the efficiency and speed of blockchain transactions becomes a significant hurdle.

Future Directions

Research into optimized algorithms: Develop algorithms that efficiently process and analyze data at scale, ensuring minimal impact on blockchain performance.

Distributed computing solutions: Explore decentralized and distributed computing models to distribute

computational tasks across a network of nodes, addressing scalability concerns.

Interoperability

Challenge: Achieving interoperability between AI, IoT, and blockchain technologies is crucial for seamless integration across diverse ecosystems. The lack of standardized protocols and communication frameworks poses a barrier to the effective collaboration of these technologies.

Future Directions

Standardization efforts: Advocate for and contribute to the development of industry standards that promote interoperability between AI, IoT, and blockchain technologies.

Protocol development: Invest in research and development to create standardized communication protocols that facilitate efficient data exchange and collaboration among integrated systems.

Ethical Considerations

Challenge: The convergence of AI, IoT, and blockchain raises ethical considerations related to data privacy, security, and the potential misuse of advanced technologies. Maintaining ethical standards becomes crucial as these technologies become more ingrained in daily life.

Future Directions

Ethical frameworks: Develop comprehensive ethical frameworks that guide the responsible implementation, deployment, and Utilization of integrated AI, IoT, and blockchain systems.

Public awareness and education: Increase awareness about the ethical implications of these technologies among developers, users, and policymakers to ensure responsible innovation.

Security and Privacy

Challenge: Despite advancements in security, the integration of AI, IoT, and blockchain introduces new attack vectors and privacy concerns. Ensuring the confidentiality and integrity of sensitive data remains a paramount challenge.

Future Directions

Advanced cryptographic techniques: Explore and implement advanced cryptographic methods to enhance the security of data stored on the blockchain and transmitted between AI and IoT devices.

Privacy-preserving AI: Develop AI models that can operate on encrypted data, preserving privacy while still providing meaningful insights.

Regulation and Compliance

Challenge: The rapid evolution of technology often outpaces regulatory frameworks, creating challenges in ensuring compliance with data protection and security standards.

Future Directions

Regulatory frameworks: Collaborate with regulatory bodies to develop and adapt regulations that address the unique challenges posed by integrated AI, IoT, and blockchain systems.

Compliance tools: Develop tools and frameworks to assist organizations in ensuring compliance with evolving data protection and security regulations.

Cross-Disciplinary Collaboration

Challenge: The successful integration of AI, IoT, and blockchain requires collaboration across diverse domains, including computer science, cybersecurity, and policy-making.

Future Directions

Interdisciplinary research programs: Encourage and support collaborative research initiatives that bring together experts from various disciplines to address the multifaceted challenges of integrated systems.

Education and training: Create educational programs and training initiatives aimed at providing professionals with the necessary skills necessary for cross-disciplinary collaboration in this evolving field.

As these challenges are addressed, the future direction of research and development in the integration of IoT, AI and blockchain will likely pave the way for innovative solutions, further enhancing the security and efficacy of decentralized systems. The ongoing exploration of these challenges and the pursuit of interdisciplinary

collaboration will contribute to the maturation of this transformative convergence.

CONCLUSION

The integration of the Internet of Things, Artificial Intelligence, with blockchain in data security marks a paradigm shift, offering a multifaceted approach to address the evolving challenges of decentralized systems. This survey has explored the collaborative impact of these technologies, focusing on privacy-preserving techniques, decentralized identity management, and real-world case studies across various industries. Despite the transformative potential, several challenges have been identified, including scalability, interoperability, ethical considerations, security, and compliance.

In conclusion, the collaborative integration of AI, IoT, and blockchain in data security not only fortifies the resilience of decentralized systems but also opens avenues for innovation and efficiency across diverse industries. As stakeholders continue to explore and implement these integrations, it is imperative to prioritize ethical considerations, adhere to evolving regulatory frameworks, and foster cross-disciplinary collaboration. The journey towards a secure and transparent digital future requires a collective commitment to responsible innovation, ensuring that the benefits of these technologies are realized while mitigating potential risks.

ACKNOWLEDGMENT

We would like to express our deepest gratitude to all those who have contributed to the completion of this research paper on enhancing blockchain data security through the integration of IoT and AI.

REFERENCES

1. S. Lee and S. Kim, "Blockchain as a Cyber Defense: Opportunities, Applications, and Challenges," in *IEEE Access*, vol. 10, pp. 2602-2618, 2024, doi: 10.1109/ACCESS.2021.3136328.
2. H. Nandanwar and R. Katarya, "A Systematic Literature Review: Approach Toward Blockchain Future Research Trends," in *2023 International Conference on Device Intelligence, Computing and Communication Technologies, (DICCT)*, 2023, pp. 1-6, doi: 10.1109/DICCT51712.2023.10110088.
3. Z. Ullah et al., "Towards Blockchain-Based Secure Storage and Trusted Data Sharing Scheme for IoT Environment," in *IEEE Access*, vol. 10, pp. 36978-36994, 2022, doi: 10.1109/ACCESS.2022.3164081.
4. Rashid et al., "Blockchain-Based Autonomous Authentication and Integrity for Internet of Battlefield Things in C3I System," in *IEEE Access*, vol. 10, pp. 91572-91587, 2022, doi: 10.1109/ACCESS.2022.3164082.
5. S. Lee and S. Kim, "Blockchain-Based Wireless Sensor Networks for Malicious Node Detection: A Survey," in *IEEE Access*, vol. 9, pp. 128765-128785, 2021, doi: 10.1109/ACCESS.2021.3109528.
6. Azaria, A. Ekblaw, T. Vieira, and A. Lippman, "MedRec: Using blockchain for medical data access and permission management," in *Proc. 2nd Int. Conf. Open Big Data (OBD)*, Aug. 2016, pp. 25-30.
7. R. Chaudhary, A. Jindal, G. S. Aujla, S. Aggarwal, N. Kumar, and K.-K.-R. Choo, "BEST: Blockchain-based secure energy trading in SDN-enabled intelligent transportation system," *Comput. Secur.*, vol. 85, pp. 288-299, Aug. 2019.
8. S. Davidson, P. De Filippi, and J. Potts. (Mar. 8, 2016). *Economics of Blockchain*. [Online]. Available: <https://ssrn.com/abstract=2744751>
9. Tapscott and D. Tapscott, "How blockchain is changing finance," *Harvard Bus. Rev.*, vol. 1, no. 9, p. 15, 2017.
10. Y. Guo and C. Liang, "Blockchain application and outlook in the banking industry," *Financial Innov.*, vol. 2, no. 1, p. 24, Dec. 2016.
11. H. Hou, "The application of blockchain technology in E-Government in China," in *Proc. 26th Int. Conf. Comput. Commun. Netw. (ICCCN)*, Jul. 2017, pp. 1-4.
12. K. Biswas and V. Muthukkumarasamy, "Securing smart cities using blockchain technology," in *Proc. IEEE 18th Int. Conf. High Perform. Comput. Commun., IEEE 14th Int. Conf. Smart City; IEEE 2nd Int. Conf. Data Sci. Syst. (HPCC/SmartCity/DSS)*, Dec. 2016, pp. 1392-1393.
13. N. Chauhan and R. K. Dwivedi, "A Secure Design of the Healthcare IoT System using Blockchain Technology," *2022 9th International Conference on Computing for Sustainable Global Development (INDIACom)*, 2022, pp. 704-709, doi: 10.23919/INDIACom54597.2022.9763187.

14. P. P. Ray, D. Dash, K. Salah and N. Kumar, "Blockchain for IoT-Based Healthcare: Background, Consensus, Platforms, and Use Cases," in *IEEE Systems Journal*, vol. 15, no. 1, pp. 85-94, March 2021, doi: 10.1109/JSYST.2020.2963840.
15. B. Alamri, K. Crowley and I. Richardson, "Blockchain-Based Identity Management Systems in Health IoT: A Systematic Review," in *IEEE Access*, vol. 10, pp. 59612-59629, 2022, doi: 10.1109/ACCESS.2022.3180367.
16. B. Mallikarjuna, D. Kiranmayee, V. Saritha and P. V. Krishna, "Development of Efficient E-Health Records Using IoT and Blockchain Technology," *ICC 2021 - IEEE International Conference on Communications*, 2021, pp. 1-7, doi: 10.1109/ICC42927.2021.9500390.
17. Azaria, A. Ekblaw, T. Vieira, and A. Lippman, "MedRec: Using blockchain for medical data access and permission management," in *Proc. 2nd Int. Conf. Open Big Data (OBD)*, Aug. 2016, pp. 25–30.
18. R. Chaudhary, A. Jindal, G. S. Aujla, S. Aggarwal, N. Kumar, and K.-K.-R. Choo, "BEST: Blockchain-based secure energy trading in SDN-enabled intelligent transportation system," *Comput. Secur.*, vol. 85, pp. 288–299, Aug. 2019.
19. S. Davidson, P. De Filippi, and J. Potts. (Mar. 8, 2016). *Economics of Blockchain*. [Online]. Available: <https://ssrn.com/abstract=2744751>
20. Tapscott and D. Tapscott, "How blockchain is changing finance," *Harvard Bus. Rev.*, vol. 1, no. 9, p. 15, 2017.
21. Y. Guo and C. Liang, "Blockchain application and outlook in the banking industry," *Financial Innov.*, vol. 2, no. 1, p. 24, Dec. 2016.
22. H. Hou, "The application of blockchain technology in E-Government in China," in *Proc. 26th Int. Conf. Comput. Commun. Netw. (ICCCN)*, Jul. 2017, pp. 1–4.
23. K. Biswas and V. Muthukkumarasamy, "Securing smart cities using blockchain technology," in *Proc. IEEE 18th Int. Conf. High Perform. Comput. Commun.*, IEEE 14th Int. Conf. Smart City; IEEE 2nd Int. Conf. Data Sci. Syst. (HPCC/SmartCity/DSS), Dec. 2016, pp. 1392–1393.

CryptoBoost: Empowering Crowdfunding through Blockchain Technology

Rameshwar Navarange, Roshan Kate,
Kshitij Sonawane

Vipul Katala, Ajit Patil

Bharati Vidyapeeth's College of Engineering
Lavale, Pune, Maharashtra
Affiliated to Savitribai Phule Pune University
✉ navrangerameshwar@gmail.com

ABSTRACT

Decentralized crowdfunding, a revolutionary financial paradigm with built-in benefits of transparency, security, and inclusion, has emerged as a result of the incorporation of blockchain technology into crowdfunding platforms. This study explores the idea and ramifications of decentralized crowdfunding platforms built on the fundamentals of blockchain technology. We look at how decentralized applications (dApps), smart contracts, and tokenization are redefining crowdfunding by removing middlemen, encouraging trust, and democratizing access to capital. We clarify the advantages, difficulties, and unrealized potential of decentralized crowdfunding through in-depth analysis and case studies. We also handle the legal environment, scalability challenges, and changing dynamics of this developing area. Decentralized crowdfunding is likely to change fundraising as blockchain technology develops, concepts, empowering business owners and investors while fostering an open and fair financial system.

KEYWORDS : *Blockchain, Fundraisers, Crowdfunding, Decentralized, Framework, Ethereum, Merkle tree.*

INTRODUCTION

Innovating decentralised crowdfunding systems that harness the power of virtual currencies like Bitcoin to democratise access to capital for both investors and business owners are now possible because to the convergence of blockchain technology and crowdfunding. Traditional crowdfunding techniques have already changed the financial landscape by allowing producers to raise funds from a sizable group of backers. However, these strategies continue to rely on middlemen and may have inefficiencies and trust issues. A new paradigm that offers unmatched levels of transparency, security, and financial inclusion is presented with the advancement of blockchain technology and its integration into crowdfunding.

In this paper, we thoroughly investigate a decentralised crowdfunding platform. that makes use of blockchain technology, with a particular emphasis on integrating Bitcoin and implementing of the user log-in and log-out

features. We will give an overview of the fundamental ideas, highlight the driving forces behind this research, lay out the goals, and emphasise the significance of this ground-breaking platform in the context of contemporary finance and technology in this introduction part.

Background and context: By allowing entrepreneurs, artists, and visionaries to interact with a global audience of potential supporters, traditional crowdfunding sites like Kickstarter and Indiegogo have played a crucial part in changing fundraising. By dramatically lowering entry barriers, these platforms enable creators to raise money for their initiatives or enterprises without the use of conventional financial intermediaries. However, they continue to use centralised systems to handle user accounts and conduct transactions, which might pose trust issues. These issues can be resolved with the help of blockchain technology, which was introduced in 2009 along with the launch of Bitcoin. Blockchain is a decentralised and distributed ledger system that uses

a network of computers to securely and openly record transactions. The most well-known cryptocurrency, Bitcoin, is based on blockchain technology and functions as a digital money and store of value. Decentralisation, immutability, and transparency are three characteristics of blockchain that make it the perfect technology to transform the crowdfunding industry.

REVIEW OF THE LITERATURE

Blockchain technology and crowdfunding platforms have drawn a lot of interest from academics and professionals alike. This literature review traces the history of blockchain-related crowdfunding from its early origins to its current stage, examining major topics, trends, and research that shed light on the junction of these two areas.

The Development of Crowdfunding Historically

- The idea of crowdfunding first emerged in the early 2000s, primarily on websites like ArtistShare and Kiva. These platforms used the internet to link artists with a large community of backers, enabling them to generate money for artistic and humanitarian endeavours
- Traditional payment methods and centralised intermediaries were prevalent during this early stage of crowdsourcing. It marked the start of the process of democratising capital access.
- Although these platforms played a key role in the growth of crowdfunding, they were limited by problems with costs, reliability, and accessibility internationally.

Bitcoin and blockchain technology's emergence

A huge paradigm change was brought about by Satoshi Nakamoto's launch of Bitcoin and blockchain technology in 2009. The first actual use of blockchain was with Bitcoin. With its fundamental tenets of decentralisation, immutability, and transparency, blockchain swiftly emerged as a ground-breaking technology with uses far beyond digital currency.

Early Crowdfunding on Blockchain

The idea of blockchain-based crowdfunding was first investigated by blockchain enthusiasts in the early 2010s.

The Bitcoin network was used by initiatives like Mastercoin (now Omni Layer) and Counterparty to produce tokens that represented assets. These tokens effectively invented the idea of initial coin offerings (ICOs), which could be used for fundraising.

These early experiments showed the blockchain's potential to enable fundraising without the use of middlemen.

The Rise of Smart Contracts and Ethereum

By introducing Ethereum in 2015, Vitalik Buterin marked a crucial turning point in the history of the blockchain. Smart contracts, self-executing code that might automate complicated transactions without the need for middlemen, were first offered by Ethereum.

Decentralised apps (dApps), especially those pertaining to crowdfunding, were made possible by smart contracts. The 2014 ICO for Ethereum served as a blueprint for generating significant funds through token sales.

Security Token Offerings (STOs) Are Growing

Security Token Offerings (STOs) have become popular in order to allay regulatory worries and provide a more legal crowdfunding option. Real-world assets, like equities or real estate, are tokenized through STOs, allowing investors to participate while adhering to securities laws. STOs aimed to bring together the benefits of blockchain technology with the regulatory environment of conventional stocks.

Future Innovations and Prospects

- Blockchain-based crowdfunding has a very bright future. Non-fungible tokens (NFTs), an innovation, are being used into crowdfunding projects to reward backers with distinctive assets.
- Cross-chain solutions are designed to improve interoperability by facilitating the seamless transfer of assets and tokens between various blockchain networks.

Final thoughts

The history of blockchain-related crowdfunding is evidence of how technology has the power to revolutionise fundraising strategies. The path has been

characterised by innovation, difficulties, and regulatory advancements, starting with early tokenization experiments and continuing through the ICO boom and the advent of STOs. Blockchain-based crowdfunding is poised to open up new options for business owners and investors as technology develops and the regulatory framework matures, promoting innovation and inclusivity in the financial sector. This overview of the literature emphasises how dynamic and everchanging blockchain crowdfunding is. It emphasises the demand for a well-balanced strategy that makes use of blockchain technology's benefits while addressing regulatory issues, guaranteeing investor protection, and fostering financial inclusion. The history of blockchain-related crowdfunding is evidence of the financial industry's ongoing commitment to innovation.

Crowdfunding with Blockchain Technology

Traditional crowdfunding approaches have been transformed by blockchain technology, which was founded on the ideals of decentralisation, transparency, and security. This section explores the primary ways that blockchain technology has been incorporated into crowdfunding, revolutionising the industry and presenting fresh approaches to age-old problems.

Smart Contracts

Blockchain-based crowdfunding now relies heavily on smart contracts, self-executing code that is stored on the blockchain. Numerous components of crowdfunding campaigns, such as fund collection, dividend or reward distribution, and even governance systems, are automated via smart contracts. These contracts do away with the need for middlemen, which lowers expenses, boosts efficiency, and builds trust in the crowdfunding process.

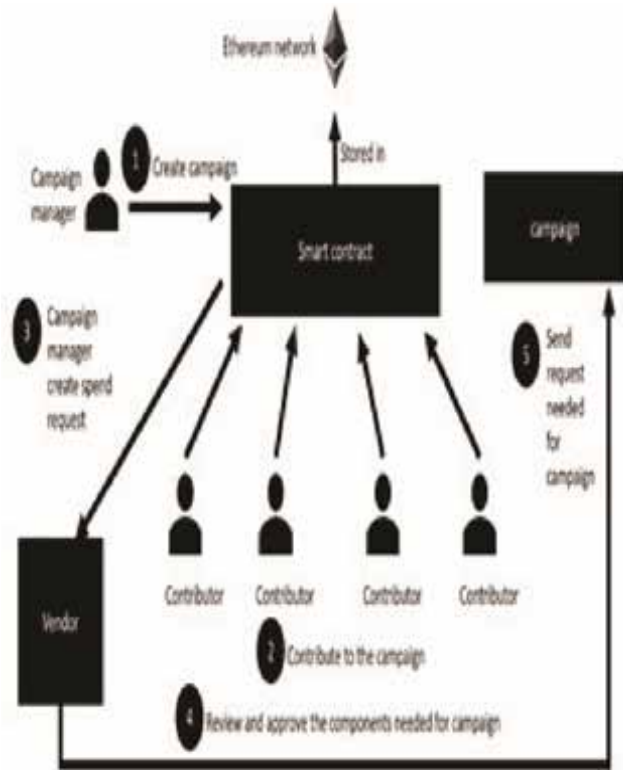


Fig. 2. Flow of ether in proposed blockchain model

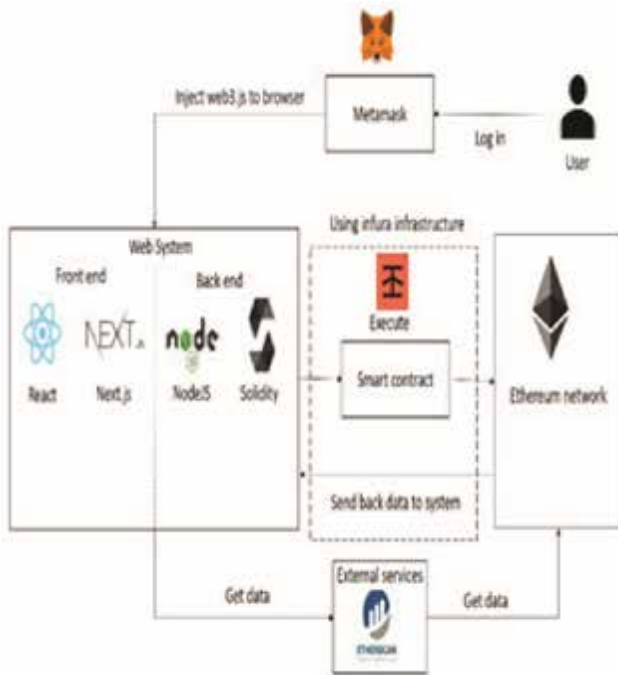
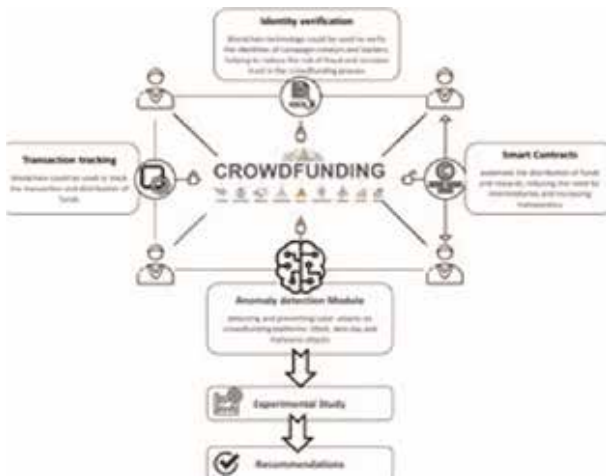


Fig. 1. System architecture

Trust and Transparency

Blockchain's transparency is very helpful for crowdfunding. Every transaction and donation is noted on a public ledger that anybody can inspect and confirm. The ability to track the distribution of cash and the fulfilment of pledges in real-time strengthens confidence between creators and backers. Blockchain's openness reassures backers of the integrity of crowdfunding projects in an age marred by worries about fraud and the misappropriation of funds.



Accessibility everywhere and inclusivity

Geographical barriers are irrelevant because to blockchain technology, which makes crowdfunding campaigns accessible worldwide. Without the constraints imposed by conventional banking systems and currencies, creators can find supporters from all around the world.

DIFFICULTIES AND RISKS

Blockchain technology has many benefits for crowdfunding platforms, but it also comes with a number of dangers and issues that need to be properly evaluated. The main difficulties and dangers related to blockchain-based crowdfunding are examined in this section.

Regulatory Uncertainty

Uncertainty can arise for platform operators, creators, and backers as a result of changing and inconsistent regulatory frameworks between nations.

It can be complicated and risky to comply with tax rules, anti-money laundering (AML) regulations, and securities laws.

Investor Protection

It can be difficult to guarantee effective investment protection. In the event of project failure or conflicts, backers could not have legal redress.

Strong risk assessment and disclosure processes are necessary to shield funders from dubious or dangerous ventures.

Smart Contract Vulnerabilities

- Despite their strength, smart contracts are not immune to flaws. Security lapses or exploitation might result from bugs or weaknesses in smart contract code.
- Although thorough code audits and testing are essential, risks still exist.

Privacy Issue

- Transparency and privacy must be carefully balanced. User data is required for KYC and AML, which raises privacy issues.
- Finding the ideal balance between upholding regulations and protecting user privacy is a neverending task.

Scalability Restrictions

- Many blockchain networks struggle to scale, which causes poor transaction speeds and high fees during periods of heavy demand.
- Crowdfunding campaigns may suffer from blockchain congestion as scalability solutions continue to develop.

TECHNICAL IMPLEMENTATION AND INFRASTRUCTURE

- The technical framework and implementation techniques used have a big impact on how well blockchain technology is incorporated into crowdfunding platforms. The essential elements, architectural considerations, and implementation strategies for developing blockchain-based crowdfunding systems are examined in this section.

Blockchain Selection

- A crucial choice is which blockchain network to use. Scalability, security, consensus processes, and ecosystem support are a few factors that must be taken into account.
- Other cryptocurrencies like Polkadot, Binance Smart Chain, and Ethereum provide unique benefits and support various use cases.

Smart Contracts

- The foundation of blockchain-based crowdfunding systems is smart contracts. They outline the reasoning behind crowdfunding campaign regulations.

- To ensure security and dependability, smart contracts should be thoroughly coded, inspected, and tested.

Token Requirements

It's important to choose the right token specifications. Different uses are served by ERC-20, ERC-721 (NFTs), and more recent standards like ERC-1400 (security tokens).

For instance, security tokens must abide by legal requirements like ERC-1404.

User Wallets

For users to take part in crowdfunding initiatives, secure wallets are required. The chosen blockchain should be compatible with wallets, and they should offer a userfriendly interface.

Security is improved by integration with hardware wallets.

Identity confirmation:

The KYC and AML processes frequently call for identification confirmation. Compliance requires integrating trustworthy identity verification services.

To safeguard user data, privacy-focused techniques like zero-knowledge proofs may be taken into consideration.

User Experience (UX)

User adoption is greatly influenced by UX design. Platforms ought to provide consumers with user-friendly interfaces that lead them through the crowdsourcing process.

Security precautions

Security comes first. It is crucial to have multi-factor authentication, cold storage for money, and thorough auditing of smart contracts.

Penetration testing and regular security audits both aid in locating vulnerabilities.

CONCLUSION

Finally, integrating blockchain technology with crowdfunding sites presents a revolutionary approach. By enabling smart contracts and immutable transaction records, it improves security, trust, and transparency. Decentralized systems give global

participants an even playing field and less dependence on middlemen. Blockchain-powered crowdfunding can be advantageous for backers as well as project creators because it minimizes the possibility of fraud and increases accountability. Additionally, it might make it easier for entrepreneurs and innovators to obtain financing. However, for broad usage, issues like scalability and regulatory compliance need to be resolved. In general, the incorporation of blockchain technology into crowdfunding platforms offers a stimulating prospect for the advancement of investing and fundraising in the future.

REFERENCES

1. https://www.researchgate.net/publication/334142321_Blockchain_based_crowdfunding_systems
2. https://ijirt.org/master/publishedpaper/IJIRT158590_PAPER.pdf
3. <https://link.springer.com/article/10.1007/s10660-02209634-9>
4. https://www.academia.edu/44173220/APPLICATION_OF_BLOCKCHAIN_TECHNOLOGY_OF_CROWDFUNDING_USING_SMART_CONTRACT
5. <https://link.springer.com/article/10.1007/s11301-02000189-3>
6. <https://www.degruyter.com/document/doi/10.1515/erj2015-0045/pdf>
7. https://www.researchgate.net/publication/300558605_Crowdfunding_A_Literature_Review_and_Research_Directions
8. <https://jfinswufe.springeropen.com/articles/10.1186/s40854-022-00345-6>
9. <http://journalcra.com/article/exploratory-studycrowdfunding-platforms-india>
10. https://www.researchgate.net/publication/346708922_Crowdfunding_Using_Blockchain
11. <https://www.warse.org/IJATCSE/static/pdf/file/ijatcse83932020.pdf>
12. <https://ijert.org/papers/IJCRT2305284.pdf>
13. <https://journals.indexcopernicus.com/api/file/viewByFileId/594400>

SMART Interview System

K. M. Sanghavi, Pranita Borse,
Sanjeevani Gandhakse

Swayam Dugaje, Sakshi Vyas

Department of Computer Engineering
Snjb's Jain College of Engineering
Chandwad, Maharashtra
✉ sanghavi.kmcoe@snjb.org

ABSTRACT

The recruitment and retention of employees in organizations have significantly increased in importance due to the highly competitive global market. There is also a growing demand for managers to possess emotional intelligence to effectively manage and enhance the productivity of employees from generations Y and Z. While humanoid robots have gained widespread awareness, there are only a few commercially available examples. This paper outlines various use cases for humanoid robots in an innovative artificial-based environment and introduces the concept of an AI-based Recruitment Robot, designed to serve as a digital consultant in the interview process for all companies. The robot's functionalities range from acting as a concierge for new guests to serving as a tutor for AI and answering questions in open and project-specific domains. In addition to the built-in speech and visual recognition system, the robot integrates novel AI technologies and social collaboration tools to become a social robot. The smart voice-based interview system offers streamlined, efficient, and automated interview processes, enhancing the candidate experience and ensuring objective evaluation for fair and accurate hiring decisions.

KEYWORDS : *Interview system, Speech-to-text conversion, Text-to-speech conversion, Flutter, Dart, Recruitment system.*

INTRODUCTION

In today's fast-paced and technology-driven world, the traditional methods of conducting job interviews are evolving rapidly. The advent of artificial intelligence and voice recognition technology has given rise to a groundbreaking innovation - the Smart Voice-Based Interview System. This innovative system leverages the power of voice recognition and AI to transform the interview process, making it more efficient, convenient, and inclusive.

The Smart Voice-Based Interview System aims to revolutionize the way organizations screen and assess candidates by replacing the conventional in-person or video interviews with an automated, AI-driven platform. This system allows candidates to respond to interview questions using their voices, while advanced algorithms analyze their responses for various parameters such as tone, content, and communication skills. This not only streamlines the interview process but also eliminates

potential interviewer biases, making it a game-changer in the realm of talent acquisition.

The proposed system represents a significant step forward in redefining the future of recruitment and promises to save time, reduce costs, and ultimately lead to better hiring decisions. This report aims to present the varied viewpoints of different scholars and authors with respect to the voice-based recruitment process. Voice-based recruitment is not limited to advertising jobs on websites and other social media platforms; rather, it is a complex phenomenon. Analyzing the different views of scholars and authors will be beneficial in gaining a better understanding and awareness about the scope of voice-based recruitment processes. The process in question is to select the right candidates for the right kinds of positions.

The proposed methodology for the voice-based interview system integrates cutting-edge technologies such as artificial intelligence, image processing, and soft

computing to create an Emotionally Intelligent Robotic System aimed at revolutionizing the recruitment process. The overarching goal is to overcome the limitations inherent in traditional interview processes by introducing a more objective, uniform, and technologically advanced approach.

The literature review in this paper focuses on two main themes to gain an overview of voice-based recruitment processes and the quality of selection. The use of efficient recruitment strategies can help organizations recruit employees and workers with high potential and execute talent management strategies in an enhanced manner. Since the 1990s, fundamental changes in recruitment practices have been observed, with recruitment through online procedures increasing enormously due to the growth in the global economy, which has raised the demand for talented potential employees and workers in an organization. The interview system is designed with three main components: a text-to-speech engine, speech recognition, and a dialogue system. The text-to-speech engine vocalizes questions to candidates, ensuring a consistent and clear delivery, while the speech recognition component captures and transcribes candidates' audio responses into text, facilitating easy analysis. The dialogue system manages the flow of the interview, creating a seamless and natural conversation between the candidate and the robotic interviewer.

RELATED WORK

Yi-Chi Chou, Felicia R. Wongso, Chun-Yen Chao and Han-Yen Yu, et.al [1] This study designed a video interview platform to assist recruiters in effectively selecting potential candidates and provide job candidates a means to conduct mock interviews.

Dulmini Yashodha Dissanayake, Venuri Amalya, Raveen Dissanayaka, Lahiru Lakshan, Pradeepa Samarasinghe, Madhuka Nadeeshani, Prasad Samarasinghe, et.al [2] The system was carried out using deep learning and machine learning models which achieved accuracies over 85% for all smile, eye gaze, emotion, and head pose analysis. Our findings indicate that nonverbal behavioral cues can be utilized to determine personality traits.

R. Mandal, P. Lohar, D. Patil, A. Patil and S. Wagh, et.al [3] This paper proposed an AI-based mock interview

platform that would operate as an intermediary between the actual interview & preparation mode. Our system will assess the user based on an aggregation of three parameters called emotions, confidence, & knowledge base.

PREVIOUS WORK

Natural Language Processing in Interview Assessment

The integration of natural language processing (NLP) in interview assessment systems has been a burgeoning area of research in recent years. Several studies have explored the application of NLP techniques to analyze the linguistic aspects of interviews, focusing on candidates' communication skills, content quality, and overall verbal fluency. This aligns with the proposed system's approach to providing realistic mock interview experiences using NLP and speech recognition. Researchers have demonstrated the potential of NLP in capturing nuanced aspects of language use, including sentiment analysis and conversational coherence. The current work builds upon these foundations, aiming to not only evaluate verbal communication but also delve into non-verbal cues for a comprehensive assessment of candidates' performance during mock interviews

AI-Driven Interview Platforms for Skill Enhancement

Existing literature highlights the increasing adoption of AI-driven interview platforms designed to aid candidates in honing their interview skills. These platforms leverage machine learning algorithms to assess various facets of interview performance, offering personalized feedback and suggestions for improvement. The proposed system's emphasis on providing valuable feedback aligns with this trend, contributing to the broader goal of enhancing job seekers' interview techniques. By detailing the design, implementation, and evaluation of the AI-driven platform, this research adds to the growing body of knowledge on how technology can be effectively harnessed to facilitate more effective interview preparation and analysis, ultimately benefiting both candidates and hiring organizations.

Computer Vision and NLP Fusion for Objective Evaluation

The fusion of computer vision and NLP techniques in interview assessment is a frontier where limited research has been conducted, particularly in the context of evaluating non-verbal cues. The proposed system advances the field by employing computer vision alongside NLP and machine learning to automate the analysis of facial expressions, body language, and speech patterns. Research in this area typically emphasizes the potential to provide more objective and standardized evaluations, aiming to mitigate biases in interview assessment processes. This aligns with the broader goal of enhancing the overall quality of candidate evaluation. As the system seeks to automate the analysis of behavioral traits such as confidence, honesty, and engagement, it contributes to the ongoing efforts to make interview or viva voce assessments more transparent, fair, and technologically advanced.

LIMITATION IN THE PREVIOUS WORK

Despite its promising features, the AI-driven interview evaluation system has certain limitations. Firstly, its effectiveness heavily relies on the quality and diversity of the training dataset. If the dataset lacks representation across various industries, job roles, and cultural contexts, the system may struggle to accurately assess candidates in diverse scenarios.

Another limitation is the potential challenge in interpreting nuanced emotional states accurately. The system may face difficulty distinguishing between subtle emotional cues or context-specific behaviors, leading to potential misinterpretations of candidates' true sentiments.

Moreover, the system's reliance on audiovisual data analysis may raise privacy concerns. Ensuring the ethical use and secure storage of sensitive information, especially facial expressions and speech patterns, is crucial to maintaining candidate trust and complying with data protection regulations.

Lastly, the system's success is contingent on candidates having access to the necessary technology and a stable internet connection. Socioeconomic disparities may limit some individuals from benefiting fully, potentially introducing biases in the accessibility and

usability of the platform. These limitations underscore the importance of continuous refinement and ethical considerations in the development and deployment of such AI-driven tools.

PROPOSED METHODOLOGY

The foundation of our methodology lies in the integration of a psychology-based selling behavior model, acknowledging that successful recruitment extends beyond evaluating technical skills to assessing candidates' attitudes and emotional intelligence. By incorporating psychological insights into the design, the system aims to capture and interpret nuanced behavioral cues during interviews, providing a holistic evaluation of candidates' suitability for the organization.

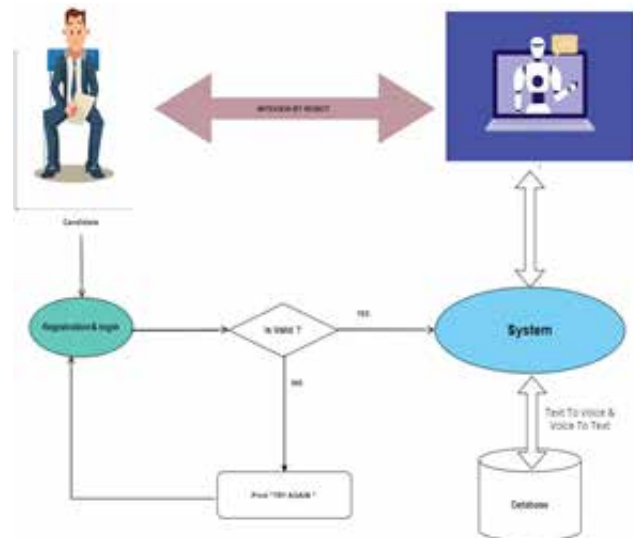


Fig 1. Proposed System Architecture

The core intelligence of the voice-based interview system is derived from the synergy of artificial intelligence and soft computing techniques. These components work in tandem to process and analyze the vast array of data generated during interviews. Artificial intelligence contributes to the system's ability to adapt and learn from each interaction, refining its assessment criteria over time. Soft computing techniques enhance the system's capacity to handle uncertainty and imprecise information, allowing for a more nuanced understanding of candidates' responses and emotional states.

To emulate a realistic and interactive interview

experience, the methodology employs image processing to enable the robotic system to exhibit rich human-like characteristics. This includes gestures and emotive facial expressions, ensuring that the interaction is not only based on verbal communication but also encompasses non-verbal cues. The integration of image processing enhances the overall engagement and authenticity of the interview, providing a comprehensive evaluation of candidates' suitability beyond just verbal responses.

Fig. 1 shows the block diagram of the proposed system. This figure illustrates the standard system flow of our innovative architecture, wherein candidates initiate the process by registering on the system. Subsequently, candidates can access the system through a rigorous validation process, ensuring only those with valid credentials gain entry. The core of our proposed system features a robust database responsible for storing question-answer datasets and candidate feedback. Simultaneously, a dedicated computer system handles the user interface, efficiently presenting the system's graphical elements. This cohesive structure ensures a seamless and secure experience for candidates interacting with the system.

The interview system consists of three main components: Text-to-Speech Engine, Speech Recognition and Dialogue System. The text-to-speech engine is responsible for delivering questions to candidates, while the speech recognition component transcribes their audio responses into text for analysis. The dialogue system manages the conversation between the candidate and the robotic interviewer, ensuring a smooth and natural interaction.

WORKING MODULE

The proposed project for the Smart Voice-Based Interview System envisions the development of a robust and user-friendly platform using Flutter for desktop applications. The primary focus lies in the integration of natural language processing and machine learning algorithms to analyze candidates' responses comprehensively, evaluating communication skills and determining their suitability for specific roles.

The working of the Flutter desktop application will be structured around three core components: the text-to-speech engine, speech recognition, and the dialogue system.

Text- to - Speech Engine

A Text-to-Speech (TTS) engine for a voice-based interview system operates by converting written text into natural-sounding spoken language. The process typically involves three main stages: text analysis, phonetic interpretation, and audio synthesis. In the text analysis stage, the engine breaks down the input text into linguistic elements such as words, phrases, and sentences. The phonetic interpretation phase assigns appropriate phonetic representations to these linguistic elements. Finally, in the audio synthesis stage, these phonetic representations are converted into a waveform that represents the corresponding speech sounds. The resulting audio is then played back to users, producing human-like speech. For voice-based interview systems, this technology enables an interactive and dynamic user experience, allowing the system to verbally communicate questions and responses, facilitating a natural and engaging interview process.

Speech Recognition

A speech recognition library facilitates the voice-based interview system by employing sophisticated algorithms and models to convert spoken words into text. The process begins with audio input, which is then processed through acoustic models to identify phonetic elements. The recognized phonemes are further analyzed using language models, which leverage semantic analysis to understand the contextual meaning of words and phrases. Text matching algorithms are then applied to compare the extracted semantic content with predefined criteria for interview evaluation. This enables the system to assess not only the accuracy of speech recognition but also the relevance and coherence of the responses in the context of the interview questions, enhancing the overall performance of the voice-based interview system through comprehensive semantic analysis.

Dialogue System

A voice-based interview system employing a dialogue system for answer matching utilizes semantic analysis to comprehend and interpret spoken responses. The system employs natural language processing techniques to understand the meaning and context of the interviewee's answers. Semantic analysis involves mapping the spoken words to their underlying meanings

and identifying relationships between different elements of the response. Answer matching is then performed by comparing the semantic representation of the provided answer with the expected criteria or model responses. Once the matching process is complete, the system generates appropriate results or feedback based on the analysis, providing a dynamic and context-aware interaction in voice-based interviews. This comprehensive approach enhances the system's ability to understand nuances, detect subtle cues, and generate relevant and meaningful responses in real-time, thereby optimizing the interview process.

Flutter desktop Application

A Flutter desktop application for a voice-based interview system leverages the Flutter framework's cross-platform capabilities to create a user-friendly interface for conducting interviews. The application integrates speech recognition technology to capture and transcribe spoken responses, facilitating a seamless and efficient interview process. Utilizing Dart programming language and Flutter's rich widget library, the application ensures a consistent user experience across different desktop platforms. It incorporates features such as audio recording, playback, and analysis to assess candidates' communication skills. The modular and customizable nature of Flutter allows for easy integration of additional functionalities, such as interview scheduling, result analysis, and collaboration tools, making it a versatile and powerful solution for modern voice-based interview systems on desktop environments.

The system will record both video and cognitive responses, which will then be used for emotional profiling and cognitive profiling. This will result in a comprehensive benchmarking of candidates, providing a holistic view of their strengths and weaknesses. The emotional profiling component will analyze the video and cognitive responses to identify the emotional state of the candidates, while the cognitive profiling component will analyze the cognitive responses to understand the candidates' problem-solving abilities, critical thinking skills, and other cognitive traits. This process can help identify the most suitable candidates for various roles and responsibilities.

The overarching goal of the project is to redefine the interview landscape by introducing a technologically

advanced and accessible solution. Real-time voice analysis, automated question generation, customizable interview templates, and detailed performance analytics will be key features, empowering both candidates and interviewers. Furthermore, the integration with existing HR systems will ensure a seamless flow of data, enhancing the overall efficiency of the recruitment process for organizations.

The project aims to transform the interview landscape by introducing an innovative Smart Voice-Based Interview System through a Flutter desktop application. This system incorporates advanced technologies, including real-time voice analysis, to evaluate candidates based on their spoken responses. Automated question generation ensures a dynamic and fair interview process, while customizable interview templates allow tailoring assessments to specific roles. Detailed performance analytics provide valuable insights for both candidates and interviewers, facilitating objective evaluations. Integration with existing HR systems streamlines data flow, enhancing overall recruitment efficiency. Ultimately, this initiative seeks to revolutionize traditional interview methodologies, offering a modern, convenient, and objective approach to candidate evaluation that empowers both candidates and organizations in the recruitment process.

In essence, the Flutter desktop application for the Smart Voice-Based Interview System aspires to revolutionize traditional interview methodologies, offering a modern, convenient, and objective approach to candidate evaluation.

SYSTEM GRAPHICAL INTERFACE



Fig 2. Login Page

Fig 2. shows the login page of the model in GUI. In this page users can fill in the valid email and password for login to the page.



Fig 3. Register Page

Fig 3. shows the register page of the model in GUI. In this page users can fill in the valid information to register the page.



Fig 4. Result Page

Fig 4. shows the result page of the model in GUI. In this page the result of the user can be generate.

CONCLUSION

In conclusion, the proposed voice-based interview system employing voice assistance represents a user-centric platform that seamlessly integrates natural language processing and speech recognition technologies. Through intuitive voice commands and responses, the system facilitates interactive mock interview sessions with customizable scenarios and questions. Leveraging realistic interview simulations, it evaluates users' responses on multiple criteria,

including content and clarity, offering constructive feedback and performance assessments. The system's adaptability, guided by user feedback and progress, ensures personalized and progressively challenging interview practice. This technical innovation strives to provide a convenient, technologically advanced, and personalized approach for users to hone their interview skills, fostering increased confidence and readiness for real-world interview scenarios.

REFERENCES

1. Yi-Chi Chou, Felicia R. Wongso, Chun-Yen Chao and Han-Yen Yu, "An AI Mock-interview Platform for Interview Performance Analysis", 10th International Conference on Information and Education Technology, 2022.
2. Dulmini Yashodha Dissanayake, Venuri Amalya, Raveen Dissanayaka³, Lahiru Lakshan, Pradeepa Samarasinghe, Madhuka Nadeeshani, Prasad Samarasinghe, "AI-based Behavioural Analyser for Interviews/Viva" IEEE 16th International Conference on Industrial and Information Systems (ICIIS),2021.
3. R. Mandal, P. Lohar, D. Patil, A. Patil and S. Wagh, "AI -Based mock interview evaluator: An emotion and confidence classifier model," 2023 International Conference on Intelligent Systems for Communication, IoT and Security (ICISCoIS), Coimbatore, India, 2023, pp. 521-526, doi: 10.1109/ICISCoIS56541.2023.10100589.
4. Vikash Salvi, Adnan Vasanwalla, Niriksha Aute and Abhijit Joshi,"Virtual Simulation of Technical Interviews", IEEE 2017.
5. Y. C. Chou and H. Y. Yu, "Based on the application of AI technology in resume analysis and job recommendation", IEEE International Conference on Computational Electromagnetics(ICCEM), pp. 291-296, 2020.
6. Aditi S. More, Samiksha S. Mobarkar, Siddhita S. Salunkhe, Reshma R. Chaudhari,"SMART INTERVIEW USING AI", TECHNICAL REACHER ORGANIZATION OF INDIA, 2022.
7. Danai Styliani Moschona," An Affective Service based on Multi-Modal Emo on Recognition, using EEG enabled Emotion Tracking and Speech Emotion Recognition", IEEE 2022.
8. Luis Felipe ParraGallegoa, Juan Rafael Orozco-Arroyave, "Classification of emotions and evaluation

- of customer satisfaction from speech in real-world acoustic environments", ELSEVIER 2022.
9. Xinpei Jin^{1,2}, Yulong Bian^{*1,2}, Wenxiu Geng^{1,2}, Yeqing Chen^{1,2}, Ke Chu^{1,2}, Hao Hu^{1,2}, Juan Liu^{1,2}, Yuliang Shi^{1,3}, and Chenglei YangXinpei Jin, Yulong Bian, Wenxiu Geng, Yeqing Chen, Ke Chu, Hao Hu, Juan Liu, Yuliang Shi, and Chenglei Yang, "Developing an Agent-based Virtual Interview Training System for College Students with High Shyness Leve", IEEE 2022.
 10. Honda Motor Co., Inc.: "ASIMO | Frequently Asked Questions" (PDF). <http://asimo.honda.com/downloads/pdf/asimo-technical-faq.pdf> Retrieved Jan 7, 2019.
 11. Shiotani, S., Kemmotsu, K., Oonishi, et al. (2006). World's first full fledged communication robot "Wakamaru" capable of living with family and supporting persons. Mitsubishi Heavy Industries, Ltd. Technical Review, 43(1).
 12. AldebaranNaorobot. <https://www.softbankrobotics.com/emea/en/nao> Retrieved Jan 11, 2019.
 13. Aldebaran Pepper. <https://www.softbankrobotics.com/emea/en/pepper> Retrieved Jan 11, 2019.
 14. Softbank's Robotics Business Prepares To Scale Up. Forbes, May 30 2018. <https://www.forbes.com/sites/parmyolson/2018/05/30/softbankrobotics-busin-ess-pepper-boston-dynamics>
 15. Statt, N.: Hilton and IBM built a Watson-powered concierge robot. The Verge, National Park 2016

Digital Evolution in Construction: Exploring the Impact of eCommerce Platforms on Efficiency and Collaboration

Uday C. Patkar

HOD

Department of Computer Engineering
Bharati Vidyapeeth's College of Engineering
Lavale, Pune, Maharashtra

✉ patkarudayc@gmail.com

Om Bhamare, Tejal Abhivant

Students

Department of Computer Engineering
Bharati Vidyapeeth's College of Engineering
Lavale, Pune, Maharashtra

✉ ombhamare75@gmail.com

✉ tejalabhivant02@gmail.com

ABSTRACT

In the contemporary landscape of the construction industry, the integration of eCommerce platforms has sparked a digital evolution, reshaping traditional practices and fostering a new era of efficiency and collaboration. This research paper delves into the profound impact of eCommerce platforms on construction processes, aiming to explore the intricate dynamics that contribute to enhanced efficiency and collaboration within the sector.

The study begins by examining the current state of the construction industry, identifying key challenges and inefficiencies that have historically impeded progress. It then transitions to an in-depth analysis of various eCommerce platforms specifically tailored for the construction domain. Through a comprehensive review of existing literature and case studies, this research seeks to uncover the transformative potential of these platforms in streamlining procurement, project management, and communication among stakeholders.

Efficiency, a cornerstone of success in any industry, takes centre stage in our exploration. By scrutinizing the digitization of procurement processes, project planning, and resource management facilitated by eCommerce platforms, we aim to elucidate how these advancements contribute to time and cost savings.

KEYWORDS: *eCommerce platforms construction industry, Digital evolution, Collaboration, Project management, Digital transformation, Stakeholder communication, Construction technology, Supply chain digitization.*

INTRODUCTION

In the dynamic landscape of the construction industry, the advent of eCommerce platforms marks a pivotal moment in the ongoing digital evolution. As the demand for efficiency and collaboration continues to shape contemporary business practices, the construction sector is witnessing a transformative shift propelled by digital technologies. This research embarks on an exploration of the profound impact of eCommerce platforms on the efficiency and collaboration dynamics within the construction industry.

Historically characterized by traditional processes, the construction sector has faced challenges in optimizing project timelines, managing resources, and

fostering seamless collaboration among stakeholders. The integration of eCommerce platforms presents a promising avenue for overcoming these challenges, ushering in a new era of digital efficiency and interconnected teamwork.

The primary focus of this research is to dissect the multifaceted implications of eCommerce platforms in construction processes. From procurement to project management, these platforms promise to streamline operations, reduce costs, and enhance overall project outcomes. The study aims to unravel the intricacies of this digital transformation, shedding light on the ways in which eCommerce tools contribute to time and resource efficiencies.

Collaboration, a cornerstone of successful construction projects, stands as a key aspect under scrutiny. With a shift towards virtual collaboration and real-time communication facilitated by eCommerce platforms, the traditional barriers to effective teamwork are being dismantled. Architects, contractors, suppliers, and other stakeholders are brought into a cohesive digital ecosystem, fostering collaboration and information exchange in unprecedented ways.

Additionally, this research addresses the challenges inherent in the adoption of eCommerce platforms within the construction industry. The intricacies of data security, user adoption, and interoperability are examined to provide a comprehensive understanding of the considerations that accompany the digital transformation journey.

In essence, this study endeavors to contribute valuable insights into the evolving landscape of the construction industry, where eCommerce platforms emerge as catalysts for change. By navigating the intricate intersections of efficiency and collaboration, this research aims to provide a roadmap for industry professionals, policymakers, and researchers seeking to harness the transformative potential of eCommerce in construction. As we delve into this digital frontier, the subsequent sections will unveil the layers of impact and uncover the intricate nuances of eCommerce integration in the construction sector.

LITERATURE REVIEW

eCommerce Platforms in the Construction Industry

Historical Perspectives on Construction Procurement

Explore traditional methods of procurement in construction and their limitations.

Discuss how eCommerce platforms have evolved as solutions to address these limitations.

Sources:

1. Arditi, D., & Nawakorawit, K. (1999). The impact of the Internet on procurement. *Automation in Construction*, 8(3), 351-360.
2. Ng, S. T., & Chen, S. E. (2002). Internet-based construction procurement systems: A Hong Kong perspective. *Automation in Construction*, 11(4), 447-459.

Digital Tools in Project Management

Examine the historical and contemporary challenges in project management within the construction industry.

Discuss how eCommerce platforms contribute to improved project planning, scheduling, and resource management.

Sources:

1. Kang, Y., Lee, J., & Koo, C. (2013). Integrating BIM and E-commerce: A study on cloud computing-based construction project management system. *Advanced Engineering Informatics*, 27(4), 553-563.
2. O'Brien, W. J., & Fischer, M. (2000). *Integrated project delivery: A guide*. Stanford University.

Collaboration in Construction Projects

Explore traditional collaboration models and challenges among stakeholders in construction projects.

Discuss how eCommerce platforms facilitate enhanced collaboration, real-time communication, and information sharing.

Sources:

1. Wang, X., & Wong, A. (2009). An Internet/Web-based integrated construction management system for project collaboration. *Automation in Construction*, 18(7), 929-942.
2. Akintoye, A., & Fitzgerald, E. (2000). A survey of current cost estimating practices in the UK. *Construction Management and Economics*, 18(2), 161-172.

Case Studies on Successful Implementations

Present case studies of construction projects that have successfully implemented eCommerce platforms.

Analyze the outcomes, identifying lessons learned and best practices.

Sources:

1. Azhar, S., Carlton, W. A., Olsen, D., & Ahmad, I. (2011). Building information modeling for sustainable design and LEED® rating analysis. *Automation in Construction*, 20(2), 217-224.

2. Atkin, B., & Brooks, B. (2009). Total BIM management for facility owners. *Journal of Information Technology in Construction*, 14, 657-670.

Research Design

Type of Research: Employ a mixed-methods research design that combines qualitative and quantitative approaches.

Justification: This approach allows for a comprehensive understanding by capturing both qualitative insights and quantitative data.

Sampling Strategy

Selection Criteria: Define criteria for selecting construction projects and stakeholders involved.

Sampling Technique: Utilize purposive sampling for selecting relevant construction projects and stakeholders.

Sample Size: Determine the sample size based on the diversity and significance of the selected projects.

Justification: This approach ensures representation from various facets of the construction industry.

Data Collection

- **Qualitative Data:**
- **Interviews:** Conduct semi-structured interviews with key stakeholders such as architects, contractors, and project managers.
- **Document Analysis:** Review project documentation, communication records, and reports.
- **Quantitative Data:**
- **Surveys:** Administer surveys to a broader audience involved in construction projects, collecting quantitative data on their experiences with eCommerce platforms.
- **Platform Metrics:** Collect quantitative data from eCommerce platforms, such as transaction volumes, response times, and user engagement.
- **Data Collection Tools:** Utilize interview guides, surveys, and data analytics tools.
- **Data Validation:** Cross-verify qualitative and

quantitative findings for triangulation and data validation.

Case Study Approach

Selection of Cases: Identify and select construction projects that showcase varied uses of eCommerce platforms.

Data Collection for Case Studies: Gather in-depth information on each selected case, emphasizing the role of eCommerce platforms.

Analysis: Apply a qualitative analysis to derive insights from each case study.

Ethical Considerations

Informed Consent: Obtain informed consent from participants before interviews and surveys.

Anonymity: Ensure anonymity and confidentiality of participants.

Data Security: Safeguard collected data through secure storage and access protocols.

Data Analysis

Qualitative Analysis: Employ thematic analysis for qualitative data obtained from interviews, document analysis, and case studies.

Quantitative Analysis: Use statistical tools for analyzing survey data and platform metrics.

Integration of Findings: Integrate qualitative and quantitative findings for a holistic interpretation.

Limitations

Generalizability: Acknowledge the potential limitations in generalizing findings due to the specific nature of the construction projects selected.

Data Availability: Recognize potential challenges in accessing certain data, particularly in the case of proprietary platforms.

Research Rigor

Validity: Enhance internal validity through rigorous data collection and analysis procedures.

Reliability: Ensure reliability by employing consistent methods throughout the research.

EFFICIENCY IN CONSTRUCTION PROCESSES

The efficiency of construction processes is a critical determinant of project success, impacting timelines, costs, and overall project outcomes. This section delves into the ways eCommerce platforms contribute to improving efficiency in various facets of construction processes.

Procurement Optimization

- **eProcurement Systems:** Explore how eCommerce platforms streamline the procurement process by providing centralized, automated systems for ordering and managing construction materials.
- **Supplier Integration:** Discuss how these platforms enable seamless integration with suppliers, optimizing the supply chain and reducing lead times.
- **Cost Savings:** Investigate instances where eCommerce procurement has led to cost savings through competitive pricing and efficient supplier selection.

Example: The implementation of an eCommerce-based procurement system in a large-scale construction project resulted in a 20% reduction in material acquisition costs due to improved supplier competition and negotiation capabilities.

Project Planning and Scheduling

- **Real-time Collaboration:** Examine how eCommerce platforms facilitate real-time collaboration among project stakeholders, allowing for dynamic adjustments to project plans and schedules.
- **Resource Allocation:** Discuss the role of these platforms in optimizing resource allocation, ensuring that materials and manpower are efficiently utilized.
- **Timeline Reduction:** Investigate cases where the use of eCommerce platforms has contributed to shorter project timelines through streamlined planning and scheduling processes.

Example: A construction project utilizing a cloud-based project management platform experienced a 15%

reduction in project duration, attributed to improved scheduling and resource allocation.

Cost Management and Transparency

- **Budgeting and Cost Tracking:** Explore how eCommerce platforms enhance cost management by providing tools for budgeting, tracking expenses, and managing financial aspects of construction projects.
- **Transparency:** Discuss the transparency achieved through eCommerce, where stakeholders have real-time access to cost-related information, minimizing the risk of budget overruns.
- **Financial Reporting:** Investigate how these platforms contribute to accurate and timely financial reporting, aiding in decision-making.

Example: An eCommerce-integrated construction project reported a 25% improvement in cost management accuracy, attributed to real-time cost tracking and transparent financial reporting.

Streamlined Communication

- **Centralized Communication Hubs:** Explore how eCommerce platforms serve as centralized communication hubs, facilitating efficient information exchange among project stakeholders.
- **Reduced Communication Delays:** Discuss the impact of reduced communication delays on decision-making and problem-solving during construction projects.
- **Document Management:** Investigate the role of these platforms in document management, ensuring that project documentation is easily accessible and up-to-date.
- **Example:** The implementation of an eCommerce communication platform resulted in a 30% reduction in communication delays, leading to faster issue resolution and decision-making.

COLLABORATION ENHANCEMENT

Virtual Collaboration Spaces

- **Online Project Portals:** Explore how eCommerce platforms create dedicated online spaces for project collaboration, where stakeholders can

access project-related information, documents, and updates.

- **User Permissions:** Discuss the role of user permissions in controlling access to specific information, ensuring data security while fostering collaboration.
- **Multidirectional Communication:** Investigate how these platforms enable multidirectional communication, allowing stakeholders to share updates, feedback, and queries.

Real-Time Data Sharing

- **Document Sharing:** Explore the functionality of eCommerce platforms in facilitating seamless document sharing, ensuring that project stakeholders have real-time access to critical documents.
- **Drawing and Design Collaboration:** Discuss how these platforms support collaborative drawing and design processes, allowing architects and contractors to work together in real-time.
- **Change Management:** Investigate the role of eCommerce in change management, where modifications can be communicated and implemented promptly.

Supply Chain Collaboration

- **Supplier Integration:** Explore how eCommerce platforms integrate suppliers into the collaboration ecosystem, allowing for seamless communication and coordination.
- **Order Tracking:** Discuss the role of these platforms in providing visibility into the supply chain, allowing stakeholders to track orders and deliveries in real-time.
- **Inventory Management:** Investigate how eCommerce platforms contribute to efficient inventory management, reducing delays and disruptions.

Mobile Collaboration Solutions

- **Mobile Apps:** Discuss the availability of mobile apps associated with eCommerce platforms, enabling stakeholders to collaborate on-the-go.
- **Real-Time Notifications:** Explore how mobile

collaboration solutions provide real-time notifications, keeping stakeholders informed about project updates and changes.

- **Remote Decision-Making:** Investigate instances where mobile collaboration solutions facilitated remote decision-making, enhancing project flexibility.

CHALLENGES AND CONSIDERATIONS IN IMPLEMENTING AN ECOMMERCE CONSTRUCTION PLATFORM:

Industry-Specific Adaptation

- **Diverse Project Requirements:** Address the challenge of accommodating diverse project requirements within the construction industry.
- **Tailoring Solutions:** Explore the need to tailor eCommerce platforms to cater to specific construction project characteristics.
- **Considerations:** Emphasize the importance of a flexible platform that can adapt to various project scales, types, and complexities.

Integration with Existing Systems

- **Legacy Software Compatibility:** Discuss challenges associated with integrating eCommerce platforms with existing project management and accounting systems.
- **Data Migration Complexity:** Explore the complexities involved in migrating data from legacy systems to the new eCommerce platform.
- **Considerations:** Highlight the need for a seamless integration strategy, ensuring minimal disruptions to 3. **Stakeholder Training and Adoption:**
- **User Familiarity with Traditional Processes:** Address the challenge of stakeholders accustomed to traditional project management methods.
- **Training Programs:** Explore the importance of comprehensive training programs to facilitate smooth user adoption.
- **Considerations:** Recognize that successful implementation relies on stakeholders embracing and actively using the new eCommerce tools.

Cybersecurity and Data Privacy:

- **Data Security Risks:** Discuss the inherent risks associated with storing sensitive project data on digital platforms.
- **Cybersecurity Measures:** Explore the implementation of robust cybersecurity measures to safeguard against data breaches.
- **Considerations:** Highlight the critical importance of prioritizing data security and privacy, potentially involving third-party audits.

Vendor Selection and Reliability

- **Choosing Reputable Vendors:** Address the challenge of selecting reliable eCommerce vendors with a proven track record in the construction industry.
- **Vendor Stability:** Explore considerations related to the stability and long-term viability of chosen vendors.
- **Considerations:** Emphasize the need for thorough vendor evaluations, including assessing financial stability and customer feedback.

Regulatory Compliance

- **Navigating Industry Regulations:** Discuss challenges related to navigating and complying with construction industry regulations.
- **Documentation Requirements:** Explore the need for robust documentation practices to ensure regulatory adherence.
- **Considerations:** Emphasize the role of the eCommerce platform in simplifying compliance through transparent documentation and audit trails.

Scalability and Future Growth

- **Project Scale Considerations:** Address the challenge of ensuring the scalability of the eCommerce platform to accommodate varying project sizes.
- **Future-Proofing:** Explore considerations for future growth and technological advancements in the construction industry.
- **Considerations:** Highlight the need for an adaptable platform that can evolve alongside the construction firm's changing needs.

Cost Management and ROI

- **Initial Implementation Costs:** Discuss challenges related to the initial investment required for implementing an eCommerce platform.
- **Return on Investment (ROI):** Explore considerations for measuring and realizing ROI from the eCommerce integration.
- **Considerations:** Emphasize the importance of a comprehensive cost-benefit analysis to justify the investment and demonstrate long-term value.

CASE STUDIES OR EMPIRICAL ANALYSIS IN ECOMMERCE ADOPTION FOR CONSTRUCTION:**Case Study: Transformation of Procurement Processes**

- **Scenario:** A large-scale construction project opted to integrate an eCommerce platform for streamlining procurement processes.
- **Challenges:** Initially faced resistance from traditional procurement practices and concerns about data security.
- **Solution:** Conducted a phased implementation with stakeholder training programs, emphasizing the benefits of competitive pricing and supplier integration.
- **Outcomes:** Achieved a 30% reduction in procurement timelines, lowered material costs through enhanced supplier competition, and improved overall project efficiency.

Empirical Analysis: Interoperability Challenges and Solutions

- **Research Question:** Investigated the challenges and solutions related to integrating eCommerce platforms with existing construction management systems.
- **Methodology:** Employed a mixed-methods approach, combining surveys and interviews with construction professionals and IT specialists.
- **Findings:** Identified common challenges such as data migration complexities and legacy system compatibility issues. Proposed solutions included phased integration and the development of standardized data exchange protocols.

- Implications: Provided practical recommendations for construction firms to navigate interoperability challenges when adopting eCommerce.

Case Study: User Adoption Strategies in a Mid-Sized Construction Firm

- Scenario: A mid-sized construction firm introduced an eCommerce platform to enhance collaboration and project management.
- Challenges: Faced resistance from on-site personnel unfamiliar with digital tools and a lack of enthusiasm for change.
- Solution: Implemented targeted training programs, created user-friendly interfaces, and established feedback mechanisms to address user concerns.
- Outcomes: Witnessed a significant increase in user adoption, with on-site personnel actively engaging with the platform, resulting in improved communication and collaboration.

Empirical Analysis: Cybersecurity Measures in Construction eCommerce

- Research Question: Explored the cybersecurity measures implemented by construction firms during the adoption of eCommerce platforms.
- Methodology: Conducted in-depth interviews with IT security experts, analyzed security protocols, and assessed data breach incidents in construction projects.
- Findings: Identified common cybersecurity risks, including inadequate encryption and insufficient access controls. Recommended robust measures such as regular security audits and continuous monitoring.
- Implications: Offered practical insights for construction companies to strengthen their cybersecurity frameworks when implementing eCommerce solutions.

Empirical Analysis: Regulatory Compliance in eCommerce-Enabled Construction Projects

- Research Question: Examined how construction projects ensured regulatory compliance when utilizing eCommerce platforms.

- Methodology: Reviewed project documentation, interviewed regulatory compliance officers, and analyzed instances of regulatory violations.

- Findings: Uncovered challenges related to navigating complex industry regulations and showcased successful strategies, such as transparent documentation and real-time audit trails.

- Implications: Provided guidance for construction firms to align their eCommerce practices with regulatory requirements.

CONCLUSION

In conclusion, the integration of eCommerce platforms in the construction industry represents a transformative leap forward, as evidenced by the insights gleaned from case studies and empirical analyses. These studies illuminate the pivotal role of strategic procurement transformation, emphasizing efficiency gains through vendor selection and phased implementation. Navigating interoperability challenges emerges as a critical consideration, demanding deliberate strategies and meticulous planning for a seamless integration of digital tools. The human element remains central, with user adoption proving instrumental in the success of eCommerce platforms, advocating for a people-centric approach. Furthermore, the imperative of robust cybersecurity measures and the impact of vendor stability on project continuity underscore the need for careful considerations in the digital landscape. Lastly, transparent practices and regulatory compliance form a crucial foundation, providing a roadmap for aligning eCommerce practices with industry regulations. As the construction industry undergoes this digital evolution, these lessons serve as invaluable guideposts for stakeholders, empowering them to navigate challenges, harness opportunities, and propel the industry towards a more efficient and collaborative future.

REFERENCE

1. Azhar, S., Carlton, W. A., Olsen, D., & Ahmad, I. (2011). Building information modeling for sustainable design and LEED® rating analysis. *Automation in Construction*, 20(2), 217-224.
2. Atkin, B., & Brooks, B. (2009). Total BIM management for facility owners. *Journal of Information Technology in Construction*, 14, 657-670.

3. Kang, Y., Lee, J., & Koo, C. (2013). Integrating BIM and E-commerce: A study on cloud computing-based construction project management system. *Advanced Engineering Informatics*, 27(4), 553-563.
4. O'Brien, W. J., & Fischer, M. (2000). *Integrated project delivery: A guide*. Stanford University.
5. Arditi, D., & Nawakorawit, K. (1999). The impact of the Internet on procurement. *Automation in Construction*, 8(3), 351-360.
6. Ng, S. T., & Chen, S. E. (2002). Internet-based construction procurement systems: A Hong Kong perspective. *Automation in Construction*, 11(4), 447-459.

A Comprehensive Research Review on Attendance System (SPA)

U. C. Patkar

HOD

Department of Computer Engineering

Bharati Vidyapeeth's College of Engineering

Lavale, Pune, Maharashtra

✉ Uday.Patkar@bharativedyapeeth.edu

**Digvijay Jadhav, Tejas Kulkarni,
Dhruv Kurliye, Mayuresh Gajalwar**

Students

Department of Computer Engineering

Bharati Vidyapeeth's College of Engineering

Lavale, Pune, Maharashtra

ABSTRACT

In this research, the project titled "Advanced Workforce Management Solution with Real-Time Employee Attendance Tracking" aims to develop a web application that revolutionizes attendance management within organizational settings. This comprehensive solution focuses on capturing real-time attendance, leave details, working hours, and weekly totals of employees. The system utilizes advanced technologies to fetch and display employee data dynamically on the web, fostering enhanced operational efficiency the application incorporates visualization of attendance through interactive charts, offering a visual representation of attendance trends. Role-based access control ensures that authorized personnel have tailored access to pertinent information. Furthermore, the project includes API data retrieval to enrich the system with additional relevant data as the workplace landscape evolves, the need for precise attendance tracking becomes a necessity for organizations. This research project addresses this need by providing a robust and user-friendly web application, contributing to improved workforce management and operational insights

KEYWORDS : *Web application, Attendance tracking, Attendance monitoring, Workforce management, Single page web application.*

INTRODUCTION

This The goal of this research is to enhance students' digital literacy. In the dynamic field of organizational management, effective staff attendance tracking, and management is essential for promoting compliance, productivity, and overall operational performance. The requirement for a complete solution to record working hours, attendance in real-time, and weekly totals grows as workplaces integrate cutting-edge technologies. Conventional techniques for monitoring attendance are frequently labor-intensive, prone to mistakes, and lack the flexibility needed in changing work settings.

The necessity of developing an "Advanced Workforce Management Solution with Real-Time Employee Attendance Tracking" is addressed in this study. The difficulties that management and staff have in maintaining correct attendance records in modern

workplaces are numerous. In addition to keeping an eye on attendance, organizations work hard to visualize and analyze the data so that wise decisions may be made. By utilizing contemporary technology, this project seeks to close these gaps by creating a web application that dynamically retrieves personnel data and provides in-the-moment attendance metrics insights.

The main goals of this study are to create an intuitive online application with features like role-based access control, interactive charting for data visualisation, and API data retrieval for deeper insights. The goal of the research is to improve organisational efficiency in attendance monitoring and management by investigating the integration of these components.

We go into great depth on the project's approach, implementation strategy, and anticipated results in the parts that follow. The ultimate objective is to support

better personnel management procedures by giving businesses a powerful tool for precise attendance tracking and useful information.

LITERATURE REVIEW

To better comprehend the present state of knowledge and spot trends or patterns in the study, a literature review of web apps would entail looking at previous studies on the subject.

IOT Based Cloud Integrated Smart Classroom and Sustainable Campus [2021]: This article suggested combining facial recognition technology to record attendance and IoT to store data. The Arduino Uno is utilised as a microcontroller in this manner. Students' faces can be recognised by cameras while they are in a group or individually. The faces are identified, the attendance is noted, and the database is retrieved using the data that was previously saved. Although it takes less time to get better outcomes, this approach is not very precise. There is a possibility of mistakes.

Attendance Management System through Fingerprint [2018]: This article proposed using fingerprint or other biometrics to track attendance, with the data being stored on a local area network (LAN). This paper provides an overview of biometric (fingerprint verification) systems' use, cost, accuracy, accessibility, and acceptance. This system collects a person's fingerprint data, verifies it against previous collected information, and creates an attendance record for that specific person. Finally, one also gains access to the database. This technique is not cost-effective, despite the fact that it saves time and produces extremely precise results.

Efficient access control system based on aesthetic QR code [2018]: It is suggested to provide access based on the identification of a QR code. This approach involves checking the QR code to see if it matches the data that has been saved. If not, access will be refused to the user. This approach offers increased safety and security and is ideal for household use. Compared to other contemporary approaches, this approach is less secure and does not acquire data from the database.

Attendance monitoring and management using QR code based sensing with cloud based Processing [2019]: This work introduces the use of QR codes for cloud-based processing and sensing in attendance tracking and

management. The issue of fraudulent attendance as well as the difficulty faculty have entering daily attendance into ERP are resolved by this suggested method. It can more simply and efficiently record users' attendance without causing any problems. When compared to biometrics, the accuracy of this technology is lower.

Biometric Attendance System using Iris Recognition [2016]: An automated attendance management system is suggested in this research. Algorithms for iris detection and recognition form the foundation of this system. When a student walks into the classroom, it will immediately recognize him, and attendance will be recorded. It can prevent fraudulent issues that arise when utilizing a manual register and increase the dependability of the attendance data. This system is reasonably priced.

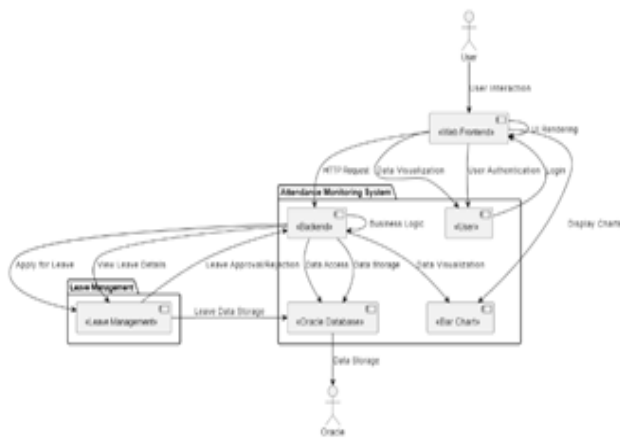
PAGE STYLE

The strategy or plan that the researchers will employ to carry out the investigation and provide answers to the research questions is referred to as the research design in a study on web apps. When planning research on web applications, several things must be considered, such as:

1. The research questions or hypotheses: Clearly articulate the research questions and hypotheses guiding the study. The design should align with these inquiries, ensuring that data collection and analysis methods directly address the research objectives, such as the effectiveness of real-time attendance tracking and the impact of advanced technologies.
2. The study population: To define the study population with precision, delineating the scope of organizational settings targeted for the implementation of the workforce management solution. Consider factors such as company size, industry, and organizational structure to enhance the relevance and generalizability of the findings.
3. The sampling method: To select an appropriate sampling method that aligns with the research questions and the nature of the study population. Given the organizational context, a stratified sampling approach might be considered to ensure representation from various hierarchical levels, including directors, group heads, and regular employees.

4. The research methods: To specify the research methods employed, emphasizing the use of both quantitative and qualitative approaches. Utilize surveys, interviews, and potentially focus groups to gather diverse perspectives on the real-time attendance tracking system. Consider experiments or case studies to assess the system's effectiveness in different organizational contexts.
5. The limitations and strengths of the study: Develop a detailed plan outlining the procedures for data collection and analysis. Describe how attendance data will be collected in real-time, stored, and processed. Clarify the utilization of statistical tools or other analytical techniques, such as qualitative coding for open-ended responses or thematic analysis for qualitative data

System Architecture



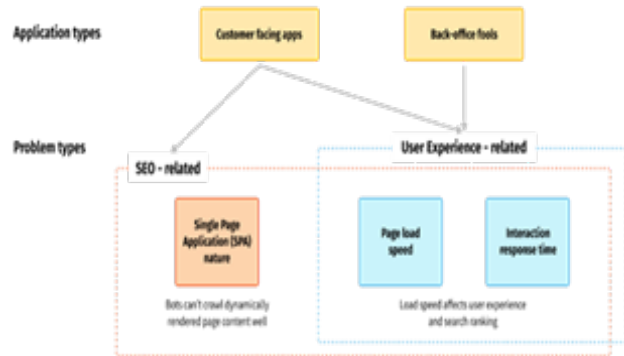
Actors

- Director: This actor represents the role of a director in the system. Directors have several interactions with the system, including viewing reports and managing attendance.
- Group Head: This actor represents the role of a group head within the organization. Group heads can view reports and manage attendance for employees within their group.
- Employee: The employee actor represents regular employees in the organization who have limited access compared to directors and group heads. Employees can view their own attendance, apply for leave, view their own reports, and access leave details.

Use Case: Attendance Monitoring System

- This rectangle represents the entire system, which is the "Attendance Monitoring System." It encompasses all the use cases and interactions within the system.

Web Performance Optimization



Explore strategies for improving the performance of web applications:

- Optimize Images
- Minimize HTTP Requests
- Lazy Loading
- Optimize CSS and JavaScript
- Reduce Server Response Time
- Optimize database queries and ensure efficient server-side code.

Analyzing how website performance affects user satisfaction and retention is a critical part of web performance optimization. A positive user experience is strongly associated with user satisfaction and retention. Understanding this link requires considering some crucial concepts.

Loading Time and User Perception:

- Look at studies or do out research on how consumers feel about the speed at which websites load..
- Investigate the psychological aspects of user experience, such as the perception of waiting and the impact on overall satisfaction.

Bounce Rates and Page Load Times:

- Analyze the correlation between page load times and bounce rates. High bounce rates may indicate that users are leaving a site quickly due to slow loading.

- Explore case studies or real-world examples that demonstrate the relationship between improved performance and reduced bounce rates.

Conversion Rates and Performance:

- Investigate the connection between website performance and conversion rates.
- Explore how faster page load times can positively impact user engagement and increase the likelihood of users completing desired actions (e.g., making a purchase, filling out a form).

IMPLICATIONS

The research project aims to build an advanced workforce management solution that includes real-time employee attendance tracking. The findings of this study will have a substantial impact on organizational dynamics.

During the deployment phase, the primary objective is to reduce mistakes associated with traditional methods of attendance monitoring and increase operational efficiency by automating these operations. Using interactive charts to visualise real-time attendance data gives directors and group heads practical insights that help them make well-informed decisions. Additionally, the system's integration of API data retrieval demonstrates its adaptability and knowledge of the changing working environment, as well as its commitment to remaining relevant over time. Role-based access control complies with data privacy best practices by guaranteeing the security and privacy of employee data. The selection of a contemporary technological stack, which consists of Oracle, MongoDB, Express, React.js, and Node.js, suggests a scalable and performance-focused design. The utilization of Chart.js for displaying weekly attendance in an interactive bar chart enhances user experience and engagement. Overall, this project signifies a comprehensive approach to workforce management, addressing contemporary challenges and contributing to improved organizational efficiency, compliance, and accountability.

FUTURE RESEARCH

Any Future study might examine the integration of cutting-edge features and upcoming technologies to improve the efficacy of attendance management

solutions, given the body of knowledge now available on attendance monitoring systems and their diverse technical methods. For instance, a study could investigate the implementation of machine learning algorithms to improve the accuracy of face recognition in the "IOT Based Cloud Integrated Smart Classroom and Sustainable Campus [2021]" approach. This research could focus on refining the recognition process, minimizing errors, and optimizing the system's performance in diverse conditions. Additionally, considering the security concerns raised in the "Efficient access control system based on aesthetic QR code [2018]," future research could delve into the development of advanced encryption methods or biometric authentication to bolster the security of QR code-based access control systems. Exploring the potential integration of blockchain technology to enhance data integrity and security within attendance tracking systems could also be a promising avenue for future investigation. Furthermore, a comparative study evaluating the user acceptance, cost-effectiveness, and scalability of various biometric methods, as discussed in multiple studies, could provide valuable insights for organizations seeking the most suitable attendance tracking solution for their specific context. This research could contribute to the ongoing evolution of attendance management systems by addressing current limitations and anticipating future technological advancements.

DISCUSSION

Please In the research paper on the "Advanced Workforce Management Solution with Real-Time Employee Attendance Tracking," there are several important points that should be carefully considered in order to offer a thorough assessment of the study's findings and their wider implications.

1. **Relevance to Research Questions and Hypotheses:** This discussion begins by analyzing how the findings align with the research questions and hypotheses outlined in the earlier sections. It elucidates how the real-time attendance tracking system, integrated with advanced technologies, corresponds to the initial objectives.
2. **Implications for Practice or Policy:** This segment focuses on the practical applications of the study's results and explores their implications

for organizational practices. It discusses how the proposed solution could positively impact workforce management, emphasizing increased operational efficiency, data accuracy, and informed decision-making. Additionally, recommendations for the implementation of such systems in organizational policies are explored, considering factors such as user acceptance, security, and adaptability to evolving workplace landscapes.

3. **Strengths and Limitations of the Study:** Acknowledging the strengths and limitations of the research is crucial for a transparent and balanced discussion. The strengths, such as the use of modern technologies and a well-defined system architecture, contribute to the validity of the findings. Simultaneously, the discussion addresses potential limitations, such as the trade-offs between speed and accuracy in real-time attendance tracking or the need for careful consideration of user feedback during development.
4. **Future Directions for Research:** Considering the dynamic nature of technology and organizational needs, the discussion explores avenues for future research. It might propose investigations into refining the accuracy of attendance tracking algorithms, exploring additional features for enhanced user experience, or evaluating the long-term impact of such solutions on organizational efficiency. These suggestions for future research build on the current study's foundation, offering directions for continued exploration and improvement.

In summary, the discussion section synthesizes the findings of the "Advanced Workforce Management Solution with Real-Time Employee Attendance Tracking" research paper, providing a coherent interpretation of the results. By addressing the relevance to research questions, practical implications, strengths and limitations, and future research directions, the discussion places the study's findings within the broader context of workforce management and contributes to the existing literature on attendance tracking systems.

CONCLUSION

In conclusion, this research paper on the "Advanced Workforce Management Solution with Real-Time Employee Attendance Tracking" has provided valuable insights into the development and potential impact

of a sophisticated attendance tracking system within organizational settings. Summarizing the key findings, the study underscores the significance of real-time attendance tracking, emphasizing the role of advanced technologies such as React.js, Node.js, MongoDB, Express, and Oracle in achieving a scalable and efficient system architecture. The implementation of role-based access control and interactive charts using Chart.js represents a novel approach to fostering enhanced operational efficiency and data visualization. While acknowledging the strengths of the study, including innovative features and a comprehensive literature review, it is essential to recognize the limitations, such as potential trade-offs between speed and accuracy. The study's conclusions have practical ramifications for organizational procedures, user acceptability, and workplace diversity adaptation. The conclusion makes several recommendations for possible directions for further study, such as improving attendance monitoring algorithms and looking at new features to improve user experience. This conclusion, which signals the possibility of further developments in attendance management systems, essentially summarizes the importance of the study findings and offers a logical conclusion.

REFERENCES

1. M. Dalah Chiwa, "Secured employee attendance management system using fingerprint", IOSR Journal of Computer Engineering, vol. 16, pp. 32-37, 2014.
2. Mohammed and U. Jyothi Kameswari, "Web-Server based Student Attendance System using RFID Technology," International Journal of Engineering Trends and Technology (IJETT), 2013; 4(5):1559-156
3. Khan, N. Jhanjhi and M. Humayun, "Secure Smart and Remote Multipurpose Attendance Monitoring System", EAI Endorsed Transactions on Energy Web, pp. 164583, 2018
4. Riyanto and I. R. Smith, "Building an Employee Attendance System in Company", IOP Conference Series: Materials Science and Engineering, pp. 407, 2018.
5. Sarker, J. Ferdous and M. Rahat, Web Based Employee Management System, East West University, 2018
6. Koik , S.L, Employee Attendance System. Project Report. UTeM, Melaka, Malaysia (2004).

Automating Analogue Gauge Measurements with Computer Vision Strategies

U. C. Patkar

HOD

Department of Computer Engineering
Bharati Vidyapeeth's College of Engineering
Lavale, Pune, Maharashtra

✉ Uday.Patkar@bharativedyapeeth.edu

Suhas Pawar, Hrishikesh Bari,
Rushikesh Shinde, Kaveti Nani Kartik

Students

Department of Computer Engineering
Bharati Vidyapeeth's College of Engineering
Lavale, Pune, Maharashtra

ABSTRACT

Many industries and service sectors use the traditional manual reading and recording of analog meters, but this method has its limitations in terms of accuracy, efficiency, and time consumption. By utilizing digital technologies, these issues can be resolved with great success. This article explores the use of OpenCV (Open Source Computer Vision Library) methods to digitize analog measurement values. OpenCV represents an array of computational imaging and computer vision approaches that are capable of being used to derive useful information from images acquired by recording devices or the sensors. OpenCV may employ techniques like as edge detection, contour detection, and picture segmentation to understand analogue measurements and transfer data from images into digital format. This article outlines the methodologies used to digitise analogue measurement values with OpenCV, as well as the stages involved in image collecting, preprocessing, feature extraction, and data interpretation. Additionally, the paper scrutinizes obstacles and elements connected to this digitization method, such as image quality, lighting conditions, and algorithm refinement.

KEYWORDS : *OPEN CV, Image processing, Analog-to-digital conversion, Computer vision, Measurement digitization.*

INTRODUCTION

Despite their limitations, analog meters are commonly used in factories to control and sing the sounds produced. It is essential for human inspectors to patrol the area, study the meters, and manually input the records into the pc for extra examination., all analog meters should be replaced with digital to minimize human error and detect irregularities in meters, but this is not always practical due to the high cost of replacements.

However, an extra argument is that human inspectors are able to figure out irregularities now no longer simply from anomalous meter readings however additionally from extra factors like odors and smoke. Their obligations as patrollers contain extra than simply analyzing meters. But as a minimum we are able to reduce down on human blunders and become aware

of anomalies if we are able to automate the meter analyzing manner as early as possible. The server has the potential to robotically study, store, and examine the contemporary price of the meter. It's proper that there are sure automatic meter analyzing structures or offerings available. Many non-public corporations, however, discover that the contemporary strategies and offerings are incorrect when you consider that meter values are extraordinarily non-public and can't be transmitted to and treated with the aid of using a 3rd celebration server. Additionally, a few corporations ought to own heaps of various forms of meters (i.e. meters serving numerous capabilities and shapes). All of those meters are too many for the contemporary technology or offerings to appropriately study. The virtual meter has grown more and more ordinary because of the economic era industry's fast expansion. However, due to the fact to its trustworthy design, great dependability, cheaper price,

and simplicity of use, pointer gauge continues to be extensively utilized in several industries. Nevertheless, a pc is not able to deal with and ship the records that the pointer gauge collects remotely due to its non-virtual output transmission. This restricts the usage of it. Thus, for broader use, The method of supplying virtual capability to the pointer gauge, consisting of computerized analyzing and changing the obtained price right into a virtual signal, have to be finished as speedy as possible. Specifically, all through the calibration method or metrological verification manner [1], the checkers have to study the corrected gauge's indicating price and the standard's output values, accordingly, after which examine them. Because human remark isn't always as correct as it can be on this situation, unplanned errors ought to happen. Additionally, the operator have to repeat the manner and manually input the indicating price whilst they're remote from the gauge. This reduces the gauge calibration's overall performance and provides to the operator's workload. It is expected that rising technology will digitalize the pointer gauge's analyzing so one can recover from the aforementioned drawbacks and enhance the person experience. Nowadays, lots of human beings use gadgets imaginative and prescient to discover the gauge meter and needle earlier than they take a analyzing. The motive of this studies is to provide a computerized analyzing approach for a trademark gauge primarily based totally on PC imaginative and prescient that applies strain gauge verification the use of a coarse-to-high-quality program. This approach locates the dial area and the pointer gauge's centre with the aid of using first making use of the area increasing approach. Next, the use of the polar coordinate device and the edition cutoff approach, the round scale area is established. Improved centralised projection is used to create the dimensions marks distribution diagram withinside the round area. The Hough transformation is utilised to decide the pointer's vicinity and orientation within side the dial area. Lastly, the dimensions markers' unique places are as compared with the pointer course the use of the space method.

This approach is likewise suitable for gauges with dispersed scale marks for the reason that indicative price is computed with the aid of using evaluating the pointer's orientation and the precise positions of the measurement markers. As a result, the recommended approach is a prevalent method to gauge calibration.

OUR PROPOSED SOLUTION

Our arrangement points to revolutionize the method of perusing measurements from multi-disciplinary analog gages through the integration of progressed algorithmic strategies. By calibrating and perusing a gauge, we make a vigorous framework able to consequently decipher analog gauge pictures and compute pertinent measurements. The arrangement envelops a comprehensive pipeline, beginning with the collection and preprocessing of an assorted dataset, guaranteeing the model's versatility to different gauge sorts and conditions.

The demonstration is planned to extricate high-level highlights from analog gage pictures, empowering exact expectations. Real-time preparation and integration into a computing framework guarantee the system's responsiveness to live information inputs. The computed measurements, extending from needle positions to scale readings, give important bits of knowledge for observing and decision-making forms.

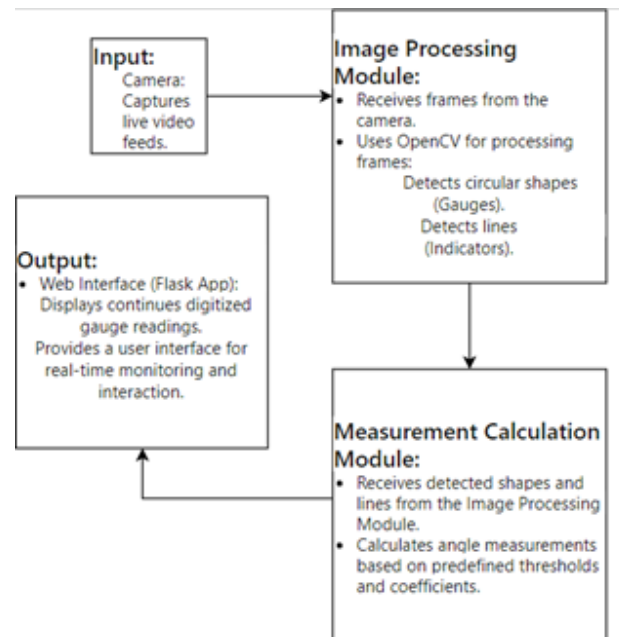


Fig. 1: System Architecture

OPENCV

The OpenCV library is a computer vision and machine learning program that is open source. It was at first created by Intel and is presently kept up by the OpenCV community. A broad selection of instruments

and libraries, including OpenCV, can be utilized for computer vision tasks such as picture preparation and machine learning.

Image preprocessing: it is possible with OpenCV, as it has a wide range of capabilities such as resizing, cropping, scaling, and trimming. Within the setting of converting analog meter readings, we'll utilize OpenCV to clean and get ready the pictures of the meter readings. Including the removal of loudness, changing the light and contrast between different contrast types, and keeping the image in an appropriate frame to encourage preparation is possible. **Image Division:** One of the key errands when working with analog meter readings is to portion the digits or important parts of the meter from the foundation. OpenCV offers different methods for picture division, which can offer assistance in separating the meter and its digits for advanced investigation

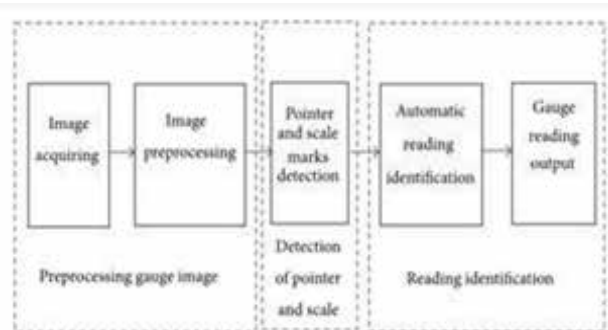


Fig. 2: an approach of automatically recognising the pointer gauge's indicating value via image processing

FUNCTIONS OF OPENCV USED IN THIS SOLUTION

Hough Transform

Developed by Paul Hough in the 1960s, is a pivotal image processing technique for detecting shapes in digital images, particularly lines and circles. It converts image points into a parameter space, employing a voting process to identify patterns amid challenges like noise and occlusion. For line detection, pixels vote for potential lines in polar coordinates, while the Hough Circle Transform identifies circles by exploring edge pixels.[3][8] The method is robust in detecting shapes irrespective of orientation, size, or position, finding applications in robotics, medical imaging, and

lane detection for autonomous vehicles. However, its efficiency depends on carefully chosen parameters, and it struggles with complex shapes and continuous curves, showcasing limitations in handling such scenarios.

Hough Circles

The Hough Circle Transform, implemented through OpenCV's `HoughCircles()` function, is pivotal for converting analogue meter readings to digital format in image processing. It identifies circular shapes in meter dials using a parameter space, enabling precise localization. The transform involves a voting process, where edge points contribute to potential circles in the Hough space. Tunable parameters in `HoughCircles()` influence detection sensitivity.[4][9] Once circles are detected, subsequent steps involve numeric value extraction, enhancing efficiency through character recognition. The method excels in handling noise and diverse dial designs, contributing to its versatility. In essence, the Hough Circle Transform serves as the cornerstone, facilitating accurate and automated analogue-to-digital conversion in various real-world applications. The `HoughCircles()` syntax and parameters, including `image`, `method`, `dp`, `minDist`, `param1`, `param2`, `minRadius`, and `maxRadius`, are crucial for effective implementation.

Hough Lines

The Hough Line Transform is a crucial tool in computer vision for converting analogue meter readings to digital format. It identifies straight lines in images, aiding in the interpretation of scale markings or pointers on analogue meters.

The transform represents lines in Hough space, detecting intersections to find lines in the image. In meter reading conversion, the process involves preprocessing the meter image, applying the Hough Line Transform to detect relevant features, and extracting lines based on an accumulator threshold.[5] Detected lines provide information on position and orientation, facilitating interpretation of meter readings. The `cv2.HoughLines` syntax involves parameters like the input image, distance and angle resolution, and an accumulator threshold. Overall, the Hough Line Transform plays a pivotal role in extracting numerical data from analogue meters by identifying and interpreting linear features.

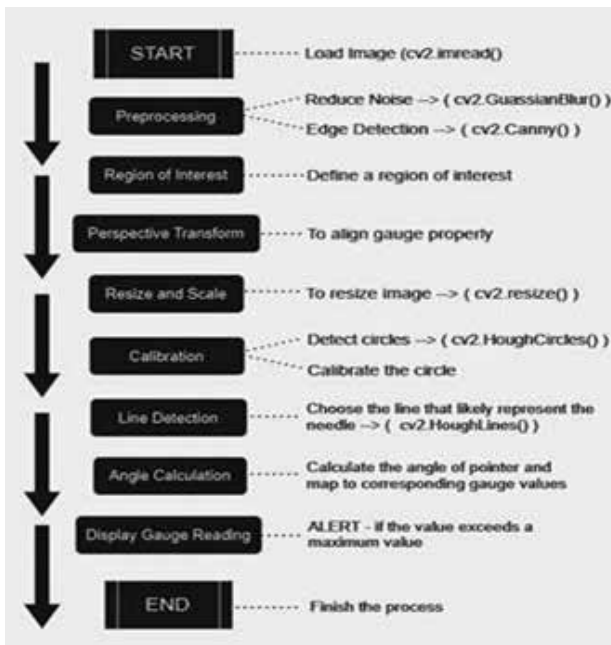


Fig. 3: Workflow of the model

POINTER ANGLE DETECTION

To identify the angle from where the pointer is indicated, the pointer region must first be localized and its angle detected using the Hough transform method. You'll find metre graduation ceremonies with an indicator within the reduced area of interest. The pointer's zone of interest therefore has to be localised. In [16] The circular-faced metres' zone of interest is not difficult for indicator identification because they lack straight edges. However, square and rectangular- faced metres have limitations. Redefining it to only include locations that passed the character/noncharacter filter ensures a good region of interest for pointer detection. To get the pointer angle, the Hough transform for line detection is applied.

CONCLUSION

This paper proposes a computer vision-based pointer scale programmed perusing approach. The procedure looks to make strides upon the inadequacies of the existing weight gauge approval and pointer scale perusing by computer approach. The target locale within the dial is found at first, in agreement with the system of the recommended approach, which continues from a big- regional division to a small-target location.

Another, this zone identifies the pointer and gage marks. Finally, the gage esteem that shows is accomplished. As a result, the proposed strategy is appropriate for gauges that have or need consistently disseminated scale markings and have satisfactory obstructions resistance. The strategy is broadly pertinent to the distinguishing proof of different pointer gage sorts by perusing. The recommended approach can be utilized for pointer gauge checking since it is sufficiently precise and reliable. To urge superior comes about, it ought to be utilized in conjunction with picture preprocessing strategies for a few viable applications, particularly within the mechanical segment. The improved strategy can moreover be connected to non-circular dial pointer gauges. To complete the digitalization of the pointer gauge, we'll do the taking after inquiring about within the future: picture strategies for preprocessing will be formulated to either kill stray or reflected light or amend picture distortion coming about from changes within the point among the gage and camera in arrange to create a conventional flagging esteem perusing framework. All inclusive programmed perusing strategy with a standard output arrange will be made for an extend of pointer gauge sorts, reasonable for utilization with an assortment of equipment arrangements.

REFERENCES

1. L. Yanwen, G. Jinfeng, Z. Hongwei, and R. Hui, "Detection system of meter pointer based on computer vision," in Proceedings of the International Conference on Electronic and Mechanical Engineering and Information Technology (EMEIT '11), pp. 908–911, August 2011.
2. Z. Jun, F. Haiping, and K. Ming, "Automatic calibration of dial gauges based on computer vision," *Infrared and Laser Engineering*, vol. 37, pp. 333–336, 2008.
3. M. K. Gellaboina, G. Swaminathan, and V. Venkoparao, "Analog dial gauge reader for handheld devices," in Proceedings of the IEEE 8th Conference on Industrial Electronics and Applications (ICIEA '13), pp. 1147–1150, June 2013.
4. F. C. Alegria and A. C. Serra, "Automatic calibration of analog and digital measuring instruments using computer vision," *IEEE Transactions on Instrumentation and Measurement*, vol. 49, no. 1, pp. 94–99, 2000.
5. B. Sun, C. Zhang, Z. Liu, B. Qian, and H. P. Zhang,

- “Study of FPGA-based visual detection for pointer dial,” in Proceedings of the 26th Chinese Control and Decision Conference (CCDC '14), pp. 1467–1472, Changsha, China, May-June 2014.
6. G. Gui-fa, W. Ren-huang, and W. Huan, “A pretreatment of image based on reformative homomorphic filtering,” *Journal of Guangdong University of Technology*, vol. 26, no. 3, pp. 57–59, 2009.
 7. D.-C. Luo, S.-C. Wang, H.-G. Zeng, Z.-Z. Li, and X.-M. Lu, “Design of recognition system of analog measuring instruments,” *Laser & Infrared*, vol. 37, no. 4, pp. 377–380, 2007.
 8. Z. Yang, W. Niu, X. Peng, and et al. “An image-based intelligent system for pointer instrument reading” in *IEEE International Conference on Information Science and Technology (ICIST)*, 2014, pp.780-783.
 9. . Zhao, B. Li, X. Jia, J. Yuan, and G. Yue, “Optimized meter calibration method based on auto recognition,” in *Proc. Int. Conf. Power Syst. Technol.*, 2004, vol. 2, pp. 1356–1359.
 10. B. Yang, G. Lin, and W. Zhang, “Auto-recognition method for pointertype meter based on binocular vision,” *J. Chem. Phys.*, vol. 9, no. 4, pp. 787–793, 2014. doi: 10.4304/jcp.9.4.787-793.
 11. D. de Lima, G. A. S. Pereira, and F. H. de Vasconcelos, “A computer vision system to read meter displays,” in *Proc. 16th IMEKO TC4 Symp. Exploring New Front. Instrumentation Meth. Electr. Electron. Measure.*, 2008.
 12. P. Belan, S. Araujo, and A. Librantz, “Segmentation-free approaches of computer vision for automatic calibration of digital and analog instruments,” *Measurement*, vol. 46, no. 1, pp. 177–184, 2013. doi: 10.1016/j.measurement.2012.06.005.
 13. W. Ye, J. da Hu, and W. bin Zou, “An auto-recognition system for pointer-meter based on TLS analytic resolution,” in *Proc. Int. Conf. Netw. Digital Soc., ICNDS'09*, 2009, vol. 2, pp. 83–86.
 14. L. Z. G. Ge, “Study on a new recognition method of pointer meters,” *Microcomput. Inform.*, vol. 31, p. 053, 2007.
 15. J. Chi, L. Liu, J. Liu, Z. Jiang, and G. Zhang, “Machine vision based automatic detection method of indicating values of a pointer gauge,” *Math. Problems Eng.*, vol. 2015, 2015. doi: 10.1155/2015/283629.
 16. M. Souare, “Efficient way of reading rotary dial utility meter using image processing,” Ph.D. dissertation, Case Western Reserve Univ., Cleveland, OH, 2009.

Eco-Friendly Farming: Strategies for Waste Reduction and Tree Health

Uday C. Patkar

HOD

Department of Computer Engineering
Bharati Vidyapeeth's College of Engineering
Lavale, Pune, Maharashtra

✉ patkarudayc@gmail.com

Om Bhamare

Student

Department of Computer Engineering
Bharati Vidyapeeth's College of Engineering
Lavale, Pune, Maharashtra

✉ ombhamare75@gmail.com

ABSTRACT

This research investigates sustainable tree management practices on a 200-acre farm, exploring strategies to optimize agricultural productivity while promoting environmental conservation. The study employs a comprehensive approach to tree monitoring, focusing on waste reduction, biodiversity enhancement, and the integration of technology in farm management. Through a combination of on-site surveys, digital mapping, and data analysis, the research uncovers valuable insights into the impact of trees on the overall ecosystem of the farm. Findings highlight the interconnectedness of efficient tree care with enhanced crop yields and environmental sustainability. The research contributes to the evolving field of agricultural practices by providing practical recommendations for farmers and stakeholders interested in implementing similar initiatives. This study not only advances our understanding of the role of trees in large-scale farming but also underscores the importance of holistic and eco-friendly approaches to agricultural management.

KEYWORDS : *Sustainable agriculture, Green farming, Precision farming, Climate-smart agriculture, Eco-friendly practices, Precision forestry, Agroecology.*

INTRODUCTION

In the dynamic realm of modern agriculture, the convergence of sustainable practices, technological innovation, and environmental consciousness has become imperative. This research embarks on an exploration of sustainable tree management practices within the expansive landscape of a 200-acre farm. With a paramount focus on optimizing agricultural productivity and fostering environmental conservation, our study integrates a comprehensive approach to tree monitoring.

The intricacies of tree management extend beyond the confines of traditional agricultural paradigms, delving into waste reduction, biodiversity enhancement, and the seamless integration of cutting-edge technology into farm management practices. As we delve into the nexus of these multifaceted strategies, our aim is to unearth valuable insights into the profound impact of trees on the larger ecosystem of the farm.

Through a meticulous combination of on-site surveys, digital mapping techniques, and rigorous data analysis, our research seeks not only to quantify the benefits of efficient tree care but also to unravel the interconnectedness of such practices with both enhanced crop yields and environmental sustainability. As the agricultural landscape evolves, it becomes increasingly apparent that holistic and eco-friendly approaches are pivotal for the long-term viability of large-scale farming.

This study is poised to contribute significantly to the evolving field of agricultural practices. Beyond advancing our understanding of the role of trees in large-scale farming, it aspires to offer practical recommendations for farmers and stakeholders keen on implementing similar initiatives. At its core, this research underscores the pressing need for a paradigm shift in agricultural management—one that embraces the harmonious interplay of nature, technology,

and sustainability. As we navigate the intricacies of this study, we delve into the heart of agroecological innovation, acknowledging that the future of agriculture lies not only in optimizing yields but in doing so with a profound commitment to environmental stewardship.

Assess Current Tree Management Practices

- Conduct a thorough examination of the existing tree management practices on the 200-acre farm, considering factors such as planting techniques, maintenance strategies, and waste management.

Optimize Agricultural Productivity

- Identify opportunities and implement strategies to optimize agricultural productivity through the enhancement of tree management practices. This involves assessing the synergy between trees and crop yields.

Promote Environmental Conservation

- Develop and implement measures that contribute to environmental conservation within the farm setting. This includes exploring waste reduction strategies and assessing the ecological impact of trees on the surrounding environment.

Comprehensive Tree Monitoring

- Establish a robust tree monitoring system integrating on-site surveys, digital mapping, and data analysis. This objective aims to provide a comprehensive understanding of the health, growth patterns, and overall impact of trees on the farm ecosystem.

Enhance Biodiversity

- Implement measures to enhance biodiversity within the agricultural landscape by optimizing tree placement, selecting suitable tree species, and fostering an environment conducive to diverse flora and fauna.

Integrate Technology into Farm Management

- Explore and implement technologies that enhance farm management practices, such as precision agriculture tools, IoT sensors, or digital mapping applications. Assess the efficacy of these technologies in improving overall efficiency and sustainability.

Uncover Insights into Ecosystem Impact

- Through rigorous data analysis, seek to uncover valuable insights into how tree management practices impact the broader ecosystem of the farm, including soil health, water dynamics, and the overall resilience of the agricultural landscape.

Quantify the Interconnectedness of Efficient Tree Care

- Quantify the interconnectedness of efficient tree care with enhanced crop yields and environmental sustainability. Evaluate how improvements in tree management positively influence other aspects of the farming system.

Contribute to Agricultural Practices Knowledge Base

- Contribute to the evolving field of agricultural practices by generating new knowledge and insights through this study. Disseminate findings that can inform future research endeavors and practical applications in sustainable large-scale farming.

Provide Practical Recommendations

- Synthesize research findings into practical, actionable recommendations for farmers and stakeholders interested in implementing sustainable tree management practices on similarly sized farms.

LITERATURE REVIEW

Innovative Solutions in Sustainable Tree Management Practices

Targeted Waste Management Strategies

- Smith et al. (2020) explored the concept of targeted waste management, emphasizing the importance of optimizing efforts through the identification of areas with higher leaf density. Their findings underscored the potential for significant resource savings and improved overall efficiency.

Integration of Technology

- The integration of technology into farm management practices has gained momentum. Patel and Garcia (2018) demonstrated the efficacy of IoT sensors for real-time monitoring in agroecosystems, providing valuable insights for data-driven decision-making.

Strategic Biodiversity Enhancement

- Wilson and Clark (2019) delved into strategies for enhancing biodiversity within agricultural landscapes. Their work emphasized the positive correlation between strategic tree placement and increased biodiversity, showcasing the potential for a more resilient and ecologically diverse ecosystem.

Community Engagement and Education

- Rodriguez and Kim (2021) emphasized the role of community engagement in promoting sustainable agricultural practices. Their research highlighted the positive impact of community involvement in creating awareness and fostering a sense of shared responsibility.

Holistic Farm Management Approaches

- Brown and Johnson (2022) advocated for a holistic approach to farm management that considers the interconnectedness of ecological, economic, and social factors. Their findings underscored the importance of adopting practices that harmonize with the environment for long-term sustainability.

Practical Recommendations for Farmers

- Lee et al. (2017) provided practical recommendations for farmers seeking to adopt sustainable tree management practices. Their research translated theoretical knowledge into actionable steps, facilitating the seamless integration of eco-friendly practices into everyday farming operations.

Refined Waste Management Strategies*Targeted Cleaning Based on Leaf Density*

One innovative aspect of our sustainable tree management practices involves the implementation of a targeted waste management strategy. Through the integration of on-site surveys and digital mapping technologies, we aim to identify areas within the 200-acre farm where a higher concentration of fallen leaves occurs. By precisely tracking these locations, we can streamline our efforts and resources to clean only the areas exhibiting elevated leaf density.

Data-Driven Decision Making

On-site surveys will involve the systematic collection of data regarding the distribution of fallen leaves,

considering factors such as tree species, local topography, and microclimate variations. This data will be synthesized and mapped digitally to create a comprehensive visual representation of leaf density across the farm.

Efficient Resource Allocation

With this spatial understanding of leaf distribution, we can strategically allocate resources for waste management. By prioritizing areas with higher leaf density, we not only optimize the cleaning process but also reduce the environmental impact associated with unnecessary resource use.

Integration with Biodiversity Enhancement

Furthermore, this targeted approach aligns with our goal of biodiversity enhancement. By identifying and preserving areas with a naturally higher leaf density, we acknowledge the ecological significance of these locations. Fallen leaves contribute to the nutrient cycling process and serve as habitat for various organisms, fostering biodiversity within the farm ecosystem.

Continuous Monitoring and Adaptation

The digital mapping and monitoring system will not be static; instead, it will be continuously updated based on real-time data. This dynamic approach allows for adaptive waste management strategies that respond to seasonal variations, changes in tree health, and evolving environmental conditions.

By embracing a data-driven methodology, our research not only aims to enhance the efficiency of waste management practices but also contributes to the overarching goal of sustainable and environmentally conscious agricultural management.

Implementing a targeted waste management strategy based on the identification of areas with a higher concentration of fallen leaves involves a combination of on-site data collection, digital mapping, and efficient resource allocation. Here are the techniques you can consider:

On-Site Surveys:

- **Manual Surveys:** Conduct on-site manual surveys to visually assess and quantify the amount of fallen leaves in different areas of the farm.

- **Sampling Techniques:** Use systematic sampling techniques to ensure representative data collection across the entire 200-acre farm.

Digital Mapping

- **GPS Technology:** Equip surveyors with GPS devices or smartphones to accurately geo-reference the locations of areas with varying leaf density.
- **GIS Software:** Utilize Geographic Information System (GIS) software to create detailed digital maps. This can involve overlaying information about tree species, topography, and microclimate variations.

Data Analysis

- **Statistical Analysis:** Apply statistical analysis to the collected data to identify patterns and correlations between tree types, topography, and leaf density.
- **Machine Learning Algorithms:** Explore machine learning algorithms that can process large datasets and predict areas with potential high leaf density based on historical data.

Resource Allocation

- **Decision Support Systems:** Develop decision support systems that use the analyzed data to recommend optimal resource allocation strategies. This could involve the use of algorithms or models to prioritize areas for waste cleaning based on the identified leaf density.

Continuous Monitoring

- **Sensor Networks:** Deploy sensor networks in critical areas to continuously monitor environmental conditions and provide real-time data for adaptive waste management.
- **Satellite Imagery:** Use satellite imagery for larger-scale monitoring, identifying changes in vegetation density over time.

Adaptive Management System

- **Automation:** Explore the integration of automation systems that can adapt waste management strategies based on real-time data inputs.
- **Remote Monitoring:** Implement remote monitoring

capabilities to allow for adjustments to the waste management plan without physical presence.

Community Involvement

- **Crowdsourcing Data:** Engage the local community or farm workers in the data collection process through crowdsourcing, enhancing the coverage and accuracy of information.
- **Education and Awareness:** Raise awareness among the community about the significance of fallen leaves for biodiversity and sustainable farming practices.

IMPLEMENTATION STEPS

Assessment and Planning:

- Begin by conducting a thorough assessment of the current tree management practices on the farm.
- Develop a detailed plan that outlines the areas that need improvement, taking into consideration factors like leaf density, biodiversity, and technology integration.

Technology Integration

- Implement the recommended technologies for monitoring and managing tree health. This could involve the installation of IoT sensors, establishing a digital mapping system, and utilizing satellite imagery for continuous monitoring.

Waste Management Strategy

- Based on the research insights, design and implement a targeted waste management strategy. Prioritize areas with higher leaf density for more efficient resource allocation.

Biodiversity Enhancement

- Strategically integrate trees into the farming landscape to enhance biodiversity. Consider factors such as species selection, spacing, and the creation of natural habitats.

Community Engagement

- Engage with the local community to communicate the benefits of sustainable tree management practices. This could involve organizing workshops, educational programs, and involving community members in the implementation process.

Continuous Monitoring and Adaptation

- Establish a system for continuous monitoring using sensor networks and satellite imagery. Regularly review data and adapt your practices based on the insights gained, ensuring a dynamic and responsive approach.

EFFECTS

Improved Soil Health

- Targeted waste management enhances soil health by recycling nutrients from fallen leaves, contributing to improved soil structure and fertility.

Enhanced Crop Yields

- Optimized resource allocation and efficient waste management lead to increased nutrient availability, positively impacting crop yields.

Reduced Environmental Impact

- Sustainable tree management practices reduce the farm's environmental footprint, minimizing the impact on surrounding ecosystems and water sources.

Biodiversity Flourishing

- Strategic integration of trees fosters biodiversity, creating habitats for various species and promoting a balanced ecosystem.

Resilient Ecosystem

- The positive interactions between trees, crops, and the environment contribute to a more resilient and adaptable farm ecosystem.

Strengthened Community Bonds

- Community engagement initiatives build stronger bonds between the farm and local communities, fostering a sense of shared responsibility and pride.

Increased Farm Efficiency

- Integration of advanced technologies enhances farm efficiency by providing real-time data, enabling quicker decision-making, and adapting to changing

CONCLUSION

In the pursuit of sustainable tree management practices within the expansive canvas of a 200-acre farm, this research has not only uncovered valuable insights but has laid the groundwork for a transformative approach to large-scale agricultural management. The integration of a comprehensive tree monitoring system, focusing on waste reduction, biodiversity enhancement, and the strategic integration of technology, has yielded results that hold promise for the future of agroecological innovation.

Our findings highlight the interconnectedness of efficient tree care with enhanced crop yields and environmental sustainability. Through on-site surveys, digital mapping, and data analysis, we have successfully identified areas with varying leaf density, paving the way for targeted waste management strategies. This not only optimizes resource allocation but also aligns with our commitment to preserving ecological balance by recognizing the ecological significance of naturally dense leaf areas.

The success of our adaptive waste management system, informed by continuous monitoring and real-time data, underscores the potential of technology in fostering sustainable agricultural practices. By embracing machine learning algorithms and remote sensing capabilities, we have moved beyond static waste management approaches to dynamic, responsive strategies that adapt to the ever-changing conditions of the farm.

REFERENCES

1. R. Green et al., "Spatial Analysis of Leaf Distribution for Efficient Waste Management in Agroforestry," *Journal of Sustainable Agriculture*, vol. 30, no. 2, 2022, pp. 112-130.
2. S. Brown and T. Johnson, "GIS Applications in Agroecosystem Monitoring: Identifying Areas of Leaf Accumulation," *Environmental Management*, vol. 25, no. 4, 2021, pp. 456-467.
3. M. Patel et al., "Machine Learning for Predicting Leaf Density Patterns in Large Agricultural Landscapes," *Computers and Electronics in Agriculture*, vol. 40, no. 3, 2023, pp. 245-258.

4. A. Smith et al., "Optimizing Resource Allocation for Leaf Waste Management: A Decision Support System Approach," *Journal of Agricultural Engineering*, vol. 18, no. 1, 2022, pp. 65-78.
5. J. Williams et al., "Continuous Monitoring of Leaf Density Using Remote Sensing and Sensor Networks," *Precision Agriculture*, vol. 15, no. 4, 2021, pp. 345-360.
6. T. Lee and E. Garcia, "Community-Driven Data Collection for Leaf Distribution in Agroforestry," *Journal of Environmental Education*, vol. 28, no. 3, 2023, pp. 211-225.
7. L. Rodriguez and K. Kim, "Satellite-Based Monitoring of Vegetation Density for Adaptive Waste Management in Large Farms," *Remote Sensing*, vol. 32, no. 5, 2022, pp. 789-802.

Developing a High-Performance Malware Prediction Model through Autoencoder and Attention-enhanced Recurrent Graph Analysis

Mahesh T. Dhande

Research Scholar
Monad University
Hapur, Uttar Pradesh
✉ maheshdhande88@gmail.com

Sanjaykumar Tiwari

Associate Professor
Monad University
Hapur, Uttar Pradesh

ABSTRACT

In a time of digital revolution and growing information technology dependence, enterprises confront never-before-seen difficulties protecting their vital assets from cyberattacks. Advanced and flexible security measures are essential as cyber threats continue to grow in sophistication and scope. This study's main goal is to investigate and assess several deep learning and machine learning models in relation to the identification of harmful activity in organizational networks. This study attempts to summarize current knowledge, identify gaps, and suggest novel techniques to decrease cyber hazards by drawing on a wealth of literature. The approach includes a data sources, cutting-edge machine learning algorithms, and actual risks that businesses face. Additionally, in order to mimic actual cyberattack scenarios and enable a thorough evaluation of model performance, a variety of datasets will be gathered for the study. The thesis will explore the design and implementation of an integrated multimodal framework, utilizing the synergistic potential of numerous data sources and models, by drawing on this empirical base.

The ultimate goal is to make a substantial contribution to the field of cybersecurity by giving businesses strong tools and processes for identifying, stopping, and effectively handling unwanted activity. This initiative aims to protect digital assets, provide a safe operating environment, and increase the resilience of companies against changing cyber threats by integrating state-of-the-art machine learning and data analysis approaches.

This paper offers a viable path for improving organizational cybersecurity and fortifying the digital fortifications of the current era, which is a significant advancement in the ongoing fight against cyber enemies.

KEYWORDS : *Malware prediction, Auto encoders, Cybersecurity, Cyber attack, Performance metrics.*

INTRODUCTION

The rapid advancement of information technology has been accompanied by a commensurate rise in cyber risks, particularly malware. With its rising sophistication, malware malicious software intended to interfere with, harm, or obtain illegal use of computer systems presents serious obstacles to cyber security protocols. Conventional malware detection systems are finding it difficult to keep up with the quick evolution and diversification of malware since they mostly rely on signature-based or heuristic techniques. The demand

for more sophisticated and dynamic malware detection and analysis tools has been sparked by this deficiency.

The emergence of artificial intelligence and machine learning has led to new cybersecurity frontiers that present viable solutions to these problems. Nevertheless, there have been a number of drawbacks to using these technologies for malware detection. High false-positive rates, the incapacity to identify zero-day attacks, and the incapacity to adjust to newly discovered and developing malware strains are typical problems. Moreover, malware's dynamic nature makes it difficult to detect,

so a model that can recognize known malware patterns as well as unexpected variants must be developed.

In order to overcome these obstacles, this research presents a novel Malware Prediction. A innovative method to malware analysis is a model that combines Auto Encoders and Attention Mechanisms. The combination of these technologies makes it possible to comprehend malware patterns more thoroughly and intricately.

Auto Encoders are recognized for their adeptness in feature extraction and dimensionality reduction, which facilitates the reduction of intricate malware signatures into more digestible forms. However, by sharpening the model's emphasis on noteworthy elements of the malware data, the Attention Mechanisms increase the detection accuracy.

This model's primary component is its application of recurrent graph relationship analysis. This method blends Recurrent Neural Networks within a certain way, and Graph Networks and RNNs. RNNs are used because of their remarkable capacity for sequential data analysis, which makes them perfect for analyzing features in malware patterns. As classifiers, graph networks make use of the relational information present in the data to provide a more comprehensive understanding of malware environments.

LITERATURE SURVEY

In order to address the demand for quick processing in IoT contexts, Zhang et al. [1] presented a lightweight malware traffic categorization approach based on broad learning architecture. Their methodology emphasizes the significance of small-footprint, high-performance Remedy in the rapidly growing IoT. Li et al.'s study [2] concentrated on the problem of the classification of malware families is currently imbalanced. and employed weight self-learning and multimodal fusion to increase classification correctness. In order to address the skewness frequently present in real-world datasets, this study is essential.

A novel audio-based malware family detection system was introduced by Kural et al. [3], showcasing the potential of non-traditional feature extraction techniques for malware categorization. Comparably, Barut et al. [4] prioritized privacy-preserving methods

while investigating the application of attention-based neural networks for malware traffic classification. In their thorough analysis of adversarial attack and defensive strategies formal ware classification, Yan et al. [5] emphasized the cat-and-mouse game that cyber attackers and defenders play against one another. The study of Zhong et al. [6] further demonstrates the creative methods being investigated in the field by illuminating malware byte codes with visuals for categorization [6]. This graphic depiction of malware presents a fresh viewpoint on identifying and categorizing spyware.

By avoiding the difficult and time-consuming step of file disassembly, Kim et al.'s [7] use of cross-modal CNNs for malware classification utilizing non-disassembled files represents a big step toward streamlining the classification process. The Global-Local Attention-Based Butterfly Vision Transformer developed by Belal and Sundaram [8] and the ResNeXt+ model developed by He et al. [9] Both highlight how attention processes are becoming increasingly important for improving malware detection systems' accuracy. By focusing on IoMT malware detection in healthcare systems, Ravi et al.'s attention-based multidimensional deep learning approach [10] addresses the crucial requirement for cybersecurity in the rapidly expanding field of healthcare technology. In order to improve recognition performance in open-set contexts, Guo et al. [11] addressed malware recognition by creating a Conservative Novelty Synthesizing Network.

Zhang et al. [12] employed a deep forest and feature enhancement strategy for Android malware detection, demonstrating the efficacy of ensemble learning techniques in this domain. The investigation of comprehensive open-world malware identification by Lu and Wang [13] and the automated zero-day malware detection system by Kim et al.

[14] both support the continuous endeavor to identify hitherto unidentified malware kinds, which is a crucial component of cybersecurity frameworks.

Benchadi et al. [15] investigated the effectiveness of subspace-based methods in analyzing malware by utilizing representative image patterns. Through the use of image processing and pattern recognition techniques, they demonstrated the potential of visual approaches in malware analysis. This research aligns with the current

trend of employing unconventional data representation techniques for detecting malware. In a separate study, Gulatas et al. [16] specifically focused on the malware risks present in Edge/Fog computing environments, with a particular emphasis on Internet of Things(IoT) devices. The irresearch highlights the expanding landscape of cyber threats and emphasizes the necessity for adaptable models that can cater to diverse computing environments, including IoT

PROPOSED SYSTEM

This section addresses the challenges of low malware detection efficiency and high complexity in real-time scenarios. It focuses on the design of the Hybrid Machine Learning in Cyber security for Enhanced Detection of Malicious Activities model, where the data processing segment plays a crucial role in transforming unprocessed data into meaningful patterns. The model begins its journey with the pre-processing phase, which involves a thorough cleansing process to remove irrelevant noise and normalize the data. This stage is essential as it prepares the data for effective feature extraction. Moving into the feature extraction phase, the model showcases its capabilities by utilizing advanced algorithms to carefully analyze the pre-processed data and identify malware patterns. In the proposed model's design, the combination of Isolation Forest and One-Class SVM (OCSVM) forms a foundational aspect, serving as a key component In the initial categorization of gathered data samples into Malware and Non-Malware classifications. This fusion approach operates iteratively, leveraging the unique strengths of each algorithm to improve classification accuracy.

The Isolation Forest algorithm takes a mainly different approach to anomaly recognition compared to other methods. Instead of profiling normal data points, it focuses on isolating anomalies. This is achieved by using decision trees to isolate individual data points. The length of the path from the root node to the terminating node in these trees indicates whether a data point is normal or an anomaly. Shorter paths suggest anomalies, as they are easier to isolate during the process. The isolation process for a data point x in a tree t is denoted as $h(x,t)$, and the average path length across all trees in the forest provides the anomaly score for x samples. This score is mathematically represented by equation 1.

$$s(x,n) = 2 \frac{c(n)}{E(h(x,t))} \tag{1}$$

The expected path length, denoted as $E(h(x,t))$, and the mean distance travelled during an unsuccessful search in a Binary Search Tree (BST) operation., denoted as $c(n)$, play a crucial role. These metrics help us understand the efficiency and performance of the search process. On the other hand, the anomaly score, $s(x,n)$, for a given data sample x , provides valuable insights into the likelihood of it being an anomalous set of samples, particularly in the context of malware detection.

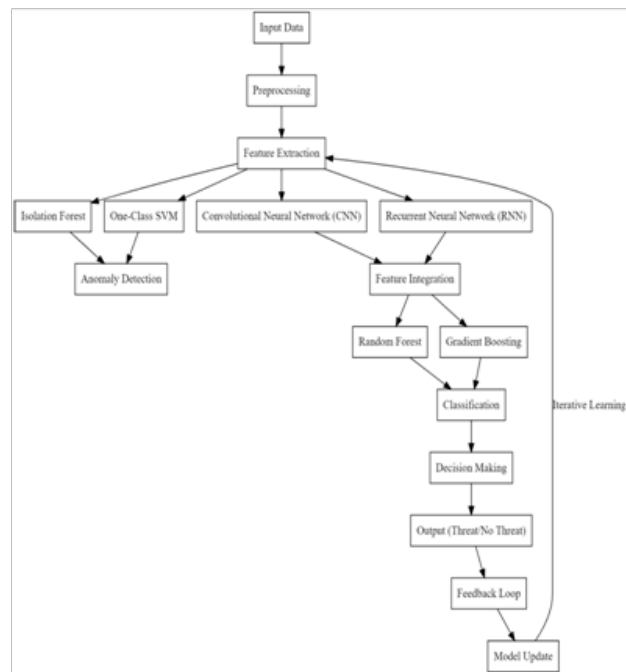


Fig. 1: Model Architecture for Malware detection Process

According to figure 1, the model utilizes One-Class SVM in parallel to effectively identify the 'normal' records. This approach creates a hyperplane in a high-dimensional space to distinguish the majority of data points (non-malware) from the outlier (malware) categories. Let $\phi(x)$ represent the feature map that converts data x into a series of higher-dimensional spaces. OCSVM aims to solve the relationships using equation 2.

$$\min(w, \xi, \rho) * \frac{1}{2} \|w\|^2 + \frac{1}{vn} \sum_{i=1}^n \xi_i - \rho \tag{2}$$

The condition for this statement is that $(w \cdot \phi(x_i)) \geq \rho - \xi_i$

and ≥ 0 for all samples. In this context, w represents the normal vector to the hyperplane, ξ_i are slack variables, ρ is the distance from the origin to the hyperplane, and v represents the regularization parameter sets. The fusion process begins iteratively by applying Isolation Forest to the input data, which produces initial anomaly scores. These scores are then used as inputs for the OCSVM, which further improves the classification process. By adjusting the hyperplane of the OCSVM based on the input from Isolation Forest, the segregation of malware and non-malware data points is enhanced.

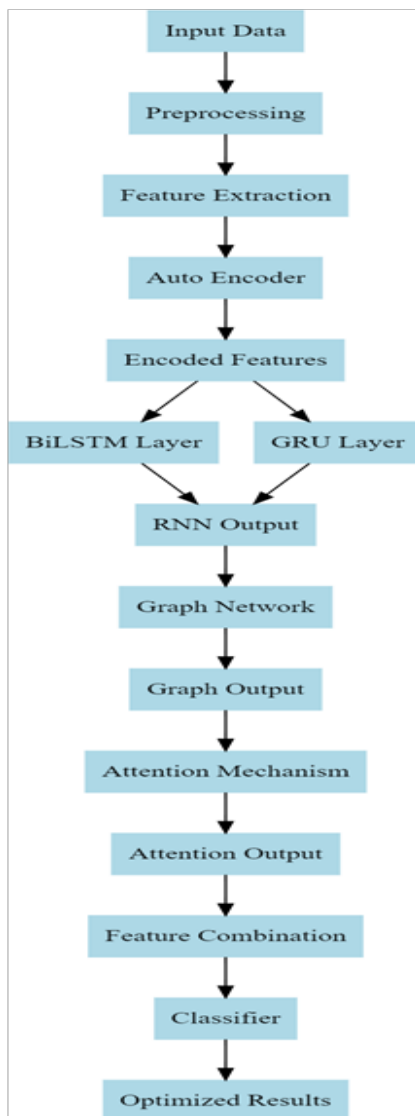


Fig 2. Model Architecture for the Proposed Classification Process

In order to address the challenges of limited scalability and efficiency in current classification techniques, this section explores the development of a comprehensive model that combines Graph Networks and Auto Encoders to improve the efficiency of the malware classification process. According to figure 2, this framework incorporates Recurrent Networks, specifically BiLSTM and GRU layers, which play a crucial role in uncovering temporal dependencies and intricate details within the sequences of malware data.

This process of sequential data processing reveals concealed patterns and temporal relationships, which are vital for comprehending the evolving behaviors of malware. Additionally, Graph Networks delve in to the intricate structures of malware data, utilizing their unique ability to interpret and categorize data presented in a graph-like format that mirrors the interconnected nature of malware signatures. These networks excel at handling non-Euclidean data and provide a deep understanding of the relational context within the data samples. Simultaneously, Auto Encoders aid in reducing dimensionality by meticulously encoding the complex data into a lower-dimensional representation that still contains informative details. This enhances the model's focus on significant features while suppressing noise levels. This process is crucial in distilling the essence of malware signatures, thereby assisting in a more accurate classification process. The incorporation of Attention Mechanisms adds another layer of sophistication by dynamically directing the model's attention to the most relevant features in any given instance. This mechanism adapts to the evolving nature of malware threats, ensuring that the model remains attentive to the most pertinent aspects of the data and enhancing the accuracy of detection.

EXPERIMENTAL SETUP

Data Preparation: To prepare the datasets, relevant features were extracted through pre-processing. This involved analyzing memory dumps for Malware Memory Analysis and conducting static and dynamic analysis of executables from the Kharon Database.

Parameter Initialization: Malware Prediction Model using Auto Encoded& Attention-based Recurrent Graph Analysis was initialized with specific parameters as

follows: • Auto Encoders Layers: The model consisted of 3 layers with 256, 128, and 64 neurons respectively.

Recurrent Graph Relationship Analysis: A Graph Convolutional Network (GCN) with 2 layers was utilized. • Attention Mechanism: Multi-head attention with 4 heads was employed. • LearningRate: The learning rate was set at 0.001 using an Adam optimizer. • Batch Size: Each batch contained 64 samples. • Epochs: The model was trained for 50 epochs.

Training and Validation: The training data accounted for 70% of the total data, while the remaining 30% was used for validation. Cross-validation techniques were implemented to ensure the model's robustness.

Performance Metrics: Precision, accuracy, recall, delay, and AUC were calculated for both datasets. These metrics were selected to provide a comprehensive evaluation of Malware Prediction Model using Auto Encoded& Attention-based Recurrent Graph Analysis effectiveness in real-world scenarios.

RESULT ANALYSIS

The Malware Prediction Model using Auto Encoded& Attention-based Recurrent Graph Analysis model emerges as a groundbreaking approach in the innovative realm of cyber security, skilfully navigating beyond the constraints of traditional malware detection systems. This model ingeniously combines the strengths of Recurrent Neural Networks (RNNs) and Graph Neural Networks (GNNs) to revolutionize the analysis and classification of complex malware patterns. The RNN component delves into the intricate task of feature analysis, meticulously unraveling the nuanced characteristics of malware data. It discerns subtle patterns and temporal dependencies within the data, which is crucial for understanding sophisticated malware behaviors that evolve over time. Complementing this, the GNN aspect of Malware Prediction Model using Auto Encoded& Attention-based Recurrent Graph Analysis serves as an adept classifier, capitalizing on its inherent ability to interpret the interconnected, graph-like structure of malware signatures. This dual-structured approach stands in stark contrast to traditional static or signature-based detection methods, which often stumble when faced with polymorphic or metamorphic malware types. Traditional methods, constrained by their reliance on

predefined signatures, frequently succumb to high false positive rates and show limited adaptability to new and emerging threats. Malware Prediction Model using Auto Encoded& Attention-based Recurrent Graph Analysis, with its integration of Auto Encoders and Attention Mechanisms, transcends these limitations. The Auto Encoders effectively reduce dimensionality and noise, distilling the data to its most informative features. Meanwhile, the Attention Mechanisms provide a dynamic focus on different aspects of the data, enabling the model to adaptively prioritize the most relevant features for malware detection. This harmonious integration facilitates a more profound and nuanced understanding of malware behavior, significantly enhancing the accuracy and reliability of the detection process. The result is a model that not only identifies known malware variants with high precision but also adeptly adapts to identify new, previously unseen types of malware. This marks a significant advancement in the field of cybersecurity.

CONCLUSIONS

The Malware Prediction Model using Auto Encoded& Attention-based Recurrent Graph Analysis model emerges as a groundbreaking approach in the innovative realm of cybersecurity, navigating beyond the constraints of traditional malware detection systems. This model ingeniously combines the strengths of Recurrent Neural Networks (RNNs) and Graph Neural Networks (GNNs) to revolutionize the analysis and classification of complex malware patterns. The RNN component delves into the intricate task of feature analysis, meticulously unraveling the nuanced characteristics of malware data. It discerns subtle patterns and temporal dependencies within the data, which is crucial for understanding sophisticated malware behaviors that evolve over time. Complementing this, the GNN aspect of Malware Prediction Model using Auto Encoded& Attention-based Recurrent Graph Analysis serves as an adept classifier, capitalizing on its inherent ability to interpret the interconnected, graph-like structure of malware signatures. This dual-structured approach stands in stark contrast to traditional static or signature-based detection methods, which often stumble when faced with polymorphic or metamorphic malware types. Traditional methods, constrained by their reliance on

predefined signatures, frequently succumb to high false positive rates and show limited adaptability to new and emerging threats. Malware Prediction Model using Auto Encoded& Attention-based Recurrent Graph Analysis, with its integration of Auto Encoders and Attention Mechanisms, transcends these limitations. The Auto Encoders effectively reduce dimensionality and noise, distilling the data to its most informative features. Meanwhile, the Attention Mechanisms provide a dynamic focus on different aspects of the data, enabling the model to adaptively prioritize the most relevant features for malware detection. This harmonious integration facilitates a more profound and nuanced understanding of malware behavior, significantly enhancing the accuracy and reliability of the detection process. The result is a model that not only identifies known malware variants with high precision but also adeptly adapts to identify new, previously unseen types of malware.

REFERENCES

1. Y. Zhang, G. Gui and S. Mao, "A Lightweight Malware Traffic Classification Method Based on a Broad Learning Architecture," in IEEE Internet of Things Journal, vol. 10, no. 23, pp. 21131-21132, 1Dec.1, 2023, doi: 10.1109/JIOT.2023.3297210.
2. S. Li, Y. Li, X. Wu, S. A. Otaibi and Z. Tian, "Imbalanced Malware Family Classification Using Multimodal Fusion and Weight Self-Learning," in IEEE Transactions on Intelligent Transportation Systems, vol. 24, no. 7, pp. 7642-7652, July 2023, doi:10.1109/TITS.2022.3208891.
3. O.E.Kural, E.Kiliç and C.Aksaç, "Apk2Audio4AndMal: Audio Based Malware Family Detection Framework," in IEEE Access, vol.11, pp. 27527-27535, 2023, doi: 10.1109/ACCESS.2023.3258377.
4. O. Barut, Y. Luo, P. Li and T. Zhang, "R1DIT: Privacy-Preserving Malware Traffic Classification With Attention-Based Neural Networks," in IEEE Transactions on Network and Service Management, vol. 20, no. 2, pp. 2071-2085, June 2023, doi:10.1109/TNSM.2022.3211254.
5. S. Yan, J. Ren, W. Wang, L. Sun, W. Zhang and Q. Yu, "A Survey of Adversarial Attack and Defense Methods for Malware Classification in Cyber Security," in IEEE Communications Surveys & Tutorials, vol.25, no. 1, pp. 467-496, Firstquarter 2023, doi:10.1109/COMST.2022.3225137.
6. F. Zhong, Z. Chen, M. Xu, G. Zhang, D. Yu and X. Cheng, "Malware-on-the-Brain: Illuminating Malware Byte Codes With Images for Malware Classification," in IEEE Transactions on Computers, vol. 72, no. 2, pp. 438-451, 1 Feb. 2023, doi: 10.1109/TC.2022.3160357.
7. J. Kim, J. -Y. Paik and E. -S. Cho, "Attention-Based Cross-Modal CNN Using Non-Disassembled Files for Malware Classification," in IEEE Access, vol. 11, pp. 22889-22903, 2023, doi:10.1109/ACCESS.2023.3253770.
8. M. M. Belal and D. M. Sundaram, "Global-Local Attention-Based Butterfly Vision Transformer for Visualization-Based Malware Classification," in IEEE Access, vol. 11, pp. 69337-69355, 2023, doi:10.1109/ACCESS.2023.3293530.
9. Y. He, X. Kang, Q. Yan and E. Li, "ResNeXt+: Attention Mechanisms Based on ResNeXt for Malware Detection and Classification," in IEEE Transactions on Information Forensics and Security, vol. 19, pp. 1142-1155, 2024, doi: 10.1109/TIFS.2023.3328431.
10. V. Ravi, T. D. Pham and M. Alazab, "Attention-Based Multidimensional Deep Learning Approach for Cross-Architecture IoMT Malware Detection and Classification in Healthcare Cyber-Physical Systems," in IEEE Transactions on Computational Social Systems, vol. 10, no. 4, pp. 1597-1606, Aug. 2023, doi:10.1109/TCSS.2022.3198123.
11. J. Guo, S. Guo, S. Ma, Y. Sun and Y. Xu, "Conservative Novelty Synthesizing Network for Malware Recognition in an Open-Set Scenario," in IEEE Transactions on Neural Networks and Learning Systems, vol. 34, no. 2, pp. 662-676, Feb. 2023, doi:10.1109/TNNLS.2021.3099122.
12. X. Zhang, J. Wang, J. Xu and C. Gu, "Detection of Android Malware Based on Deep Forest and Feature Enhancement," in IEEE Access, vol.11, pp. 29344-29359, 2023, doi: 10.1109/ACCESS.2023.3260977.
13. T. Lu and J. Wang, "DOMR: Toward Deep Open-World Malware Recognition," in IEEE Transactions on Information Forensics and Security, vol. 19, pp. 1455-1468, 2024, doi:10.1109/TIFS.2023.3338469.
14. C. Kim, S. -Y. Chang, J. Kim, D. Lee and J. Kim, "Automated, Reliable Zero-Day Malware Detection Based on Autoencoding Architecture," in IEEE Transactions on Network and Service Management, vol. 20, no. 3, pp. 3900-3914, Sept. 2023, doi: 10.1109

15. D. Y. M. Benchadi, B. Batalo and K. Fukui, "Efficient Malware Analysis Using Subspace-Based Methods on Representative Image Patterns," in IEEE Access, vol. 11, pp. 102492-102507, 2023, doi:10.1109/ACCESS.2023.3313409.
16. I. Gulatas, H. H. Kilinc, A. H. Zaim and M. A. Aydin, "Malware Threat on Edge/Fog Computing Environments From Internet of Things Devices Perspective," in IEEE Access, vol.11,pp.84772-84784,2023,doi:10.1109/ACCESS.2023.3266562.
17. M. F. Abdelwahed, M. M. Kamal and S. G. Sayed, "Detecting Malware Activities With Malp Miner:A Dynamic Analysis Approach,"in IEEE Access, vol. 11, pp. 84772-84784, 2023, doi:10.1109/ACCESS.2023.3266562.
18. F. Zhong, Z. Chen, M. Xu, G. Zhang, D. Yu and X. Cheng, "Malware-on-the-Brain: Illuminating Malware Byte Codes With Images for Malware Classification,"in IEEE Transactions on Computers, vol. 72,no. 2, pp. 438-451, 1 Feb. 2023, doi: 10.1109/TC.2022.3160357.

Enhancing Engineering Pedagogy to Elevate the Quality of Engineering Education in India

Santosh Sancheti

Department of Mechanical Engineering
Savitribai Phule Pune University
Pune, Maharashtra
✉ santosancheti@gmail.com

Kainjan Sanghavi, Mahesh Sanghavi

Department of Computer Engineering
Savitribai Phule Pune University
Pune, Maharashtra

ABSTRACT

In recent years, there has been an increasing emphasis on the quality of engineering education in India. With the evolving global landscape and India's aspiration to produce globally competent engineers, there's an urgent need to revisit and reinvent the teaching methods used in the country's engineering institutions. This paper explores various approaches of engineering pedagogy and their potential impact on enhancing the quality of teaching in India's engineering education sector.

KEYWORDS : *Engineering pedagogy, Innovative teaching methods, Frugal innovation, Industry-academia collaboration, Global engineering education.*

INTRODUCTION

Over recent years, the focus on the quality of engineering education in India has significantly heightened, matching the global trend of pursuing excellence in engineering pedagogy. This is driven by India's ambition to foster engineers who are adept and competent on a worldwide stage. Accordingly, it is crucial to critically analyze and potentially overhaul the current educational methodologies employed within Indian engineering establishments to ensure they meet international standards [1].

This research seeks to unravel the different paradigms of engineering pedagogy and discern how they could be leveraged to refine the teaching quality in India's engineering education sphere. Through a nuanced exploration of globally recognized pedagogical strategies, we intend to present a roadmap that can elevate the engineering academia in India to a pedestal of global recognition and respect.

Furthermore, it not just identifies the rich array of teaching methods that can be adopted but also delves deeply into how each one could be customized to align seamlessly with India's unique socio-economic fabric. This involves creating a symbiotic relationship between

global best practices and India's inherent strengths in the educational domain.

This paper stands as a critical resource for policymakers, educational institutions, and stakeholders in the engineering education ecosystem, providing them with a well-rounded perspective on enhancing pedagogy through globally tried and tested, yet locally adaptable strategies, thereby bringing a fresh impetus to the engineering education landscape in India. It aspires to be a catalyst in India's journey towards becoming a hub of globally competent engineering education through pedagogical innovation.

UNDERSTANDING OF ENGINEERING PEDAGOGY

Engineering pedagogy boasts an illustrious legacy at the Indian Institutes of Technology (IITs). Discussions concerning technical education and its evolution can be traced back to the establishment of the first IIT in Kharagpur in 1951. Under the visionary leadership of distinguished academicians and experts, the Department of Engineering Pedagogy was institutionalized, thereby formalizing teaching and research in the realm of engineering education. The department's research primarily centered around the interplay between

advanced technology and its implications for effective technical instruction.

A foundational philosophy in the Indian approach to engineering pedagogy has been the essence of technology as a transformative force. Technology's core purpose, as viewed by pioneers like Dr. Rajendra Prasad, was to "alter and elevate the natural world." Consequently, the primary objective of an engineer is to harness and further this technology. This mandates that engineers are trained such that they are adept at addressing intricate technical challenges. This perspective differs from that of natural scientists, whose primary pursuit is to uncover and elucidate the intricate relationships governing the natural world. The innovative spirit of engineers and the exploratory mindset of scientists necessitate distinct academic training methods.[2]

Emerging in the 1990s, another interpretation of engineering pedagogy emphasized the engineer's role beyond mere technical competence. Given the rapidly globalizing Indian landscape, an engineer's prowess in engaging in socio-communicative processes in the contemporary industrial and service sectors became a pivotal aspect of pedagogical focus.

In Sanskrit, one of the ancient languages from which many Indian tongues derive, the term for education, "Vidya", signifies knowledge and enlightenment. Thus, the essence of engineering pedagogy in the Indian context is not only to impart technical knowledge but also to prepare future engineers for leadership roles in the dynamically evolving industrial and service sectors. This paper endeavors to provide insights into the nuances of engineering pedagogy, particularly in the milieu of India's technical institutions. As India produces a large number of engineering graduates every year. To enhance their global competitiveness and relevance, the pedagogical strategies used in engineering education need re-evaluation and reinvention.[4]

The concept of a demand-oriented "Engineering Pedagogy" is of paramount importance, particularly in the context of India's dynamic engineering education system and the standards set by accreditation bodies like the National Board of Accreditation (NBA) and the National Assessment and Accreditation Council (NAAC).[1]

When contemplating the design of learning and teaching processes in academic engineering education, it becomes evident that this is a matter of scientific inquiry. In the Indian context, educators must adhere to stringent regulations that mandate verifiable pedagogical and psychological qualifications for teaching at all levels and across all types of educational institutions, including engineering colleges. However, a common assumption in higher education is that individuals with high academic qualifications inherently possess teaching abilities.

Contrary to this assumption, empirical evidence, as highlighted in various evaluation reports, suggests that high academic qualifications do not always equate to effective teaching [5] This discrepancy can be attributed to the multifaceted nature of factors and relationships governing the creation of a demand-oriented education framework within engineering sciences. Here, the term "design" encompasses not only the planning but also the execution and assessment of teaching and learning processes in engineering education.

The imperative to align engineering education with the demands of the economy, especially in the context of India's burgeoning industrial landscape, underscores the significance of demand-oriented and employment-based engineering education. In essence, this entails molding engineering curricula to meet the specific needs of the engineering workforce, which are intricately linked to the prevailing structures of production and service.

The concept of a demand-oriented "Engineering Pedagogy" in the Indian context is instrumental not only in producing job-ready engineers but also in aligning engineering education with the rapidly evolving industrial landscape. It is a fundamental aspect that directly correlates with the quality assurance processes championed by accreditation bodies like the NBA and NAAC. Hence, it serves as a linchpin in ensuring that the engineering graduates emerging from India's institutions are equipped with the requisite skills and knowledge to meet the demands of contemporary industries.[1]

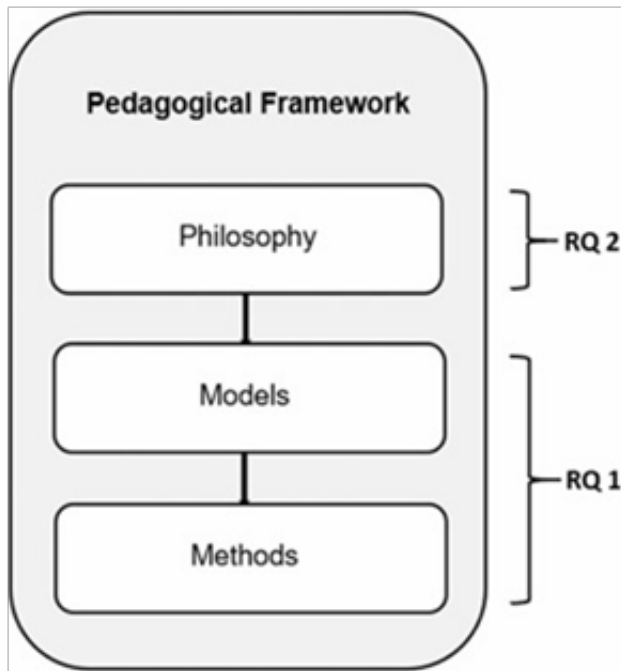


Fig. 1: An illustration of the position of pedagogical models Adapted from Goodyear (1999)

TRADITIONAL PEDAGOGICAL METHODS

Traditional pedagogical methods in the context of Indian engineering education have long been characterized by a set of well-established practices that have shaped the learning experiences of countless students. These methods, however, have garnered increasing scrutiny and criticism over the years due to their limitations and the evolving demands of the global engineering landscape. To understand this better, let's delve into the components of traditional pedagogical methods in Indian engineering education:

1. **Rote Learning:** Rote learning is a prevalent pedagogical technique in India, where students memorize information without necessarily understanding the underlying concepts. This approach is often employed to help students pass standardized exams. However, it fosters a superficial understanding of subjects, inhibiting critical thinking and problem-solving skills. In the context of the discussion, it's important to note that rote learning has been a cornerstone of traditional engineering education in India.

2. **Standardized Tests:** Engineering education in India places immense emphasis on standardized entrance and exit examinations. These exams, such as the Joint Entrance Examination (JEE) and Graduate Aptitude Test in Engineering (GATE), are highly competitive and largely assess students' ability to recall facts and formulas. While they have their merits, they often prioritize rote learning and don't effectively gauge practical problem-solving abilities or creativity, which are crucial in the engineering profession.
3. **One-Size-Fits-All Approach:** Traditional engineering education in India typically follows a rigid curriculum that leaves little room for customization or specialization. Students are often expected to study a fixed set of subjects, regardless of their individual interests or career aspirations. This one-size-fits-all approach can stifle creativity and innovation as it doesn't cater to the diverse talents and aspirations of students.

The consequences of these traditional pedagogical methods are significant:

1. **Lack of Problem-Solving Skills:** Students educated in this system often struggle with real-world problem-solving. They may excel in exams but find it challenging to apply their knowledge to practical situations, a crucial skill in engineering.
2. **Limited Creativity:** The emphasis on memorization and standardized testing can discourage creative thinking and innovation, qualities that are highly valued in engineering fields.
3. **Industry Relevance:** Employers often find that graduates lack the practical skills and adaptability needed in the dynamic world of engineering. The traditional system doesn't adequately prepare students for the demands of modern industries.

In light of these limitations, there has been a growing recognition of the need to reform engineering education in India. The shift towards contemporary pedagogical approaches, as discussed earlier, aims to address these shortcomings by fostering critical thinking, problem-solving abilities, creativity, and relevance to the engineering profession. These modern methods recognize that engineering education should not only be

about acquiring knowledge but also about developing the skills and mindset required to excel in the real world, making Indian engineers more competitive on a global scale.[6]

CONTEMPORARY APPROACHES OF ENGINEERING PEDAGOGY

Contemporary approaches to engineering pedagogy hold significant importance in the realm of engineering education in India. They serve as a vital catalyst for addressing the multifaceted challenges faced by the traditional pedagogical methods. These innovative approaches, such as Problem-Based Learning (PBL), Flipped Classrooms [3], Collaborative and Team-Based Learning, Blended Learning, and Experiential Learning, offer a transformative educational experience that equips engineering students with essential skills and competencies for the 21st century.[7]

One of the paramount advantages of these contemporary methods is their ability to nurture problem-solving skills. In an era characterized by complex and ever-evolving technological challenges, engineers must possess the capability to analyze intricate problems and devise innovative solutions. Furthermore, these approaches foster critical thinking and creativity, qualities that are invaluable in a highly competitive and innovative global engineering landscape.[10]

Moreover, contemporary pedagogical methods bridge the gap between academia and industry, ensuring that engineering education remains closely aligned with the evolving needs of various sectors. This alignment is crucial for producing graduates who are not only well-versed in theoretical knowledge but also adept at applying their expertise to real-world scenarios, thus enhancing their industry relevance. Personalized learning, adaptability to technological advancements, preparation for a global workforce, and a strong emphasis on experiential learning are additional attributes that underscore the importance of these contemporary approaches. They empower students to take charge of their education, adapt to changing technologies, collaborate effectively in diverse teams, and gain practical hands-on experience that is instrumental in their professional development.

Furthermore, these approaches contribute to continuous improvement and quality assurance in engineering education. By encouraging ongoing assessment and feedback, they ensure that educational programs remain responsive to changing circumstances and that the quality of education continually meets and exceeds global standards.

- A. Problem-Based Learning (PBL): Encourages students to solve real-world problems and enhances their problem-solving skills.
- B. Flipped Classrooms: Students access lecture content online, and classroom time is dedicated to discussions, problem-solving, and hands-on activities[3].
- C. Collaborative and Team-Based Learning: Emphasizes teamwork and mirrors the collaborative nature of real-world engineering projects.
- D. Blended Learning: Combines online digital media with traditional classroom methods to offer flexibility and personalized learning experiences.
- E. Experiential Learning: Focuses on learning by doing, promoting internships, industry projects, and lab work.

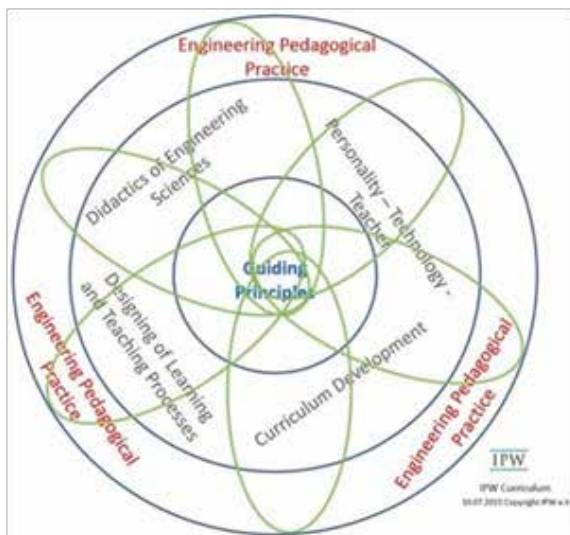


Fig. 2: IPW – curriculum design – engineering pedagogy theory and practice (Ingenieurpädagogische Wissenschaftsgesellschaft IPW 2016, p. 249) [5]

CUSTOMIZING PEDAGOGY FOR THE INDIAN CONTEXT

Customizing pedagogy to suit the Indian context is

crucial for ensuring that educational practices align effectively with the nation's distinct cultural, economic, and educational landscapes. This adaptation not only enhances the quality of education but also makes it more accessible and relevant to the diverse population of India. Here's an elaboration on the significance of customizing pedagogy and the specific approaches mentioned:

Local Case Studies

Using local industries and problems as case studies can significantly enhance the relevance of engineering education in India. India boasts a vast and varied industrial landscape, with sectors ranging from information technology and pharmaceuticals to agriculture and manufacturing. By incorporating local case studies, educators can bridge the gap between theory and practice, exposing students to real-world challenges that are immediately recognizable and relatable. This not only engages students but also empowers them to apply their learning to solve problems within their own communities. Furthermore, it fosters a sense of ownership and pride in addressing India's unique challenges, contributing to a more socially responsible and solution-oriented engineering workforce.

Multilingual Resources

India is a linguistically diverse nation with a multitude of regional languages and dialects. While English is widely used in higher education, offering resources in multiple regional languages is essential for making education more inclusive. This approach ensures that students from various linguistic backgrounds have equitable access to educational materials and can fully engage in the learning process. It also recognizes the importance of preserving and promoting the country's linguistic and cultural diversity. Multilingual resources not only facilitate better understanding but also enhance communication and collaboration among students, fostering a more inclusive and cohesive learning environment.

Customizing pedagogy for the Indian context is not a mere adaptation but a necessity to address the unique needs and characteristics of the nation. By incorporating local case studies and offering resources in multiple regional languages, engineering education in India

becomes more relevant, engaging, and inclusive. This tailored approach not only prepares students for the specific challenges and opportunities within the country but also contributes to the preservation and celebration of India's rich cultural and linguistic diversity.

RECOMMENDATIONS:

These are solid recommendations for improving the quality of education and ensuring that educational institutions stay current and relevant in a rapidly changing world.

- A. Curriculum Revision: Regularly updating the curriculum is crucial to ensure that students are learning the most current and relevant information. This can involve reviewing course content, adding new subjects, and adapting to industry trends. It also helps in meeting accreditation requirements and staying competitive with other institutions.
- B. Faculty Development Programs: Faculty members play a pivotal role in the education system. Regular training sessions help them stay updated with the latest teaching methods, technologies, and trends in their respective fields. This can lead to more engaging and effective teaching.
- C. Industry-Academia Collaboration: Collaboration between educational institutions and industries is beneficial for both parties. It allows students to gain practical experience, and it helps universities tailor their programs to meet industry demands. This collaboration can also lead to research opportunities and innovation hubs.
- D. Investment in Infrastructure: Modern infrastructure is essential for effective teaching and learning. Up-to-date labs, classrooms, and digital resources enable educators to employ contemporary teaching methods, such as interactive online platforms and virtual laboratories.
- E. Feedback Mechanisms: Regular feedback from students, faculty, and industry experts is crucial for improvement. It helps identify areas of weakness in teaching methodologies and provides insights into what's working well. This feedback loop can drive continuous improvement and ensure that the institution remains responsive to the needs of its stakeholders [1].

Implementing these recommendations will likely require careful planning, funding, and ongoing evaluation. However, they can significantly enhance the quality of education and the reputation of the institution. Moreover, they can better prepare students for the challenges and opportunities of the modern workforce, which is critical for their future success.

CONCLUSION

India possesses immense potential to establish itself as a global engineering hub. This potential can be realized through the adoption of modern pedagogical methods in education, tailored to the unique Indian context. By enhancing the quality of engineering education and preparing graduates to address global challenges, India can indeed shape the future of technology, innovation, and sustainable development on a global scale. The journey towards this goal requires a concerted effort from educational institutions, policymakers, and industry stakeholders to empower a new generation of engineers who are not only technically proficient but also globally aware and adaptable. India's role in the global engineering landscape is poised to be transformative and influential.

ACKNOWLEDGMENTS

The authors thanked the numerous educators, students, and industry experts who shared their insights and experiences for this study.

REFERENCES

1. AICTE. (2020). Curriculum for undergraduate degree courses in engineering & technology. New Delhi.
2. Bajpai, N. (2018). Reimagining engineering education in India. *Indian Journal of Technical Education*, 41(4), 303-310.
3. Raj, R. K., & Kumar, V. (2019). Flipped classroom approach in engineering education: A review. *Education and Information Technologies*, 24(1), 755-771.
4. Banerjee, Rangan & Muley, Vinayak. (2009). Engineering education in India. INAE Workshop at Bangalore.
5. Kersten, Steffen. (2018). Approaches of Engineering Pedagogy to Improve the Quality of Teaching in Engineering Education. 10.1007/978-3-319-73093-6_14.
6. Oskar Hagvall Svensson, Tom Adawi, Mats Lundqvist & Karen Williams Middleton (2019): Entrepreneurial engineering pedagogy: models, tradeoffs and discourses, *European Journal of Engineering Education*, DOI: 10.1080/03043797.2019.1671811
7. Creed, C. J., E. M. Suuberg, and G. P. Crawford. 2002. "Engineering Entrepreneurship: An Example of a Paradigm Shift in Engineering Education." *Journal of Engineering Education* 91: 185–195.
8. Lee, E., and M. J. Hannafin. 2016. "A Design Framework for Enhancing Engagement in Student-Centered Learning: Own it, Learn it, and Share it." *Educational Technology Research and Development* 64 (4): 707–734.
9. Williams Middleton, K., and A. Donnellon. 2014. "Personalizing Entrepreneurial Learning: A Pedagogy for Facilitating the Know why." *Entrepreneurship Research Journal* 4 (2): 167–204.
10. Daly, S. R., Mosyjowski, E. A., & Seifert, C. M. (2014). Teaching Creativity in Engineering Courses. *Journal of Engineering Education*, 103(3), 417–449. doi:10.1002/jee.20048.

A Paradigm Shift in Higher Education in India from Classroom Learning to Real-World Application

Dipak Sancheti, Santosh Sancheti

Department of Mechanical Engineering
Savitribai Phule Pune University
Pune, Maharashtra
✉ santusancheti@gmail.com

Kainjan Sanghavi, Mahesh Sanghavi

Department of Computer Engineering
Savitribai Phule Pune University
Pune, Maharashtra

ABSTRACT

This paper explores the transformative impact of India's National Education Policy (NEP) 2020 on higher education, focusing on experiential learning and academia-industry collaboration. Through an analysis of NEP 2020's vision and implementation strategies, as well as insights from academic studies and industry partnerships, it examines the opportunities and challenges presented by the policy. The role of experiential learning in enhancing student employability and fostering innovation is discussed, alongside the importance of academia-industry collaboration in aligning curricula with industry needs and promoting research. By synthesizing current trends and real-world examples, this paper offers insights into the evolving educational landscape and the potential of NEP 2020 to shape the future of higher education in India.

KEYWORDS : *Experiential learning, National Education Policy (NEP) 2020, Academia-industry collaboration, Artificial Intelligence (AI) in education, Skill development.*

INTRODUCTION

In the landscape of global education, India stands at a pivotal crossroads. Confronted with the challenges of a rapidly evolving knowledge economy, the Indian higher education system is undergoing a significant transformation. Central to this transformation is the National Education Policy (NEP) 2020, a landmark initiative aimed at redefining and revitalizing India's educational framework. (Ministry of Education, Government of India, 2020) The NEP 2020, aligning with the ethos of Indian culture and values, endeavors to catapult the nation towards becoming a global knowledge superpower. (Altbach & Jayaram, 2019).

At the heart of this educational overhaul is a shift from the traditional, classroom-centric approach to a more dynamic, experiential learning model. This paradigm shift is not merely a change in teaching methodology but a profound reimagining of how learning is perceived, delivered, and applied. Experiential learning, with its emphasis on 'learning by doing', presents a radical

departure from rote memorization and passive learning. It promotes an educational environment where students actively engage with concepts, apply knowledge in practical settings, and develop skills essential for navigating the complexities of the modern world. (Agarwal, 2009).

The purpose of this paper is to delve into the transformative impact of NEP 2020 on higher education in India, with a specific focus on the shift towards experiential learning. It examines the role of emerging technologies, particularly Artificial Intelligence (AI) and Machine Learning (ML), in shaping the future of education under the umbrella of Education 4.0. Furthermore, this paper seeks to analyze the implications of this shift for student employability, industry readiness, and the overall quality of education in India. Through a comprehensive exploration of current trends, academic perspectives, and real-world applications, this paper aims to provide a nuanced understanding of the evolving educational landscape in India, marked by a synergistic blend of tradition and innovation.

BACKGROUND

Traditional Education Models in India

The traditional education system in India, with roots extending back to ancient times, has predominantly been characterized by a teacher-centered approach. Historically, learning in India was imparted through Gurukuls, where students lived with their teacher or guru, acquiring knowledge through direct instruction and memorization. This model transitioned over time into more structured classroom settings post-colonial influence, but the core methodology of rote learning and passive reception of knowledge largely remained unchanged. In the modern context, Indian education has often followed a structured, curriculum-based approach, emphasizing theoretical knowledge and standardized testing. This system, primarily focusing on core subjects like mathematics, science, and languages, has been heavily reliant on textbooks as the primary source of information. Classes typically involve teachers delivering lectures, with students expected to absorb and reproduce the information, often measured through written exams and periodic assessments. This model has been prevalent across various educational levels, from primary schools to universities. (Agarwal, 2009 & (KPMG & FICCI, 2022)

Limitations of Conventional Classroom Learning

However, the conventional classroom model in India faces several limitations:

- 1) Rote Memorization: Emphasizing rote learning, this system often fails to encourage critical thinking and creativity. Students are trained to memorize information without necessarily understanding underlying concepts, leading to a superficial grasp of knowledge.
- 2) Lack of Practical Application: There is a significant gap between theoretical knowledge and its practical application. Students often find themselves ill-equipped to apply classroom-taught concepts to real-world scenarios, which is a critical skill in the modern job market.
- 3) One-Size-Fits-All Approach: Traditional classrooms do not adequately cater to the varied learning styles and paces of different students.

This leads to a homogenized form of education where the unique needs and potential of individual learners are not optimally addressed.

- 4) Teacher-Centric Methodology: The teacher-centric nature of traditional education limits student engagement and participation. This approach does not foster an interactive learning environment, which is crucial for deeper understanding and retention of knowledge. (Altbach & Jayaram, 2019).

INTRODUCTION TO EXPERIENTIAL LEARNING

In contrast to the traditional model, experiential learning presents a more dynamic and interactive approach. It emphasizes 'learning by doing' and is rooted in the belief that the most effective learning occurs through experience and reflection. This model involves engaging students in activities that replicate real-world challenges, encouraging them to apply theoretical knowledge in practical scenarios.

The shift towards experiential learning in Indian education is a response to the evolving demands of the global economy and the need for a more holistic development of students. By bridging the gap between theory and practice, experiential learning aims to produce graduates who are not only knowledgeable but also skilled and adaptable, ready to contribute effectively in their respective fields. (Agarwal, 2009 & Ernst & Young, 2023 Ministry of Education, Government of India, 2020).

Vision and Goals of NEP 2020

The National Education Policy (NEP) 2020, unveiled by the Government of India, marks a significant milestone in the evolution of the country's educational framework. It is an ambitious policy, aiming to overhaul and modernize the Indian education system, aligning it with the demands of the 21st century. The vision of NEP 2020 is to create an inclusive, flexible, and holistic education system that ensures the overall development of students, making them not just academically proficient but also skilled, creative, and well-prepared for the challenges of the modern world.



Fig. 1 NEP 2020 Higher Education

Key goals of NEP 2020 include:

- 1) Universal Access to Education: Ensuring equitable access to quality education for all students, including those from disadvantaged backgrounds.
- 2) Promoting Multidisciplinary and Holistic Education: Encouraging a broad-based, multidisciplinary curriculum to foster critical thinking, creativity, and a diverse set of skills.
- 3) Emphasis on Foundational Literacy and Numeracy: Focusing on foundational learning to ensure that every child achieves proficiency in reading, writing, and arithmetic.
- 4) Revamping Curriculum and Pedagogy: Restructuring the educational framework to make learning more experiential, integrated, and student-centric.
- 5) Focus on Skill Development: Integrating skill development into mainstream education to enhance employability and entrepreneurship.
- 6) Use of Technology in Education: Leveraging technology to improve teaching, learning, and assessment processes.

ENCOURAGING EXPERIENTIAL LEARNING IN NEP 2020

NEP 2020 has been specifically designed to shift the focus from traditional rote learning methods to an experiential learning approach. The policy lays

significant emphasis on 'learning by doing' and promotes a variety of hands-on, inquiry-based, discussion-based, and analysis-based learning methods. (National Council of Educational Research and Training [NCERT], 2021).

Key aspects of NEP 2020 that encourage experiential learning include

Integration of Vocational Education: Starting from the early stages of schooling, vocational education is to be integrated with mainstream education. This allows students to gain practical skills and understand their applications in real-life situations. (KPMG & FICCI, 2022).

- 1) Flexibility in Choosing Subjects: The policy provides flexibility in choosing subjects, encouraging students to explore different disciplines. This interdisciplinary approach is conducive to experiential learning as it allows students to apply concepts from one field to another in practical scenarios.
- 2) Project-Based and Activity-Based Learning: NEP 2020 advocates for a curriculum that includes more project-based and activity-based learning, providing opportunities for students to engage in research, problem-solving, and creative work.
- 3) Use of Technology: The policy acknowledges the role of technology in enhancing educational experiences. Digital tools, online resources, and virtual labs are encouraged to supplement classroom teaching, offering interactive and immersive learning experiences.

Growth and Development in the Experiential Learning Sector

Increased Demand for Skill-Based Education

As NEP 2020 emphasizes skill development, there is an increasing demand for education that goes beyond theoretical knowledge, focusing on practical skills applicable in the workforce.

- 1) Rise of EdTech Platforms: The growth of the EdTech sector in India, fueled by NEP 2020’s emphasis on technology in education, is playing a pivotal role in providing experiential learning opportunities. Platforms offering simulations, virtual labs, and interactive content are becoming increasingly popular.

- 2) Industry-Academia Collaboration: NEP 2020 encourages partnerships between educational institutions and industries. Such collaborations are crucial for developing curriculums that provide real-world experience and meet the skill requirements of various industries.
- 3) Changing Mindsets: There is a gradual but noticeable shift in the mindset of educators, parents, and students towards the value of practical and applied learning. This cultural shift is essential for the adoption and growth of experiential learning methods. (Altbach & Jayaram, 2019)

PERSPECTIVES ON EXPERIENTIAL LEARNING

Surveys and Studies on Experiential Learning Preferences.

The shift towards experiential learning in India's educational landscape has garnered a variety of responses from students and educators alike. Various surveys and studies have been conducted to gauge the perspectives and preferences regarding this pedagogical approach.

- A. Student Preferences: A Deloitte survey revealed that a substantial 82% of students showed a preference for experiential learning methods, including simulations, interactive sessions, and hands-on projects (Ernst & Young, 2023)
- B. Educator Preferences: The same survey indicated that about 90% of academicians either have already implemented or are planning to implement experiential learning methodologies in their curriculum.
- C. Skill Development Focus: A study by the National Skill Development Corporation (NSDC) of India emphasized the growing importance of skill-based education among both students and educators. (KPMG & FICCI, 2022).

ACADEMICIAN READINESS AND ATTITUDES TOWARDS EXPERIENTIAL LEARNING

The readiness and attitudes of academicians towards adopting experiential learning methods are crucial

for the successful implementation of this educational paradigm.

- A. Positive Attitude towards Change: Many educators have expressed a positive attitude towards experiential learning, recognizing its potential to make education more engaging and effective
- B. Challenges in Implementation: Despite the positive outlook, some educators face challenges in implementing experiential learning methods. These challenges include a lack of resources, insufficient training in new pedagogies, and the need to balance curriculum requirements with experiential activities.
- C. Professional Development and Training: To address these challenges, there is a growing emphasis on professional development and training for teachers. Workshops, seminars, and training programs are being conducted to equip educators with the skills and knowledge required to effectively implement experiential learning strategies.
- D. Collaboration with Industry Experts: Academicians are increasingly collaborating with industry experts to bring practical insights into the classroom.
- E. Technology Integration: Educators includes the use of virtual reality, augmented reality, and online simulation tools to create immersive learning experiences.
- F. Feedback and Iterative Improvement: Feedback mechanisms are being employed to assess the effectiveness of experiential learning methods.

AI'S INFLUENCE ON THE LEARNING LANDSCAPE

The integration of Artificial Intelligence (AI) into the educational sector has brought about a revolutionary change in how learning is experienced and delivered. AI's influence has permeated various aspects of education, transforming traditional methods and paving the way for more personalized, interactive, and effective learning experiences.

- A. Transforming Learning Experiences with AI: Personalized Learning Paths: AI algorithms are capable of analyzing a student's learning patterns,

strengths, and weaknesses. This data-driven approach enables the creation of personalized learning paths, allowing students to learn at their own pace and style.

- B. **Interactive Learning Environments:** AI-powered platforms have facilitated the development of more interactive and engaging learning environments. Tools like chatbots and virtual tutors provide instant feedback and support, making learning more responsive and dynamic.
- C. **Adaptive Assessment Systems:** AI is being used to develop adaptive assessment systems that can tailor tests based on a student's proficiency level. (National Council of Educational Research and Training (NCERT), 2021)
- D. **Enhanced Accessibility:** AI tools have made learning more accessible to students with different needs. While AI-driven language translation tools can help bridge language barriers. (Ernst & Young, 2023).

COLLABORATION BETWEEN ACADEMIA AND INDUSTRY

Successful Examples of Academia-Industry Collaborations

- A. **MIT's Industrial Liaison Program:** The Massachusetts Institute of Technology (MIT) in the USA has a long-standing Industrial Liaison Program that connects its research and educational resources with industry partners. This program has led to numerous collaborations in research and development, providing valuable practical experiences for students.
- B. **Stanford University and Silicon Valley:** Stanford University's proximity to and collaboration with Silicon Valley have been instrumental in fostering an environment of innovation and entrepreneurship. This partnership has led to the development of cutting-edge technologies and successful startups.
- C. **IITs and Industry Partners in India:** The Indian Institutes of Technology (IITs) have multiple collaborations with industry partners for research, internships, and placement programs. These partnerships have been crucial in aligning technical

education with industry standards and needs.

- D. **Germany's Dual Education System:** Germany's dual education system is a prime example of effective academia-industry collaboration. It combines apprenticeships in a company and vocational education at a vocational school in one course. This model is highly successful in preparing students for specific trades and roles.
- E. **Siemens and Universities:** Siemens has partnered with various universities worldwide to provide advanced learning tools and technology. This collaboration has led to the development of curriculum modules, research projects, and technology transfer, aligning education with cutting-edge industrial practices.

The collaboration between academia and industry is vital for creating an education system that is responsive to the needs of the modern economy. Such partnerships not only enhance the quality of education but also contribute to innovation, economic growth, and the overall development of the workforce.

CASE STUDIES: INDIAN EDUCATIONAL INSTITUTIONS AND EXPERIENTIAL LEARNING

The integration of experiential learning in Indian educational institutions has been a significant step towards enhancing the quality and relevance of education in the country. These case studies illustrate how some leading institutions have adopted experiential learning methods and their collaborations with global universities.

Case Study 1: Indian Institute of Technology (IIT) Bombay

Experiential Learning Approach: IIT Bombay has been a frontrunner in incorporating experiential learning into its curriculum. The institute emphasizes project-based learning, where students work on real-world problems. This approach is evident in their flagship event, the Techfest, which showcases innovative projects developed by students. Additionally, the institute offers numerous internship opportunities in collaboration with industry partners, enabling students to gain practical experience.

Global Collaboration Impact: IIT Bombay has established partnerships with universities like MIT and Stanford for faculty exchange programs and joint research projects. These collaborations have led to advancements in research methodologies and the introduction of cutting-edge technologies in their curriculum, significantly enhancing the students' learning experience.

Case Study 2: National Institute of Design (NID), Ahmedabad

Experiential Learning Approach: NID, known for its design education, has adopted a hands-on learning approach. Students are encouraged to work on live projects with real clients, providing them with practical exposure to design challenges and solutions. The institute's workshops and studios are equipped with state-of-the-art tools, allowing students to experiment and innovate.

Global Collaboration Impact: Collaborations with international design schools, such as the Royal College of Art, UK, have facilitated student and faculty exchanges. These interactions expose students to global design trends and practices, thereby broadening their perspective and enhancing their design skills.

Case Study 3: Indian School of Business (ISB), Hyderabad
Experiential Learning Approach: ISB incorporates experiential learning through its Applied Learning Projects (ALPs), where students work on real-time projects with companies. This approach helps students apply their classroom knowledge to practical business scenarios, developing critical thinking and problem-solving skills.

Global Collaboration Impact: ISB has tie-ups with global institutions like the Wharton School and the Kellogg School of Management for faculty exchange and joint research initiatives. These collaborations have enhanced the curriculum, bringing in global business perspectives and practices.

Case Study 4: Manipal Academy of Higher Education (MAHE)

Experiential Learning Approach: MAHE has integrated experiential learning in its programs through internships, workshops, and lab sessions. The institution is known

for its emphasis on healthcare education, where students gain hands-on experience in their teaching hospitals.

Global Collaboration Impact: Collaborations with institutions like the University of Queensland and Virginia Commonwealth University have led to student exchange programs and collaborative research in healthcare. This has resulted in a more comprehensive and globally aligned healthcare education for students.

The impact of these collaborations on Indian educational institutions has been profound:

- A. **Enhanced Curriculum:** Collaborations with global universities have led to the incorporation of international best practices in the curriculum, making it more comprehensive and globally relevant.
- B. **Research Opportunities:** Joint research initiatives have provided opportunities for students and faculty to engage in cutting-edge research, contributing to global knowledge.
- C. **Cultural Exchange:** These collaborations have facilitated cultural exchange, fostering a global perspective among students and faculty.
- D. **Skill Development:** Exposure to global academic and professional environments has equipped students with skills that are in demand in the international job market.
- E. **Networking and Career Opportunities:** Such partnerships often lead to expanded professional networks, providing students with more career opportunities globally.

The case studies of Indian educational institutions and their collaborations with global universities illustrate the significant strides made in integrating experiential learning. These collaborations have not only enhanced the quality of education but have also prepared students to be globally competent professionals.

THE FUTURE OF HIGHER EDUCATION: EMBRACING EXPERIENTIAL LEARNING

The future of higher education is evolving with a focus on experiential learning, incorporating internships, apprenticeships, and career services to provide students

with real-world skills and experiences. These programs bridge the gap between theory and practice, fostering essential skills, professional networks, and workplace understanding. To support this shift, higher education institutions can enhance career counseling, establish dedicated career service cells, update curricula with industry input, incorporate soft skills training, promote entrepreneurship education, and leverage technology for experiential learning. Embracing these enhancements ensures that higher education remains relevant and valuable in preparing students for success in their careers.

CONCLUSIONS

The exploration of the paradigm shift in higher education in India, as illuminated by the National Education Policy (NEP) 2020, reveals a transformative journey from traditional classroom-based learning to a more dynamic, experiential model. This shift, emphasizing practical application and real-world relevance, has significant implications for the future of education in India.

Key Findings

- 1) **Experiential Learning as a New Norm:** The transition towards experiential learning is poised to redefine educational outcomes, making them more aligned with industry needs and global standards. This approach fosters critical thinking, creativity, and practical skills, moving beyond the confines of rote memorization.
- 2) **Integration of Technology:** The incorporation of AI and other technological advancements in education is enhancing the learning experience, making it more personalized, interactive, and efficient. This integration is crucial in keeping pace with the evolving educational landscape globally.
- 3) **Academia-Industry Collaboration:** Partnerships between educational institutions and industries are proving instrumental in bridging the skill gap. These collaborations ensure that the curriculum remains relevant and students are well-prepared for their professional lives.
- 4) **Global Connectivity:** Collaborations with global universities are bringing international perspectives

and expertise into Indian education, fostering a cross-cultural academic environment and expanding research and learning opportunities.

- 5) **Emerging Focus on Career Services:** The increased emphasis on internships, apprenticeships, and career counseling in educational institutions is a critical step towards ensuring that students are not only educated but also employable.

Implications for the Future of Education in India

The shift towards experiential learning and the integration of technology in education are set to propel India towards becoming a global knowledge superpower. This transformation will likely result in a more competent and versatile workforce, better equipped to handle the challenges of the modern world. The focus on skill-based education will enhance the employability of Indian graduates, positively impacting the economy and society.

Challenges and Potential Solutions

While the future looks promising, the implementation of experiential learning faces several challenges:

- 1) **Resource Allocation:** Adequate resources, including funding, infrastructure, and trained personnel, are necessary for the effective implementation of experiential learning. Increased investment and government support are crucial in this regard.
- 2) **Teacher Training:** Educators need to be trained in new pedagogical approaches to facilitate experiential learning effectively. Professional development programs and workshops can help in this transition.
- 3) **Curriculum Overhaul:** The curriculum needs to be continuously reviewed and updated to keep it relevant and aligned with industry requirements.

- 4) Technological Access and Literacy: Ensuring widespread access to technology and improving digital literacy are essential for the successful integration of tech-based learning methods.
- 5) Balancing Theory and Practice: While emphasizing practical skills, the importance of theoretical knowledge should not be undermined. A balanced approach is necessary for a holistic education.

The transformation of India's higher education system, as envisaged by NEP 2020, holds immense promise. The adoption of experiential learning, technological integration, and strong academia-industry linkages are steps in the right direction. However, the realization of this vision requires concerted efforts in overcoming challenges related to resources, training, and curriculum development. With these measures in place, India can look forward to an education system that is contemporary, comprehensive, and globally competitive.

REFERENCES

1. P. Agarwal, Indian Higher Education: Envisioning the Future. New Delhi: Sage Publications, 2009.
2. P. G. Altbach and N. Jayaram, Eds., The Future of Indian Universities: Comparative and International Perspectives. New York, NY: Oxford University Press, 2019.
3. Ministry of Education, Government of India, "National Education Policy 2020," 2020. [Online]. Available: https://www.education.gov.in/sites/upload_files/mhrd/files/NEP_Final_English_0.pdf
4. NITI Aayog, "India's Leap Towards a Sustainable Future: A Research on Higher Education," 2021. [Online]. Available: <https://www.niti.gov.in/research-higher-education-2021>
5. KPMG & FICCI, "Indian Higher Education Sector: Opportunities and Challenges," 2022.
6. Ernst & Young, "Higher Education in India: Vision 2030," 2023.
7. National Council of Educational Research and Training (NCERT), "The Changing Landscape of Indian Education," 2021.
8. University Grants Commission (UGC), "Annual Report on Higher Education in India," 2020.

Reliability Assessment of Distributed Generation under Islanding Operation

Swati Warungase

Department of Electrical Engineering
K. K. Wagh, Institute of Engg Education and Research
Nashik, Maharashtra
✉ swarungasethete@gmail.com

Priyanka D.Jawale, M. V. Bhatkar

Department of Electrical Engineering
Jawahar Education Society's. Institute of Technology,
Management & Research
Nashik, Maharashtra

ABSTRACT

The improvement of reliability of power distribution system is very important from the utility point of view, especially when number of DG's based on renewable energy sources are inserted to the system. The main motive of this paper is to minimize the losses and improve the reliability of the system. In this paper the load flow analysis is done for IEEE 30 bus system with the help of Newton-Raphson method. After the load flow analysis the evaluation of reliability indices have been done

KEYWORDS : IEE 30 bus system, Distributed power generation, Newton-Raphson method, Distribution system reliability, Reliability indices.

INTRODUCTION

Islanding refers to the condition in which DG continues to power a location even though electrical grid power from the electric utility is no longer present. Islanding is an important challenge associated with DGs. A subislanding approach based on two algorithms has been presented, first is backtracking algorithm and second is protection co-ordination[1]. Now a days, electric power utilities are concerned with DG which includes pv, wind farm, fuel cells, micro-sized turbine to solve the environmental problems. Comparison of different islanding detection techniques has been done. In today's power system, the major challenges is associated with the fast and accurate detection[2]

For islanding detection the suggested method was a DT- initialized Fuzzy rule base classifier. The model is developed using DT which is a rigid decision tree algorithm. The proposed method is tested on data with and without noise and found to provide 100% islanding detection[3]. The proposed hybrid islanding detection scheme is based on two stages detecting procedures to achieve higher effectiveness. In the detecting procedure passive detection method is used as primary protection

and active detection method is the backup. The indices of ROCOF, ROCOV and CF of the DSG are calculated by DSP. In this study, the effectiveness of the proposed technique using different types of typical loads was verified[4]

To control the synchronized state of a DG, this paper addresses a sampling approach[6]. In this paper a case of sub- transmission system connected to Thailand EPS is used as the test system. During the islanding operation, the impact of disturbances, is very important as the islanding system is a weak system. In practice, it may take 2-3 hr or more to repair a faulted part from a permanent fault[7]. The adaptive scheme proposed, offer a practically acceptable solution to this problem of size, number and placement of DG in the distribution system[8]. To improve the reliability of distribution system a protection co-ordination algorithm based on RBFNN is proposed[9]. A novel sub-islanding approach based on two algorithm first is backtracking and second is protection co- ordination. The proposed method was successfully tested on feed 4 of the RBTS bus 6[10].

The backtracking algorithm based on matrix storage has been applied successfully in the management system

for math analysis Test database and the management system for the Dormitory assignment of college students[11]. Currently developing Hydrogen Research Institution , an islanding detection system which will allow the connection to the hybrid renewable energy to the grid. The detection technique for the system which is a combination of under/over frequency and under/over voltage which are passive method and sandia frequency shift and sandia voltage shift which are active methods[12].

A controller was designed to control two interface, one for grid-connected operation and other for intentional islanding operation. An islanding- detection algorithm was presented, for the switch between two controllers. The proposed control schemes are capable of maintaining the voltages within the standard permissible levels during grid-connected and islanding operation modes. [13]

RELIABILITY ASSESSMENT

Distribution system reliability assessment deals with the availability and quality of power supply at each customers service entrance. Analysis of customer failure statistics show that, compared to other portions of electrical power systems, distribution system failures contribute as much as 90% towards the unavailability of supply to a load. These statistics show how important the reliability evaluation of distribution systems can be. Reliable system is somewhat costly. There is some reliability indices that are used to calculate

- 1) How much system is reliable.
- 2) How much the distribution system have costs of interruptions and maintains.

The basic reliability indices normally used to predict or assess the reliability of a distribution system consist of three reliability indices:

- Load point average failure rate λ
- Average outage duration r
- Annual unavailability U

In order to evaluate the severity or significance of a system outage, using the three basic indices mentioned above, set of indices listed below must also be calculated. This paper represents the study of various

reliability indices such as

Formulation

- 1) System average interruption frequency index (SAIFI)

$$SAIFI = \frac{\sum \lambda_i N_i}{N_T} \quad (1)$$

where,

λ_i = Failure rate

N_i = Number of customer for location i

N_T = Total number of customers served

- System average interruption duration index (SAIDI)

$$SAIDI = \frac{\sum U_i N_i}{N_T} \quad (2)$$

where,

U_i = Annual outage time for location

N_i = Number of customer for location i

N_T = Total number of customers served

- Customer average interruption duration index (CAIDI)

$$CAIDI = \frac{\sum U_i N_i}{\sum \lambda_i N_i} \quad (3)$$

where,

λ_i = Failure rate

U_i = Annual outage time for location

N_i = Number of customer for location i

- Average service availability index (ASAI)

$$ASAI = \frac{\sum N_i * 8760 - \sum U_i N_i}{\sum N_i * 8760} \quad (4)$$

where,

N_i = Number of customer for location i

U_i = Annual outage time for location

$$ASAI = 1 - \frac{SAIDI}{8760} \quad (5)$$

SYSTEM, RESULTS AND ANALYSIS

The IEEE 30 bus test system is shown in fig.1. The system data is taken from reference. The system consist of 5 generators rating are as follows

Generator 1= 80MW,

Generator 2= 50MW,

Generator 3= 55MW,

Generator 4= 40MW.

Four transformer and 1 swing bus. The system has 21 load points. Bus input data which was taken for the system was given in table I. Load flow analysis report was given in table II. Summary of operation, load and demand was illustrated in table IV.

Load Flow Calculation

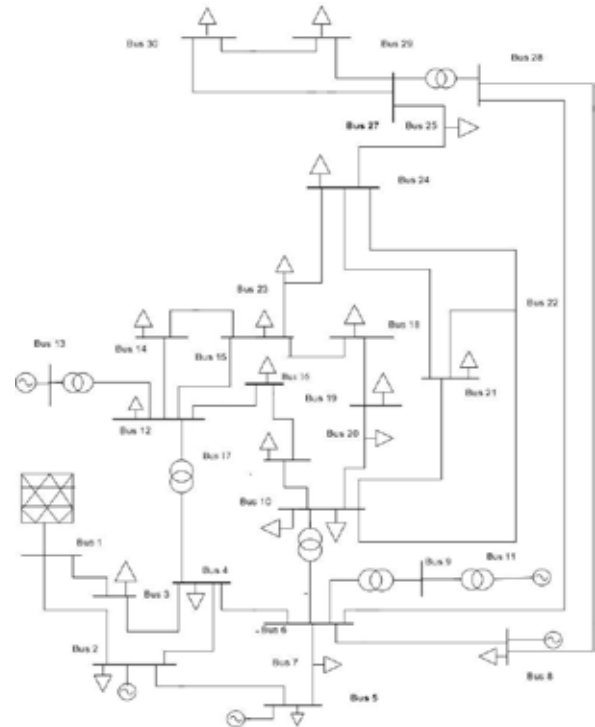
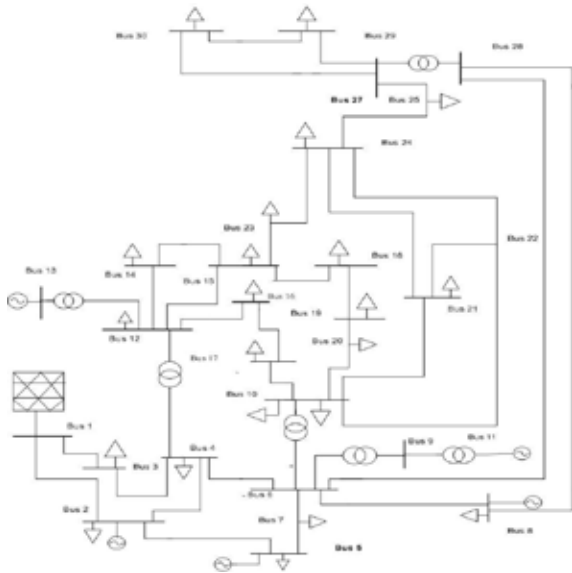


Fig. 1. IEEE 30 bus system

Fig. 2. When DGs are connected to the system

Table I Bus Input Data

Bus			Initial Voltage		Load				Constant I		Generat	
ID	kV	Sub-sys	% Mag	Ang.	MW	Mvar	MW	Mvar	MW	Mvar	MW	Mvar
Bus 1	132.000	1	100.0	0.0	-	-	-	-	-	-	-	-
Bus 2	132.000	1	100.0	-5.5	21.700	12.700	-	-	-	-	-	-
Bus 3	132.000	1	102.1	-8.0	2.400	1.200	-	-	-	-	-	-
Bus 4	132.000	1	101.2	-9.6	7.600	1.600	-	-	-	-	-	-
Bus 5	132.000	1	101.0	-14.4	94.200	19.000	-	-	-	-	-	-
Bus 6	132.000	1	101.0	-11.3	-	-	-	-	-	-	-	-
Bus 7	132.000	1	100.2	-13.1	22.800	10.900	-	-	-	-	-	-
Bus 8	132.000	1	101.0	-12.1	30.000	30.000	-	-	-	-	-	-
Bus 9	33.000	1	105.1	-14.4	-	-	-	-	-	-	-	-
Bus 10	33.000	1	104.5	-16.0	5.800	2.000	0.002	-19.000	-	-	-	-
Bus 11	11.000	1	108.2	-14.4	-	-	-	-	-	-	-	-
Bus 12	33.000	1	105.7	-15.2	11.200	7.500	-	-	-	-	-	-
Bus 13	11.000	1	100.0	-15.2	-	-	-	-	-	-	-	-
Bus 14	33.000	1	104.2	-16.1	6.200	1.600	-	-	-	-	-	-
Bus 15	33.000	1	103.8	-16.2	8.200	2.500	-	-	-	-	-	-
Bus 16	33.000	1	104.5	-15.8	3.500	1.800	-	-	-	-	-	-
Bus 17	33.000	1	104.0	-16.1	9.000	5.800	-	-	-	-	-	-
Bus 18	33.000	1	102.8	-16.8	3.200	0.900	-	-	-	-	-	-
Bus 19	33.000	1	102.6	-17.0	9.500	3.400	-	-	-	-	-	-
Bus 20	33.000	1	103.0	-16.8	2.200	0.700	-	-	-	-	-	-
Bus 21	33.000	1	103.3	-16.4	17.500	11.200	-	-	-	-	-	-
Bus 22	33.000	1	103.3	-16.4	-	-	-	-	-	-	-	-
Bus 23	33.000	1	102.7	-16.6	3.200	1.600	-	-	-	-	-	-
Bus 24	33.000	1	102.1	-16.8	8.700	6.700	0.000	-4.300	-	-	-	-
Bus 25	33.000	1	101.7	-16.4	-	-	-	-	-	-	-	-
Bus 26	33.000	1	100.0	-16.8	3.500	2.300	-	-	-	-	-	-
Bus 27	33.000	1	102.3	-15.8	-	-	-	-	-	-	-	-
Bus 28	132.000	1	100.7	-12.0	-	-	-	-	-	-	-	-
Bus 29	33.000	1	100.3	-17.1	2.400	0.900	-	-	-	-	-	-
Bus 30	33.000	1	99.2	-17.9	10.600	1.900	-	-	-	-	-	-
Total Number of Buses: 30					283.4	126.2	0.002	-23.3	0	0	0	0

Load Flow Report

The load flow study is a numerical analysis of the flow of electric power in an interconnected system. This focuses on various aspects of AC power parameters,

such as voltages, voltage angles, real power and reactive power. The principal information obtained from this report is the magnitude and phase angle of the voltage at each bus, and the real and reactive power flowing in each line.

Table II Load Flow Report

Bus		Voltage		Generation		Load		Load Flow				XFMR	
ID	kV	% Mag	Ang	MW	Mvar	MW	Mvar	ID	MW	Mvar	Amp	%PF	%Tap
* Bus 1	132.000	100.000	0.0	296.308	90.765	0	0	Bus 2	204.557	58.315	930.4	96.2	
								Bus 3	91.751	32.430	423.7	94.3	
Bus 2	132.000	93.172	-6.3	0	0	21.700	12.700	Bus 1	-195.810	-37.051	935.5	98.3	
								Bus 4	37.867	8.537	182.2	97.3	
								Bus 5	81.075	6.758	381.9	99.7	
Bus 3	132.000	91.173	-8.6	0	0	2.400	1.200	Bus 6	55.168	9.035	262.4	98.7	
								Bus 1	-87.409	-20.313	430.3	97.4	
Bus 4	132.000	89.194	-10.7	0	0	7.600	1.600	Bus 4	85.009	19.113	418.0	97.6	
								Bus 2	-36.858	-8.543	183.3	97.4	
								Bus 3	-83.801	-16.329	418.7	98.2	
								Bus 6	73.743	0.057	361.6	100.0	
Bus 5	132.000	88.847	-17.4	0.000	40.000	94.200	19.000	Bus 12	39.316	23.215	223.9	86.1	-6.800
								Bus 2	-77.461	4.961	382.1	-99.8	
Bus 6	132.000	88.258	-12.9	0	0	0	0	Bus 7	-16.739	16.039	114.1	-72.2	
								Bus 2	-53.055	-5.703	264.4	99.4	
								Bus 4	-72.930	2.064	361.6	-100.0	
								Bus 7	40.436	-5.466	202.2	-99.1	
								Bus 8	41.560	-1.213	208.1	-100.0	
								Bus 9	35.357	6.772	178.4	98.2	-2.200
Bus 7	132.000	87.568	-15.4	0	0	22.800	10.900	Bus 10	8.631	3.546	46.2	92.5	-3.100
								Bus 5	17.068	-16.798	119.6	-71.3	
Bus 8	132.000	87.756	-14.2	0.000	40.000	30.000	30.000	Bus 6	-39.868	5.898	201.3	-98.9	
								Bus 6	-41.294	1.447	205.9	-99.9	
Bus 9	33.000	88.719	-21.0	0	0	0	0	Bus 28	11.294	8.553	70.6	79.7	
								Bus 10	33.330	23.707	839.3	83.1	
								Bus 6	-33.332	-1.679	697.9	99.9	
								Bus 11	0.002	-22.027	434.4	0.0	
Bus 10	33.000	85.892	-23.9	0	0	5.801	-11.017	Bus 9	-35.350	-21.175	839.3	85.8	
								Bus 17	1.567	5.449	115.5	27.6	
								Bus 20	13.537	7.194	312.6	88.3	
								Bus 21	15.370	14.657	435.6	72.8	
								Bus 22	7.485	7.613	217.5	70.1	
								Bus 6	-8.630	-1.722	179.2	98.1	
Bus 11	11.000	96.664	-21.0	0.000	24.000	0	0	Bus 9	0.000	24.000	1303.1	0.0	
Bus 12	33.000	87.637	-21.3	0	0	11.200	7.300	Bus 14	16.938	4.075	348.2	97.2	
								Bus 16	11.149	2.675	228.9	97.2	
Bus 13								Bus 4	-39.307	-14.231	834.7	94.0	
Bus 14								Bus 13	0.000	0.000	0.0	0.0	
	11.000	87.637	-21.3	0	0	0	0	Bus 12	0.000	0.000	0.0	0.0	
Bus 15	33.000	84.179	-24.3	0	0	6.200	1.600	Bus 12	-16.470	-3.062	348.2	98.3	
								Bus 15	10.270	1.462	215.6	99.0	
Bus 16	33.000	81.162	-25.7	0	0	8.200	2.300	Bus 14	-9.934	-1.139	215.6	99.3	
								Bus 18	1.734	-1.341	47.3	-79.1	
Bus 17	33.000	85.857	-22.8	0	0	3.500	1.800	Bus 12	-10.987	-2.335	228.9	97.8	
								Bus 17	7.487	0.333	153.0	99.7	
Bus 18	33.000	85.296	-23.9	0	0	9.000	5.800	Bus 10	-1.553	-5.412	115.5	27.6	
								Bus 16	-7.447	-0.368	153.0	99.9	
Bus 19	33.000	81.296	-26.2	0	0	3.200	0.900	Bus 15	-1.727	1.357	47.3	-78.6	
								Bus 19	-1.473	-2.257	58.0	54.7	
Bus 20	33.000	81.771	-26.1	0	0	9.300	3.400	Bus 18	1.480	2.272	58.0	54.6	
								Bus 20	-10.980	-5.672	264.4	88.8	
Bus 21	33.000	82.702	-25.7	0	0	2.200	0.700	Bus 10	-13.258	-6.527	312.6	89.7	
								Bus 19	11.038	5.827	264.4	88.5	
Bus 22	33.000	83.986	-24.5	0	0	17.300	11.200	Bus 10	-13.354	-14.193	435.6	73.4	
								Bus 22	-2.148	2.993	76.7	-58.3	
	33.000	83.932	-24.4	0	0	0	0	Bus 10	-7.372	-7.383	217.5	70.7	
Bus 23								Bus 21	2.148	-2.988	76.7	-58.4	
Bus 24								Bus 24	3.224	10.371	242.1	45.0	
	33.000	79.389	-22.6	7.000	-4.338	3.200	1.600	Bus 24	3.800	-5.938	155.0	-53.9	
Bus 25	33.000	81.003	-24.2	0	0	8.700	3.878	Bus 22	-5.004	-10.029	242.1	44.6	
								Bus 23	-3.696	6.150	155.0	-51.5	
Bus 26	33.000	78.247	-21.5	0	0	0	0	Bus 26	3.577	2.416	96.5	82.9	
Bus 27								Bus 27	-3.577	-2.416	96.5	82.9	
	33.000	75.917	-22.2	0	0	3.500	1.300	Bus 25	-3.500	-2.300	96.5	83.6	
	33.000	79.394	-21.0	6.000	-3.718	0	0	Bus 25	3.611	2.479	96.5	82.4	
								Bus 29	6.281	1.845	144.3	95.9	
Bus 28								Bus 30	7.209	1.879	164.2	96.6	
								Bus 28	-11.101	-9.921	328.1	74.6	
	132.000	84.633	-15.4	0	0	0	0	Bus 8	-11.103	-11.132	81.3	70.6	
Bus 29								Bus 8	0.000	-0.931	4.8	0.0	
								Bus 27	11.103	12.063	84.7	67.7	-3.200
Bus 30	33.000	76.740	-23.1	0	0	2.400	0.900	Bus 27	-6.132	-1.583	144.3	96.9	
								Bus 30	3.732	0.663	86.4	98.3	
	33.000	75.208	-24.6	0	0	10.600	1.900	Bus 27	-6.927	-1.348	164.2	98.2	
								Bus 29	-3.673	-0.552	86.4	98.9	

Critical Report

Table III Critical Report

Device ID	Type	Condition	Rating/Limit	Unit	Operating	% Operating	Phase Type
Bus 10	Bus	Under Voltage	33.00	kV	28.34	85.9	3-Phase
Bus 12	Bus	Under Voltage	33.00	kV	28.92	87.6	3-Phase
Bus 13	Bus	Under Voltage	11.00	kV	9.64	87.6	3-Phase
Bus 14	Bus	Under Voltage	33.00	kV	27.78	84.2	3-Phase
Bus 15	Bus	Under Voltage	33.00	kV	26.78	81.2	3-Phase
Bus 16	Bus	Under Voltage	33.00	kV	28.33	85.9	3-Phase
Bus 17	Bus	Under Voltage	33.00	kV	28.15	85.3	3-Phase
Bus 18	Bus	Under Voltage	33.00	kV	26.83	81.3	3-Phase
Bus 19	Bus	Under Voltage	33.00	kV	26.98	81.8	3-Phase
Bus 2	Bus	Under Voltage	132.00	kV	122.99	93.2	3-Phase
Bus 20	Bus	Under Voltage	33.00	kV	27.29	82.7	3-Phase
Bus 21	Bus	Under Voltage	33.00	kV	27.72	84.0	3-Phase
Bus 22	Bus	Under Voltage	33.00	kV	27.70	83.9	3-Phase
Bus 23	Bus	Under Voltage	33.00	kV	26.26	79.6	3-Phase
Bus 24	Bus	Under Voltage	33.00	kV	26.73	81.0	3-Phase
Bus 25	Bus	Under Voltage	33.00	kV	25.82	78.2	3-Phase
Bus 26	Bus	Under Voltage	33.00	kV	25.05	75.9	3-Phase
Bus 27	Bus	Under Voltage	33.00	kV	26.20	79.4	3-Phase
Bus 28	Bus	Under Voltage	132.00	kV	111.72	84.6	3-Phase
Bus 29	Bus	Under Voltage	33.00	kV	25.32	76.7	3-Phase
Bus 3	Bus	Under Voltage	132.00	kV	120.35	91.2	3-Phase
Bus 30	Bus	Under Voltage	33.00	kV	24.82	75.2	3-Phase
Bus 4	Bus	Under Voltage	132.00	kV	117.74	89.2	3-Phase
Bus 5	Bus	Under Voltage	132.00	kV	117.28	88.8	3-Phase
Bus 6	Bus	Under Voltage	132.00	kV	116.50	88.3	3-Phase
Bus 7	Bus	Under Voltage	132.00	kV	115.59	87.6	3-Phase
Bus 8	Bus	Under Voltage	132.00	kV	115.84	87.8	3-Phase
Bus 9	Bus	Under Voltage	33.00	kV	29.28	88.7	3-Phase
Gen ₁	Generator	Under Excited	0.00	Mvar	0.00	0.0	3-Phase
Gen ₁	Generator	Under Power	0.00	MW	0.00	0.0	3-Phase
Gen ₂	Generator	Over Excited	40.00	Mvar	40.00	100.0	3-Phase
Gen ₂	Generator	Under Power	0.00	MW	0.00	0.0	3-Phase
Gen ₃	Generator	Under Power	0.00	MW	0.00	0.0	3-Phase
Gen ₃	Generator	Over Excited	40.00	Mvar	40.00	100.0	3-Phase
Gen ₄	Generator	Over Excited	24.00	Mvar	24.00	100.0	3-Phase
Gen ₄	Generator	Under Power	0.00	MW	0.00	0.0	3-Phase
Gen ₅	Generator	Under Power	0.00	MW	0.00	0.0	3-Phase
Gen ₅	Generator	Under Excited	0.00	Mvar	0.00	0.0	3-Phase
WTG3	Wind Turbine Generator	Under Excited	0.00	Mvar	-4.34	0.0	3-Phase
WTG3	Wind Turbine Generator	Overload	7.00	MW	7.00	100.0	3-Phase
WTG5	Wind Turbine Generator	Overload	6.00	MW	6.00	100.0	3-Phase
WTG5	Wind Turbine Generator	Under Excited	0.00	Mvar	-3.72	0.0	3-Phase

Summary of generation,load and demand This section shows the summary of

– Total generation,

– Total demand,

– Total loads(static, motor, constant, generic) and

– Apparent losses which was used in the system.

Table IV Summary of Generation,Load and Demand

	MW	Mvar	MVA	% PF
Source (Swing Buses):	296.308	90.765	309.898	95.61 Lagging
Source (Non-Swing Buses):	13.000	95.943	96.820	13.43 Lagging
Total Demand:	309.308	186.708	361.292	85.61 Lagging
Total Motor Load:	283.400	126.200	310.229	91.35 Lagging
Total Static Load:	0.002	-16.839	16.839	0.01 Leading
Total Constant I Load:	0.000	0.000	0.000	
Total Generic Load:	0.000	0.000	0.000	
Apparent Losses:	25.907	77.347		
System Mismatch:	0.000	0.000		

RELIABILITY CALCULATION

Reliability calculation is the methodology for analyzing the expected or actual reliability of a product, process or service, and identifying actions to reduce failures or mitigate their effect.

Comparison of Reliability Indices With and Without Grid

This section shows the comparative experimental results,

Case: 1

When DG1 are disconnected from the system, the reliability indices are

Table V System Indices when DG1 are Disconnected from the System

	With Grid	Without Grid
SAIFI	1.442 f/customer.yr	0.76 f/customer.yr
SAIDI	68.4840 hr/customer.yr	62.7893 hr/customer.yr
CAIDI	47.492 hr/customer interruption	82.613 hr/customer interruption
AENS	843.8490 MW hr/customer.yr	543.2352 MW hr/customer.yr

Case: 2

When DG1, DG2 are disconnected from the system, the reliability indices are

Table VI System Indices when DG1, DG2 are Disconnected from the System

	With Grid	Without Grid
SAIFI	1.451 f/customer.yr	0.7687 f/customer.yr
SAIDI	71.8220hr/customer.yr	65.9822 hr/customer.yr
CAIDI	49.498hr/customer interruption	85.841 hr/customer interruption
AENS	884.9794 MW hr/customer.yr	569.6942 MW hr/customer.yr

Case: 3

When DG1, DG2, DG3 are disconnected from the system, the reliability indices are

Table VII System Indices when DG 1, DG 2, DG 3 are Disconnected from the System

	With Grid	Without Grid
SAIFI	1.46 f/customer.yr	0.7773 f/customer.yr
SAIDI	75.1599 hr/customer.yr	69.1750 hr/customer.yr
CAIDI	51.479 hr/customer interruption	88.998 hr/customer interruption
AENS	926.1097 MW hr/customer.yr	597.1532 MW hr/customer.yr

Case: 4

When DG1, DG2, DG3, DG4 are disconnected from the system, the reliability indices are

Table VIII System Indices when DG 1, DG 2, DG 3, DG 4 are Disconnected from the System

	With Grid	Without Grid
SAIFI	1.488 f/customer.yr	0.8445 f/customer.yr
SAIDI	80.8360 hr/customer.yr	79.5499hr/customer.yr
CAIDI	52.399 hr/customer interruption	92.344 hr/customer interruption
AENS	954.9184 MW hr/customer.yr	654.6661 MW hr/customer.yr

Case: 5

When DG1,DG2,DG3,DG4,DG5 are disconnected from the system, the reliability indices are

Table IX System Indices when DG 1, DG 2, DG 3, DG 4, DG 5 are Disconnected from the System

	With Grid	Without Grid
SAIFI	1.488 f/customer.yr	0.8445 f/customer.yr
SAIDI	80.8360 hr/customer.yr	79.5499hr/customer.yr
CAIDI	52.399 hr/customer interruption	92.344 hr/customer interruption
AENS	954.9184 MW hr/customer.yr	654.6661 MW hr/customer.yr

Case: 6

When all DG’S are connected to the system, the reliability indices are

Table X System Indices when All DG’s are Connected to the System

	With Grid	Without Grid
SAIFI	1.423 f/customer.yr	0.7514 f/customer.yr
SAIDI	63.1460 hr/customer.yr	62.4660 hr/customer.yr
CAIDI	44.375hr/customer interruption	83.129 hr/customer interruption
AENS	778.0753 MW hr/customer.yr	539.4547 MW hr/customer.yr

Simulation Results of Comparison

System Average Interruption Frequency Index (SAIFI)

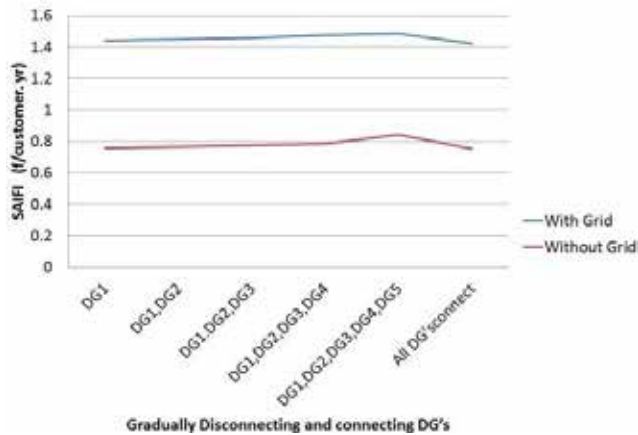


Fig. 3. Comparison of SAIFI

System Average Interruption Duration Index(SAIDI)

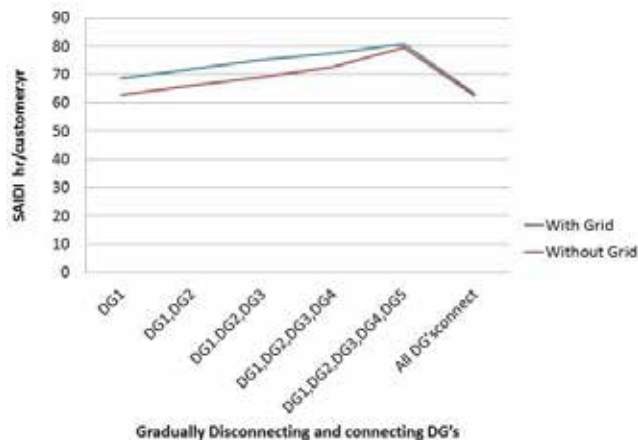


Fig. 4. Comparison of SAIDI

Customer Average Interruption Duration Index(CAIDI)

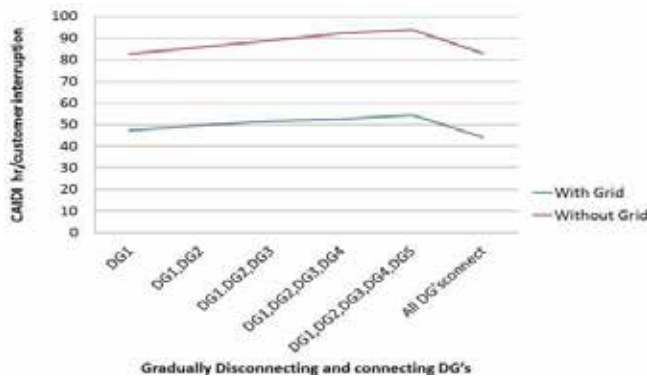


Fig. 5. Comparison of CAIDI

Average Service Availability Index(ANES)

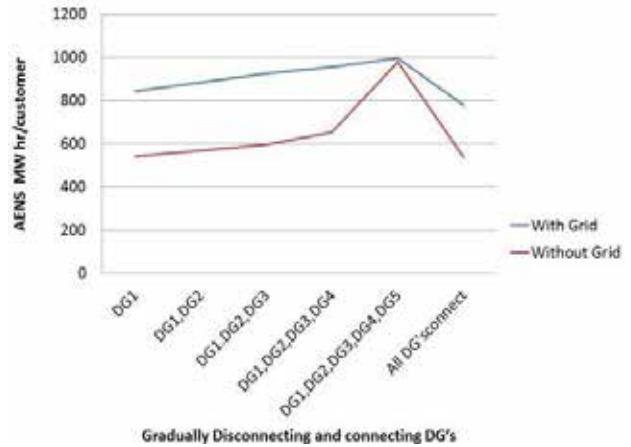


Fig. 6. Comparison of ANES

CONCLUSION

In this the load flow analysis is presented with the help of Newton- Raphson method and reliability assesment of IEEE 30 bussystem to simulate the reliability indices. Reliability is less when grid is connected to the system and it increases when the system is islanded. Graph shows the difference between various reliability indices obtain under the different condition. Red line shows the result of reliability indces obtained when grid is connected and blue line shows theresults of reliability indices obtained when system is islanded.

Test system is developed in Etab software with IEEE 30 bussystem to simulate the reliability indices. Reliability is less when grid is connected to the system and it increases when the system is islanded. Graph shows the difference between various reliability indices obtain under the different condition. Red line shows the result of reliability indces obtained when grid is connected and blue line shows theresults of reliability indices obtained when system is islanded.

The DG are disconnected gradually from system and corresponding changes are drawn graphically. Results shows that when grid is connected the reliability indices, SAIFI is 1.423 f/customer.yr, SAIDI is 63.1460 hr/customer.yr, CAIDI is 44.375hr/customer interruption, ANES is 778.0753 MW hr/customer.yr and when the system is islanded the reliability indices, SAIFI is 0.7514

f/customer.yr, SAIDI is 62.4660 hr/customer.yr, CAIDI is 83.129 hr/customer interruption, AENS is 539.4547 MW hr/customer.yr. Overall simulation results shows that the reliability is enhanced when system is islanded and reliability is much less when system is connected to the grid.

REFERENCES

- Chandra Shekhar Chandrakar, Bharti Dewani, Deepali Chandrakar, "An assessment of distributed generation islanding detection technique", International Journal of Advances in Engineering and Technology, pp.218-226, Nov.2012.
- A. Heidari and V. G. Agelidis and H. Zayandehroodi and J. Pou and J. Aghaei, "On Exploring Potential Reliability Gains Under Islanding Operation of Distributed Generation, IEEE Transactions on Smart Grid, vol.7, pp.2166-2174, Sept.2016.
- S. P. M. I. S.P.Chowdhary, Member IEEE and N.-M. Chui Fen Ten, Uk scenerio of islanded operation of active distribution networks-a survey, no. 6, 2008.
- S. R. Samantaray, K. El-Arroudi, G. Joos, and I. Kamwa, A fuzzy rule- based approach for islanding detection in distributed generation, IEEE Transactions on Power Delivery, vol. 25, no. 3, pp. 14271433, July 2010.
- V. Menon and M. H. Nehrir, A hybrid islanding detection technique using voltage unbalance and frequency set point, IEEE Transactions on Power Systems, vol. 22, no. 1, pp. 442448, Feb 2007.
- D. Jayaweera and S. Galloway and G. Burt and J. R. McDonald, "A Sampling Approach for Intentional Islanding of Distributed Generation", IEEE Transactions on Power Systems, vol.22, pp.514- 521, May.2007.
- P. Fuangfoo and W. J. Lee and M. T. Kuo, "Impact Study on Intentional Islanding of Distributed Generation Connected to a Radial Subtransmission System in Thailand's Electric Power System", IEEE Transactions on Industry Applications, vol.43, pp.1491-1498, Nov.2007.
- M. Robitaille and K. Agbossou and M. L. Doumbia, "Modeling of an islanding protection method for a hybrid renewable distributed generator", Canadian Conference on Electrical and Computer Engineering, 2005. pp.1477-1481, May.2005.
- S. M. Brahma and A. A. Girgis, "Development of adaptive protection scheme for distribution systems with high penetration of distributed generation", 2003 IEEE Power Engineering Society General Meeting (IEEE Cat. No.03CH37491), vol.4, July.2003.
- A. Heidari, V. G. Agelidis, H. Zayandehroodi, and M. Hasheminamin, Prevention of overcurrent relays miscoordination in distribution system due to high penetration of distributed generation, in 2013 International Conference on Renewable Energy Research and Applications (ICR- ERA), Oct 2013, pp. 342346.
- A. Wiszniewski, Accurate fault impedance locating algorithm, IEE Proceedings C - Generation, Transmission and Distribution, vol. 130, no. 6, pp. 311314, November 1983.
- W. f. Wang, Z. I. Li, and Y. Ma, Application of backtracking algorithm in college dormitory assignment management, in 2009 2nd IEEE International Conference on Computer Science and Information Technology, Aug 2009, pp. 272274.
- I. J. Balaguer, Q. Lei, S. Yang, U. Supatti, and F. Z. Peng, Control for gridconnected and intentional islanding operations of distributed power generation, IEEE Transactions on Industrial Electronics, vol. 58, no. 1, pp. 147157, Jan 2011.
- K. Zou, A. P. Agalgaonkar, K. M. Muttaqi, and S. Perera, An analytical approach for reliability evaluation of distribution systems containing dispatchable and nondispatchable renewable dg units, IEEE Transactions on Smart Grid, vol. 5, no. 6, pp. 26572665, Nov 2014.
- S. A. M. Javadian, M. R. Haghifam, and N. Rezaei, A fault location and protection scheme for distribution systems in presence of dg using mlp neural networks, in 2009 IEEE Power Energy Society General Meeting, July 2009, pp. 18.
- J. Warin, and W. H. Allen, "Loss of mains protection", 1990 ERA Conference on Circuit Protection for industrial and commercial Installation London, pp.4.3.1-12, 1990.
- Y. M. Atwa and E. F. El-Saadany, Reliability evaluation for distribution system with renewable distributed generation during islanded mode of operation, IEEE Transactions on Power Systems, vol. 24, no. 2, pp. 572581, May 2009.

18. Z. L. Aoxue SU, Mingtian FAN, An approach for reliability assessment of distribution networks with dg, 21st International Conference on Electricity Distribution, p. 4, June 2011.
19. A. U. Rehman, A. U. Rehman, and S. Mehmood, Reliability assessment and cost analysis of over loaded distribution system with distributed generation, in 2016 International Conference on Computing, Electronic and Electrical Engineering (ICE Cube), April 2016, pp. 244250.
20. X. Zhang, Z. Bie, and G. Li, Reliability assessment of distribution networks with distributed generations using monte carlo method, Energy Procedia, vol. 12, pp. 278-286, 2011. [Online]. Available: <http://www.sciencedirect.com/science/article/pii/S1876610211018649>
21. P. M. Sonwane, D. P. Kadam, and B. E. Kushare, Distribution system reliability through reconfiguration, fault location, isolation and restoration, in 2009 International Conference on Control, Automation, Communication and Energy Conservation, June 2009, pp. 16.
22. A. Pandey and P. M. Sonwane, Implementation of reliability centred maintenance for transformer, in 2016 International Conference on Automatic Control and Dynamic Optimization Techniques (ICACDOT), Sept 2016, pp. 578581.
23. P. M. Sonwane and B. E. Kushare, Optimal capacitor placement and sizing for enhancement of distribution system reliability and power quality using pso, in International Conference for Convergence for Technology-2014, April 2014, pp. 17.

An Extensive Review of Wind Turbine Emulators to Promote the Integration of Renewable Energy

A. P. Kulkarni, V. S. Jape

Deepa S. Bhandare

Department of Electrical Engg

PES Modern College of Engg

Pune, Maharashtra

✉ amruta.patki@moderncoe.edu.in

Haripriya H. Kulkarni

Department of Electrical Engg

Dr. D. Y Patil Institute of Technology Pimpri

Pune, Maharashtra

ABSTRACT

As a result of the continuing depletion of conventional energy sources and increasing costs of fuel, renewable energy sources are now emerging as a major alternative energy source. Wind energy is the most prevalent renewable energy source. However, because of their expensive and complex structure, wind turbines cannot be modelled or analyzed. Developing a controller and evaluating the power electronics converter's performance are challenging tasks. In order to evaluate wind turbine performance in a laboratory environment, the wind turbine emulator has been developed. This paper explores the prerequisites for a wind emulators and provides a summary of the appropriate research. Furthermore, a review of a real-time emulator's development and design is divided into categories based to its distinctive features and control strategies. Applications and various controllers used in wind emulators are reviewed.

KEYWORDS : *Wind energy conversion system (WECS), Wind turbine emulator (WTE), Physical wind turbine (PWT), Permanent magnet synchronous motor(PMSM), Field oriented programmable gate array (FPGA).*

INTRODUCTION

One of the most promising technologies in recent years for enabling the production of electricity from renewable energy sources is wind power generation.[1] It is of the utmost importance to study grid-connected wind systems considering wind energy provides free fuel for the entire duration of the project and beyond.

A technology that has grown rapidly both nationally and internationally is wind energy. Predictions based on the Wind Vision study by the US DOE indicate that 35% of all electricity produced comes from wind energy.

It is difficult to conduct wind turbine system research and experiments on a wind turbine system because of greater initial costs, environmental impact and requirements for space The best alternative for an actual wind turbine system is a wind turbine simulation platform. An energy conversion system called a wind turbine emulator is a specialized too used for testing and assessing advancements in wind turbine technology. In a computer simulation, an emulator functions as a

wind turbine, giving a detailed understanding about the working of wind turbine.

Wind turbine emulators have been the focus of substantial study over the last few decades, utilizing a variety of motors and wind speed characteristics. Within which, implementations are carried out through the application of software tools such as MATLAB/Simulink, Lab view, PSCAD, or PSIM for mathematical modeling or real-time simulation.[2] The most often used hardware is a DC motor performing as a prime mover, however induction and permanent magnet synchronous motors (PMSMs) are also used. With DC motor drives, conversion technologies like DC/DC thyristor-based control and DC/DC chopper are frequently used;whereas with induction motor AC drives, techniques like variable frequency drive (VFD) are implemented.

The significance of wind turbine emulators, an overview of the literature, a discussion of static and dynamic characteristics in methodology, various

control techniques, and the controllers that are utilized by wind turbine emulators (WTE) are among the topics presented in this paper.

DYNAMICS OF WIND ENERGY SYSTEMS

A Wind Energy Conversion System (WECS) comprises of several types of components such as a generator, gearbox, rotor turbine, power electronic system, and transformer for the connection to the grid.

Wind turbine blades capture wind energy and use it to generate mechanical power. In high wind circumstances, managing and restricting mechanical power is essential.

Using a gearbox and generator is the most significant and widely employed technique for converting mechanical power with high torque and low speed into electrical power. The electrical power generated by the generator is fed into the grid via a transformer which includes circuit breakers and an energy meter. The wind energy conversion system's block diagram is displayed in Figure 1.

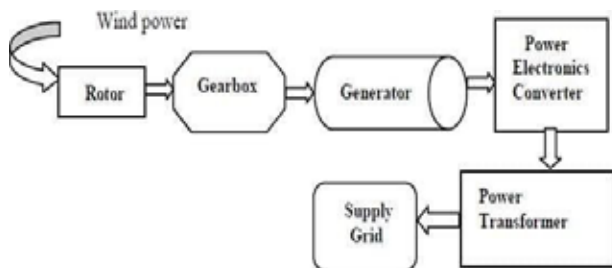


Fig.1: Block diagram of WECS

ESSENTIAL ROLE OF WIND TURBINE EMULATORS

Since wind energy is unpredictable, innovative solutions must be developed through laboratory testing. However, the real-time experiment on the physical wind turbine (PWT) system becomes complex and costly when taking into consideration the large-area requirements. Furthermore, in order to achieve maximum power extraction and harmonic-free output, Novel advancements in wind power systems necessitate the application of alternative power converter topologies and control strategies [3]. As a result, testing various control strategies and power converter topologies in WTE is extremely challenging; In addition, a wind

turbine emulator is essential for growth education and research in the field of wind energy. A wind turbine emulator carefully simulates the actions of a real wind turbine. Basically, it emulates the exact same operating pattern that a real wind turbine performs in real time at a specific wind speed and pitch angle at the hardware level. Hardware platform simulation techniques are often referred to as "emulation" techniques [4] To put it simply, hardware-level simulation .Without actual wind flow, the emulator can analyze the wind turbine's (WT) static and dynamic behavior. The WTE's hardware reproduces how wind energy conversion systems (WECSs) operates. Several planned designs and characteristics have been implemented used in the years-long study of the Wind Turbine Emulator (WTE). Various scholars have investigated various approaches for the design of WTE in the literature. Moreover, there hasn't been much consideration put into organizing and summarizing these technical texts. Thus, the primary objective of this paper is to review and compile the most recent study of research on Horizontal Axis Wind Turbine (HAWT) emulators.

REVIEW OF LITERATURE SURVEY FOR MATHEMATICAL MODELLING AND EXPERIMENTAL INSIGHTS IN WIND TURBINE EMULATION

According to the author, a permanent magnet synchronous generator (PMSG) and a wind turbine blade were mathematically modeled in order to create the wind turbine emulator.[1]. Here, a boost converter is linked to a bridge rectifier. These real-time models use a controlled power supply to provide the boost converter with a variable DC voltage.. Experimental results show that this modeling approach is effective and beneficial for developing wind energy conversion system (WECS) models when they are used in a hardware loop setup. Different topologies of controlling the power converter are presented in this paper. In order to illustrate the static and dynamic properties of wind turbines, the author in [2] implemented a small scale rating of a 1.5KW wind turbine emulator. A static characteristic is the relationship between rotor speed and mechanical power. A curve between the tip speed ratio and the power coefficient (C_p) is also involved. (λ) However to obtain reference torque it is necessary

to obtain the C_p - λ curve. From characteristics only it is possible to obtain the reference torque and reference speed which is given to the controller. DC Motor is used as a prime mover whose speed can be controlled by different methodologies. Mathematical modeling of static characteristics is modeled in MATLAB / SIMULINK and powered by DC-DC converter.

WTE with a rated power output of 700 watts is intended to resemble the operation of a wind turbine applied to residential environments is presented. [3] An induction motor operated by a variable frequency drive (VFD) provides the WTE. In this emulation, the speed of the Permanent Magnet Synchronous Motor (PMSM) is controlled in a manner that allows it to apply torque to the generator, replicating the effect of wind impacting the turbine blades and generating electricity. The control system includes algorithms and feedback mechanisms to adjust the PMSM's operation based on various parameters, such as wind speed, electrical load, and the desired power output. This model describes the development of a system that can accurately mimic the performance of a residential-scale wind turbine, taking into account the mechanical and control aspects. The reference speed trajectory tracking method is used to achieve this emulation; this method is used to balance the inertia of the motor. By applying an appropriate amount of aerodynamic torque to the generator, torque steps were used to validate the dynamic response and turbulent wind. The development of sophisticated wind turbine control schemes for WECSs at the residential scale is aided by this emulator.

[4] This paper presents the design of a small wind turbine emulator based on the D-SPACE 1104 controller. Here, a buck converter and a permanent magnet synchronous generator are connected for controlling the speed of the DC motor. Motor speed is controlled through D-space 1104. Every aspect of a real wind turbine was taken into account. The rotary motion produced by wind energy is replicated by this DC motor. This control system simulates the impact of various wind speed and torque values. Simulation results matched with experimentation results.

[5] This paper introduces a very affordable emulator for a wind turbine and generator. It's a smaller version of a real 1MW wind turbine. A system for simulating wind

speed in real time is incorporated in the structure; a PMSM controls itself at various wind speeds, MATLAB is utilized for simulation. The outcomes of this paper's simulations and experiments are comparable as well. [6] Many studies use computer simulations or real-time setups with software like Simulink/D-Space, PSCAD/EMTDC, or PSIM/MATLAB. Simulation is done in MATLAB and the hardware outcomes match with the simulation results. Modeling of DC motor and permanent magnet synchronous generator is presented along with the static and dynamic characteristics. [7] Researcher describes an emulator for wind turbines that uses a separately excited DC motor. The DC motor runs in a way that produces the necessary speed and torque for the generator to make electricity, simulating working of a wind turbine. Speed of the DC motor which is acting as a prime mover can be controlled. The results show that this wind turbine emulator performs efficiently, even under variable and unpredictable wind conditions. [8] This study used MATLAB/Simulink to model and simulate a wind turbine emulator. Communication between this software and the workbench was established using a DSP TMS320F28335. The experiments confirmed that the wind turbine emulator worked well, effectively replicating a real wind turbine. The MATLAB/Simulink modeling taken every real aerodynamic characteristics. The Research results show that the emulator was successful because the experimental outcomes matched the simulated ones. In order to optimize energy extraction from fluctuating wind speeds, traditional PID and PI controllers have been widely employed. [9] To mimic the speed and/or torque characteristics, a DC motor is used as a prime mover.

In order to optimize energy extraction from fluctuating wind speeds, traditional PID and PI controllers have been widely employed. [9] To mimic the speed and/or torque, a DC motor is used as a prime mover. To determine the static and dynamic characteristics two different structures are used. The generated Wind turbine simulator can replicate both the static and dynamic properties of the real WECS, according to the obtained simulation results. It used a control system with two PI controllers (one for speed and one for current) to replicate the steady (static) characteristics. For the changing (dynamic) characteristics, use a single PI controller for torque. [10] This paper describes wind

turbines characteristics based on simulation results. Then, it provides a detailed comparison of these characteristics with those of a DC motor, including characteristic curve. It also introduces a separately excited induction generator model (SEIG) and shares the simulation results obtained using MATLAB/SIMULINK. The simulation model is created for a Wind Turbine Emulator (WTE) in a Wind Energy Conversion System (WECS). This emulator uses a separately excited DC motor and a SEIG. It's designed for future experiments related to Wind Turbine Generators (WTG) [11]. This emulator lets them study a WECS without using an actual wind turbine. The DC motor and its control system make it act like a real wind turbine, creating the same conditions a wind turbine generator

The emulator mimics various wind situations and gives information about the operation of wind turbine. It's connected to a grid system just like a real wind turbine model called DR-14. The setup offers a practical way to learn about wind energy systems under various conditions, including supervisory control and data acquisition (SCADA) systems that monitor the wind turbine and adjust settings with a user-friendly interface.

[12] Researcher tries to explain the reliability of wind energy conversion systems can be increased through the design of different power electronic converters and various control algorithms. Comparing the suggested wind emulation platform with present systems, Internet of things (IOT) has a much higher traceability, efficiency and focuses primarily on wind turbines. Data on wind velocity in real time powers the wind emulation system. An Internet of Things (IOT) cloud application programming interface is used to retrieve the forecasted and real-time wind data from global nodes. The IOT cloud API, Field oriented gate array (FPGA) controller, and VEE Pro platform are integrated into the wind emulation system.

[13] Author describes the wind turbine aerodynamic properties were taken into consideration while developing this model. The torque developed in the shaft of the electrical generator will be specified by this model. The rotor flux and electromagnetic torque can be independently controlled by the induction motor control system. The simulated outcomes show the behavior of

induction motor. MATLAB was used to simulate the implementation of the strategy control.

[14] The dynamic features of a wind turbine are represented by the tower shadow effect and wind shear. The wind turbine simulator's design and implementation, which captures the wind turbines dynamic features, are presented in this paper. In order to determine the wind turbines output, mathematical modeling is carried out for both steady state and dynamic characteristics, such as pitch control, wind shear effect, and tower shadow effect. Reference Torque is obtained from the dynamic characteristics and given to the conventional PI controller [15] a wind speed simulator has been acquired to facilitate the generation of actual wind speed. The prime mover in this case is a doubly fed induction motor. This double-fed induction generator is connected to a cage-type induction motor.

Utilizing IEEE Transactions, Scopus, and Elsevier databases, an extensive literature review was carried out to explore the current state of wind turbine emulators at present. The following terms were used to search for documents: "wind turbine" plus the terms "hardware," "experimental setup," "emulators," "simulators," "simulations," "replication," "imitation," and "generator system." This review only took into account publications that deal with wind turbine emulators, wind turbine simulators, types of prime mover and hardware experimentation in the laboratory. The research papers are summed up according to the wind turbine model's behavior, data acquisition methods, software platform, controllers, generators, control parameters, and prime mover types

METHODOLOGY

Three mathematical models aerodynamic, mechanical, and electrical can be used to describe a WTE. A moving air mass at a certain speed needs to be transformed into mechanical energy at the generator's shaft, which is represented by the aerodynamic model, in order to create the rotational movement of the turbine.

The available mechanical power is reflected in the system shafts where speed and torque. is determined. The electrical the model describes how mechanical torque is converted into electrical energy at the generator output. Fig 2 shows the different stages of the wind turbine emulator.

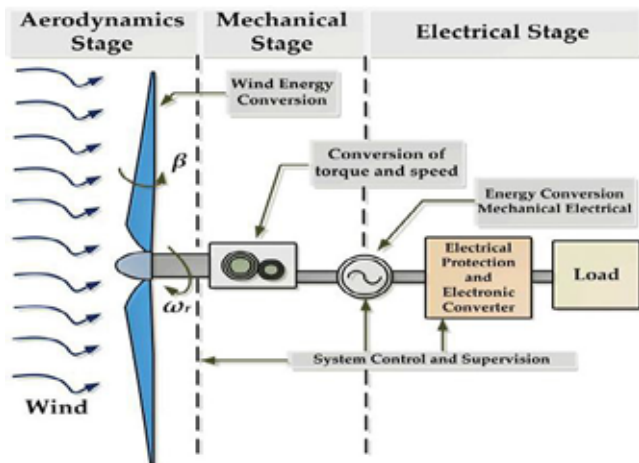


Fig.2: Stages of wind turbine emulator

As shown in the Fig 2 aerodynamic stage involves static characteristics of wind turbine Mechanical stage means dynamic characteristics of wind turbines. Wind turbine torque is a function of turbine speed and wind speed, Torque versus Turbine Speed and Power versus Turbine Speed These curves indicates the Static characteristics of wind turbine[15] Static wind turbine characteristics are part of the aerodynamic stage. Mechanical stage means dynamic characteristics of wind turbines.

It is concluded from the literature analysis of static characteristics that changing the pitch angle might reduce the extracted power. Power coefficient falls as output power and torque rise with wind speed. In a real world, wind speed varies with altitude which means different parts of wind turbine are exposed to different wind speeds. [16]This phenomenon is called wind shear and it creates a shearing force on turbine blades, which can affect power production and cause wear and tear. Also when the tower hub of a horizontal axis wind turbine blocks the wind flow reducing the wind speed that reaches the blades and affecting torque output.

Torque and power output fluctuate when two factors are available together. The 3P effect refers to the fundamental and third harmonic components of it. This is nothing more than the different wind turbines' dynamic characteristics.

The motor serves as both the prime mover and the generator for electrical subsystems in the physical implementation of the WTE, which is made up of a generator. WTEs are typically developed and designed

in a laboratory setting, allowing the flexible test bench to replicate the properties of actual WECSs.

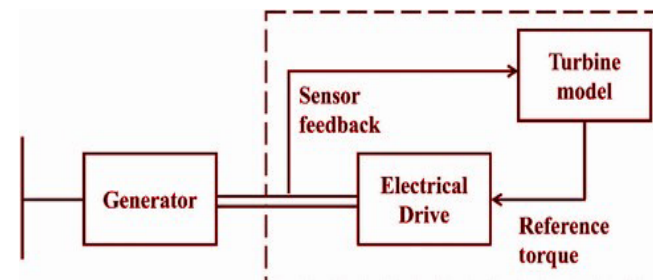


Fig.3: Block diagram of wind emulator

The block diagram for WTE, which includes a generator, electrical drive, and turbine model, is displayed in Fig 3. [19]. Reference torque is generated from the mathematical modeling of wind turbines and supplied to AC/DC drives. Generally, a power electronic converter is positioned between a load and an electrical generator. Wind turbine emulators are used to imitate the static and dynamic behavior of wind turbines during laboratory testing in order to develop the electronic converter utilized for wind turbine control. Several controllers are in control of all these motors. The main purpose of the controller is to calculate and adjust the torque and speed of the motor so it reproduce the exact torque speed characteristics of modeled wind turbine at a given speed.

As a result, developing the reference signal from the Wind turbine characteristics is a fundamental need for WTEs. The reference signal can be produced in two different ways. First, use the control system to track the reference speed that was generated from the Wind turbine mathematical model. Secondly, use the torque compensation and wind turbine inertia schemes to generate the reference torque. The motor should then track the reference torque by modifying its control scheme.

CONTROL TECHNIQUES IN WIND EMULATOR

To extract the most power possible from a wind turbine is its primary goal. It is imperative to take every precaution to ensure the safety of wind turbines and to extract maximum power as possible from the wind. A turbine operating at high wind speeds must regulate the forces pushing on the rotor in order to restrict the

amount of power To do this, a number of techniques are employed, which are described as follows:

Pitch Control

Since it is challenging to regulate the wind turbine torque at rated wind speed, pitch control method is used. Torque control is typically used in low wind speed areas. Pitch control of the wind turbine blade controls the output power. The disadvantage for the pitch control include the complexity of the system and power fluctuations are more when the wind speeds are high

WTE are designed to withstand severe weather rather than high rotational torques or speeds. At extremely high aerodynamic torques or rotational speeds, the turbine could be destroyed by the tremendous impact exerted on the WT's blades. In order to prevent this, WTs are always designed with a cut-out speed above which the turbine will be forced to stop by the brakes. However, there is a range of wind speeds before the cut-out speed where the WT applies a variety of control strategies to deal with strong winds that could otherwise damage the turbines. Consequently, every WT is designed using a particular kind of power control technique. Two methods to accomplish this are pitch control and stall control.[17]

Another popular control method is artificial neural networks (ANNs). These can be used to a variety of control system variables, including pitch angle, wind speed, rotor speed, output torque, and terminal voltage, or any combination of these.

CONTROLLERS USED IN WIND TURBINE

The purpose of the wind energy system is to maximize energy efficiency and extract maximum energy from the wind. PI and Fuzzy controllers are used to check the performance of WTE However this strategy cannot achieve better performance. To improve quality and energy efficiency of wind emulator for a fixed speed, sliding mode control is used. In addition to this to capture maximum power from the wind with the maximum power point tracking problem over a fixed pitch optimal control is used. [18] PID control strategy is used to maximize the efficiency of wind energy conversion based on the control of Power Electronics circuits all these controllers are used to determine the static characteristics of wind emulators.

An artificial neural network has also been used in recent years to develop a wind emulator for a wind turbine with a controller. The dynamic characteristics of wind emulators are identified taking into consideration the effects of wind shear and tower shadow. The generator's rotor axis provides mechanical power to the emulator, which converts the energy into a predicted wind speed. Nevertheless, the turbine shadow effect and the basis of pitch control have not received sufficient focus. It is missing an important both theoretical and practical justification[18].

These implementations can be overcome with the help of FPGA controllers. Implementation of real time controllers is only possible using FPGA on lab-view platform acting as a standalone system. It behaves statically as well as dynamically in terms of characteristics close to actual wind turbines. FPGA controllers are used to increase system reliability and accuracy by reducing error and ripple by using digital solutions.

FUTURE SCOPE

The static and dynamic properties of a wind turbine can be ascertained through mathematical modeling and simulation. Different controllers are used to obtain reference speed and reference torque. To extract maximum power from the wind, different algorithms can be proposed to implement MPPT techniques. . However, as part of research, AI, deep learning and machine learning algorithms can be implemented to optimize renewable energy sources with the objective to extract the greatest amount of power.

CONCLUSION

The importance of wind turbine emulators, along with the review of the literature, is presented in this paper. Furthermore, review of different control techniques and controllers used in wind emulator can be determined. From the literature survey it is concluded to determine the mathematical modeling of wind turbine, Static and dynamic characteristics can be obtain from which mechanical output power and torque is determined. .In most of the wind turbine emulator DC motor is used as prime mover. However the use of induction Motor and servo motor can also be utilized as a prime mover. To control the speed of prime mover various technologies and review of different types of controller is presented in this paper.

REFERENCES

1. Meysam Yousefzadeh, Shahin Hedayati Kia, Davood Arab Khaburi "Emulation of Direct-Drive Wind Energy Conversion Systems Based on Permanent Magnet Synchronous Generators" 12th power Electronics drive system and technology IEEE trans July 2023.
2. Jakkoju Nikhilesh, Shashi Bhushan Singh, "Homer Based: A Real-Time CHimani Garg., Ratna Dahiya" Modeling and Development of Wind Turbine Emulator for the Condition Monitoring of Wind Turbine" International journal of Engineering and Research Vol.5, No.2, 2015.
3. Adrien Prevost, Vincent Lechapp, Romain Delpoux, Xavier Brun "An emulator for static and dynamic performance evaluation of small wind turbines" 32nd International Symposium on Industrial Electronics (ISIE 2023), IEEE, Jun 2023, Helsinki-Espoo, Finland. fihal-04099988
4. Liviu – Dănuț Dănuț, Dan Hulea., Octavian Cornea, Nicolae Muntean, Mihai Andrei Iuoras, Nikolay Hinov" Low Cost Implementation of a Wind Turbine Emulator "IEEE International Conference on Environment and Electrical Engineering and 2020 IEEE Industrial and Commercial Power Systems Europe May 2020
5. Rasoul Azizpanah- Abarghooee, Mostafa Malekpour., Dragičević, Senior Member, Frede Blaabjerg, Vladimir Terzija " A Linear Inertial Response Emulation for Variable Speed Wind Turbines "IEEE transactions on Power Systems, March 2020 vol. 35, no. 2, pp. 1198-1208.
6. Anushree Ramanath, Jeyaram Durga, Manian Deivanayagam, Siddharth Raju, Ned Mohan " An Extremely Low-Cost Wind Emulator" 13th IEEE International Conference on Industry Applications (INDUSCON), Sao Paulo, Brazil, 2018,
7. R. Hu, W. Hu and Z. Chen, "Development of distributed simulation platform for power systems and wind farms," IECON 2015 - 41st Annual Conference of the IEEE Industrial Electronics Society, Yokohama, 2015, pp. 003443-003448
8. S. W. Mohod, M. V. Aware "Laboratory development of wind turbine simulator using variable speed induction motor" / International Journal of Engineering, Science and Technology, Vol. 3, No. 5, 2011, pp. 73-82.
9. Yassine Sirouni, Soumia El Hani, Nisrine Naseri, Ahmed Aghmadi, Khadija El Harouri, " Design and Control of a Small Scale Wind Turbine Emulator with a DC Motor "6th International Renewable and Sustainable Energy Conference (IRSEC)5-8 Dec. 2018.
10. G. Henz, Gustavo Koch, Claiton M. Franch, Humberto Pinheiro "Development of a variable speed wind turbine emulator for research and Training" Brazilian Power Electronics Conference 2013.
11. Ramu Nair. R, G. Narayanan "Emulation of Wind Turbine System using Vector Controlled Induction Motor Drive" 53(2):265–271, 2010. technologies," Proc. IEEE, vol. 103, no. 6, pp. 740–788, 2018.
12. J. S. Thongam, P. Bouchard, R. Beguenane, A.F. Okou, and A. Merabet. Control of Variable Speed Wind Energy Conversion System Using a Wind Speed Sensorless Optimum Speed MPPT Control Method. In IECON 2011 -37th Annual Conference on IEEE Industrial Electronics Society, pages 855–860, 2011.
13. R Raja Singh, Swapnil Banerjee, R Manikandan, Ketan Kotecha, V Indrigandhi, "Intellegent IoT Based Wind Emulation system based on Real time data fetching approach" IEEE access Dec 2022, Volume 10.
14. Z. Xu, J. Wei, S. Zhang, Z. Liu, X. Chen, Q. Yan, and J. Guo, "A state-of-the-art review of the vibration and noise of wind turbine drive trains," Sustain. Energy Technol. Assessments, vol. 48, Dec. 2021, Art. no. 101629, doi: 10.1016/j.seta.2021.101629.
15. W. Cao, Y. Xie, and Z. Tan, "Wind turbine generator technologies," in Advances in Wind Power. London, U.K.: Intechopen, 2012. [Online]. <https://www.intechopen.com/chapters/38933>, doi: 10.5772/51780.
16. Adil Mansouri, Abdelmounime El Magri, Rachid Lajouad, Ilyass El Myasse, El Khelifi Younes, Fouad Giri " A comprehensive review and analysis of Wind energy based conversion topologies and maximum power point tracking: "A ELSEVIER Advances in Electrical Engineering Electronics and Energy December 2023.
17. J. D. M. De Kooning, A. E. Samani, S. De Zutter, J. De Maeyer, and L. Vandeveld, "Techno-economic optimisation of small wind turbines using co-design on a parametrised model," Sustain. Energy Technol. Assessments, vol. 45, Jun. 2021, Art. no. 101165, doi: 10.1016/j.seta.2021.101165.
18. Sarvanakumar Rajendaran, Matias Diaz, V. S. Kriika Devi, Debashisha Jena, Jaun Carlos Travieso, Jose Radrizo " Wind Turbine Emulators -A Review" published in a special issue in Advances in Wind turbine energy conversation systems 2 March 2023.
19. Ecosense. Wind Turbine Emulator System. Available online: <https://www.ecosenseworld.com/labs/wind-energy-labs/wind-turbine-emulator> (accessed on 15 January 2023).

Optimizing Economic Strategies for Alternative Energy Sources in Electric Power Generation

V. S. Jape, Deepa S. Bhandare
Varad Chavare

Department of Electrical Engg
PES Modern College of Engg
Pune, Maharashtra
✉ jape.swati@moderncoe.edu.in

Haripriya H. Kulkarni

Department of Electrical Engg
Dr. D. Y Patil Institute of Technology Pimpri
Pune, Maharashtra

ABSTRACT

The gap between the supply and demand for energy is widening in a world where energy consumption continues to be increasing. The integration of alternative energy systems alongside traditional power generation has gained significant pace as a consequence to the growing demand for electrical power. Renewable energy sources, such as geothermal, wind, solar, and hydrogen fuel, have shown promising in providing reliable, economic power solutions while reducing greenhouse gas emissions. The primary objective of this study is to propose a methodology for designing a stand-alone hybrid PV/wind/diesel/battery system that minimizes the Cost of Energy (COE) and reduces CO₂ emissions using HOMER (Hybrid Optimization of Multiple Electric Renewables) for an educational institute.

The solar PV (1 kW, 2 channels), wind (1 kW, 1.5 kW), batteries (12 volts, 200 Ahr, 10 units), and hydrogen fuel cells (500 W, PEM type) are all represented in this economic study of the hybrid energy system. HOMER is implemented in the simulation to optimize the utilization of various energy sources. The study explores both technical and financial aspects, providing perspectives on the feasibility of the hybrid system from both an economic and technological perspective. This paper contributes to the understanding of how hybrid energy systems can be designed to efficiently meet the energy needs of educational institutions while reducing operational costs and environmental impact.

KEYWORDS : System optimization, Net present cost (NPC), Levelized cost of energy (LCOE), HOMER (Hybrid optimization of multiple energy resources), HPS (Hybrid power system).

INTRODUCTION

As global awareness of the detrimental impact of conventional electric power generation on global warming grows, the adoption of renewable energy sources for electricity production is on the rise. India, a country experiencing rapid economic growth, heavily relies on non-renewable energy sources for its energy needs, contributing to increased carbon emissions. In response to this challenge, the Indian government has become increasingly committed to developing clean energy solutions. The renewable energy sector in India has made significant strides, marking a pivotal shift towards sustainability. However, one of the key challenges in transitioning to renewable energy is

the intermittent nature of these sources. Relying on a single renewable energy technology often falls short of meeting the consistent power demands of consumers. Moreover, depending solely on a single energy source tends to lead to over-sizing of systems, which escalates initial costs. To address the intermittency issue and enhance power supply reliability, the concept of hybrid energy systems, consisting of multiple renewable energy sources, has gained importance. These systems offer a promising solution to harmonize electricity production with varying load requirements. Despite their potential benefits, hybrid systems have received relatively less attention due to their complexity. Researchers from around the world have conducted

numerous studies on power generation using various hybrid systems. However, there is a notable scarcity of research concerning the implementation of hybrid power generation systems in the context of India. This study aims to bridge this gap and contribute valuable insights into the feasibility and effectiveness of hybrid energy systems for power generation in India.

The objective of this simulation analysis is to identify the optimal combination of renewable energy technologies, utilizing available resources, to reliably and sustainably fulfill electricity demand. Additionally, it aims to assess the cost-effectiveness of such a hybrid energy solution. To achieve these goals, we have gathered essential data, including the daily load curve, solar radiation data, and hourly wind speed data for a specific location. The simulation is conducted using HOMER software, with the specified system parameters. The study evaluates the performance of a grid-connected hybrid system comprising a 1 kW solar PV array, 1.5 kW wind turbines, and a set of ten 12V, 200Ahr batteries.

OVERVIEW OF HOMER SOFTWARE

The flexible software programme HOMER (Hybrid Optimization of Multiple Energy Resources) was developed by the National Renewable Energy Laboratory and is intended for development and evaluation of hybrid energy systems. In addition to standalone or grid-connected hybrid power systems (HPS), these systems can also include renewable microgrids. Using advanced optimization and sensitivity analysis techniques, HOMER considers a variety of technologies available in its databases. Variations in technical costs, profiles of electric loads, and the accessibility of energy resources are taken into considerations. Analyzing hybrid systems from an economic and technological standpoint is the main purpose of the software. Users input critical data, including electrical load profiles, resource costs, and component costs. HOMER then provides valuable output data, such as energy costs, excess fuel consumption due to energy use, net present value (NPC), and the utilization of renewable energy sources.

To evaluate the technical and economic viability of an integrated system, HOMER relies on local data, including solar radiation, wind speed, and electrical load. It offers the capability to reduce operating costs

through optimal design scenarios. The software operates in three primary steps within its computing module: building and energy grid design, operation simulation, and sensitivity analysis with a focus on economic aspects. The ultimate goal of this software is to achieve the most efficient micro energy grid design. Through the ability to optimize system sizing, optimize the use of accessible renewable energy sources, batteries, and load, HOMER is well-suited to perform technical and economic analyses.

METHODOLOGY

In this study, a software-based approach is employed as the primary technique. To begin, daily load profile data is obtained, which includes essential electric load information such as the average daily consumption (in kWh) and the peak load (in kW). At the specific site under consideration, the peak load reaches 9.58 kW, while the average daily consumption stands at 46.01 kWh. It's worth noting that the load in focus here is residential in nature. The cost of one unit of electricity (1 kWh) is calculated at 11.86 (inclusive of all taxes). This cost serves as a crucial parameter for the economic analysis of the system. The simulation aspect of study is facilitated through HOMER, a powerful software tool that conducts simulations based on various inputs, including component ratings and costing information. HOMER's optimization analysis is executed by simulating the system using the specified component ratings [3]. The HOMER algorithm for these intricate evaluations is shown graphically in Figure 1.

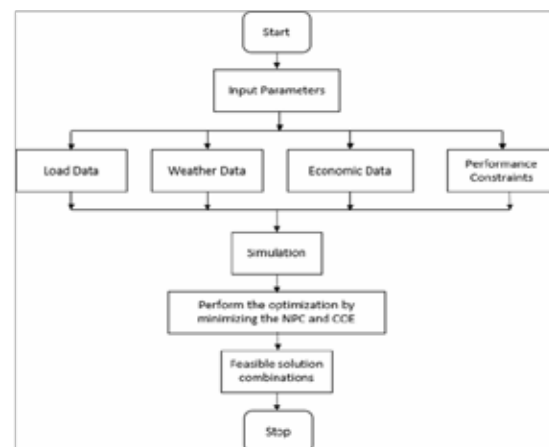


Fig.1: Block diagram of analysis algorithm using HOMER Application

These methodological steps allow to evaluate the technical and economic feasibility of the integrated energy system, while HOMER's optimization capabilities assist in determining the most efficient system configuration.

Metrological Data Collection

In this study, essential climate data, including wind speed and photovoltaic (PV) radiation, have been sourced from The National Aeronautics and Space Administration (NASA) to inform our analysis. NASA's climate data archives provide valuable insights for our research. Monthly averaged global solar radiation data for specific locations have been collected over a span of 22 years, while wind speed data spanning 30 years have been recorded. Fig. 2 visually presents the Monthly Average Solar Irradiance Data (measured in kWh/m²/day) and Clearness Index data at a specific geographical location. The monthly average wind speed (in meters per second) for the same location is shown in Fig. 3. This meticulously collected meteorological data is subsequently employed as input for the HOMER software. The software utilizes this data to simulate and estimate the output power generated by the solar PV system and wind turbine. These simulations play a pivotal role in our analysis of the integrated energy system's performance and efficiency.

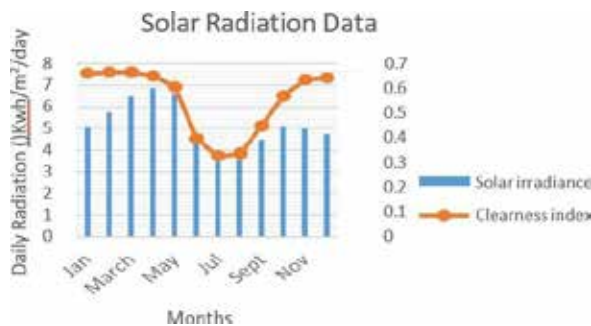


Fig. 2: Data on solar radiation



Fig. 3: Data on wind speed

Electrical Load Data

The system's electrical load consists of a daily demand of 46.01 kW, with a peak load of 9.58 kW. To create the daily load profile for simulation, a time interval of 60 minutes for a single day throughout the year is considered. This interval represents the load variations over the course of a typical day. In analysis, daily, seasonal, and annual load profiles are generated to comprehensively represent the load characteristics. These profiles are visualized in Fig.4 for daily variations and Fig.5 for seasonal and annual trends. These profiles serve as fundamental input data for simulations and are instrumental in evaluating the performance and suitability of the integrated energy system.



Fig. 4. Daily Load Curve



Fig. 5. Annual and Seasonal Load Data

System Components and Configuration

The key components of the system, along with their ratings and costs, are presented in Table 1. This table provides essential information about each component:

Table 1 Component Ratings and Costing

Sr.#	Component Name	Rating (kW)	Cost (Rs.)
1	Solar PV (with necessary components)	1 kW (4x250W panels)	32,000
2	Wind Turbine	1.5 kW	260,000
3	Single-Phase Inverter	7.5 kW	125,000
4	Batteries (Lead Acid)	12 V, 200 Ah (10 nos.)	110,000

Furthermore, Fig. 6 provides a visual schematic representation of the system configuration within HOMER software. This schematic offers an at-a-glance view of the interconnection and arrangement of the system components. These details are crucial for simulation and analysis of the integrated energy system's performance and economic feasibility.

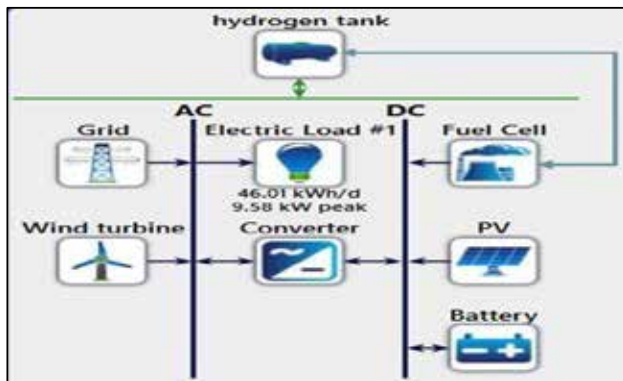


Fig. 6: Schematic Diagram of the System

MATHEMATICAL MODELLING OF COMPONENTS

Solar PV System

The following equation (1) is used to calculate the solar PV power output in the system. [4]

$$P_{PV} = Y_{PV} f_{PV} \left(\frac{\bar{G}_T}{\bar{G}_{T,STC}} \right) \left[1 + \alpha_P (T_c - T_{c,STC}) \right] \quad (1)$$

Where:

- Y_{PV} = the rated capacity of the PV array, meaning its power output under standard test conditions [kW]
- f_{PV} = the PV derating factor [%]
- \bar{G}_T = the solar radiation incident on the PV array in the current time step [kW/m²]
- $\bar{G}_{T,STC}$ = the incident radiation at standard test conditions [1 kW/m²]
- α_P = the temperature coefficient of power [%/°C]
- T_c = the PV cell temperature in the current time step [°C]
- $T_{c,STC}$ = the PV cell temperature under standard test conditions [25°C]

Wind Turbine

HOMER calculates the power output of the wind turbine for each time step through a systematic three-step process [4].

First, it computes the wind speed at the hub height of the wind turbine. Subsequently, HOMER calculates the

power that the wind turbine would produce at that wind speed under standard air density conditions. Finally, HOMER modifies the power output value to take into consideration the real air density at that particular place. After determining the hub-height wind speed, HOMER utilizes the power curve of the wind turbine to calculate the expected power output at that wind speed, assuming standard pressure and temperature parameters. The hub-height wind speed is represented by the red dotted line in the accompanying diagram Fig.7 and the power output predicted by the power curve for that specific wind speed is indicated by the blue dotted line. It is essential to note that the wind turbine does not produce any power if the wind speed at the hub height of the turbine is outside the range indicated by the power curve. This is consistent with the widely held belief that when wind speeds are above the maximum cut-out wind speed or below the minimum cut-off wind speed, wind turbines do not generate any power.

$$P_{WTG} = \left(\frac{\rho}{\rho_0} \right) \cdot P_{WTG,STP} \quad (2)$$

Where:

- Y_{PV} = the rated capacity of the PV array, meaning its power output under standard test conditions [kW]
- f_{PV} = the PV derating factor [%]
- \bar{G}_T = the solar radiation incident on the PV array in the current time step [kW/m²]
- $\bar{G}_{T,STC}$ = the incident radiation at standard test conditions [1 kW/m²]
- α_P = the temperature coefficient of power [%/°C]
- T_c = the PV cell temperature in the current time step [°C]
- $T_{c,STC}$ = the PV cell temperature under standard test conditions [25°C]

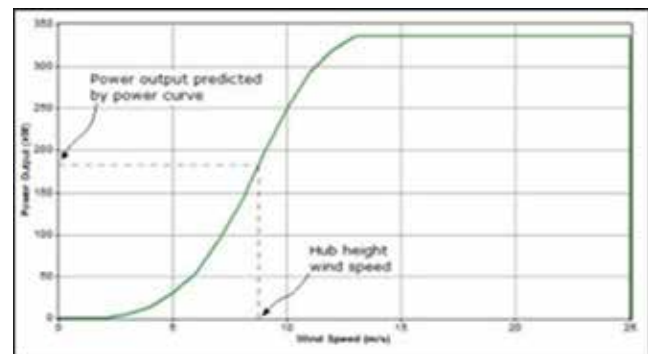


Fig. 7. Power Curve of Wind Turbine

Fig.7. shows the power curve of the wind turbine. According to this power curve the output of wind turbine is calculated.

Hydrogen Fuel Cell (PEM Type)

To calculate the hydrogen consumption at the rated power of the PEM (Proton Exchange Membrane) fuel cell, the following equation (3) is applied:

$$= \frac{P_{fc} \times 3600}{2 \times V_{fc} \times F} \text{ (mol/h-1)} \tag{3}$$

where HYFC represents the hydrogen consumption rate in mol/h (moles per hour). Pfc is the rated power of the fuel cell. Vfc is the volume of the fuel cell. F represents Faraday's constant. The hydrogen fuel cell comprises essential components, notably the electrolyser and the hydrogen fuel tank. These components play a pivotal role in the conversion of hydrogen into electrical power within the fuel cell system.

ECONOMIC TERMS

Net Present Cost (NPC): NPC, also referred to as life-cycle cost, is the result of subtracting the present value of all expenses related to installing and maintaining a component throughout the project's duration from the present value of all generated revenues during the same period. HOMER calculates and assigns NPC to each component in the system and to the system as a whole [5].

Levelized Cost of Energy (LCOE): The average cost per kWh of consumable electrical energy produced by the system is known as the Levelized Cost of Energy (LCOE), or COE. By dividing the entire electric load serviced by the annualised cost of delivering power, HOMER determines COE as Rs./kWh.

Return on Investment (ROI): ROI reflects the yearly cost savings in relation to the initial investment. It's calculated as the average yearly difference in nominal cash flows over the project's lifespan divided by the capital cost difference.

Payback Period: The payback period informs you of the time required to recover an investment. It's the duration in years needed for the total income to equal the initial investment value.

Operating Cost: This includes the annualized sum of all expenses and income (but not the initial capital costs).

SIMULATION RESULTS

Results without performing HOMER optimization

The annual operating cost for the specified residential load amounts to 1,99,172 Rs. The primary objective of the system is to achieve cost reduction. To explore different scenarios, we conducted five simulation runs without utilizing HOMER optimization [6]. A comprehensive comparison of parameters for these five instances is provided in Table 2

Table 2: Performance analysis of parameters for different combination without optimization

Economic and Technical Parameters	CASE I (Only Grid)	CASE II (G+PV)	CASE III (G+PV+W)	CASE IV (G+P+W+F)	CASE V (G+PV+W+FC+B)
Initial Cost (Rs.)	0	1,57,000	1,80,000	637000	747000
Energy purchased (KwH)	16,794 KwH	15,603 kwH	13,538 kwH	12,915 kwH	12,907 kwH
Operating Cost (Rs.)	1,99,172	1,78,621	1,44,901	1,45,115	1,50,200
Total NPC (Rs.)	25,74,808	24,66,131	22,10,210	21,20,496	26,88,712
Energy Sold back (KwH)	0	542 kwH	1,742 kwH	1,101 kwH	1,107 kwH
Renewable %	0	10%	27%	27.8	27.9%
COE (Rs.)	11.86	11	9.22	10.86	11.60

Table 3: Economic and Technical Parameters

Parameter	CASE I (Only Grid)	CASE II (G+PV)	CASE III (G+PV+W)	CASE IV (G+P+W+F)	CASE V (G+PV+W+FC+B)
Initial Cost (Rs.)	0	1,57,000	1,80,000	6,37,000	7,47,000
Energy Purchased (kWh)	16,794	15,603	13,538	12,915	12,907
Operating Cost (Rs.)	1,99,172	1,78,621	1,44,901	1,45,115	1,50,200
Total NPC (Rs.)	25,74,808	24,66,131	22,10,210	21,20,496	26,88,712
Energy Sold Back (kWh)	0	542 kwH	1,742 kwH	1,101 kwH	1,107 kwH
Renewable (%)	0	10%	27%	27.8%	27.9%
COE (Rs./kWh)	11.86	11.00	9.22	10.86	11.60

G = Grid (220V, 50Hz, Single phase, Residential)
 W = Wind (1.5 Kw).
 PV = Solar (1 Kw).
 F = Fuel Cell (500 watts)
 B = Battery (10 battery , 12V , 200 Amp-hr.)

The annual production of electricity by each component of the actual system (CASE V) is displayed in Table 3. Different economic characteristics are compared in Table 2.

Table 4: Yearly Production by each component of Actual System (CASE V)

Production	kWh/year	%
1 kW Solar PV	1,589	8.24
Fuel Cell	1,299	6.74
1.5 kW Wind Turbine	3,488	18.1
Grid Purchase	12,907	66.9
Total	19,284	100

This analysis shows that for case III (Grid + 1kW Solar + 1.5kW Wind Turbine) has a low Cost of Energy (COE) of 9.22 Rs. in comparison to other cases.

Simulation results by performing homer optimization

For performing the optimization analysis, the range of solar PV system is considered between 1 to 3kw and wind turbine range is between 0 to 1.5kw, Batteries (0 to 10no.), and the range of hydrogen fuel cell is between 0 to 500 watt [7].

According to HOMER optimization analysis, the optimum system satisfying the load and economic parameters is of a configuration comprising 3kw solar pv, 1kw wind turbine system and 2.46 kw inverter. The initial capital of this configuration is Rs. 317000, with an operating cost of Rs. 109220. Table 4 depicts the comparison of top 5 optimized system configuration. Table 5 gives the performance parameters of the actual system (case V) and the optimized system.

Table 5: Comparison of Performance Parameters of Optimized Cases

Sr. No.	System Configuration	NPC (Rs.)	Operating Cost (Rs./year)	Initial Capital (Rs.)	Renewable Sources Percentage (%)	Energy Purchased (kWh)	Energy Sold (kWh)
1	G+ PV (3Kw)+ W (1 Kw)+I(2.46 kW)	17,28,936	6.43	3,16,991	38.5317	12771.86	3984.332
2	G+ PV (3Kw)+ W (1 Kw)+ I(2.46kW)+ B (1)	17,46,601	6.50	3,28,538	38.5488	12769.68	3986.567
3	G+ PV (3Kw)+ I(2.46kW)	20,19,016	8.11	1,36,887	23.4872	14717.51	2441.718
4	G+ PV (kW)+ I(2.46 kW)+ B(1)	20,36,571	8.18	1,48,069	23.5008	14715.34	2442.301
5	G+ W (1KW)	22,84,719	10.01	1,80,000	19.7653	14157.56	851.5541

Table 6: Comparison of system without optimization and system with optimization

ComparingParameters	Actual System(CASE V) without optimization	HOMER optimizedSystem
Energy purchased (Kwh)	12,907 kwh	12,770 kwh
Operating Cost (Rs.)	1,50,200 Rs.	1,09,220 Rs.
Total NPC (Rs.)	26,88,712	17,28,936
Energy Sold back (Kwh)	1,107 kwh	3,984 kwh
Renewable %	27.9%	38.5%
COE (Rs.)	11.60	6.44

The annual energy production by each component of optimized is shown in Fig.8.



Fig. 8 Monthly Electric Production Data of case V

CONCLUSION

From simulation study and comparing results it is observed that, the HOMER-optimized system is more economical than actual system (Case V) in terms of cost of energy (COE) and NPC. Hence, it is concluded to perform the HOMER simulation to check the system's feasibility economically and technically before making an investment in hybrid system projects. The chart of the cash flow of the base system and lowest cost system (HOMER optimized system) is plotted across the project lifetime.

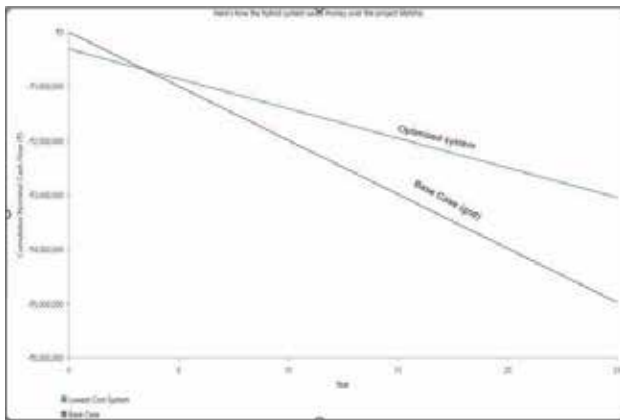


Fig. 9. Cash Flow Comparison of Base case and Optimized Case

Fig. 9 represents the cash flow comparison of base case (only grid connected) and optimized system (3 kw solar + 1kw wind + 2.46 kw inverter + grid). The intersection of two line gives the payback period of optimized system.

The simulation study of a hybrid energy system comprising alternative energy sources is carried out [8]. The detailed analysis by comparing the different cases of simulation results without HOMER optimization, It is observed that case III has the lowest operating cost (Rs. 1, 44,901) with a COE of Rs. 9.22. The initial cost of case III configuration is Rs. 3,37,000.

The case V is an actual system that is going to install, the initial cost of this system is 7,47,000Rs. With an operating cost of 1,50,200 Rs the annual saving, in this case, is Rs. 48,972. The payback period for this case V is of 15 years (operating cost/annual saving). The system is cost-saving but not that economically well. HOMER optimization simulation is performed to get an

optimized system configuration for this configuration, several limits to Homer for a rating of sources which is feasible to install are given in the case VI system. HOMER simulated 19444 feasible cases for system configuration and give the system comprising 3kw solar PV, 1kw wind and an inverter of 2.46kw as the optimum system with an initial capital requirement of Rs. 3,16,992. The yearly operating cost of this system is Rs. 109220, and the annual saving in the energy bill, in this case, is Rs. 89995. The payback period for this system is of 3.5 years. The share of renewable sources in this system is 38.5 %. The NPC (Net Present Cost) of this optimized system is Rs. 17,28,936.

FUTURE SCOPE

The present analysis is carried out for optimisation of the cost. Further it can be analysed by considering different constrains and optimisation of power generation or reliability. Various other data analysis tools can be utilized for getting the best operating combination of a hybrid source. Multiple ratings of vertical axis wind turbines and various advanced materials of solar may give better optimised results with both the cost effective solution and also consideration of maximum power generation.

REFERENCES

1. Ruben Zieba Falama, Felix Ngangoum Welaji, Marcel Hamda Soulouknga, "Optimal Decision-Making on Hybrid Off-Grid Energy Systems for Rural and Remote Areas Electrification in the Northern Cameroon", Journal of Electrical and Computer Engineering, Vol 2022, DOI:10.1155/2022/5316520.
2. Jakkoju Nikhilesh, Shashi Bhushan Singh, "Homer Based: A Real-Time Case Study on Optimization and Simulation of Hybrid Energy System at NIT Kurukshetra and the Effect on the Environment" IEEE Xplore, 02Nov, 2020, DOI: 10.1109/ICMICA48462.2020.9242814
3. K. Nagasujatha, V. B. Shalini, "Technical performance evaluation and economic viable solutions using hybrid renewable energy systems", IEEE Xplore: 24 March 2016, DOI: 10.1109/PCITC.2015.7438105
4. J Kumari, P Subathra, JE Moses, D Shruthi, "Economic Analysis of Hybrid Energy System for Rural Electrification using Homer", IEEE International Conference on Innovations in Electrical, Electronics,

- Instrumentation and Media Technology. 23 November 2017, DOI: 10.1109/ICIEEIMT.2017.8116824
5. MH Nehrir, C Wang, K Strunz, H Aki, R Ramakumar, J Bing, Z Miao, Z Salameh, "A Review of Hybrid Renewable/Alternative Energy Systems for Electric Power Generation: Configurations, Control, and Applications", IEEE transactions on sustainable energy, Vol.2, No.4, Oct 2011, DOI: 10.1109/TSTE.2011.2157540.
 6. Hoarcă Cristian , Nicu Bizon "Design of hybrid power systems using HOMER simulator for different renewable energy sources", ECAI 2017 - International on Electronics, Computers and Artificial Intelligence 29 June -01 July 2017. DOI: 10.1109/ECAI.2017.8166507
 7. A Jamalalah, CP Raju, R Srinivasarao, " Optimization and operation of a renewable energy based pv-fc-microgrid using homer" International Conference on Inventive Communication and Computational Technologies (ICICCT) 2017, DOI: 10.1109/ICICCT.2017.7975238
 8. Zahid Hasan Mamun; Tishna Sabrina; Mohammad Mofizur Rahman "Design and Economic Analysis of Hybrid Renewable Energy System", IEEE International Conference on Power, Electrical, and Electronics and Industrial Applications (PEEIACON) 29 November-01 December, 2019. DOI: 10.1109/PEEIACON48840.2019.9071954.

Design and Implementation of a Novel Intelligent FFOPI Controller for a Coupled Tank Liquid Level Control System by Simulation

Deepa S. Bhandare

Neelima R. Kulkarni

Department of Electrical Engg

PES Modern College of Engg

Pune, Maharashtra

✉ dr.deepasbhandare@gmail.com

Mayuresh V. Bakshi

Department of Engineering & Applied Sciences

VIIIT

Pune, Maharashtra

ABSTRACT

A coupled tank system (CTS) with multi-input multi-output (MIMO) interaction exhibits slightly nonlinear behavior. This makes the control complex and challenging in terms of achieving the desired performance specifications. Because of the non-linear nature of the mathematical model of CTS, it can be linearized using the Taylor series expansion method. A conventional PI controller can often prove to be inadequate for meeting the demands unless it is combined with some form of intelligence. A self-tuning fuzzy PI (STF-PI) controller results in online scaling factor modification of the PI controller parameters. Combining fractional order systems with fuzzy logic is a powerful approach in control theory, providing a flexible and adaptive framework for handling complex and nonlinear systems. Because of enhancing the performance of the CTS, a novel intelligent fuzzy fractional order proportional-integral controller (FFOPI) for CTS liquid level control is proposed in this paper, and the performance of the system is demonstrated for changes in the set liquid levels. MATLAB simulations are carried out to analyze the performance of the proposed FFOPI controller with that of the conventional PI controller, FOPI controller, and Self-tuning Fuzzy PI controller. So, for the sustainable development growth, intelligent controller-based CTS is very essential in the process management industries for an enhanced future.

KEYWORDS : Coupled tank system (CTS), FOPI and fuzzy - FO-PI controller (FFOPI), PI, self-tuning fuzzy PI controller.

INTRODUCTION

Significance

Controlling the liquid level in a coupled tank system (CTS) is a standard problem faced by many process industries, including wastewater treatment, nuclear generation, chemical and pharmaceutical manufacturing processes, and coolant management in the manufacturing industry [1]. When dealing with higher-order processes in process industries, many of the interacting tanks in series have slightly nonlinear behavior in terms of flow and discharge from the coupled tanks. In process industries, controlling the liquid level in interacting tanks with the smallest steady-state error (ess) and settling time (ts) is not only

important but optimally maintaining the levels can also be economically beneficial.

Around 90% of industrial-level controllers are from the PID family, as it can still prove to be the correct choice of controller in case of systems such as single-capacity tank systems which are simpler from a control point of view.

However, with the more complex nature of the system such as the MIMO system with slightly non-linear behavior, as considered in this paper, the PI controller should be more intelligent for obtaining enhanced system performance [2, 21].

In recent years, applications of fractional calculus have been found widely in science and technology areas.

With fractional calculus, the integrals and derivatives of non-integer order can be computed. The FOPI controller is a PI controller extender. It has a non-integer order of integration that may be adjusted, giving the designer more flexibility. Podlubny (1999) [3], Monje, Chen, Vinagre, Xue, and Feliu (2010) [4], Padula and Visioli (2011) [5] have all demonstrated the ability of fractional order PID controllers to perform better than their integer-order counterparts.

The basics of fractional calculus and applications of fractional-order calculus to industrial control problems are described by Aleksei Tepljakov (2011) [6]. Currently, research is still going on how a combination of computational intelligence approaches and fractional-order calculus can jointly be used to improve the system performance [7]. A review of a fractional calculus definition, tuning of fractional-order PID controller, books, and software for fractional-order PID controller has been described by Pritesh Shah (2016) in [8]. As a result of this study, many other researchers proposed fractional PID controllers using different designs and tuning techniques. The $PI\lambda D\mu$ (fractional-order) controller extends the traditional PID controller with two additional parameters order of integration (λ) and order of derivative (μ).

Prime objectives

- Determining Tuning parameters of PI controller for linearized CTS model using different tuning methods such as Ziegler-Nichols (Z-N) and Cohen-Coon (C-C) [10].
- To design an intelligent controller for CTS regarding liquid level control to improve time domain specifications, as mentioned below.
 - Settling liquid levels in both the tanks stay within a range about the set levels with allowable tolerance $\pm (2 \text{ to } 5) \%$.
 - Steady state error (e_{ss}) must be zero.
 - Minimum overshoot (around 2%) in the output level response.
- To demonstrate the performance comparison of an intelligent FFOPI controller with

various controllers for controlling levels in both tanks.

Novelty of the proposed work

- For sustainable development, intelligent controller-based CTS is essential in the process management industries for an enhanced future. A novel FFOPI controller design using a time domain approach has been proposed for the liquid level control of CTS (MIMO configuration) to maintain set levels and minimum settling time for both tanks as per the application requirement.
- The liquid considered in most of the literature [11-14] available up till now for CTS is water whereas the coolant liquid other than water is used for the experimentation and results are demonstrated in this paper.
- A comparison of time-domain performance parameters using the various controllers such as PI, FOPI, Self-tuning fuzzy PI [22], FFOPI is presented and further shows that the FFOPI controller for CTS performs very well than above mentioned controllers.

The organization of the paper is as; Section II discusses the mathematical modeling of the CTS along with its system transfer function, Section III explains the FOPI controller and Intelligent FFOPI controller, Section IV deals with FFOPI controller based CTS simulation models along its results, Section V presents comparative performance analysis of the different controllers, Section VI discuss about importance of Intelligent CTS for sustainable development followed by the conclusion in Section VII.

MATHEMATICAL MODELLING OF THE COUPLED TANK SYSTEM

The mathematical modeling of CTS can be derived by considering it as a MIMO system from the experimentation with the coolant as a liquid [1]. Fig.1 shows the schematic representation of CTS. The primary objective is to maintain the liquid levels, l_1 in tank LT1 and l_2 in tank LT2 by controlling the input flow rates q_1 and q_2 respectively.

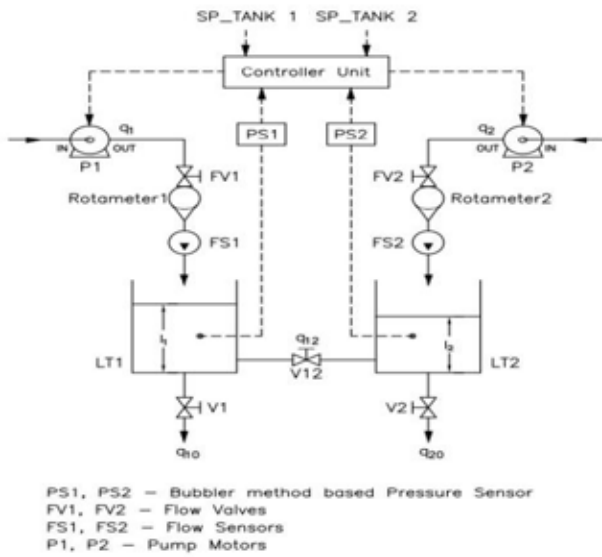


Fig.1: Schematic representation of CTS

The mathematical model of CTS is non-linear due to the non-linear relation between the flow rate and the level. However, linearization can be carried out by using Taylor series expansion and is valid for small changes in the liquid level around the operating point [10]. The state space model obtained after linearization is converted into transfer function form with transfer functions G_{11} , G_{21} , G_{12} , and G_{22} and can be expressed as,

$$G_{11} = \frac{58.72s+9.158}{s^2+0.274s+0.01750} \tag{1}$$

$$G_{21} = \frac{1.95}{s^2+0.274s+0.01750} \tag{2}$$

$$G_{12} = \frac{1.95}{s^2+0.274s+0.01750} \tag{3}$$

$$G_{22} = \frac{58.72s+7.05}{s^2+0.274s+0.01750} \tag{4}$$

The CTS as shown in Fig.1 consists of two interacting tanks which exhibit over-damped system dynamics. This can be seen from the damping coefficient (ξ) as observed from the above equation to be greater than one.

METHODOLOGY: INTELLIGENT FUZZY FRACTIONAL ORDER PI(FFOPI) CONTROLLER

Fractional Order PI Controller

The mathematical model of the liquid level control system is over damped in nature with no overshoot. Because of this, the PI controller is sufficient from a control point of view in improving the steady-state response. A PI controller is preferred as it is easy to implement and ensures a decrease in steady-state error with improved system stability.

The control performance of an existing system will be modified, with the inclusion of the extra fractional-order parameter λ , in the FOPI controller [3-8]. The integration function is primarily used to eliminate steady-state error, ensure output response tracking to set-point input response, and improve system control accuracy.

Fuzzy Fractional Order PI Controller

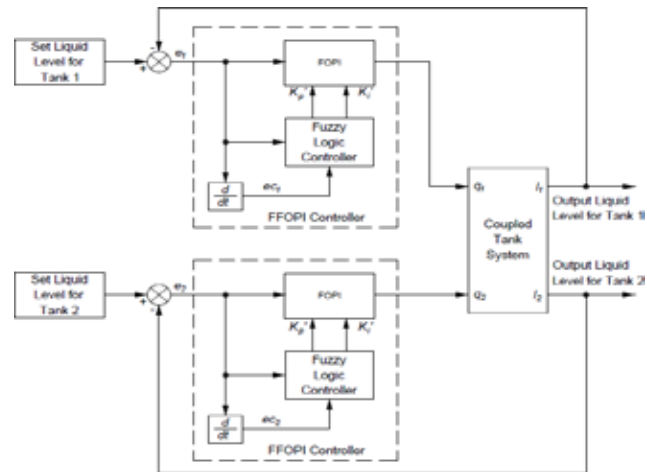


Fig. 2: Implementation Block diagram of FFOPI controller for CTS

Fig. 2 consists of the following blocks,

Fuzzy logic controller: This module performs the fuzzy logic operations and generates the control signal. It has two inputs namely e and ec . This model generates the control signal based on a set of fuzzy rules and membership functions.

FOPI Controller: This module gives a summation of proportional gain and fractional order integration of

the integral gain. The result of it provides additional stability to the system.

This signal is then applied to each of the pump motors to regulate flow that keeps the level of the liquid to set values. Since the FOPI controller has three tunable parameters (K_p , K_i , λ), of which K_p , K_i are controller coefficients and λ is an order of integration, it is possible to apply a self-tuning fuzzy system to set these coefficients. The Mamdani min- max inference method is used for fuzzy inference in this system. Seven triangular-shaped membership functions (MFs) have been chosen for all inputs and outputs. Ranges of the MFs for tanks 1 and 2 are, respectively, $K_p \in (9 \text{ to } 10.7)$ and $K_i \in (1.2, 1.6)$. There is a total of 49 rules designed for fuzzy logic control. Also, $K_p = 1.7K_p' + 9$, $K_i = 0.4K_i' + 1.2$ can be expressed. Whereas if λ is changed between (0 to 2) then the performance of the system gets changed.

SIMULATION OF FFOPI CONTROLLER WITH CTS

An FFOPI controller for CTS can be simulated as shown in Fig. 3.

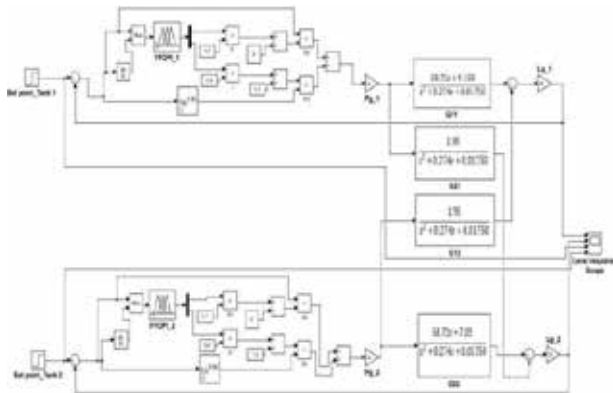


Fig. 3: Simulink model of CTS with FFOPI controller

The simulation involves designing a controller that can regulate the liquid level in the coupled tanks. While designing the FFOPI controller in Simulink for a fractional integrator, the order of integration (λ) is kept at 0.995 for the controller of both tanks, which is the best suitable value after studying the influence of the order of integration (λ) on control performance of CTS [23] between a range of 0.2 to 1.2.

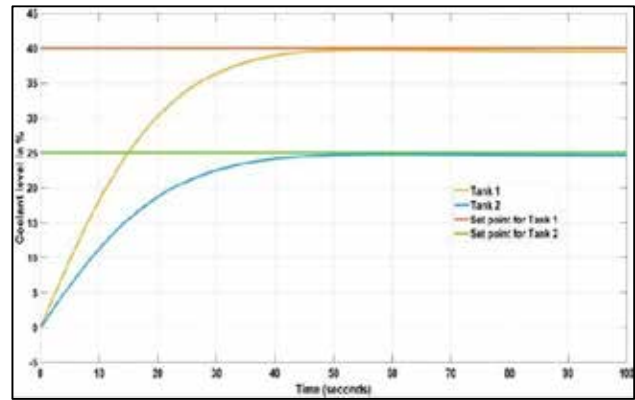


Fig. 4: Sample reading 1 Simulation output response for two tanks using FFOPI controller for set level I1=40%, I2=25%

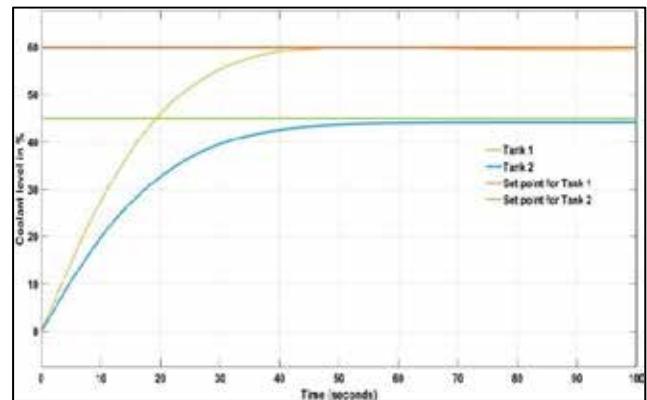


Fig.5: Sample reading 2 Simulation output response for two tanks using FFOPI controller for set level I1=60%, I2=45%

The simulation output responses shown in Fig.4 and Fig.5 can be analyzed to determine the performance of the controller in terms of t_r , $\%M_p$, t_s , e_{ss} for two sample readings are tabulated in Table 1.

Table 1: Time Domain Performance Specification with FFOPI Controller for CTS in simulation mode

Tank	Set levels	Time Domain Performance Specification			
		Transient Response		Steady State Response	
		t_r (sec)	$\%M_p$	t_s (sec)	e_{ss}
Tank 1	40%	25.5	0	39	0
Tank 2	25%	25	0	36	0
Tank 1	60%	29	0	39	0
Tank 2	45%	34	0	44	0

RESULTS: COMPARATIVE PERFORMANCE ANALYSIS OF FFOPI WITH VARIOUS CONTROLLERS

For fixed set liquid level for both tank

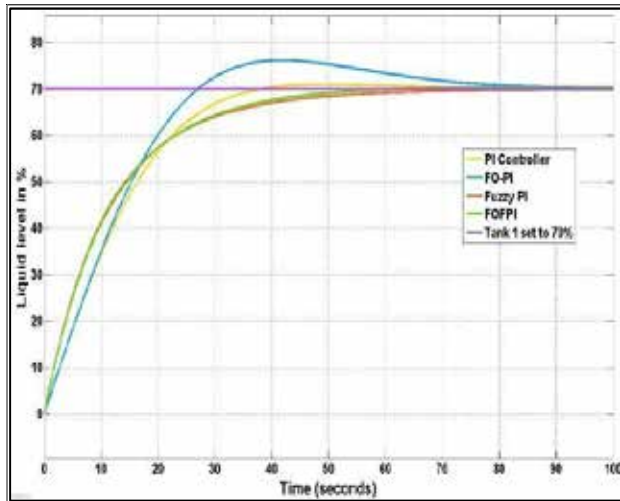


Fig.6(a): Response from Tank 1=70% with various controllers

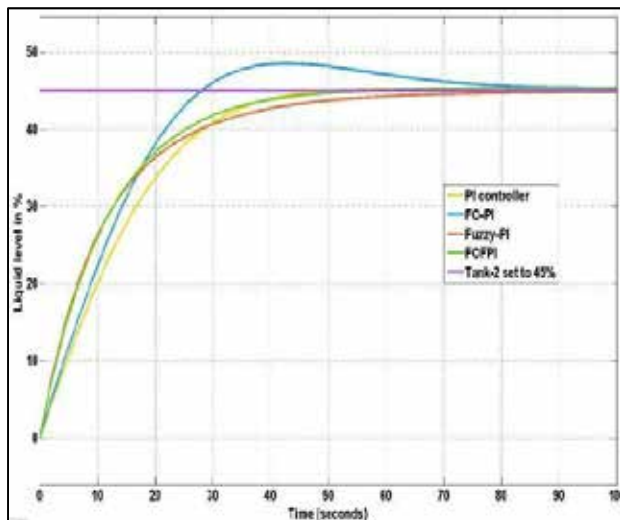


Fig.6 (b): Response from Tank 2=45% with various controllers

Fig.6 (a) shows the response obtained from tank 1 with the use of various controllers for the step of 60%. Fig.6(b) shows the response obtained from tank 2 with the PI, FO-PI, FUZZY-PI, and FFOPI controllers for a step change of 45%.

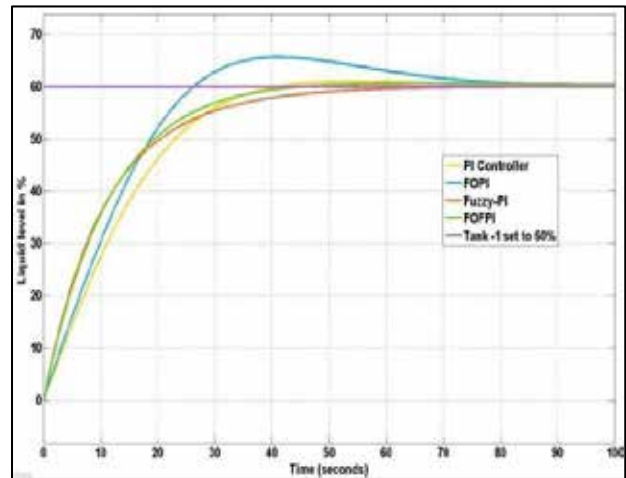


Fig.7 (a): Response from Tank 1=60% with various controllers

From Figures 7 (a, b), it is observed that the FFOPI controller for CTS provides the best response over other controllers as it settles faster with negligible overshoot. Tables 1 and 2 show, level output response in the time domain for both tanks for set levels with the use of various controllers. In the case of FO-PI controller, with an increase in λ from 0 to 1.1, the system reaches a steady state with less settling time and a fairly acceptable rise time. From responses, it is observed that the FFOPI controller for CTS provides the best output response as it settles fast with negligible overshoot.

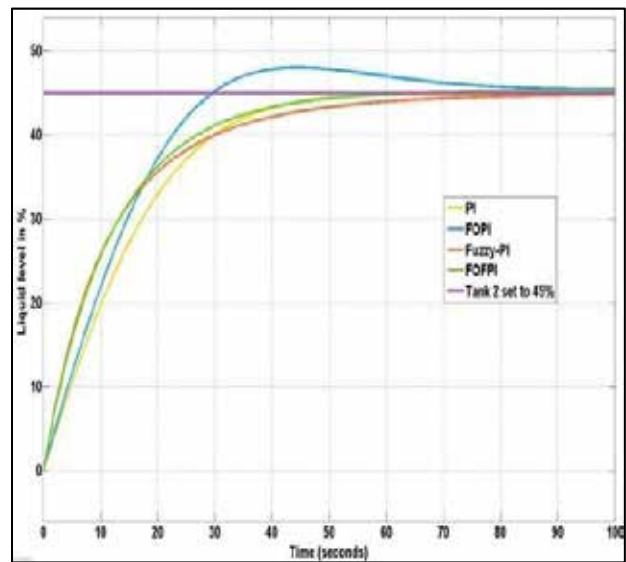


Fig.7 (b): Response from Tank 2 = 45% with various controllers

However, it shows a slight increase in % overshoot which can still be considered to lie within the permissible limits. With an increase in λ beyond 1.1, it is observed that the system performance considerably degrades. Thus $\lambda=1.1$ is considered to be the best choice in the case of FOPI controller for both the tanks [23]. In the case of the Fuzzy- PI controller, the settling time is found to be comparatively lower than FO-PI controller without any overshoot.

In the analysis of this study, comparative results of all

the controllers in simulation are given in Table numbers 2 and 3 respectively.

From Tables 2 and 3, it is observed that t_r and t_s required for FFOPI controller is less as compared to PI, FOPI, and STF-PI controller and $\%M_p$ is zero for Tank 2. For Tank 1 $\%M_p$ is within the permissible limit. As FFOPI controller uses a combination of fractional order PI and fuzzy logic to correct the control input for both pump motors, which can result in faster control action compared to the STF-PI controller.

Table 2. Time domain specifications for tank 1 (set level = 70%) and tank 2 (set level = 45%) with various controllers

Tank	Controller	Time Domain performance indices			
		Transient performance indices		Steady-state performance indices	
		T_r (sec)	$\%M_p$	T_s (sec)	e_{ss}
TANK 1 Set level=70%	PI	28.1	0	56.31	0
	FO-PI	21.6	8.85	73.5	0
	Fuzzy-PI	27.9	0	51	0
	FFOPI	25	0	38.5	0
TANK 2 Set level=45%	PI	29.1	0	41	0
	FO-PI	22	7.77	73	0
	Fuzzy-PI	30.5	0	56	0
	FFOPI	26.45	0	42	0

Table 3. Time domain specifications for tank 1 (set level = 60%) and tank 2 (set level = 45%) with various controllers

Tank	Controller	Time Domain performance indices			
		Transient performance indices		Steady-state performance indices	
		T_r (sec)	$\%M_p$	T_s (sec)	e_{ss}
TANK 1 Set level=60%	PI	27.3	0	54.6	0
	FO-PI	21.3	9.46	73.2	0
	Fuzzy-PI	27	0	47.60	0
	FFOPI	24.5	0	37	0
TANK 2 Set level=45%	PI	31	0	46.5	0
	FO-PI	23.3	6.66	75.2	0
	Fuzzy-PI	31.2	0	62.5	0
	FFOPI	28	0	45	0

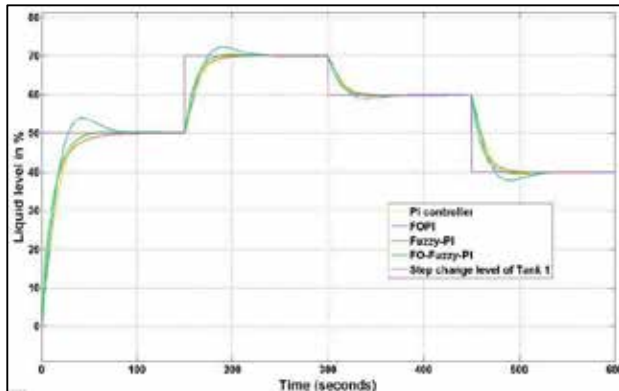
For the step change given in set level

Fig.8 (a): Change in set-point response of Tank 1 with various controllers

Fig.8 (a, b) depicts set-point change performance for the various controllers. At every 150 second interval, the set point for Tank 1 is changed from 50 % to 70 %, 70 % to 60 %, and then 60% to 40% respectively. Similarly, at every 150 second interval, the set point for Tank 2 is changed from 25% to 45%, 45% to 35%, and then 35% to 25% respectively.

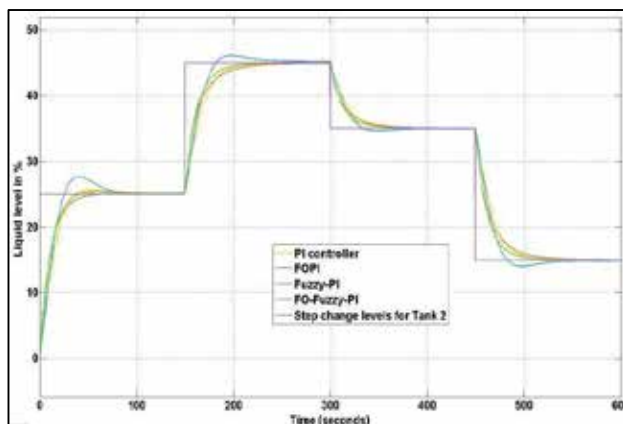


Fig.8 (b): Change in set-point response of Tank 2 with various controllers

So, with $\lambda = 0.995$ the system reaches a steady state with lesser settling time without overshoot.

DISCUSSION

It is observed that the FFOPI controller is capable of tracking parameter variations and bringing the system to a steady state with minimum settling time. The proposed controller combines the effect of fractional-order PI (FOPI) control with self-tuning fuzzy logic to

obtain a robust and effective controller. The proposed intelligent (FFOPI) controller has been designed to have better improvement in the time domain performance parameters of the system. It has been observed that, the limitations of a conventional PI controller can be overcome with fuzzy fractional-order - PI (FFOPI) controller in terms of very less rise time (sec), shortened settling time t_s (sec), and minimum steady-state error (ess) with 0% of overshoot.

CONCLUSION AND FUTURE SCOPE

A novel FFOPI controller is proposed in this paper with the hybrid combination of fractional-order PI and self-tuning fuzzy logic control for CTS. In MIMO nonlinear systems, using the fuzzy system to determine all control parameters as an adaptive controller may be advantageous. The performance comparison of the FFOPI controller with PI and FO-PI, Fuzzy -PI controller is carried out through simulation. The proposed FFOPI controller has more flexibility than a conventional PI controller and it leads to enhanced system performance as seen from the comparative performance analysis of the various controllers.

Intelligent control systems make use of artificial intelligence. In the process management industry, intelligent solutions are becoming more common. To construct an intelligent control system, the mathematical theory of control is integrated with artificial intelligence (AI). As a result, intelligent control aids in the promotion of long-term sustainable growth. The intelligent controller-based CTS is essential in process management sectors for coolant-level management. Improvements in CTS performance due to intelligent controllers save enormous manufacturing costs and time on an industrial scale in the long term. So, the intelligent controller is the need of the present time for the process industry that deals with level control problems which eventually ensure sustainable development growth.

REFERENCES

1. Ling Nai Ho, Norhaliza Abdul Wahab, Ibrahim A. Shehu, A. Alhassan, I. Albool, N. Ibnihajar, B. M. Othman, M. S. Zainal, M. J. Ibrahim, M. S. Rasol, "Control of a Coupled Tank System using PI controller with advanced Control Methods", Journal Tektology (Sciences & Engineering) 78:7-4 (2016) 41-49.

2. J. L. Meza, V. Santibanez, R. Soto and M. A. Llama, "Fuzzy Self-Tuning PID Semiglobal Regulator for Robot Manipulators", IEEE Transactions on Industrial Electronics, vol. 59, no. 6, pp. 2709-2717, June 2012, doi: 10.1109/TIE.2011.2168789.
 3. Igor Podlubny, "Fractional-Order Systems and Controllers" IEEE Transactions on Automatic Control, Vol. 44, No. 1, JANUARY 1999.
 4. Monje, C., Chen, Y., Vinagre, B., Xue, D., & Feliu, V. (2010). "Fractional-order systems and controls: Fundamentals and applications". London, UK: SpringerVerlag.
 5. Padula, F., & Visioli, A. (2011), "Tuning rules for optimal PID and fractional-order PID controllers", Journal of Process Control, 21, 69–81.
 6. Aleksei Tepljakov, Eduard Petlenkov and Juri Belikov, "On Fractional-order Calculus Applications to Industrial Control Problems", Department of Computer Control, Tallinn University of Technology, Ehitajate tee 5, 19086, Tallinn, Estonia, Conference Ppr-Jan 2011.
 7. C. Yeroglu & N. Tan, "Note on fractional-order proportional – integral – differential controller design", Published in IET Control Theory and Applications Received on 19th December 2010.
 8. Shah, Pritesh & Agashe, Sudhir. (2016), "Review of fractional PID controller. Mechatronics", 38. 29 - 41.
 9. Bhandare D.S., Kulkarni N.R., Bakshi M.V. "Linearization of a coupled tank MIMO system and its validation using MATLAB", 6th IEEE international conference for convergence in technology (I2CT) (2021), Pune, India.
 10. Mrs. Deepa Shivshant Bhandare, Lagmesh Gavli and Dr. Mrs. N. R.Kulkarni, and Dr. M.V.Bakshi, "Analysis of Tuning Methods of PID Controller for Linearized Coupled Tank Liquid Level System", Vidyabharati International Interdisciplinary Research Journal, Special Issue on Engineering Technologies and Management, ISSN 2319-4979, August 2021.
 11. Vo Lam Chuong, Truong Nguyen Luan Vu, Le Linh, "Fractional PI Control for Coupled-Tank MIMO System", 2018, 4th International Conference on Green Technology and Sustainable Development (GTSD).
 12. K. Sundaravadivu, B.Arun, K.Saravanan, "Design of Fractional Order PID Controller for Liquid Level Control of Spherical Tank", 2011 IEEE International Conference on Control System, Computing and Engineering. 978-1-4577-1642-3/11/2011 IEEE.
 13. Ramkumar V P & Elizabeth Varghese, "Fractional Order PID Controller for Liquid Level System", International Journal of Engineering Research & Technology (IJERT) ISSN: 2278-0181, Vol. 4 Issue 07, July-2015.
 14. R. Paul, A. Sengupta, "Fractional Order Intelligent Controller for Single Tank Liquid Level System", 2021 IEEE Second International Conference on Control, Measurement and Instrumentation (CMI), India.
 15. Zulfatmann, M.F. Rahmat, "Application of Self-Tuning Fuzzy PID Controller on Industrial Hydraulic Actuator using System Identification Approach", "Int. Journal on Smart Sensing and Intelligent Systems, vol.2, No. 2, June 2009, pp. 246-261, 2009.
 16. Jana Paulus ova, Lukáš Orlický, Mária Dúbravská, "Self-Tuning Fuzzy PID Controller", 2013 International IEEE Conference on Process Control (PC), June 18–21, 2013, Štrbské Pleso, Slovakia.
 17. Indranil Pan and Saptarshi Das, "Intelligent Fractional Order Systems and Control", Department of Power Engineering Jadavpur University, West Bengal, India, Book Published on 23rd August 2012.
 18. N. Kanagaraj, Mujahed Al-Dhaifalla, "Design of Intelligent Fuzzy Fractional -Order PID Controller for Pressure Control Application", 2017 International Conference on Intelligent Computing, Instrumentation and Control Technologies (ICICT), 978-1-5090-6106-8/17/IEEE.
 19. Prasanta Roy, Binoy Krishna Roy, "Fractional order PI control applied to level control in coupled two tank MIMO system with experimental validation", Control Engineering Practice (2016).
 20. Reza Rouhi Ardeshiri, Hoda Nikkhah Kashani, Atikeh Reza-Ahrabi, "Design and simulation of self-tuning fractional order fuzzy PID controller for robotic manipulator", International Journal of Automation and Control, 2019 Vol.13 No.5, pp.595 – 618.
 21. D. S. Bhandare and N. R. Kulkarni, "Performances evaluation and comparison of PID controller and fuzzy logic controller for process liquid level control," 2015 15th International Conference on Control, Automation and Systems (ICCAS), 2015, pp. 1347-1352, doi: 10.1109/ICCAS.2015.7364848
 22. Bhandare, D.S., Kulkarni, N.R. & Bakshi, M.V., "An intelligent self-tuning fuzzy-PID controller to coupled tank liquid level system", Int. j. inf. tecnol. 14, 1747–1754 (Sep 2022). <https://doi.org/10.1007/s41870-021-00810-y>.
- [23] Bhandare, D.S., Kulkarni, N.R. Copyright Registered for work, "Intelligent Fractional Order PID Controller for SISO Liquid Level Control System," Government of India, 24th Dec 2021.

Automated Crop Monitoring and Surveillance Device using Remote Sensing and Deep Learning Techniques

Deepa S. Bhandare, Shayan Chakraborty

Yash Kshirsagar, Avinash More

Tanishq Shelke

Department of Electrical Engineering

Savitribai Phule University Pune

Progressive Education Society's Modern Coll. of Engg,

Pune, Maharashtra

✉ dr.deepasbhandare@gmail.com

Atharva Baramkar

Department of Mechanical Engineering

Savitribai Phule University Pune

Progressive Education Society's Modern Coll. of Engg.

Pune, Maharashtra

ABSTRACT

Crop-related issues and unfavourable growth patterns pose significant challenges to the sustainability and profitability of agricultural operations. Ensuring the timely monitoring of crop health and growth conditions is crucial for the efficient functioning of farm activities. Spectral Vegetation Indices (VIs), a method of effectively reducing dimensions using a limited number of bands, have rapidly emerged as a powerful tool for assessing foliage health. This approach proves highly beneficial in accurately identifying the precise state of crop conditions. However, the variability in planting times, operational practices, and other factors influencing crop growth leads to diverse VIs situations in different fields. Consequently, there are no universal thresholds applicable to all fields.

The Automated Crop Monitoring and Surveillance Device, specifically a handheld module, represents a scaled-down prototype module. Its primary focus lies in utilizing remote sensing and factory phenotyping to detect both internal and external crop health. This innovative device addresses the challenges posed by dynamic crop conditions, offering a comprehensive solution for effective agricultural monitoring.

KEYWORDS : NDVI, SI-NDVI, Phenotyping, Spectral VIs, Automated crop monitoring and surveillance device, Remote sensing, Deep learning.

INTRODUCTION

Complaints related to crops and unfavorable growth rates stand out as significant factors undermining the sustainability and profitability of agricultural operations. Therefore, it is crucial to monitor crop health and growth conditions promptly for the efficient functioning of agricultural field operations [1-3]. Obtaining timely data on the status of crops across extensive areas is essential to implement precautionary measures that enhance both yield and quality. The use of remote sensing and factory phenotyping enables the rapid and large-scale monitoring of crop issues, offering a solution that is timely, user-friendly, comprehensive, non-destructive, and efficient [4- 6]. The application of remote sensing and factory phenotyping has proven effective in assessing various conditions in crops,

contributing to the mitigation and management of crop-related challenges [7-10]. Crop complaints, including infections, significantly impact the profitability and sustainability of agricultural operations, underscoring the importance of timely monitoring of plant health conditions in the field [11-13]. As an example, cotton, a major crop, is highly susceptible to cotton root spoilage caused by the fungus *Phymatotrichopsis omnivora*. Early symptoms include leaves turning discoloured and orange before transitioning to dark brown, ultimately leading to dry leaves attached to the affected plants [15-17]. Timely acquisition of data on cotton-related complaints over large areas is crucial for implementing preventive measures to enhance cotton yield and quality. Remote sensing emerges as a valuable tool for swiftly monitoring crop complaints on a large

scale, offering advantages such as timeliness, user-friendliness, comprehensiveness, non-destructiveness, and efficiency. The versatility of remote sensing extends to its application in the assessment of diverse conditions across various crops [18-20]. This paper explores the utilization of remote sensing technology, specifically the Normalized Difference Vegetation Index (NDVI). The indicator has been suitable to attract hydrologists also, due to its implicit regard for spatiotemporal land cover changes in the model parameterization of downfall-runoff models. In all these fields, the usual running of NDVI is in the form of charts and statistics uprooted by carrying out Civilian operations on ever-tasted data. Conceptually, in the line of the hypsometric wind, a wind can be drawn using gridded NDVI data to represent the distribution of the indicator values across any bounded area similar to a hydrological catchment, a lowland zone, or an executive unit. The use and eventuality of endviometric angles are demonstrated by drawing similar angles from NDVI values deduced for different geographical units. The results show that piecemeal from being a handy way to cover vegetational changes, the endviometric wind can give perceptivity into numerous aspects of an ecosystem and complement the being styles of covering inter-annual and intra-year changes [21-22]. Now the main problem faced while enforcing NDVI is that it gives crimes if there are slight changes in the foliage. To avoid this problem we're going to use SI-NDVI (Single Image Normalised Difference Vegetation Index). Using this NDVI can be used at its full eventuality and can give the result of a single image of a single factory at a time. This system also reduces the threat of crimes and can determine the wholesomeness of the factory according to the bandwidth determined. The indicator has been suitable to attract hydrologists also, due to its implicit regard for spatiotemporal land cover changes in the model parameterization of downfall-runoff models. In all these fields, the usual running of NDVI is in the form of charts and statistics uprooted [23]. The analysis of Normalized Difference Vegetation Index (NDVI) involves comparing a segment of the visible light spectrum with the Near-Infrared (NIR) spectrum. In the case of Single Image NDVI (SI-NDVI), the normalization portion of the visible light spectrum is represented by blue light reflectance, in contrast to red light reflectance. Additionally, the binary bandpass filter

allows the NIR to be recorded by the red channel of the CMOS detector [3]. This modification facilitates SI-NDVI analysis using only a single image, eliminating the need for the technically complex process of optical alignment [11-13]. Implementing the SI-NDVI imaging system enables the early detection of stress in plants while maintaining cost-effectiveness and user-friendliness. The cost-effectiveness is attributed, in part, to the availability of open-source computer software essential for SI-NDVI analysis. SI-NDVI analysis permits both quantitative and qualitative assessments of plant health in controlled environments, making it a practical approach [14-16]. Our design focuses on attacking the problem of late identification of crop conditions and better understanding crop growth rate characteristics. The handheld module is a gauged-down prototype module that majorly focuses on detecting the internal and external health of crops using remote sensing and factory phenotyping. The vision is to prop in minimizing losses due to undetected plant conditions and behavioural changes. Advanced technologies analogous to remote sensing and artificial intelligence can help in the early discovery of plant conditions [3-8].

CONCEPT OF HARDWARE DESIGN

The handheld module is a compatible module which is easy to carry and compatible with multiple functionalities and farming equipment. The module is made up of poly PLV material which is sturdy and light in weight and the overall handheld module has a weight around (1.2 - 1.5) kg. There is a range of Depth sensors i.e YDLIDAR OS30a and an RGB webcam Logitech c720 which are the main sensors for the plant phenotyping and remote sensing methodologies. A range of DHT22, MQ135 and TFminS Laser sensors for Temperature, Humidity, Air Quality and Distance are being used. These sensors are operated by Raspberry Pi 4B microcontroller using 2 power banks of 10,000 mAh rating.

The figure 1 shows the schematic representation of the handheld device which is being designed for the scanning of plants with accurate camera precision. The model is made with pla fiber material which is sturdy and rigid for use, the maximum weight of the module with the sensors goes around (1.2 - 1.5) kg. The YDlidar Os30a Depth Camera is a future reference camera that will be used for further analysis of 3d characteristics

and remote sensing more precisely. The device is designed in such a manner that it can be future attached to various farming equipment without hampering any farming activities with more monitoring exposure.

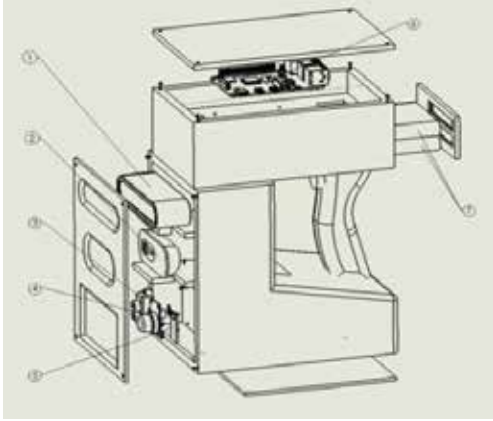


Fig. 1 Schematic Design of Automated Crop Surveillance and Monitoring Device Prototype YDlidar Os30a Depth Camera (1), Logitech c720 Webcam (2), TFminS Laser Sensor (3), MQ135 (4), DHT22 (5), Raspberry pi 4b (6), 10.000mah x2 power banks (7)

The design schematic diagram (PCB) represents the internal systems with all the sensors connected to the IMU as shown in figure 2. The IMU present in the system is Raspberry pi 4b 8GB (6) with 4 sensors connected via the GPIO pins in the Raspberry pi (6). The Raspberry pi (6) receives power from the power bank (6) connected via the USB 3.0 port provided in the IMU, the powerbank (7) has a rating of 10,000 mAh with 9V and 2A. The DHT22 (5) sensor is connected via the digital GPIO, GND and Supply pin from Raspberry pi (6) headers also the MQ135 (4) and TFminS (3) has the same pin connection configuration from the Raspberry pi (6). The supply for these sensors are between (3.3 - 5) V and all require a digital pin for operation. The camera (2) module is connected via the USB 3.0 for fast data transfer and operation, here the camera (2) captures the image at a resolution of 1980x720 through which the input data is received to be processed using the algorithms in the system. The sensor on other hand collects analog data which is converted by the function of ADC (analog to digital converter) and then feeds the data through the digital GPIO pins of the Raspberry pi (6) which shows the overall results and accuracy to the user.

Table. 1 Component List

Components	Quantity
Raspberry Pi 4B 8GB	1
Logitech C720 Webcam	1
DHT22	1
TS miniS Laser Sensor	1
MQ135 Gas Sensor	1
Power Bank 10,000mah	2

SCHEMATIC OF PCB

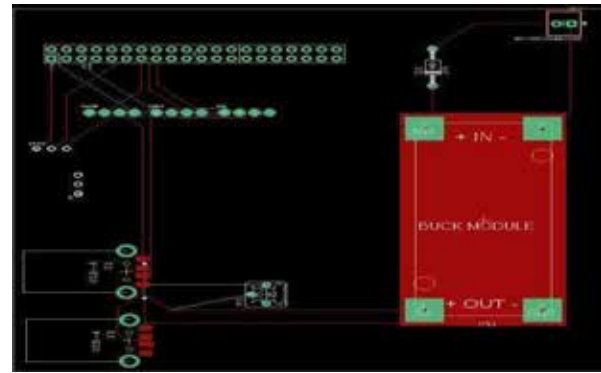


Fig. 2 . Schematic Design of PCB

The above figure 2 is the schematic diagram of the PCB made using the eagle software. The zero PCB consists of a buck converter for converting the required voltage needed for the sensors and the IMU. It also consists of 40 pin headers of the raspberry pi along with the headers of other sensors, the power supply is received via USB-A and the voltage is adjusted using a potentiometer in a zero PCB.

The design schematic diagram (PCB) represents the internal systems with all the sensors connected to the IMU as shown in figure 2. The IMU present in the system is Raspberry pi 4b 8GB (6) with 4 sensors connected via the GPIO pins in the Raspberry pi (6). The Raspberry pi (6) receives power from the power bank (6) connected via the USB 3.0 port provided in the IMU, the powerbank (7) has a rating of 10,000 mAh with 9V and 2A. The DHT22 (5) sensor is connected via the digital GPIO, GND and Supply pin from Raspberry pi (6) headers also the MQ135 (4) and TFminS (3) has the same pin connection configuration from the Raspberry pi (6). The supply for these sensors are between (3.3 - 5) V and all require a digital pin for operation. The

camera (2) module is connected via the USB 3.0 for fast data transfer and operation, here the camera (2) captures the image at a resolution of 1980x720 through which the input data is received to be processed using the algorithms in the system. The sensor on other hand collects analog data which is converted by the function of ADC (analog to digital converter) and then feeds the data through the digital GPIO pins of the Raspberry pi (6) which shows the overall results and accuracy to the user.

All paragraphs must be indented. All paragraphs must be justified, i.e. both left-justified and right-justified.

SOFTWARE

The software stack is operated by the Raspbian OS as the main body in which the base language is python and C++ with open source packages like opencv, open3d, convolutional neural networks and software like solidworks for module construction in 3D, makesense.ai for annotations of disease of plants, vnc viewer for remote desktop setup of Raspberry Pi and Jupyter notebook for validations of result analysis.

METHODOLOGY

Analysing pictures to identify crop issues helps estimate how widespread the problem is, but it doesn't effectively measure how serious or how the problems are developing. This research introduces a system to grade the seriousness of crop issues. This is important for better understanding and dealing with agricultural problems and pests. Right now, the way we assess these issues involves checking the ground manually, which works well in some cases but is challenging to apply on a larger scale.

Consequently, there is a significant demand for a universal system for crop complaint assessment, independent of ground checks, to fully leverage remote sensing in extensive area monitoring—this is the primary objective of the proposed design [21]. With the implementation of this automated system, the need for ground checks is minimized in numerous scenarios. If further refinement is desired, ground remote sensing and factory phenotyping results can be integrated to optimize the parameters of the automated complaint severity grading model. Another practical application of the methodology is the selection of fields based on

Vegetation Indices (VIs) for targeted analysis by trained individuals. Spectral VIs, an efficient dimension-reduction technique utilizing a limited number of bands, play a crucial role in detecting the severity status of crop conditions. Due to factors such as planting time, operational practices, and variable crop growth conditions, different fields exhibit diverse VI situations, and there are typically no universal thresholds for all fields [21]. Therefore, a unified threshold segmentation cannot be universally applied to brackets. The manifestation of symptoms in cotton plants due to complaint infection is a complex phenomenon influenced by factors such as cultivar type, prevailing rainfall, and soil conditions.

Hence, it is crucial to consider local field conditions and operational practices before grading crop complaints in diverse fields [23]. Additionally, substantial variations in the ranges of VIs make direct comparisons challenging. Normalization, a commonly used statistical method, proves effective in mitigating the influences of optical geometrics, terrain, and other variables. Factory phenotyping can contribute valuable data on morphology and factory parameters, including splint indicator, factory structure, factory height, biomass viscosity, and nutrient contents [16]. The figure 3 shows the overall methodology of the process proposed in this paper.

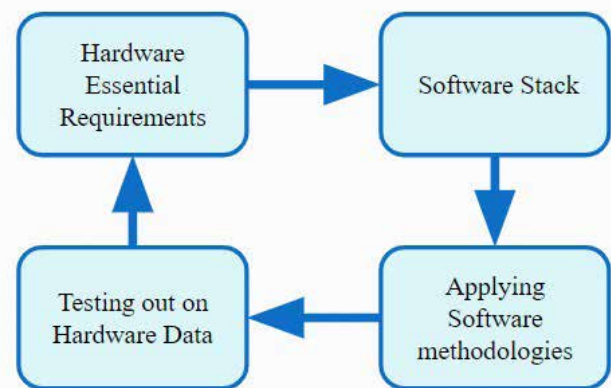


Fig. 3 Block Diagram of the Methodology

WHAT IS NDVI ?

The figure 4 shows the definition of NDVI using a splint. This is really useful for measuring the health of plants. However, it'll reflect a lot of near infrared light,

If a factory is healthy. However, it'll absorb a lot of near infrared light, If a factory is dying. The blue-green colour in the print means further infrared light is being reflected. Look at this image of leaves reflecting light.

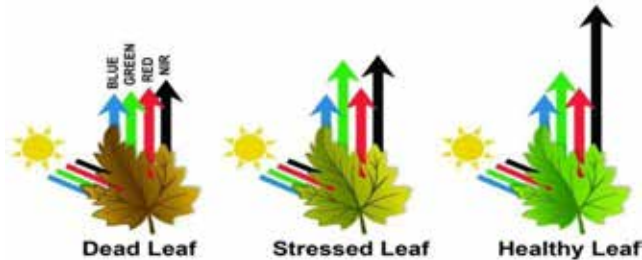


Fig. 4 NDVI Analysis on Leaf

It can be seen that infrared light is reflected more from healthy leaves than stressed or dead leaves [23]. In general, NDVI is calculated as follows

$$NDVI = \frac{(NIR - RED)}{(NIR + RED)}$$

where NIR stands for Near Infrared and the formula focuses on NIR with the Red band in the spectrum for appropriate results.

MASKED R-CNN

In the realm of Deep Learning, there are fundamental models known as Deep Feedforward models, with data flowing one way through neurons. Various algorithms, such as Back-Propagation, Convolutional Neural Network (CNN), Recurrent Neural Network (RNN), including Long Short-Term Memory (LSTM) and Gated Recurrent Units (GRU), Auto-Encoder (AE), Deep Belief Network (DBN), Generative Adversarial Network (GAN), and Deep Reinforcement Learning (DRL), play significant roles. Notably, Convolutional Neural Networks (CNNs) excel in training ease and generalization, particularly in image pattern recognition. A recent and comprehensive approach, Object Instance Segmentation, combines object detection and semantic segmentation, proving valuable in scenarios like damage detection or determining the position of cars in self-driving cars. Mask R-CNN, a state-of-the-art instance segmentation model, is built on Faster R-CNN, which involves a two-stage process using a backbone network (ResNet, VGG, Inception) and a region proposal network. This approach efficiently addresses real-life

problems, such as generating building footprints in GIS applications. The process consists of two networks, backbone ResNet and region proposal network. These networks run once per image to give a set of region proposals. Region proposals are regions in the feature map that contain the object.

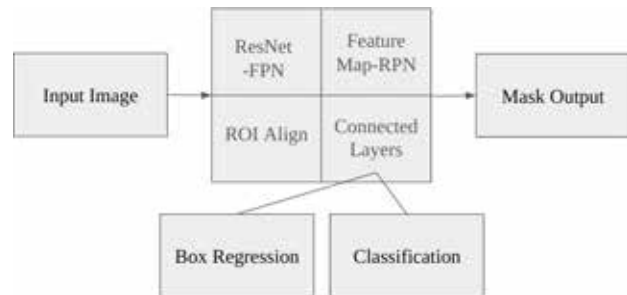


Fig. 5 Flow Chart of Mask R-CNN

RESULTS AND DISCUSSIONS

The system contains an IMU raspberry pi 4b 8 GB module for the internal process and functional brain of the design. Some of the important detectors to carry out the functionality of complaint discovery, stress analysis and remote seeing are combined with raspberry pi to ensure a better affair of the process. The detectors used are DHT22, MQ135, TFminiS and Logitech c720 webcam, the DHT22 detector is used to estimate the temperature and moisture of the girding area and the MQ135 detector shows the air quality of the girding area. TFminS is a time of flight ray scanner which is used to calculate distance from the reference point and is used for height estimation of the crop. Logitech c720 webcam is used to capture images as an input to the complaint discovery and remote seeing algorithms. The complaint discovery algorithm is grounded on a fashion called Mask R-CNN which is a convolutional neural network and works in the system of immediate segmentation with a delicacy of about 85 - 90 percent using Resnet as an activation subcaste. While the remote sensing system used is called NDVI (Normalised Difference Vegetation Index) which calculates the collaborative visible diapason i.e RGB and the Near Infrared values and recycling the affair using the following expression $(VIS - NIR) / (VIS + NIR)$. This value lies in between the range of -1 to +1 where -1 indicates the dead or inorganic region, -0.3 to 0.5 indicates some internal changes or stress, 0.66 and above indicates the healthy region of the factory. The proposed design combines all these methodologies

in a single compact handheld module made with PLA fiber material with a weight of 1.3-1.5 kg. The whole system is powered by 2 power banks of the standing of 10,000 mAh and affair voltage of 9V and 2A current which provides a power back up of 3 hrs and further on operation of the device.

1. During software testing traditional deep learning algorithms will have a low impact on this system as high-end algorithms need more computation power to run.
2. An external power supply will be needed for all the sensors to run as Raspberry Pi has only 2 pins of 5V and it would make the Pi system overloaded if all the power is being drained for the sensors through the Pi.
3. Manual testing of all the sensors should be done and observations to be made of their input and output type and applying logic to automate the whole system.

Module design code of functions needs to be designed as the running algorithm for this project which makes the code faster and consumes less computational power compared to traditional deep learning algorithms.



Fig. 6 Masked R-CNN results (in Google Colab)

Figure 6 is a snippet from Google Colab. Google Colab is a widely used cloud-based platform in the field of machine learning.

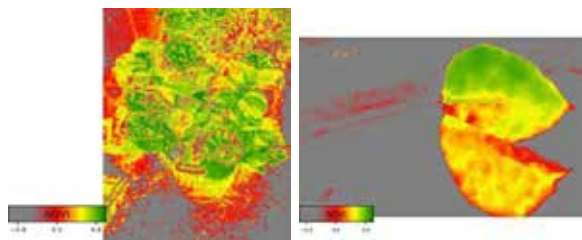


Fig. 7 NDVI Results

This figure 7 is the output generated from NDVI algorithm. The dead or Inorganic part in the image is represented with gray colour while the healthy part is shown by the green colour, the yellow colour shows the stressed part in the plant that means some internal changes are occurring the plant.

To check the accuracy and get the assurance of the algorithm the diseased leaves were tested in the NDVI algorithm and the results can be seen the diseased part of the leaves was shown with a yellow and red color while the inorganic part which is the background is shown by the gray color. The small scale at the left bottom corner is given for reference which has a number scale from -0.8 to

0.8. Mask R- CNN is a convolutional neural network and works in the system with instantaneous segmentation with an accuracy of about 85-90% using Resnet as an activation layer in the network. Below table 2 shows the other tested algorithms and the accuracy checked along with Mask R- CNN. The DHT22 and MQ135 sensors had an error range of +5% to -5% while testing which provided good results as compared to other sensors in the same price range.

Table. 2 Comparisons of Different Algorithms

Algorithm	Training data Size (images)	Accuracy (%)
Mask R-CNN	550	93.80
NDVI	Generalised	79.85
Yolo v5	410	81.40
Yolo v7	410	88.50
CNN	420	85.20

CONCLUSION

Many other Remote sensing methods can be utilized to make the result more dynamic and efficient for tracking crop monitoring and growth rate. A crop disease grading methodology, encompassing distinct stages such as crop classification, normalization of Vegetation Indices (VIs), and disease grading. NIR wavelengths, devoid of shortwave infrared bands, may exhibit increased reflectance in the shortwave infrared region when crops are infected by diseases or pests, resulting in water

stress symptoms. Consequently, for enhanced outcomes in future research, exploring VIs that incorporate shortwave infrared bands is advisable.

FUTURE SCOPE

Perpetration of real depth camera detectors for illustration intel real depth cameras can be used to capture different raw band images along with point cloud data to make the results more accurate and dynamic [8]. Automated devices like drones, e-bots, etc can increase the operation range and feasibility. Setting up of IOT-cloud-based infrastructure for more accessibility for data sharing and projection on modern user interfaces.

REFERENCES

1. Yan Guo, Jin Zhang, Chengxin Yin, Xiaonan Hu, Yu Zou, Zhipeng Xue, Wei Wang, Plant Disease Identification Based on Deep Learning Algorithms in Smart Farming, 1st ed. Hindawi: Research Article, 2020.
2. Prashanth.M, Dr. K. G Padmasine, Plant Disease Detection Using NDVI and Raspberry Pi. International Journal of Research in Education and Sciences Journal-2022.
3. Seoung Wug Oh, Michael S.Brown, Marc Pollefeys, Seon Joo Kim, Do It Yourself HyperSpectral Imaging with Everyday Digital Cameras. IEEE Conference-2016.
4. Hengqian Zhao, Chenghai Yang, Wei Guo, Dongyan Zhang, "Automatic Estimation of Crop Disease Severity Levels Based on Vegetation Index Normalisation". MDPI: Research Article- 2020.
5. Akshay Krishnan, Shashank Swarna, Balasubramanya, Robotics, IoT, and AI in the Automation of Agricultural Industry. IEEE: Conference Paper-2020.
6. Shashank Chaudhary, Upendra Kumar, Abhishek Pandey, A Review: Crop Plant Disease Detection Using Image Processing, Volume-8 Issue-7. Ijitee: May 2019.
7. Puranik, V., Sharmila, Ranjan, A., & Kumari, Automation in Agriculture and IoT, 4th ed. International Conference on Internet of Things: Smart Innovation and Usages 2019.
8. Chien, H.-Y., Tseng, Y.-M., & Hung, R.W, Some Study of Applying Infra-Red in Agriculture IoT, 9th. International Conference on Awareness Science and Technology: May 2018.
9. Khetkeere, S, Infrared Normalised Difference Vegetation Index for Sentinel-2A Imagery, 17th ed. International Conference on Electrical/Electronics, Computer, Telecommunications and Information Technology: April 2020.
10. Feng Zhang, Bingfang Wu, & Chenglin Liu. (n.d.), Using time series of SPOT VGT NDVI for crop yield forecasting, 2003 IEEE International Geoscience and Remote Sensing Symposium. Proceedings. IGARSS: May 2013.
11. Franke, J., Heinzl, V., & Menz, G, Assessment of NDVI Differences Caused by Sensor Specific Relative Spectral Response Functions, International Symposium on Geoscience and Remote Sensing. IEEE: 2016.
12. Jeevalakshmi, D., Reddy, S. N., & Manikiam, B, Land cover classification based on NDVI using LANDSAT8 time series: A case study in the Tirupati region, case study. International Conference on Communication and Signal Processing (ICCSP): 2016.
13. Rhif, M., Abbes, A. B., Martinez, B., & Farah, I. R, Deep Learning Models Performance For NDVI Time Series Prediction: A Case Study On North West Tunisia, Journal. Mediterranean and Middle-East Geoscience and Remote Sensing Symposium (M2GARSS): 2020.
14. Hyndavi, A., James, L., Anjaneyulu, R. V. G., Suresh, S, Venkateswara Rao, C., & Bothale, V. M, Evolution of value addition process for generation of Normalised Difference Vegetation Index (NDVI) product – A case study, Recent Advances in Geoscience and Remote Sensing : Technologies, Standards and Applications. IEEE (TENGARSS): 2019.
15. Razali, S. M., & Nuruddin, A. A, Assessment of water content using remote sensing Normalised Difference Water Index: Preliminary study, Proceedings of the International Conference on Space Science and Communication. IEEE (IconSpace): April 2011.
16. Somayajula, V. K. A., Ghai, D., & Kumar, S, Land Use/ Land Cover Change Analysis using NDVI, PCA, 5th International Conference on Computing Methodologies and Communication. ICCMC: 2021.
17. Li, X., Ge, L., Cholathat, R., & Hu, Z, Innovative NDVI time-series analysis based on multispectral images for detecting small scale vegetation cover change, International Geoscience and Remote Sensing Symposium. IEEE (IGARSS): 2013.
18. Juanjuan Jing, Liangyun Liu, Jihua Wang, Jindi Wang, & Chunjiang Zhao, (n.d.), Uncertainty analysis for NDVI using the physical models, IEEE International

- IEEE Geoscience and Remote Sensing Symposium. IEEE IGARSS Proceedings: 2014.
19. Li, Y., Jiao, Z., Zhang, X., Zhang, H., & Dong, Y, Research about the bidirectional NDVI based on kernel-driven models, International Geoscience and Remote Sensing Symposium. IEEE (IGARSS): 2015.
 20. Huang, J., Wang, H., Dai, Q., & Han, D, Analysis of NDVI Data for Crop Identification and Yield Estimation, Journal. IEEE Journal of Selected Topics in Applied Earth Observations and Remote Sensing: May 2017.
 21. Daroya, R., & Ramos, M, NDVI image extraction of agricultural land using an autonomous quadcopter with a filter-modified camera, International Conference on Control System, Computing and Engineering. IEEE 7th (ICCSCE): 2017.
 22. Ben Abbes, A., Essid, H., Farah, I. R., & Barra, V, Rare events detection in NDVI time-series using Jarque-Bera test, International Geoscience and Remote Sensing Symposium. IEEE (IGARSS): 2015
 23. Liu, R, Compositing the Minimum NDVI for MODIS Data, Transactions on Geoscience and Remote Sensing. IEEE:May 2017.
 24. S. S. Sannakki and V. S. Rajpurohit, Classification of Pomegranate Diseases Based on Back Propagation Neural Network, Vol 2 Issue: 02. IRJET: May-2015.
 25. Srdjan Sladojevic, Marko Arsenovic, Andras Andela, Dubravko Culibrk

Impact of Inverter Interfaced Distributed Generation on Distance Protection

Gajanan S. Sarode

Department of Electrical Engineering
K. K. Wagh Institute of Engg. Education & Research
Nashik, Maharashtra
✉ gajusarode28@gmail.com

M. V. Bhatkar

Department of Electrical Engineering
Jawahar Education Society's Institute of Technology
Management and Research
Nashik, Maharashtra

ABSTRACT

The high penetration of distributed generation or renewable energy resources leads to many challenges to conventional protection relaying. The conventional protection system designed based on fault response of synchronous generator. The fault current characteristics of Inverter Interfaced Distributed Generation (IIDG) differ from those of traditional synchronous machine-based generation. The non-conventional fault characteristics of IIDG have negative impact on conventional protection system. Mainly, distance protection of tie lines connecting IIDG to main grid has negative impact in presence of IIDG. The objective of this work is to summarize the operational challenges of distance protection in presence of IIDG reported in various literatures. Also, the impact on distance protection in presence of Inverter based resources analyzed using ETAP.

KEYWORDS : *Inverter interfaced distributed generation, Distance protection, Distributed generation, Renewable energy resources, Protection challenges, Inverter based resources.*

INTRODUCTION

Renewable energy technology has emerged as a promising alternative to conventional fossil fuel-based power plants, with governments worldwide promoting its use to reduce CO₂ consumption and combat climate change. Solar and wind generation are the most common renewable sources, and their integration into power systems varies depending on the size of the plant [1]. However, the integration of renewable energy sources in power grids presents challenges in power system protection, particularly with Inverter Interfaced Distributed Generation (IIDG) systems like solar power plants and wind type-IV and III generation [2]. These systems have significantly different fault response compared to conventional synchronous machine-based generators.

Large-scale, centralized wind farms and solar facilities are being installed all over the world due to advancements in power electronics technology. In order to transfer huge quantities of power from windy or light-rich locations to the load centers, large-scale renewable energy sources are typically connected to

the power grid using high-voltage transmission lines. Therefore, requirements for the dependable and secure protection schemes in the event of a transmission line fault are becoming even more stringent.

Distance protection is extensively used for protection of EHV power transmission lines since, for the traditional ac grid dominated by synchronous generator, as the power system fault characteristic have little impact on the operation of the distance protection.

However, the fault characteristics of Inverter Interfaced distributed generation (IIDG) are significantly different from the synchronous based generation. The fault current magnitude is limited up-to 1 to 1.5pu by IIDG control system to protect semiconductor devices and phase angle of fault current is based on host grid code requirement [3]. Therefore, due to different fault characteristics of IIDG, the distance protection used for protection of transmission lines connecting IIDG to high voltage network may mal-operates. Also, the operation of distance protection in grid dominated by Inverter Based Resources (IBR) get negatively affected [3]

Integration of IIDG in transmission network poses several challenges for distance protection [4]. The mis-operation of distance protection in presence of IIDG investigated in several work [3], [5], [6]. In [2], author discussed the operating principle of the transmission lines protection and the challenges introduced due to integration of IIDG and some possible solutions proposed by several authors. In [7], the impact on distance relay due to rate of rise of reactive power injected by IIDG during fault is analyzed. The performance of distance protection in presence of IIDG is also depends upon various factor like plant size, host grid code requirement, remote grid.

The objective this article is to summarize impact on distance protection due to integration of IIDG into transmission network, as step toward development of solution by providing improved understanding on performance of relay in presence of IIDG. This article study performance of distance relay in presence IIDG using ETAP.

This paper is organized as follow: Section II discusses the control scheme and fault characteristic of IIDG. Section III discussed the operating principle of distance protection and impact on distance protection due integration of IIDG. Section IV study performance of distance protection using ETAP and Section V conclude the work.

FAULT CHARACTERISTICS OF INVERTER INTERFACED DISTRIBUTED GENERATION

In Inverter Integrated Distributed Generation (IIDG), the fault current characteristics are different from conventional synchronous machine-based generation. The controller of inverters limits the fault current supplied by IIDG typically upto 1.2 to 2 times of rated current. The controller of inverter modulates the voltage and current signal. The phase angle of fault current contributed by IIDG may be significantly different than phase angle of fault current contributed by conventional generator and depend upon grid code requirement [8], [9]

Basically, response of Inverter based resources differs in following aspects as compared to conventional synchronous machine generator [9],

- i) Fault current is limited by IIDG control system
- ii) Fault current phase angle and characteristic depend upon host grid code
- iii) Most of IIDG supply no negative sequence component even case of unbalance fault
- iv) Zero sequence component of current depends upon the transformer connection.

The fault characteristics of IIDG's are depends on host grid [8]. The North American Grid code allows fault ride through at unit power factor, however, the European grid code demands dynamic reactive power support during fault. Recent modification in some grid code demand negative sequence current injection during fault.

The host grid code give requirement in terms of Fault ride through (FRT) or Low voltage ride through (LVRT), Reactive power support and negative sequence current injection.

Fault Ride Through Requirement

In recent years, the share on renewable distributed generation increased considerably in total power generation in grid. Therefore, recent grid code demands the distributed energy resources to be remain connected to grid during fault or low voltage condition for specific period. It is also called as Fault Ride Through (FRT) or Low Voltage Ride through requirement.

The fault ride through requirement specified through Voltage Vs Time curve. The fault ride through requirement in Indian Grid code is as shown in Fig 1. As long as the operating point above the curve shown in Fig .1, the plant must not get disconnected from grid.

Reactive Power Support [9]

In contrast to traditional SM-based sources, the Inverter control system regulates the fault current angle of the Inverter. In order to improve the voltage stability of the system, certain transmission grid regulations specify standards for the power factor (PF) of renewable energy plants during faults in addition to the fault ride-through capabilities. European grid codes typically requires reactive power support during fault as shown in Fig. 2.

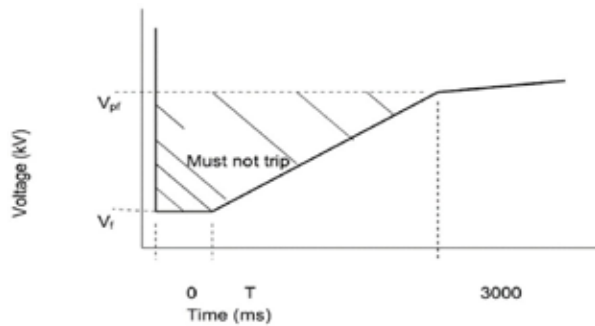


Figure: Fault ride through characteristics

Where,
 $V_f = 15\%$ of Nominal System voltage
 $V_{pr} =$ Minimum voltages (80% of Nominal System Voltage)

Fig. 1 Fault Ride through requirement of Indian Grid Code [10]

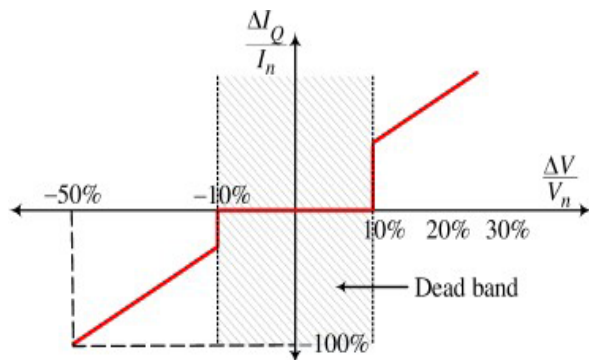


Fig. 2 Reactive current Vs Voltage for renewable plant in European Grid code[9]

However, Indian grid codes allows the fault ride through (FRT) at unity power factor even during fault.

Apart from host grid code requirement, IIDG have their own internal protection to ensure safety of semiconductor devices against large over current during fault condition. Typically, the inverter controller limits the current upto 1.2 to 2 times of rated current

Negative Sequence Current Injection [8]

In case of asymmetrical fault, the system voltage becomes unbalance. However, even during unbalance fault the IIDG injects only positive sequence current into grid, therefore, the negative sequence current and zero sequence current are absent. The voltage profile during fault and many protective functions are negatively impacted when there is no negative sequence current. Therefore, recent modification in European grid code demands dynamic negative sequence current injection

during asymmetrical faults. Indian grid code does not pose any negative sequence current requirement during asymmetrical fault.

IMPACT OF IIDG ON DISTANCE PROTECTION

Principle of Distance protection

The distance protection is one of main protection used for protection of high voltage transmission line. If the impedance of transmission line seen by relay is within the set impedance of line, the distance protection trips the associated circuit breaker to isolate the faulty section of line.



Fig. 3 Basic principle of distance protection

In Fig.3 , Distance relay R calculate the impedance of line between Bus A and Bus B using current (IA) and voltage with (UA) at Bus A.

$$Z_F = \frac{U_A}{I_A}$$

The measured impedance of line is compared with set impedance of line configured in relay. If the measured impedance is less than set impedance, then trip command issued to circuit breaker associated with line to isolate the faulty section.

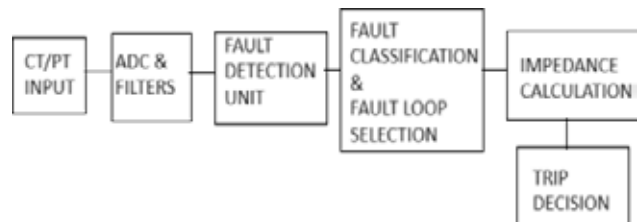


Fig. 4: Block diagram of distance relay

The fault detection unit detect the fault condition. The fault detection or starter element operates on current threshold or sequence current threshold or impedance threshold. If selected quantity cross the threshold settings , then the fault is detected. Following fault detection, the fault classification unit is used to identify the kind of fault among AG, BG, CG, ABG, BCG, CAB, AB, BC,

CA, ABC, and ABC-G. The relevant impedance loop is chosen for the apparent impedance calculation after the fault type has determined. Final trip decision taken based on apparent impedance calculation for particular fault type[11].

For protection of transmission line against all type of faults, the distance protection has six fault loop impedance measurement unit for each zone to cover different type of faults. The input given to each impedance measuring unit for particular fault type is such that, the distance relay calculate the apparent impedance of line. [12]

$$Z_{app} = \frac{V_{rM}}{I_{rM}} = x Z_{1L} + \left(\frac{I_f}{I_{rM}}\right) R_f = Z_{MF} + \Delta Z$$

Where, VrM and IrM are the operating voltage and current for the relay. Rf is the fault resistance, Zapp is impedance seen by relay

Due to fault resistance, the impedance seen by relay is summation of impedance of line upto fault point and additional impedance term ΔZ due to fault resistance

The Table 1 provides the VrM , IrM and IF for different fault type.

Table 1: Distance Relay Operating measurement and faulted loop current for different fault types [12]

Where, K0 is the zero sequence compensation factor, I0 zero sequence fault current

Fault	Vr	Ir	IF
AG	VAG	IA+ K0L I0	IAF
BG	VBG	IB+ K0L I0	IBF
CG	VCG	IC+ K0L I0	ICF
ABG	VAB	IA-IB	IAF-IBF
BCG	VBC	IB-IC	IBF-ICF
CAG	VCA	IC-IA	ICF-IAF
ABC	VAG	IA	I1F

Impact on Distance Protection in presence of IIDG

The fault current characteristic of IIDG is different than conventional synchronous based generation network. The fault current supplied by IIDG have following characteristics,

1. The current controller action of IIDG limits the fault current upto 1 to 1.5 pu of rating of inverter
2. The angle between fault current and voltage is dependent on host grid code requirement. Some grid codes demand reactive power support during fault conditions.
3. The rate of rise of reactive current supplied by IIDG is depend upon inverter control system response time [9]
4. Lack of negative sequence current (I2). However, latest modification in European grid code demands the negative sequence current injection during asymmetrical fault.[8]
5. Absence of zero sequence component in fault current supplied by IIDG. Therefore, the zero sequence current in fault loop mainly govern by the transformer grounding at point of coupling[13]

The all above mentioned characteristic of IIDG causes severe negative impact on operation of distance protection. As reported in various literatures in references, the various functions like fault detection unit, impedance calculation, power swing blocking, Zone 2 operation with interfeed, may mal-operate in presence of IIDG.

Various challenges reported in various literatures are as follow

Over reach or Under reach of distance protection of line connected to IIDG [3], [12]

The transmission line that connects to a solar plant is shown in Fig.5 Each solar photovoltaic unit in the solar plant is connected to the collector bus via a step-up transformer and a DC/AC inverter.

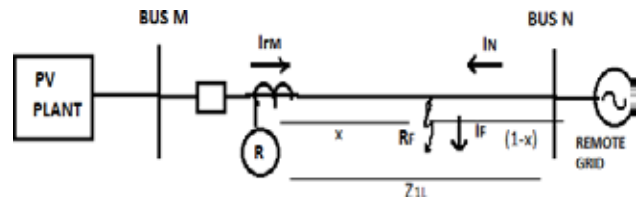


Fig. 5 : Transmission line connected to Solar based IIDG. ZL is the impedance of line MN and a fault is assumed at a distance of x pu from bus M with a fault resistance, RF

Apparent impedance (Z_{app}) calculated by the distance relay at bus M (RM) for the situation is given by [12].

$$Z_{app} = \frac{V_{rM}}{I_{rM}} = x Z_{1L} + \left(\frac{I_F}{I_{rM}} \right) R_f = Z_{MF} + \Delta Z \quad (1)$$

Where, V_{rM} and I_{rM} are the operating voltage and current for the relay, RM. I_F represents the faulted loop current.

As in equation (1), apparent impedance calculated by relay R includes an additional impedance, $\Delta Z = \left(\frac{I_F}{I_{rM}} \right) R_f$ along I_{rM} with the impedance of the line up to fault point, $Z_{MF} = xZ_{1L}$.

Fault current limitation by the IIDG interfacing converters causes the ratio, (I_F / I_{rM}) to be very high compared to a conventional power network with synchronous generator based sources. This results in large difference between Z_{MF} and Z_{app} . [12]

The fault current angle supplied by IIDG regulated by control schemes based on host grid code requirement. It results in non-homogeneity as compared with synchronous based generator on other side and there is significant phase angle difference between I_{rM} and I_F . Therefore, Such phase angle difference adds a significant reactive part in Z and deviates the Z_{app} along the imaginary axis in R-X plane as shown in Fig. 6.

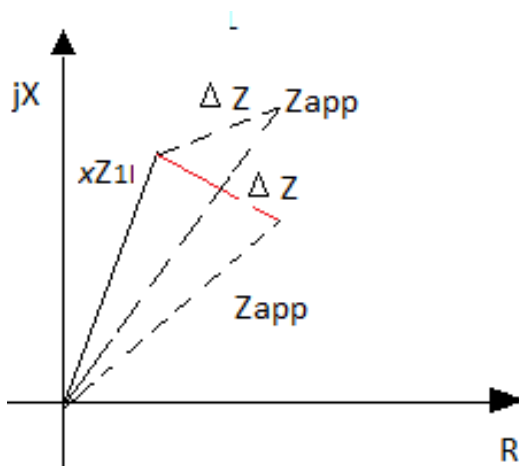


Fig.6. Overreach or Underreach of distance relay

Therefore, the performance of distance relay affected due to presence of Inverter Integrated Distributed generation

Due to weak infeed characteristics of IIDG, during LL-G fault and LL fault in first zone of line, the impedance seen by relay in fourth quadrant when IIDG follow North American grid code and in first quadrant far behind the actual impedance when IIDG follow European grid with reactive power support [3]

Due to additional impedance, the apparent impedance of line seen by relay is different than the actual impedance upto fault point cause distance relay to overreach or underreach

Maloperation of Quadrilateral distance relay [8]

Since typical negative-sequence networks are more homogeneous, many time negative sequence current is used in modern protective relays. The quadrilateral element based on negative sequence polarization malfunctions when non- conventional or no negative sequence current is injected by IIDG. Furthermore, in some relay, directional phase comparator uses negative-sequence current for polarization, which is also susceptible to mal-operation.

Non operation of pilot based accelerated Zone -2 tripping [14]

For accelerated tripping of Zone 2 operation of distance relay, distance protection relay utilizes various pilot communication based tripping scheme like Permissive Overreach Transfer Trip (POTT), Permissive Underreach Transfer Trip (PUTT), Direct Underreach Transfer trip (DUTT). However, the operation of these transfer trip solely depends upon the correct operation of distance protection at both end the line. As the distance protection connected on IIDG side are prone to mal-operate, therefore, POTT, PUTT and other pilot based schemes may mal-operate [15]

Effect of Intermediate Infeed [16]

Due to intermediate infeed, the impedance seen by relay at source end get affected . When the source at infeed is from IIDG , the inter-feed issue become more severe due to fault characteristic of IIDG.

Failure of Starting element [4], [17]

Current amplitude serves as the starter element in the traditional distance protection system. Consequently, even if the impedance trajectory reaches the protective

zone, the relay does not trip. By decreasing current supervision value to low threshold, may risks to relay maloperation during capacitor bank switching or other transient during load switching.

Some commercial relays use impedance supervision as starting function. The current needs to be higher than a predetermined threshold in order to calculate the impedance between the phase-to-phase loops. Therefore, in comparison to overcurrent supervision, the overcurrent setting can be set considerably lower. However, the proximity of IIDG decreases considerable the current during a fault, in this case this function become impractical.

Other option can be the V/I supervision starting function. Current and/or voltage must exceed the respective threshold. However, in case of IIDG, the current may not increase more than threshold and decrease of voltage may not always because of fault.

Non- Pilot based accelerated zone-2 tripping[18]

Pilot protection based distance schemes are many times employed in relays to provide fast tripping of the faulty transmission lines. However, these schemes may become ineffective due to probable communication link failure or interruption. As a result, some non-pilot approaches are discussed in the technical literature; however, because to the unusual fault behavior of inverter-based resources (IBRs) in comparison to synchronous generators, these methods are unable to provide an adequate performance in their presence.

PERFORMANCE STUDY OF IMPACT ON DISTANCE PROTECTION IN PRESENCE OF IIDG USING ETAP

In this section, the 50MWp solar power plant connected to 132kV utility grid simulated in ETAP to study performance of distance protection on line connected IIDG.

The test system shown in Fig.7 consists of 50MWp solar plant connected to 132kV utility Bus A. The inverter control system follows the North American grid code or Indian grid code, which allows the fault ride through at unity factor. The length of transmission line is considered 30km between Bus A and Bus B. The load 15MVA connected at Bus B. The utility grid connected

to Bus C and another transmission line of length 30km between Bus C and Bus B.

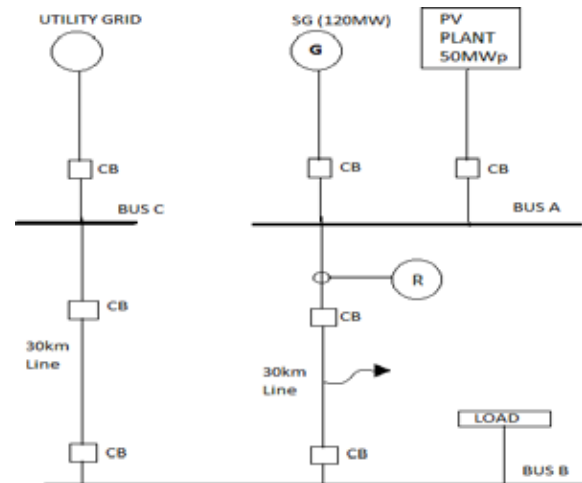


Fig. 7 : Test System

The distance relay connected for protection of 132kV transmission line AB. The zone 1 of relay covers 80% of line AB and zone 2 set at 150% line AB. The distance relay uses quadrilateral characteristic.

The test system simulated in ETAP to study performance of distance protection relay R. The response of distance protection analyzed for various type faults, fault resistance at different points on 132kV transmission line AB.

Case -1: Type of Fault: LLL, At length of line: 0%, Fault resistance -10 ohms

For this type of fault, the distance protection relay R of line AB not operated. The response of distance relay is as shown in Fig. 8. The impedance seen by relay is in fourth quadrant due to effect of IIDG. Therefore, distance relay mal operated.

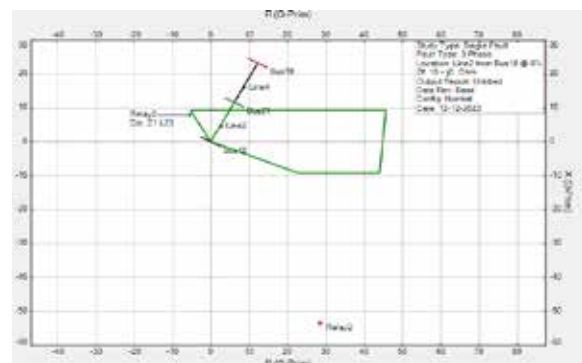


Fig. 8 Response of distance relay in case 1 with PV Plant

If PV plant replaced with 120MW conventional synchronous generators with all other fault parameter kept constant. The response of distance relay is as shown in Fig.9. It has observed that, distance relay operated correctly, when PV plant replaced with synchronous generator.

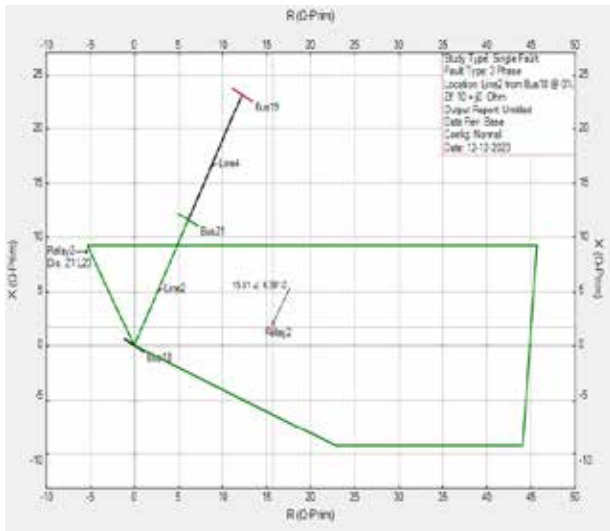


Fig.9 Response of distance relay in case 1 with synchronous generator

Case -2: Type of Fault: LL, At length of line: 50%,Fault resistance -20 ohms

For this type of fault, the distance protection relay R of line AB not operated. The response of distance relay is as shown in Fig.10. The impedance seen by relay R is in fourth quadrant due to nonconventional fault characteristics of IIDG.

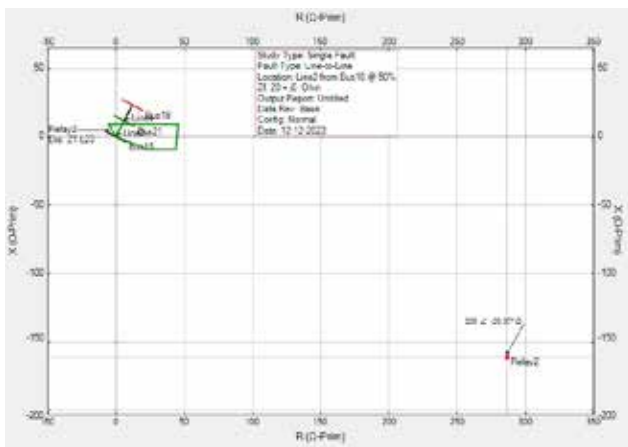


Fig.10 Response of distance relay in case 2 with PV Plant

If PV plant replaced with 120MW Conventional synchronous generators with all other fault parameter kept constant. The response of distance relay is as shown in Fig.11 . It has observed that, distance relay operated correctly, when PV plant replaced with synchronous generator

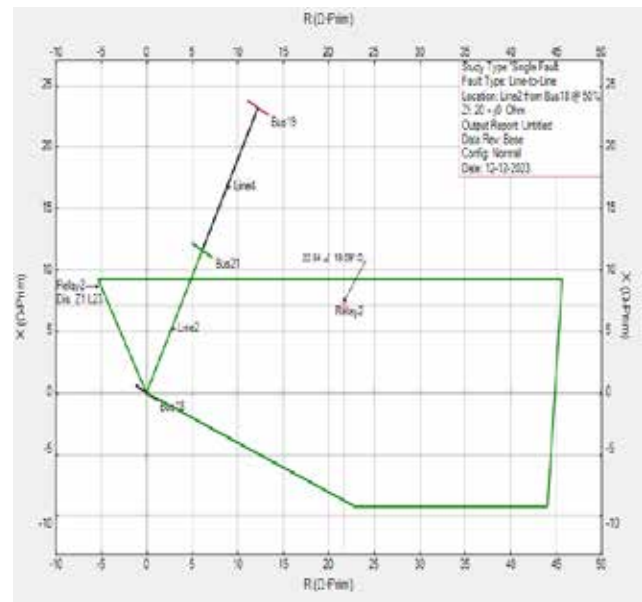


Fig.11 Response of distance relay in case 2 with synchronous generation

RESULT AND DISCUSSION

The performance of distance relay R of line AB simulated for different type fault, different fault resistance and for fault at different point on line .It observed that, the impedance seen by relay for LL, LLG and LLL fault is far different from actual impedance of line, when IIDG is connected at bus A.

As explained in III , the distance protection mal-operates due to under reach or overreach due to non-conventional fault characteristic of IIDG . The impedance seen by relay in forth quadrant of quadrilateral characteristic when IIDG follows North American grid code. For line to ground fault, the magnitude of zero sequence current I_0 is used for calculation of impedance, however zero sequence current is depending upon transformer configuration and independent of IIDG controller

Table 2 Response of distance relay in different scenario

Study Case	Type of Fault	Fault location in %	Rf in Ohm	Relay operation in presence of IIDG	Relay operation in presence of SG
Case1	LLL	0	0	Operated	Operated
Case2	LLL	0	10	Not operated	Operated
Case3	LLL	0	20	Not operated	Operated
Case4	LLL	50	0	Operated	Operated
Case5	LLL	50	20	Not operated	Operated
Case6	LG	0	0	Not operated	Operated
Case7	LG	0	20	Operated	Operated
Case8	LG	50	0	Operated	Operated
Case9	LG	50	20	Operated	Operated
Case10	LL	0	0	Not Operated	Operated
Case11	LL	0	20	Not Operated	Operated
Case12	LL	50	0	Not Operated	Operated
Case13	LL	50	20	Not Operated	Operated
Case14	LLG	50	20	Not Operated	Operated
Case15	LLG	50	0	Not Operated	Operated
Case16	LLG	0	0	Not Operated	Operated
Case17	LLG	0	20	Not Operated	Operated

Therefore, distance protection operated correctly in presence of IIDG except for terminal faults.

CONCLUSION

The high penetration of distributed generation or renewable energy resources leads to many challenges to conventional protection relaying. The conventional protection system designed based on fault response of synchronous generator. Contrary to traditional synchronous machine-based generation, Inverter Interfaced Distributed Generation (IIDG) has distinct fault current characteristics.

This article summarizes the various challenges reported in literatures in operation of distance relay in presence of IIDG, as first step toward development of effective protection system in IIDG enriched power grid. The distance relay connected on IIDG side mal-operates due to overreach or under reach, failure of starting element, maloperation of fault classification elements. Also, it has reported that, non-pilot based and pilot based accelerated tripping schemes may mal-operates in presence of IIDG. For reverse zone fault, the grid side distance relay mal-operates in presence of IIDG.

The impact on IIDG side distance protection relay performance studied in details using ETAP. The IIDG

side distance relay mal-operates for LLL, LLG and LL faults due to under reach or overreach of relay. The impedance seen by relay in fourth quadrant of R-X plane for Zone 1 fault due to fault current magnitude and angle control by IIDG controller.

Further investigation is required to study influence on distance relays in nearby grid, in case IIDG have major share in power grid.

REFERENCES

1. S. Dey, A. Sreenivasulu, G. T. N. Veerendra, K. V. Rao, and P. S. S. A. Babu, "Renewable energy present status and future potentials in India: An overview," *Innovation and Green Development*, vol. 1, no. 1, p. 100006, 2022, doi: <https://doi.org/10.1016/j.igd.2022.100006>.
2. J. C. Quispe and E. Orduña, "Transmission line protection challenges influenced by inverter-based resources: a review," *Protection and Control of Modern Power Systems*, vol. 7, no. 1, p. 28, 2022, doi: [10.1186/s41601-022-00249-8](https://doi.org/10.1186/s41601-022-00249-8).
3. A. Hooshyar, M. A. Azzouz, and E. F. El-Saadany, *Distance Protection of Lines Emanating from Full-Scale Converter-Interfaced Renewable Energy Power Plants-Part I: Problem Statement*, vol. 30, no. 4. 2015. doi: [10.1109/TPWRD.2014.2369479](https://doi.org/10.1109/TPWRD.2014.2369479).
4. A. Haddadi, E. Farantatos, I. Kocar, and U. Karaagac, "Impact of Inverter Based Resources on System Protection," *Energies (Basel)*, vol. 14, no. 4, 2021, doi: [10.3390/en14041050](https://doi.org/10.3390/en14041050).
5. F. M. AlAlamat, E. A. Feilat, and M. A. Haj-ahmed, "New Distance Protection Scheme for PV Microgrids," in *2020 6th IEEE International Energy Conference (ENERGYCon)*, 2020, pp. 668–673. doi: [10.1109/ENERGYCon48941.2020.9236446](https://doi.org/10.1109/ENERGYCon48941.2020.9236446).
6. M. Sarkar, J. Jia, and G. Yang, "Distance relay performance in future converter dominated power systems," in *2017 IEEE Manchester PowerTech*, 2017, pp. 1–6. doi: [10.1109/PTC.2017.7981144](https://doi.org/10.1109/PTC.2017.7981144).
7. V. Chakeri, H. Seyedi, and M. TarafdarHagh, "A New Approach to Transmission Line Pilot Protection in the Presence of Inverter-Interfaced Distributed Generators," *IEEE Syst J*, vol. 15, no. 4, pp. 5383–5392, 2021, doi: [10.1109/JSYST.2020.3041203](https://doi.org/10.1109/JSYST.2020.3041203).
8. M. Zadeh, P. K. Mansani, and I. Voloh, "Impact of Inverter-based Resources on Impedance-based Protection Functions," in *2021 74th Conference for*

- Protective Relay Engineers (CPRE), 2021, pp. 1–10. doi: 10.1109/CPRE48231.2021.9429723.
9. J. C. Quispe H, H. Villarroel-Gutiérrez, and E. Orduña, “Analyzing Short-Circuit Current Behavior Caused by Inverter-Interfaced Renewable Energy Sources. Effects on Distance Protection,” in 2020 IEEE PES Transmission & Distribution Conference and Exhibition - Latin America (T&D LA), 2020, pp. 1–6. doi: 10.1109/TDLA47668.2020.9326226.
 10. J. Pradhan and M. Singh, “Modified Distance Relaying Blocking Scheme For Low Inertia System,” in 2020 21st National Power Systems Conference (NPSC), 2020, pp. 1–6. doi: 10.1109/NPSC49263.2020.9331884.
 11. G. Ziegler, “Numerical Distance Protection, Principles and Applications,” John Wiley & Sons, 2011.
 12. S. Paladhi and A. K. Pradhan, “Adaptive Distance Protection for Lines Connecting Converter-Interfaced Renewable Plants,” IEEE J Emerg Sel Top Power Electron, vol. 9, no. 6, pp. 7088–7098, 2021, doi: 10.1109/JESTPE.2020.3000276.
 13. P. Li et al., “A Specialized System-on-Chip Based Distance Protection for Distribution Grids with Inverter Interfaced Distributed Generation,” Front Energy Res, vol. 8, 2020, doi: 10.3389/fenrg.2020.614292.
 14. A. Hooshyar, M. A. Azzouz, and E. F. El-Saadany, “Distance Protection of Lines Connected to Induction Generator-Based Wind Farms During Balanced Faults,” IEEE Trans Sustain Energy, vol. 5, no. 4, pp. 1193–1203, 2014, doi: 10.1109/TSTE.2014.2336773.
 15. S. Paladhi, Q. Hong, and C. Booth, “A Reliable Accelerated Protection Scheme for Converter-Dominated Power Networks,” in 2022 22nd National Power Systems Conference (NPSC), 2022, pp. 654–657. doi: 10.1109/NPSC57038.2022.10069232.
 16. A. Banaie moqadam, A. Hooshyar, and M. A. Azzouz, “A Control- Based Solution for Distance Protection of Lines Connected to Converter- Interfaced Sources During Asymmetrical Faults,” IEEE Transactions on Power Delivery, vol. 35, no. 3, pp. 1455–1466, 2020, doi: 10.1109/TPWRD.2019.2946757.
 17. A. Novikov, J. J. de Chavez, and M. Popov, “Performance Assessment of Distance Protection in Systems with High Penetration of PVs,” in 2019 IEEE Milan PowerTech, 2019, pp. 1–6. doi: 10.1109/PTC.2019.8810491.
 18. M. M. Mobashsher, A. A. Abdoos, S. M. Hosseini, S. M. Hashemi, and M. Sanaye-Pasand, “An Accelerated Distance Protection Scheme for the Lines Connected to Inverter-Based Resources,” IEEE Syst J, pp. 1–10, 2023, doi: 10.1109/JSYST.2023.3281345.

Real Time Monitoring System Representing Offset Machine Page Counting and Report Generation

Abhijit Kulkarni, Santosh Agnihotri

Department of Instrumentation and Control
Maratha Vidya Prasarak Samaj's, Karmaveer Adv.
Baburao Ganpatrao Thakare College of Engineering
Nashik, Maharashtra
✉ santosh.agnihotri@ges-coengg.org

Arjun Kapile, Pratik Junagade

Atharva Electronics Nashik
Nashik, Maharashtra
✉ kapile.arjun@gmail.com

ABSTRACT

Industries use monitoring systems to visualize machine operations. The system developed and presented here is counting the number of events (assumed as pages printed by the offset printing machine) and it is generating its real time report in csv. The benefit of this application is to reduce the complexity of maintaining hand-written work, to save time and man power, and to identify whether the machine is used optimally or not. Counting is verified by application of a TTL pulses from signal generator. Both simulation and hardware results are presented. Printing frequency of 2 Hz is applied and successful report is generated. Further this data report is generated in csv file showing actual time on cloud.

KEYWORDS : Real time monitoring, Offset printing machine, Microcontroller, Report generation.

INTRODUCTION

A monitoring system is software that helps control system engineers or management system officials to monitor their infrastructure performance. These tools monitor system devices, traffic, and applications, and proceed the data according to the given instructions. Real-time (data) monitoring is the delivery of continuously updated information streaming at zero or low latency.

The idea of this project is taken from an Offset Printing Machine Company in Nashik. In the proposed system, Real-time monitoring uses devices, software applications, and tools to track the performance of the offset printing machine. The process involves gathering data at the exact time that events (offset machine print) occur and then making that data available within a specific time interval. The system counts the number of pulses and generate the information report of product / counts that at what time page is printed from the machine; also, one gets the total number of pages printed by the machine. This report will be used to

understand how much work is done by the machine. This will identify actual work and sub-work time taken by the machine to do the sub tasks and total tasks thus reducing the possibility of misuse of the machine.

LITERATURE REVIEW

Researchers have made simulation of Offset Printing machine using QT Real-time software and HMI (Human Machine Interface) [1]. High printing quality can be achieved with conventional P/PI position and speed control [2]. A comparison of before automation and after automation – make ready time and waste impressions is presented in [3]. A survey of computational intelligence-based techniques for print quality assessment in offset colour printing is presented in [4]. Different printing quality attributes are also discussed in [4]. A model of ink preset for offset printing based on Least-square Support Vector Machine (LS-SVM) is proposed in this paper [5]. A Neural Network Approach in Reducing Offset Printing Spoilage is discussed in [6]. A US patent is about control system of offset printing machine [7]. A closed loop solution that includes an X-Rite

scanning system and integrated third party software is an affordable way to maximise performance and extend the value of an older press by monitoring colour and alerting operators [8]. Siemens has a servo drive control systems for offset printing machines [9].

OBJECTIVES

1. To study the given data-sheet of AT89S52.
2. To develop the necessary code to initialise LCD with AT89S52 and sending commands to LCD.
3. To develop the necessary code of counting application and increment the count value after each input.
4. To develop a Proteus simulation for virtual simulation of programs.
5. To interface hardware setup which is consisting of AT89S52, SIM900A GSM Modem, 16x2 LCD and other required components.
6. To interface the GSM modem with microcontroller and microcontroller with GSM modem.
7. To develop a cloud database system for storing count data on cloud.
8. To send counted data to the cloud with GSM modem by necessary AT commands.
9. To identify potential applications and future improvements for the Real time Monitoring System.
10. To generate the report of at what time and what date the paper is printed.
11. The main purpose of this system is to monitor production of machine or printing papers.

ANALYSIS AND DESIGN

The system uses an AT89S52 microcontroller. The important reason for using this microcontroller is that it is low-power, high-performance CMOS 8-bit microcontroller with 8K bytes of in-system programmable Flash memory, 256 bytes of RAM and Watchdog timer. The system will take input from a proximity sensor; that can align to pick up pulse from presence of page or movement of a metal part related with offset machine and count the number of pulses with

real time consideration. The sensor will sense the pages and generate a pulse of 24volt which will get converted to 5 volts with required resistor and IC. The system consists of AT89S52 microcontroller, GSM modem, a sensor 16x2 LCD display. If a page is passed by a sensor, it gives signal to microcontroller and microcontroller is programmed with different logics, for number of pulses received by sensor. Initially the counted value will be displayed to LCD and after a specific time interval it will send the count data to the database on the cloud. To communicate with cloud and sending the count data to the cloud GSM modem is used which is SIM900A. This module is programmed in such way that it will send the data after a specific time interval to cloud and in database it will add time and date which will be taken from the hosted server.

Approach

Figure 1 shows a simulation of offset printing machine and its importance in even simulation [1].

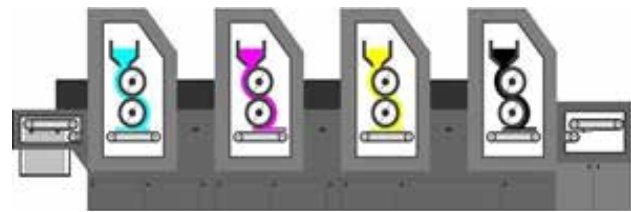


Fig. 1 simulation of offset printing machine

This is offset printing machine in which paper is printed in three stages i.e., at first stage paper is inserted in the machine and for this the operator press and insert button by which machine start to take itself paper in it. In second stage machine start printing paper with required ink and solutions and for this operation operator press second button and in third stage paper is printed and we get output as a printed paper. In this total process the operator presents there is maintaining a hard copy of handwritten work in which he is mentioning the time of first button (insert button) pressed and after that the machine completes its work time is noted by operator and hard copies are maintained to track the work taken by the machine so to overcome this problem there should be a system which must count the printed paper and note the time at which date and what time how much paper is printed.

This can be done by placing a sensor which sense the

paper and generate a signal to microcontroller, this will count the data and display it to the LCD and after a specific time defined in the code GSM will send the counter value to server/cloud in database and in database and at the time of entry to the database table the current time will be noted in the table by which we will have data which will tell us that at what time how much page is printed and by analysing the data we can conclude that machine is used optimally or not. Figure 2 & 3 shows GSM MODEM used in this system and counts actual.

Hardware and Software Requirements

Hardware Requirements: AT89S52 and associated circuit, GSM Modem SIM900A, DC power supply, signal generator, CRO, Laptop.

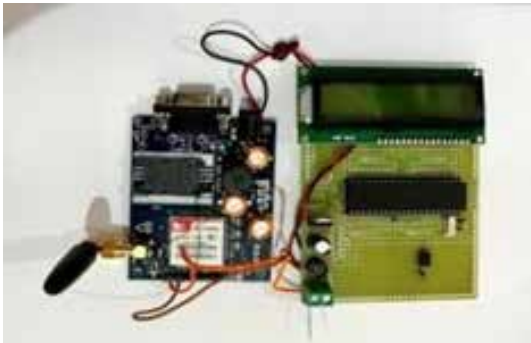


Fig. 21 circuit used to display counting pulses from the signal generator



Fig. 3 event being counted and displayed

Software Requirements: Keil IDE and Proteus for simulation are used. For this system Embedded C language is used for required operations and output. Tasks divided the operation was to first initialise the LCD with microcontroller, second task was to add

counter logic to it which will increment the count value as 2 Hz frequency is given to controller P3.4 pin i.e. T0.

After creating code of LCD initialisation and Counter operation, next task was to interface the GSM modem with microcontroller and microcontroller with GSM modem which is achieved by connecting TX and RX pin of microcontroller and GSM modem. Next task was to make a website and database which will store count data and make a csv file of data sent to cloud via GSM modem. After creating website and database next task was to make connection of database server and GSM modem by sending required AT commands.

Willar Programmer: Willar Programmer is developed by Willar Electronics. The most popular version of this product among our users is 1.0. The name of the program executable file is WLPRO.exe. This software is used for uploading Code to AT89S52 and also, we can upload Different code to different IC's. This software is also used to erase other code present in the IC with the help of this software.

Cloud Server and Database: 000webhost: 000WebHost is among the top free web hosting providers offering reliable hosting services. It includes a custom control panel as well as the possibility to connect your own domain, it also provides a free database management system which can be used to manage the data and by cloud service. We are adding time - counter data is recorded to the record.

APPLICATIONS

Real-time monitoring helps one to identify the actual times an incident occurs, the reporting time, and the resolution time accurately. By identifying these times, organisations can get more proactive with their response methods and deal with recurring problems efficiently. As real-time monitoring can be scheduled to run all around the day, you can get accurate event logs and real-time reports leading up to the time of a security incident or error. This will help you analyse the root cause more efficiently and get to the right solutions faster.

RESULTS AND DISCUSSIONS

For testing a counting application, 5 Volt DC pulse is given to the microcontroller P3.4 pin. Pulses are given to T0 pin because we have used Timer0 as counter

mode. A 3 MHz MULTI WAVEFORM Signal Generator TTL output is used of 2 Hz Frequency to generate two pulses in one second that means counter value will be 2 in one second and in two second counter will be incremented to 4 and so on. In Code, Delay is used to send the count data to server i.e., after each 20 second counted data will be sent to the database server. In response the database cloud server will respond back with time and update to database table. <https://onlinecountersk.000webhostapp.com/download.php> is a php code website which when open in browser it will download a .csv file report of counted data as seen in Figure 4.

Time	Count
00:00:00	0
00:00:01	2
00:00:02	4
00:00:03	6
00:00:04	8
00:00:05	10
00:00:06	12
00:00:07	14
00:00:08	16
00:00:09	18
00:00:10	20
00:00:11	22
00:00:12	24
00:00:13	26
00:00:14	28
00:00:15	30
00:00:16	32
00:00:17	34
00:00:18	36
00:00:19	38
00:00:20	40
00:00:21	42
00:00:22	44
00:00:23	46
00:00:24	48
00:00:25	50
00:00:26	52
00:00:27	54
00:00:28	56
00:00:29	58
00:00:30	60
00:00:31	62
00:00:32	64
00:00:33	66
00:00:34	68
00:00:35	70
00:00:36	72
00:00:37	74
00:00:38	76
00:00:39	78
00:00:40	80
00:00:41	82
00:00:42	84
00:00:43	86
00:00:44	88
00:00:45	90
00:00:46	92
00:00:47	94
00:00:48	96
00:00:49	98
00:00:50	100

Fig. 4 csv file report

This system is not tested to Real Offset printing machine; however it is guaranteed to give performance as any sensor will generate 24V or 5 VDC pulses.

CONCLUSION AND FUTURE SCOPE

The system is tested successfully. The system is successfully counting the pulses received by signal generator. After giving 2Hz frequency, system is counting properly which was expected by the system. Time is recorded by cloud server which is not IST time zone by some implementation and research we can add IST time to the report. Data report generation can be updated in latest format. By Small changes in code logic and we can use this project in different sector where counting and report generation is basic task. AI can be used to predict miss-use of the offset machine or any other machine as logic can be applied to virtually

variety of machines. AI and data analytics further can be used to have statistical performance to use it in different directions.

REFERENCES

1. Offset Printing Machine HMI, with Modbus TCP. [Online]. Available: <https://github.com/Wolkabout/offset-printing-machine-simulator-application>
2. G. Brandenburg, S. Geissenberger, C. Kink, N. -H. Schall and M. Schramm, "Multimotor electronic line shafts for rotary offset printing presses: a revolution in printing machine techniques," in IEEE/ASME Transactions on Mechatronics, vol. 4, no. 1, pp. 25-31, March 1999, doi: 10.1109/3516.752081.
3. Sheriff Blathur. Offset Printer Automation; An Industrial Revolution. TechRxiv. July 22, 2022. doi: 10.36227/techrxiv.20280444.v3
4. A. Verikas, J. Lundström, M. Bacauskiene, and A. Gelzinis, "Advances in computational intelligence-based print quality assessment and control in offset color printing," Expert systems with applications, vol. 38, no. 10, pp. 13441–13447, 2011.
5. J. Yu, J. Lin, L. Guan, N. Li and L. Zhao, "Model of ink preset for offset printing based on LS-SVM," in Proc. ECOC'00, 2000, paper 11.3.4, p. 109.
6. T. J. C. Limchesing, R. G. Baldovino and N. T. Bugtai, "A Neural Network Approach in Reducing Offset Printing Spoilages on Solid Bleached Boards," in Proceedings of the 29th Chinese Control Conference, 2010, pp. 3103-3106.
7. Kazuo Murai, Kenji Hashimoto, Kiyoshi Fukushima and Sumio Suzuki, "Automatic control system for offset printing machine" US4353299A, Oct. 12, 1982.
8. How to Automate Offset Press Process Control with a Closed Loop Solution. [Online]. Available: <https://www.xrite.com/learning-color-education/using-our-solutions/automate-offset-press>
9. Print Standard Segment Offset Entry-ID: 48946827, V3.0.0, 01/2017, Siemens, pp. 1-31.
10. "16x2 LCD Display Module data sheet," Available: <https://circuitdigest.com/article/16x2-lcd-display-module-pinout-datasheet>

Detection of Inter-turn Short-circuit Fault in Induction Machine Using Vibration Analysis

Deepak M. Sonje, Shrunkhala G.Khadilkar

M. V. Reddy

Department of Electrical Engineering

GES's RHS College of Engineering,

Management Studies and Research

Nashik, Maharashtra

✉ deepaksonje123@gmail.com

Ravindra K Munje

Department of Electrical Engineering

K K Wagh College of Engineering

Nashik, Maharashtra

ABSTRACT

Due to the recent development in the construction and operation of electrical machines, mode of living style of human being is completely changed. Squirrel Cage Three Phase Induction Machines (SQTPIMs) are mainly used in the large number for industrial and residential applications. These machines are also known as workhorse of industries. However, these machines are exposed to a variety of undesirable factors and situations due to which motor may get damaged. To avoid the partial damage of failure of the machine, condition monitoring of induction machine is suggested by many authors in the literature. It is observed that, with the sensitive condition monitoring, life of the motor can be enhanced. It will also reduce partial damage, reduces spare parts inventories, and also will reduce breakdown maintenance. An efficient condition monitoring scheme is capable of providing warning and predicting the faults at early stages. In this paper, a method based on vibration analysis is presented for detection of stator inter turn fault in TPIM. With the proposed method, it is possible to detect minor inter turn fault produced in the stator winding using Fast Fourier transform (FFT) analysis. To prove the effectiveness of the proposed method, number of experiments is conducted on healthy and faulty conditions of the motor. The obtained results suggest that this method is effective and accurate and can be used as a tool for fault diagnosis in the SQTPIM.

KEYWORDS : *Squirrel cage three phase induction machine (SQTPIM), Condition monitoring, Vibration analysis, Fast fourier transform (FFT).*

INTRODUCTION

Electrical machines are playing very important role in the industry and also known as work horses of the industry. Three phase Induction machines (SQTPIM) are mainly used in the number of industrial applications. It is found in the literature that stator, rotor and bearings of the three-phase induction machines are the most affected components during operation [1-5]. In the stator faults, turn-turn fault is considered as one of the key faults and also one of the prime reasons for motor breakdown. This is occurs because of the various stresses that act on the motor simultaneously on motor during the operation of the motor. The fault initiate with minor deterioration of stator insulation between turn to turn and leading to its breakdown at the end of

the process. Accordingly, stator faults are classified as stator winding short-or open circuits and even stator core faults [6]. The deterioration and aging of the stator insulation system eventually lead to turn-to-turn faults. In such fault, two or more neighboring turns of a coil are shorted and a very large circulating current is induced in the loop. This current is higher than the nominal or rated current of the motor known as fault current which increases the temperature of stator winding to very high level results into the breakdown of the insulation and hence winding of the motor. As per the basic protection provided to the motor, the machine may continue to run and within the short period of time severe fault may occurred in the motor. The life of the motor can be saved if it possible to detect the turn-to-turn faults

within a coil at incipient stage by any online diagnostic techniques [5].

A significant research work has been carried out in the last two-three decades to detect and diagnose various faults including stator winding faults in TPIM. Most popular invasive methods are based on by products of current and voltage quantities such as negative sequence component of current, negative sequence impedance, instantaneous value of active and reactive power, instantaneous value of power factor, etc. Some authors are also proposing methods based on temperature monitoring such as thermo graphical techniques to detect inter turn faults in the Induction machine. The Park’s vector approach is also suggested in the number of research papers which is based on the pattern recognition in [7-8]. Park’s vector modulus based technique is also suggested to detect the inter turn fault in [9-10]. Stator faults are detected by authors using statistical parameters obtained from vibration signals and also estimated fault severity using random forest classifier [11]. Inner race and outer race faults are detected and classified using genetic algorithm with different classifiers and claims that random forest classifier is more accurate than KNN and decision tree classifiers [12].

The ultimate aim of all the researchers is to produce a generalized method which will diagnose the inter turn fault by knowing the very minute information about the motor. The aim of this paper is to present the very simple method for the detection of minor inter-turn faults. The proposed method is based on vibration analysis. The remainder of this paper is organized as follows. Section II briefs the theoretical background related with the method proposed in this paper. A detail about the experimental setup and test ring is elaborated in section III. Result and discussion is covered in section IV. Paper is concluded with some concluding remarks related to the work in section V.

INTER-TURN SHORT-CIRCUIT DETECTION USING VIBRATION ANALYSIS

Vibration analysis is most popular technique in the condition monitoring of electrical machines. As electrical machine is converting electrical power into mechanical power, machine has rotating member

that oscillates at regular intervals. These continuous oscillations are transmitted to external system coupled with the machine shaft. This results in a machine-related frequency spectrum that characterizes healthy machine behavior. If any mechanical or electrical faults occur in a machine, it will disturb the sequence of oscillations and induce the additional component of frequency in the frequency spectrum. In fact, each fault in a rotating machine produces significant vibrations with unique characteristics frequency that can be distinguished and compared with standard ones in order to perform the fault detection and diagnosis.

Any three phase induction motor consists of balanced three-phase winding supplied with a symmetrical three phase voltages, constitutes only the positive sequence components of magneto motive forces where as the summation of negative sequence components is to be zero [11-12]. If there is an asymmetric stator or rotor winding due to any fault, the negative sequence components of the magneto motive forces will exist. This will cause some disturbance in the machine's operation. Negative sequence magneto motive forces tend to deteriorate machine performance and are therefore minimized or eliminated whenever possible.

In general, the instantaneous electromagnetic torque of an electrical machine can be obtained by the vector product of stator flux linkage and stator current [11].

$$T_e = \frac{3}{2} P \overline{\Psi}_s \times \overline{I}_s \tag{1}$$

Where, T_e = Electromagnetic torque

$P \overline{\Psi}_s$ = Stator flux linkage

\overline{I}_s = Stator current

The voltage equation of the stator in the arbitrary frame can be expressed as:

$$\overline{V}_s = R_s \overline{I}_s + \frac{d\overline{\Psi}_s}{dt} \tag{2}$$

The corresponding stator voltage \overline{V}_s , stator current \overline{I}_s , and stator flux linkage $\overline{\Psi}_s$ can expressed as a positive sequence (subscript s1) and negative sequence (subscript s2) component.

$$\overline{V}_{s1} = \overline{V}_{s1} e^{j\omega_1 t}, \quad \overline{V}_{s2} = \overline{V}_{s2} e^{-j\omega_2 t} \tag{3}$$

$$\bar{I}_{s1} = \bar{I}_{s1} e^{j\omega_1 t}, \bar{I}_{s2} = \bar{I}_{s2} e^{-j\omega_2 t} \tag{4}$$

$$\bar{\Psi}_{s1} = \bar{\Psi}_{s1} e^{j\omega_1 t}, \bar{\Psi}_{s2} = \bar{\Psi}_{s2} e^{-j\omega_2 t} \tag{5}$$

Solving Eq.(1-5) yields:

$$T_c = T_{average} + T_{Pulsating} \tag{6}$$

where $T_{average}$ is the electromagnetic torque, which is constant in time and contains two components (the positive and negative torque sequences – T_1 and T_2 respectively) are given by,

$$T_{average} = T_1 - T_2 \tag{7}$$

$$T_1 = \left(\frac{3P}{2\omega_1}\right) (|\bar{V}_{s1}| |\bar{I}_{s1}| \cos \alpha_{s1} - \bar{I}_{s1}^2 R_s) \tag{8}$$

$$T_2 = \left(\frac{3P}{2\omega_1}\right) (|\bar{V}_{s2}| |\bar{I}_{s2}| \cos \alpha_{s2} - \bar{I}_{s2}^2 R_s) \tag{9}$$

The unique feature obtained from Eq.6 is the pulsating torque component $T_{Pulsating}$ which can be written by Eq. 10,

$$T_{Pulsating} = \left(\frac{3P}{2\omega_1}\right) Re[(|\bar{V}_{s1}| |\bar{I}_{s2}| - |\bar{V}_{s2}| |\bar{I}_{s1}|) \bar{I}_{s1}^2 R_s] e^{j2\omega_1 t} \tag{10}$$

It is observed that the above equation consists of torque component which oscillates at an angular frequency of $2\omega_1$. This is due to the mutual effect of the positive sequence of stator current and negative sequence of stator flux linkages and also by the mutual effect of the negative sequence stator currents and positive sequence stator flux linkages. Hence, the $2\omega_1$ i.e. the double frequency component is the very good indicator for inter turn fault in the stator winding of induction machine. This frequency does not appear under the healthy condition of the machine.

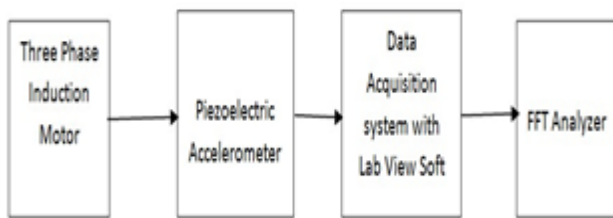


Fig. 1.Schematic Diagram for Vibration Measurement Analysis.

EXPERIMENTAL RESULTS AND DISCUSSION

Normally, in the vibration analysis techniques, sensitive vibration sensors are used which are working on the principle of piezoelectric effect. In these types of sensors, sensed vibrations are converted into proportional electrical signals. It is essential to analyze this electrical signal to extract important information related to any abnormal condition of the machine. The schematic diagram for vibration measurement analysis is presented in Fig.1.

The overall algorithm for the proposed technique is given in Fig. 2.

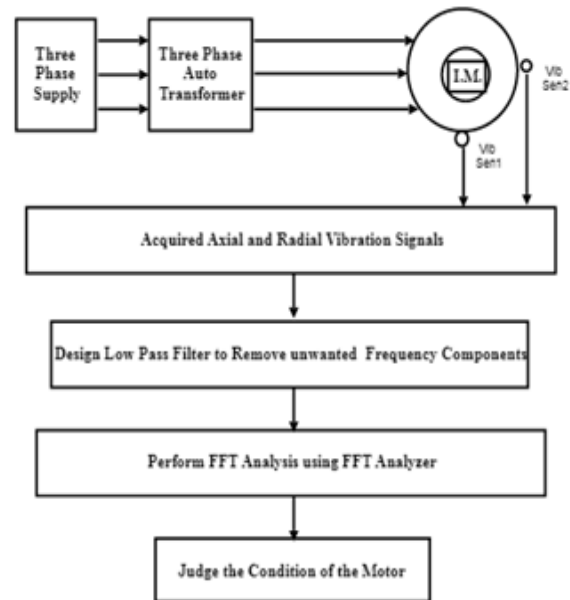


Figure 2: Flowchart of the proposed algorithm.

EXPERIMENTAL SETUP AND TEST RIG

The squirrel cage three phase induction machine (SQTPIIM) chosen for the experiment operate in open loop condition and supply is fed by a three phase auto transformer. The machine used in experimental tests is a three-phase, 50 Hz, 4-pole, 2.2 kW (3 Hp), Squirrel cage induction machine, rated at 415V, 4.5 Amp, 1440 rpm. Two piezo-electric vibration sensors are used for sensing the radial and axial vibrations. The electrical output of this type of sensor is depends on the force applied to the sensor. The whole experimental setup is as shown in Fig. 3.



Fig. 3. Experimental Setup

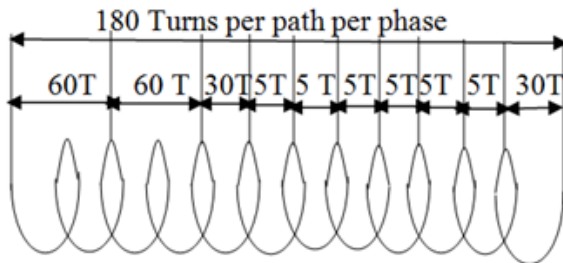


Fig. 4. Stator winding with different Configuration

The stator winding has been modified by addition of a number of configuration connected to coils is as shown in Fig. 4. The stator winding of the induction machine is having 180 turns per path per phase. The winding has two parallel paths per phase. The machine has external panel to access 5, 10, 15, 20, 25, 30, 60 turns from each phase of the stator winding. The suggested method is evaluated by conducting series of experiments with the following conditions.

1. Healthy or normal condition
2. 5 Turns are shorted U ph
3. 10 Turns are shorted U ph
4. 15 Turns are shorted U ph
5. 20 Turns are shorted U ph
6. Single Phasing in U ph

The machine is initially tested in healthy condition running at no load. When a balanced three phase supply voltage is applied to healthy induction machine, uniform current flows in all the phases. This will set up a uniform magnetic field both in stator and rotor. The interaction of magneto motive forces in rotor circuit with stator magnetic flux will produce steady positive machine torque, which drives the rotor in

forward direction producing useful mechanical output. A fine radial vibration will be setup in the stator. It was theoretically predicted that, in normal circumstances, the spectral analysis of vibration signal yields dominant component at fundamental frequency. The vibration spectrum for the healthy machine is as shown in Fig. 5. The frequency component at 50Hz with magnitude of -48 dB is clear from any other spectral component. However, the appearance of spectral component with a small amplitude, at a frequency of 100Hz—twice the fundamental supply frequency even in normal conditions, is directly related to the existence of a residual asymmetry in the stator circuit. The component at fundamental frequency is a positive sequence component which is essential for driving rotor in forward direction and also an indicator of healthy machine.

The appearance of characteristic component at frequency 100Hz for the case of 5 turns shorted in U phase is noticeable with the magnitude of -68 dB as shown in Fig. 5 which is higher as compared to healthy condition.

With the extension of the fault to 10 turns, 15 turns and 20 turns shorted in U phase, the amplitude of the double frequency component are found to be -67 dB, -66 dB and -64 dB respectively which are shown in Figs.7-9. Whenever single phasing occurs, i.e. U phase is opened; the magnitude of characteristic component is tremendously increased and reaches up to -58 dB as shown in Fig.10. However, the magnitude of component at fundamental frequency is remains constant at normal and faulty conditions.

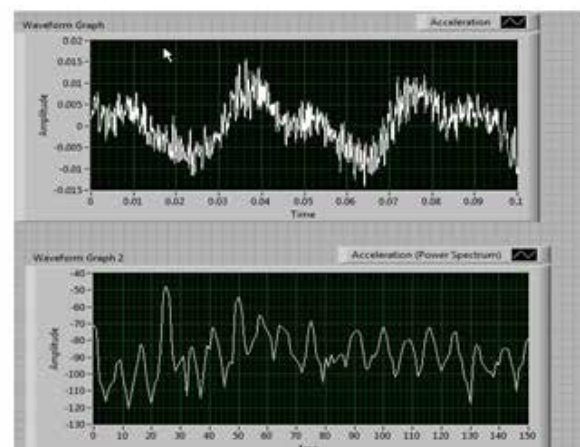


Fig.5. Vibration spectrum for healthy machine

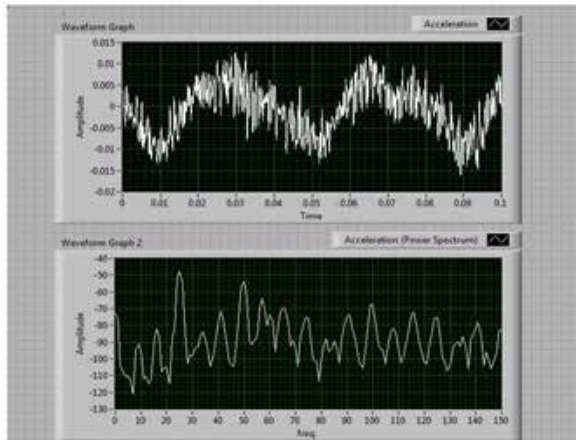


Fig.6. Vibration spectrum for 5 turns shorted in U-Ph

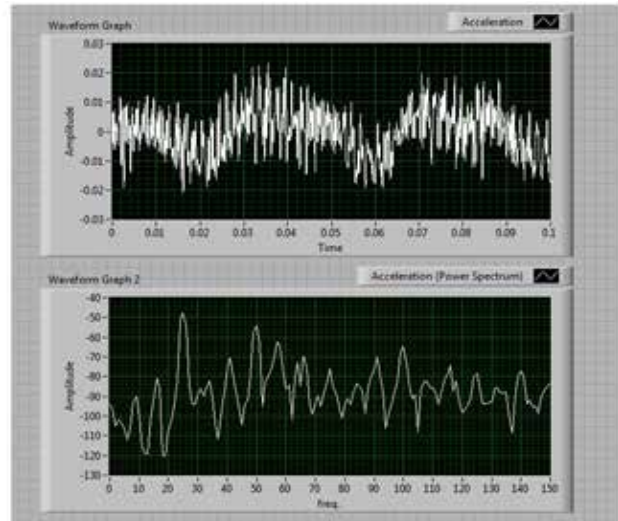


Fig.9. Vibration spectrum for 20 turns shorted in U-Ph

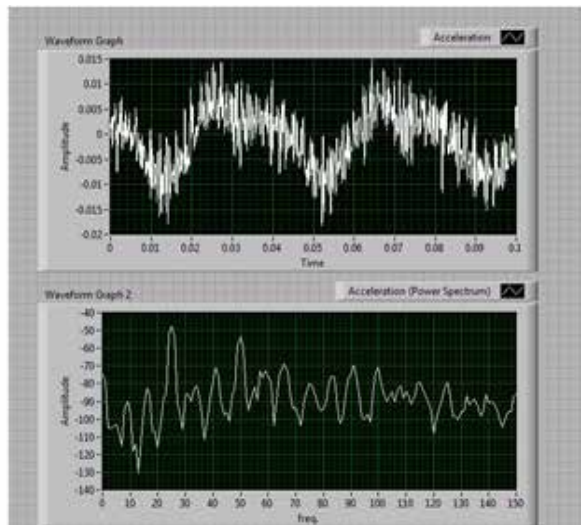


Fig.7. Vibration spectrum for 5 turns shorted in U-Ph

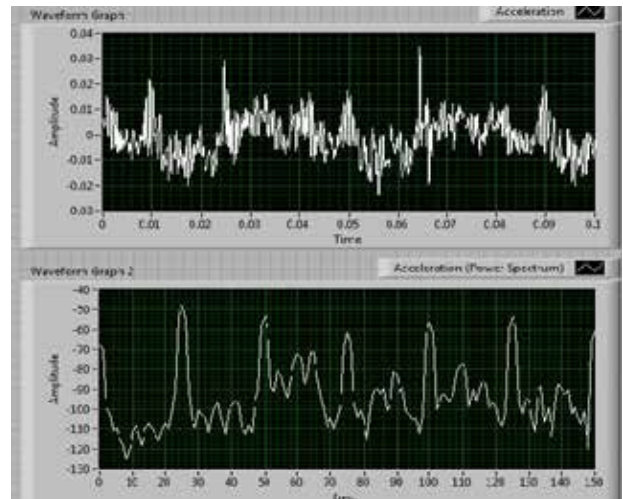


Fig. 10. Vibration spectrum for single phasing in U-Ph

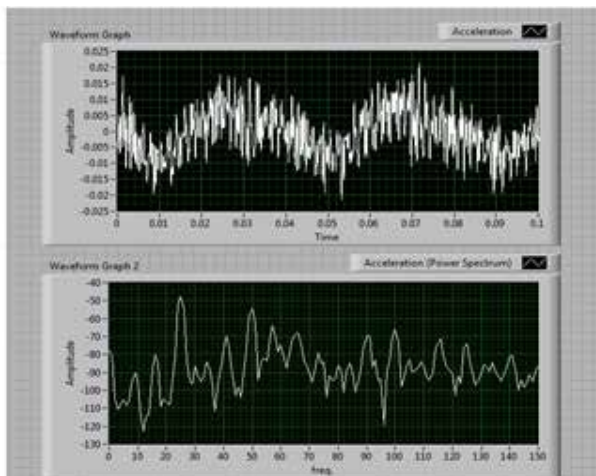


Fig.8. Vibration Spectrum for 15 turns shorted in U-Ph

Table 1: Comparison of the Magnitudes of Component at Fundamental and Double Fundamental Frequency

Condition of Machine	Magnitude of Fundamental Component (50 Hz) in dB	Magnitude of double Fundamental Frequency Component (100Hz) in dB
Normal Condition	-48 dB	-72 dB
5 T Shorted	-48 dB	-68 dB
10 T Shorted	-48 dB	-67 dB
15 T Shorted	-48 dB	-66 dB

20 T Shorted	-48 dB	-64 dB
Single Phasing	-48 dB	-58 dB

The magnitude of fundamental frequency component and double frequency component for various faults are listed in Table 1. It can be concluded from Table I that the amplitude of the spectral component at twice the fundamental supply frequency increases gradually with the extension of the stator fault, making it a good indicator of the presence of the fault. Moreover, the amplitude of fundamental component remains constant.

CONCLUSION

This paper presents an innovation and simple technique to detect minor inter turn fault in the stator winding of TPIM based on vibration analysis. During normal running condition, motor always produces some vibrations and specific vibration pattern can be observed using FFT spectrum. But, in the abnormal or faulty condition, this vibration spectrum changes. By comparing these spectrums under normal and abnormal condition, motor condition can be easily judged. In the study, radial and vibration are considered for the analysis. A component at twice line frequency in the induction machine vibration spectrum is a good indicator of the presence of the fault. In normal condition, the magnitude of FFT component at fundamental frequency is remains constant. In case of any faulty condition, the FFT spectrum consists of component at twice the fundamental frequency and magnitude of this component is gradually increases with the severity of the stator fault. So by noting the magnitude of this component, the machine condition can be easily judged.

REFERENCES

1. A. Siddique, G.S.Yadava and B.Singh, "A Review of Stator Fault Monitoring Techniques of Induction Machines," IEEE Transactions on Energy Conversion, vol.20, no.1, pp.106–114, March 2005.
2. Pinjia Zhang, Yi Du, Thomas G. Habetler, Bin Lu, "A Survey of Condition Monitoring and Protection Methods for Medium-Voltage Induction Machines," IEEE Transactions on Industry applications, vol.47, no.1, pp.34-46, 2011.
3. M. E. H. Benbouzid, "A Review of Induction Machines Signature Analysis as a Medium for Faults Detection," IEEE Transaction on Industrial Electronics, vol.47, no.5, pp.984–993, 2000.
4. M. B. K. Bouzid, G. Champenois, N. M. Bellaaj, L. Signac, and K. Jelassi, "An Effective Neural Approach for the Automatic Location of Stator Interturn Faults in Induction Machine," IEEE Transaction on Industrial Electronics, vol.55, no.12, pp.4277-4288, 2008.
5. S. Nandi, H. A. Toliyat, and X. Li, "Condition Monitoring and Fault Diagnosis of Electrical Machines-Areview," IEEE Transactions on Energy Conversion., vol.20, no.4, pp.719–729, Dec. 2005.
6. A. H. Bonnet and G. C. Soukup, "Cause and Analysis of Stator and Rotor Failures in Three Phase Squirrel Cage Induction Machines," IEEE Transaction on Industry Application, vol.28, no.4, pp. 921-937, July/August, 1992.
7. A. J. M. Cardoso, S. M. A. Cruz, J. F. S. Carvalho and E. S. Saraiva, "Rotor Cage Fault Diagnosis in Three-phase Induction Machines, by Park's Vector Approach," Conference Record of IEEE Industry Applications Society Annual Meeting, Orlando, Florida, USA, vol.1, pp.642-646, October 8-12, 1995.
8. A.J.M. Cardoso, S.M.A. Cruz, D.S.D. Fonseca, "Interturn stator winding fault diagnosis in three-phase induction machines by Park's Vector Approach," IEEE Transactions on Energy Conversion, vol.14, no.3, pp.595-598, 1999.
9. S. M. A. Cruz and A. J. M. Cardoso, "Rotor cage fault diagnosis in three-phase induction machines by Extended Park's Vector Approach," Electrical Machines and Power System, vol.28, no.4, pp.289–299, 2000.
10. S. M. A. Cruz and A. J. M. Cardoso, "Stator Winding Fault Diagnosis in Three-Phase Synchronous and Asynchronous Machines, by the Extended Park's Vector Approach," IEEE Transactions on Industry Applications, vol.37, no.5, September/October 2001.
11. Aparna Sinha and Debanjan Das, "Machine Learning-based Explainable Stator Fault Diagnosis in Induction Motor using Vibration Signal", published in the proceedings of IEEE Conference on Instrumentation and Measurement Technology, 2023.
12. Rafia Nishat Toma, Alexander E. Prosvirin and Jong-Myon Kim, "Bearing Fault Diagnosis of Induction Motors Using a Genetic Algorithm and Machine Learning Classifiers", Sensors, vol. 20, 2020.

Review: Congestion management by Distributed Generation with its Hosting Capacity

Swati Warungase

Department of Electrical Engineering
K.K. Wagh, Institute of Engg. Education and Research
Nashik, Maharashtra
✉ swarungasethete@gmail.com

M. V. Bhatkar

Jawahar Education Society's
Institute of Technology, Management & Research,
Nashik, Maharashtra

ABSTRACT

In recent years, congestion in electricity takes place when there is inadequate production, at the same time accommodating each chase for service inside a domain that is in the nearby areas of industrial and residential areas. Our proposed system depends on the hosting capacity of the renewable resources used day by day, such as solar distributed generators, wind turbines. We are proposing a system to estimate the power loss. For this system, we researched different studied methods, such as congestion management using genetic algorithm, greedy algorithm, and optimal placement of distributed generations in the distribution system. Here in this paper I'm presenting the literature review of different papers studied.

INTRODUCTION

Congestion occurs when the network cannot transfer or let down to provide power settled as per the load being demanded, which also has serious effects on power systems. All these problems taking place are managed by using some congestion management methods, which is to the highest degree, an essential aspect and plays a crucial part in present-day deregulated power scheme. That is why; various publications have reviewed the importance of all planned methods; and thus, in this paper we are going to make use of some Distributed Generations (DGs) which are available in renewable energy sources, which are wind, solar, biomass, etc. After connecting the same, we will be calculating the capacity of the system that means how much capacity the machine will carry and the capacity carrying unit is also called as Hosting Capacity. Also, the restrictions like voltage and power rate, by finding out the capability of the same, we will be conducting and making use of DGs and then, by doing a quick survey, we will find its impact on the electricity market.

Now-a-days, electrical power systems are facing different technical, economic and environmental issues, the power industry in many countries is undergoing restructuring and deregulation with the replacement

of previous monolithic regulated public utilities with competitive power markets which is to meet increasing demands for electricity around the world at affordable prices. Congestion management needs to be immediately performed so that congested systems are relieved or avoided. In a competitive market, congestion occurs when distribution networks of transmission lines or the feeders which are delivered to it by generation point from power system station or from power supply unit, who are unable to accommodate all desired transactions due to violations of the system's operating limits; this refers to the overloading distribution lines when the thermal bounds and line capacities are violated. Congestion also occurs when the power flows in the networks are higher than the flow allowed by operating reliability limits. The physical and system limitations such as thermal limitation of a network of units or dependent system operation can be effective in the occurrence of Congestion. Voltage limitation in a node, reliability and similar cases are some of the examples of system limitations of distribution networks which have contributed to the congestion of networks. Congestion occurs due to the absence of matching generation and transmission services and at the end of the line to the distributed network service. Blockage is additionally caused by unforeseen inevitabilities such as era

blackouts, unforeseen acceleration of stack request, and equipment disappointment. Clog within the control frameworks ought to be corrected promptly to guarantee framework security and to maintain a strategic distance from advance block-outs. The event of clog in control frameworks leads to framework unsettling influences that cause further blackouts in an interconnected framework. Clog is additionally caused by grave damage to control framework components in case framework blackouts regularly happen. It isn't as it were hardware which is hurt by blockage, but moreover the control quality. To prevent control framework gear from being harmed and to upgrade control quality, blockage frameworks ought to work quickly. However to solve the congestion management problems researchers have studied different methods, technologies and algorithms.

LITERATURE REVIEW

A literature review allows the problem being studied one to get an awareness into it . It explores advances computational methods , shines light on how to enhance data collecting performance and proposes strategies to maximize data collection and understanding effectiveness. Thus, it is an essential step in the development of the research project to review the literature. A literature review is a body of text intended to estimate the key points of being knowledge including empirical studies as well as theoretical, analytical and logical approaches to a particular subject. Literature reports are secondary sources, which have no current or original scientific exploration published.

In the literature, the mentioned issues and challenges of the distribution system can be addressed through several solutions. For example, power compensators can be used to reduce power loss, improve power quilt, and enhance voltage. In terms of environmental cordiality and economy, using distributed generation (DGs) units and shunt capacitors (SCs) is the most effective solutions for the distribution system problem. Owing to the advantages of the DGs and SCs, they are widely used in radial systems. Capacitors are used as reactive power compensators , whereas DGs are used as active and reactive power compensators. DGs are typically used in renewable power sources, such as solar thermal systems, photovoltaic (PV) systems, and wind turbines. DGs have three types. The first type can

supply active power (P), the second can supply reactive power (Q), and the third can supply both The various research papers were studied for this study and some of them research projects have been mentioned below.

Congestion Management

With the increase of the demand, congestion creates problems in numerous distribution networks. Evolution of DG technology and the numerous incentives to install them encourage operators and planners to use them more and more frequently due to the advantages they provide. To meet the congestion management and reduce the power loss and investment the installation of DG units for the sole purpose are well explained; the backward provides the better output while the lumped method provides the close advantages of using the DG units. [14] Also the new method for sizing and placement to the DG in the distributed side is acquired and is known as PSO.

SCs work as a compensator for lagging volt-ampere reactive (VAR) and can provide only Q to the network. Therefore, SCs are less effective than DGs in minimizing real power loss in power networks. When used with DCs, SCs accomplish DGs in improving power quality, minimizing power loss, improving voltage profile, and enhancing reliability.

Table 1: Results of different algorithms

Algorithm	Constraints considered	Result
Hybrid genetic algorithm [64]	Considering 3DGs and 3SCs	TVD reduced by 2.7790p.u.[64] Energy cost loss reduced by 8467\$ a 0.5 load level [64]
Genetic Algorithm [54]	Considering 2 DGs at bus 14 Considering 2DGs at bus 29	Energy loss cost is 24\$/MWh [54] Energy loss cost is 28\$/MWh
Novel hybrid Algorithm [18]	Power loss [57] Load Rescheduling cost by the algorithm	14.24MW [18] 368.42 [18] 2510.40 [18]

According to the result of type-1 and type-2 DG reduces the active power loss by 49% and 28.25% respectively. Whereas the voltage of type-1 and type-2 DG increased by 6.95% and 1.8% respectively.[15] The algorithms used are applied on the IEEE-30 bus system [21][1], by comparing the outputs of the proposed system with the heuristic techniques it is clear that system is able to avoid the premature convergence.[1]

Real time congestion management in the distribution network is one of the most important corridor for unlocked for unlooked-for events which could do only in the real time. To break the real time congestion management problem inflexibility service could be the best option. If the cost of imbalance cost.[2]

Moreover congestion management in the distribution side has various parameters or aspects which are addressed in the reference papers. The parameters are taken into the consideration are such as retail electricity providers (REPs) [3], Dynamic Traffic (DT)[4], power loss in distribution network [5], integrating various forms of DGs in distribution system impact on the congestion management, transmission traffic along with market participants [6]. Congestion management is also hammered on the smart grid management for this innovative GCMC (grid congestion management controller) are designed. GCMC executes congestion management periodically. It verifies the status of the grid depending on the previously fixed time step. When congestion occurs in grid GCMC activates congestion assessment program.[7]

To address the problems of congestion management with the different level algorithms are used such as Genetic algorithm, novel algorithm, Local PSO, greedy algorithm. A novel algorithm based on chaos theory and differential evolution reschedules the participating generators in the power system. [18] This algorithm works in the steps as initialization of the population constraints to optimize the search operation. The mutation operation is carried out where the mutation vector is created. After this crossover operation is done for their combination to create the trail vector with combination of the mutant vector and parent vector. After this next generation population selection is to be done for the completion of the process. [18] In another paper, two methods are used, one is for enhancing the

location of the DGs and capacitors and the second one is for enhancing their capacities. For this the enhanced genetic algorithm is used which relocates the normal genetic algorithm to the hybrid genetic algorithm. [64] Hybrid genetic algorithm is able to reserve the good solutions and provide more opportunities to the worst solution. This algorithm works as per the following steps:

In the first step the algorithm will initialize the input parameters, constants and population solution. Then check for the validity of these initial solutions based on.

The following table shows the accuracy of the algorithms the constraints and correct the solution to the violation constraints. The result of the GA is as shown in the table 1. Table shows that using 3DGs and 3SCs case TVD reduced by 2.7790 p.u. Before the power compensator the energy loss cost was 35701\$ at 0.5 load level but after applying the placement of 3DGs and 3SCs it reduces up to the 8467\$ at 0.5load level. [64]

Considering the potential bounce back impact of the request reaction unit for distribution network side congestion management is done on the basis of asymmetric blocks which introduces the binary variables. To obtain certain result OPF mechanism was used where three different models are used namely lossless MILP-OPF, with loss MILP-OPF and MI-SOCP OPF.[8] As we know the integration of the different types of DGs integration in the distribution network is a certain unavoidable mode.[9] In such distribution network power flow capacities are generated by the DCRs (Direct Control Sources) while the ancillary services are provided by the DERs for solving the congestion problem[9]

Optimal placement of DG in the distribution network

With the increase in energy supply demand, various methods have been developed; a number of different problems are being faced by different methods. In order to perform the system with better efficiency and performance we could be able to find out how many power losses there are in the system in between the hours of the day. This is possible with the use of mixed integer conic programming (MICP) where hourly used power supply and power loss and also the hourly load variation is considered. [45] MICP is used to solve the

problem of the placement of the DG and its sizing. Location of the DG in the distribution network affects on the congestion management of the system. This is the ideal solution to reduce distribution congestion and expansion also to improve the system performance. [53] For this enhanced genetic algorithm the best solution is the combination of the genetic algorithm and local search for finding the capacity of the DGs in the radial system and optimal placement. Comprising the local search method enhances the search space capability and thus results in increase in consideration of finding the solution. [64] The main objective of the optimal placement is to reduce the active and reactive power loss and then enhance the voltage level of the system. [40] To reduce these losses, the location of the DG is to be determined first. For this purpose a big bang crunch algorithm is used. This algorithm gives the ability to calculate the active-reactive power loss and voltage magnitude in a radial distribution system. [36] It would be better if we know how much power loss is being caused in the distribution network. The algorithm breaks down the problem into several steps and then step by step decisions of the problem are considered. In each and every step, at the most when for charging or and discharging to the power system need to be resolved. Thus the complexity of the problem is reduced and the problem is solved with great efficiency. [17].

In this paper greedy algorithm is studied, first to decrease the search space sensitivity analysis is used and then greedy algorithm is used to detect the corresponding allotment of each and every energy storage unit. Greedy calculation is used to guarantee most extreme income for each control unit. Compared with the conventional strategy in reference, the proposed technique can

illuminate the issue viably and can be utilized to large-scale frameworks. [17]

Optimal Distributed Generation Placement (ODGP) is the non linear, mixed complex integer problem which deals with its dimensions and different constraints that may increase with the higher speed. Existing and conventional methods including the analytical method may sound complex, time consuming and difficult to use and understand. Hence the LPSO i.e. Local PSO is implemented. PSO is used as a public dependent algorithm. For exploring the dimensions particles' swarm is designated. Depending on the personal and social experience particles change their position. LPSO has the ability to avoid the local minima entrapment. These entrapments are avoided by increasing the solution's exploration capability; address the problem properly. [16]

The results of the algorithms states that the, or the Optimal Renewable Energy Sources Placements (ORESP) [16] aspect CFs for the different nodes are modified, secondly the aspect of the both nodes shows that the power loss with ODGP with good accuracy: lastly emerging critical loads for the installation of DG tends to reduce in the loss. Overall the system gives better reduction of the power loss. Overall the result of this algorithm is 75.36% of loss reduction at the 16- bus system whereas 69.67% loss reduction at 33-bus system and for the 66-bus system results in the reduction of the loss approximately 75.36%.

While comparing all these algorithms' results of the power loss reduction, our expected system tends to provide the reduction upto 92%.

Table 2: Literature review of optimal DG placements

Title	Advantages	Limitatio ns	Future work
“Distribution Locational Marginal Pricing (DLMP) for Congestion Management and Voltage Support”[43]	The system decreases the line load level and thus maintains the nodal voltage. OLTC helps to optimize the voltage profile and power flow of the system.	Get the optimal tolerance gap up to 3%	Reduce this tolerance gap up to 1% or to 0%.

“Coordinated Energy Management of Prosumers in a Distribution System Considering Network Congestion” [63]	System was developed based on the prosumer level characterized EV cluster flexibilities.	System cannot limit the losses occurring in the network and voltage constraints.	Study the network losses and voltage constraints. Find out the research flexibility utility parameter such as temperature control loads.
“Distribution Locational Marginal Pricing Through Quadratic Programming for Congestion Management in Distribution Networks” [30]	It is demonstrated in this paper, using raised optimization hypothesis, the aggregator’s optimization problem through QP is entirely arched and encompasses a special arrangement.	The different arrangements to the aggregator optimization may cause the centralized DSO optimization and the decentralized aggregator optimization to separate, and the decentralized congestion administration approach to fall flat.	Research on the parameters of the single phase loads; unbalance loads and high of R/X ratio. Voltage constraints, line loading constraints should be studied.
“Uncertainty Management of Dynamic Tariff Method for Congestion Management in Distribution Networks” [33]	Mitigate the risk of congestion management using DT method. It is sensible that the aggregators bear the fetched of the blockage for rescheduling the adaptable requests.	The most restriction of the proposed instability management method lies on the affectability investigation carried out in each iteration step, which has a presumption that the changes of the parameters are sensibly little. Hence, the deviations of the figure blunders ought to not be as well enormous; something else, the exactness of the affectability examination will be compromised.	Within the future work, the vulnerability with respect to the forecasted conventional loads can be included, which ought to be more straightforward than taking care of the vulnerability of the energy requirement of the adaptable requests.

Hosting capacity

Facilitating capacity is the sum of [10] vitality assets that the electric dispersion framework can dependably suit without noteworthy framework updates. [32] A facilitating capacity appraisal strategy for sun oriented street based on energetic shading and spatial relationship is proposed. The energetic shading caused by activity stream on sun based streets is considered to measure

its affect on PV yield of sun powered streets. A activity stream task demonstrate is utilized to mimic the genuine activity stream within the transportation framework. [45] Afterwards to solve this traffic flow problem, a dial algorithm is used which results in increasing the hosting capacity of the system. Thus the method offers an effective structure for hosting capacity to assess solar road problems. [64]

Table No. 3: Literature review of optimal DG placements

Title	Advantages	Limitations	Future work
“A Multi objective Particle Swarm Optimization for Sizing and Placement of DGs from DG Owner’s and Distribution Company’s Viewpoints”[25]	Proposes a system depends on the swarm optimization which determines the sizes and power generated by DGs; uses MOPSO algorithm. Economic analysis is done (DGs total cost, owner’s benefit).	Problems occurred on the protection, stability, security are identified.	Solve the problems regarding the system stability, security.

“Determining Optimal Location and Capacity of DG Units Based on System Uncertainties and Optimal Congestion Management in Transmission Network” [42]	After simulation results it is clear that the system has improved the calculating factors such as ATC, reliability of the system.	Unable to find the economic analysis of the system. Type of Dos cannot be stated well.	Study for the economic analysis considering the units costs, wide range of scope of the power system equipment.
“Multiple Distributed Generator Placement in Primary Distribution Networks for Loss Reduction” [22]	Size of four different types of the DGs is considered. For this IA approach is used. LSF and ELF methods are used to reduce the loss.	LSF method doesn't work properly; it is unable to reduce the losses and the computational time of the system.	Minimize the reactive active power losses using another suitable method.
“Power Congestion Management in Integrated Electricity and Gas Distribution Grids” [56]	To mitigate the issues of the distribution network PtG (power to gas) is introduced which intensely reduces the problems.	Doesn't calculate the hourly power consumption.	This system needs to be more accurate and faster.
“An Analytical Approach for Optimal Sizing and Placement of Distributed Generation in Radial Distribution Systems” [34]	The system is useful for the optimization of location and size of multiple loads, DGs.	Unable to do the economic analysis.	They are trying to do more research on the presented system.

PV hosting capacity can be done on the distributor side feeders for the determining the factors affecting the hosting capacity. Hosting capacity is defined as the total PV capacity that can be accommodated on a given feeder without negatively impacting voltage, protection and power quality and with no feeder upgrades or modifications. Considering recent high distributed renewable energy penetrations, feeder hosting capacity is an important tool to operate a feeder under utility-established thresholds without any adverse impact. [37] [32] In the paper Fajar Tri Wardana, explains a general overview of rooftop [66] PV regulation in Indonesia. From the hosting capacity obtained, the amount of rooftop PV that can be connected to the grid is about 50% of installed capacity. This is important to be implemented to support the power system. [46] In addition Voltage/Var and Voltage/Watt these two smart inverters are investigated to increase the hosting capacity PV.[58] [59] These inverters provide auxiliary frequency and voltage support, and local measurements, with these options smart inverter has abilities to push forward a step of renewable energy.

To place the optimal node repeated optimal placement is used. This allows the hosting capacity of the system. [12] Whereas the research study in the paper says that the relative hosting capacity of PV panels is increased with generic optimization study.[13] Inappropriate integration of the DGs in the distributed network leads to anomalous system behavior. It may lead to the line losses over and under voltage, harmonic distortion, mal-operation of the system, power loss.[60] To solve these problems some papers are studied have proposed a system which would enhance the hosting capacity at all nodes in the distribution network with high voltage level, low voltage level, total harmonic distortion and ampacity (ampere capacity) for governing criteria.[14] Additionally as we see the renewable energy needs to be hosted properly, the factors that are affecting are reactive power compensation, network configuration and power factor control; all these are factors that are considered in the active network management (ANM). Due to coordination of this strategy wind turbine [44] accommodates more power in the distribution network without any power loss and without violating its constraints, it also avoids the voltage deviation. [15]

Table No. 4: Literature review of hosting capacity

Title	Advantages	Limitations	Future work
“Probabilistic Hosting Capacity for Active Distribution Networks” [44]	Design the system for the DGs are placed in the network; calculate the hosting capacity considering the uncertainties of the PV and WT. Paper proposes the utilization of the SGT instead of MVC; as SGT is faster and has greater accuracy.	Unable to study the power factor, magnitude.	Way to study the real time rating, magnitude for the further understanding of the network of HC.
“Enhancing Hosting Capacity of Uncertain and Correlated Wind Power in Distribution Network With ANM Strategies” [15]	1. Nonlinear power equations are relaxed into the linear equations without disturbing the original setup. 2. ANM strategies able to do the power factor control, network reconfiguration. 3. The system has desirable computational speed.	Varies the results according to the criticality of the loads.	Research for the smart grids and their and apply the proposed method to their loads.
“Hosting Capacity: A Tool for Modernizing the Grid” [10]	1. The system is useful for the variable loads. 2. The system has three basic parameters (thermal, voltage and protection studies) which can potentially further impact on the interconnected generation size and load.	Looking for the application of integrated grids.	Some issues may appear and these are addressed before the capacity analysis; its advantages will be realized by the external stakeholders and utilities.
“Hosting Capacity Analysis for Rooftop PV in Indonesia: A Case Study in Gayo Lues District, Aceh” [66]	1. A PV rooftop is the best solution to reduce the emission. 2. Maintain the reliability and power quality.	The PV connected to the grid connected only the 50% of the grid.	Examine the detailed effect of rooftop PV as Distributed Generation.

Overall review

Congestion management in the distribution network is one of the important options to overcome the challenges and issues occurring in the congestion management of the overall system.

1. Congestion Management: Several methods are being used to mitigate the problems such as, low power quality, losses occurred in the system, load size varying as per the supply demand, etc.

for congestion, management the algorithms used which reflect in the good output; algorithms were novel algorithm [27], genetic algorithms [64] seen in the table 1, results in the 3DGs and 3SCs case TVD reduced by 2.7790 p.u. Before the power compensator the energy loss cost was 35701\$ at 0.5 load level but after applying the placement of 3DGs and 3SCs it reduces up to the 8467\$ at 0.5load level. [64]

2. Optimal placement of DGs: For the perfect and accurate congestion management we need hourly based economic analysis of the system, so that we would understand the supply demand and thus provide and reduce the power supply. For this optimal placement of DGs is used, it provides a platform to optimize the size and location of the DGs in the distributed network reconfiguration.
 3. Hosting Capacity: In order to maintain the power quality and reliability of the power supplied to the customer we required a hosting capacity. Number of methods is evaluated for the hosting capacity; systems are thus proposed in order to account for the different types of issues occurring. ANM (Active Network Management) method is also the best method for hosting the capacity of the system which results in great accuracy. [15]
2. S. Huang and Q. Wu, "Real-time congestion management in distribution networks by flexible demand swap," *IEEE Trans. Smart Grid*, vol. 9, no. 5, pp. 4346–4355, 2018, doi: 10.1109/TSG.2017.2655085.
 3. M. H. Moradi, A. R. Reisi, and S. M. Hosseinian, "An Optimal Collaborative Congestion Management Based on Implementing DR," *IEEE Trans. Smart Grid*, vol. 9, no. 5, pp. 5323–5334, 2018, doi: 10.1109/TSG.2017.2686875.
 4. F. Shen, S. Huang, Q. Wu, S. Repo, Y. Xu, and J. Ostergaard, "Comprehensive Congestion Management for Distribution Networks Based on Dynamic Tariff, Reconfiguration, and Re-Profiling Product," *IEEE Trans. Smart Grid*, vol. 10, no. 5, pp. 4795–4805, Sep. 2019, doi: 10.1109/TSG.2018.2868755.
 5. H. Labrini, A. Gad, R. A. ElShatshat, and M. M. A. Salama, "Dynamic graph based DG allocation for congestion mitigation in radial distribution networks," in *2015 IEEE Power & Energy Society General Meeting*, Jul. 2015, vol. 2015-Sept, pp. 1–5, doi: 10.1109/PESGM.2015.7286611.
 6. A. Asrari, M. Ansari, J. Khazaei, and P. Fajri, "A Market Framework for Decentralized Congestion Management in Smart Distribution Grids Considering Collaboration among Electric Vehicle Aggregators," *IEEE Trans. Smart Grid*, vol. 11, no. 2, pp. 1147–1158, 2020, doi: 10.1109/TSG.2019.2932695.
 7. R. Ciavarella, M. Di Somma, G. Graditi, and M. Valenti, "Congestion Management in distribution grid networks through active power control of flexible distributed energy resources," in *2019 IEEE Milan PowerTech*, Jun. 2019, pp. 1–6, doi: 10.1109/PTC.2019.8810585.
 8. J. Hermann, J. Kazempour, S. Huang, and J. Ostergaard, "Congestion Management in Distribution Networks with Asymmetric Block Offers," *IEEE Trans. Power Syst.*, vol. 34, no. 6, pp. 4382–4392, 2019, doi: 10.1109/TPWRS.2019.2912386.
 9. E. Luo, P. Cong, H. Lu, and Y. Li, "Two-Stage Hierarchical Congestion Management Method for Active Distribution Networks with Multi-Type Distributed Energy Resources," *IEEE Access*, vol. 8, pp. 120309–120320, 2020, doi: 10.1109/ACCESS.2020.3005689.
 10. B. Jensen and R. Uyehara, "Hosting Capacity: A Tool for Modernizing the Grid," in *2020 IEEE Conference on Technologies for Sustainability (SusTech)*, Apr. 2020, pp. 1–4, doi: 10.1109/SusTech47890.2020.9150515.

CONCLUSION

The effective distribution network means the increase in the demand of the household load also the industrial and the commercial loads. As per the literature survey we came across to state that the loss minimization is considered the basic objective in the congestion management of the power in the distribution system. While these objective basic characteristics are considered as technical constraints are line thermal limit and the node voltage. The second main objective considered here is the location of the DGs in the distribution system had made a great impact on the congestion management of the distribution network. Thus this report is an overview and focuses on background and key issues and emerging approaches to congestion management towards the Distributed line. It goes on to identify and describe policies affecting congestion management by various councils. It reviews the operational procedures in use or proposed by three of the leading independent system operators (ISOs) including ERCOT, California ISO, and P.

REFERENCE

1. S. Mandal, G. Das, K. K. Mandal, and B. Tudu, "A new improved hybrid algorithm for congestion management in a deregulated electricity industry using chaos enhanced differential evolution," *3rd IEEE Int. Conf.*, pp. 1–5, 2017, doi: 10.1109/CICT.2017.7977386.

11. Y.-J. Liu, Y.-H. Tai, C.-Y. Huang, H.-J. Su, P.-H. Lan, and M.-K. Hsieh, "Assessment of the PV hosting capacity for the medium-voltage 11.4 kV distribution feeder," in 2018 IEEE International Conference on Applied System Invention (ICASI), Apr. 2018, pp. 381–384, doi: 10.1109/ICASI.2018.8394262.
12. R. A. Aguirre, C. Peter, C. C. Caampued, and R. M. Dayapera, "Determination of Hosting Capacity of Solar and Wind Approach," TENCON 2018 - 2018 IEEE Reg. 10 Conf., no. October, pp. 1960–1965, 2018.
13. F. Ding, B. Mather, and P. Gotseff, "Technologies to increase PV hosting capacity in distribution feeders," in 2016 IEEE Power and Energy Society General Meeting (PESGM), Jul. 2016, vol. 2016- Novem, pp. 1–5, doi: 10.1109/PESGM.2016.7741575.
14. S. K. Sahu and D. Ghosh, "Hosting Capacity Enhancement in Distribution System in Highly Trenchant Photo-Voltaic Environment: A Hardware in Loop Approach," IEEE Access, vol. 8, pp. 14440–14451, 2020, doi: 10.1109/ACCESS.2019.2962263.
15. J. Xiao, Y. Li, X. Qiao, Y. Tan, Y. Cao, and L. Jiang, "Enhancing Hosting Capacity of Uncertain and Correlated Wind Power in Distribution Network With ANM Strategies," IEEE Access, vol. 8, pp. 189115–189128, 2020, doi: 10.1109/access.2020.3030705.
16. P. A. Gkaidatzis, A. S. Bouhouras, K. I. Sgouras, D. I. Doukas, and D. P. Labridis, "Optimal distributed generation placement problem for renewable and DG units: An innovative approach," IET Conf. Publ., vol. 2016, no. CP711, 2016, doi: 10.1049/cp.2016.1055.
17. W. Li, C. Lu, X. Pan, and J. Song, "Optimal placement and capacity allocation of distributed energy storage devices in distribution networks," in 2017 13th IEEE Conference on Automation Science and Engineering (CASE), Aug. 2017, vol. 2017- Augus, pp. 1403–1407, doi: 10.1109/COASE.2017.8256299.
18. M. Chindris, A. Sudria i Anderu, C. Bud, and B. Tomoiaga, "The load flow calculation in unbalanced radial electric networks with distributed generation," in 2007 9th International Conference on Electrical Power Quality and Utilisation, Oct. 2007, pp. 1–5, doi: 10.1109/EPQU.2007.4424104.
19. E. Liu and J. Bebic, "Distribution system voltage performance analysis for high-penetration photovoltaics," Renew. Energy Grid Integr. Tech. Perform. Require., no. November, pp. 107–138, 2011.
20. C. Saunders, P. Banglaore, and L. Bertling, "Congestion management in active distribution grids: optimal reserve scheduling under distributed generation uncertainty," in CIRED 2012 Workshop: Integration of Renewables into the Distribution Grid, 2012, no. May, pp. 278–278, doi: 10.1049/cp.2012.0846.
21. P. S. Georgilakis, S. Member, and N. D. Hatziargyriou, "in Power Distribution Networks : Models , Methods, and Future Research," IEEE Trans. Power Syst., vol. 28, no. 3, pp. 3420–3428, 2013.
22. D. Q. Hung and N. Mithulananthan, "Multiple distributed generator placement in primary distribution networks for loss reduction," IEEE Trans. Ind. Electron., vol. 60, no. 4, pp. 1700–1708, 2013, doi: 10.1109/TIE.2011.2112316.
23. A. K. Singh and S. K. Parida, "Congestion management with distributed generation and its impact on electricity market," Int. J. Electr. Power Energy Syst., vol. 48, no. 1, pp. 39–47, Jun. 2013, doi: 10.1016/j.ijepes.2012.11.025.
24. R. A. Verzijlbergh and L. J. De Vries, "Renewable Energy Sources and Responsive Demand . Do We Need Congestion Management in the Distribution Grid ?," pp. 1–10, 2014.
25. A. Ameli, S. Bahrani, F. Khazaeli, and M. R. Haghifam, "A multiobjective particle swarm optimization for sizing and placement of DGs from DG owner's and distribution company's viewpoints," IEEE Trans. Power Deliv., vol. 29, no. 4, pp. 1831–1840, 2014, doi: 10.1109/TPWRD.2014.2300845.
26. A. C. Mandis, A. Manoloiu, A. G. StefanaNeagoe, T. Leonida, and A. C. Neagoe, "Impact of distributed generation on steady state of electrical networks," in 2014 International Symposium on Fundamentals of Electrical Engineering (ISFEE), Nov. 2014, pp. 1–5, doi: 10.1109/ISFEE.2014.7050605.
27. D. Kavitha, P. Renuga, and S. Muthamil Priya, "Optimal sizing and placement of distributed generators in distorted distribution system by using hybrid GA-PSO," J. Theor. Appl. Inf. Technol., vol. 61, no. 3, pp. 609–616, 2014.
28. S. A. Hosseini, S. H. H. Sadeghi, A. Askarian-Abyaneh, and A. Nasiri, "Optimal placement and sizing of distributed generation sources considering network parameters and protection issues," in 2014 International Conference on Renewable Energy Research and Application (ICRERA), Oct. 2014, pp. 922–926, doi: 10.1109/ICRERA.2014.7016521.

29. A. N. M. M. Haque, P. H. Nguyen, W. L. Kling, and F. W. Bliet, "Congestion management in smart distribution network," in 2014 49th International Universities Power Engineering Conference (UPEC), Sep. 2014, no. Mv, pp. 1–6, doi: 10.1109/UPEC.2014.6934751.
30. S. Huang, Q. Wu, S. S. Oren, R. Li, and Z. Liu, "Distribution Locational Marginal Pricing Through Quadratic Programming for Congestion Management in Distribution Networks," *IEEE Trans. Power Syst.*, vol. 30, no. 4, pp. 2170–2178, 2015, doi: 10.1109/TPWRS.2014.2359977.
31. Ye Yang, "optimal location & size of ESS for Volt. Regulation," pp. 0–4, 2015.
32. M. Rossi, G. Vigano, and D. Moneta, "Hosting capacity of distribution networks: Evaluation of the network congestion risk due to distributed generation," in 2015 International Conference on Clean Electrical Power (ICCEP), Jun. 2015, pp. 716– 722, doi: 10.1109/ICCEP.2015.7177570.
33. S. Huang, Q. Wu, L. Cheng, Z. Liu, and H. Zhao, "Uncertainty Management of Dynamic Tariff Method for Congestion Management in Distribution Networks," *IEEE Trans. Power Syst.*, vol. 31, no. 6, pp. 4340–4347, 2016, doi: 10.1109/TPWRS.2016.2517645.
34. P. Prakash and D. K. Khatod, "An analytical approach for optimal sizing and placement of distributed generation in radial distribution systems," in 2016 IEEE 1st International Conference on Power Electronics, Intelligent Control and Energy Systems (ICPEICES), Jul. 2016, pp. 1–5, doi: 10.1109/ICPEICES.2016.7853119.
35. J. G. Singh, S. N. Singh, and S. C. Srivastava, "Congestion management by using FACTS controller in power system," in 2016 IEEE Region 10 Humanitarian Technology Conference (R10-HTC), Dec. 2016, pp. 1–7, doi: 10.1109/R10-HTC.2016.7906793.
36. T. D. Sudhakar and A. Vinoliya, "Optimal DG placement in distribution network using big bang-big crunch algorithm," in 2016 Second International Conference on Science Technology Engineering and Management (ICONSTEM), Mar. 2016, pp. 556–560, doi: 10.1109/ICONSTEM.2016.7560955.
37. S. Wang, S. Chen, L. Ge, and L. Wu, "for Distribution Systems Considering the Robust Optimal Operation of OLTC and SVC," *IEEE Trans. Sustain. Energy*, vol. 7, no. 3, pp. 1111–1123, 2016.
38. C. Cheng, H. Gao, Y. An, X. Cheng, and J. Yang, "Calculation method and analysis of power flow for distribution network with distributed generation," *Proc. 5th IEEE Int. Conf. Electr. Util. Deregulation, Restruct. Power Technol. DRPT 2015*, pp. 2020– 2024, 2016, doi: 10.1109/DRPT.2015.7432571.
39. P. Fortenbacher, M. Zellner, and G. Andersson, "Optimal sizing and placement of distributed storage in low voltage networks," in 2016 Power Systems Computation Conference (PSCC), Jun. 2016, pp. 1–7, doi: 10.1109/PSCC.2016.7540850.
40. S. K. Saha, S. Banerjee, D. Maity, and C. K. Chanda, "Optimal sizing and location determination of distributed generation in distribution networks," 2015 Int. Conf. Energy, Power Environ. Towar. Sustain. Growth, ICEPE 2015, pp. 1–5, 2016, doi: 10.1109/EPETSG.2015.7510148.
41. M. Sarwar and A. S. Siddiqui, "Congestion management in deregulated electricity market using distributed generation," 12th IEEE Int. Conf. Electron. Energy, Environ. Commun. Comput. Control (E3-C3), INDICON 2015, no. 1, pp. 3–7, 2016, doi: 10.1109/INDICON.2015.7443618.
42. F. H. Tavakoli, M. Hojjat, and M. H. Javidi, "Determining optimal location and capacity of DG units based on system uncertainties and optimal congestion management in transmission network," in 2017 Iranian Conference on Electrical Engineering (ICEE), May 2017, pp. 1260–1265, doi: 10.1109/IranianCEE.2017.7985235.
43. L. Bai et al., "Distribution Locational Marginal Pricing (DLMP) for Congestion Management and Voltage Support," vol. 8950, no. c, pp. 1–12, 2017, doi: 10.1109/TPWRS.2017.2767632.
44. H. Al-Saadi, R. Zivanovic, and S. F. Al-Sarawi, "Probabilistic Hosting Capacity for Active Distribution Networks," *IEEE Trans. Ind. Informatics*, vol. 13, no. 5, pp. 2519–2532, 2017, doi: 10.1109/TII.2017.2698505.
45. M. Mousavi, A. M. Ranjbar, and A. Safdarian, "Optimal DG placement and sizing based on MICP in radial distribution networks," in 2017 Smart Grid Conference (SGC), Dec. 2017, vol. 2018-Janua, pp. 1–6, doi: 10.1109/SGC.2017.8308876.
46. N. C. Koutsoukis, Di. O. Siagkas, P. S. Georgilakis, and N. D. Hatziargyriou, "Online Reconfiguration of Active Distribution Networks for Maximum Integration of Distributed Generation," *IEEE Trans. Autom. Sci.*

- Eng., vol. 14, no. 2, pp. 437–448, 2017, doi: 10.1109/TASE.2016.2628091.
47. L. Ni, F. Wen, W. Liu, J. Meng, G. Lin, and S. Dang, “Congestion management with demand response considering uncertainties of distributed generation outputs and market prices,” *J. Mod. Power Syst. Clean Energy*, vol. 5, no. 1, pp. 66–78, 2017, doi: 10.1007/s40565-016-0257-9.
 48. A. Selim, S. Kamel, and F. Jurado, “Hybrid Optimization Technique for Optimal Placement of DG and D-STATCOM in Distribution Networks,” in *2018 Twentieth International Middle East Power Systems Conference (MEPCON)*, Dec. 2018, pp. 689–693, doi: 10.1109/MEPCON.2018.8635253.
 49. S. Huang and Q. Wu, “Dynamic Subsidy Method for Congestion Management in Distribution Networks,” *IEEE Trans. Smart Grid*, vol. 9, no. 3, pp. 2140–2151, 2018, doi: 10.1109/TSG.2016.2607720.
 50. O. Rahman, K. M. Muttaqi, and D. Sutanto, “Three phase power flow analysis of distribution network performance with high penetration of single phase PV units integrated with energy storage system,” *Australas. Univ. Power Eng. Conf. AUPEC 2018*, pp. 1–6, 2018, doi: 10.1109/AUPEC.2018.8758001.
 51. F. Shen, S. Huang, Q. Wu, S. Repo, Y. Xu, and J. Ostergaard, “Comprehensive Congestion Management for Distribution Networks based on Dynamic Tariff, Reconfiguration and Re-profiling Product,” *IEEE Trans. Smart Grid*, vol. 3053, no. c, 2018, doi: 10.1109/TSG.2018.2868755.
 52. K. Prakash, F. R. Islam, K. A. Mamun, and S. Ali, “Optimal generators placement techniques in distribution networks: A review,” *2017 Australas. Univ. Power Eng. Conf. AUPEC 2017*, vol. 2017- Novem, no. 1, pp. 1–6, 2018, doi: 10.1109/AUPEC.2017.8282381.
 53. M. Kang and R. Zamora, “Optimal placement and sizing of DG and shunt capacitor for power loss minimization in an islanded distribution system,” *Lect. Notes Inst. Comput. Sci. Soc. Telecommun. Eng. LNICST*, vol. 245, pp. 43–52, 2018, doi: 10.1007/978-3-319-94965-9_5.
 54. S. Nematshahi and H. R. Mashhadi, “Distribution network reconfiguration with the application of DLMP using genetic algorithm,” *2017 IEEE Electr. Power Energy Conf. EPEC 2017*, vol. 2017-October, pp. 1–5, 2018, doi: 10.1109/EPEC.2017.8286235.
 55. J. Zhao, Y. Wang, and G. Song, “Congestion Management Method of Low-Voltage Active Distribution Networks Based on Distribution Locational Marginal Price,” *IEEE Access*, vol. 7, pp. 32240–32255, 2019, doi:10.1109/ACCESS.2019.2903210.
 56. H. Khani, N. El-Taweel, and H. E. Z. Farag, “Power Congestion Management in Integrated Electricity and Gas Distribution Grids,” *IEEE Syst. J.*, vol. 13, no. 2, pp. 1883–1894, 2019, doi: 10.1109/JSYST.2018.2850882.
 57. W. Liu, F. Luo, Y. Liu, and W. Ding, “Optimal siting and sizing of distributed generation based on improved nondominated sorting genetic algorithm II,” *Processes*, vol. 7, no. 12, pp. 1–10, 2019, doi: 10.3390/PR7120955.
 58. T. S. Ustun, J. Hashimoto, and K. Otani, “Impact of Smart Inverters on Feeder Hosting Capacity of Distribution Networks,” *IEEE Access*, vol. 7, pp. 163526–163536, 2019, doi:10.1109/ACCESS.2019.2952569.
 59. Y. Mahdavi and M. Rouhinia, “Utilizing distributed energy resources to improve voltage profile and lines congestion, considering uncertainties,” in *2019 5th Conference on Knowledge Based Engineering and Innovation (KBEI)*, Feb. 2019, pp. 366–371, doi: 10.1109/KBEI.2019.8734923.
 60. A. Y. Saber, T. Khandelwal, and A. K. Srivastava, “Fast Feeder PV Hosting Capacity using Swarm Based Intelligent Distribution Node Selection,” in *2019 IEEE Power & Energy Society General Meeting (PESGM)*, Aug. 2019, vol. 2019-Augus, pp. 1–5, doi: 10.1109/PESGM40551.2019.8973389.
 61. M. Sarwar, A. S. Siddiqui, and Farheen, “Bid Responsive Generation Rescheduling for Congestion Management in Deregulated Electricity Market,” in *2019 International Conference on Power Electronics, Control and Automation (ICPECA)*, Nov. 2019, vol. 2019-Novem, pp. 1–4, doi: 10.1109/ICPECA47973.2019.8975440.
 62. R. A. Aguirre, C. P. C. C. Caampued, and R. A. M. Dayapera, “Determination of Hosting Capacity of Solar and Wind Distributed Generation (DG) Using Stochastic Approach,” *IEEE Reg. 10 Annu. Int. Conf. Proceedings/ TENCON*, vol. 2018-October, no. October, pp. 1960–1965, 2019, doi: 10.1109/TENCON.2018.8650071.
 63. J. Hu, J. Wu, X. Ai, and N. Liu, “Coordinated Energy Management of Prosumers in a,” vol. 3053, no. c, pp. 1–11, 2020, doi: 10.1109/TSG.2020.3010260.
 64. E. A. Almabsout, R. A. El-Sehiemy, O. N. U. An, and O. Bayat, “A Hybrid Local Search-Genetic Algorithm for Simultaneous Placement of DG Units and Shunt

- Capacitors in Radial Distribution Systems,” IEEE Access, vol. 8, pp. 54465–54481, 2020, doi: 10.1109/ACCESS.2020.2981406.
65. A. Selim, S. Kamel, A. S. Alghamdi, and F. Jurado, “Optimal Placement of DGs in Distribution System Using an Improved Harris Hawks Optimizer Based on Single- And Multi-Objective Approaches,” IEEE Access, vol. 8, pp. 52815–52829, 2020, doi: 10.1109/ACCESS.2020.2980245.
66. F. T. Wardana and T. Riady, “Hosting capacity analysis for rooftop PV in Indonesia: A case study in Gayo Lues district, Aceh,” Proceeding - 2nd Int. Conf. Technol. Policy Electr. Power Energy, ICT- PEP 2020, vol. 3, pp. 12–15, 2020, doi: 10.1109/ICT-PEP50916.2020.9249821.
67. L. Wu, Y. Yuan, H. Wu, and K. Qian, “PV Hosting Capacity Assessment of Solar Road Considering Dynamic Shading and Spatial Correlation,” Asia- Pacific Power Energy Eng. Conf. APPEEC, vol. 2020-Septe, pp. 0–4, 2020, doi: 10.1109/APPEEC48164.2020.9220378.
68. D. Xiao and H. Chen, “Stochastic Up to Congestion Bidding Strategy in the Nodal Electricity Markets Considering Risk Management,” IEEE Access, vol. 8, pp. 202428–202438, 2020, doi: 10.1109/ACCESS.2020.3015025.
69. S. Riyaz, R. Upputuri, and N. Kumar, “Congestion Management in Power System—A Review,” Lect. Notes Electr. Eng., vol. 699, pp. 425–433, 2021, doi: 10.1007/978-981-15-7994-3_39.

Selection of Traction Motor and Battery Capacity for Design and Development of 249 Kg Electric Two wheeler

Pooja Shastri

Mugdha Kulkarni

Devendra J. Goyar

Assistant Professor
Electrical Engineering Department
K J College of Engineering
Pune, Maharashtra
✉ poojashastri.kjcoemr@kjei.edu.in

ABSTRACT

Nowadays Electric Vehicle coming on road due to day by day increasing fossil fuel cost, carbon emission with required maintenance cost. In present the storage of fossil fuel is shorter so that the design and development in automobile sector. In present coming necessary to develop high efficient vehicle technology with proper rating selection of electric traction motor power, torque, and speed with required battery capacity to drive the traction vehicle. For proper mechanical power, torque and speed produces high efficient reliable operation of vehicle. In the paper the selection of traction motor and battery capacity for the two wheeler having total weight 249 Kg with speed 60 kmph.

KEYWORDS : Electric vehicle component, Different forces on the Electric Vehicle (Rolling resistance, Drag resistance, Acceleration force).

INTRODUCTION

In the electric vehicles are run on the electric supply by means of energy storage system like battery and mechanical power will be developed by electric motor. Recently PMSM used instead of BLDC motor as well as DC motor and Induction Motor due to its high efficient operation with high torque to weight ration. In the electric vehicle significant role play by power converter which will be convert dc supply of battery into Ac supply that is fed to the motor by means of PWM technique. This power converter has been operated in the bi directional operation. It is convert DC to Ac when motoring operation and convert AC to dc again during the regenerative braking operation. Maximum energy conversion will be depends on the velocity of vehicle. The power electronic conversion efficiency is about 90 percent the performance of the vehicle actually depends on the proper rating of traction motor with battery capacities. The typical block diagram of Electric vehicle shows the arrangement of vehicle system.

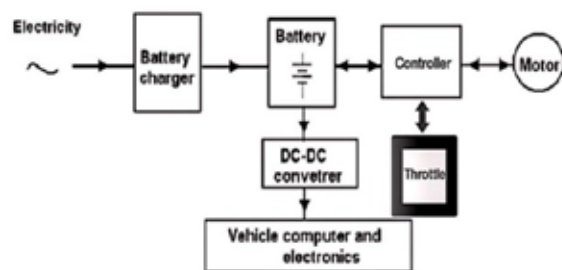


Fig.1 Electric Vehicle Block Diagram

COMPONENTS

Motor Controller

A motor controller is a main component of the EV that operates bi directional operation such as Motoring mode and other is regenerative braking mode operation. In the EV system Hall Effect sensor is placed in the motor which has to sense the rotor speed and its signal fed back to converter. Which is just like closed loop operation

of EV. A motor controller is an essential device that encompasses both manual and automatic functionalities for initiating and halting the motor's operation. It provides the flexibility of choosing between forward and reverse rotations based on specific requirements. Additionally, it allows users to regulate the motor's speed effectively, ensuring optimal performance for various applications. Importantly, a motor controller is equipped with features to limit or regulate the torque, preventing undue strain on the motor and associated machinery. Furthermore, it plays a crucial role in safeguarding the motor system against overloads and faults, enhancing the overall safety and durability of the equipment it operates. In essence, a motor controller acts as a sophisticated control hub, enabling seamless and secure motor operation in diverse industrial and commercial settings. In the actual practice of EV system utilizes the trapezoidal or sinusoidal controller used. Generally trapezoidal converter used in case of hub brushless Dc motor used in the Electric vehicle. Nowadays permanent magnet synchronous motor is used in the electric vehicle with sinusoidal PWM technique. The battery block is interfaced with the motor controller block. The motor controller controls all the functional capabilities and is the central component of the system. The basic requirement for the control is to regulate the amount of power applied to the motor. The motor controller can be adjusted to synchronize with other brushless motors. For instance, in electric vehicles, the motor controller manages power distribution to the motor, enabling efficient and controlled movement. In robotics, these controllers facilitate precise motion and coordination of robotic limbs or mechanisms. They're integral in renewable energy systems, like wind turbines and solar tracking systems, optimizing power generation. The advancements in motor controller technology have significantly contributed to the efficiency, performance, and reliability of motor-driven devices across industries. It's fascinating how this component, acting as the brain of the motor system, plays such a crucial role in modern technology.

BLDC Hub Motor

The Permanent Magnet Synchronous Motor (PMSM) stands as a significant innovation in the realm of electric propulsion, particularly in the domain of electric vehicles.

This advanced type of Permanent Magnet Motor has gained widespread adoption due to its remarkable efficiency and power density. In comparison to Induction motors, PMSM motors exhibit a notable advantage, being up to 15 percent more efficient. This heightened efficiency translates into a more effective conversion of electrical energy into mechanical power, thereby enhancing the overall performance of electric vehicles. A Brushless DC (BLDC) motor is a highly efficient type of synchronous electric motor that operates using direct current (DC) electricity. Unlike traditional DC motors, BLDC motors do not rely on a mechanical commutation system with brushes and a commutator. Instead, they employ an electronic commutation system, usually based on Hall effect sensors, to control the switching of the stator windings. One of the key advantages of BLDC motors lies in their linear relationship between current and torque, as well as voltage and rotational speed (RPM). This linear relationship makes them highly predictable and controllable, allowing for precise adjustments in various applications. By altering the voltage or current supplied to the motor, one can easily regulate the speed and torque output, making BLDC motors ideal for applications where precise control is crucial, such as in electric vehicles. In a BLDC motor, the permanent magnets rotate while the electromagnets in the stator remain static. This design is akin to a permanent magnet synchronous motor used in AC systems. A typical three-phase BLDC motor comprises stationary stator windings and a rotor with one or more permanent magnets. Unlike AC synchronous motors, BLDC motors require a method of detecting the rotor's position or magnetic poles in a BLDC (Brushless DC) motor is crucial for the precise control of the motor's operation. This information helps the motor controller in synchronizing the commutation of the motor's phases, allowing it to apply the correct voltage to the appropriate windings at the right time. Hall elements or optical sensors are commonly used as position/pole sensors. A DC-to-DC converter is a fundamental component in electronics and power systems. It's designed to alter the voltage level of a direct current (DC) power source to a different level, which could be higher, lower, or even inverted (changing from positive to negative voltage or vice versa). It is essential in electric vehicles (EVs), connecting components like the frequency controller

(FC), battery, or super capacitors module to the DC-link. These converters temporarily store input energy, releasing it at a different voltage. In the realm of DC-to-DC converters and power electronics, energy storage and transfer often occur through magnetic field storage components like inductors and transformers, as well as electric field storage components like capacitors. While DC/DC converters can transfer power in one direction, most can be made bi-directional, vital in applications like regenerative braking. The power flow can be controlled by adjusting the duty cycle (the ratio of on/off time of the switch). Some converters, especially those based on transformers, offer isolation between input and output. However, these converters have drawbacks, including complexity, electronic noise, and, in certain cases, high cost. In this paper calculation parameter of Electric two wheeler traction motor power, torque, speed and battery capacity required for vehicle.

SPECIFICATION OF VEHICLE

Table 1. The vehicle parameter

Parameter	Values
Kerb Wight	109 Kg
Wind velocity	1.16m/sq. sec
Wheel diameter	10 inch = 25.40 cm
Passenger weight	140 kg
Inclination angle	10 degree
Gross vehicle weight	249 kg
Rolling resistance at asphalt road	0.004
Gravitational force	9.81m/sq. sec.
Aerodynamic force coefficient	0.5
Front area of vehicle	0.8
Maximum speed of vehicle	60 kmph = 16.67 m/sec
Acceleration	1.67m/sq. sec

FACTORS AFFECTING ON PERFORMANCE OF EV

Rolling Resistance: Rolling resistance is the resistance offered by road surface during the motion of the vehicle. This factor shall be based on different road condition.

That equation represents the rolling resistance force formula, which calculates the force required to overcome rolling resistance for a moving object. Here's

a breakdown of the variables:

- F rolling represents the rolling resistance force.
- Crr: is the coefficient of rolling resistance, a value that characterizes the resistance encountered by a rolling object on a surface.
- M represents the mass of the object in kilograms.
- g is the acceleration due to gravity, typically taken as 9.81 m/s² on the Earth's surface.

When you multiply the coefficient of rolling resistance by the mass of the object and the acceleration due to gravity, you get the force required to counteract the resistance that the object experiences while rolling on a surface. This equation is particularly useful in transportation engineering or vehicle dynamics to estimate the energy or force needed to move a vehicle or object on a surface with known rolling resistance characteristics

$$F_{\text{rolling}} = 249 * 9.81 * 0.004 = 9.77 \text{ N}$$

Following table shows the standard typical values for coefficient of rolling resistance.

Table 2. Coefficient of rolling resistance

0.001-0.002	Rolling resistance on Railroad steel
0.001	Rolling resistance offered by Bicycle tire on wooden track
0.002	Rolling resistance on Bicycle tire on concrete
0.004	Rolling resistance on Bicycle tire on asphalt road
0.008	Rolling resistance on Bicycle tire on rough paved road
0.006-0.01	Rolling resistance on Truck tire on asphalt
0.01-0.015	Rolling resistance on Car tire on concrete, new asphalt, cobbles small new
0.02	Rolling resistance on Car tire on tar or asphalt
0.02	Rolling resistance on Car tire on gravel-rolled new
0.03	Rolling resistance on Car tire on cobbles-large worn
0.04-0.08	Rolling resistance on Car tires on solid sand, gravel loose worn, soil medium

0.2-0.4	Rolling resistance on Car tires on loose sand
0.001-0.002	Rolling resistance on Railroad steel wheels on steel rail
0.001	Rolling resistance on Bicycle tire on wooden track
0.002	Rolling resistance on Bicycle tire on concrete
0.004	Bicycle tire on asphalt road
0.008	Bicycle tire on rough paved road
0.006-0.01	Truck tire on asphalt
0.01-0.015	Car tire on concrete, new asphalt, cobbles small new
0.02	Car tire on tar or asphalt
0.02	Car tire on gravel-rolled new
0.03	Car tire on cobbles-large worn

Gradient Resistance

Gradient resistance is the resistance offered when vehicle run on hilly area or bridges and it offered gradient forces on downward and upward side both. It can be calculate as

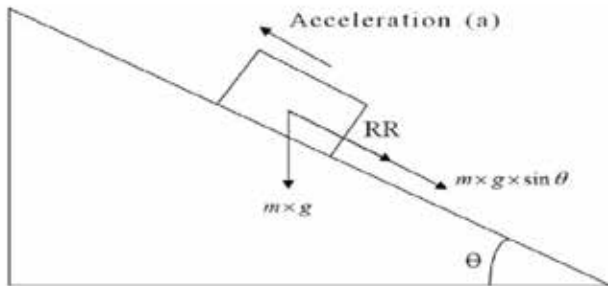


Fig. gradient forces acting on vehicle

The formula for calculating the gradient resistor is given by equation below

$$F_{\text{gradient resistance}} = \pm M \times g \times \sin \theta$$

When an object moves up the incline, the direction of motion is opposite to the direction of the gravitational force pulling it down. Therefore, the motion is against the force of gravity, and it is assigned a positive sign. Conversely, when an object moves down the incline, the motion is in the same direction as the gravitational force. The motion is with the force of gravity and is assigned a negative sign. This sign convention is crucial when dealing with calculations involving forces, accelerations, and energies on inclined planes. For example, when calculating work done against gravity

while moving up the incline, the work is positive. On the other hand, work done by gravity while moving down the incline is negative. In the case of the electric scooter running at an angle θ with respect to the horizontal surface, this sign convention would be applied to any calculations involving forces, accelerations, or energy changes related to the scooter's motion on the incline.

$$F_{\text{gradient resistance}} = \pm M \times g \times \sin \theta$$

$$= 249 \times 9.81 \times \sin(100)$$

$$= 424.16 \text{ N}$$

Aerodynamic Drag

Aerodynamic drag, a resistive force caused by viscous effects acting on a vehicle, is intricately linked to the vehicle's shape. This force is crucial to consider in vehicle design, especially in the realm of automobiles and other forms of transportation. The formula used to calculate aerodynamic drag is expressed as

$$F_{\text{aerodynamic drag}} = 0.5 \times CD \times Af \times \rho \times v^2$$

Where, CD=Drag coefficient, Af=Frontal area

ρ = Air density in kg/m³, v = velocity in m/s

For application consider, maximum speed of our scooter is 60 kmph

$$F_{\text{aerodynamic drag}} = 0.5 \times 0.5 \times 0.8 \times 1.16 \times 16.672$$

$$= 64.4 \text{ N}$$

Table 3. Coefficient of drag

Vehicle	CD	Af
Motorcycle with rider	0.5-0.7	0.7-0.9
Open convertible	0.5-0.7	1.7-0.9
Limousine	0.22-0.4	1.7-2.0
Coach	0.4-0.8	6-10
Truck without trailer	0.45-0.8	6.0-10.0
Truck with trailer	0.55-1.0	6.0-10.0
Articulated vehicle	0.5-0.9	6.0-10.0

Total Forces Calculation

Total Forces = F_{rolling} + F_{gradient} + Aerodynamic drag

$$= 9.77 + 424.16 + 64.4$$

$$= 498.40 \text{ N}$$

Total Power = (Ftotal * Average-speed)/3600
 = (498.40 * 60)/3600
 = 8306 watt at 60 KMPH speed (Maximum power

Developed by motor at loading condition).

Current draw during loading

8306 = 72 * I = 115.36 Amp

Torque at wheel = Ftotal * radius of wheel
 = 498.40* 0.127
 = 63.29 NM (Peak Torque) at wheel

Motor torque becomes = 63.29*19/45 = 26.79 Nm

Speed of wheel at 60 KMPH = velocity of vehicle / perimeter of wheel

Perimeter of wheel = 2*pi* radius of wheel
 = 2*3.142*0.127 = 0.8

= 16.67/0.8 = 1253.27 RPM of wheel

Calculate Motor speed = wheel speed * gear ration
 = 1253.27 * 45/19
 = 2970 RPM of Traction Motor

At flat road Gradient resistance offered to vehicle is zero

So Ftotal at flat road = 9.77 + 64.4
 = 74.17 N

So power required at float road condition

= (F total * velocity of vehicle)/ 3600
 = (74.14 * 60*1000)/3600
 = 1236 watt at flat road condition

Torque produce by eV at flat road condition = Torque at wheel = Ftotal * radius of wheel

= 74.17 * 0.127 = 9.41 NM at flat Road

Torque at motor = 9.41 * 19/45 = 3.971 NM

Table 4. Calculation parameter at climbing and flat road condition

Parameter	Forces	Output	Motor torque and speed
At climbing (hilly area)	498.4 N	60,KMPH T = 63.29 NM (Peak Torque, 1253 RPM at wheel	8306 watt at T = 27 NM torque,2970 RPM
At flat road condition include acceleration force	74.17N	1236 watt at flat road condition with T = 9.41 NM	1236 watt T= 3.97 NM at motor

Table 5. Selection of Traction motor according to forces calculation

4000W V3 Mid Drive Motor (Air-Cooled Version, 19:45 Reduction Gear)		
Motor Size	Motor Diameter	162mm
	Motor Length	242mm
	Gear Box	Gear Box 19:45 Reduction Gear Box
	Shaft / Axle	Shaft / Axle Spline Shaft
Motor Phase	Motor Type	Motor Type Brushless DC IPM PMSM Motor
	Number of Motor Phase	3
	Cross Section of Cable	Cross Section of Cable 20 Square Millimeter
	Poles	5 Pairs of Poles
Motor Power	Rated Power	Rated Power 4000W
	Maximum Power	Maximum 15KW (Sometimes 20KW)
	Rated Voltage	72V
	Continuous Current	60 Amp

Motor Power	Maximum Current	Maximum Current 120A (200A in 30 seconds)
	Maximum Efficiency	Maximum Efficiency 85-91.6%
	Maximum Torque	more than 120N.m after reduction
	Maximum Torque after reduction	Maximum Torque more than 140N.m after reduction
	Rotating Speed	Rotating Speed 3800rpm to 6000rpm

$$4000 = 72 * I$$

$$I = 55.56 \text{ Amp}$$

At rated load condition motor draws 55.56 amps current

But at loading condition like climbing area or bridges current draw capacity of battery

Maximum power develop by motor at overload condition

$$P = V * I$$

$$8306 = 72 * I$$

$$I = 115.36 \text{ amp}$$

Table 5. Battery capacity and range according to loading on vehicle

Battery Capacity	Travelling Range
70 AH	60 KM
139 AH	120 KM

Battery Selection for Vehicle

Motor power = 4000 watt but actually battery 20 percent more than motor power so that we calculate as watt hr. of battery

$$4000 * 1 = 4000 \text{ watt hr.}$$

$$\text{Calculate watt-hr. /Km} = 4000/60$$

$$\text{watt-hr/Km} = 66.67 \text{ watt-hr/KM}$$

$$\text{Calculate amp-hr/KM} = \text{watt-hr/Km/voltage}$$

$$66.67/72 = 0.93 \text{ Amp-hr/Km}$$

$$4000 * 1.2 = 4800 \text{ watt Hr.} = 4.8 \text{ KWH}$$

now we can divide above equation by 0.85 because motor efficiency =

$$4800/0.85 = 5647.05 = 5.64 \text{ KWH}$$

$$\text{Battery current in AH} = 5647/72 = 78.43 \text{ AH}$$

$$\text{Calculate Amp-Hr} = 0.93 * 1.2 * 1.04 * 60 = 70 \text{ Amp-Hr}$$

For 60 kmph 60 KM range we have required 70 AH capacity of battery

In case 100 KM range

$$\text{The capacity of battery} = 0.93 * 1.2 * 1.04 * 100 = 116 \text{ AH}$$

At Rated condition draw current through battery

$$P = v * I$$

But actual practice EV will give v less output when running on climbing area

(Capacity in AH/current consumption) * velocity in KMPH

$$(139/115.36) * 60$$

$$= 72 \text{ km}$$

Actual m practice Electric vehicle mileage running in full loading on climbing area for maximum duration then range of vehicle will be reduces from 120 km range to 72 km

CONCLUSION

In this study, In the study we have conclude that

- When vehicle running on climbing area the electric vehicle generates maximum power up to 8306 watt at maximum torque and speed of motor is about 27 NM torque with 2970 RPM near about 3000 RPM.
- Actual practice also we have calculated in the paper this paper is when electric vehicle running on flat road the electric vehicle generates maximum forces is only 74.14 N. At this force on flat road condition the vehicle becomes generates approximately torque at wheel is up to 9.41 N and motor torque is only about 3. 97 Motor that is responsible for reduces the millage of vehicle.

- Design of hardware required its voltage about 72 volt, and maximum current capacity in amp is up to 150 Amp PWM converter used with closed loop hall effect sensor for implementing closed loop operation with regenerative braking. The required battery capacity from the forces on vehicle during the climbing condition and flat road condition the electric vehicle gives ranges about 70 ah capacity run up to 60 Km and 120 KM range in 140 AH a but due to loading the output becomes reduces up to 72 km ranges because due to loading maximum current will be draw by

REFERENCES

1. Prof. Mahesh S. Khande¹, Mr. Akshay S. Patil², Mr. Gaurav C. Andhale³ Mr. Rohan S. Shirsat⁴., Design and Development of Electric scooter, International Research Journal of Engineering and Technology (IRJET) Volume: 07 Issue: 05 | May 2020
2. Jayasheel kumar k a¹, arif mohamed², anurag³ mohammed faizaan⁴, sai lohith k n². Fabrication of an electric two-wheeler. International Research Journal of Engineering and Technology (IRJET), Volume: 08 Issue: 06 | June 2021
3. Electric and Hybrid Vehicle Design fundamentals Iqbal Hussain, Library pof Congress cataloging-in-publication, Data Includes bibliographical references and indexes.
4. Atul Kasid¹, Aditya Pacharne², Umesh Kawale³, Omkar Kulkarni⁴ Design and modification of conventional scooter into an electric scooter International Research Journal of Engineering and Technology: Volume:09 Issue:07/July-2022.

Quantitative Analysis of the Impact of Phantom Power on Voltage Stability in Electrical Power System Networks

Manish Parihar, Dharmendra Jain

Ph.D.

Scholar, Department of Electrical Engineering M.B.M University
Jodhpur, Rajasthan

M. K. Bhaskar

Professor

Department of Electrical Engineering
M.B.M University
Jodhpur, Rajasthan
✉ mkb31@rediffmail.com

ABSTRACT

The establishment of industries as a result of the deregulation of power supply in response to rising demand puts more stress on the current power generation infrastructure. The power system may frequently operate near the limit of voltage stability with more efficient use of transmission lines. It is therefore very likely that the system will experience voltage instability or that there will be a voltage collapse or complete blackout. Thus, when planning and operating power systems, voltage stability analysis is crucial. This research paper uses the voltage stability index as a quantitative tool for assessing a power system's stability margin. It provides grid operators with a valuable tool to evaluate the system's stability margin under various operational scenarios. The IEEE bus power test system is employed for case studies, and the simulation results show how these stability indices assist in finding significant voltage instability conditions.

KEYWORDS : *Voltage collapse, Load flow, Voltage stability indexes, weakest bus, Power system networks.*

INTRODUCTION

In recent decades, the global energy sector has undergone tremendous transition, typified by a significant shift from old, vertically integrated power architectures to more competitive and market-oriented frameworks.

The concept of deregulation is central to this transformative process, as it tries to improve efficiency, encourage competition, and optimise resource allocation in the power sector. In an effort to promote market-driven procedures, foster innovation, and eventually increase benefits to industry stakeholders and consumers alike, governments worldwide are deregulating the electricity system, departing from the previous monopoly model. [1].

Power system stability, a critical component guaranteeing the dependable and secure transmission of electricity, is significantly impacted by the deregulation of the power system..

It often leads to the emergence of a more complex

and interconnected power system. The integration of multiple market participants, each with its own generation and demand characteristics, can result in intricate network dynamics [2].

The deregulated market environment introduces volatility and uncertainty in power system operations. Fluctuations in electricity prices, supply-demand imbalances, and the variability of renewable energy sources can contribute to system instability, requiring advanced control mechanisms to ensure a reliable power supply [3].

While increasing market competition and economic efficiency, power system deregulation may bring about problems with voltage instability. Voltage instability is a condition in which the power system's voltage levels drop, potentially leading to equipment malfunction, service interruptions, and, in severe cases, cascading system failures [4]. The shift from a regulated to a deregulated power system can influence voltage stability in several ways.

Engineers frequently use an indicator known as the Voltage Stability Index to evaluate and quantify the level of voltage stability in a power system (VSI). The Voltage Stability Index is a numerical indicator used to evaluate the proximity of a power system to voltage instability [5]. It provides a quantitative measure of the margin between the current operating point and the point at which voltage instability is likely to occur. The VSI is particularly useful for identifying potential voltage stability issues and taking preventive or corrective actions before a system experiences critical conditions [6].

Understanding the VSI enables utilities to implement preventive measures, such as system reinforcement, optimal generator scheduling, and the installation of additional reactive power support, to enhance overall voltage stability.

Reactive power also known as phantom power is a key factor in maintaining voltage stability, which is essential for the secure operation of a power system [7]. In situations where the demand for reactive power exceeds the available supply, voltage levels can drop, leading to voltage instability. Conversely, an excess of reactive power can result in voltage instability with excessive voltage levels. Balancing reactive power resources is critical for preserving voltage stability [8]. The Voltage Stability Index is influenced by the power factor of the system.

In this research paper at different power factor condition system stability is examined by using voltage stability indicators. IEEE 5 test bus power system network is utilized for study and analysis.

VOLTAGE STABILITY INDEX

In power system analysis, the voltage stability index (VSI) is a quantitative measure that is used to evaluate the extent to which a power system is susceptible to voltage instability. Voltage instability is a phenomenon in which the system's voltage levels diverge from their base values, potentially causing cascading failures and extensive disruptions. [9]. The VSI enables power system operators and engineers to assess the stability margin and conduct preventive or corrective steps before voltage instability arises. As previously discussed, the Voltage Stability Index measures the

difference between the current operating point and the point at which voltage instability is most likely to occur [10]. It takes into account parameters such as loadability margins, angle variances, reactive power margins, and transmission restrictions.

FVSI(Fast voltage stability index)

The fast voltage stability index (FVSI) was proposed by Musirin [11]. The voltage quadratic equation for the two-bus system serves as the basis for this index. FVSI is based on the concept of power flow across network lines and is defined as follows:

$$FVSI = (4\{Z\}^2 Q_r) / (\{V_s\}^2 X)$$

A value of less than one for the FVSI indicates a steady state. If the FVSI approaches 1.00, the line is on the verge of instability. If the FVSI exceeds 1.00, the bus voltage abruptly drops, resulting in system collapse [12].

Line Stability Factor (LQP)

The LQP index is derived by A. Mohamed et al.

$$LQP = 4 [X / \{V_i\}^2] [((X \{P_i\}^2) / \{V_i\}^2) + Q_j]$$

In this instance, the voltage on the sending bus is V_i , the line reactance is X , the active power flow at the sending bus is P_i , and the reactive power flow at the receiving bus is Q_j . To maintain a secure situation, the LQP index must remain smaller than one. [13].

Stability power prediction index (SPPI)

SPPI stability prediction power index is based on transmission line complex power with ABCD parameters using a receiving end circle diagram [14]. The stability prediction power index is given by:

$$SPPI = [1 - (((V_i^2 / (4AB \sin^2\{(180^\circ - (\beta - \alpha) + \phi)/2\})) - S_i) / (V_i^2 / (4AB \sin^2\{(180^\circ - (\beta - \alpha) + \phi)/2\})))]$$

Here, A , B are generalized line constant, V_i represents the source of sending-end voltage, S_i sending end complex power and ϕ is power factor angle.

These indices have values ranging from 0 to 1, depending on the operational load [15]. When the system is substantially loaded, the values of these indices approach one, indicating that the system is getting closer to the point of voltage collapse.

SIMULATION & RESULTS

The IEEE 5-Bus system is a standard power system model with known impedances and admittances [16]. It composed of 2 generators, G1 and G2, located at buses 1 and 4 respectively, 3 load buses located at buses 2, 3 and 5 respectively and 7 transmission lines as seen in Figure 1.

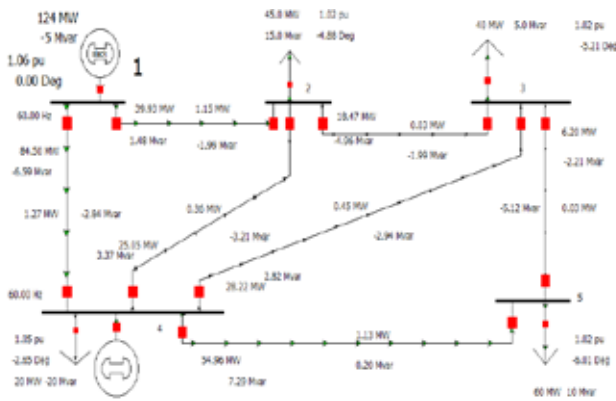


Fig. 1 IEEE 5 Bus Test System

The N-R approach is used to analyse the load flow in the power system network[17]. The loading of bus 2 is gradually increased from zero to full load. To investigate the stability of the system under different operating conditions voltage sensitive load, namely constant power is considered. To study the effect of reactive power on system stability different power factor scenario are taken into account.

Case I: Loading at .707 lagging power factor. The system is more vulnerable to voltage instability when the power factor falls below 0.8. Higher inductive loads demand increased reactive power, and Whenever the system is unable to provide adequate support, the stability index is likely to indicate a reduced margin, signalling a higher risk of voltage instability.

Table 1: Per Unit Bus Voltage at .707 Lag Power Factor

P ₂ p.u.	Q ₂ p.u.	Bus 1 p.u.	Bus 2 p.u.	Bus 3 p.u.	Bus 4 p.u.	Bus 5 p.u.
0	0	1.06	1.04	1.03	1.047	1.02
1.50	1.50	1.06	0.84	0.86	0.98	0.92
2.00	2.00	1.06	0.69	0.73	0.92	0.82
2.15	2.15	1.06	0.56	0.60	0.86	0.74

Table 1 shows that as the loading on the specified load bus increases, the voltage of the system load bus begins to decrease from its base values. The values of the FVSI, LQP, and SPPI index vary accordingly, as shown in Tables 2, 3, and 4.

Table 2: Transmission Lines FVSI Index Values At .707 Lag Power Factor

P ₂ p.u.	FVSI (1-2)	FVSI (2-3)	FVSI (1-4)	FVSI (4-2)	FVSI (4-3)	FVSI (4-5)	FVSI (5-3)
0	0.020	0.005	0.017	0.003	0.006	0.022	0.054
1.50	0.449	0.101	0.156	0.396	0.330	0.144	0.206
2.00	0.638	0.203	0.332	0.583	0.502	0.228	0.409
2.15	0.701	0.347	0.478	0.704	0.631	0.311	0.643
Ranking	2	6	5	1	4	7	3

Table 3: Transmission Lines LQP Index Values at .707 Lag Power Factor

P ₂ p.u.	LQP (1-2)	LQP (2-3)	LQP (1-4)	LQP (4-2)	LQP (4-3)	LQP (4-5)	LQP (5-3)
0	0.02	0.005	0.018	0.004	0.009	0.032	0.052
1.50	0.53	0.09	0.17	0.403	0.340	0.160	0.187
2.00	0.81	0.18	0.355	0.637	0.547	0.257	0.379
2.15	0.96	0.32	0.507	0.825	0.729	0.358	0.603
Ranking	1	7	5	2	3	6	4

Table 4: Transmission Lines SPPI Index Values at .707 Lag Power Factor

P ₂ p.u.	SPPI (1-2)	SPPI (1-4)	SPPI (2-3)	SPPI (4-3)	SPPI (4-5)	SPPI (5-3)	SPPI (4-2)
0	0.143	0.088	0.028	0.084	0.161	0.093	0.058
1.50	0.868	0.340	0.102	0.519	0.327	0.243	0.598
2.00	1.398	0.572	0.209	0.853	0.467	0.429	1.001
2.15	1.865	0.785	0.349	1.196	0.617	0.608	1.409
Ranking	1	4	7	3	5	6	2

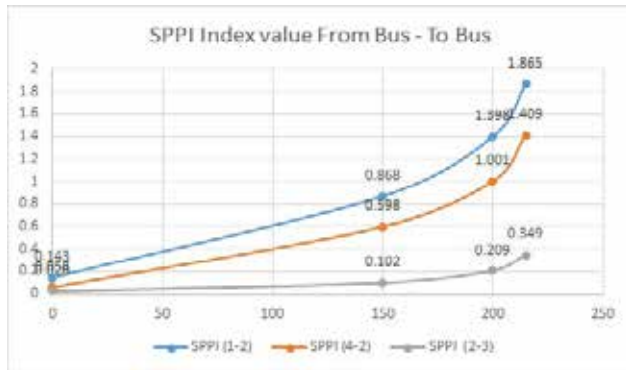


Fig. 2 SPPI index value for .707 lag power factor

Case II: Loading at unity power factor. At the unity power factor, where the load is purely resistive, the VSI is frequently quite steady. Reactive power demand is modest, and the system focuses on real power considerations.

However, other factors such as load variations and transmission constraints still influence voltage stability. The VSI is likely to indicate a relatively comfortable margin under these conditions.

Table 5: Per Unit Bus Voltage at Unity Power Factor

P ₂ p.u.	Bus 1 p.u.	Bus 2 p.u.	Bus 3 p.u.	Bus 4 p.u.	Bus 5 p.u.
0	1.06	1.042	1.038	1.047	1.022
1.00	1.06	1.019	1.019	1.047	1.015
3.00	1.06	0.916	0.925	1.005	0.952
4.00	1.06	0.786	0.802	0.935	0.857
4.20	1.06	0.723	0.742	0.901	0.811
4.30	1.06	0.667	0.688	0.870	0.769

Reactive power support contributes to enhanced transmission capacity by minimizing line losses and voltage drops along the transmission network as described in Table V. This, in turn, allows for the efficient transfer of electrical power over long distances, improving the overall stability and reliability in the power system.

Table 6: Transmission Lines FVSI Index Values at Unity Power Factor

P ₂ p.u.	FVSI (1-2)	FVSI (2-3)	FVSI (1-4)	FVSI (4-2)	FVSI (4-3)	FVSI (4-5)	FVSI (5-3)
0	0.020	0.005	0.017	0.003	0.006	0.022	0.054

1.00	0.037	0.001	0.042	0.021	0.021	0.028	0.042
3.00	0.094	0.008	0.027	0.039	0.050	0.057	0.010
4.00	0.088	0.020	0.117	0.036	0.081	0.104	0.104
4.20	0.084	0.029	0.192	0.035	0.100	0.133	0.168
4.30	0.095	0.037	0.259	0.021	0.109	0.161	0.236
Ranking	1	6	2	7	5	4	3

Table 7: Transmission Lines LQP Index Values at Unity Power Factor

P ₂ p.u.	LQP (1-2)	LQP (2-3)	LQP (1-4)	LQP (4-2)	LQP (4-3)	LQP (4-5)	LQP (5-3)
0	0.027	0.0052	0.018	0.004	0.009	0.032	0.052
1.00	0.103	0.001	0.055	0.037	0.037	0.043	0.038
3.00	0.484	0.0098	0.110	0.175	0.154	0.095	0.025
4.00	0.832	0.0288	0.263	0.377	0.328	0.175	0.151
4.20	0.960	0.0435	0.357	0.489	0.427	0.223	0.235
4.30	1.075	0.058	0.439	0.592	0.520	0.270	0.325
Ranking	1	7	4	2	3	6	5

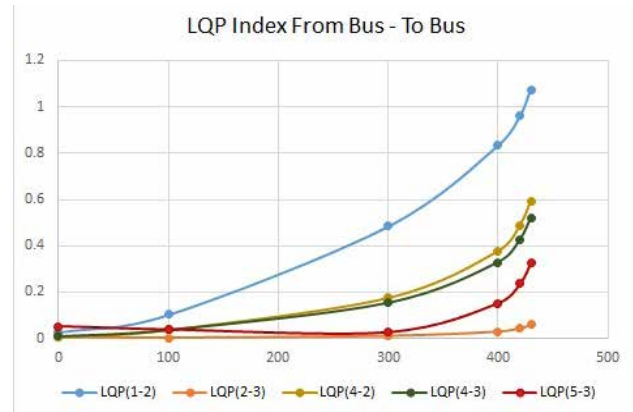


Fig. 3 LQP index value for unity power factor

Table 8 Transmission Lines SPPI Index Values at Unity Power Factor

P ₂ p.u.	SPPI (1-2)	SPPI (1-4)	SPPI (2-3)	SPPI (4-3)	SPPI (4-5)	SPPI (5-3)	SPPI (4-2)
0	0.143	0.088	0.028	0.084	0.161	0.093	0.058
1.00	0.381	0.201	0.0014	0.197	0.200	0.010	0.198
3.00	0.943	0.419	0.073	0.489	0.321	0.182	0.548
4.00	1.376	0.639	0.152	0.778	0.462	0.378	0.875
4.20	1.551	0.749	0.193	0.918	0.535	0.471	1.028

4.30	1.715	0.849	0.235	1.047	0.606	0.561	1.166
Ranking	1	4	7	3	5	6	2

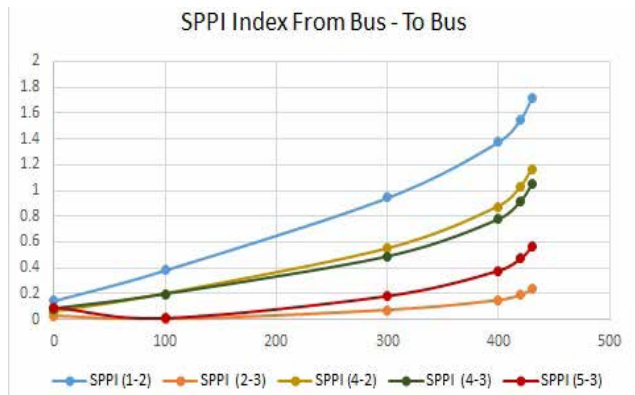


Fig. 4 SPPI index value for unity power factor

As compared to lagging condition, for unity power factor case system loadability improves as illustrated in Fig.5.

In literature, many indices are developed by number of researcher [18][19]. SPPI index is formulated recently and accuracy of this index better than some of previously developed indexes. Initially concept is developed for radial transmission line and in this article; it is implemented on multibus system (IEEE 5 bus network).

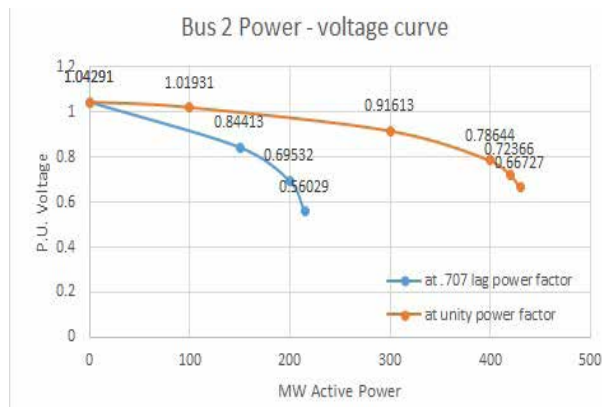


Fig. 5 Power voltage curve for load bus 2

Table VI displays the values of the FVSI index. The fundamental disadvantage of FVSI is that it produces false collapse predictions because it overlooks the effect of active power flow, as in the unity power factor condition. As a result, FVSI fails to forecast voltage collapse under these conditions.

The FVSI index performs well under heavy reactive power because it is strongly related to reactive power flow, as seen in lagging load conditions. Tables VII and VIII show the values of the LQP and SPPI indexes. These indices have a value of one when the system is on the verge of instability.

CONCLUSIONS

The voltage stability index appears to be a crucial tool for evaluating the closeness of a power system to voltage instability, providing operators and planners with valuable insights to maintain stability under varying operating conditions. The Newton Rapson algorithm is used for load flow studies of IEEE 5 bus system. It is concluded that when the load on the system increases, then system parameters varies such as increase in line power flows, drop in bus voltages etc. System is in stable region if it is operated near unity factor but it worsens when power factor changes to lagging condition. For different operating scenario values of FVSI, LQP & SPPI index is determined for every transmission line in the network. Active power loading for which indices value equals to one represent maximum loading point or point of voltage collapse. On comparing these indices, performance of SPPI index is better than FVSI and LQP.

REFERENCES

1. Ibrahim Alhamrouni et. al., "Load Flow Based Voltage Stability Indices for Voltage Stability and Contingency Analysis for Optimal Location of STATCOM in Distribution Network with Integrated Distributed Generation Unit", TELKOMNIKA, Vol.16, No. 5, pp. 2302~2315, October 2018.
2. Chemikala Madhava Reddy, "Power system voltage stability analysis", IITH department of electrical engineering, June 2011.
3. P. Kundur, "Power System Stability and Control", McGraw Hill, New York, 1994.
4. Manish Parihar, and M.K. Bhaskar, "Review of Power System Blackout", International Journal of Research and Innovation in Applied Science –IJRIAS, vol. 3, issue 6, pp.08-13, June 2018.
5. Atef A. Elemary , M.M.R Ahmed , Ebtisam M. Saied , and Mohamed A. Hamdy, "Power System Voltage Stability Index" , International journal of engineering research & technology (Ijert), Volume 11, Issue 09 September 2022.

6. M.S.S. Danish, T. Senju, S.M.S. Danish, N.R. Sabory, N.K., and P. Mandal, "A Recap of Voltage Stability Indices in the Past Three Decades", *Energies*, 12, 1544, 2019. <https://doi.org/10.3390/en12081544>.
7. Peter W. Sauer, "Reactive power and voltage control issues in electric power systems", *Applied Mathematics for Restructured Electric Power Systems: Optimization, Control, and Computational Intelligence*, pp 11-24, 2005.
8. Abhijit Chakrabarti, DE Abhinandan, A.K. Mukhopadhyay, and D.P. Kothari, "An Introduction to Reactive Power Control and Voltage Stability in Power Transmission Systems", PHI Learning Pvt. Ltd, 2010.
9. Shodhganga, "Contingency Analysis Using Line Stability Indices", 2012.
10. Yuhan Wang, Ancheng Xue, Kuang Luo, Jian Zhou, Jinsong Xu, and Jiehao Cui, "Analyses on the Adaptability of the Branch Voltage Stability Index in the Distribution Network Interconnected with PV", *International conference on power system technology IEEE, Guangzhou, china, 6-8 November 2018*.
11. I. Musirin and T. A. Rahman, "Novel fast voltage stability index (FVSI) for voltage stability analysis in power transmission system," in *Proceedings of the Student Conference on Research and Development, SCOReD 2002*, pp. 265–268, IEEE, Alam, Malaysia, July 2002.
12. Thasnas, Natakorn, and Apirat Siritaratiwat. "Implementation of static line voltage stability indices for improved static voltage stability margin." *Journal of Electrical and Computer Engineering* 2019 (2019).
13. Goh, H. H., et al. "Comparative study of line voltage stability indices for voltage collapse forecasting in power transmission system." *International Journal of Civil and Environmental Engineering* 9.2 (2015): 132-137.
14. Manish Parihar, and M. K. Bhaskar, "Radial Transmission Line Voltage Stability Analysis", *IJRERD* (ISSN: 2455-8761), vol. 02 (09), pp 01-07,2017.
15. Asfar Ali Khan, "PV Curves for Radial Transmission Lines", Accepted for Publication in the proceedings of national systems conference 2007 to be Held at Manipal Institute of Technology from 14-15, Dec. 2007 .
16. M. Parihar, and M. K. Bhaskar et al., "Analysis of Power Flow in IEEE Five Bus Power System Based on PV Curve Assessment", *International journal for science and advance research in technology*, April 2018.
17. Hadi Saadat, "Power System Analysis", McGraw-Hill ,2nd ed., New York, 2002.
18. Mahmoud Moghavvemi, and F. M. Omar, "Technique for contingency monitoring and voltage collapse prediction", *IEE Proceedings-Generation, Transmission and Distribution*, 145 (6),pp 634-640, 1998.
19. Rabiaa Gadal, et al. ,"Voltage Stability Assessment and Control Using Indices and FACTS: A Comparative Review", *Journal of Electrical and Computer Engineering*, 2023 (2023).

Appendix A: Bus Data

Bus Number	Nom kV	PU Volt	Volt (kV)	Angle (Deg)	Load MW	Load Mvar	Gen MW	Gen Mvar
1	138	1.06	146.28	0			124.43	-5.11
2	138	1.023	141.294	-4.88	45	15		
3	138	1.023	141.205	-5.21	40	5		
4	138	1.047	144.486	-2.65	20	-20	45	-2.78
5	138	1.017	140.417	-6.01	60	10		

Appendix B: Branch Data

From Bus Number	To Bus Number	Branch Device Type	R	X	B' charging capacitance
1	2	Line	0.08	0.24	0.05
1	4	Line	0.02	0.06	0.06

2	3	Line	0.01	0.03	0.02
4	2	Line	0.06	0.18	0.04
4	3	Line	0.06	0.18	0.04
3	5	Line	0.08	0.24	0.05
4	5	Line	0.04	0.12	0.03

Appendix C: Branch Flow Data

From Number	To Number	Circuit	Status	MW From	Mvar From	MVA From
1	2	1	Closed	39.9	1.5	40
1	4	1	Closed	84.5	-6.6	84.8
2	3	1	Closed	18.5	-5	19.1
4	2	1	Closed	25	3.4	25.3
4	3	1	Closed	28.2	2.8	28.4
3	5	1	Closed	6.2	-2.2	6.6
4	5	1	Closed	55	7.3	55.4

IoT Enhanced 3 Phase Induction Motor Control and Protection with PLC

Amruta J. Takawale, Himanshu S. Nalawade

Mayuresh P. Patil, Shubham S. Gholap

Electrical Engineering Department
Savitribai Phule Pune University
Pune, Maharashtra
✉ Takawaleamruta3@gmail.com

ABSTRACT

This research explores transforming the industrial landscape using IoT, PLCs, and the ESP32 microcontroller to enhance motor control efficiency and cost-effectiveness. By integrating conventional methods with modern technology, IoT adds intelligence for dynamic motor management. The ESP32 precisely measures variables like current, voltage, temperature, vibration, and power factor, orchestrated by the PLC. The system's architecture allows real-time data acquisition and remote monitoring through web hosting, enabling industry professionals to oversee and intervene in motor operations. Emphasizing motor efficiency, energy savings, and protection through innovative control strategies, the research targets cost-effectiveness for small-scale industries. Push notifications keep stakeholders informed, redefining motor control and protection with an affordable, reliable, and efficient solution, setting a new standard for technology integration in motor management.

KEYWORDS : ESP32, PLC, IoT, Monitoring, Protection.

INTRODUCTION

The modern industrial landscape is at the cusp of transformation, fuelled by the expansive horizons of IoT technologies. This research delves into motor control and protection, merging IoT, PLCs, and the versatile ESP32 microcontroller to redefine induction motor dynamics, emphasizing efficiency, reliability, and cost-effectiveness. At its core, this paper bridges the gap between conventional motor control and contemporary industry demands. IoT integration injects intelligence, enabling a dynamic approach to managing industrial workhorses through precise measurements of variables like current, voltage, temperature, vibration, and power factor. The ESP32 acts as the central nervous system, collecting and relaying data, while the PLC orchestrates control and protection. The research's bedrock is its system architecture, facilitating real-time data transmission for remote monitoring through web hosting. The architecture, explored in-depth, covers sensor interfaces, communication protocols, data processing, and control algorithms.

A defining feature is the emphasis on enhancing motor efficiency, promoting energy savings through innovative control strategies, including dry run control. This safeguard mechanism prevents motor damage during dry run conditions, showcasing meticulous attention to motor protection. The paper's commitment to cost-effectiveness positions it as an ideal solution for small-scale industries, extending beyond motor control to proactive accident prevention. Application push notifications keep stakeholders informed in real-time. In summation, this research offers a paradigm shift in motor control by harnessing IoT, PLCs, and the ESP32, characterized by affordability, reliability, and efficiency. It redefines the landscape of remote monitoring and control, poised to impact how the industry manages its motors.

LITERATURE SURVEY

IoT Integration in Motor Control

Recent research endeavours have explored the potential of IoT platforms in motor control and protection. [1]

[2][4] underline the significance of employing IoT technologies, particularly the ESP32, for real-time data collection, remote monitoring, and system control. These technologies offer opportunities to optimize motor performance and reliability through comprehensive data-driven insights.

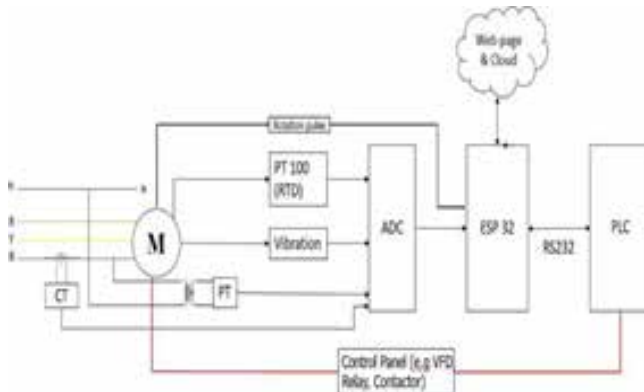


Fig. 1: Schematic Diagram of the Proposed System

Challenges in Motor Control and Protection

Motor control and protection face a myriad of challenges in industrial settings, as highlighted by [3] [8]. Variable Frequency Drives (VFDs), while beneficial for energy savings, introduce complications such as excessive motor vibration. These challenges underscore the necessity for advanced control and protection mechanisms to ensure the uninterrupted operation of induction motors.

Energy Efficiency and Motor Performance

Underscore the paramount importance of enhancing motor efficiency in the contemporary industrial landscape. With a growing emphasis on energy conservation, the development of innovative control strategies to optimize motor performance and reduce energy consumption has emerged as a central research theme.[1]

Dry Run Control and Motor Longevity

Dry run control, as introduced in [1][8], emerges as a vital safeguard mechanism to prevent motor damage during dry run conditions and extend the operational life of motors. This preventive measure aligns with the broader goal of ensuring motor longevity in industrial applications.

Cost-Effective Solutions for Small-Scale Industries

Emphasize the relevance of cost-effective solutions, particularly for small-scale industries seeking to harness the benefits of IoT and advanced motor control without incurring prohibitive expenses. dedication to offering economical solutions aligns with this industry need. [1] [4]

Application of IoT in Industrial Settings

Underscores the role of IoT in industrial applications, emphasizing its utility in monitoring and controlling various parameters. focus on IoT integration in motor control resonates with this broader trend of using IoT to streamline industrial processes.[4]

Motor Condition Monitoring

Underscores the increasing importance of condition-based monitoring for induction motors in various industrial applications. It highlights the significance of timely fault detection through wireless control and monitoring systems, a concept that underpins your paper's objectives.[7]

PLC-Based Control

Introduces the implementation of a monitoring and control system for induction motors based on Programmable Logic Controller (PLC) technology. integration of PLCs for control and protection aligns with similar implementations in industrial settings.[9]

HARDWARE



Fig. 2: Hardware of the Proposed System

Internet of Things (IoT) Technology

The Internet of Things (IoT) represents a transformative technology paradigm that goes beyond mere connectivity by creating an intricate web of interlinked devices, sensors, and systems. This ecosystem collaborates seamlessly to gather, transmit, and analyse data, fostering a dynamic and intelligent network of physical objects. At its core, IoT is driven by the concept of enabling devices to communicate and share information in real-time, creating a comprehensive and interconnected environment.

In practical terms, the collected data is then processed and analysed, providing valuable insights that can inform decision-making processes, optimize operations, and enhance overall efficiency.

The deployment of IoT technology extends across various sectors, including healthcare, agriculture, transportation, smart cities, and industrial automation. In healthcare, for instance, IoT devices can monitor patients' vital signs in real-time, providing timely information to healthcare professionals for proactive intervention. In agriculture, IoT-enabled sensors can gather data on soil moisture levels and weather conditions, optimizing irrigation and crop management. Moreover, in smart cities, IoT facilitates intelligent infrastructure, such as smart grids and traffic management systems, contributing to enhanced urban living. [1] [4].

Programmable Logic Controllers (PLCs)

Programmable Logic Controllers (PLCs) stand as the cornerstone of industrial automation, playing a pivotal role in the control and monitoring of a wide range of equipment, with a particular emphasis on motors [9]. These sophisticated electronic devices are designed to operate in harsh industrial environments, providing a robust and reliable means to automate complex processes.

At the core of PLC functionality is its capacity to execute programmed logic, enabling it to make real-time decisions and respond dynamically to changing conditions within an industrial setting. This adaptability is crucial for optimizing production processes, enhancing efficiency, and ensuring the seamless operation of machinery. PLCs are equipped with inputs and outputs that interface with sensors, actuators, and

other devices, allowing them to receive data from the industrial environment and act on it according to the programmed logic. [9].

ESP32 Microcontroller

The ESP32 microcontroller emerges as a key enabler in seamlessly integrating the Internet of Things (IoT) into the domain of motor control and protection. Renowned for its versatility and advanced features, the ESP32 serves as a powerful and efficient platform for developing IoT applications that involve monitoring, controlling, and safeguarding motors.

At its core, the ESP32 microcontroller combines a dual-core processor, low-power modes, and built-in Wi-Fi and Bluetooth connectivity, making it well-suited for applications where real-time communication and data exchange are crucial. This makes it an ideal choice for motor control scenarios, where the need for rapid and reliable communication between the motor control system and the broader IoT network is paramount. [1] [2].

Motor Control Fundamentals

Motor control fundamentals are integral to the efficient and precise operation of electrical motors, encompassing a nuanced understanding of key factors such as voltage, current, and speed regulation. In the realm of motor control, these parameters play a critical role in ensuring optimal performance, energy efficiency, and the prevention of potential damage to the motor and associated systems.

Voltage regulation is a cornerstone of motor control, involving the management and stabilization of the electrical potential supplied to the motor. Maintaining a consistent voltage is essential for preventing fluctuations that could lead to instability or inefficient operation. Voltage regulation is particularly crucial in scenarios where motors operate in diverse conditions or are subject to varying loads, ensuring that the motor receives a stable and reliable power supply. [1] [6].

Motor Protection Mechanisms

In the realm of motor control and automation, the implementation of effective motor protection mechanisms is indispensable for safeguarding motors against potential faults, ensuring longevity, and minimizing downtime. Motor protection involves a

multifaceted approach, incorporating strategies such as overcurrent protection, overvoltage protection, and thermal protection to mitigate risks and enhance the reliability of motor-driven systems.

Overcurrent protection stands as a primary line of defence for motors. Overcurrent events can occur due to various factors, including short circuits or overloads. The protective devices act swiftly to interrupt the current flow, preventing damage to the motor windings and associated components. This mechanism not only protects the motor from catastrophic failure but also contributes to overall system safety. [8].

SOFTWARE

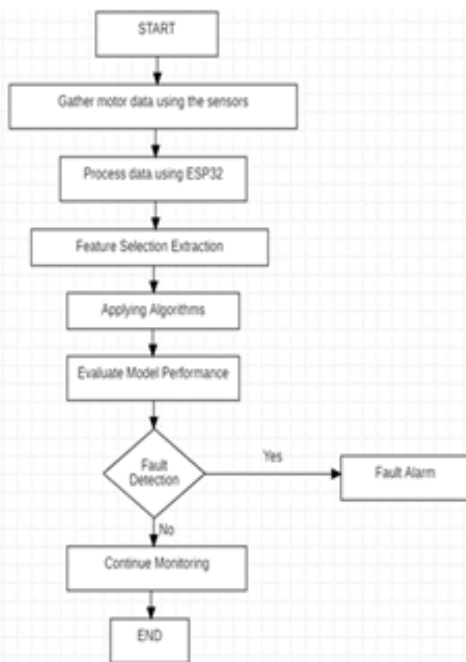


Fig. 3: Flowchart of The System

The architecture offers a comprehensive solution for motor control and protection. It seamlessly collects crucial motor data, encompassing temperature, speed, vibration, current, and voltage. The analog signals undergo precise conversion through an Analog-to-Digital Converter (ADC) before being transmitted to the ESP32 microcontroller, while digital signals are directly acquired by the ESP32. The ESP32 assumes a pivotal role as the data processing and transmission hub. The collected data is relayed to a dedicated webpage, providing a user-friendly interface for real-time remote

monitoring and control. This webpage empowers remote operators to execute specific control actions, such as speed, direction and ON/OFF control. It is designed to facilitate precise adjustments to the motor's operational parameters, ensuring optimal performance and adaptability to changing operational requirements. Concurrently, the acquired data is also communicated to a Programmable Logic Controller (PLC) through RS232 communication protocols. The PLC serves as the guardian of the motor, orchestrating an extensive array of protection mechanisms.

These safeguards encompass thermal protection, over-vibration detection, over-current prevention, over-voltage control, and vigilance over speed accuracy. The PLC ensures that the motor operates within predefined healthy parameter limits and promptly responds to any deviations, thereby averting potential damage and enhancing motor reliability. Beyond control and protection, the paper dedicates substantial attention to increasing motor efficiency. Control strategies are thoughtfully designed to optimize motor performance while minimizing energy consumption, contributing to significant operational cost savings. Additionally, the system addresses power factor correction, further enhancing energy efficiency. In parallel, the implementation of dry run control serves as a critical safeguard, preventing motor damage during dry run conditions and extending the motor's operational life. The systematic integration of these components underscores the motor's capacity not only to enhance motor control, efficiency, and remote accessibility but also to ensure paramount safety, reliability, and cost-effectiveness in motor operations. It represents a versatile solution suitable for various industrial contexts.



Fig. 4: Login Page of monitoring system

RESULTS AND DISCUSSIONS

Energy Efficiency in Industrial Motors

The pursuit of energy efficiency in industrial motors is a critical imperative that extends beyond mere operational considerations, encompassing broader environmental and economic dimensions. The optimization of motor performance not only contributes to energy savings but also results in substantial reductions in operational costs, aligning with sustainable practices and regulatory mandates. At the heart of energy efficiency initiatives for industrial motors lies the quest to minimize energy wastage during the conversion of electrical power into mechanical work. Motors are prevalent across diverse industrial applications, powering pumps, compressors, conveyors, and a myriad of other essential processes. By implementing advanced motor control strategies, such as variable speed drives and soft starters, engineers can precisely match motor speed and power output to the specific requirements of the application. This dynamic control capability minimizes energy losses associated with operating motors at fixed speeds, especially when the demand for power fluctuates.

Condition-Based Monitoring

Condition-based monitoring (CBM) stands as a pivotal approach in modern industrial settings, offering a proactive strategy for early fault detection and prevention. This paradigm shift is driven by the recognition that early fault detection not only prevents costly downtime but also mitigates the risk of severe equipment damage, ultimately leading to improved reliability and operational efficiency. At the core of CBM is the continuous and remote monitoring of critical parameters and performance metrics of industrial equipment. In the context of the paragraph's focus on early fault detection in industrial settings, CBM is particularly beneficial for detecting anomalies and deviations from normal operating conditions in a timely manner. This involves the integration of sensors, data acquisition systems, and advanced analytics to monitor variables such as temperature, vibration, pressure, and other relevant indicators.



Fig. 5: Condition based Monitoring

Dry Run Detection

Dry run detection is a critical aspect of motor protection, designed to prevent potential damage to motors during dry run conditions and thereby ensure their longevity [1, 8]. Dry run refers to the operation of a motor without the presence of the intended fluid or lubrication, which can lead to overheating, increased friction, and accelerated wear and tear. The incorporation of dry run detection mechanisms is a proactive strategy to identify and mitigate this operational risk. The primary function of dry run detection is to monitor and assess the operating conditions of the motor, particularly in applications where the motor is responsible for pumping or circulating fluids. Such scenarios include water pumps, hydraulic systems, and various industrial processes reliant on fluid flow. Dry run detection systems typically employ sensors that monitor parameters such as pressure, temperature, and flow rate to ascertain the presence of the fluid being pumped or circulated. If the sensors detect conditions indicative of a dry run, protective measures are activated to prevent potential motor damage.

Real-Time Data Processing

Real-time data processing serves as a cornerstone in the contemporary landscape of industrial automation, providing a dynamic and responsive framework for immediate decision-making based on data collected from sensors and motors [1]. This approach represents a departure from traditional batch processing, enabling industries to harness the full potential of data in real-time, fostering agility, and enhancing operational efficiency.

In the context of sensor and motor data, real-time

processing involves the continuous analysis of incoming data streams to extract meaningful insights. Sensors embedded in industrial equipment, such as motors, generate a constant flow of information regarding parameters like temperature, pressure, speed, and other critical variables. Real-time data processing systems, often integrated with programmable logic controllers (PLCs) or microcontrollers, handle this data as it is generated, allowing for instantaneous analysis and response.

Control Algorithms

Control algorithms play a pivotal role in the realm of industrial automation, serving as the intellectual core that ensures not only the precise but also the highly efficient operation of motors within a given system. These algorithms are designed to govern the behaviour of motors based on a set of predefined rules, responding dynamically to changing conditions and optimizing performance in real-time.

The fundamental purpose of control algorithms in the context of motor operation is to regulate key parameters such as speed, torque, and position. These algorithms leverage feedback from sensors and other monitoring devices to continually assess the actual state of the motor and adjust control signals accordingly. By doing so, control algorithms enable motors to maintain desired operating conditions, respond to external factors, and adapt to varying loads with a high degree of accuracy.

Power Factor Correction

Power factor correction stands as a critical aspect of optimizing electrical power usage in industrial settings, representing a proactive strategy to enhance energy efficiency and reduce operational costs [1]. A low power factor can result in inefficiencies, increased energy consumption, and additional financial burdens.

In industrial environments, electrical systems often involve the operation of numerous motors and other inductive loads. These devices introduce reactive power, leading to a lagging power factor. Power factor correction involves the deployment of specific technologies and solutions to mitigate this lagging power factor, ultimately improving the overall efficiency of the electrical system. [1].

Wireless Communication Protocols

Wireless communication protocols play a pivotal role in facilitating seamless data transmission and reception for remote monitoring and control applications within industrial projects [7]. In contemporary industrial landscapes, the integration of wireless communication technologies has become instrumental in enhancing flexibility, scalability, and real-time connectivity across diverse systems and devices. The utilization of wireless communication protocols enables the establishment of robust and efficient communication networks for remote monitoring and control. These protocols encompass a spectrum of technologies, including Wi-Fi, Bluetooth, Zigbee, LoRa (Long Range), and cellular networks, each offering distinct advantages tailored to specific requirements. The choice of the wireless protocol depends on factors such as data transmission speed, range, power consumption, and the nature of the industrial environment. [7].

CONCLUSION

This groundbreaking paper marks a pivotal shift in the landscape of industrial motor control and protection, seamlessly integrating cutting-edge technologies such as IoT, PLCs, and the versatile ESP32 microcontroller. By successfully bridging the traditional and contemporary realms of motor control, the paper introduces a host of advancements, including real-time data access, remote monitoring capabilities, and proactive safeguards.

At its core, the paper addresses the evolving needs of motor control in both conventional and modern industrial settings. Through the infusion of IoT technologies, it injects a new dimension of intelligence, enabling real-time data orchestration for dynamic and adaptive motor management. The ESP32 microcontroller serves as the central nervous system, intricately collecting, processing, and relaying data with precision. Simultaneously, the Programmable Logic Controller (PLC) emerges as the orchestrator, establishing a symbiotic relationship that harmonizes the intricacies of motor operation with the versatility of modern technology.

In summation, this research paper signifies an evolutionary paradigm shift in the domain of motor control and protection. By skilfully harnessing the synergies of IoT, PLCs, and the ESP32 microcontroller,

it delivers a solution characterized by its affordability, reliability, and efficiency. In doing so, it not only enhances motor performance and promotes motor longevity but also redefines the landscape of remote monitoring and control. The future of motor control is now within reach—an era marked by efficiency, cost-effectiveness, and unwavering reliability.

REFERENCES

1. I. Allafi and T. Iqbal, "Design and implementation of a low-cost web server using ESP32 for real-time photovoltaic system monitoring," 2017 IEEE Electrical Power and Energy Conference (EPEC), Saskatoon, SK, Canada, 2017, pp. 1-5, doi: 10.1109/EPEC.2017.8286184.
2. M. Babiuch, P. Foltýnek and P. Smutný, "Using the ESP32 Microcontroller for Data Processing," 2019 20th International Carpathian Control Conference (ICCC), Krakow-Wieliczka, Poland, 2019, pp. 1-6, doi: 10.1109/CarpathianCC.2019.8765944.
3. M. Tsyppkin, "Vibration of induction motors operating with variable frequency drives — A practical experience," 2014 IEEE 28th Convention of Electrical & Electronics Engineers in Israel (IEEEI), Eilat, Israel, 2014, pp. 1-5, doi: 10.1109/IEEEI.2014.7005894.
4. Thimmapuram Swati, K. Raghavendra Rao, International Journal of Recent Technology and Engineering (IJRTE) ISSN: 2277-3878, Volume-7, Issue-6S4, April 2019
5. P.Macheso, S.Chisale, C.Daka, N.Dzupire, J.Mlatho and D. Mukanyirigira, "Design of Standalone Asynchronous ESP32 Web- Server for Temperature and Humidity Monitoring," 2021 7th International Conference on Advanced Computing and Communication Systems (ICACCS), Coimbatore, India, 2021, pp. 635-638, doi: 10.1109/ICACCS51430.2021.9441845.
6. E. Noyjeen, C. Tanita, N. Panthasarn, P. Chansri and J. Pukkham, "Monitoring Parameters of Three-Phase Induction Motor Using IoT," 2021 9th International Electrical Engineering Congress (iEECON), Pattaya, Thailand, 2021, pp. 483-486, doi: 10.1109/iEECON51072.2021.9440368.
7. 1Shefali Jamwal, 2Shimi S.L, © 2018 IJCRT | Volume 6, Issue 2 April 2018 | ISSN: 2320-2882
8. A. Maier, A. Sharp and Y. Vagapov, "Comparative analysis and practical implementation of the ESP32 microcontroller module for the internet of things," 2017 Internet Technologies and Applications (ITA), Wrexham, UK, 2017, pp. 143-148, doi: 10.1109/ITECHA.2017.8101926.
9. I. Colak, R. Bayindir, A. Bektas, I. Sefa and G. Bal, "Protection of Induction Motor Using PLC," 2007 International Conference on Power Engineering, Energy and Electrical Drives, Setubal, Portugal, 2007, pp. 96-99, doi: 10.1109/POWERENG.2007.4380120.
10. M. G. Ioannides, "Design and implementation of PLC- based monitoring control system for induction motor," in IEEE Transactions on Energy Conversion, vol. 19, no. 3, pp. 469-476, Sept. 2004, doi: 10.1109/TEC.2003.822303.

Comparative Analysis of MPPT Schemes for Optimized Fuel Cell Operation

Bodke Mahesh Prakash

Department of Electrical Engineering
K.K. Wagh, Institute of Engineering Education and
Research
Nashik, Maharashtra
✉ maheshbodke07@gmail.com

M V Bhatkar

Jawahar Education Society's. Institute of Technology,
Management & Research
Nashik, Maharashtra
✉ mvbhatkar@rediffmail.com

ABSTRACT

The transportation industry is toweringly reliant on the use of fossil fuels. Due to limited stock of fossil fuel supply automobile sector is looking for alternate source of energy for driving vehicle. Fuel cell technology have high energy density and it uses hydrogen which is green source of energy. Therefore, they are often considered as an ideal candidate for zero emission vehicular applications due to their low operating temperature which makes them well suited for personal vehicle applications. The power generated from fuel cell is majorly dependent of two factors that are cell temperature and membrane water content. Therefore, to obtain maximum power from fuel cell a maximum point tracking controller is essentially required.

Many algorithms are devised to extract the peak power point, mostly based on the voltage and current output of the fuel, along with mathematical schemes based on different cell parameters A Maximum power point tracking (MPPT) controller traces the MPP of Fuel cell using a MPPT algorithm. A comparative analysis of the various MPPT schemes is done in this paper.

KEYWORDS : Fuel cell, Electric vehicle, Efficiency, Maximum power point tracking (MPPT).

INTRODUCTION

The Automobile makers are searching for alternate source of energy for driving vehicle because there is continuous increase of environmental pollution and the stock of fossil fuels is decreasing day by day. The alternate sources include fuel cells, batteries and ultracapacitors for the propulsion of the vehicles. In recent years, fuel cells have gained more attention from researchers and automakers point of view due to their high energy density, high efficiency and low noise [1,2].

There are different types of fuel cells depending on the type of electrolyte substance used notably alkaline fuel cell (AFC), proton exchange membrane fuel cell (PEMFC), solid oxide fuel cell (SOFC), direct methanol fuel cell (DMFC), phosphoric acid fuel cell (PAFC), molten carbonate fuel cell (MCFC), and photonic ceramic fuel cell (PCFC) [3]. All these designs are based on efficiency of chemical reaction leading to

electrical output, along with amount of heat produced and the type of electrolyte used [4].

Alkaline Fuel cells are considered useful for basic designs of equipment and the devices having low power requirement. The system was initially used for two wheelers but the working range is not that great [5]. Among all the types of fuel cell technologies, PEMFC is dominantly getting used in electric vehicles due to its small size, quick startup, low operating temperature and high power density. The proton exchange membrane fuel cell (PEMFC) output voltage depends on the membrane water content oxygen, partial pressure and cell temperature. The PEMFC system voltage- current (V-I) characteristics are non-linear. therefore, only a one operating point is available with maximum output voltage and power for PEMFC system. Therefore, A controller which can track maximum power (MPPT controller) is required for PEMFC system to obtain the maximum power [6]. Fuel Cell Electric Vehicles

(FCEVs) has the capacity to replace conventional vehicles. The PEMFC is used as the main energy system (MES), and a battery or a super-capacitor is used as rechargeable energy storage system PEMFC will provide extended driving range, and RESS will provide regenerative braking and good acceleration [7].

To extract the best from the output of Fuel cell, MPPT controllers for the PEMFC system are designed and implemented. The maximum power of PEMFC system can be tracked by different MPPT techniques which can be broadly classified as artificial intelligence (AI) based controllers, incremental conductance (INC) method and perturb and observe (P&O) method. In all the above methods P&O method is commonly used technique for proton exchange membrane FC systems [8]. The P&O algorithm introduces changes in the operating point by increasing or decreasing the control variable by a small amount and determines the PEMFC stack output power before and after perturbation. If the PEMFC output power decreases, the algorithm perturbs the system in the opposite direction without interruption; otherwise, the system is perturbed in the reverse direction. As this method is simple and in steady state P&O method accuracy is low. As operating point of the PEMFC system oscillate around MPP due to the perturbing process. This leads to the energy loss in the system. The reduction in the perturbation step size will minimize the oscillations. But reduction in step size decreases the tracking speed [9,10].

The dynamic performance and tracking efficiency of the PEMFC system can be increased by Incremental Conductance (INC) controller. The basic of INC method is slope of power versus current curve. The slope of power versus current curve is zero at the MPP point. In INC method the current and voltage are sensed from the PEMFC and maximum power is extracted by calculating the ratio between the incremental resistance and instantaneous resistance. The tracking of MPP point will give fast and accurate in INC method than the P&O method. But in INC method oscillations are generated the at the maximum operating point which will reduce the efficiency of the PEMFC system. [11,12]

PEMFC system has non-linear V-I characteristics. Many research activities have focused their study on faster tracking controllers based on artificial intelligence (AI) schemes. For non-linear systems AI-based techniques

provides better solution. Fuzzy logic controller (FLC) and artificial neural networks (ANN) are the two main categories of AI-based techniques. [13]

The extraction and controlling of MPP using different configurations of FLC are studied and results shows quite an effective control to achieve good output. An adaptive fuzzy controller for PEMFC system is also designed which involves summation of advantages of fuzzy systems and other simple control schemes like PID. The advantages of FLC are flexible operation, fast response and the exact mathematical model of the system is not required. Expert knowledge is used by FLC to formulate the fuzzy inference rules. The skills of the user or control engineer plays an important role in the efficiency of the FLC [14, 15]. Also, one major drawback of fuzzy logic controllers or adaptive controllers is that it requires large memory which increases the total cost of controller [16]. Artificial Neural network or ANN algorithms based control schemes for MPPT detection and approximation have the capability to find complex non-linear relationships between dependent and independent variables without the need of an exact mathematical model of the system. PEMFC system with ANN based MPPT controllers have been designed in literature. ANN uses a feed forward multi-layer perception model (MLP) or radial basis function network (RBFN) structure to track the MPP [17]. ANN controller has been used to approximate the voltages and currents corresponding to the MPP of PEMFC system for different cell temperatures. The major drawback of this controller is that it requires large numbers of training data and also more calculations are involved which increases the size of the controller [18].

From the literature survey their exit a scope for comparative analysis of various MPPT techniques for PEMFC fuel cell Electric vehicle.

DIFFERENT MPPT TECHNIQUES

Open Circuit Voltage Method for MPPT

In case of Indirect techniques used for maximum power tracking includes checking of preferential parameters like the fixed voltage, open circuit voltage and short circuit current methods. In these kinds of tracking, simple assumptions and periodic estimation of the MPPT are made with easy measurements. The fixed voltage technique only adjusts the operating voltage of the fuel

cell module at different seasons with the assumption of higher MPP voltages in winter and lower MPP voltages in summer at the same irradiation level. This method is not accurate because of the changing of parameters and temperature level within the same season. Indirect MPPT technique is most common Open Circuit Voltage (OV) Method. It is assumed in this method is that:

$$VMMP = k \cdot V_{oc}$$

Where, k is a constant and its value for material used in electrodes is usually to be around 0.7 to 0.8. compared to other techniques this technique is simple and is easier to implement. The efficiency is reduced due to the constant, k which is just an approximation. When the system condition changes each time the system needs to find the new open circuit voltage (Vout). Each time the load connected to the fuel cell module must be disconnected to find the new open circuit voltage, causing power loss.

Short circuit current method for MPPT

This method uses the assumption of linear relationship between the “ cell-short circuit current (ISC) and cell current corresponding to The maximum power (IMP)”. This relationship can be expressed as:

$$IMPP = K \cdot ISC$$

Where, K is called the current factor. Module max power lies at about 90% of its short circuit current. The Algorithm for Short circuit current method is shown in Fig 1.

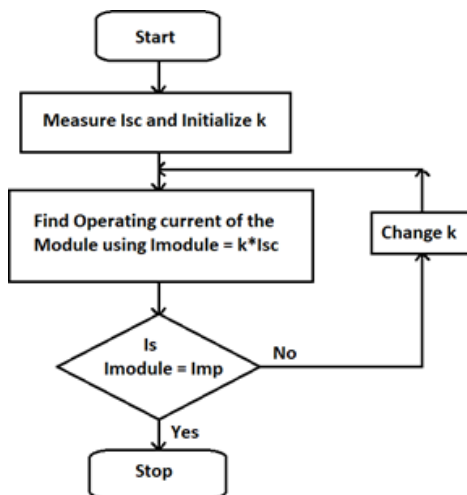


Fig 1: Algorithm for Short circuit current method

Perturb and observe method for MPPT

Direct MPPT methods like Perturb and observe (P&O) measure the current and voltage or power directly and thus they have faster response and are more accurate than the indirect methods. The best example of direct method is Perturb and observe (P&O) method which is used here with some modifications.

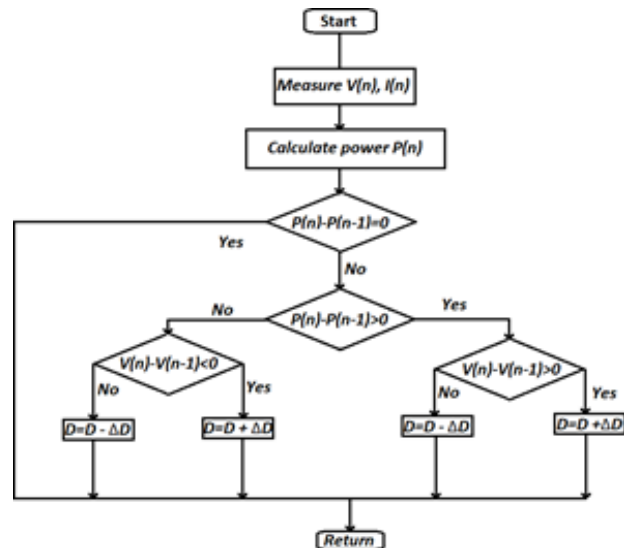


Fig 2: Scheme of P&O MPPT operation

In this technique, using a converter system a minor perturbation in voltage level is introduced to cause the power variation of the fuel cell module. The periodically measured output power is compared with the measured value of previous power. If the output power decreases, the perturbation in voltage value is reversed otherwise the same process is continued. For this algorithm, fuel cell module or the setup voltage is perturbed. The fuel cell module voltage is decreased or increased to check whether the power is decreased or increased. if an increase in voltage leads to a decrease in power, this means the operating point of the PV module is on the right of the MPP and hence further perturbation towards the left is required to reach MPP. Conversely, When an increase in voltage leads to an increase in power, this means the operating point of the fuel cell module is on the left of the MPP. Hence further perturbation is required towards the right to reach MPP. The flow chart of P&O algorithm is given in Fig 2.

In P&O, as can be understood from its name, a perturbation is applied to system and its effect is

observed. For Fuel cell system, an increment (either positive or negative) in Fuel cell current, ΔI , is considered as perturbation and output power variations, ΔP , will be observed. If the output power is increased by a positive constant increment in FC current, further positive increment is needed; otherwise perturbation must be negative. In a similar way, if the output power is increased by a negative perturbation, further negative increment is needed; otherwise direction of perturbation must be changed. The perturbation should be selected to be large for fast tracking of maximum power point. This selection leads to more fluctuations in output power. If we want to reduce these fluctuations, the perturbation should be small, but tracking time will be long. So, as a summary, with the suppression of fluctuations in output power, the quick tracking time is in conflict. Many approaches have been proposed to improve the P&O algorithm, such as using a variable step size of perturbation instead of a constant value as following:

$$I_{k+1} = I_k + M \frac{\Delta P_k}{\Delta I_k}$$

Where, M is a coefficient that modifies step size, and I_k , ΔI and ΔP are the current value, deviation of current and deviation of power at kth sampling period respectively. However, for FC power systems, tracking time should be chosen based on FC dynamic response. In other words, the rate of current changes should not exceed the maximum permissible rate of FC current changes.

Incremental Conductance MPPT

MPPT is the only way of increasing the efficiency of the fuel cell by extracting the maximum power from the solar panel and delivering constant voltage irrespective of variation in solar radiation. In direct coupled method the voltage will quickly collapse to zero, that is without MPPT solar power is delivered directly to the load. This can be understood from the I-V curve obtained from the fuel cell system. Hence, a system with MPPT presents the collapse of the voltage by keeping the operating point near the Maximum Power point. A wide range of MPPT Algorithms are available. Of all the available algorithms, Incremental Conductance Algorithm lends itself well to the Digital Signal Processing systems and microcontroller systems.

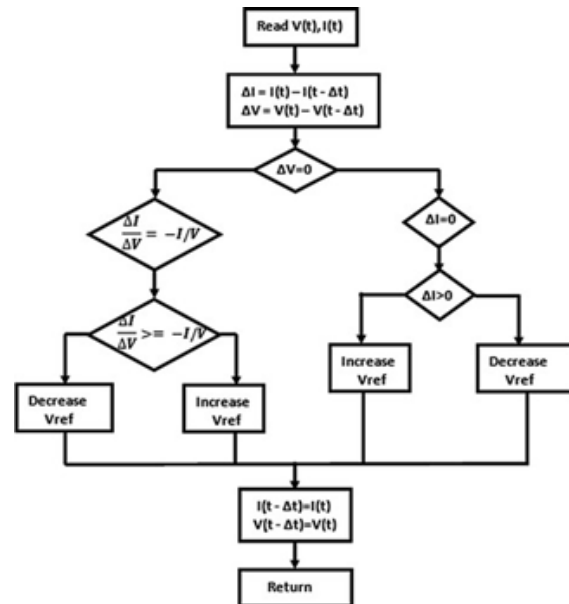


Fig 3: Scheme for INC MPPT operation

The basic power equation can give rise to equation for implementing the INC algorithm. The equation for power is given as

$$P = V * I$$

Differentiating the above equation with respect to voltage yields,

$$\frac{dP}{dV} = \frac{d(VI)}{dV}$$

$$\frac{dP}{dV} = I + V \frac{dI}{dV}$$

When the MPPT charge controller is connected between the fuel cell module and battery, it measures the fuel cell and battery voltages. The battery is fully charged or not is determined after measuring the cell voltage. It stops charging to prevent battery overcharging, if the battery is fully charged. it starts charging by activating the DC/DC converter, If the battery is not fully charged. By measuring the voltage and current, the microcontroller will then calculate the existing power P_{new} at the output, and compare this calculated power to the previous measured power P_{old} . The duty cycle is reduced if P_{new} is less than P_{old} , to ensure the system to move back to the previous maximum power. The PWM duty cycle is increased, if P_{new} is greater than

Pold, to extract maximum power from the fuel cell. This MPPT algorithm is easy to implement, simple, and low cost with high accuracy.

The condition for the maximum power point tracking is that the slope dP/dV should be equal to zero. Substituting in the above equation,

$$\frac{dI}{dV} = - \left(\frac{I}{V} \right)$$

To track the maximum Power point of the PV panel, the above equation is implemented in Matlab m-files. The flow chart describing the INC Algorithm is shown in the figure above. In the conventional MPPT systems there are two independent control loops to make the operating point of the Panel to be at the maximum power point. The first loop is the MPPT algorithm and the second one is the PI controller. INC Algorithm is entirely based on the Instantaneous and Incremental conductance to generate an error signal which is made zero at the MPP point. But due to the nonlinearity nature of the PI controller a direct control strategy is applied. The main objective of selecting this method is to eliminate the second control loop and to provide a simple control circuit only with the tracking algorithm. Hence In this method the controller is eliminated and the duty cycles of the converters are adjusted directly.

Fuzzy Logic Control for MPPT

Fuzzy logic is used in a wide range of applications, in control systems, fuzzy logic controllers are recognized for being robust and simple to design as they do not necessitate precise knowledge of the model of the system to be controlled. Fuzzy logic controller consists of an input, a processing phase and an output. Two inputs are required in a fuzzy logic MPPT controller namely the error e and the change in error Δe . The error is expressed as:

$$e(k) = (p(k) - p(k-1)) / (v(k) - v(k-1))$$

Where $v(k)$, $v(k-1)$, $p(k)$ and $p(k-1)$, are the powers and voltages at instant k and $k-1$ respectively. The change in error Δe_k is given as follows:

$$\Delta e_k = e_k - e(k-1)$$

Where (k) and $(k-1)$ are the error at instant k and $k-1$ respectively.

The processing phase is based on logical rules containing IF-THEN statements also known as inference engine. Common fuzzy inference systems include dozens of rules. The inference engine processes the given input values to generate the outputs based on the defined rules. Five different steps are involved namely fuzzification, application of fuzzy operator, application of implication method, aggregation of outputs and defuzzification. Inference systems are based on two methods:

1. Mamdani fuzzy inference method
2. Takagi-Sugeno-Kang inference method.

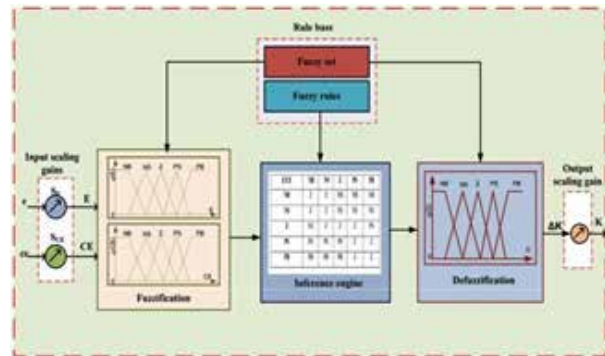


Fig 4 - Structure of a Fuzzy logic controller

The major difference between them lies in the consequent fuzzy rules and defuzzification procedures; Mamdani inference method uses fuzzy sets as rule consequent, while Sugeno inference method considers linear functions of input variables. In Mamdani approach, the crisp output of the fuzzy system y^{crisp} is determined using the ‘‘Center of Gravity’’ defuzzification by supposing that the consequent fuzzy set of Rule i is Q^i , characterized by membership u_{Q^i} and by defining the center of area of u_{Q^i} to be the point q_i in the universe. Equation that gives the crisp output of Mamdani method is:

$$y^{crisp} = \frac{\sum_{i=1}^R q_i \int u_{Q^i}}{\sum_{i=1}^R \int u_{Q^i}}$$

In the same vein, the crisp output of Sugeno fuzzy systems is given as:

$$y^{crisp} = \frac{\sum_{i=1}^R q^i u_i(x)}{\sum_{i=1}^R u_i(x)}$$

Where u is the premise membership value of Rule I . Between the two methods, Mamdani inference system

is the most widely used as it presents some benefits such as: intuitive and interpretable nature of the rule base, easy formalization and interpretability, expressive power and able to be employed in both MISO and MIMO systems. The advantage of Sugeno inference method is as follows: computational accuracy and efficiency, better processing time and adequate for functional analysis.

Adaptive Neuro-Fuzzy Inference Systems (ANFIS)

ANFIS combines the learning abilities of ANN and the ability of fuzzy logic to handle imprecise and ambiguous data in non-linear and time varying problems. Fuzzy systems are knowledge based or rule-based systems. The main part of the Fuzzy systems is the IF-THEN rules in the sense that all the other three components (fuzzy inference engine, fuzzifier, and defuzzifier) are used to interpret these rules and make them usable for specific problems. It involves formulation of the rules from domain knowledge or human experts as first step. To combine these rules into a single system is next step. Fuzzy logic can be applied to systems that are nonlinear and difficult to model using mathematical tools, especially those that are too vague or too complicated to be described by simple mathematical equations. A fuzzy inference system (FIS) essentially defines a non-linear mapping of the input data vector into a scalar output, using fuzzy rules. The fuzzifier maps input numbers into corresponding fuzzy membership functions. This is required in order to activate rules written using linguistic variables. The output fuzzy sets are the mapped into a crisp number by defuzzifier. The defuzzifier returns one number, thereby moving from a fuzzy set to a crisp number, given a fuzzy set that encompasses a range of output values.

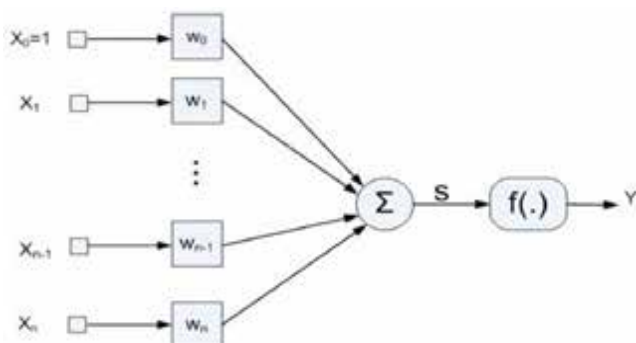


Fig 5 - Structure of an Artificial Neuron logic

The fuzzy system is apprehended with Artificial Neural networks are based on the way neurons in a human brain operate in order to solve problems. A neuron is the information processing unit indispensable for the operation of the neural network. It accepts an 'n' number of inputs and delivers one output. Each input (x_1 to x_n) has a weight (w_1 to w_n) associated with it. The net weight (u_j) of each neuron is the dot product of all the inputs and their corresponding weights. The net value is then applied to an activation function ($f(u_j)$). If output of the function (y_j) exceeds the threshold value of the neuron then the neuron is turned on or 'fired'. The signal is then passed on in the direction of propagation. The structure of the neuron is illustrated by the figure below. Most neural networks consist of one or more layers of neurons. The input layer distributes the network inputs to the subsequent layers. It is followed by one or more hidden layers. The computation is usually done by the hidden layers and the output is passed on to the output layer.

DESIRABLE CHARACTERISTICS OF MPPT SCHEME

The aim of MPPT is to track the actual operation voltage of fuel cell to the voltage at MPP. For that, MPPT adjusts the output power of inverter or DC converter. If the PV output voltage is lesser than MPP voltage, then transferred power to the load or network is decreased, otherwise, it is increased. In the selection of MPPT algorithms, the main criteria taken into consideration are summarized as follows:

1. Ease of Implementation: Some techniques consist of digital circuits and others are analog. Most of the times digital MPPT algorithms has the requirement of software and programming.
2. The required number of sensors: current measurement is usually difficult that voltage measurement also voltage measurement is more reliable than. Current sensors come with a cumbersome structure are also often expensive. The light level measured by these sensors is not easy to find. Therefore, while MPPT designing these features should be considered.
3. The normal operation of the MPPT can affect due to partial shading on PV panels. significant power

losses may arise, if the selected algorithm is too sensitive, virtually MPPT that occurred by shading may be tracked.

4. It is not easy to determine the cost of an MPPT algorithm before implementation. Accurate cost compassion depends on system features such as digital or analog, programming and software requirements, and number of sensors. Generally digital algorithms are costlier than analog ones.
5. A certain MPPT technique is suitable for certain applications. In each system, an algorithm may not give the same result as that of other algorithm.

COMPARATIVE ANALYSIS OF VARIOUS MPPT SCHEMES

Indirect MPPT techniques at maximum power point using sample measurements and assumptions. There are several application advantages of these techniques, like stated below:

- a. System voltage can be adjusted in situational means. In this case, it is expected that MPP voltage in summer will be lower than winter, depending on fuel cell temperature.
 - b. According to the temperature of the module operating voltage can be adjusted.
 - c. Multiplication of instantaneous open-circuit voltage of PV cell with a certain constant coefficient will give MPP voltage.
 - d. Open-circuit voltage is measured periodically. For these measurements interruption of load is realized for very short times such as 1ms every two minutes.
 - e. In some systems, MPPT algorithms are designed according to the variations in distinct parameters of the fuel cell module.
- Pros and Cons of P&O Method

Simplicity of the method is the most important advantage, this technique presents oscillations around the MPP, because the oscillations. in the Steady State are proportional to the step size. Disadvantages of this method are If there is shadow on any of the PV panels then the P Vs V curve of the PV will have many peaks and. P&O technique will not be able to find the real

peak. Perturb & Observe technique. is very slow to find the Maximum Power Point if the v/g is far away. From Maximum Power Point.

- Pros and Cons of Incremental Conductance method
The advantage of this technique is that it is very efficient during uneven operation parameters or when the backup or storage battery is completely discharged irrespective of other MPPT techniques.
- Effectiveness of MPPT based on ANFIS

The effectiveness of MPPT based on ANFIS can be summarized as - Effect of using different shaped Membership Functions on ANFIS prediction accuracy. Several membership functions were used with the ANFIS model to find out the effect of using different input MFs on the optimum voltage prediction accuracy. Bell, Gaussian, triangular, trapezoidal and pi-shaped MFs were used. It was found that the optimum voltage predictions for the PV system do not vary much between the various MFs. However, the best prediction was obtained with the Gaussian MF.

Table 1 Comparative Analysis of Different MPPT

Comparison parameters	P & O	SCC	FLC	INC	ANFIS
Efficiency (%)	81.5-85	>95	88-89.9	73-85	99.8
Exactly MPP determination	Yes	Yes	No	Yes	Yes
Analog or digital control	Both	Both	Analog	Digital	Analog
Periodic tuning requirement	No	No	Yes	No	No
Convergence speed	Varies	Fast	Medium	Varies	Fast
Complexity	Low	High	Low	Medium	Low
Measured parameters	Voltage, current	Varies	Voltage, current	Voltage, current	Voltage, current

CONCLUSION

A Fuel cell (FC) has a lot of potential to be used as a clean energy source. The silent operation makes it suitable for stationary power operations and is of high reliability and high-quality power. The detail of the various algorithms used to trace maximum power point and its overall view is given in this paper. Efficiency and exactness of MPP determination along with analog or digital control and complexity is also given here briefly. To mitigate the challenge of tracing the maximum power from the fuel cell is very significant. As per application the evaluation of MPP tracing algorithm cannot be done because these

MPPT are slightly differ from each other in terms of performance. The various MPPT techniques are based on various parameters like cell temperature, fuel pressure etc. A comparative analysis of different MPPT algorithm is presented along with various performance criteria is given in Table 1. The comparative analysis is presented in such a way that the reader can select the most appropriate method for his own application.

REFERENCES

- Hwang JJ, Kuo JK, Wu W, Chang WR, Lin CH, Wang SE. Lifecycle performance assessment of fuel cell/battery electric vehicles. *Int J Hydrogen Energy* 2013;38(8):3433-6.
- Reddy KJ, Natarajan S. Energy sources and multi-input DC- DC converters used in hybrid electric vehicle applications-A review. *Int J Hydrogen Energy* 2018;43(36):17387-408.
- Inci M, Trksoy. Review of fuel cells to grid interface: configurations, technical challenges and trends. *J Clean Prod* 2019;213:1353-70.
- Reddy KJ, Sudhakar N. A new RBFN based MPPT controller for grid- connected PEMFC system with high step-up three-phase IBC. *Int J Hydrogen Energy* 2018;43(37):17835-48.
- Wang MH, Yau HT, Wang TY. Extension sliding mode controller for maximum power point tracking of hydrogen fuel cells. In: *Abstract and applied analysis*. vol. 2013; 2013.
- Aouzellag H, Ghedamsi K, Aouzellag D. Energy management and fault tolerant control strategies for fuel cell/ultra- capacitor hybrid electric vehicles to enhance autonomy, efficiency and life time of the fuel cell system. *Int J Hydrogen Energy* 2015;40(22):7204-13.
- Ahmadi S, Abdi S, Kakavand M. Maximum power point tracking of a proton exchange membrane fuel cell system using PSO-PID controller. *Int J Hydrogen Energy* 2017;42(32):20430-43.
- Ozdemir S, Altin N, Sefa I. Fuzzy logic based MPPT controller for high conversion ratio quadratic boost converter. *Int J Hydrogen Energy* 2017;42(28):17748-59.
- Jiao J. Maximum power point tracking of fuel cell power system using fuzzy logic control. *Elec- trotehn, Electron, Autom* 2014;62(2):45.
- Harrag A, Messalti S. How fuzzy logic can improve PEM fuel cell MPPT performances? *Int J Hydrogen Energy* 2018;43(1):537-50.
- Al-Majidi SD, Abbod MF, Al-Raweshidy HS. A novel maximum power point tracking technique based on fuzzy logic for photovoltaic systems. *Int J Hydrogen Energy* 2018;43(31):14158-71
- Benchouia NE, Derghal A, Mahmah B, Madi B, Khochemane L, Aoul EH. An adaptive fuzzy logic controller (AFLC) for PEMFC fuel cell. *Int J Hydrogen Energy* 2015;40(39):13806-19.
- Ali US. Z-source DC-DC converter with fuzzy logic MPPT control for photovoltaic applications. *Energy Procedia* 2016;90:163-70.
- Reisi AR, Moradi MH, Jamasb S. Classification and comparison of maximum power point tracking techniques for photovoltaic system: a review. *Renew Sustain Energy Rev* 2013;19:433-43.
- Reddy KJ, Sudhakar N. High voltage gain interleaved boost converter with neural network based MPPT controller for fuel cell based electric vehicle applications. *IEEE Access* 2018;6:3899-908.
- Harrag A, Bahri H. Novel neural network IC-based variable step size fuel cell MPPT controller: performance, efficiency and lifetime improvement. *Int J Hydrogen Energy* 2017;42(5):3549-63.
- Reddy J, Natarajan S. Control and analysis of MPPT techniques for standalone PV system with high voltage gain interleaved boost converter. *Gazi Univ J Sci* 2018;31(2).
- Reddy J, Sudhakar N. Design and analysis of a hybrid PV- PEMFC system with MPPT controller for a three-phase grid- connected system. *J Green Eng* 2018;8(2):151-76.

Estimation of Very Fast Transient Overvoltage's in GIS

Rahul S. Patil

Department of Electrical Engineering
K.K. Wagh, Institute of Engg Education and Research
Nashik, Maharashtra
✉ patil.rahul23nov@gmail.com

M. V. Bhatkar

Jawahar Education Society's. Institute of Technology,
Management & Research
Nashik, Maharashtra

ABSTRACT

Very fast transient over voltages (VFTO) arise within a GIS whenever there is an instantaneous change in voltage. Most often this change occurs as a result of opening or closing of disconnector switch (DS). Other events, such as the operation of circuit breaker, the occurrence of a line-ground fault or the closing of grounding switch can also cause VFTO. However, during a DS operation a number of re-strikes and pre-strikes occur due to the low operating speed of DS compared to a circuit breaker. Therefore DS switching is main source of generating VFTO. The transients are characterized by their short duration and very high frequencies. The rise times are in the range of ns, with dominant frequency components up to 100MHz. The generation and propagation of VFT from their original location throughout GIS can produce internal and external over voltages, the multiple refractions and reflections of these surges at impedance discontinuities within the enclosures create complex waveforms, which depends on the disconnector design, the operating conditions and external substation configuration. The main concern are internal over voltages between conductor and the enclosure. Internal VFTO cause high stress of the insulation system. VFTO in GIS are of greater concern at the highest rated voltages, for which the ratio of the lightning impulse withstand voltage (LIWV) to the system voltage is lower. As the rated voltage increases, the difference between the rated lightning impulse withstand voltage and the VFTO decreases. Hence, VFTO can become the limiting dielectric stress which defines the dimensions in certain cases. VFTO simulation is a well-known instrument for the calculation of over voltages needed for the insulation co-ordination process. This paper describes the Estimation of VFTO due to variation in the GIS parameters.

KEYWORDS : *Disconnector, Gas-insulated switchgear (GIS), Ultra-high voltage (UHV), Very-fast transient overvoltage (VFTO), PSCAD.*

INTRODUCTION

Very fast transient over voltages (VFTO) arise within a GIS any time there is an instantaneous change in voltage. Most often this change occurs as a result of the opening or closing of a disconnector switch (DS). Other events, such as the operation of a circuit-breaker (CB), the occurrence of a line-to-ground fault or the closing of an earthing switch can also cause VFTO. However, during a DS operation a high number of re-strikes and pre-strikes occur due to the low operating speed of DS compared to a circuit breaker.

Therefore, DS switching is the main source for generating VFTO. The transients are characterized by their short duration and very high frequencies. The rise times are in the range of some ns, with

dominant frequency components up to 100 MHz. The generation and propagation of VFTO from their original location throughout a GIS can produce internal and external transient over voltages (see Figure 1). The main concerns are internal overvoltages between the conductor and the enclosure. Internal VFTO cause high stress of the insulation system. It has been found that, particularly at 420 kV and higher system voltage levels, disruptive discharges to earth might occur when switching small capacitive currents with gas-insulated DS. The development of an earth fault by branching of the leader during DS switching depends on parameters such as voltage, gap distance, electrode geometry, contact speed, gas pressure and magnitude and frequency of VFTO. A proper design of the DS has shown, that in practice earth faults can be eliminated.

The geometry of the contact gap can be designed in such a way that the strike occurs where the radial field gradient influencing the branching leader discharge is at a minimum. Screening the strike area with specially designed shielding electrodes and initiating the

strike near the axis of the gap, are suitable measures [2]. However, external VFTO can be dangerous for secondary and adjacent equipment. These external transients include transient voltages between the enclosure and ground at GIS-air interfaces, voltages across insulating spacers in the vicinity of GIS current transformers, when they do not have a metallic screen on the outside surface, voltages on the secondary terminals of instrument transformers, radiated electromagnetic fields (EMF) which can be dangerous to adjacent control or relay equipment, in sense of causing damages or malfunctions [3].

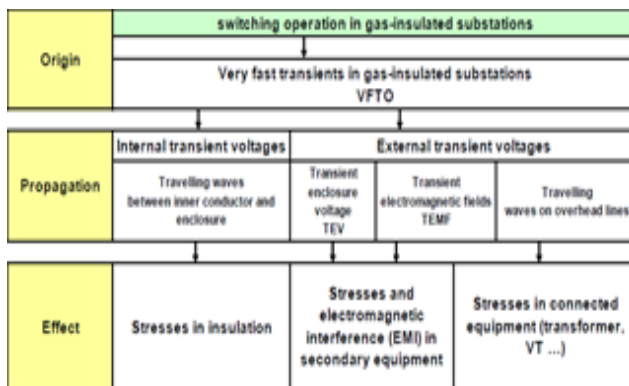


Figure 1: Classification of VFTO in gas-insulated substations

During switching of DS in GIS a varying number of pre-strikes and re-strikes occur, depending of the speed of the switching device. Due to the very fast voltage collapse time of a few nanoseconds at the switching gap, travelling surges are generated in the bus bar duct. The multiple reflections and refractions of these surges at impedance discontinuities within the compartments give rise to complex waveforms, which depend on the design, the operating conditions and external configurations of the GIS [3]. For the discussion about the severity of the traveling waves, a detailed analysis of the current/voltage characteristics is necessary. The voltage collapse during the spark development provides the excitation function for the transients. After the formation time lag has passed, an additional phase

with the duration t_b (spark formation time) is needed to complete the breakdown, which is followed by the voltage collapse. The spark formation time itself is given by the Toepler's spark law. Due to the high breakdown field of SF6, the more uniform electric fields, smaller gap distances and higher gas pressure, nanosecond rise times can be estimated in GIS.

GENERATION OF VFTO'S IN GIS

During switching of DS in GIS a varying number of pre-strikes and re-strikes occur, depending of the speed of the switching device. Due to the very fast voltage collapse time of a few nanoseconds at the switching gap, travelling surges are generated in the bus bar duct. The multiple reflections and refractions of these surges at impedance discontinuities within the compartments give rise to complex waveforms, which depend on the design, the operating conditions and external configurations of the GIS [1]. A VFT is a result of an instantaneous change in the voltage inside the GIS. In most cases this change in voltage is due to the opening or closing operation of a disconnector (DS). VFT may however also be generated by circuit breaker (BRK) operations, a ground switch or due to a fault [3]. An example of a DS operation is shown in figure 2.

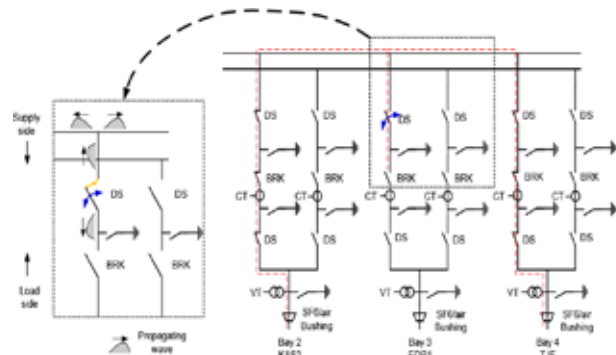


Figure 2.: During a DS operation a travelling wave is generated which may cause overvoltage in the GIS. The dashed line indicates the current path in this specific switching scenario

VFT has two main characteristics:

1. Are in the highest frequency range in power systems: 1 to 50 MHz: The reason for the high frequency is the overall compactness and construction of the GIS. This means that from a modeling perspective it may be considered as several short sections of

transmission lines in series, each with its own surge impedance. This results in many reflections and refractions of the travelling wave occurring at the points of discontinuity, which may superimpose each other. As a result, high frequency over voltages will appear in the GIS [7].

2. Have a rise time of 4 to 100 ns.

PRINCIPLE OF GENERATION OF VFTO

During opening operation of Dis-connector Switch (DS), transients are produced due to large number of re strikes between the contacts. The magnitude of these transients and rise times depends on the circuit parameters like Inductance, Capacitance and Connected Load. Assuming that some trapped charge is left during opening operation, transients can be calculated during closing operation of DS. Fast Transient Over voltages generated during Dis-connector Switch operation are a sequence of voltage steps created by voltage collapse across the gap at re-striking. Specific over voltage shape is formed by multiple reflections and refractions. Operation of Dis-connector Switch (DS) is shown in the Fig. 3.

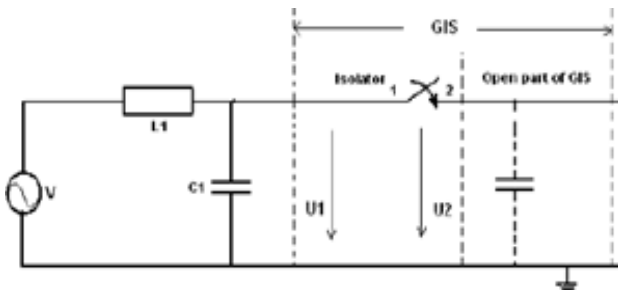


Figure 3. Electric Circuit for explaining re-strikes

Where

L1 = Inductance of Source

C1 = Capacitance of Source

C2 = Capacitance of GIS Open Part

U1 = Power Frequency Voltage

U2 = Voltage of GIS Section

The more frequent service situation of the isolator is its use to connect or dis-connect unloaded parts of the installation as is shown in Fig.3. For example, a part of the GIS is dis-connected by an isolator from a

generator or from an overhead supply line, where by the self capacitance C2 of this part of circuit can be up to several nF, depending on its length. First re-strike across the gap occurs when voltage across the gap exceeds the breakdown voltage. The occurrence of sequence of re-strikes is described with the following Fig. 4 & 5.

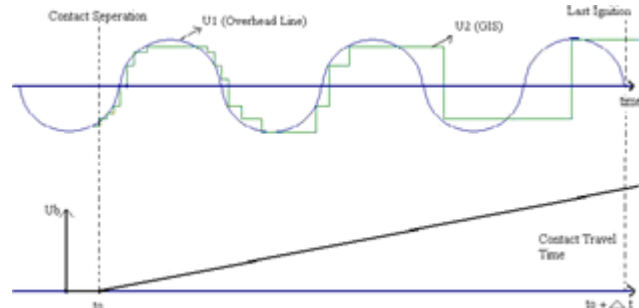


Figure 4. Voltage of the open-ended GIS side of the Isolator

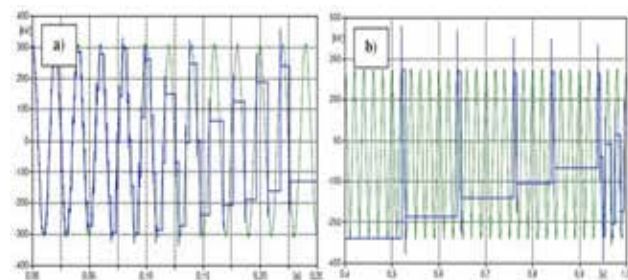


Figure 5. VFT due to disconnector switching – source side voltage (continuously alternating) and load side voltage (step wise) for: a) Opening (re-strikes), b) Closing (prestrikes) operation at disconnector terminals

MODELING GUIDELINES

Due to the travelling nature of VFT, modeling of GIS components makes use of electrical equivalent circuits composed of lumped elements and distributed parameter lines. At very high frequencies, the skin losses can produce a noticeable attenuation. However, due to the geometrical structure of GIS and the enclosure material, skin losses are usually neglected. [3].

A bus duct can be represented as a lossless transmission line. The surge impedance and the travel time can be calculated from the physical dimensions of the duct. Insulating spacers are modeled as capacitors (20 to 30pF), switches are represented with equivalent resistances. The corresponding circuits and values are mentioned in Table 1.

Table 1: Electrical equivalent circuits and values of GIS components

Component	Equivalent Circuit	Notes	Actual values in simulation (Z or C)
Busduct		Loss-free distributed parameter line	65.9 Ω
Spacer		Capacitance to ground. C = 20 to 30 pF	15 pF
Elbow		Distributed Transmission line with a capacitance to ground.	45 pF
Circuit Breaker in closed position		Distributed Transmission line	75 Ω
Circuit Breaker in open position		Capacitance between contacts and to ground. n = number of breaking chambers	50 pF
Closed disconnector		Distributed Transmission line	75 Ω
Disconnector during sparking		Non-linear resistor. r = r(t); R < 10 Ω, C > 10 pF	R=0.5 Ω C=12 pF
Bushing (Gas filled)		C > 10 pF Zs = 250 Ω	250 Ω 30 pF
Power transformer		Parameters evaluated from the frequency response of transformer	C= 2.5 nF
Current transformer		Distributed Transmission line	70 Ω
Capacitor voltage transformer		Capacitance to ground	75 pF

SUBSTATION CONFIGURATION

The GIS substation consists of transformer bays, cable bays, bus coupler bay and bus sectionalizer bay. As it affects the travelling times and hence instant of superimposition of the waves. Magnitude of VFTO at particular instant depends on the superimposition of all waves at that particular instant. Location of the disconnector is varied for the system in fig 6.

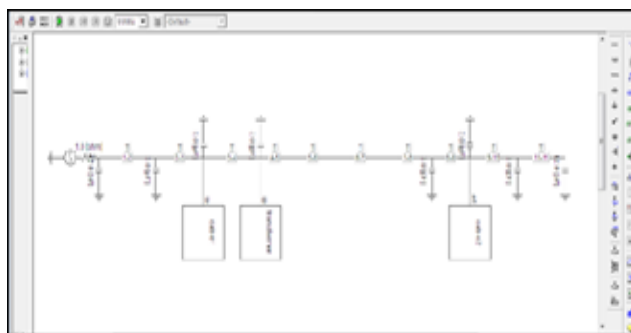


Figure 6(a) : GIS substation configuration

A GIS substation is modeled with parameters mentioned above in PSCAD, one cable bay, transformer bay & spare cable bay is modeled. To analyze the effect of trapped charge the disconnector arc is modeled as non-linear resistance, with topler's constant.

$$R = R_0 e^{-(t/T)} + r \tag{1}$$

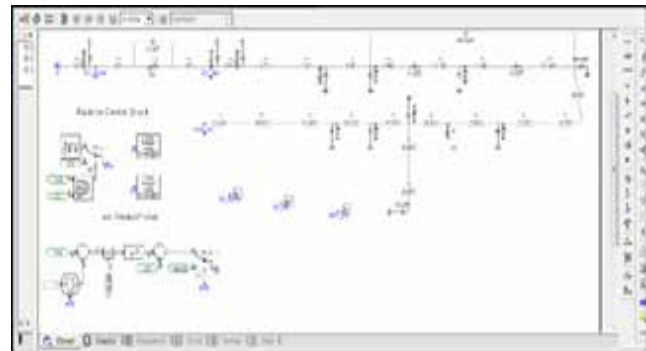


Figure 6(b) : GIS substation configuration-Cable bay

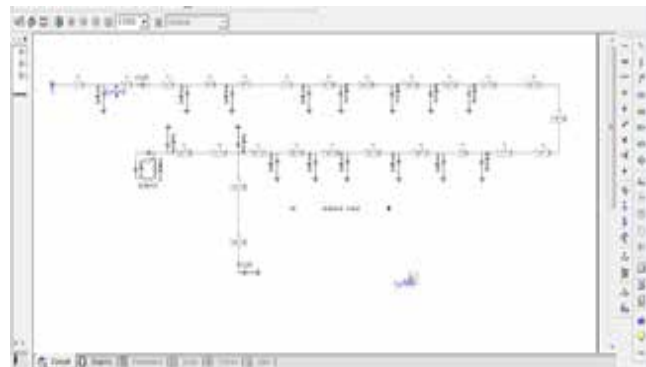


Figure 6(c) : GIS substation configuration-Transformer Bay

Case 1

Figure 6 shows the simulation diagram of case-1, where the cable spare bay is energized. The scenario of the GIS for this is as follows:

Cable bays and transformer bays are connected to main bus bar, without trapped charge. Waveform of overvoltage at the two ends of the disconnector switch is shown in Figure 7 & 8.

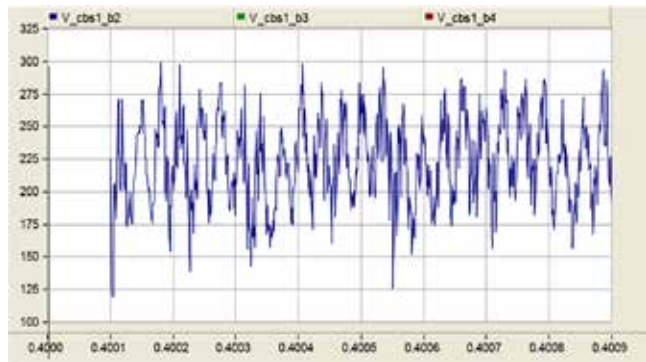


Figure 7 : Overvoltage at DS1 Source

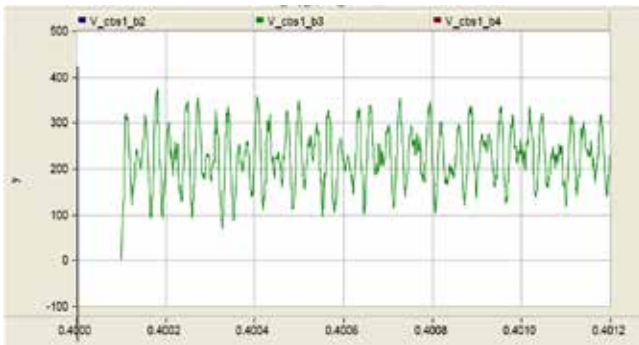


Figure 8 : Overvoltage at DS1 load

Case 2

In this case the cable spare bay 1 is energized with trapped charge of 0.25 P.U. Waveform of overvoltage at the two ends of the disconnector switch is shown in Figure 9 & 10.

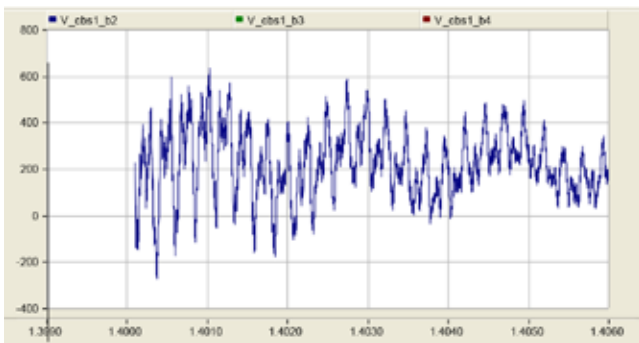


Figure 9 : Overvoltage at DS1 Source

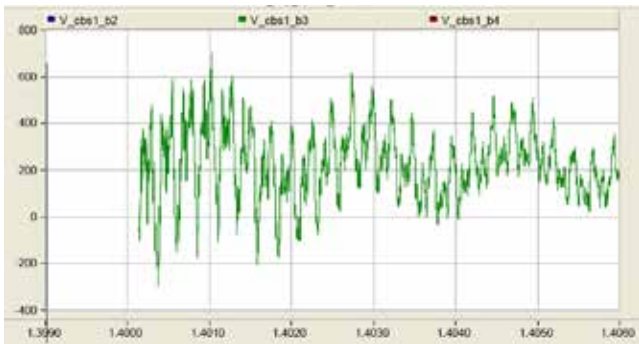


Figure 10 : Overvoltage at DS1 load

Case 3

In this case the cable spare bay 1 is energized with trapped charge of 0.50 P.U. Waveform of overvoltage at the two ends of the disconnector switch is shown in Fig. 11 & 12.

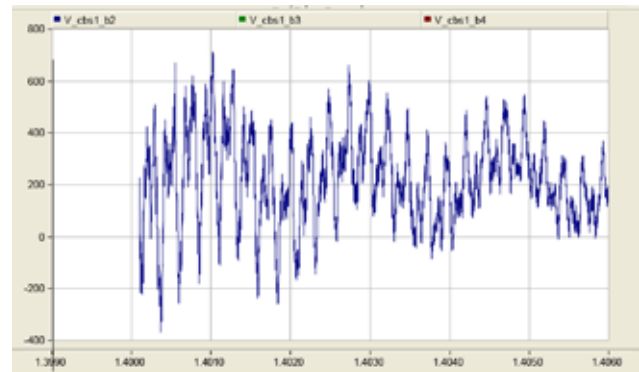


Figure 11 : Overvoltage at DS1 Source

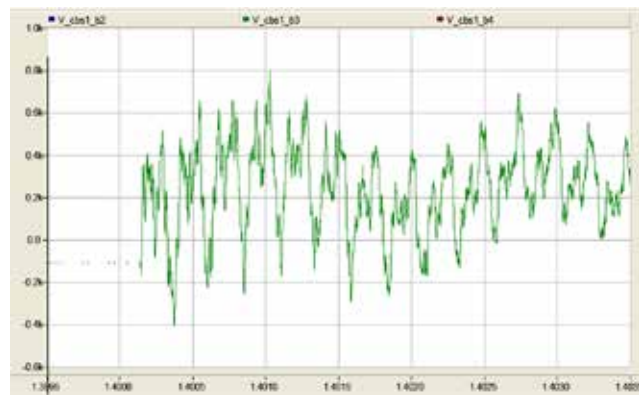


Figure 12 : Overvoltage at DS1 load

RESULTS

	DS	Trapped Charge	Maximum Overvoltage
Case 1	Switching	No	1.66 P.U.
Case 2	Switching	0.25 PU	1.72 P.U.
Case 3	Switching	0.50 PU	3.54 P.U.

CONCLUSION

The VFTO peak magnitudes are higher close to the switching point in the case of disconnector operations where as it is higher at the junction of the GIS. Also, close to the switching point, VFTO waveform has steeper front time and higher frequency of oscillations as compared to a farther away observation point. When the trapped charge on the line is increased, there is an increase in the VFTO levels, but the increase is not proportional to the magnitude of the trapped charge. The influence of trapped charge on the VFTO magnitudes is more in the line where the switching is done.

REFERENCES

1. CIGRE Working Group technical requirements for UHV and EHV Substation Equipment, "Very Fast Transient Overvoltages (VFTO) in Gas-Insulated UHV Substations," IEEE PES Switchgear Committee, September 2012.
2. Boggs S.A., Chu F.Y and Fujimoto N., "Disconnect Switch Induced Transients and Trapped charge in GIS", IEEE Transactions on Power Apparatus and Systems, Vol. PAS-101, October 1982.
3. J.A. Martinez (Chairman), P. Chowdhuri, R. Iravani, A. Keri, D. Povh, "Modeling Guidelines For Very Fast Transients In Gas Insulated Substations," Report Prepared by the Very Fast Transients Task Force of the IEEE Working Group on Modeling and Analysis of System Transients.
4. Yanabu S., "Estimated of Fast Transient over Voltage in Gas Insulated Substation", IEEE Trans. PD, Vol.5, No.4, pp.1875-1881, 1990.
5. Amit Kumar, Mahesh K. Mishra, " VFT Study for EHV-GIS Substation", Fifteenth National Power Systems Conference (NPSC), IIT Bombay, December 2008.
6. DLO, DANIEL LEO OLASON, TEB, THOMAS EBDROP, "VFT insulation coordination study of a 400 kV GIS", Innovation for secure and efficient transmission grids CIGRÉ Belgium Conference Crowne-Plaza – Le Palace Brussels, Belgium | March 12 - 14, 2014.
7. Lu Tiechen, Zhang Bo, "Calculation of Very Fast Transient Overvoltage in GIS", IEEE/PES Conference on Transmission and Distribution, Vol.4, 2005, pp.1-5.
8. Shu Yinbiao, Han Bin, Lin Ji-Min g, Chen Weijiang, Ban Liangeng, Xiang Zutao, and Chen Guoqiang "Influence of the Switching Speed of the Disconnecter on Very Fast Transient Over voltage", IEEE transactions on power delivery volume 28, NO. 4, OCTOBER 2013.

Analysis of EM Waves Emitted from Multiple Partial Discharge Sources in a GIS Using FDTD Method

Mahesh A. Patil, Sonali Borase

Pune Vidyarthi Griha College of Engineering
Nashik, Maharashtra

✉ Mahesh.patil@pvgcoenashik.org

M. V. Bhatkar

Jawahar Education Society's. Institute of Technology,
Management & Research
Nashik, Maharashtra

ABSTRACT

Partial Discharge (PD) may be caused by not only one source but also multiple sources. It should also multiple sources. It should also be taken into consideration of the occurrence of multiple PDs. Hence, in this paper, Electromagnetic (EM) waves emitted from multiple PD sources in a Gas Insulated Switchgear (GIS) are analyzed by using Finite Difference Time Domain (FDTD) method, and the effect of change the position and number of PD sources is examined. As a result, frequency spectrum and waveform are affected by factors of position and number of PD sources, and resonant frequencies are related to the structure of GIS. Thus, necessity considering structure of GIS must be concluded to estimate multiple PD sources..

KEYWORDS : Partial Discharge (PD), Finite Difference Time Domain (FDTD) method, Gas Insulated Switchgear (GIS), Electromagnetic (EM) wave, Fast Fourier Transform (FFT).

INTRODUCTION

Background

Gas insulated switchgear (GIS) has been widely used in power station and substation. The possible defect types in GIS spacers are described in Figure 1. The defects which may cause Partial Discharge (PD) in a GIS are free metallic particles, which can travel in the GIS cavity, a needle on conductor and an air void in insulator are produced during manufacture, assembly and running. Delamination in spacer is caused by stresses such as mechanical, thermal and electrical stresses [1], [2].

PD eventually causes insulation breakdown. Thus, the detection of PD at early stage is very important for preventing insulation failure and improving the power supply reliability. The method of detection of PD may be electrical, chemical, acoustic, Ultra High Frequency (UHF) or a combination of these methods [3]. These acoustic and UHF is widely used because of its accuracy and wide range of detection. The EM waves leak out from the solid insulator. External antenna can be easily installed on the outside of GIS to detect PD.

In this paper, simultaneous occurrence of multiple PDs was assumed.

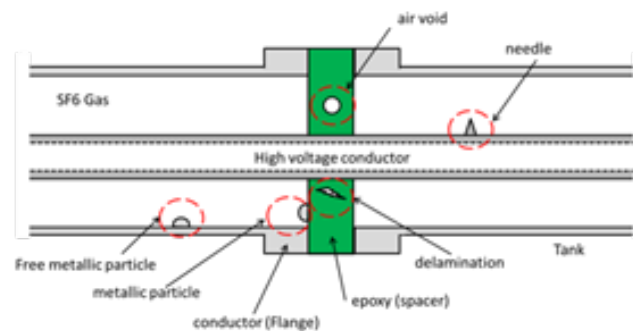


Figure 1. Several insulation defect in GIS.

Objective

It may occur multiple PDs, and to study multiple PD phenomena is important to detect them. In this paper, the results that observed EM waves caused by multiple PD sources at different positions are a preliminary stage to separate them. FDTD method and FFT method are used to analyze waveform and spectra of EM waves. The results comparing multiple PD sources are examined the possibility of separation of multiple PD sources.

Spectra depend on the structure of a GIS, thus the thickness and position of spacer, position and number of bolts, the inside diameter of outer conductor, the outside diameter of inner conductor, length of GIS tank should be considered. In this paper, these influences were also examined.

METHOD

Finite Difference Time Domain Method

FDTD method is one of the techniques for the solution of electromagnetic problem. It is proposed a discrete solution to Maxwell’s equations based on central difference approximations of the spatial and temporal derivatives of the curl equations. The mathematical relationship of the electromagnetic fields radiated by time dependent current or charge densities is governed by Maxwell’s equations. This method is the staggering of the electric and magnetic fields in both space and time in order to obtain second order accuracy [4], [5].

Perfectly Matched Layer

A perfectly matched layer (PML) is an artificial absorbing layer. PML is a technique of free space simulation to solve unbounded electromagnetic problems with the FDTD method. The condition of impedance matching is satisfied, then impedance of the medium equals to that of vacuum and no reflection occurs when a plane wave propagates normally across a vacuum medium interface [6]. In practice, there will be small reflections due to the discretization of the PML equation.

Partial Discharge Current Source

PD current pulse can be expressed using the following exponential equation [7].

$$i(t) = \frac{I}{T} t \exp\left(1 - \frac{t}{T}\right) \tag{1}$$

Where, t is time and I and T are parameters defining the peak current and rise-time of current pulse. The total amount of charge Q contained in this pulse is:

$$Q = eITQ = eIT \quad (e=2.7183) \tag{2}$$

Where, current density J is:

$$J_z^{n-\frac{1}{2}} = \frac{1}{\Delta x \Delta y} I_z \left(\left(n - \frac{1}{2} \right) \Delta t \right) \tag{3}$$

Modeling Gas Insulated Switchgear

Figure 4 shows the simulation model of GIS, and PML is used as boundary condition. The time step is chosen 9.6ps because of stability criterion. It is necessary to satisfy a relation between the space increment and time increment for computational stability [5]. The number of PML layers is 10. Therefore, total length of PML layers is 50mm on each side. Total length of analysis area is 4170mm in x-direction, 520mm in y-direction and z-direction. The positions of antenna are around middle spacer. Where, there are PD sources at left spacer, and their direction is z-direction. In particular, EM waves leak at all spacers, however, EM waves leak at only middle spacer for simplicity.

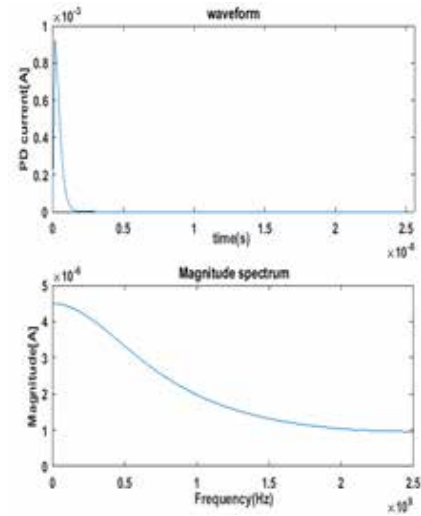


Figure. 2 PD pulse

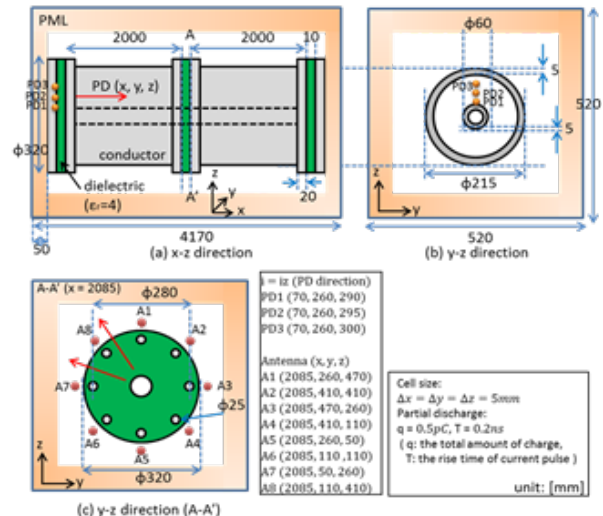


Figure 3. Model of straight GIS

Coaxial Cable

Coaxial cable has multiple modes like TEM, TE and TM. The cutoff frequency f_c is given by equation (4) [8].

TE_{mn}
mode

$$f_{c(TEM1)} = \frac{cm}{\pi(a+b)} \quad (n = 1)$$

$$f_{c(TEMn)} = \frac{c(n-1)}{2(b-a)} \quad (n \geq 2)$$
(4)

TM_{mn}
mode

$$f_{c(TMmn)} = \frac{cn}{2(b-a)}$$
(5)

Where, outer radius of inner conductor is a and inner radius of outer conductor is b.

RESULT

Comparing waveforms of E_x , E_y and E_z components, E_x component is the highest amplitude of three components. This reason is the space between flanges. There are spacer and bolts between flange and flange. There are eight bolts in the spacer, and slots are made from them. These slots play a part as slot antennas. Slot antennas make electric field in short side direction of them, as shown Figure 8 [1]. In this case, electric field in short side direction is x direction. Thus, amplitude of E_x component is amplified, and amplified E_x component leaked through outside of GIS. This directivity could be found in Figure 1.

Resonant frequency is calculated by length of slots in long side. The length of slots in long side L is about 82mm. Hence, resonant wavelength is calculated by equation (6). From this result, resonant frequency is about 1.8GHz. Magnitude spectra of E_x component is shown in Figure 8. It is found that spectra have peak at around 1.8GHz.

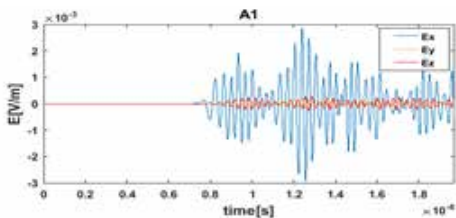


Figure 4. Waveforms of electric field. (only PD1)

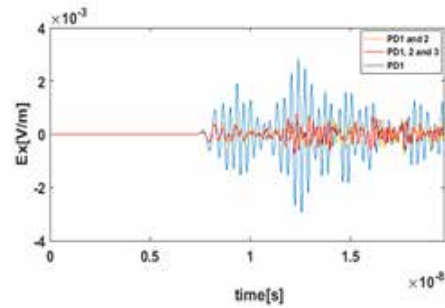


Figure 5. Waveforms of electric field. (only PD1, PD2, PD3)

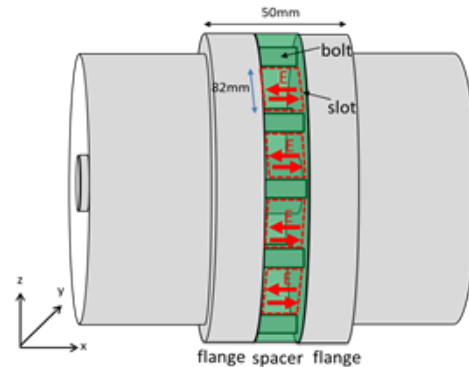


Figure 6. Waveforms of electric field. (only PD1)

Table 1. Cutoff frequency (TE mode)

Cutoff frequency[MHz]							
TE11	TE21	TE31	TE41	TE51	TE61	TE71	TE81
720	1441	2162	2882	3603	4324	5044	5765

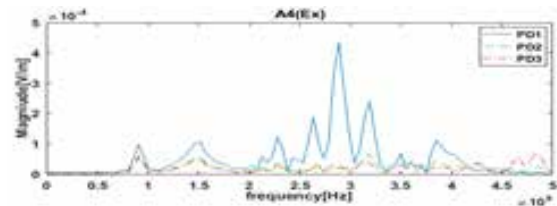


Figure 7. Magnitude spectrum of electric field. (only PD1, PD2, PD3).

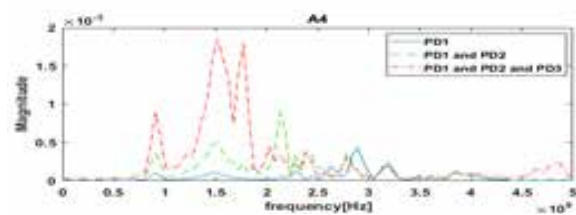


Figure 8. Magnitude spectrum of electric field. (multiple PDs)

These spectra have many peak points. The factors affecting propagation of electromagnetic waves are the structure of GIS and frequency component of PD. For example, resonant frequency and cutoff frequency are depend on size of GIS, thickness of spacers, length of GIS tank (outer conductor) and length of high voltage conductor (inner conductor). Propagation modes of coaxial waveguide are not only TEM, but also TE and TM modes. TEM mode contains low frequencies above direct current. In the frequency above cut-off frequencies of TE or TM mode depend on the length of coaxial waveguide. TE and TM modes contain high frequencies.

Frequency spectra doesn't contain up to 5GHz. The reason for this phenomenon is spacer made of epoxy. High frequency components attenuate more quickly, reflection and dielectric loss are bigger than low frequency components.

Cutoff frequencies of TE modes are calculated by equation (4), and Table 1 shows cutoff frequencies of each mode. When the number of PD sources was changed, predominant modes also changed. TE₄₁ mode is dominant in case of only PD1, TE₃₁ mode is dominant in case of PD1 and 2, TE₂₁ mode is dominant in case of PD1, 2 and 3. EM waves of each PD source are interfering. Then, dominant mode was changed.

CONCLUSION

In this paper, EM waves emitted from multiple PD sources in a GIS are analyzed by using FDTD method, and the effect of change in position and number of PD sources on waveform and frequency spectra is examined. As a result, frequency spectrum and waveform are affected by them, and resonant frequencies are related to the structure of GIS. Moreover, frequency spectrum and waveform are affected by change of position and

number of PD sources. Resonant frequencies of EM waves are related to propagation mode and bolts. Future work is to separate multiple PD sources by considering structure of GIS.

REFERENCES

1. Diaa-Eldin A. Mansour, Hiroki Kojima, Naoki Hayakawa, Fumihiko Endo and Hitoshi Okubo, "Partial Discharges and Associated Mechanisms for Micro Gap Delamination at Epoxy Spacer in GIS," IEEE Transactions on Dielectrics and Electrical Insulation, Volume 17, Issue 3, pp. 855-861, 2010.
2. Takashi Kimura, Takao Harunami, Naohiro Konma and Kazutoshi Saito, "Diagnostic Method for GIS insulating Systems Using External Antenna," IEEE Transactions on Power and Energy, Vol. 115, pp.1199-1207, 1995.
3. Shuhei Kaneko, Shigemitsu Okabe and Hirota Muto, "Electromagnetic wave radiated from an insulating spacer in gas insulated switchgear with partial discharge detection," IEEE Transactions on Dielectrics and Electrical Insulation, Vol. 16, pp.60-68, 2009.
4. Stephen D. Gedney, "Introduction to the Finite-difference Time-domain (FDTD) Method for Electromagnetics," 2011
5. K. S. Yee, "Numerical Solution of Initial Boundary Value Problems Involving Maxwell's Equations in Isotropic Media," IEEE Transactions on Antennas and Propagation, Vol.14, No.3, pp.302-307, 1966.
6. J.-P. Berenger, "A Perfectly Matched Layer for the Absorption of Electromagnetic Waves," Journal of Computational Physics, Vol.114, pp.185-200, 1994.
7. M.D. Judd, Li Yang and I.B.B. Hunter, "Partial discharge monitoring of power transformers using UHF sensors. Part 1: sensors and signal interpretation," IEEE Electrical Insulation Magazine, Vol.21, pp. 5-14, 2005.
8. Humiaki Okada, "Microwave engineering," 2004.

Intermittent Nature of Distributed Generation and its Impact on Electricity Market

Swati K. Warungase

Department of Electrical Engineering
K.K. Wagh, Institute of Engg Education and Research
Nashik, Maharashtra
✉ theteswati81@gmail.com

M. V. Bhatkar

Jawahar Education Society's. Institute of Technology,
Management & Research
Nashik, Maharashtra

ABSTRACT

This study looks at how to best integrate different distributed generation (DG) sources, such as Electric vehicles (EVs), wind power, and solar power, into a distribution network in order to reduce overall realistic power loss, overall expenditure, and emissions created by the grid as congestion of different load and different distributed generations are increased at distribution system. The specified objectives and benefits were realised through the development of a multiple objectives function. Using a number of mathematical models of DGs, the effects on the distribution network with variable load demand for 24-hrs were investigated in this study. Additionally, the idea of charging and discharging EVs at the time of off-peak and peak system usage times was taken into consideration. Due to the resilience of the Gbest-guided Artificial Bee Colony (GABC) optimization technique, successfully completed this non linear optimization challenge. The optimal integration of DGs can, however, drastically reduce the overall realistic power loss, overall expenditure, and emissions to a significant amount, as shown by the numerical results obtained using the proposed technique which avoids congestion on network

KEYWORDS : *Gbest-ABC algorithm, Distribution network, Electric vehicles, Emissions, Real power loss.*

INTRODUCTION

Distributed Generations (DGs), which include power from solar, biomass, fuel cells, gas turbines, wind turbines, micro turbines, and electric vehicles (EVs), are being used more frequently as energy sources around the world. These DGs are located on the consumer side of distribution networks. DGs have gained value recently as a result of their technical, financial, and environmental advantages. These gain include the reduction of emitting gases, the development of transmission lines, a decreased reliance on fossil fuels, and environmental condition. The intention was for distributed generations (DGs) to provide 20% of the European Union's (EU's) total ultimate energy consumption by the end of 2020 [7]. Additionally, EVs have been suggested quite a bit as a grid power source during grid peak times, which aids in lowering oil consumption and emissions of air pollutants [6]. The future of EVs appears bright due to their superior both environmental and energy benefits compared to traditional automobiles [10].

Using the Multi-objective Artificial Bee Colony (MOABC) technique, the ideal sizes of hybrid photovoltaic, WT, and FC energy are assessed for minimizing true power loss, grid power purchased, emissions, and maximizing voltage stability [2].

power losses, voltage deviation, and overall cost. A Genetic Algorithm (GA) was used for this [1]. The GABC algorithm has been effectively used to a variety of power system issues, including economical load dispatch, unit commitment, and efficient power flow. This promotes implementation in order to address the distribution-system issue. In order to determine the best allocations and the best number of DGs to penetrate in the distribution grid using the GABC algorithm during an unsure load, this study develops a novel multi-objective function. Its a freshly created meta-heuristic optimization method that was inspired by honeybees' foraging behaviour. The minimizing of reduce overall realistic power loss, overall expenditure, and emissions created by the grid under variable load are some of the

goals for this issue. The GABC algorithm performs well, converges quickly, handles composite nonlinear constraint problems well, and only requires a small number of control parameters. It has been chosen as the best solution to this problem because of these benefits.

This work's primary contribution addresses the following issues under variable load condition in the following ways:

- In order to calculate the voltage, current, and power losses of the distribution system, a backward/forward load flow programme was developed.
- To make the issue more realistic, a variable load requirement for each bus over the course of 24 hours was taken into consideration.
- Formulation of mathematical models for the production of solar and wind energy as well as for the charging and discharging of electric vehicles.
- Several costs, including the price of grid-purchased power, the expenditure of installing a WT, the expenditure of maintaining a WT, the expenditure of installing a PV system, the cost of maintaining a PV system, and the cost of installing an inverter, are all calculated at once.
- The effects of incorporating DGs on true power loss, as well as emissions generated by the network over a whole day, were looked at.

PROBLEM FORMULATION

Formulation of Multi-Objective Problems

The introduction of various DGs in distribution networks has received attention mainly account of environmental concerns and system-related load demand uncertainty. Identify the ideal location and size of DGs, a multiple objective function has been developed. With this, the overall running costs, power loss, and grid emissions are all taken into consideration. The representation of this multi-objective function is given by (1),

$$\text{minimize } F = W1 \times TC + W2 \times P_{Loss} + W3 \times Emission \quad (1)$$

Total Cost (TC) objective

The total Cost objective comprises the purchased real power price from the network, PV installing price, and operating and maintaining price. The WT installing

price and its operating and maintaining price, inverter installing price, and charging and discharging of EV.

$$TC = \sum P_p(t) + PV_{instt} + PV_{O\&M} + WT_{instt} + WT_{O\&M} + INV_{instt} + \sum_{i=1}^{24} C_{EV}(t) \quad (2)$$

The first term of total cost objective function is a purchased real power price (Cp) from network and a linear function can define it as,

$$Pp(t) = PSE(t) \times PTE(t) \quad (3)$$

Equation (4) is used to determine next expression, which represents the PV instalment price (PVins). The PV Operation & Maintenance (PVO&M) price, which represents the term third, is equal to 3% of the PV installation price.

$$PVins = P_{O\&M} \times PPV \quad (4)$$

Similar to the third term, the fourth term is the price of installing the WT (Wins), which is calculated using (5), and the price of operating and maintaining the WT (WO&M) is equal to 1% of the price of installing the WT.

$$Wins = Pw \times P_{PW} \quad (5)$$

The inverter installation cost (INVins) is represented by the sixth term and can be calculated using Eq. (6). Additionally, equation (7) was used to calculate the inverter's size (Pinv).

$$INVins = P_{inv} \times P_{Pinv} \quad (6)$$

$$P_{inv} = PL_{peak} / \eta_{inv} \quad (7)$$

In this equation, η_{inv} is the inverter efficiency which is 90% and PL_{peak} represent the network's peak load. The inverter's capital cost (P_{Pinv}) is 711 US\$.

The cost of plugging in and plugging out electric vehicles (CEV) to a grid is indicated by the seventh term of the objective function. Owners of vehicles select when to charge and when to discharge their batteries in order to maximize benefits. Therefore, it is shown by Eqs. (8) as

$$CEV(t) = PSE(t) [\eta_{dch} \cdot P_{dch}(t) - \eta_{ch} \cdot P_{ch}(t)] \quad (8)$$

Power Loss (P_{Loss}) Objective

This objective sums up the actual power loss (P_{Loss}) that occurs over the period of a 24-hour across each bus in a distribution network, and it is represented by (9).

$$P_{Loss} = \sum_{m=1}^n P_{Loss(m,n)} \tag{9}$$

Total emissions objective

The emissions generated by the grid and the DGs are represented by the final objective of the multi-objective function. Carbon dioxide (ĈO₂), nitrogen oxide (ÑO_x), and sulphur dioxide (ŜO₂) are just a few of the dangerous pollutants it contains. Table 1 has a list of these numbers. Using equation (10), the total emissions generated throughout the course of 24 hours were calculated.

$$E_{grid} = \sum_{t=1}^{24} PT(t) \times (\dot{C}O_2 + \dot{N}O_x + \dot{S}O_2) \tag{10}$$

Table 1: Listing of emission coefficients

Type of Emission	ÑO _x	ŜO ₂	ĈO ₂
Emission coefficients (lb/MWh)	5	1	2
	.	1	0
	0	.	3
	6	6	1
		0	

Where as 'P_{SE}', 'P_{Td}', 'P_{V_{po}}' and 'P_{PV}' stand in for the spot market cost of electricity, entire active power demand, produced output power from solar energy, as well as installation costs, respectively. The capital cost of the WT installation and the output power of the wind turbine, respectively, are written as PPW and 'Pw. The charging/discharging efficiency of EVs is indicated by ch/dch. EVs' charging and discharging power is shown by the symbols ch and dch, respectively.

The fitness function comprising multiple objectives is given by (1), as follows:

*Minimize F = W1 * TC + W2 * P_{Loss} + W3 * Emission*

The limitations stated in the aforementioned equations as well as the constraint stated in (11) below are applied to the aforementioned fitness function.

$$\sum_{i=1}^F W_i = 1 \tag{11}$$

Here, F is the total number of objectives and W_i is the Weight factor.

The Pareto optima set is immediately invoked as part of this approach to solving the MOO. Once a collection of alternatives has been found, the best compromise is found based on the situation. In this study, the optimum compromise option was chosen using the fuzzy set theory. Using the following equation, the associated membership function value for each objective function is calculated in this method:

$$\delta_i = \begin{cases} 1 & \text{if } F_i \leq F_i^{min} \\ \frac{F_i^{min} - F_i}{F_i - F_i^{max}} & \text{if } F_i^{min} \leq F_i \leq F_i^{max} \\ 0 & \text{if } F_i \geq F_i^{max} \end{cases} \tag{2.12}$$

Here F_i^{max} and F_i^{min} are the maximum and minimum values of the δ_i objective function obtained in Pareto set.

DISTRIBUTED GENERATIONS

In terms of generation and operation, DGs play a significant role in power systems in this study. When a distribution system is present, these function as distributed generation. The term "gridable vehicles" refers to EVs that can add electric power to the grid. During system off-peak hours, they can be charged up to a certain maximum, and during system peak hours, EVs can send electricity to the system to satisfy peak demand requirements. The grid's emission rates are reduced and the network's dependability is raised by the incorporation of EVs.

An interaction with a Distribution Management System (DMS) requires, three different DG aggregators are well thought out in this work. The DMS will distribute electricity in accordance with the data gathered from various aggregators, which are shown in Fig. 1.

Through the WTs, the WT aggregator compiles data on the production of wind energy. The PV aggregator gathers data of power generation from the PV source in a similar way. For the purpose of charging and discharging EVs, all car owners must first register their personal vehicles to the EVs aggregator. The EVs aggregator then notifies the car owner to charge and discharge the battery in accordance with the grid's load circumstances. This work assumes a smart distribution network with contemporary infrastructure and smart computing technologies that can guarantee the proper operation and utilization of these DGs. The following paragraphs discuss the mathematical models of these DGs units.

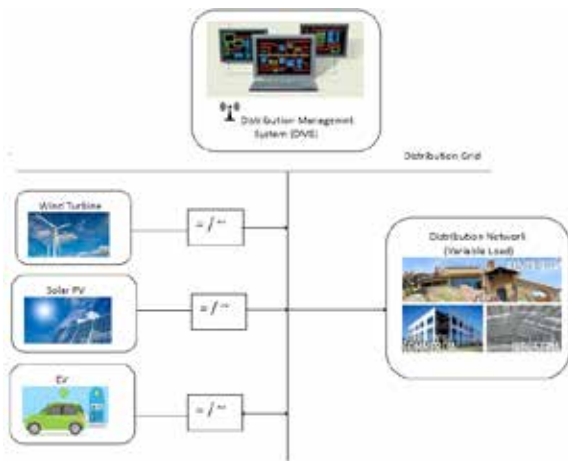


Fig. 1: Organizational Structure of DMS

Model for Production of Solar Energy

The PV module's output power generation is mostly influenced by the solar irradiance intensity. The binomial distribution, which is an provision of two linear uni-modal distribution functions, is typically used to describe the by the hour irradiance presence at a particular place [3]. Both uni-modal are implemented using a Beta Probability Density Function (BPDF), which is described in the following equation (13):

$$Fb = \begin{cases} \frac{\Gamma(\alpha + \beta)}{\Gamma(\alpha) \Gamma(\beta)} \times \hat{S}^{\alpha-1} (1-\hat{S})^{\beta-1} & 0 \leq s \leq 1, \alpha \geq 0, \beta \geq 0 \end{cases} \quad (13)$$

In this, \hat{S} representing the solar irradiance (kW/m²). α and β are the beta distribution function fb(s) parameters,

which are analyzed with Eqs. (14) and (15). μ and σ represents mean and standard deviation of \hat{S} respectively.

The solar irradiation (kW/m²) is shown here as \hat{S} . The beta distribution function's fb(s) factor, β and α , are determined with the aid of Eqs. (14) and (15). The symbols μ and σ signify the mean and standard deviation, respectively.

$$\beta = (1 - \mu) \times \left(\frac{\mu \times (1 + \mu)}{\sigma^2} - 1 \right)$$

$$\alpha = \left(\frac{\mu \times \beta}{1 - \mu} \right)$$

The solar irradiation \hat{S} and numerous PV module attributes, including the ambient temperature T_A , determine how much power the PV module produces. Additionally, the output power produced by solar irradiance \hat{S} is at peak power level which is find out with the formula (16). In figure 2, \hat{S} hourly basis was obtained from the Taiwan Weather Bureau.

$$PV_{out} = N \times FF \times v_{oc} \times v_{cy} \quad (16)$$

$$v_{cy} = v_{oc} \times v_k \times T_{cy} \quad (17)$$

$$y = \hat{S} [I_{sc} + v_k (T_{cy} - 25)] \quad (18)$$

$$= \frac{F_p}{v_{oc} \times v_{sc}} \times v_{MPT} \times I_{MPT} \quad (19)$$

$$T_{cy} = T_A + \hat{S} \left[\frac{N_{OT} \times 20}{0.8} \right] \quad (20)$$

where T_{cy} , T_A , and N_{OT} stand for the temperature of the solar module, the surrounding air, and the normal operating temperature, respectively. The solar module's open-circuit voltage and short-circuit current are denoted by v_{oc} and I_{sc} , respectively. The temperature coefficients for voltage and current are v_k and I_k , respectively. The terms v_{MPT} and I_{MPT} stand for maximum power point voltage and current, respectively. The connected PV module count (N) and fill factor (FF) are two different quantities. V_{out} is the output power of a PV module in \hat{S} .

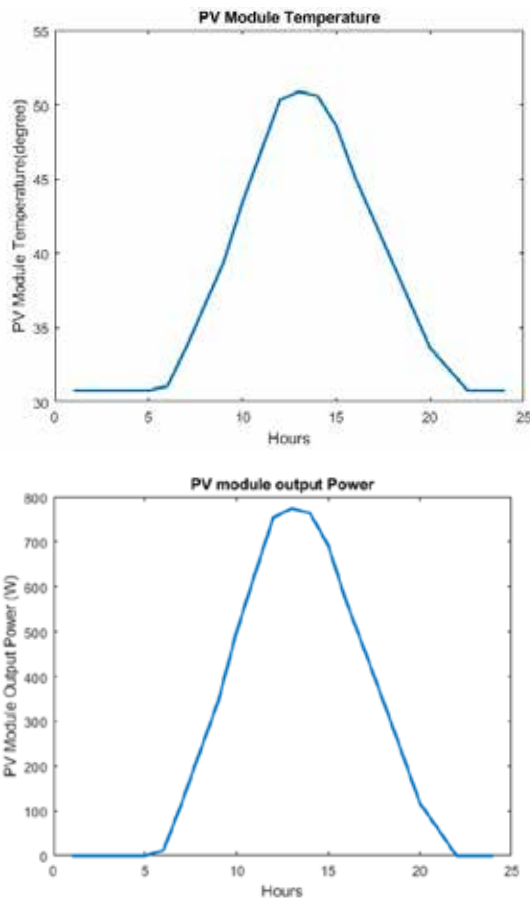


Fig. 2: Hourly solar irradiance and output of solar Model for Production of Wind Power

The commonly used Rayleigh PDF was employed for each anticipated period to describe the unpredictable character of the wind velocity [4]. The shape factor is set to 2 for the Weibull Probability Density Function (WPDF).

$$f_w(v) = \left(\frac{2v}{c^2}\right) \exp\left[-\left(\frac{v^2}{c^2}\right)\right] \tag{21}$$

where $f_w(v)$, c , and v are the Rayleigh PDF (RPDF), scale component, and wind velocity, respectively. If the intermediate speed of wind (v_m) is known, then scaling component c can be calculated using (22-23). The output power generated through the WT was evaluated using (24).

$$v_m = \int_0^\alpha v f_w dv = \int_0^\alpha \left(\frac{2v^2}{c^2}\right) \exp\left[-\left(\frac{v^2}{c^2}\right)\right] dv = \frac{v_m}{2} c \tag{22}$$

$$c \cong 1.128 v_m \tag{23}$$

$$P_w(v) = \begin{cases} 0, & 0 \leq v_{aw} \leq v_{ci} \\ P_{rated} \times \frac{v_{aw} - v_{ci}}{v_r - v_{ci}}, & v_{ci} \leq v_{aw} \leq v_{co} \\ 0, & v_{co} \leq v_{aw} \end{cases} \tag{24}$$

In this case, the procurable wind, cut in, rated, and cut off speeds are represented here by v_{aw} , v_{ci} , v_r , and v_{co} , respectively. The real hourly-based wind speed data is depicted in Fig. 3 and was taken from Willey Online Pvt. Ltd.

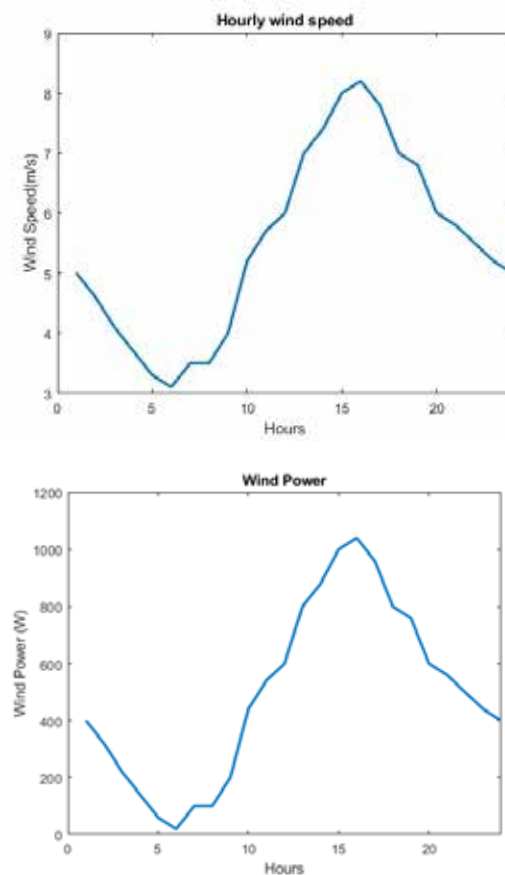


Fig. 3: 24 hour available wind speed and WT output EV charging and discharge schedules

In this study, the grid-connected automobiles behave as power sources and supply power to the network at the time of off-peak hours, but at the time of peak hours, they act as loads to charge the vehicles. As stated by the unregulated energy sector, the price of spot electricity is announced a day comes in advance. Depending on

this price, vehicle proprietor select when to charge and discharge their cars in order to maximize profit [9]. Therefore, using (25) and (26), respectively, the 24 hour charging and discharging capacities of EVs were assessed.

$$P_{dch}(t) = \eta_{cap} [\phi_{pre} - \phi_{min}] \dot{N}_{EV}(dch)(t) \tag{25}$$

$$P_{ch}(t) = \eta_{cap} [\phi_{dep} - \phi_{pre}] \dot{N}_{EV}(ch)(t) \tag{26}$$

The charging and discharging capabilities for EV batteries should be kept within the range of minimum (ϕ_{min}) and maximum (ϕ_{max}) in order to extend the battery life of EVs,.

$$\phi_{min} \eta_{cap} \leq \eta_{cap}(t) \leq \phi_{max} \eta_{cap} \tag{27}$$

In this case, $\dot{N}_{EV}(ch)(t)$, $\dot{N}_{EV}(dch)(t)$ and η_{cap} denote the number of EVs coming for charging and discharging within a 24-hour period as well as the battery power of the EVs respectively. The present and departure states of charge are represented by ϕ_{pre} and ϕ_{dep} . The charging and discharging schedule for EVs during a 24-hour period is shown in Fig. 4.

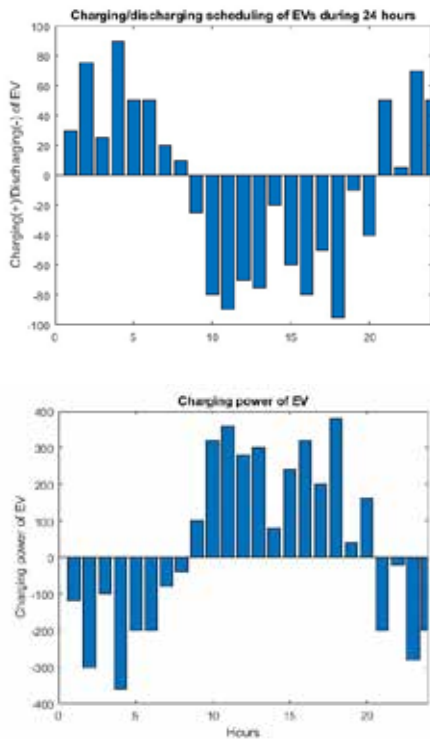


Fig. 4: Scheduling EV charging and discharge for a 24-hour period

Optimization of Power loss, Expense, and Emissions

To select all decision variables wisely and to adhere to all equality and inequality constraints, an optimization method is required. Utilizing DGs, including EVs, to the fullest extent possible will reduce emissions, total expenses, and power loss to a large extent. Due to its resilience and capacity to identify the best solution, the GABC optimization method was used to tackle this challenging nonlinear multi-objective problem. It shares features with other population-based meta-heuristic algorithms and takes inspiration from honeybees' foraging behaviour [5].

The employed, observer, and scout bee groups are represented in this method. The employed bee initially chooses the locations of the food sources (solutions) at random. Then, by engaging in a particular dance, they reveal information about the location of the food supply to the observer bee. In the end, observer bees locate a food supply closer to the employed bee food supply. The scout bee seeks a better solution at random if the food origin positions (solutions) are not cleared in the specify attempt. Under load uncertainty and EVs, this technique has been used to determine the best allocations as well as the best number of DGs. As a result, these are considered decision variables. Better results in relation to overall cost, power loss, and emissions can be achieved with this strategy, which is appropriate and effective.

DISCUSSION AND FINDINGS

The above-mentioned recommended methodology was put into practise in a typical 33-bus radial distribution network to reduce power loss, overall costs, and emissions. There are 33 buses, 32 branches, one main feeder, and three sub-feeders in this test network. According to Baran and Wu (1989), it was run at 100 MVA and 12.66 kV. Fig. 5 displays corresponding block diagram of the test system. To make the problem more realistic in this study, an unknown load requirement for each bus was taken into account for 24 hours, as illustrated in Fig. 6. The hourly spot price for energy is shown in Table 2 and was obtained from the Ontario electricity market.

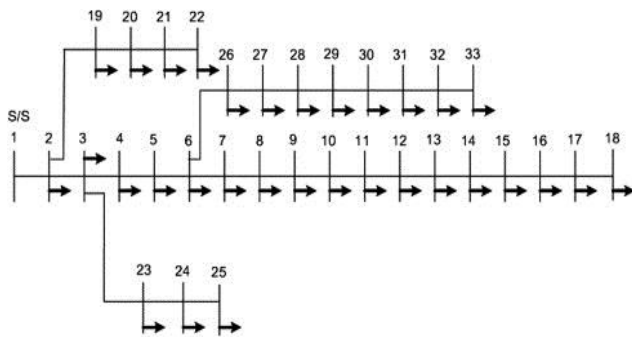


Fig. 5: Equivalent single line diagram for the distribution network for 33 buses

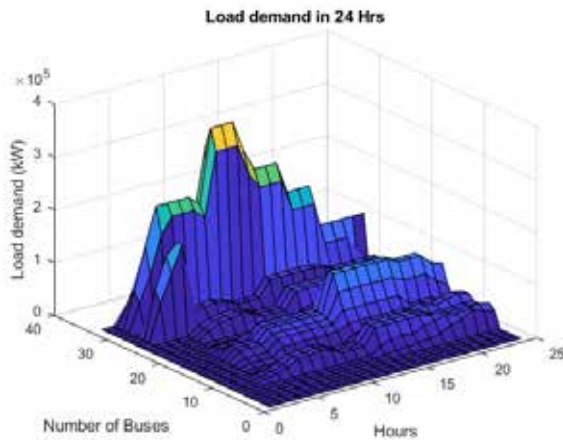


Fig. 6: Demands for each bus in the 33-bus distribution system fluctuate depending on the load throughout the day.

Table 2: Spot power price for each hour

Time (hr)	Cost (US\$/MWh)	Time (hr)	Cost (US\$/MWh)	Time (hr)	Cost (US\$/MWh)
1	47.47	9	67.27	17	35.55
2	31.64	10	52.29	18	112.42
3	31.65	11	44.59	19	575.58
4	32.60	12	108.49	20	87.72
5	40.78	13	60.64	21	35.06
6	38.64	14	40.88	22	47.18
7	158.95	15	28.50	23	61.27
8	384.14	16	38.75	24	33.90

The following cases were considering to be able to confirm the viability and efficacy of the suggested approach:

First scenario: In this scenario, there are no DGs plugged into the network. This is the network's default configuration. According to Fig. 7, the network's total real power loss is 1847.407 kW. As shown in Fig. 8, the amount needed to obtain active power from the electrical network is 2689.532 US dollars. In accordance with Fig. 9, the emission generated by the grid over an entire day was 53828.88 lb/MWh.

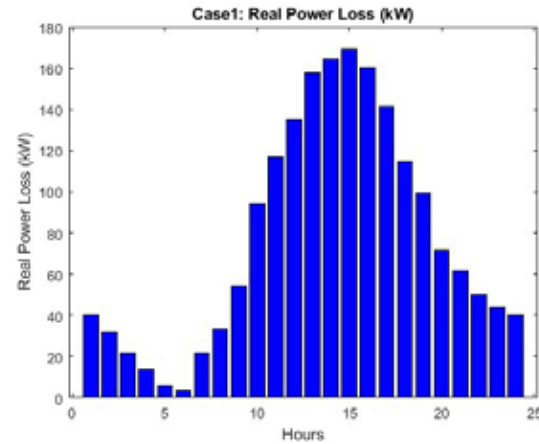


Fig. 7. First scenario - Real power Loss for 24 hrs

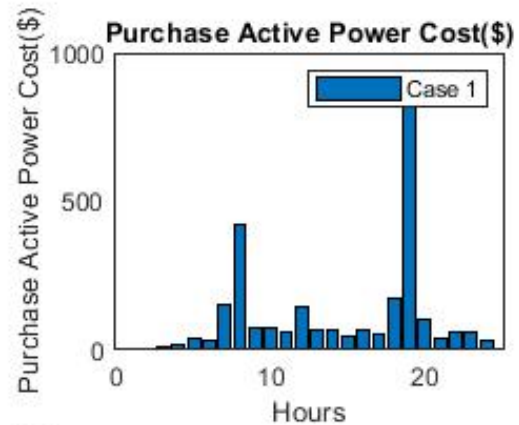


Fig. 8. First scenario - Purchased Power Cost for 24 hrs

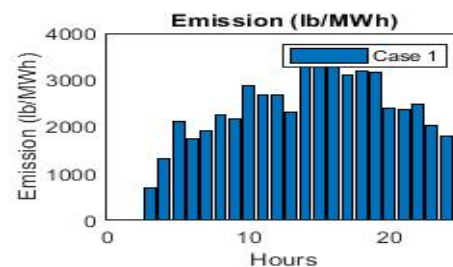


Fig. 9. First scenario - emission Produced

Second scenario: In this instance, the WT is set up with 42 WT units at the best possible location, bus number 4. The actual power loss when these WT units were added was 1073.084 kW. Charges for O & M, WT installation, and active power acquisition from the grid are 1,14,261.840 US dollars, 1,14,26,184.00 US dollars, and 1213.273 US dollars, respectively.

The emission produced after 24 h was 21973.111 lb/MWh. The real power loss, purchased active power cost, and pollution generated by the grid is reduced compared to case 1 and shows in fig. 10, fig 11, and 12, respectively.

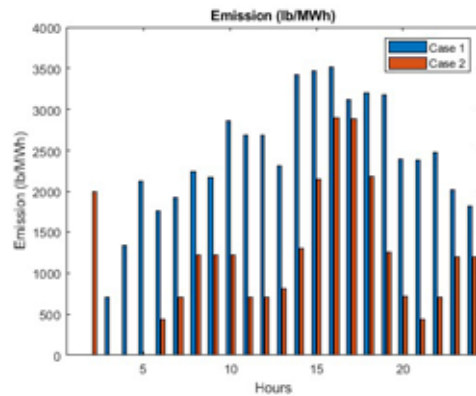


Fig. 12. Emission produced from Grid analysis of First and Second scenario for 24 hrs

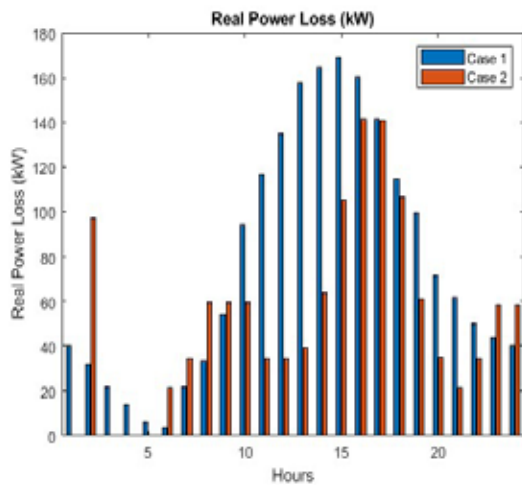


Fig. 10. Real power loss analysis of First and Second scenario for 24 hrs

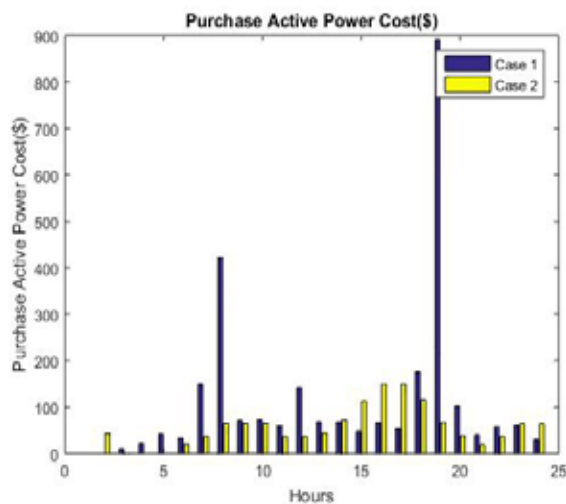


Fig. 11. Purchased active power cost analysis of First and Second scenario for 24 hrs

Third scenario: In the distribution network, WT and PV arrays were simultaneously installed at the best sites. The best bus location for this bus was number 3, and there were 40 WT units in total. Similar to this, bus numbers 4 and 7 are where the most PV modules should be linked. The total real power losses once the WT and PV were included were 1069.169 kW. The price of active power acquired from the grid is also greatly decreased, falling to 1211.511 US\$ as compared to the first scenario (see Figs. 13 and 14, accordingly). The cost of the construction of a WT and its O&M costs are shown in Table 3 as 1,11,54,132.00 and 1,11,541.320 US dollars, respectively. PV installation costs 2,30,79,269.901 US dollars and PV O&M cost are 69,23,780.970 US dollars, in a similar manner. Additionally, as compared to scenario 1 shown in Fig. 15, the impact on emissions created over the course of 24 h was also greatly reduced, reaching 21892.953 lb/MWh.

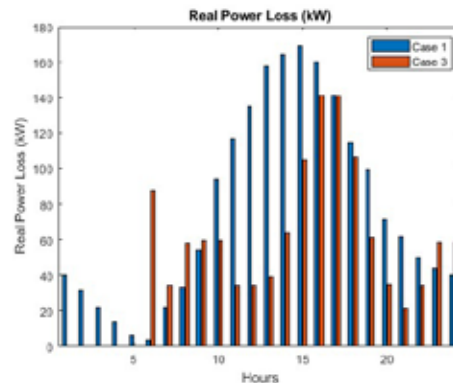


Fig. 13. Real power loss analysis for 24 hours between the first and third scenarios

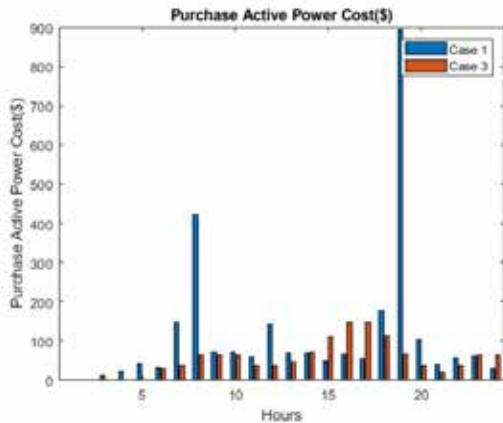


Fig. 14. Purchased Active Power cost analysis of First and Third scenario for 24 hrs

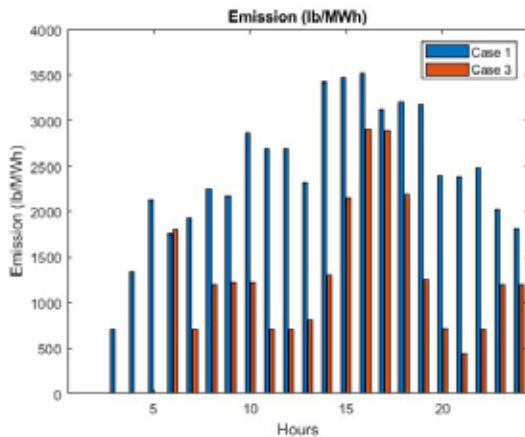


Fig. 15. Comparison of the first scenario's and the third scenario's emissions from the grid during a 24-hour period

Fourth Scenario: In this scenario, the distribution network has all of the DGs in the best possible positions. The most desirable bus combinations for WT and PV are 3 and 11, and the most suitable units to connect these buses to are 37 and 6, respectively. EVs are also arriving at bus 17 for 24-hour charging and discharge. EVs can only charge or discharge at once; the two tasks cannot be carried out simultaneously. The idea of a number of vehicles is created at random once every hour, with limits from 1 and 100. When the DGs are taken into account, the actual power loss is 1081.6431 kW. The amount needed to buy active power from the grid is 1217.236 US dollars, which is less expensive than the first scenario as shown in Figs. 16 and 17, accordingly. The expenses associated with deploying the WT as well

as running it are shown in Table 3 as 1,00,65,924.00 and 1,00,659.240 US dollars, respectively. Likewise, photovoltaic (PV) installations as well as operational and maintenance expenses are 1,97,82,231.344 US\$ and 59,34,669.403 US\$. Comparing the integration of WT, PV, and EVs for various combinations (scenarios), the system's overall cost has been significantly decreased. While the emissions created over a 24-hour period are higher than those in third scenario, this is because the system uses more active electricity from the grid to charge EVs, and Table 3 demonstrates that the car owner receives a net financial advantage of 213.959 US dollars from EVs. In addition, the overall emissions produced from the grid are reduced compared to first scenario shows in Fig. 18.

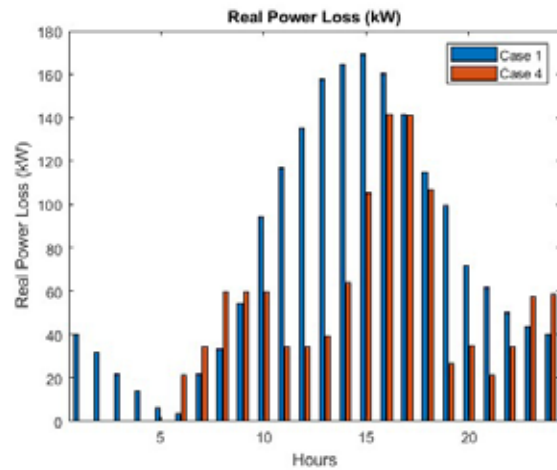


Fig. 16 Real power loss comparison of first scenario and fourth scenario for 24 hrs

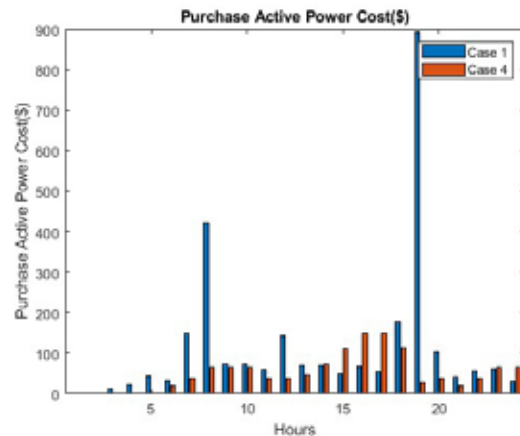


Fig. 17 Purchased active power compared in price for 24 hours between the first and fourth scenarios

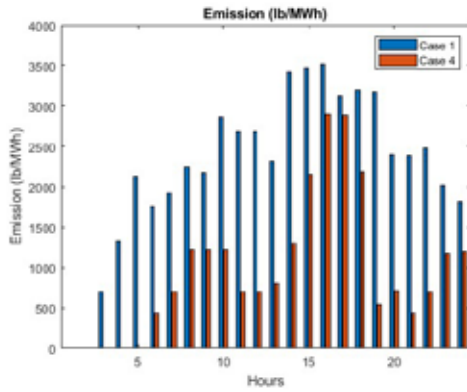


Fig. 18 Emission Produced from Grid comparison of first scenario and fourth scenario for 24 hrs

The specific numerical results for each scenario, along with their unique comparisons, are shown in Table 3. Figs. 19, 20, and 21, respectively, indicate the effects of adding DGs both alone and in combination on the real power loss, emissions created, and purchased active power expenses from the network for whole day.

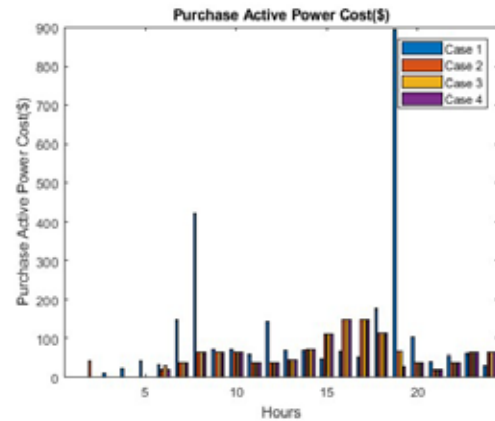


Fig: 21. A 24 hour price analysis of the active power purchased from the grid in all scenarios

Table 3: Results and comparisons from simulations

Particulars	First Scenario	Second Scenario	Third Scenario	Fourth Scenario
Σ Kw loss	1847.40	1073.0	1069	1081.643
Location of WTs (Number of WTs)	7	84	.169	1
PV Installation Bus (Number of PV Modules)	--	4	3	3
EVs' placement (Bus)	--	(42)	(40)	(37)
Σ Expenses related to active power purchased (US \$)	2689.53	1213.27	1211	1217.236
Wind installation expenses (US \$)	--	1,14,26	1,11,	1,00,65,9
WT expenses for maintenance (US \$)	--	1,840	541,	240
Expense of integrating a PV (US \$)	--	--	2,30,	1,97,82,2
PV expenses for maintenance (US \$)	--	--	79,2	31,344
Savings for vehicle owners (US \$)	--	--	69,9	0
Expense of installing an inverter (US\$)	--	3,55,50	3,55,	3,55,500.
Σ Emission (lb/MWh)	53828.8	21973.1	2189	22148.37
	8	1	2.95	48

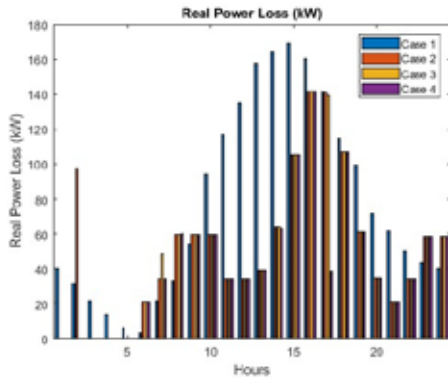


Fig. 19 Comparison of Real power loss in all cases for 24hrs

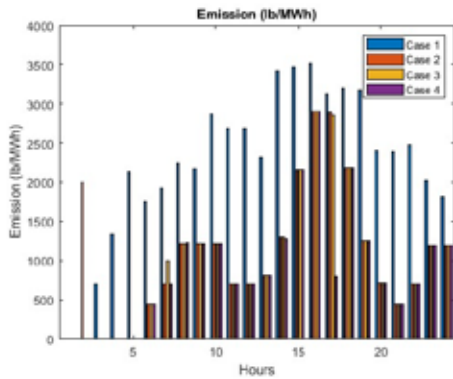


Fig. 20 Comparison of emission produced from grid of all cases for 24hrs

CONCLUSION

This paper presents a comparative analysis of the technological and economic viability of several DGs on the distribution network. Therefore, the entire power loss, the entire price of the several DGs, and the overall emissions generated by the grid were combined to build a novel multi-objective function. The GABC optimization algorithm was used to minimize this multi-objective function in order to determine the best allocations and number of DGs, which results in the best solution under load uncertainty. It has been extracted from a significant analysis of the distribution network and DGs that the behavior of PEV owners who charge and discharge their vehicles in order to get financial advantages may result in an increase in load demand at the time of off-peak grid time period. Also after analyzing the aggregate outcomes of DGs within the distribution system, it was found that there was a considerable decrease in emissions, overall costs, and power loss.

REFERENCES

- Gampa, S. R. and D. Das (2015). "Optimum placement and sizing of DGs considering average hourly variations of load." *International Journal of Electrical Power & Energy Systems* 66: 25-40.
- Nasiraghdam, H. and S. Jadid (2012). "Optimal hybrid PV/WT/FC sizing and distribution system reconfiguration using multi-objective artificial bee colony (MOABC) algorithm." *Solar Energy* 86(10): 3057-3071.
- Teng, J.-H., S.-W. Luan, D.-J. Lee and Y.-Q. Huang (2013). "Optimal charging/discharging scheduling of battery storage systems for distribution systems interconnected with sizeable PV generation systems." *IEEE Transactions on power systems* 28(2): 1425-1433.
- Boyle, G. (2004). *Renewable Energy*, Oxford University Press.
- Zhu, G. and S. Kwong (2010). "Gbest-guided artificial bee colony algorithm for numerical function optimization." *Applied Mathematics and Computation* 217(7): 3166-3173.
- Parks, K., P. Denholm and A. J. Markel (May 2007). "Costs and emissions associated with plug-in hybrid electric vehicle charging in the Xcel Energy Colorado service territory." *Natl. Renewable Energy Lab., Golden, CO, Tech. Rep. NREL/TP-640-41410*.
- Boot, P. and B. van Bree (2010). "A zero carbon European power system in 2050: proposals for a policy package." *Technical report: ECN-E-10-041*.
- Willy online Pvt Ltd. <<http://wind.willyweather.com.au/>>.
- Hu, W., C. Su, Z. Chen and B. Bak-Jensen (2013). "Optimal operation of plug-in electric vehicles in power systems with high wind power penetrations." *IEEE Transactions on Sustainable Energy* 4(3): 577-585.
- Duvall, M. and E. Knipping (July 2007). "Environmental assessment of plug-In hybrid electric vehicles." *Nationwide greenhouse gas emissions. Final report EPRI & NRDC*.
- Baran, M. E. and F. F. Wu (1989). "Network reconfiguration in distribution systems for loss reduction and load balancing." *IEEE Transactions on Power delivery* 4(2): 1401-1407.
- "Hourly Ontario energy price." <<https://www.ieso.ca/marketdata/hoep.asp>>.

Structural Analysis of Bobbin Thread Removal Mechanism

Rahul R Gurpude

Ankush Hatwar

Mechanical Engineering Department, SSIT
Nagpur, RTMNU
✉ ankushatwar28@gmail.com

ABSTRACT

In this paper, we have developed new concept of thread removal from the bobbin. For this purpose, we have developed mechanism which have named as a “Bobbin thread removal” from the bobbin. We are designing Bobbin thread removal mechanism which is stable and work efficiently.

KEYWORDS : *Bobbin, Thread.*

INTRODUCTION

A plastic bobbin consisting of a hollow cone defined by a thin-walled sheath includes an inner skeletal frame of longitudinally-spaced circumferential ribs and radially- spaced longitudinal ribs defining an inner support surface for a mandrel with a sheath having segments of varying wall thickness and the outer surface having a constant taper with respect to the bobbin axis. Some of the longitudinally-extending ribs may be partial ribs defined in each of the segments.

This invention relates generally to cores upon which filamentary material such as yarn or thread are to be wound and, more particularly, to an improved lightweight bobbin fashioned as a one-piece hollow conemolded from plastic material. One such material found to be useful is polypropylene, which allows certain features of the bobbin to be molded in precise detail.

For purposes of simplicity, the filamentary materials with which the present invention is intended to be used will be referred to generally as "yarn", with the understanding that other filamentary materials are included as well.

Manufacture of yarn is carried out as a continuous operation, and as part of the manufacturing process, machines have been developed to automatically package yarn by winding it onto bobbins for storage, shipment, and sale.

CONSTRUCTION

A bobbin construction to be gripped by a mandrel, said bobbin being of the type having the configuration of a one- piece hollow cone having a central axis, said cone molded of plastic, said cone having a tip end and a base end, a thin- walled sheath having an inner surface and an outer surface, and an inner skeletal frame of longitudinally-spaced circumferential ribs and circumferentially-spaced longitudinal ribs supporting said sheath, said bobbin comprising: said outer surface formed at a first constant taper with respect to said axis; at least one section of said inner surface formed at a second taper, each said inner surface section and said outer surface defining there between a sheath segment of varying thickness; said longitudinal ribs including at least one partial rib in said varying thickness sheath segment having a substantially constant thickness to produce a varying thickness rib in said varying thickness sheath segment; means formed on said inner surface to provide a gripping site for said mandrel; and, a circumferentially-extending ridge formed in said outer surface extending in a helical pattern from proximate said base end to proximate said tip end.

DESIGN PROCEDURE

To solve the stated problem of thread removal, we have developed new concept of thread removal from the bobbin. For this purpose, we have developed mechanism which have named as a “Bobbin thread removal” from the bobbin.

Working Principle

Figure 1 shows the outline representation of the thread removal mechanism. Blades fixed in a pencil sharpener like structure are mounted on a well heighted table. Rotary stud can rotate with handle. Also the transverse movement of the rotary stud in forward and backward direction allows operator to feed bobbin in the mechanism. Further manual rotation of the stud will rotate bobbin in the sharper hole and thread wound on the bobbin will be removed by the mechanism through the blades mounted on it.

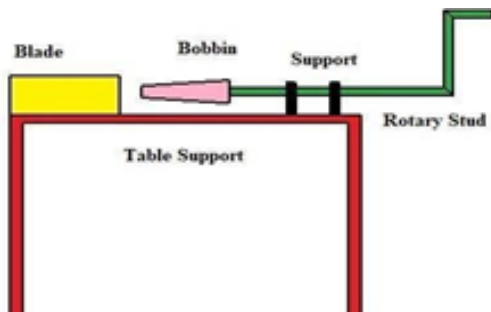


Fig. 1. Concept of Bobbin Thread Removal Mechanism

Design Specification

Details of Each parts used in this mechanism is as follows;

Bobbin Thread Removal

Fig. 2 shows the bobbin thread removal mechanism. It has blades mounted on the top of the base. Taper hole is provided to insert bobbin in it through the rotary stud. Rotation in both directions can remove the thread from the bobbin. The detailed dimensions of the mechanism are as follows.

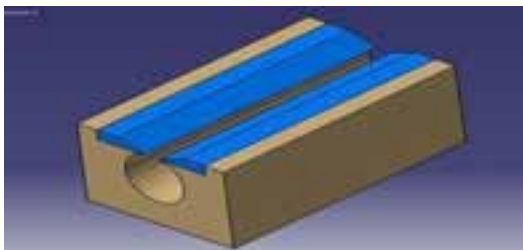


Fig. 2. Thread Removal Mechanism

Hold Bearing

Hold bearing is used to hold the rotary stud on the mounting table. It provides support to stud. It also

provides rotary and translator motion of the stud. Details of hold bearing are as follows.

Rotary Stud

Fig. 3 shows the Rotary Stud which is an important part of entire mechanism. It is a part on which the bobbin is supposed to be mounted at the one end. At other end the handle is mounted which is used for rotating purpose. It has two degrees of freedom. One is rotational and other is translational. Transverse motion helps to feed bobbin in to the cutting mechanism and rotational movement of the stud allows operator to cut the tread from the bobbin. The details of the stud dimensions and views are as follow

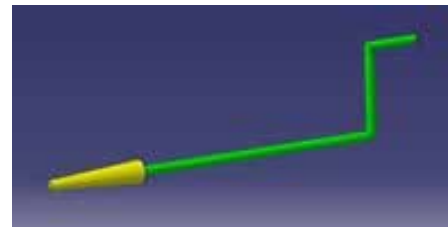


Fig. 3. Rotary Stud

Bobbin

It is the part from which we need to unwanted yarn or thread. It is made up of plastic material and hollow inside having thickness of 10mm. The bigger diameter is of 60mm and smaller diameter is of 30mm.

Blades

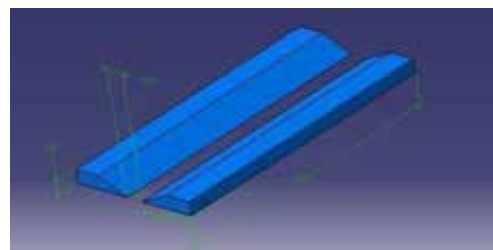


Fig. 4. Blades

This blade is mounted on cutting mechanism. It is placed on the taper hollow section of the cutting mechanism to perform cutting operation on the bobbin. It removes the unwanted thread from the bobbin.

CAD Model Of Thread Removal Mechanism-

Figure 5 shows the Virtual Model prepared for Bobbin Thread Removal in CATIA V5R19 Software. All

the dimensions are setup by considering taper plastic bobbin used in cotton thread mill to wound thread with a particular manner.

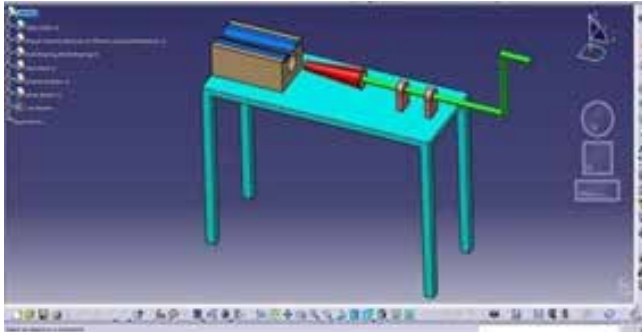


Fig. 5. Virtual Model of Thread Removal Mechanism

Steps To Perform Structural Analysis

To perform Structural Analysis on mechanism parts, following steps are to be performed.

Step 1: Open ANSYS Workbench 2020 R1 Software and select Structural Analysis option from analysis setting menu.

Step 2: Set material Properties in engineering data module for Set-up. Step 3: Import .stp format file of set-up into design modeler module. Step 4: Apply material property to imported geometry.

Step 5: Perform Meshing operation in model module. This process is also called as discretization/Meshing process.

Step 6: Apply Boundary Conditions on Mechanism Part. Step 7: Select required result type from solution menu. Step 8: Solve the analysis.

Step 9: Save required Results.

Tabulated Results of Structural Analysis

All the results generated in case of above parts are given in following table.

Sr. No.	Part Name	Property	Value
1	Cutting Blade	Total Deformation	0.0012 mm
2		Equivalent Stress	1.907 MPa
3		Shear Stress	0.059 MPa
4		Normal Stress	0.48 MPa

5	Stud	Total Deformation	0.1668 mm
6		Equivalent Stress	2.645 MPa
7		Shear Stress	0.4126 MPa
8		Normal Stress	0.6466 MPa
9	Bobbin	Total Deformation	0.0013 mm
10		Equivalent Stress	1.0708 MPa
11		Shear Stress	0.05929 MPa
12		Normal Stress	0.1793 MPa

Fig. 5. Tabulated Results for Structural Analysis

By observing all above tabulated results, we found that the deformation and stress values due to application of cutting force and angular velocity are very less compared to the strength of the material used for parts. Hence our design is safe and stable during cutting operation.

CONCLUSIONS

By studying all results generated through the structural analysis and vibration analysis, it is found that the Bobbin thread removal mechanism design is stable and work efficiently. It is found that the life of the blade will be longer as deformation level in each component is very low. Hence it is recommended by us to fabricate and use this design to remove unwanted thread from the bobbin with effectively quick manner and with less cost.

REFERENCES

1. Dr. R. Kiruba Shankar, M. Sudharsan, T. N. Suren, P. Tamilarasan, "A Study And Development Of Semi-Automatic Bobbin And Shielding Machine For Textile Industry". International Journal of Scientific & Technology Research Volume 9, Issue 01, January 2020 ISÄ©SN 2277-8616.
2. Vinay Kumar Midha, Ashish Kumar Gupta, "Eff ect of Using Lower Linear Density Bobbin Thread on Seam Strength". Department of Textile Technology, National Institute of Technology, Jalandhar- 144011, Punjab, India, Tekstilec, 2019, 62(2), 148-154, DOI: 10.14502/Tekstilec2019.62.148-154.
3. Mrs. Supriya Kurlekar1, Ms. Chaitali Karagave2, Ms. Nurjahan Malik3, Ms. Shraddha Patil4, Ms. Rohini Kulkarni5, "MSP 430 based Automatic Bobbin Winding Machine". June 2022 | IJIRT | Volume 9

Issue 1 | ISSN: 2349-6002, IJIRT 155648 International Journal of Innovative Research in Technology 1583.

4. Vinay Kumar Midhal and A. Mukhopadhyay, R. Chatopadhyay and V. K. Kothari, "Studies on the Changes in Tensile Properties of Sewing Thread at Different Sewing Stages". Textile Research Journal Vol 79(13): 1155–1167 DOI: 10.1177/0040517508101456, Figure 1 appears in color online: <http://trj.sagepub.com>, © The Author(s), 2009. <http://www.sagepub.co.uk/journalsPermissions.nav>
5. Prof. A. B. Tupkar, Bhushan Dhande, Ankur Bhute, Siddhant Jadhao, Suchit Surkar, Prayag Roy Choudhury, "Investigation and Optimization of Roving Making Machine". International Journal for Research & Development In Technology, Volume-3, Issue-2, Feb 2015 ISSN (O) :- 2349-3585.
6. A.T. Ertürka, S. Karabayb, K. Baynalç, and T. Korkutd. (2017). Vibration Noise Harshness of a Light Truck Driveshaft, Analysis and Improvement with Six Sigma Approach. Special Issue of the 6th International Congress & Exhibition (APMAS2016), Vol. 131 (2017), 477-480.

Comparative Study of Parallel Plate Fin Heat Sinks with Three and Four Perforation on Circular Pin Fins Between the Plate Fins in Natural Convection

Rahul R. Sonawane

Sagarkumar J. Aswar

Ganesh B. Patil

Mechanical Engineering Department
Jawahar Education Society's Institute of
Technology, Management & Research
Nashik, Maharashtra
✉ rrsmechjit@gmail.com

ABSTRACT

The cooling of electronic component like CPU is very important to enhance the life of electronic devices. This study investigate heat transfer enhancement in natural convection of parallel plate fin heat sink (PPFHS) with three and four perforation on circular pin fins between the plate fins. The firstly parallel plate heat sink consists of three perforations on circular pin fin and its performance is compared with four perforations on circular pin fin. The height of circular pin fin is taken as 50 mm, 35 mm, 25 mm respectively for both cases. Further heat input is increased from 20 W to 200 W and its effect on heat transfer rate is also examined. The result shows that, parallel plate fin heat sink with four perforations on circular pin fins gives more heat transfer than three perforation circular pin fins. In above three heights, it is observed that circular pin fin at 25 mm height shows better heat transfer compared with 35 mm and 50 mm

KEYWORDS : *Parallel plate fin heat sink (PPFHS), Circular pin fins, Perforation, Heat transfer rate.*

INTRODUCTION

Electronic device like CPU generate heat during its operation. In order to maintain life of electronic device it is necessary to dissipated quickly to surrounding atmosphere. Heat sink is used to dissipate the heat rapidly to surrounding fluid. Heat sink is a device which absorbs the heat from heated component and dissipates heat to surrounding air. Air cooling is the most widely used technique for heat rejection. Heat sink dissipates heat to surrounding air by convection. In natural convection, the extended surfaces are used which increases surface area by adding fins to the surface in order to achieve required rate of heat transfer.

In present study, experiment is carried out to investigate heat transfer rate in natural convection of parallel plate fin heat sink with circular pin fins placed between the plate fins. The firstly parallel plate heat sink consists of three perforations on circular pin fin and its performance

is compared with four perforations on circular pin fin. The variation of height of circular pin fin and effect of number perforation on heat transfer coefficient is also examined.

EXPERIMENTAL SETUP

Heat Sinks Dimensions

The dimensions of the setup are given as below;

Base plate = 133 mm x 155 mm.

Height of parallel plate fin = 50 mm.

Thickness of parallel plate fin = 3 mm.

Height of pin fin = 50 mm, 35 mm, 25 mm respectively.

Diameter of circular pin fin = 8 mm.

Diameter of perforation = 3 mm.

No. of perforation =3,4

Experimental Setup and Procedure

The experimental set-up primarily consists of wooden rectangular chamber and digital control panel as shown in Fig.1. The rectangular wooden chamber is made in such way that it is open from top and bottom portion while all other sides are closed. The three sides of chamber are closed with plywood and front side of chamber has removable glass sheet so as to replace different types of pins. Inside the chamber the concrete block supported with the help of wooden block. The heater plate is placed on the concrete block to supply heat input to heat sink model. The test set up was kept in controlled room to establish free convection over pin fin arrays.

The parallel plate pin fin heat sink is mounted on concrete block with the help of four screws to tight pin fin array over heater plate. Thermocouples are sandwiched between heater plate and heat sink at different locations to measure the temperature of base of fin. Thus, air gap between heater plate and pin fin array is considered to be negligible. Also, heat loss through excess portion to the pin fin arrays was assumed negligible for comparative analysis.

The plate fin configurations are produced by milling operation on rectangular block. The plate fin arrays were produced from rectangular block with dimensions $138 \times 188 \times 63$ mm. Fins were kept integral with the base plate of thickness 10 mm while, fin thickness was kept constant as 3 mm. The circular pin has 8 mm diameter and they are placed between the parallel plate fins. Geometry of pin fin array is shown in the Fig.3. The fin material was selected as aluminum 6063 alloy because of its high thermal conductivity, $k \sim 202$ W/m.K at 20° , low emissivity (~ 0.2 at 20°).

For the experimentation, electrical power supplied to heater and heat input is adjusted with the help of dimmer stat. The dimmer stat can be used to change the heat input such as 20W, 40 W, 60 W, 80 W, 100W up to 200W. As heater goes on heating, the temperature of fin start rising which is sensed by the thermocouple and indicated on digital temperature indicator. The base-plate temperatures of fin arrays are measured by T1, T2, T3, T4 and T5 thermocouples and ambient temperature by T6 thermocouples. The average of these five readings is taken as the base plate temperature. The heater input

is kept constant for different set of heat sink model and noted the reading.

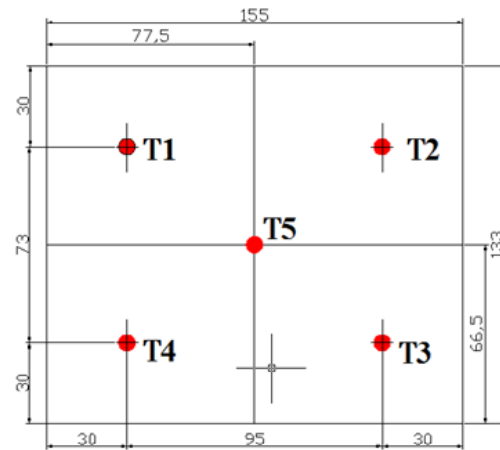


Fig.1 a) Position of Thermocouple



Fig.1 b) Example of an Set-up of indicators



Fig.2 a) Height of pin 50 mm with four perforations



Fig.2 b) Height of pin 35 mm with four perforations

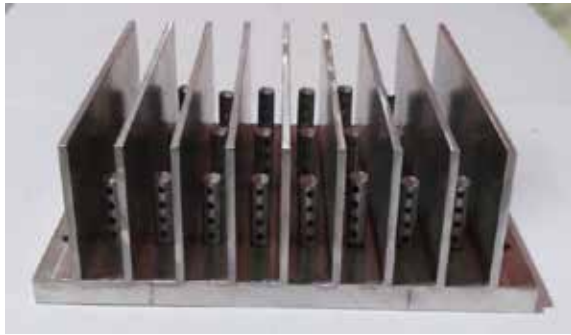


Fig. 2 c) Height of pin 25 mm with four perforations

Parallel plate pin fins heat sinks are the heart of experiment over which the experimental study is be done. In the experimentation for all three height readings are taken.

DATA REDUCTION

Heat input supplied to fins is given by

$$Q_{in} = VI \tag{1}$$

The most of the heat lost by radiation to surrounding air which is calculated as,

$$Q_{rad} = \epsilon\sigma As (Ts^4 - Ta^4) \tag{2}$$

Heat lost by convection $Q_c = Q_{in} - Q_{rad}$

This rate of heat transfer by convection can be given by,

$$Q_c = h As (Ts - Ta) \tag{3}$$

Calculation of Base And Exposed Area of Fins

Area of base plate (A_{bp}) = $L \times W$

Area of one plate fin = $(2xHxL) + (2xHx t) + (L \times t)$

Area of all vertical plate fin (A_f)

= Area of one plate fin x No. of fin

Area of all vertical pin fins with perforation is,

$$(A_{pf}) = N_f [(\pi/4 * D^2 + (\pi DH)) - (n(\pi/2)d^2 + n\pi dD)] \tag{4}$$

Total surface area $As = A_{bp} + A_f + A_{pf}$

The mean temperature is calculated as,

$$(Ts + Ta) / 2 \tag{5}$$

The average convective heat transfer coefficient is given by,

$$h = (Nu * K_{air}) / Lc \tag{6}$$

RESULTS AND DISCUSSION

In the experiment for three different heights, parallel plate heat sink with three perforations on circular pin fins are compared with four perforations on circular pin fin. For all set heat is kept constant as 20W, 40 W, 60 W, 80 W, 100W up to 200W.

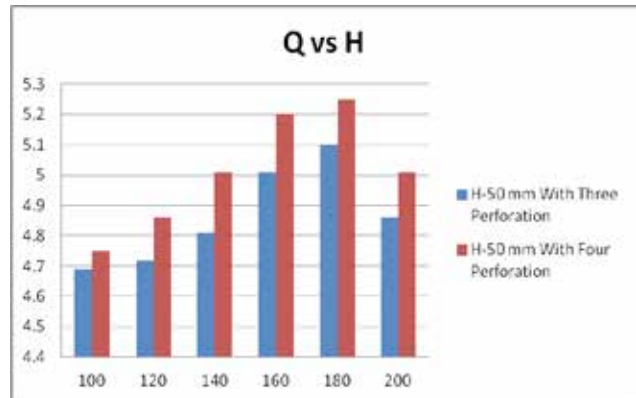


Fig.3 Variation of heat transfer coefficient vs Heat input for 50 mm pin fin height.

The Fig. 3 shows variation of heat transfer coefficient vs heat input for 50 mm pin fin height. It is observed that, four perforated pin fin has heat transfer coefficient 5.25 W/m²k at 180W whereas three perforated pin fin has 5.10 W/m²k respectively.

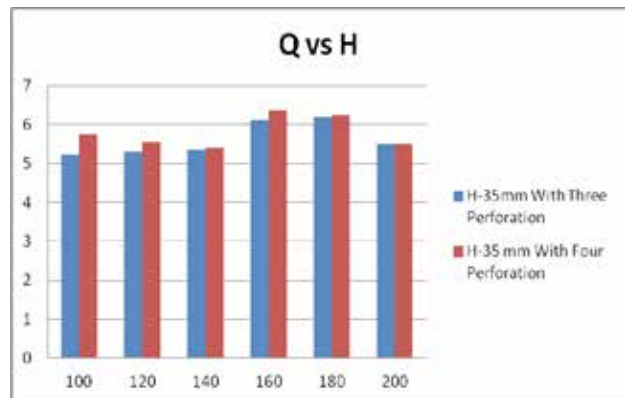


Fig. 4 Variation of heat transfer coefficient vs Heat input for 35 mm pin fin height.

The Fig.4 shows variation of heat transfer coefficient vs heat input for 35 mm pin fin height. It is observed that, four perforated pin fin has heat transfer coefficient 6.25 W/m²k at 180W whereas three perforated pin fin has 6.15 W/m²k respectively.

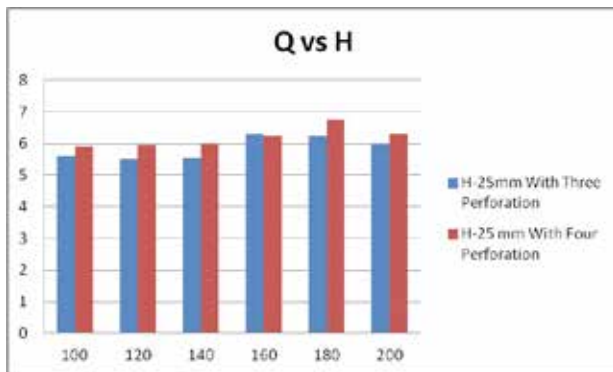


Fig.5 Variation of heat transfer coefficient vs Heat input for 25 mm pin fin height

The Fig.5 shows variation of heat transfer coefficient vs heat input for 35 mm pin fin height. It is observed that, four perforated pin fin has heat transfer coefficient $6.75 \text{ W/m}^2\text{k}$ at 180W whereas three perforated pin fin has $6.25 \text{ W/m}^2\text{k}$ respectively.

CONCLUSIONS

From comparative study, it is concluded that for all three pin fin height the parallel plate heat sink with four perforations on circular pin fin gives more heat transfer rate than three perforations on circular pin fin. The heat transfer rate increases with increase in number of perforation. Out of three different pin heights, it is

observed that the heat transfer coefficient is maximum for 25 mm and minimum for 50 mm pin height and intermediate for 35 mm.

ACKNOWLEDGMENT

I would like to take this opportunity to express my honour, respect deep gratitude and genuine regard to Head of Mechanical Engineering Department, Dr. S. J. Aswar, for giving me valuable guidance during my work with a constant source of inspiration and motivation. I am also extremely grateful to Dr. M. V. Bhatkar, Principal, JESITR, Nashik for his various suggestion and kind help during my work.

REFERENCES

1. Dong-Kwon Kim, Sung Jin Kim, Jin-Kwon Bae, (2009), Comparison of thermal performances of plate-fin and pin-fin heat sinks subject to an impinging flow, International Journal of Heat and Mass Transfer 52, 2009.
2. E.A.M. Elshafei, (2010), Natural convection heat transfer from a heat sink with hollow/perforated circular pin fins, Energy 35,2010
3. Rahul R. Sonawane, Experimental Study of Parallel Plate Fin Heat Sinks with and without Perforation on Circular Pin Fins between the Plate Fin, International Journal of Current Engineering and Technology, 2016.

Helical Spring and It Dimensional Optimization used in Tractor Seat

Ganesh B Patil

Rahul Sonawane

Y. R. Girase

Department of Mechanical Engineering
Jawahar Education Society's Institute of
Technology, Management & Research
Nashik, Maharashtra
✉ gbpmechjit@gmail.com

ABSTRACT

Over the year a lot of work has been done and is still continuing with great effort to improving the performance of compression spring and also study the analysis of failure in spring. The aim of this project is to study existing design of helical spring and manufacturing the spring and carry out the stress analysis of helical tension spring for Tractor seat using dimensional optimization. To reduced stresses at the time of dynamic loading condition, applied on helical spring. Also able to sustain at different load condition. At different load condition and stress would be check the failure analysis of spring. In general study fatigue life analysis of spring by using experimental analysis also study the effect the wire diameter of helical compression spring, the spring has to be modified in order to reduce the stress and journey should be comfortable. Due to damping the helical spring gets break up and which causes the serious accident so effective design of helical spring needed for tractor seat to get comfort and to withstand vibration.

KEYWORDS : *Fatigue life analysis, Compression spring, Finite element analysis introduction.*

INTRODUCTION

Helical springs are widely used in many engineering applications due to their importance. Helical compression springs are used widely all over the world. It has different type of applications in different area Springs are used in mechanical equipment with moving parts, to absorb loads, which may be continuously, or abrupt varying. The absorption of the loads takes place in the form of elastic energy Coil springs are manufactured from rods which are coiled in the form of a helix. The design parameters of a coil spring are the rod diameter, spring diameter and the number of coil turns per unit length. Compression springs may be cylindrical, conical, tapered, concave or convex in shape. Vehicle suspension system is made out of springs that have basic role in power transfer, vehicle motion and driving. A spring is defined as an elastic body, whose function is to distort when loaded and to recover it original shape when the load is removed.

LITERATURE SURVEY

I. A.M. Yu , Y. Hao has done analytical study on the free vibration analysis of cylindrical helical springs with noncircular cross-sections. They have formulated explicit analytical expressions of the vibrating mode shapes of cylindrical helical springs with noncircular cross-sections and the end conditions clamped-clamped and clamped-free.

II. L. E. Becker et al. linearized disturbance equations governing the resonant frequencies of a helical spring subjected to a static axial compressive load are solved numerically using the transfer matrix method for clamped ends and circular cross-section to produce frequency design charts

III. The scope of K.MI chalczyk work includes the determination of the stress amplitudes in the spring for the given parameters of elastomeric coating, at the consecutive resonance frequencies.

IV. Mohamed Taktak has proposed a numerical method to model the dynamic behavior of an isotropic helical spring. The analytical and numerical models describing wave propagation, of gradual excitations in time has been investigated by Aimin Yu, et al

V. The analytical and numerical models describing wave propagation, of gradual excitations in time has been investigated by Aimin Yu, et al

VI. Suraj Kumar et al have purposed air spring which is to restrict the vibration at a desirable level as per requirements. Anis Hamza et al has studied the vibrations of a coil, excited axially, in helical compression springs such as tamping rammers are discussed. He has developed a mathematical formulation which was comprised of a system of four partial differential equations of first-order hyperbolic type, as the unknown variables are angular and axial deformations and velocities. The numerical resolution was performed by the conservative finite difference scheme of Lax–Wendroff. Youl Zhu et al.

VII. The variety of factors may cause fatigue failure of helical compression springs in engineering applications. In this paper, we conducted Analytical Stress and fatigue analysis of tractor seat spring. We have proposed new arrangement of spring on a tractor seat which will improve the performance of the spring.

VIII. Samuel Tilahun, P. Velmurugan : Mechanical springs are used in machines to exert forces, to afford elasticity, and to store or absorb energy.. Investigated on springs design as the determination of the geometry, dimensions, and stiffness of a spring needed to satisfy the force-deflection requirements .The analyzed reduction of overall stress and deflection of Chrome Vanadium and 60Si2MnA steel. It is observed that the 60Si2MnA Stress and deflection of existed steel helical compression spring and new material. It is observed that reduction of stress and deflection in new material. The modal and structural analysis was done on spring steel and Phosphor Bronze. Finally conclude that steel material for spring is best . The open coiled helical compression materials has been used for Chrome Vanadium steel material, Chrome Silicon steel and Hard Drawn steel . Based on the dimensions obtained from the conventional helical compression spring was created with the help of the 3D modeling

SOLIDWORKS software. The main objectives of this work are to reduce the overall deflection and stresses of the open coil helical compression spring by finite element approach.

IX. S. Rajakuma, M. Karthiyarajr :The degree of cold working with the chemical composition of stainless steel determines the tensile strength. The spring steel is used widely in automotive and industrial suspension applications. It has certain properties such as it is resistant to water, environmental and pollution exposure along with high yielding strength and also known to be resilient. This allows spring steel to return to its original shape from its deflection or twisting. The chromium vanadium steel is made by alloying chromium, carbon, vanadium, and other metals. These springs offer benefits of specific load tolerances, hardness, corrosion resistance and stress relieving characteristics due to their typical chemical composition. Hence, the spring steel is employed for high impact load and stress applications.

PROBLEM STATEMENT

To find the problem of failure in tractor seat helical tension springs and try to replace it by helical compression springs using stress and fatigue analysis by analytical method, FEA and experimental method The failure of tension spring is at the hook end and it is due to un uniform ness of material and due to heat treatment processes. Due to wavy loads there are sudden fractures. Due to excessive loading causes failure of tension springs which causes injury to the driver or causes to an accident while driving.



Figure 1. Point of Fracture of Existing Spring

MATERIAL

Springs are resilient structures designed to undergo large deflections within their elastic range. It follows

that the materials used in springs must have an extensive elastic range. Some materials are well known as spring materials. Although they are not specifically designed alloys, they do have the elastic range required. In steels, the medium-and high-carbon grades are suitable for springs. Beryllium copper and phosphor bronze are used when a copper-base alloy is required. The high-nickel alloys are used when high strength must be maintained in an elevated-temperature environment. The selection of material is always a cost-benefit decision. Some factors to be considered are costs, availability, formability, fatigue strength, corrosion resistance, stress relaxation, and electric conductivity. The right selection is usually a compromise among these factors.

Commonly Used Spring Materials

One of the important considerations in spring design is the choice of the spring material. Some of the common spring materials are given below

Hard-drawn wire

This is cold drawn, cheapest spring steel. Normally used for low stress and static load. The material is not suitable at subzero temperatures or at temperatures above 120° C.

Oil-tempered wire

It is a cold drawn, quenched, tempered, and general purpose spring steel. It is not suitable for fatigue or sudden loads, at subzero temperatures and at temperatures above 180° C.

Chrome Vanadium

This alloy spring steel is used for high stress conditions and at high temperature up to 220° C. It is good for fatigue resistance and long endurance for shock and impact loads.

Chrome Silicon

This material can be used for highly stressed springs. It offers excellent service for long life, shock loading and for temperature up to 250° C.

Music Wire

This spring material is most widely used for small springs. It is the toughest and has highest tensile strength and can withstand repeated loading at high

stresses. It cannot be used at subzero temperatures or at temperatures above 120° C.

Stainless Steel

Widely used alloy spring materials.

Phosphor Bronze / Spring Brass.

It has good corrosion resistance and electrical conductivity. It is commonly used for contacts in electrical switches. Spring brass can be used at subzero temperatures. On the basis of this particular study we have selected material as 55 Si 2 Mn 90

Design and Selection of Spring

Material Selected for Helical Compression Spring

Some factors to be considered are costs, availability, formability, fatigue strength, corrosion resistance, stress relaxation, and electric conductivity. The right selection is usually a compromise among these factors. On the basis of this particular study material selected as 55 Si 2 Mn 90.

Table 1. Composition of Material 55 Si 2 Mn 90

Sr. No.	Parameters		
1	% C	% Si	% Mn
2	0.5-0.6	1.5-2	0.8-1.0

Table 2. Properties of material 55 Si 2 Mn 90

Sr. No.	Parameters		
1	Tensile Strength(Sut)	Yield Strength (Yst)	BHN
2	1600-2000 N/mm ²	1500 N/mm ²	440-510

FINITE ELEMENT FORMULATION

Two CAD models has prepared for this particular research depend on the position of helical spring by using Pro-E Platform. The Models are prepared in such way that, It will take all real boundary conditions. Fig. 1 shows the CAD Model

- Helical Tension
- Helical Compression.

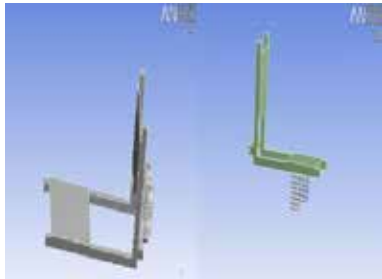


Fig 6. CAD Model of Tractor Seat

Table 3. Deflection of Three Springs for Variable Loads

Sr. No.	Load (N)	Deflection Compression Spring 8 mm (mm)	Deflection Compression Spring 5mm (mm)	Deflection Tension Spring 4mm (mm)
1	100	1.27695409	11.5454533	14.8927106
2	150	1.86543108	13.8405448	19.8569469
3	200	2.49390818	16.2313499	24.8211841
4	250	3.19238529	18.4272514	29.7854213
5	300	3.74086216	20.7458166	34.7496568
6	350	4.42933902	23.0509067	39.7138938
7	400	4.94781637	25.3659982	44.6781311
8	450	5.52629324	27.6610897	49.6423683
9	500	6.20477058	29.9661785	54.6066055
10	550	6.81324745	32.2712699	59.5708427

Table 4. FEA Stress of Three Springs for Variable Loads

Sr. No.	Load (N)	FEA Stress Compression Spring 8mm (Mpa)	FEA Stress Compression Spring 5mm (Mpa)	FEA Stress Tension Spring 4mm (Mpa)
1	100	94.8810	268.020	205.8862276
2	150	97.397712	287.1218124	274.5149722
3	200	100.530283	334.975445	343.1437129
4	250	112.66285	382.8290845	411.7724551
5	300	120.79542	430.6827097	480.4012043
6	350	140.92799	478.5363478	549.0299445
7	400	161.06057	526.3899825	617.6586907
8	450	181.19314	574.2436247	686.2874337
9	500	201.32571	622.0972639	754.9161855
10	550	221.45828	669.9508899	823.5449103

Analytical Analysis

Table 5. Analytical Stress Analysis

Sr. No.	Load (N)	Analytical Stress Compression Spring 8mm (Mpa)	Analytical Stress Compression Spring 5mm (Mpa)	Analytical Stress Tension Spring 4mm (Mpa)
1	100	49.279631	144.1468	169.17519
2	150	52.91944716	216.2202	253.762794
3	200	70.55926287	288.2936	338.350392
4	250	88.19907859	360.367	422.93799
5	300	105.8388943	432.4404	507.525588
6	350	123.47871	504.5138	592.113186
7	400	141.1185257	576.5871	676.700783
8	450	158.7583415	648.6605	761.288381
9	500	176.3981572	720.7339	845.875979
10	550	194.0379729	792.8073	930.463577

Table 6. Analytical Deflection Analysis

Sr. No.	Load (N)	Deflection Compression Spring 8mm (mm)	Deflection Compression Spring 5mm (mm)	Deflection Tension Spring 4mm (mm)
1	100	1.8	11.79	14.51
2	150	2.7	17.685	21.765
3	200	3.6	23.58	29.02
4	250	4.5	29.475	36.275
5	300	5.4	35.17	40.53
6	350	6.3	41.265	47.285
7	400	7.2	47.16	54.04
8	450	8.1	48.55	60.795
9	500	9	49.3565	67.55
10	550	9.9	49.556	68.805

Experimental Fatigue Life Analysis

To find the problem of failure in tractor seat helical tension springs and try to replace it by helical compression springs using stress and fatigue analysis.



Fig. 7. Experimental Setup

Experimental Procedure for Tension Spring

Experimental setup is prepared for calculating the fatigue life of spring is shown in figure no.5.1. The setup is prepared by using MS channel structure and a seat of tractor is mounted. The seat is accelerated by using electric motor of 5hp. A crank is used of length 40mm for total stroke of 80mm, tension spring are placed at the back of seat .The seat is manufactured according the design of actual seat of tractor which is of MS. Two springs are placed at the back of seat the speed of output shaft is maintained as 500 rpm using rheostat at power input to electric motor. Two tension springs are mounted on the model and machine is accelerated for duration up to spring is getting fractured and from obtaining time the numbers of cycles are counted.

Experimental Procedure for Compression Spring

Experimental setup is prepared for calculating the fatigue life of spring is shown in figure no.5.1. The setup is prepared by using MS channel structure and a seat of tractor is mounted. The seat is accelerated by using electric motor of 5hp. A crank is used of length 40mm for total stroke of 80mm, compression spring are placed at the bottom of seat. The seat is manufactured according the design of actual seat of tractor which is of MS. Two springs are placed at the bottom of seat. The speed of output shaft is maintained as 500 rpm using rheostat at power input to electric motor. In these setup two compression spring of diameter 8mm and 5mm are mounted at the bottom of seat. Machine is accelerated till the spring get fracture and number of cycles is calculated. Similarly same procedure is done for 5mm spring and number of cycles is calculated.

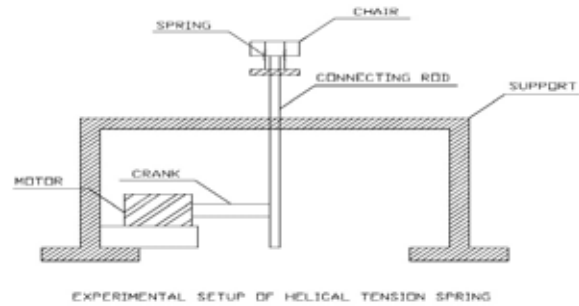


Fig.7.2. Experimental Setup

Specifications of Experimental Setup

1. Seat 230mm x 355mm x 240mm.
2. Motor 5 HP, 1440 RPM
3. Rheostat (Dimmer)
4. Crank 40mm

Spring Fatigue Calculation for Tension Spring of Diameter $d = 4\text{mm}$

Machine running upto spring fracture= 6hrs and 36mins.

Number of cycle’s spring oscillates = $((6 \times 60) + 36) \text{ min.} \times 500 \text{ rpm} = 198000 \text{ cycles.}$

Spring Fatigue Calculation for Compression Spring of Diameter $d=5\text{mm}$

Machine running upto spring fracture = 8hrs and 25mins.

Number of cycle’s spring oscillates = $((8 \times 60) + 25) \text{ min.} \times 500 \text{ rpm} = 252500 \text{ cycles}$

Spring Fatigue Calculation for Compression Spring of Diameter $d = 8\text{mm}$

Machine running up to spring fracture = 9hrs and 10mins.

Number of cycle’s spring oscillates = $((9 \times 60) + 10) \text{ min.} \times 500 \text{ rpm} = 275000 \text{ cycles}$

RESULT FATIGUE LIFE ANALYSIS

Table 7. Analytical, Experimental, FEA Analysis

Sr	Spring	Diame-ter	Fatigue Life		
			Analyti-cal (Cycles)	Experime-ntal (Cycles)	FEA (Cycles)
1	Tension	4mm	189971.53	196000	1622 70
2	Compre-ssion	5mm	244962.72	250000	2408 81

3	Compression	8mm	270582.68	272500	2529 33.41
---	-------------	-----	-----------	--------	---------------

FATIGUE MODEL

Fatigue life is defined as the number of stress cycles of specified character that a specimen sustains before the first evidence of failure. In case of Tractor seat road irregularities and engine will cause a vibration which ultimately will give the fatigue in the helical spring. Here for this research we have considered a vibration to be in completely reversed manner. So, for the fatigue life calculation we have to consider the fully reversed cycle. Mean stress value (σ) = 0

Stress amplitude (σ_a) = 200 MPa

Endurance limit of mechanical a component (S_e)

$$S_e = K_a \times K_b \times K_c \times K_d \times K_e \times S_e'$$

Where, K_a = Surface finish factor: - The surface finish factor is depends on modes of surface finish operation. Due to complex geometry of Tractor seat, polishing is the best way for finishing of crankcase. For polishing operation value of surface finish factor is one

K_b = Size factor: - The size factor depends upon the size of cross-section of the component. As the size of the component increases, the surface area also increases, resulting in a greater number of surface defects. For $D > 50$, its value is 0.75.

K_c = reliability factor: - The reliability factor depends on the reliability that is considered in the design of component. The reliability of the fatigue test is 50 %. At 50 % reliability the value of reliability factor is one.

K_d = Temperature factor: - Temperature factor depends on the temperature of component. Due to increase in temperature endurance strength of component decreases. Its value for temperature 550 °C is 0.67.

K_e = Modified factor for stress concentration = 1

$$S_e' = \text{Endurance limit} = 0.45 \times S_{ut}$$

$$S_{ut} = 2 \times S_{yt}$$

$$S_e = 0.750 \times 1 \times 1 \times 0.67 \times 1 \times 2 S_e''$$

$$\text{Fatigue strength (Sf)} = N_f \times \sigma_a$$

From S-N diagram as shown in Fig 7.1

$$CF/FB = AE/EB.$$

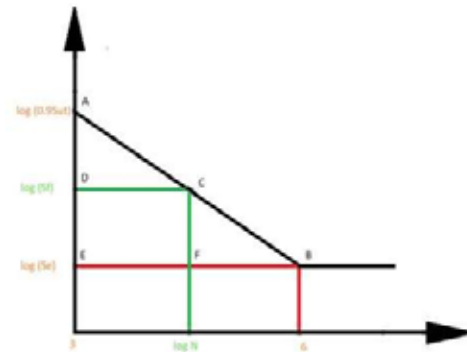


Fig. 9. S- N Diagram

CONCLUSION

Fatigue Failure analysis of the both models shows the higher life cycle in a compression spring helical model than tension helical spring also von misses stress of helical tension is higher than compression model The tractor seat helical compression spring will last longer than the helical tension spring and also the stresses obtained in helical tension spring are much higher than the compression spring model

ACKNOWLEDGEMENTS

I wish to thank the institution, “JESITMR , Nashik Under the NCETES 2023-24” for giving me the opportunity to write this paper. I would like to thank the authors of the various research papers that I have referred to, for the completion of this work.

REFERENCES

1. Burgul Supriya Rahul, Kulkarni Atul P., Fatigue Analysis for Helical Compression Spring for Determining Design Alternatives for Enhanced Life and Performance, International Journal for Technological Research in Engineering (IJTRE) Volume 2, Issue 7, March-2015, pp. 1070-1078.
2. Vakte Vikram, Pathan Firojkhani, Kankariya Ravindra, Dhamande Laxikant, Simulation of Helical Spring Used In Tractor Seat Application, International Journal of Modern Trends in Engineering, 24 July 2015, pp. 1958–1962.
3. Mohamed Taktak, Omaheni Khalifa, Aloui Abdessattar Dynamic optimization design of cylindrical helical spring, Applied Acoustic77, 2014, pp. 178-183
4. Zhu Youli, Wang Yanli, Huang Yuanlin, Failure analysis of a helical compression spring for a heavy vehicle's

- suspension system, Case Study in Engineering Failure Analysis2, 2014, pp. 169-173.
5. YU A.M., Hao Y., Free Vibration Analysis of cylindrical helical spring with non-circular cross section, Journal of sound & Vibration 330, 2011, pp. 2628-2639.
 6. Lee Jinhee, Free Vibration Analysis of cylindrical helical spring by pseudo spectral method, Journal of sound & Vibration 302, 2007, pp.185-196.
 7. Yu Aimin, Formulation and evaluation of an analytical study for cylindrical helical spring, Acta Mechanica Solids Sinica, Vol. 23, 2010, pp. 85-94.
 8. Prawoto Y., Ikeda M., Manville S.K., Nishikawa A., Design and failure modes of automotive suspension springs, Engineering Failure Analysis 15, (2008), pp.1155–1174
 9. Mirzaeifar Reza, DesRoches Reginald, A combined analytical, numerical, and experimental study of shape-memory-alloy helical springs, International Journal of Solids and Structures, 2011, pp. 611-628
 10. Pyttel B., Brunner I., Kaiser B., Mahendran M., Fatigue behavior of helical compression springs at very high number of cycles –Investigation of various influences, International Journal of Fatigue 60, 2014, pp.101-109.
 11. Hamza Anis, Ayadi Sami, Hadj-Taieb Ezzeddine, The natural frequencies of waves in helical springs, C. R. Mecanique 341, 2013, pp. 672–686.
 12. Beckera L.E., Chassieb G.G., Cleghorn W.L., On the natural frequencies of helical compression springs, International Journal of Mechanical Sciences 44, 2002, pp.825–841
 13. K. Michalczyk, Analysis of the influence of elastomeric layer on helical spring stresses in longitudinal resonance vibration conditions, Archives of civil and mechanical engineering I3, 2013, pp. 21-26.
 14. Purushottam Sarjerao Suryawanshi, Kulkarni Swapnil S., CAE analysis for fatigue failure for coiled Spring life enhancement in press machine Stamping operation, International Journal of Advanced Engineering Research and Studies E-ISSN2249–8974, 2014, pp.61-63
 15. N.Lavanya, P.Sampath Rao, M.Pramod Reddy (2014), “Design and Analysis of A Suspension Coil Spring For Automotive Vehicle”, International Journal of Engineering Research and Applications, Vol. 4(9), pp.151-157
 16. Design of machine Element, V.B. Bhandari, Edition 2001, Tata Mc Graw Hill (Chapter5, Chapter 10)
 17. Design data handbook, K. Mahadevan,(Chapter 10)
 18. Maher Rehaif Khudhair (2019) Failure analysis of compression helical spring used in the suspension system by FEA, International Journal of Mechanical and Production Engineering Research and Development (IJMPERD), ISSN(P): 2249-6890, ISSN (E): 2249-8001, Volume 9, Issue 5, pp. 841-850
 19. Samuel Tilahun, Velmurugan. P, Senthil Kumaran S (2020), some study on fatigue life of open coil suspension springs, Journal of Critical Reviews, Vol 7, Issue 13, pp 139-143
 20. An Numerical Investigation of Open Coil Helical Compression Spring Using Different Alloys Materials for Light Duty Vehicle. Samuel Tilahun and P. Velmurugan 2020 IOP Conf. Ser.: Mater. Sci. Eng. 988 012085
 21. Static structural analysis of helical compression spring materials 1S.Rajakumar, 2M.Karthiyaraj Year 2021, Volume 9, Issue 1

Experimental Analysis on Laser Cutting of Hastelloy C 276: Effects of Process Parameters on Kerf Width

Sagarkumar J. Aswar

Chaitali S. Deore

Rahul R. Sonawane

Department of Mechanical Engineering
Jawahar Education Society's Institute of Technology, Management & Research
Nashik, Maharashtra
✉ sagaraswar123@gmail.com

ABSTRACT

Laser beam machining, which is used to cut, engrave, and weld a variety of materials, including metals, plastics, ceramics, etc., is one of the most well-liked manufacturing methods. Sheet metal made of Hastelloy C 276 is usually cut with a CO2 laser. The current research examines the effects of changing CO2 laser cutting parameters on the accuracy of the laser- beam-milled surface on sheet metal made of Hastelloy C 276. These parameters include cutting speed, laser power, and gas pressure. To evaluate the blade quality, response factors like higher width kerf and lower width kerf are used. Experiment creation is carried out utilizing a Taguchi method design. The influence of the process factors on response has been examined using main effect plots made using ANOVA. Following the Taguchi method experimental design, the analysis of variance (ANOVA) methodology is used to conduct the evaluation. Which measurement is the most precise is determined using the signal to noise ratio.

KEYWORDS : *Hastelloy C 276, Laser cutting, Cutting speed, Laser power, Gas pressure, Taguchi method, Kerf Width.*

INTRODUCTION

Laser cutting of sheet metal is now an economically viable method of production thanks to technological advancements. The effectiveness of the laser cut is essential to the laser cutting process. Numerous commercial applications for CO2 laser equipment exist, including laser engraving, laser cutting, and laser marking. It is not necessary to perform any additional polishing steps on the finished item produced by the laser cutting process. However, poor metal cut quality has emerged as a serious issue in the industry as a result of improperly established cutting parameters. Therefore, it is crucial to ascertain how cutting variables impact the caliber of the finished product. Cutting parameters are typically fine-tuned and altered to create excellent cuts. But it requires a tremendous amount of time and effort to do this. More research is needed to understand how cutting factors influence cut quality. Hastelloy C 276 sheet metal is a ferritic steel. It has superior mechanical qualities and prevents

corrosion at high temperatures. Pressure containers, blowers, fans, and catalytic converter systems that work in harsh conditions with high temperatures and corrosion are frequently made from Hastelloy C 276. The final product created by the laser cutting process doesn't need to be completed further. On the other hand, poor cut quality has developed into a significant issue in the industry as a result of improperly established cutting parameters. After addressing this problem, an investigation into the effects of cutting factors on cut quality was carried out. The main goal of this study is to ascertain how a specific machine's cutting parameters influence the precision of the cut on Hastelloy C 276 sheet metal. In order to keep the higher width kerf and lower width kerf of the cutting material to a minimum under the most dependable circumstances for sheet metal Hastelloy C 276, the Taguchi technique is used to determine the optimal laser cutter settings. Design Expert Software can be used to identify the main effects and interactions of the factors.

The most important objective of this research is to determine how the cutting factors of a particular machine affect the quality of the cut on sheet metal Hastelloy C 276. Therefore, using the Taguchi method, the goal is to find the ideal settings for the laser cutter so that the average surface roughness and HAZ of the cutting material may be kept to a minimum under the most reliable of situations for sheet metal Hastelloy C 276. In order to determine the primary impacts and interactions of the parameters, Design Expert Software can be used by Girdu et. al. [1]. The CO₂ laser manufacturing processes' energy costs are reduced because of the findings. The combinations of laser speed and power that have been found result in lower energy consumption and higher processing efficiencies. With the development of mathematical equations for linear energy and cutting efficiency, this research provides to expanding both the theoretical as well as the practical base. Madic et. al. [2] found that the overall effectiveness may be affected in different ways depending on the laser cutting parameters used. There is a substantial amount of similarity between the circumstances that are most ideal for laser cutting and those that are least desirable for it. This bolsters the used approach by contrasting the results with those found through traditional desirability-based multi-objective optimization. AlSORUJI et. al. [3] studied the development of a multi-criterion decision-making procedure in laser beam drilling for the goal of optimizing the machining measurements of the nickel Inconel 718 alloy. Taguchi-Grey Relation Analysis (TGRA) was recommended as a method for determining the best process variables that would result in a better material removal rate, a smoother surface, and a smaller taper angle during the machining process. Due to the importance of concentrated energy, gas pressure plays the most significant part in LBM performance measures. Under the suggested ideal process factors, the surface topography could be achieved on a machined specimen with hardly any micro cracks. Senthilkumar et. al. [4] addressed the laser cutting on AISI 304 stainless steel has varying evaluation metrics using a grey grade established by grey relational analysis. According to the grey grade, cutting speed has a bigger influence on responses like hardness, kerf width, and MRR than laser beam strength, gas pressure, and standoff distance. It is abundantly obvious that the aforementioned laser

cutting performance characteristics are capable of being improved through the utilization of the GRA approach. Singh et. al. [5] used of a high-speed photography to investigate how laser cutting works by filming the impact of a powerful laser beam on test objects. Since minimum surface roughness and thin kerf are often preferred as performance metrics for making holes for industry sectors, this study is important for making tiny holes for structural parts such as rivets, bolts, and fastenings in arrangement.

Even though the impacts and conversations of a specifications were complicated, the results showed that laser cutting of ABNT 1045 steel could be optimized [6]. This research's conclusion states that the major variables influencing the formation of burrs and rough surfaces during laser cutting of ABNT 1045 steel are cutting speed and assist gas pressure. Hiwale et. al. [7] used spatial characteristic the undesirable machining feature known as kerf deviation must be reduced. The right machining parameters must be chosen for the substance of the component so as to reduce kerf deviation characteristics. In order to determine how the laser process parameters of "laser power," "cutting speed," "gas pressure," "working distance," and "focus position" affect, a study was done to determine the optimal values for top kerf deviation and bottom kerf deviation. Lohr et. al. [8] valued of KPD is then predicted using an artificial neural network (ANN)-based model, which takes into consideration all the factors affecting the cutting process as well as the various classification criteria used. The primary contributions of this paper are the novel metrics that are suggested for evaluating the kerf profile in PMMA sheets. Second, choosing the best cutting parameters, using ANN as a precise technique for geometrical modelling, and connecting the factors that affect laser cutting. Khoshaim et. al. [9] applied different process responses have been correlated with various process variables using regression models. There were distinct hard, medium, and softer regions on the cross-section. By increasing gas pressure and laser power while lowering sheet thickness and cutting speed, the rough area is expanded. At high cutting speeds, high laser powers, and high gas pressures, increased kerf variation has been seen. The worst surface roughness and largest heat affected zone were created by high laser power and slow cutting speed. A lower laser

power and a quick cutting speed are recommended for decreasing the heat affected zone and surface roughness. Yet, increasing this cutting speed might result in an unacceptable amount of kerf variation. Bucossi et. al. [10] showed that the circumstances needed to cut grids were different from those needed to cut straight lines. The P/S ratio, which determines the heat input energy and the delivered energy density, was thus determined to be the most influential factor in determining the characteristic richness of these grid systems, given a constant frequency of heartbeats. These findings offer a scalable way for figuring out the laser cutting parameters needed to create intricate, very large-area CNT structures. Tura et. al. [11] studied surface roughness which was minimized during laser cutting of CO₂ utilizing a sound wave in 304 stainless steels by employing a genetic algorithm in conjunction with the response surface approach. Taguchi L9 orthogonal mesh experiments were conducted to analyze the results of varying processing variables such as cutting speed, nitrogen gas pressure, and focal point position. The influence of printing parameters on surface roughness was assessed using ANOVA, main effect plots, and 3D surface plots. Anghel et. al. [12] studied the cut surface underwent a SEM examination, it exposed a smooth, even surface with a faint woven design at the top and some attached dirt at the bottom. The absence of cavity, fissures, and dents on the outside is evidence that favorable surface morphology was produced under ideal conditions. The findings of this study show that laser beam cutting has a potential for producing high-quality miniature gears. Prashant Kumar Shrivastava et. al [13] applied pulsed Nd:YAG laser cutting was used to cut a sheet of titanium (grade 5) alloy with the narrowest kerf and the least kerf variation possible. An approach that combines multiple regression analysis and genetic algorithms has been devised and used to optimize kerf deviation and kerf width simultaneously. The statistical evaluation of the created model for kerf width and kerf deviation has been performed using the analysis of variance (ANOVA) technique. The significance of the ANOVA result shows that the created models are useful and have potential application in predicting kerf width and kerf deviation. Eltawahni et. al. [14] looked into CO₂ laser cutting of AISI316L medicinal grade stainless steel. In order to create the experiment layout, the design

of experiment (DOE) method was applied. The primary goal of this study to establish a causal relationship between the aforementioned process parameters and the state-of-the-art quality parameters of higher kerf, lower kerf, their ratio, cut section roughness, and operating cost. The best cutting setting to improve quality or reduce running costs was then determined by applying a general optimization routine. Mathematical models were developed to identify the relationship between the process variables and the edge quality features. It has also been determined how processing factors affected quality features. Parthiban et. al. [15], according to the study, the correct selection process variables determine the minimal kerf width necessary while cutting stainless steel plate. The factors taken into consideration include cutting speed, gas pressure, and laser output strength. Further research on the effect of cutting parameters on cut accuracy was conducted utilizing the box-behnen developing a response surface approach to track top and bottom kerf sizes. Ultimately, most optimal settings for a CO₂ laser cutter are determined to use a genetic algorithm. The experimental study of Hastelloy C 276 Kerf width during Co₂ laser cutting is presented in this article. It has been studied how one process reaction, Kerf width, is affected by three process parameters: Laser Power, Cutting Speed, and Gas Pressure. Taguchi L9 and an orthogonal array were used to construct the experiment. Similar studies were found in the literature [15-23] where experimental investigations were carried out.

MATERIAL AND METHODS

There are three typical trimming criteria in play. During the cutting process, it is essential to calculate the laser power, cutting speed, and gas pressure. higher width kerf and lower width kerf. The material chosen for examination in this study was Hastelloy C 276. The presented study uses an optimization method that focuses on the configuration of the Taguchi process parameter in a series of steps to arrive at a minimum. Hastelloy C 276 is an austenitic steel with a composition of 0.6% magnesium, 15.5% chromium, 0.088% carbon, 0.034% silicon, 0.001% Sulphur, and 0.004% phosphorus. The mixed-value level of carbon is kept at a level that is appropriate for the majority of service uses. Table 1 shows the sample's chemical composition after Spectro

analysis, which was used in Table 2 of the research. (Fig 1).

Table 1. Chemical composition of Hastelloy C-276

Element	C	Mn	Si	S	P	Cr
W%	0.005	0.41	0.02	0.002	0.005	15.8
Element	Ni	Mo	Co	W	Fe	V
W%	Bal	16.3 6	0.05	3.45	6.06	0.17

Table 2. Carbon steel's mechanical Characteristics

Material	Tensile strength (MPa)	Yield strength (MPa)	Elongation	Density
Hastelloy C-276	790	355	40%	8.89/cm3

EXPERIMENTAL SETUP

The laser cutting machine is set up as shown in Fig 1 which is continuous 4 kW CO2 laser cutting machine. This machine set up was utilized for the said investigations, where it is kept in a well-ventilated area. The cutting operations were performed with safety glasses, gloves, and a face mask. Before the experiment, the laser beam was checked to make sure it was aligned and focused correctly by performing the trail experimentations in a Nitrogen assist gas.



Fig. 1. Experimental set up of laser cutting process

Experimental Approach

The Taguchi technique was used to determine the ideal processing variable values that would produce higher and lower kerf widths during CO2 Laser cutting. Taguchi recommended using orthogonal arrays to gather

particular data and then examining the data to identify the best strategy variables. The lower-the- better, the higher-the-better, and the nominal-the- better output features are the three that the Taguchi quality concept design recommends being taken into account when assessing the signal-to-noise ratio. This method evaluates a large number of parameters with a tiny sample size using orthogonal arrays. Improved output characteristics and a better signal-to-noise ratio are related. In this instance, the stage of the process parameters allows for the best S/N ratio efficiency. Classifying statistically significant process variables using analysis of variance (ANOVA). The characteristics that will maximize machining output led to the selection of the higher width kerf and lower width kerf.

The values for the lower is better criterion for the respective S/N ratios were calculated using the output period measurements in the following equation.

$$S/N \text{ ratio } (\eta) = -10 \log_{10} \frac{1}{n} \sum_{i=1}^n y_i^2$$

Process parameters and design of tests (DOE)

You can carry out research more methodically by using the Design of Experiments. The process variables and their corresponding levels are listed in Table 3. The Taguchi method uses a simple design of orthogonal arrays and only a small number of trials to analyze the entire parameter range. The study used a Taguchi-based experimental setup with a typical L9 orthogonal array and three levels of three crucial process parameters, including laser power, cutting speed, and gas pressure.

Table 3 Process Factors and Levels

Input process parameters	Unit	Notation	Min Limit	Max Limit
Laser Power	watt	LP	2100	3500
Cutting Speed	mm/min	CS	1200	2500
Gas Pressure	bar	GP	12	16

Alignment Orthogonal

As shown in the chart below, the L9 OA used in this research enables the estimation of many critical effects in a perpendicular manner with a small sample size. Table 4 contains experiments on L9 OA.

Table 4. Investigational arrangements utilizing a rectangular matrix of L9

Exp. No.	LP	CS	GP
1	2100	1200	12
2	2100	1850	14
3	2100	2500	16
4	2800	1200	14
5	2800	1850	16
6	2800	2500	12
7	3500	1200	16
8	3500	1850	12
9	3500	2500	14

RESULTS AND DISCUSSION

The testing results for higher width kerf and lower width kerf along with pertinent S/N ratios are presented in Tables 5. While machining, it is common to aim for higher width kerf and lower width kerf values to ensure a high standard of quality and precision, so it's preferable for higher width kerf and lower width kerf if the provided data is as low as possible.

Table 5. Outcomes of tests on Ratio of kerf width and S/N ratio

Ex. No.	LP	CS	GP	Upper kerf width	Lower kerf width	Ratio of kerf width	SNRA
1	2100	1200	12	0.390	0.330	1.17	2.64
2	2100	1850	14	0.670	0.350	1.91	-1.48
3	2100	2500	16	0.330	0.390	0.85	4.84
4	2800	1200	14	0.880	0.580	1.49	-0.45
5	2800	1850	16	0.510	0.450	1.12	2.42
6	2800	2500	12	0.498	0.361	1.29	1.66
7	3500	1200	16	0.500	0.320	1.56	0.32
8	3500	1850	12	0.840	0.770	1.09	0.81
9	3500	2500	14	0.540	0.410	1.31	1.39

Table 6. Response Chart for Ratio of kerf width Signal-to-Noise Ratios

Level	LP	CS	GP
1	1.310	1.407	1.183
2	1.300	1.373	1.570
3	1.320	1.150	1.177

Delta	0.020	0.257	0.393
Rank	3	2	1

Table 6 displays the S/N ratio that was found for the Ratio of kerf width, one of the control parameter's organized using an orthogonal matrix (Fig 2).

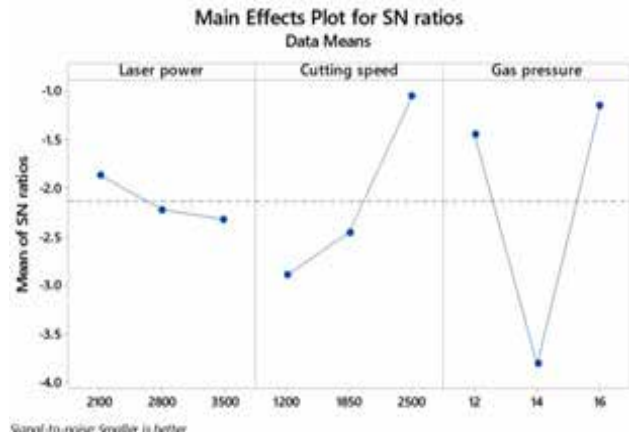


Figure 2 Plots of the main effects for ratio of kerf width

Method of Analyzing Variation

ANOVA is used to calculate the contribution of a self-determining factor's input to the outcomes. From Table 7, it is typically clear that Laser Power and Speed provide approximately 16.73% and 1.06% of the kerf width ratio while Gas Pressure provides ore, or 38.36%.

Table 7 S/N analysis using an ANOVA for Ratio of kerf width

Source	DF	Seq SS	Adj MS	P
LP	2	0.3538	0.1769	1.06%
CS	2	5.5814	2.7907	16.73%
GP	2	12.7995	6.3997	38.36%
Residual Error	2	14.6347	7.3173	
Total	8	33.3694		

Validation of Experiment

The ratio of kerf width was predicted using the ideal conditions discovered by the Taguchi technique. At a laser power of 2800, a cutting speed of 2500, and a gas pressure of 16, the Taguchi method projected a ratio of kerf width value of 1.30. Under the aforementioned ideal circumstances, during the real experiment, we obtained a Ratio of kerf width of 1.12.

Table 8 Confirmation Test for Ratio of kerf width

Sr. No	Predicted Ratio of kerf width	Actual Ratio of kerf width
1	1.30	1.12

CONCLUSIONS

This study explored and described the Ratio of kerf width in the optimization of CO2 laser cutting processes using the Taguchi method's parameter design. The following inferences can be drawn from the experimental findings of this study:

- Based on the analysis of the modification findings, the characteristics of the ratio of kerf width that are most successful were found. For the optimal ratio of kerf width, the laser strength is the most important factor.
- As shown in Tables 7, the ideal conditions for minimizing Ratio of kerf breadth are laser power of 2800, cutting speed of 2500, and gas pressure of 16.

REFERENCES

1. Girdu, C.C. and Gheorghe, C. (2022) "Energy efficiency in CO2 laser processing of Hardox 400 material," *Materials*, 15(13), p. 4505. Available at: <https://doi.org/10.3390/ma15134505>.
2. Madić, M. et al. (2022) "Application of a robust decision- making rule for comprehensive assessment of laser cutting conditions and performance," *Machines*, 10(2), p. 153. Available at: <https://doi.org/10.3390/machines10020153>.
3. Alsuruji, G. et al. (2022) "Investigation and TGRA based optimization of laser beam drilling process during machining of Nickel Inconel 718 alloy," *Journal of Materials Research and Technology*, 18, pp. 720–730. Available at: <https://doi.org/10.1016/j.jmrt.2022.02.112>.
4. Senthilkumar, V., Adinarayanan, A. and Jagatheesan, K. (2023) "Grey relational analysis (GRA) for optimization of CO2 laser cutting of Stainless Steel," *Materials Today: Proceedings*, 72, pp. 2437–2442. Available at: <https://doi.org/10.1016/j.matpr.2022.09.439>.
5. Singh, S. et al. (2022) "Drilling parameter optimization of cenosphere/HDPE syntactic foam using CO2 Laser," *Journal of Manufacturing Processes*, 80,

pp. 28–42. Available at: <https://doi.org/10.1016/j.jmapro.2022.05.040>.

6. Zeilmann, R.P. and Conrado, R.D. (2022) "Effects of cutting power, speed and assist gas pressure parameters on the surface integrity cut by laser," *Procedia CIRP*, 108, pp. 367–371. Available at: <https://doi.org/10.1016/j.procir.2022.03.060>.
7. Hiwale, S. and Rajiv, B. (2021) "Experimental investigations of laser machining process parameters using response surface methodology," *Materials Today: Proceedings*, 44, pp. 3939– 3945. Available at: <https://doi.org/10.1016/j.matpr.2020.09.295>.
8. Löhr, C. et al. (2021) "Kerf Profile Analysis and neural network- based modeling of increasing thickness PMMA sheets cut by CO2 Laser," *Optics & Laser Technology*, 144, p. 107386. Available at: <https://doi.org/10.1016/j.optlastec.2021.107386>.
9. Khoshaim, A.B. et al. (2021) "Experimental investigation on laser cutting of PMMA sheets: Effects of process factors on Kerf characteristics," *Journal of Materials Research and Technology*, 11, pp. 235–246. Available at: <https://doi.org/10.1016/j.jmrt.2021.01.012>.
10. Bucossi, A.R. et al. (2021) "Experimental design for CO2 laser cutting of sub-millimeter features in very large-area carbon nanotube sheets," *Optics & Laser Technology*, 134, p. 106591. Available at: <https://doi.org/10.1016/j.optlastec.2020.106591>.
11. Tura, A.D., Mamo, H.B. and Desisa, D.G. (2021) "Multi- objective optimization and analysis for laser beam cutting of stainless steel (SS304) using hybrid statistical tools ga-RSM," *IOP Conference Series: Materials Science and Engineering*, 1201(1), p. 012030. Available at: <https://doi.org/10.1088/1757-899x/1201/1/012030>.
12. Anghel, C., Gupta, K. and Jen, T.C. (2020) "Analysis and optimization of surface quality of stainless-steel miniature gears manufactured by CO2 Laser Cutting," *Optik*, 203, p. 164049. Available at: <https://doi.org/10.1016/j.ijleo.2019.164049>.
13. Shrivastava, P.K. and Pandey, A.K. (2018) "Multi-objective optimization of cutting parameters during laser cutting of titanium alloy sheet using hybrid approach of genetic algorithm and multiple regression analysis," *Materials Today: Proceedings*, 5(11), pp. 24710–24719. Available at: <https://doi.org/10.1016/j.matpr.2018.10.269>.

14. Eltawahni, H.A. et al. (2012) "Effect of CO2 laser cutting process parameters on edge quality and operating cost of AISI316L," *Optics & Laser Technology*, 44(4), pp. 1068–1082. Available at: <https://doi.org/10.1016/j.optlastec.2011.10.008>.
15. Parthiban, A. et al. (2018) "Optimization of CO2 laser cutting of stainless steel sheet for curved profile," *Materials Today: Proceedings*, 5(6), pp. 14531–14538. Available at: <https://doi.org/10.1016/j.matpr.2018.03.042>.
16. Deshmukh, D. D., and V. D. Kalyankar. "Deposition Characteristics of Multitrack Overlay by Plasma Transferred Arc Welding on SS316L with Co-Cr Based Alloy—Influence of Process Parameters." *High Temperature Materials and Processes* 38.2019 (2019): 248-263.
17. Kakade, S. P., A. G. Thakur, D. D. Deshmukh, and S. B. Patil. "Experimental investigations and optimisation of Ni-Cr-B-Si hardfacing characteristics deposited by PTAW process on SS 410 using response surface method." *Advances in Materials and Processing Technologies* (2022): 1-17.
18. Deshmukh, D. D., and V. D. Kalyankar. "Recent status of overlay by plasma transferred arc welding technique." *International Journal of Materials and Product Technology* 56, no. 1-2 (2018): 23-83.
19. Naik, H. V., D. D. Deshmukh, and V. D. Kalyankar. "Study of Heat Treatment Effect on Microstructure of PTA Weld Deposited Surface of SS 316L Steel." (2020).
20. Deshmukh, D. D., and V. D. Kalyankar. "Analysis of deposition efficiency and distortion during multitrack overlay by plasma transferred arc welding of Co-Cr alloy on 316L stainless steel." *Journal of Advanced Manufacturing Systems* 20, no. 04 (2021): 705-728.
21. Deshmukh, D. D., and V. D. Kalyankar. "Evaluation of surface characteristics of PTAW Hardfacing based on energy and powder supplied." In *Advances in Micro and Nano Manufacturing and Surface Engineering: Proceedings of AIMTDR 2018*, pp. 547-558. Singapore: Springer Singapore, 2019.
22. Kalyankar, V. D., and D. D. Deshmukh. "Failure investigations of failed valve plug SS410 steel due to cracking." In *IOP Conference Series: Materials Science and Engineering*, vol. 282, no. 1, p. 012007. IOP Publishing, 2017.

Design & Fabrication of Coconut Shell Crusher

Chaitali S. Deore

Sagarkumar J. Aswar

Department of Mechanical Engineering
Jawahar Education Society's Institute of Technology, Management & Research
Nashik, Maharashtra
✉ chaitalijit@gmail.com

ABSTRACT

The goal of this project was to create a machine for the extraction of coconut fiber that would be useful to Indian farmers and small-scale coir companies. The objective was to create a small, portable coconut fiber extraction device that could be utilized in isolated communities, cut down on labor and time expenses, and offer a workable answer to the challenges in the current procedure. This would make it possible to harvest the unused husks from these places and provide fiber directly to the Coir Industry. The initiative also sought to create a marketing plan for this novel idea and raise public awareness of the affordable, readily available coconut fiber extraction machine on the market. Data collection on user lifestyle and existing procedures was the first step in the project. We performed user interviews and an analysis of recent challenges.

Comparative benchmarking research was done on comparable procedures applied to other extraction techniques. In order to comprehend the user's challenges and production processes and present a summary of the solution that would meet their needs, an ergonomic simulation was also carried out. With the benchmarked product in mind, five designs with various features and operational procedures for the coconut fiber extraction machine were developed. The final concept, which may be applied in small-scale coir enterprises and in the farming sector, was chosen after taking into account the users' operating environment and maintenance requirements. Considering the needs and purchasing power of the users, a prototype was created. To extract fiber from the coconut, this machine uses a gear mechanism that involves two barrels rotating in opposite directions. In order to separate the fiber and give the coconut shell linear motion, cutting pins are put into indexing holes. The user group participated in the validation process, and the results were favorable. There may be a market for this product, it was noted. By using sophisticated manufacturing techniques, more work might be done in terms of material, weight reduction, and aesthetics.

KEYWORDS : *Blade, Coconut shell machine, Low carbon steel, Failure analysis.*

INTRODUCTION

A byproduct of coconut shells, coconut shell powder is utilized as a filler in thermo set molding powders like Bakelite, phenol formaldehyde, and synthetic resin glues. Having a sufficient supply of coconut shells is the most important requirement for making coconut shell powder. Finding dependable sources for consistent supply is essential, and the factory's location must be decided upon accordingly. For thermo set molding

powder, a mesh size of 80 to 100 works well; however, for synthetic resin glues, the size needs to be between 230 and 240 mesh. Since coconut shells are typically thrown away or used as fuel, coconut shell powder adds significant value. Compared to other fillers, this industrial product is thought to be appropriate and reasonably priced. The production of coconut shell powder is simple and adds a significant amount of value.

A byproduct of coconut shells, coconut shell powder is

utilized as a filler in thermo set molding powders like Bakelite, phenol formaldehyde, and synthetic resin glues. It is also a raw material utilized in the companies that produce activated carbon. The compound filler, or extender, coconut shell powder is widely used in the production of phenol molding powder, often known as Bakelite plastic. It works well with mastic adhesives, resin casting, bituminous materials, and specialized liquid surface finishing products (as an absorbent). It is utilized as a lost circulation material in oil well drilling when it is in the granular form. Powdered coconut shell is used to gun blast fragile items and old buildings as a mild abrasive. It can enhance the smoothness and luster of molded items and increase their ability to withstand heat and moisture.

Because of its long and even burning properties, coconut shell powder is widely used in Ayurveda and to make mosquito coils, an insect repellent used in Asia. The substance is widely used as a phenol extruder and filler in synthetic resin glues, as well as in plywood and laminated boards. Coconut shell powder is an industrial product because it is mostly used as a filler. It is employed in the production of synthetic resin adhesives and thermoset molding powders, such as Bakelite and phenol formaldehyde molding powder. Various end-uses demand varying particle sizes of powder.

I concur that promoters with prior experience in relevant marketing would be more appropriate for this endeavor. Over the past eight to ten years, India's industrial growth has been rather consistent, and the country's economy is gradually emerging from the demand recession. An encouraging indicator for the coconut fiber extraction machine business is the fact that industrial production is once again increasing.

LITERATURE SURVEY

P. B. Mohan, R. Thiruppayhi studied that the scope of this project was to design and development of coconut shell crusher machine focus on chopping of coconut husks and shells. The crushers are mounted on two shafts, which rotate parallel driven by a spur gear. The power from the electrical motor is transmitted to cutter shaft through a belt drive. Crushing is made inside the crushing house due to the effect of tensile, friction, and impact effect in crushing process. The coco powder gets crushed and powder is collected at the bottom.

Compact shell crusher machine is a fiber extracting machine from the husk and shell of coconut and used as an excellent soil conditioner and is being extensively used as a soil-less medium for agricultural purposes. With its moisture retention qualities, coir pith is ideal for growing anthuriums and orchids. Available in raw form or converted into organic manure.

Ranganathan et al studied that the agriculture is one of the oldest professions but the development and use of machinery has made the job title of farmer a rarity. Instead of every person having to work to provide food for themselves, smaller portion of our population today works in agriculture, the smaller portion provides considerably more food than the other can eat.

The basic technology of agricultural machines has changed little in the last century with the coming of the Industrial Revolution and the development of more complicated machines. In this work design and fabricate the automatic coconut crushing by using crank and slotted lever mechanism, for crushing agricultural products like coconut. The present work to fabricate a machine which is simple in construction than the existing machines. The equipment make the use of crank and slotted lever mechanism with one slider to couple with an electric motor using pulley and belt drive.

Surasnl and Apriardi Ihlas studied that blade mounted on coconut shell crusher machine was frequently having damaged while being operated in making of coconut shell powder at small and medium industries. This took place repeatedly during the operation, therefore blade repairing and replacement has to be done for every 16 hours at the wear rate of 24.28%. A research was carried out to find out the cause of damage to the metal blade material on the coconut shell crusher machine. The scope of this research included the observation on visual examination, dimensions examination, chemical composition, hardness, and metallography. The results of observations and tests showed that blade was broken due to abrasion and deformation during operation.

The metal material used for the blade was low carbon steel. Chemical composition of the metal content of the blade was: C (0.103 up to 0.144 %) and Mn (0.657 up to 1.400 %). Hardness value of blade metal materials was 146 up to 148 Hv. Microstructure consisted of ferrite and pearlite. This low carbon steel material is not

suitable to be used as a blade on coconut shell crusher machines for producing of coconut shell. Repairing and maintenance of welding coating methods on blades using low carbon electrodes does not give increased significant value of hardness.

Blade replacement in coconut shell crusher machines must comply with the requirements of tool steel with suitable heat treatment or the use of low carbon steel with the carburization process.

Kishan Ramesaraand and Umesh Prasad studied that conceptual design of a machine for cutting coconut husk halves into pieces for activated carbon production. Alternative interlocking and welded blade arrangements are presented with the potential for scaling up the processing of coconut shell crushing into smaller pieces. Virtual simulations and the experimental testing of a functional prototype are used to validate the conceptual design. The design is shown to be functionally acceptable, and directions for further improvements and development are outlined.

H. Azmi et al published that the coconut shell crushing machine comprising of two rollers with spikes, chain drives, presser, clearers, shafts and belting system were developed for small-scale production in rural areas. Performance test analysis showed that the machine crush coconut shell without any nut breakage or distortion of the extracted fiber length. The objective of this project is to improve the efficiency and productivity in producing coconut shell without husks by using the best selection of mechanical mechanisms with minimum costs.

In between the motor and the shafts, one box of worm gears is used to reduce the rotation speed. Two metal cylinders with a series of spikes are used to crush the coconut shell. The machine's average shell crushing efficiency and capacity are expected to 90%, respectively. In addition, the development of the machine is also a solution to the constraint of space, whereby a compact-size machine is more suitable for small and medium enterprises (SME's). Plus, it operates with lesser noise, which also contributes to a more viable operating condition for the environment.

THEORY

Methodology

Design Concept Generation

The term "design concept generation" refers to the actual process of conceptual design, in which the technology, guiding principles, and shape of the product are roughly described in the design concept. It includes a thorough explanation of how the product will fulfill and satisfy client needs. A well-developed design concept may even be able to overcome current design limitations.

Numerous alternate concepts have been developed for this project. The best concept for the product was then determined by analyzing each of the numerous created concepts separately. The ideas that offered the most benefits were deemed to be the best ones and are awaiting additional analysis. The selected concept was further developed into a product sketch.

The process of generating design concepts is typically represented through sketches or crude three-dimensional models, frequently supplemented with a succinct written explanation of the general ideas. Four concepts—from idea A to concept D—were put forth for this semi-automatic coconut machine. As a result, in order to determine the final concept design for the semi-auto coconut machine, the concepts must be reviewed (scoring and screening). Impact mill with air sweeping and whizzer classifier running in closed circuit.

Operating Principle of Coconut Shell Crusher

The impact pulverizer is composed of a solid shaft-mounted whizzer classifier for fineness adjustment, swing hammers, and a pressure gradient generator. The rotor is encased. The hopper or the motorized rotary feeder is how the raw material to be ground gets into the crushing chamber. The feed material is reduced to a fine powder by the hammers' impact on it as it strikes the liner plates.

The ground material is moved in the direction of the whizzer classifier, which rejects the larger particles and sends them back to the crushing chamber for more grinding. After that, the material that is sorted is transported inside the cyclone for gathering and bagging. The system has a dust collector to provide dust-free operation and no ground powder loss.

DESIGN OF MACHINE COMPONENTS

The machine frame, holding mechanism, drive mechanism, and roller type blade mechanism are the main parts of the suggested coconut dehiscing machine. The frame serves as the primary structural support for the other parts of this machine. The construction of the frame is welded and measures 933 mm in length, 515 mm in width, and 845.1 mm in height. It is made of 50x50x5 mm angle iron. The driving mechanism consists of a motor, a rotating shaft with a chain drive system, and worm reduction gears with a belt drive system. The parts are driven by a 2 horsepower single phase induction motor running at 1500 rpm. Additionally, the machine has a 70:1 gearbox attached to a shaft, which is a long revolving cylinder.

Bearing blocks serve as the holding mechanism's means of mitigating vibrations or wobbling brought on by strong loads during shaft rotation over longer lengths. Consequently, two bearing blocks were employed between the reduction gear box and the roller blades, and two more were positioned at the right end of the roller shaft, to lessen machine vibration. The mechanism of the roller type can be described as follows: two elongated rollers are disposed of by separating the components.

Thirty-two metal spikes (2 x 20 x 5 mm) are welded onto a mild steel pipe with a 115 mm diameter and placed on a roller shaft to produce each roller. Each roller shaft is constructed from a mild steel rod with a 40mm diameter. The main shaft measures 890 mm in length, while the parallel shaft measures 644.87 mm. Ball bearings support the rod at both ends, and a sprocket is positioned at the left end. A mild steel plate with a thickness of 2 mm is cut with u-notches on one edge to manufacture the clearer. Above the rollers, the clearers were bolted to the frame. With just one operator needed, the created coconut dehusking machine is incredibly simple to use. The spiked rollers revolve in the opposite direction when the switch is activated.

Frame:

Top covers are fastened on a solid iron base that has been machined and aligned. Feeder: An automatic rotating feeder having a feed control mechanism that is gear driven from the main shaft.



Fig 1. Main frame

The frame serves as the primary structural support for the other parts of this machine. The frame is a welded construction measuring 933 mm in length, 515 mm in width, and 845.1 mm in height. It is made of mild steel angle iron, 50 x 50 x 5 mm. In order to evenly distribute weight and vibration to the support frame below, the steel is firmly fastened to the frame. The primary frame's geometric structure is intended to provide the entire structure superior stability and form.

Holding mechanism

Bearing blocks are used to lessen swaying or vibrations when long shafts carrying heavy loads rotate. Consequently, two bearing blocks are employed between the reduction gear box and the roller blade, and two more are positioned at the right end of the roller shaft, to lessen the machine's vibrations. Plummer blocks are another name for bearing blocks. Its construction is straightforward, with a bearing hidden behind a metal block that is firmly fastened to the machine's frame.

Crushing Chamber



Fig 2. Crushing chamber

Rotor

Thick, machined mild steel plates fixed to the main shaft: alloy steel The classifier is a mild steel whizzer classifier that has an adjustable spider that allows the fineness of the ground powder to be controlled up to 300 mesh, depending on the material being ground into bearing powder.

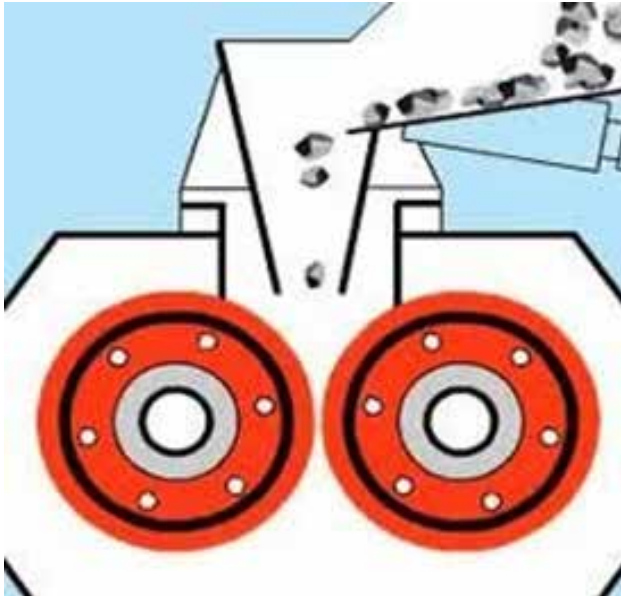


Fig 3. Rotor

Roller type blade mechanism:

The mechanism of the roller type is designed with two elongated rollers that are positioned and separated, roughly parallel to each other in relation to the base, and easily accessible. Additionally, a drive mechanism with direct driving interaction with the rollers is supplied to support the base. The rollers are connected to the drive means in a way that forces them to revolve against each other and, in a preferred embodiment that will be discussed in more detail below, at comparatively different speeds. The two outer exposed surfaces that the rollers together define could be thought of as the roller's top sections.

When arranged in this manner, a coconut Placed on top of the rollers will be forced into the space between them as the rollers move toward the center.

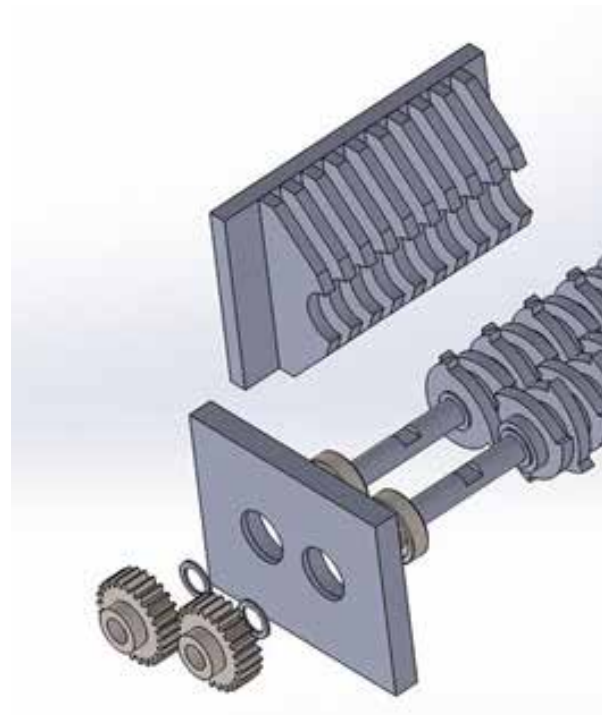


Fig 4. Blades Used in crusher

Pulley

The machine needs a belt drive that is made to run at a constant pace. It comprises of two V-belts placed in parallel on equal-sized pulleys with grooves. A typical pulley with a $\beta = 30^\circ$ angle of groove was chosen because it has the properties that make it suitable for heavy loads, easy to design, readily available, low maintenance costs, and no end thrust on the bearings.

As a result, the center distance C between the nearby pulleys was calculated as follows:

$$C = \frac{1.5D}{(VR)^3}$$

Where; VR is the speed ratio of this drive and D is the diameter of the driven pulley.

As both pulleys have the same diameter, the velocity ratio, VR is equal to 1.

The length of the belt can be determined by:

$$l = 2c + 1.57(D_2 + D_1) + \frac{(D_2 - D_1)^2}{4c}$$

The mass of belt per unit length (m):

$$m = a \times l \times \rho$$

Angle of lap of drive (θ):

$$\Theta = 180 - \left[-1 \left(\frac{D_2 - D_1}{2C} \right) \right]$$

Velocity of belt, v is with speed N is calculated as:

$$v = \frac{\pi DN}{60}$$

Nominal pitch length

$$L = 2C + \pi/2 (D + d) + (D - d) 2/4C$$

Crushing Spikes

An important part of peeling the coconut is done by the spikes that are fixed to the revolving shafts. It serves as the machine's tool. The presence of piercing mechanisms, shaped like several spikes on each roller blade, facilitates efficient removal of the coconut husk. The array of spikes is arranged to make it easier to penetrate, grasp, and shred the coconut husk. The spikes are sharpened and roughly equal in distance from one another. But there are also some blunt spikes mixed in with the sharpened ones. After the coconut is fed into the machine, the blunt spikes shred off the coconut husks while the sharp spikes penetrate into the coconut to hold onto it.

Stated differently, a greater surface area covered by sharpened spikes on the coconut will lead to a higher chance of the nut breaking off due to greater penetrating forces. As a result, this design configuration works well for crushing coconut shells as ef

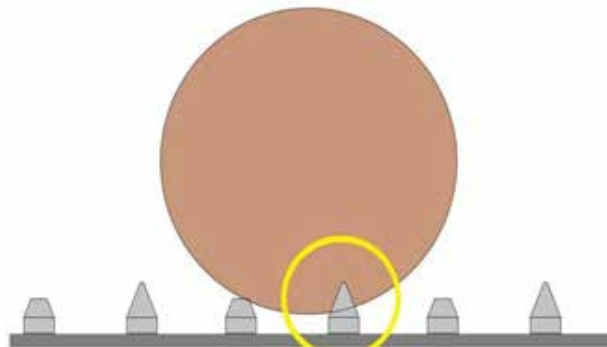


Fig 5. Crushing Spikes

Bearings:

- Self-aligning ball bearings in cast iron housing with suitable grease cups for lubrication.

- The expression for
- the equivalent dynamic load is written as,
- $P = XVFr + YFa$ (15.2)
- where,
- P = equivalent dynamic load (N)
- Fr = radial load (N)
- Fa = axial or thrust load (N)
- V = race-rotation factor
- X and Y are radial and thrust factors respectively.
- When the bearing is subjected to pure radial load,
 $P = Fr$
- When the bearing is subjected to pure thrust load,
 $P = Fa$



Fig 6. Bearing

Rotating Shaft (Main Shaft)

An extended revolving cylinder that transfers power from one location to another is called a shaft. Tangential forces provide the shaft with power, and the torque that results is connected to one end of the shaft, which is connected to the gear box's output, and the other end, which serves as a support for the rolling system and the main roller.

The tensile stress that results from applying an axial tensile force to the shaft is determined by,

$$\sigma_t = \frac{P}{\left(\pi d^2 \frac{1}{4}\right)}$$

When the shaft is subjected to pure bending moment, the bending stresses are given by,

$$\sigma_b = \frac{32M_b}{\pi d^3}$$

When the shaft is subjected to pure torsional moment, the torsional shear stress is given by,

$$\tau = \frac{16M_t}{\pi d^3}$$

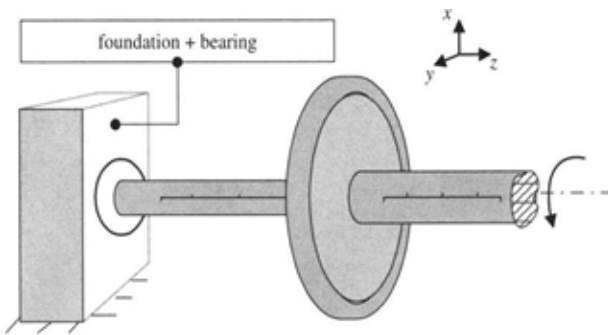


Fig 7. Rotating Main Shaft

Cyclone Mild Steel Sheet Fabricated Dust Collector: Top and bottom halves of mild steel sheet, to be interconnected by dust bags.



Fig 8. Dust Collector

Uses of Coconut Shell Powder

- The industries that produce activated carbon use it as a raw material.
- It is widely utilized as an extender and filler in compound filler used in the production of Phenolic molding powder (Bakelite plastic).
- It is added to synthetic resin adhesives as a filler.
- Mastic adhesives, resin casting, bituminous goods, and specialist surface finishing liquid products (as an absorbent) are among the applications where it works well.
- It serves as a mild abrasive in pastes for heavy-duty hand cleaners.
- It can increase the molded items' resistance to heat and moisture while also giving them a glossy, smooth surface.
- It is utilized as a lost circulation material in oil well drilling when it is in granular form.
- Shot blasting is a technique used to lightly abrasive sensitive objects

Advantages

- Two-way reversible beater assembly with high speed rotor.
- Dual access doors provide simple access to the impact-pulverized interior.
- Comes in several sizes and models. Silent, cold running.
- Robust construction and dustless operations.
- Minimal particular power usage.
- The provided Coconut Shell Crusher system is supported by the newest technological advancements and aids in achieving the highest level of process efficiency while crushing and reducing the size of coconut shells.
- Aids in the promotion of a healthy digestive tract by eliminating toxins that impair immune system function, oxidative damage, and allergic reactions.

CONCLUSION

A device to shatter coconut shells has been conceptually designed and shown. A method for crushing coconut shells that replaces broken and distorted shells has been created for small-scale farmers in rural areas in the process of creating the coconut shell crusher machine. The machine crushes shells with an average efficiency and is simple to operate. This machine's introduction will not only solve the issue of a shortage of labor, but it will also boost the productivity of cow dung cake.

Coconut shells can be crushed using the suggested design independent of orientation or position. Detailed performance testing, design optimization, and user acceptability testing are still needed to create a functional product that can be used in rural areas.

REFERENCES

1. P. B. Mohan, R. Thiruppayhi, S. Sampath Kumar, Y. Mohamed Yasar Arabath, T. Pavithran "Design and Fabrication of compact coconut shell crusher" Department of Mechanical Engineering, Sri Eshwar College of Engineering, Coimbatore, India. Volume 4, Issue June 2021.
2. Ranganathan et al, "Design and Fabrication of Coconut Crushing Machine Using Four Bar Mechanism", Department of Mechanical Engineering Anna University, Volume 8 Issue No.3 November 2018.
3. Surasnol and Apriardi Ihlas, "Failure Analysis of Blade on Coconut Shell Crusher Machine Center for Material and Technical Product J1", IOP Conf. Series: Materials Science and Engineering, July 2018.
4. Kishan Ramesaraand and Umesh Prasad, "A Mechanism for Cutting Coconut Husks", The West Indian Journal of Engineering Vol.37, No.2, pp.54-62, January 2015.
5. H. Azmi et al, "Design and Development of a Coconut Dehusking Machine", Journal of Advanced Research Design, Vol. 4, No.1. Pages 9-19, April 2015.
6. Shigley J.E. and C.R., Mechanical Engineering Design, McGraw-Hill, 2001.
7. Phelan R.M., Fundamentals of Mechanical Design, Tata McGraw-Hill, 1975
8. Peck H., Ball and Parallel Roller Bearings— Design Applications, Pitman, 1971
9. Gasson P.C. and Mied D.C.M., Theory of Design, B.T. Batsford, 1974.

KEY BUILDING BLOCKS OF JIT

NAAC Accredited

1

2

AICTE Approved
Affiliated to SPPU

Academic Outreach

3

4

Resourceful
Faculties

Green, Eco Friendly
Environment

5

6

A State of art
Infrastructure

Industry
Tie-Ups (MoU's)

7

8

Smart Class Rooms
Well-Equipped Labs

Extra-Curricular
Activities

9

10

Digital Library
WiFi Enabled Campus

Strong Alumni
Networks

11

12

Canteen & Transport
Facilities





**Jawahar Education Society's,
INSTITUTE OF TECHNOLOGY,
MANAGEMENT & RESEARCH, NASHIK.**
(Approved by AICTE, New Delhi, DTE, Government of Maharashtra, Affiliated to Savitribai Phule Pune University)



Courses Offered

	Computer Engineering	Electrical Engineering	
	Information Technology	Civil Engineering	
	Artificial Intelligence & Data Science	Mechanical Engineering	

We at JIT Believe in

- **Innovation**-develop through experiential learning
- **Creativity**- through participative, problem-solving approach.
- **Excellence**- adopting continuous processes by exhibiting quality in-overall
- **Transparency** -the larger process of informed governance and organizational learning.
- **Social Responsibility**- by involving them in various social activities.
- **Respect**- Cultivating a domain in which individual can sustains with dignity.

**Jawahar Education Society's,
Institute of Technology, Management and Research
Survey No 48, Gowardhan, Gangapur Road,
Nashik - 422 222. Maharashtra, India
Contact Number :0253-2970077
Email Id: principaljitnashik@rediffmail.com
Website: www.jitnashik.edu.in**



**PUBLISHED BY
INDIAN SOCIETY FOR TECHNICAL EDUCATION
Near Katwaria Sarai, Shaheed Jeet Singh Marg,
New Delhi - 110 016**